APR 1 - 1997

ORNL/TM-13401

ornl

ORNL
Master Copy

OAK RIDGE
NATIONAL
LABORATORY

LOCKHEED MARTIN

Performance Assessment for the Class L-II Disposal Facility

March 1997

MANAGED AND OPERATED BY
LOCKHEED MARTIN ENERGY RESEARCH CORPORATION
FOR THE UNITED STATES
DEPARTMENT OF ENERGY

ORNL-27 (3-96)

This report has been reproduced directly from the best available copy.

Available to DOE and DOE contractors from the Office of Scientific and Technical Information, P.O. Box 62, Oak Ridge, TN 37831; prices available from (423) 576-8401, FTS 626-8401.

Available to the public from the National Technical Information Service, U.S. Department of Commerce, 5285 Port Royal Rd., Springfield, VA 22161.

This report was prepared as an account of work sponsored by an agency of the United States Government. Neither the United States Government nor any agency thereof, nor any of their employees, makes any warranty, express or implied, or assumes any legal liability or responsibility for the accuracy, completeness, or usefulness of any information, apparatus, product, or process disclosed, or represents that its use would not infringe privately owned rights. Reference herein to any specific commercial product, process, or service by trade name, trademark, manufacturer, or otherwise, does not necessarily constitute or imply its endorsement, recommendation, or favoring by the United States Government or any agency thereof. The views and opinions of authors expressed herein do not necessarily state or reflect those of the United States Government or any agency thereof.

ORNL-TM/13401

PERFORMANCE ASSESSMENT FOR THE CLASS L-II DISPOSAL FACILITY

March 1997

Prepared for
ENERGY SYSTEMS WASTE MANAGEMENT ORGANIZATION
LOCKHEED MARTIN ENERGY SYSTEMS, INC.
Oak Ridge, Tennessee

Prepared by
OAK RIDGE NATIONAL LABORATORY
Oak Ridge, Tennessee 37831
managed by
LOCKHEED MARTIN ENERGY RESEARCH CORP.
for the
U.S. DEPARTMENT OF ENERGY
under Contract No. DE-AC05-96OR22464

CONTENTS

LIST OF FIGURES vii

LIST OF TABLES xi

ABBREVIATIONS AND ACRONYMS xv

EXECUTIVE SUMMARY xvii

1. INTRODUCTION 1-1

2. DESCRIPTION OF THE CLASS L-II DISPOSAL SITE 2-1
   2.1 Site Characteristics 2-1
      2.1.1 Site Location and Topography 2-1
      2.1.2 Construction Topographic Modifications 2-1
      2.1.3 Regional Climate 2-3
      2.1.4 Hydrology 2-3
      2.1.5 Geology and Soils 2-8
      2.1.6 Hydrogeology 2-16
   2.2 Waste Characteristics 2-19
   2.3 Waste Treatment, Certification, Storage, and Disposal 2-20
      2.3.1 Waste Treatment Facilities 2-23
      2.3.2 Low-Level Waste Characterization and Certification 2-23
   2.4 Class L-II Disposal Facility 2-24

3. ANALYSIS OF PERFORMANCE 3-1
   3.1 Scenario Development and Selection 3-3
      3.1.1 Release and Environmental Transport Scenarios 3-5
      3.1.2 Human Exposure Scenarios 3-10
      3.1.3 Scenarios Analyzed 3-21
   3.2 Assumptions 3-22
      3.2.1 Wastes 3-22
      3.2.2 Source Term Assumptions 3-23
      3.2.3 Site Assumptions 3-24
   3.3 Conceptual Models 3-31
      3.3.1 Waste Characteristics 3-31
      3.3.2 Site Hydrology 3-33
      3.3.3 Source Term 3-39
      3.3.4 Environmental Transport 3-47
      3.3.5 Exposure Pathway Modeling and Dose Estimation 3-55
      3.3.6 Verification and Validation of Methodology 3-57

4. RESULTS OF ANALYSIS 4-1
   4.1 Site Hydrology 4-1
      4.1.1 Terrain Analysis and Site Recharge 4-2
      4.1.2 Site Water Budgets 4-4

4.2 Source Term 4-6
4.2.1 Source Terms for Environmental Transport 4-6
4.2.2 Source Terms for Direct Intrusion 4-20
4.3 Environmental Transport 4-27
4.3.1 Transport in Shallow Subsurface and to Groundwater 4-28
4.3.2 Groundwater Transport 4-33
4.3.3 Surface Water Transport 4-39
4.3.4 Calculation of Contaminant Concentrations in Groundwater and Surface Water 4-39
4.4 Dose Analysis 4-43
4.4.1 Off-Site Exposure 4-52
4.4.2 Analysis for Inadvertent Intruders 4-55
4.5 Summary of Disposal Limits 4-74
4.5.1 Disposal Limits Based on Analyses for Off-Site Releases 4-74
4.5.2 Disposal Limits Based on Analysis for Inadvertent Intruders 4-78
4.5.3 Estimated Disposal Limits 4-81
4.5.4 Application of Disposal Limits to Mixtures of Radionuclides 4-84
4.6 Sensitivity and Uncertainty 4-85
4.6.1 Source Terms 4-86
4.6.2 Shallow Subsurface Transport 4-87
4.6.3 Groundwater 4-88
4.6.4 Surface Water Transport 4-88
4.6.5 Human Exposure Scenarios 4-88
4.7 Interpretation of Results 4-93
4.8 Continued Work 4-95
4.9 Quality Assurance 4-96

5. PERFORMANCE EVALUATION 5-1
5.1 Comparison of the Performance Assessment Results with the Performance Objectives 5-1
5.2 Application of the Results to Waste Acceptance Criteria 5-2
5.3 Improvement and Maintenance of the Performance Assessment 5-2

6. PREPARERS 6-1

7. REFERENCES 7-1

APPENDIX A. DESCRIPTION OF THE SOURCE1 COMPUTER PROGRAM A-1
A.1 Introduction A-1
A.2 Concrete Degradation Modeling A-1
A.2.1 Sulfate Attack A-2
A.2.2 Calcium Hydroxide Leaching A-3
A.2.3 Corrosion of Steel Reinforcement A-6
A.3 Concrete Structural and Cracking Analyses A-9
A.3.1 Structural Analysis A-9
A.3.2 Cracking Analyses A-19
A.3.3 Concrete Pad Degradation Model A-27
A.3.4 Leachate Collection System Degradation Model A-29

A.4 Flow Partitioning A-29
A.5 Radionuclide Release Modeling A-30
A.5.1 Advective Transport Model A-30
A.5.2 Diffusion Transport Model A-31
A.5.3 Calculation of Total Radionuclide Release A-33
A.6 References A-34

APPENDIX B. TRANSPORT-RELATED PROPERTIES OF RADIONUCLIDES IN WASTE AND CONCRETE USED IN THE PERFORMANCE ASSESSMENT OF THE CLASS L-II DISPOSAL FACILITY B-1
B.1 Introduction B-1
B.2 Background B-3
B.3 Transport Mechanisms B-4
B.3.1 Advection B-4
B.3.2 Diffusion B-5
B.4 Summary and Conclusions B-12
B.5 References B-16

APPENDIX C. ANALYSIS OF ATMOSPHERIC EMISSIONS FROM THE CLASS L-II DISPOSAL FACILITY C-1
References C-12

APPENDIX D. HYDROLOGY AND SUBSURFACE TRANSPORT MODELING D-1
D.1 Terrain Analysis D-1
D.1.1 Introduction D-1
D.1.2 Digital Terrain Analysis Methods D-2
D.1.3 Terrain Analysis of the CIIDF Site D-4
D.1.4 Hydrologic Modeling with TOPMODEL D-4
D.1.5 TOPMODEL Applications D-5
G.2 Unified Transport Model Determination of CIIDF Water Budgets D-5
D.3 The PADSIM Model D-11
D.3.1 Preferential Flow Algorithm D-11
D.3.2 Annual Increment in Soil Path Length D-12
D.3.3 Half-Life Calculations D-12
D.3.4 Chemical Adsorption D-12
D.3.5 Mass Balance Test D-14
D.4 References D-15

APPENDIX E. MODELING OF GROUNDWATER FLOW AND RADIONUCLIDE TRANSPORT AT THE CLASS L-II DISPOSAL FACILITY E-1
E.1 Porous Medium Contaminant Transport Theory E-1
E.2 Groundwater Modeling for the CIIDF E-3
E.2.1 Conceptual Model E-3
E.2.2 Computer Model E-5
E.3 References E-36

APPENDIX F. PLOTS OF MAXIMUM DRINKING WATER CONCENTRATION VS DISPOSAL INVENTORY F-1

APPENDIX G. DOSE ANALYSIS FOR OFF-SITE INDIVIDUALS AND INADVERTENT INTRUDERS G-1
G.1 Introduction G-1
G.2 Radionuclides Considered in Dose Analysis G-2
G.3 Assumed Exposure Scenarios and Exposure Pathways G-5
G.3.1 Exposure Scenarios and Exposure Pathways for Off-Site Individuals G-5
G.3.2 Exposure Scenarios and Exposure Pathways for Inadvertent Intruders G-6
G.4 Dose Conversion Factors for Internal and External Exposure G-8
G.5 Models and Parameter Values for Exposure Pathways G-14
G.5.1 Exposure of Off-Site Individuals to Radionuclides in Contaminated Water G-14
G.5.2 Exposure Pathways for Inadvertent Intruders into Disposal Facility G-19
G.6 Summary G-50
G.7 References G-55

FIGURES

Figure 2.1 Location of CIIDF on the ORR 2-2
Figure 2.2 Pre- and postconstruction topography in the vicinity of CIIDF 2-4
Figure 2.3 Location of Bear Creek watershed on the Oak Ridge Reservation 2-6
Figure 2.4 Geologic map of the Oak Ridge Reservation 2-11
Figure 2.5 Geologic map of the CIIDF modeling area 2-13
Figure 2.6 Geologic cross section through the CIIDF modeling area 2-14
Figure 2.7 Schematic profile showing subsurface flow zones and intervals, general thickness ranges, estimated relative water flux, and change in water type with depth for the aquitard of the CIIDF site in comparison to the aquifer of the Knox geological formation 2-17
Figure 2.8 Plan view of the CIIDF site 2-25
Figure 3.1 Iterative analysis method for releases to the environment for the CIIDF performance assessment 3-4
Figure 3.2 Grid cells representing the CIIDF 100-m compliance boundary 3-28
Figure 3.3 Linkage of simulation results from four simulation models for quantifying nuclide transport in the environment and surroundings of the CIIDF 3-32
Figure 3.4 The landscape surface generated from the digital elevation model of the CIIDF site as modified for facility construction 3-35
Figure 3.5 Map and frequency distribution of topographic index for the CIIDF site used for estimation of spatial variation in groundwater recharge 3-36
Figure 3.6 Flow chart of the major components of hydrologic simulation with the Unified Transport Model 3-37
Figure 3.7 The properties and structural equations of the PROSPER component of the Unified Transport Model used for calculation of evapotranspiration and soil water drainage 3-38
Figure 3.8 Logic flow of the SOURCE1 computer code 3-41
Figure 3.9 Logic flow of the concrete-degradation and -cracking subroutines 3-43
Figure 3.10 Essential features of PADSIM in the linkage between SOURCE1 and FTWORK for nuclide transport to groundwater and for lateral subsurface transport to surface water 3-50
Figure 3.11 Locations of USGS stream gauging stations in the vicinity of CIIDF 3-54
Figure 3.12 Record of stream discharge at USGS Station 03538270 3-56
Figure 3.13 Validation of FTWORK using study at the West Bear Creek site 3-62
Figure 4.1 Areas of stream channels (black), ephemeral wetlands (light grey), and remaining areas identified with differing rates of recharge from terrain analysis 4-3
Figure 4.2 Calculated release rates of ^{3}H from a CIIDF pad as a function of time 4-13
Figure 4.3 Calculated release rates of ^{14}C from a CIIDF pad as a function of time 4-14
Figure 4.4 Calculated release rates of ^{60}Co from a CIIDF pad as a function of time 4-15
Figure 4.5 Calculated release rates of ^{90}Sr from a CIIDF pad as a function of time 4-16
Figure 4.6 Calculated release rates of ^{99}Tc from a CIIDF pad as a function of time 4-17
Figure 4.7 Calculated release rates of ^{137}Cs from a CIIDF pad as a function of time 4-18
Figure 4.8 Calculated release rates of ^{238}U from a CIIDF pad as a function of time 4-19
Figure 4.9 Fraction of initial radionuclide inventory remaining in CIIDF as a function of K_d for years 100, 300, 500, 1000, and 2000 4-23
Figure 4.10 Fraction of initial radionuclide inventory remaining in CIIDF as a function of K_d for year 5000 4-24

Figure 4.11 Fraction of initial radionuclide inventory remaining in CIIDF as a function of K_d for year 10,000 4-25
Figure 4.12 Simulated ^{3}H release rates for the lateral subsurface and recharge paths from PADSIM as a function of time 4-31
Figure 4.13 Simulated ^{14}C release rates for the lateral subsurface and recharge paths from PADSIM as a function of time 4-32
Figure 4.14 Simulated ^{60}Co release rates for the lateral subsurface and recharge paths from PADSIM as a function of time 4-34
Figure 4.15 Simulated ^{90}Sr release rates for the lateral subsurface and recharge paths from PADSIM as a function of time 4-35
Figure 4.16 Simulated ^{99}Tc release rates for the lateral subsurface and recharge paths from PADSIM as a function of time 4-36
Figure 4.17 Simulated ^{137}Cs release rates for the lateral subsurface and recharge paths from PADSIM as a function of time 4-37
Figure 4.18 Simulated ^{238}U release rates for the lateral subsurface and recharge paths from PADSIM as a function of time 4-38
Figure 4.19 Drinking water concentration as a function of CIIDF inventory for ^{14}C 4-42
Figure 4.20 Drinking water concentration as a function of CIIDF inventory for ^{60}Co 4-44
Figure 4.21 Drinking water concentration vs time for ^{3}H 4-45
Figure 4.22 Drinking water concentration vs time for ^{14}C 4-46
Figure 4.23 Drinking water concentration vs time for ^{60}Co 4-47
Figure 4.24 Drinking water concentration vs time for ^{90}Sr 4-48
Figure 4.25 Drinking water concentration vs time for ^{99}Tc 4-49
Figure 4.26 Drinking water concentration vs time for ^{137}Cs 4-50
Figure 4.27 Drinking water concentration vs time for ^{238}U 4-51
Figure A.1 Schematic diagram of floor geometry used in the calculation of bending moments A-16
Figure A.2 Schematic diagram of steel and concrete geometry used in calculating stress resulting from corrosion of steel reinforcement A-26
Figure D.1 Map and frequency distribution of simulated soil water saturation deficit at the CIIDF site for 1197 and 1209 h in 1991 . . . . . D-6
Figure D.2 Map and frequency distribution of simulated soil water saturation deficit at the CIIDF site for 1245 and 3915 h in 1991 . . . . . D-7
Figure E.1 Location of CIIDF on the Oak Ridge Reservation E-7
Figure E.2 Finite difference horizontal discretization of the CIIDF groundwater model E-8
Figure E.3 Preconstruction topography of the CIIDF model domain E-9
Figure E.4 Vertical discretization of the preconstruction CIIDF groundwater model E-10
Figure E.5 Variograms of hydraulic conductivity field near the CIIDF site E-13
Figure E.6 Continuous hydraulic conductivity field kriged from data E-15
Figure E.7 Zonal hydraulic conductivity field for the CIIDF model E-16
Figure E.8 Diffuse recharge distribution for the CIIDF model E-18
Figure E.9 Preconstruction boundary conditions for the CIIDF model E-19
Figure E.10 Water table interpolated from measured values near CIIDF E-21
Figure E.11 Water table residual error for flow model calibration E-24
Figure E.12 Calibrated preconstruction water table for the CIIDF region E-25
Figure E.13 Calibrated preconstruction Darcy velocity near CIIDF E-26
Figure E.14 Proposed topographic modifications to the CIIDF site E-28
Figure E.15 Vertical discretization of the postconstruction CIIDF groundwater model E-29
Figure E.16 Postconstruction boundary conditions reflecting topographic modifications E-30

Figure E.17 Calculated postconstruction water table for the CIIDF model E-31
Figure E.18 Calculated postconstruction Darcy velocity near the CIIDF site E-32
Figure E.19 Grid cells representing the CIIDF 100-m compliance boundary E-34
Figure F.1 Maximum drinking water concentration as a function of CIIDF inventory for ^{3}H F-2
Figure F.2 Maximum drinking water concentration as a function of CIIDF inventory for ^{10}Be F-3
Figure F.3 Maximum drinking water concentration as a function of CIIDF inventory for ^{14}C F-4
Figure F.4 Maximum drinking water concentration as a function of CIIDF inventory for ^{26}Al F-5
Figure F.5 Maximum drinking water concentration as a function of CIIDF inventory for ^{36}Cl F-6
Figure F.6 Maximum drinking water concentration as a function of CIIDF inventory for ^{40}K F-7
Figure F.7 Maximum drinking water concentration as a function of CIIDF inventory for ^{41}Ca F-8
Figure F.8 Maximum drinking water concentration as a function of CIIDF inventory for ^{60}Co F-9
Figure F.9 Maximum drinking water concentration as a function of CIIDF inventory for ^{59}Ni F-10
Figure F.10 Maximum drinking water concentration as a function of CIIDF inventory for ^{63}Ni F-11
Figure F.11 Maximum drinking water concentration as a function of CIIDF inventory for ^{79}Se F-12
Figure F.12 Maximum drinking water concentration as a function of CIIDF inventory for ^{87}Rb F-13
Figure F.13 Maximum drinking water concentration as a function of CIIDF inventory for ^{90}Sr F-14
Figure F.14 Maximum drinking water concentration as a function of CIIDF inventory for ^{93}Zr F-15
Figure F.15 Maximum drinking water concentration as a function of CIIDF inventory for ^{93m}Nb F-16
Figure F.16 Maximum drinking water concentration as a function of CIIDF inventory for ^{94}Nb F-17
Figure F.17 Maximum drinking water concentration as a function of CIIDF inventory for ^{99}Tc F-18
Figure F.18 Maximum drinking water concentration as a function of CIIDF inventory for ^{107}Pd F-19
Figure F.19 Maximum drinking water concentration as a function of CIIDF inventory for ^{113m}Cd F-20
Figure F.20 Maximum drinking water concentration as a function of CIIDF inventory for ^{121m}Sn F-21
Figure F.21 Maximum drinking water concentration as a function of CIIDF inventory for ^{126}Sn F-22
Figure F.22 Maximum drinking water concentration as a function of CIIDF inventory for ^{129}I F-23
Figure F.23 Maximum drinking water concentration as a function of CIIDF inventory for ^{135}Cs F-24
Figure F.24 Maximum drinking water concentration as a function of CIIDF inventory for ^{137}Cs F-25
Figure F.25 Maximum drinking water concentration as a function of CIIDF inventory for ^{151}Sm F-26
Figure F.26 Maximum drinking water concentration as a function of CIIDF inventory for ^{152}Eu F-27
Figure F.27 Maximum drinking water concentration as a function of CIIDF inventory for ^{154}Eu F-28
Figure F.28 Maximum drinking water concentration as a function of CIIDF inventory for ^{155}Eu F-29
Figure F.29 Maximum drinking water concentration as a function of CIIDF inventory for ^{207}Bi F-30
Figure F.30 Maximum drinking water concentration as a function of CIIDF inventory for ^{210}Pb F-31
Figure F.31 Maximum drinking water concentration as a function of CIIDF inventory for ^{226}Ra F-32
Figure F.32 Maximum drinking water concentration as a function of CIIDF inventory for ^{229}Th F-33
Figure F.33 Maximum drinking water concentration as a function of CIIDF inventory for ^{230}Th F-34
Figure F.34 Maximum drinking water concentration as a function of CIIDF inventory for ^{232}Th F-35
Figure F.35 Maximum drinking water concentration as a function of CIIDF inventory for ^{231}Pa F-36
Figure F.36 Maximum drinking water concentration as a function of CIIDF inventory for ^{232}U F-37
Figure F.37 Maximum drinking water concentration as a function of CIIDF inventory for ^{233}U F-38
Figure F.38 Maximum drinking water concentration as a function of CIIDF inventory for ^{234}U F-39
Figure F.39 Maximum drinking water concentration as a function of CIIDF inventory for ^{235}U F-40
Figure F.40 Maximum drinking water concentration as a function of CIIDF inventory for ^{236}U F-41
Figure F.41 Maximum drinking water concentration as a function of CIIDF inventory for ^{238}U F-42
Figure F.42 Maximum drinking water concentration as a function of CIIDF inventory for ^{237}Np F-43
Figure F.43 Maximum drinking water concentration as a function of CIIDF inventory for ^{238}Pu F-44
Figure F.44 Maximum drinking water concentration as a function of CIIDF inventory for ^{239}Pu F-45
Figure F.45 Maximum drinking water concentration as a function of CIIDF inventory for ^{240}Pu F-46

Figure F.46 Maximum drinking water concentration as a function of CIIDF inventory for ^{241}Pu F-47
Figure F.47 Maximum drinking water concentration as a function of CIIDF inventory for ^{242}Pu F-48
Figure F.48 Maximum drinking water concentration as a function of CIIDF inventory for ^{244}Pu F-49
Figure F.49 Maximum drinking water concentration as a function of CIIDF inventory for ^{241}Am F-50
Figure F.50 Maximum drinking water concentration as a function of CIIDF inventory for ^{242m}Am . . . F-51
Figure F.51 Maximum drinking water concentration as a function of CIIDF inventory for ^{243}Am F-52
Figure F.52 Maximum drinking water concentration as a function of CIIDF inventory for ^{243}Cm F-53
Figure F.53 Maximum drinking water concentration as a function of CIIDF inventory for ^{244}Cm F-54
Figure F.54 Maximum drinking water concentration as a function of CIIDF inventory for ^{245}Cm F-55
Figure F.55 Maximum drinking water concentration as a function of CIIDF inventory for ^{246}Cm F-56
Figure F.56 Maximum drinking water concentration as a function of CIIDF inventory for ^{247}Cm F-57
Figure F.57 Maximum drinking water concentration as a function of CIIDF inventory for ^{248}Cm F-58
Figure F.58 Maximum drinking water concentration as a function of CIIDF inventory for ^{249}Cf F-59
Figure F.59 Maximum drinking water concentration as a function of CIIDF inventory for ^{250}Cf F-60
Figure F.60 Maximum drinking water concentration as a function of CIIDF inventory for ^{251}Cf F-61

TABLES

Table 1.1 Performance objectives for low-level radioactive waste disposal 1-1
Table 2.1 Surface water radionuclide measurements in Bear Creek 2-8
Table 2.2 Stratigraphic column of Cambro-Ordovician Rocks, White Oak Mountain Thrust Block, Oak Ridge, Tennessee 2-9
Table 2.3 Physical forms of low-level waste on the Oak Ridge Reservation 2-21
Table 2.4 Volume (m^3) of low-level waste generated on the Oak Ridge Reservation during 1994 . . 2-22
Table 3.1 Radionuclide-specific physical data used throughout the CIIDF performance assessment 3-2
Table 3.2 Mean radionuclide concentrations in air, 1994 3-7
Table 3.3 Summary of exposure pathways for off-site individuals due to releases by water pathways 3-13
Table 3.4 Summary of exposure scenarios for inadvertent intrusion into solid waste in disposal facility 3-20
Table 3.5 Radionuclide-specific soil/water partition coefficients used for environmental transport analyses 3-29
Table 3.6 Physicochemical parameters used in the SOURCE1 simulation of CIIDF 3-45
Table 3.7 Radionuclide-specific input data to SOURCE1 for the CIIDF PA 3-48
Table 3.8 The proportion of bypass flow for vertical and lateral flow paths and the maximum first-year transport through the soil matrix as a function of chemical adsorption 3-52
Table 3.9 Annual increment in soil matrix path length and times to full matrix exposure to nuclides as a function of K_d for the vertical and lateral flow paths 3-52
Table 3.10 Bear Creek discharges measured at USGS gauging stations 3-55
Table 4.1 Subset of representative radionuclides used to illustrate transport behavior 4-2
Table 4.2 Monthly precipitation, soil water drainage, lateral subsurface flow, and surface runoff results from the Unified Transport Model for three sets of weather conditions and various periods at the CIIDF site 4-5
Table 4.3 Simulated monthly seepage results used in source term calculations for CIIDF 4-7
Table 4.4 Abridged SOURCE1 output for ^{137}Cs 4-8
Table 4.5 Maximum annual radionuclide release rate from a CIIDF pad and year of occurrence for vertical and lateral release components of SOURCE1 calculations 4-21
Table 4.6 Vault failure times from environmental transport calculations and from direct intrusion calculations 4-26
Table 4.7 Waste distribution coefficient (K_d) values for intruder scenario inventory estimation 4-27
Table 4.8 Solubility-limited concentration for selected radionuclides 4-28
Table 4.9 Maximum annual flux and concentration of nuclides, and year of occurrence for the recharge and lateral subsurface flow paths 4-29
Table 4.10 Maximum groundwater and surface water concentrations resulting from water pathway limiting inventories 4-40
Table 4.11 Annual effective dose equivalents from drinking water pathway per unit concentration of radionuclides in water 4-53
Table 4.12 Allowable limits on concentrations of radionuclides in groundwater or surface water at off-site locations 4-54
Table 4.13 Annual effective dose equivalents from agriculture scenario for inadvertent intruders per unit concentration of radionuclides in disposal facility 4-56
Table 4.14 Waste dilution factors applied to dose analysis for agriculture scenario 4-59

Table 4.15 Reductions in inventory of elements in disposal facility due to mobilization and transport in infiltrating water—Part I 4-61
Table 4.16 Reductions in inventory of elements in disposal facility due to mobilization and transport in infiltrating water—Part II 4-62
Table 4.17 Allowable limits on concentrations and inventories of radionuclides for CIIDF based on agriculture scenario for inadvertent intruders 4-64
Table 4.18 Annual effective dose equivalents from resident scenario for inadvertent intruders per unit concentration of radionuclides in disposal facility 4-68
Table 4.19 Allowable limits on concentrations and inventories of radionuclides for CIIDF based on resident scenario for inadvertent intruders 4-69
Table 4.20 Annual effective dose equivalents from post-drilling scenario for inadvertent intruders per unit concentration of radionuclides in disposal facility 4-70
Table 4.21 Allowable limits on concentrations and inventories of radionuclides for CIIDF based on post-drilling scenario for inadvertent intruders 4-72
Table 4.22 Allowable limits on inventories of radionuclides for CIIDF based on allowable off-site releases in groundwater or surface water 4-75
Table 4.23 Allowable limits on concentrations and inventories of radionuclides in CIIDF based on analyses of scenarios for inadvertent intruders 4-79
Table 4.24 Allowable limits on concentrations and inventories of radionuclides in the CIIDF based on analyses of off-site releases and scenarios for inadvertent intruders 4-82
Table B.1 Transport-related properties of radionuclides in waste and concrete used in the performance assessment of the CIIDF B-1
Table B.2 Relationship of the dimensionless distribution coefficient (K) to some other commonly measured distribution coefficients B-6
Table B.3 Distribution coefficients and solubility limits of elements evaluated in the CIIDF performance assessment B-13
Table B.4 Transport parameters used to calculate diffusion coefficients for waste (D_w) B-14
Table B.5 Transport parameters used to calculate diffusion coefficients for concrete (D_c) B-15
Table C.1 Parameter values used to determine dose from all potential exposure pathways associated with atmospheric emissions C-6
Table C.2 Calculated annual dose per unit concentration values and annual effective dose equivalents (EDEs) from the atmospheric transport pathway C-9
Table C.3 Emission rate, ambient concentrations, and calculated atmospheric dispersion term values for CIIDF and the Oak Ridge Reservation C-11
Table D.1 Volumetric soil water content (m^3/m^3) at selected matric pressures and the saturated hydraulic conductivity for a compacted soil cap with grass vegetation and for soil layers below tumulus pads D-9
Table D.2 Volumetric soil water content (m^3/m^3) at selected matric pressures and the saturated hydraulic conductivity of a failed compacted soil cap and soil layers with grass or forest vegetation D-10
Table E.1 Estimates of hydraulic conductivity used for the generation of synthetic hydraulic conductivity fields E-12
Table E.2 Variograms used to generate synthetic hydraulic conductivity fields at the CIIDF E-14
Table E.3 Model recharge rates E-17
Table E.4 Calculated vs measured head at target wells E-22
Table G.1 Radionuclides considered in dose analysis for off-site individuals and inadvertent intruders G-3
Table G.2 Internal dose conversion factors for ingestion of radionuclides G-9

Table G.3 Internal dose conversion factors for inhalation of radionuclides G-11
Table G.4 External dose-rate conversion factors for radionuclides uniformly distributed in 15 cm of surface soil G-15
Table G.5 External dose-rate conversion factors for radionuclides uniformly distributed in infinite thickness of soil G-17
Table G.6 Annual effective dose equivalents from drinking water pathway per unit concentration of radionuclides in water G-20
Table G.7 Elemental plant-to-soil concentration ratios in vegetables G-23
Table G.8 Annual effective dose equivalents to inadvertent intruders from vegetable pathway per unit concentration of radionuclides in disposal facility for agriculture scenario G-25
Table G.9 Annual effective dose equivalents to inadvertent intruders from soil ingestion pathway per unit concentration of radionuclides in disposal facility for agriculture scenario G-28
Table G.10 Annual effective dose equivalents to inadvertent intruders from external exposure while working in vegetable garden per unit concentration of radionuclides in disposal facility for agriculture scenario G-31
Table G.11 Annual effective dose equivalents to inadvertent intruders from external exposure during indoor residence per unit concentration of radionuclides in disposal facility for agriculture scenario G-33
Table G.12 Annual effective dose equivalents to inadvertent intruders from inhalation exposure while working in vegetable garden per unit concentration of radionuclides in disposal facility for agriculture scenario G-35
Table G.13 Annual effective dose equivalents to inadvertent intruders from inhalation exposure during indoor residence per unit concentration of radionuclides in disposal facility for agriculture scenario G-38
Table G.14 Annual effective dose equivalents to inadvertent intruders from all exposure pathways per unit concentration of radionuclides in disposal facility for agriculture scenario G-43
Table G.15 Annual effective dose equivalents (rem/year per μCi) for agriculture scenario for inadvertent intruders per unit concentration of radionuclides in disposal facility from exposure to contaminated soil in vegetable garden and exposure during residence on disposal site G-46
Table G.16 Annual effective dose equivalents to inadvertent intruders per unit concentration of radionuclides in disposal facility for resident scenario G-48
Table G.17 Annual effective dose equivalents to inadvertent intruders per unit concentration of radionuclides in exhumed waste from all exposure pathways for post-drilling scenario G-51
Table G.18 Summary of radionuclide-independent parameter values used in dose analyses for off-site individuals and inadvertent intruders G-54

ABBREVIATIONS AND ACRONYMS

BCV	Bear Creek Valley
CA	composite analysis
CH	contact-handled
CIIDF	Class L-II Disposal Facility
DEM	digital elevation model
DOE	U.S. Department of Energy
DOE-ORO	U.S. Department of Energy, Oak Ridge Operations
EDE	effective dose equivalent
EPA	U.S. Environmental Protection Agency
^3H	tritium
ISCLT2	Industrial Source Complex Long-Term Air Dispersion Model
IWMF	Interim Waste Management Facility
K_d	distribution coefficient
LLW	low-level waste
LLWDDD	Low-Level Waste Disposal Development and Demonstration
NEPA	National Environmental Policy Act
NPDES	National Pollutant Discharge Elimination System
ORNL	Oak Ridge National Laboratory
ORR	Oak Ridge Reservation
PA	performance assessment
$PDCF_w$	pathway dose conversion factor for the drinking water pathway
PNL	Pacific Northwest Laboratory
SDCF	scenario dose conversion factor
SWSA	solid waste storage area
$T_{½}$	half-life
TRU	transuranic
TSD	treatment, storage, and disposal
USGS	U.S. Geological Survey
UTM	Unified Transport Model
WAC	waste acceptance criteria
WEC	waste evaluation criteria

EXECUTIVE SUMMARY

This draft radiological performance assessment (PA) for the proposed Class L-II Disposal Facility (CIIDF) on the Oak Ridge Reservation (ORR) has been prepared to demonstrate compliance with the requirements of U.S. Department of Energy (DOE) Order 5820.2A. This PA considers the disposal of low-level radioactive wastes (LLW) over the operating lifetime of the facility and the long-term performance of the facility in providing protection to public health and the environment. The performance objectives contained in the order require that the facility be managed to accomplish the following:

1. Protect public heath and safety in accordance with standards specified in environmental health orders and other DOE orders.
2. Ensure that external exposure to the waste and concentrations of radioactive material that may be released into surface water, groundwater, soil, plants, and animals results in an effective dose equivalent (EDE) that does not exceed 25 mrem/year to a member of the public. Releases to the atmosphere shall meet the requirements of 40 CFR Pt. 61. Reasonable effort should be made to maintain releases of radioactivity in effluents to the general environment as low as reasonable achievable.
3. Ensure that the committed EDEs received by individuals who inadvertently may intrude into the facility after the loss of active institutional control (100 years) will not exceed 100 mrem/year for continuous exposure or 500 mrem for a single acute exposure.
4. Protect groundwater resources, consistent with federal, state, and local requirements.

The PA has been prepared in accordance with the guidance provided by the DOE Peer Review Panel that outlines the format and content for a radiological performance assessment.

The proposed CIIDF will be located about 2.5 km (1.5 miles) north of Oak Ridge National Laboratory (ORNL) and about 5 km (3 miles) southwest of the Y-12 Plant on ORR in Bear Creek Valley. The proposed facility is located on a 10-ha (24-acre) tract of land on the slopes of a midvalley knoll. The site is to be graded, with the addition of fill material to provide capacity for the construction of 20 tumulus pads. Each pad will have the capacity for 30,000 ft^3 of waste contained in 330 concrete vaults. Waste is to be packaged in ST-5 waste containers (B-25 boxes), which will be emplaced in the concrete vaults. The annular space between each ST-5 container and concrete vault is to be filled with grout material and the vault sealed with butyl rope seal material. The vaults will be stacked in three layers and ultimately covered with an engineered earthen cover. CIIDF is to be constructed with diversion channels on the north, west, and east sides. These channels are designed to intercept surface water run-on, collect run-off, and locally depress the water table. Drains are to be installed in existing ephemeral creeks that transect the tumulus pad layout. The pads are to be sloped to a drainage channel that is connected to a drainage gallery. Underpad drainage is also piped into the drainage gallery. Gallery discharges are to be monitored prior to discharge to the National Pollutant Discharge Elimination System (NPDES) discharge point. Contaminated gallery discharges are to be collected and treated prior to release to the environment.

Approximately 10,000 m^3/year of LLW is managed each year on ORR. Of this quantity, a relatively small volume is to be disposed of at CIIDF. These wastes are expected to include a large number of radionuclides, most of which are expected to have radionuclides with half-lives less than 30 years. Wastes disposed of at CIIDF will be characterized and certified by waste generators using waste acceptance criteria that are to be developed from the results of this PA.

This PA considered radionuclides likely to be present in wastes to be disposed of at CIIDF, and considered in detail those radionuclides with half-lives greater than 5 years. Radionuclides with half-lives less than 5 years were excluded from detailed consideration based on the integrity of CIIDF, which would allow decay to render them insignificant in contributing to exposures of individuals. Each radionuclide considered in detail was analyzed to determine the maximum allowable inventory that could be present on a tumulus pad and meet the performance objectives of DOE Order 5820.2A. Mixtures of radionuclides are addressed by combining the contributions of each radionuclide to ensure that the sum is less than the allowable inventories.

The maximum allowable inventories for each pad that meet the performance objectives of DOE Order 5820.2A were determined using a series of models to represent the site-specific behavior of CIIDF. Transport of contamination to points of public exposure was determined to be controlled by groundwater and surface water transport, to the exclusion of all other exposure pathways. Inadvertent intrusion was considered by analysis of the agriculture, resident, and post-drilling scenarios. Other scenarios were discussed but shown to be less significant in the analysis of CIIDF.

The long-term performance of CIIDF was conducted a connected suite of models The water budget for the facility was determined by the Unified Transport Model (UTM), which used hourly inputs to calculate the monthly seepage into CIIDF, the annual recharge into the groundwater, and the annual surface and shallow subsurface water fluxes. Seepage estimates into the CIIDF were used to calculate releases of contamination from the facility using the SOURCE1 model. The PADSIM model divided these releases between the annual lateral transport of contamination to the shallow subsurface and groundwater recharge. Recharge of contaminated water was used as input to the FTWORK model to determine the groundwater transport of contamination and the subsequent release to surface water. Through iteration of the problem, the results from the computer modeling were used to determine the maximum concentration of each radionuclide in waste corresponding to the performance objective for water resource protection of 4 mrem/year. The calculated maximum concentration was then converted to the maximum allowable inventory for each pad at CIIDF.

Estimates of the maximum allowable inventory on each pad which satisfies the performance objectives for inadvertent intrusion were calculated for identified scenarios that are the most restrictive for the CIIDF. The maximum allowable inventory for each radionuclide was then set based on the most restrictive limit calculated from the inadvertent intruder and environmental transport calculations.

The analysis for CIIDF required the use of assumptions to supplement the available site characterization data. Assumptions were made to define the physical and chemical properties of engineered and geologic materials, the closure of the disposal facility, and the application of annual averages of data representing processes and events of short duration. These assumptions were selected to

provide a reasonable yet conservative representation of facility performance and were based on the limited information available.

The methodology used to analyze the performance of CIIDF was based on the available data about the waste anticipated to be disposed of at CIIDF, the disposal methods to be used at CIIDF, and the CIIDF site characteristics. Since the results were calculated to ensure that the performance objectives were satisfied for each radionuclide, operation of the facility with waste acceptance criteria consistent with the maximum allowable inventories ensures that the performance objectives are satisfied. A qualitative sensitivity and uncertainty analysis was conducted to identify parameters and mechanisms that contribute to uncertainty in the results. A quantitative uncertainty analysis will be prepared as part of the revision of this PA prior to operation of CIIDF.

The results determined in this PA indicate that of the 60 radionuclides analyzed, 35 were limited by the surface water or the groundwater pathway. The results were calculated to the time of maximum dose with the understanding that a time of 10,000 years would be appropriate for establishing a time of compliance. Only one radionuclide had a peak after the 10,000-year time of compliance (^{10}Be), and all but four radionuclides had reached the their peak by 1,000 years. The analysis of direct intrusion indicated that extended periods of institutional control would increase the maximum allowable inventories of 9 of the 25 radionuclides limited by intrusion.

The analysis of the performance of CIIDF did not consider sources of contamination present in Bear Creek Valley associated with historical disposals or plant operations on ORR. These sources of contamination will be considered in a separate composite analysis report that will be prepared in conjunction with the revision of this PA.

The results presented in this PA provide a reasonable basis for evaluating the performance of CIIDF and provide reasonable assurance that the performance objectives of DOE Order 5820.2A will be met for the disposal of LLW at CIIDF. Continued work to reduce uncertainties and improve the methodology used to analyze the performance of CIIDF are likely to relax the allowable limits on inventory determined in the analysis.

1. INTRODUCTION

Site-specific radiological performance assessments (PAs) are required for the disposal of low-level radioactive waste at U.S. Department of Energy (DOE) facilities. The purpose of the PA is to demonstrate compliance with the performance objectives for low-level waste (LLW) disposal stated in DOE Order 5820.2A, Chapter III, paragraph 3a (Table 1.1). PAs are to be subjected to review by the Oversight and Peer Review Panel of DOE for technical quality and consistency across the DOE complex. PAs are to include site-specific geohydrology and waste composition as part of the PA methodology. This PA has been prepared for a new disposal facility on the Oak Ridge Reservation (ORR) called the Class L-II Disposal Facility (CIIDF) that employs the tumulus technology used at the existing Solid Waste Storage Area (SWSA) 6 disposal facility (ORNL 1994).

Table 1.1 Performance objectives for low-level radioactive waste disposal

1. Protect public health and safety in accordance with standards specified in applicable EH Orders and other DOE Orders.

2. Assure that external exposure to the waste and concentrations of radioactive material which may be released into surface water, ground water, soil, plants and animals results in an effective dose equivalent that does not exceed 25 mrem/yr to any member of the public. Releases to the atmosphere shall meet the requirements of 40 CFR 61. Reasonable effort should be made to maintain releases of radioactivity in effluents to the general environment as low as is reasonably achievable.

3. Assure that the committed effective dose equivalents received by individuals who inadvertently may intrude into the facility after the loss of active institutional control (100 years) will not exceed 100 mrem/yr for continuous exposure or 500 mrem for a single acute exposure.

4. Protect ground water resources, consistent with Federal, State and local requirements.

This PA has been prepared in accordance with the guidance provided by the DOE Peer Review Panel (DOE 1989) that describes the recommended format and content for DOE LLW disposal facility radiological PAs and is consistent with the guidance provided by the DOE Peer Review Panel for preparing PAs (DOE 1991). The PA includes the disposal facility description, analysis of performance, results of the analysis, the performance evaluation, and continued work towards improving the PA. The PA has been prepared to provide limiting average concentrations of radionuclides in wastes that would be suitable for disposal at CIIDF. Other sources of contamination from nearby facilities that may contribute contamination to the environment have not been considered in this PA.

CIIDF is located in a 10-ha (24-acre) site in Bear Creek Valley. The site is in proximity to State Highway 95 to the west, Pine Ridge to the north, Bear Creek to the south, and Gum Hollow

Branch to the east. A detailed description of the site is presented in Sect. 2.1. Waste disposal operations are to be performed using the tumulus technology developed for application to ORR at SWSA 6. A complete description of the disposal technology is provided in Sect. 2.3. Waste is to be characterized, treated, and certified at facilities located outside CIIDF.

The performance objectives for waste disposal at CIIDF shown in Table 1.1 include requirements for the protection of groundwater resources consistent with federal, state, and local requirements. The State of Tennessee has not issued regulations directly affecting radioactive waste disposal, nor has the state issued formal regulations protecting groundwater resources. The State of Tennessee has issued implementing regulations for the Safe Drinking Water Act that limit the dose in drinking water for community water supplies to 4-mrem (40-μSv) annual effective dose equivalent (EDE). In the present analysis, this regulatory limit has been regarded as the appropriate limit for the protection of groundwater resources. Compliance with the performance objective of groundwater resource protection usually has been interpreted as meaning that concentrations of chemical and radioactive contaminants at any points of compliance should not exceed standards for public drinking water supplies established by the U. S. Environmental Protection Agency (EPA). In this assessment, the point of compliance is at a location more than 100 m (328 ft) from the edge of the disposal unit cover at which the groundwater contaminant concentrations are the highest. The 100-m buffer zone is consistent with the guidance provided by the DOE Peer Review Panel (DOE 1991). The protection of groundwater resources is considered to be independent of the matter of institutional control. Consequently, the 4-mrem annual EDE performance objective is applied at any time following the disposal of radioactive materials for the purposes of groundwater protection. The application of the performance objective is associated with the consumption of 2 L of water per day by an individual from a well with the highest level of contamination outside the 100-m buffer zone. Future regulatory developments may specify the appropriate limit for the protection of groundwater resources, but lacking this guidance, the 4-mrem annual limit has been adopted as the proper value for groundwater resource protection in this PA.

Bear Creek is the receiving stream for any contamination released by water pathways to the environment. Although surface water is not explicitly identified as a performance objective for LLW disposal, the geohydrological behavior of ORR results in the relatively rapid transport of contamination from wastes to surface water by shallow subsurface transport, groundwater transport, and ephemeral creek discharges. This site-specific characteristic makes surface water both an important pathway for human exposure and a major indicator of disposal facility performance. The State of Tennessee has established National Pollution Discharge Elimination System (NPDES) limits for discharges from Bear Creek that do not include radioactivity. For the purposes of this PA, the 4-mrem annual EDE for protection of groundwater resources has been extended to surface water in Bear Creek. While this extension of the performance objectives is not explicitly required, the protection of surface water resources consistent with groundwater resources is expected to encompass any additional requirements on the protection of water resources being considered by the state, EPA, or DOE.

The 4-mrem annual EDE performance objective for surface water is applied at the nearest surface water collection point that is downstream of CIIDF. This performance objective is used to calculate the limiting average concentration in waste for a individual using Bear Creek as a drinking water supply and consuming 2 L/d of contaminated surface water. Limiting average concentrations of radionuclides in waste are determined independent of the arrival time of the contaminants. If a radionuclide is associated with a limiting average concentration that occurs during the period of active institutional control, the analysis also estimates the limiting average concentration in waste at the end of the 100-year period of institutional control. The evaluation of compliance with the performance objectives for any member of the public is based on the limiting average concentrations in waste that would occur after the end of institutional controls.

Compliance with the performance objective for releases to the atmosphere meeting the requirements of 40 CFR 61 is demonstrated by analyzing the potential atmospheric emissions of volatile and nonvolatile radionuclides. As shown in Sect. 3.1 and Appendix C, releases to the atmosphere from CIIDF operations do not affect waste inventories.

The performance objective for inadvertent intrusion is analyzed using a variety of scenarios that could reasonably occur in the future. Inadvertent intrusion is considered to occur within the 100-m buffer zone at any time after the 100-year period of active institutional control. For the purposes of demonstrating compliance with the performance objective, inadvertent intrusion according to the scenarios considered is presumed to occur prior to 10,000 years after the disposal of wastes. Limiting average concentrations in waste and inventories are determined without the consideration of dose from the emanation of radon. Radon emissions from the decay of uranium are presumed to be limited by the standard of 20 $pCi/m^2 \cdot s$ incorporated into 40 CFR 61.

2. DESCRIPTION OF THE CLASS L-II DISPOSAL SITE

This section presents a brief review of the known characteristics of the CIIDF site, the characteristics of the wastes anticipated to be disposed of in CIIDF, and a summary of the CIIDF design. The descriptions presented are intended to provide the essential background for understanding the analysis of the facility performance and to summarize the work that has been performed in site characterization and facility design. The representation of the site, wastes, and disposal facility for the purposes of analysis is discussed in Sect. 3.

2.1 SITE CHARACTERISTICS

CIIDF is planned for construction in Bear Creek Valley on DOE's ORR in east Tennessee. The site has been investigated extensively, and much of the site description is based on these investigations (Lee and Ketelle 1989, Golder 1988, Ogden 1995.)

2.1.1 Site Location and Topography

The proposed CIIDF LLW disposal site is located about 2.5 km (1.5 miles) north of Oak Ridge National Laboratory (ORNL) on ORR, at latitude 35°56.77′ N and longitude 84°18.65′ W. The site lies in Bear Creek Valley about 5 km southwest (downstream) of the Y-12 Plant, as shown on Fig. 2.1. Significant local features include Bear Creek, which runs along the southern edge of the valley, and the Clinch River, located about 7.5 km southwest of the site. Further references in this PA to coordinates (easting and northing, in feet) are with respect to the Y-12 Plant grid.

Topography in and around Bear Creek Valley is typical of that in the western portion of the Valley and Ridge Physiographic Province in east Tennessee. The valley is about 800 m wide and trends northeast-southwest. Pine Ridge forms the northwestern boundary and Chestnut Ridge the southeastern, both with crest elevations of approximately 335 m (1100 ft). A line of low knobs with crest elevations about 20 m (60 ft) above the valley floor adorns the southeastern slopes of Pine Ridge, and the CIIDF site is located on the southeast slope of such a knob. The lowest topography in the vicinity of CIIDF is where Bear Creek turns abruptly to the northwest cutting through Pine Ridge, at an elevation of 245 m (800 ft) above mean sea level, giving a total topographic relief in the site of about 90 m (300 ft).

2.1.2 Construction Topographic Modifications

Construction of CIIDF, which is discussed in greater detail in Sect. 2.2, will involve several modifications of the topography in the immediate vicinity of the site. Initially, 10 ha (24 acres) is to be cleared on the southern slopes of a midvalley knoll, followed by grading for six pads and construction

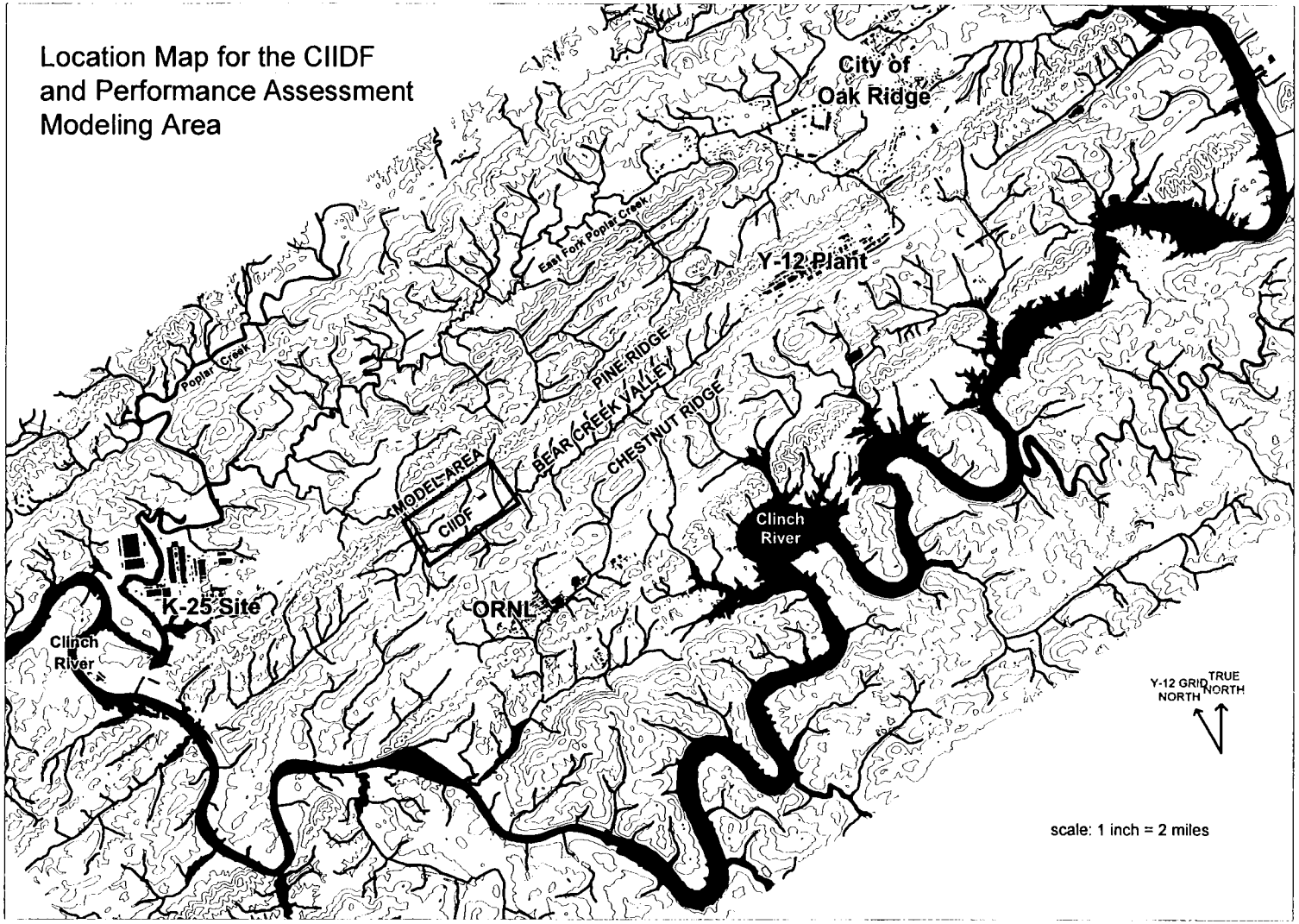

Fig. 2.1. Location of CIIDF on the Oak Ridge Reservation.

of two pads, a drainage gallery, a monitoring station, an operations building, and an access road. Eventually, the site may consist of as many as 20 pads, arranged in two rows of ten as shown in Fig. 2.2, which illustrates the pre- and postconstruction topography of the site. For the purposes of this PA, the 20-pad configuration is assumed. The major changes to the topography include two bench cuts for the two rows of pads, with drains installed where ephemeral creeks currently transect the pad layout. Plans also include a diversion trench along the northern and western edges of the pads, another to the east, and grading for the access road.

The intent of these passive controls is to isolate CIIDF hydrologically, by providing diversions for run-on by overland and shallow subsurface flow and by depressing the water table beneath the facility. These modifications are reflected in the facility design (Foster-Wheeler 1995) and are discussed further in Sect. 2.3.

2.1.3 Regional Climate

The climate of ORR is moderated by the influence of the Cumberland Mountains to the west and the Great Smoky Mountains to the east. They divert the warm winds from the Gulf of Mexico to produce warm, humid summers and cool winters. Extremes in precipitation, temperature, and winds are uncommon.

The mean annual temperature in Oak Ridge is 14.4°C (58°F). The coldest month is usually January, with temperatures averaging 3.3°C (38°F) and lows occasionally reaching −17°C (0°F). The warmest month is usually July, with temperatures averaging 25°C (77°F) and highs occasionally reaching 38°C (100°F). Daily temperature fluctuations are typically 12°C (20°F).

Prevailing winds are influenced by the topography and are either up-valley (northeasterly) or down-valley (southwesterly). Daytime winds are typically up-valley, and nighttime winds are typically down-valley. Tornadoes and high winds are rare.

Precipitation is highly variable within and between years. The 40-year annual average precipitation is 1.4 m (54 in.) with approximately 0.26 m (10.4 in.) of snowfall. Monthly precipitation is typically highest in January and February with storms of low intensity and long duration. Thunderstorms are common during the summer. October is typically lowest in precipitation.

2.1.4 Hydrology

The hydrologic processes of the CIIDF site are the result of interaction of precipitation with the landscape topography and the porous soil and subsoil materials. This interaction is modified by the extraction of soil water by vegetation in evapotranspiration. The technical aspects of these interactions are outlined in the following sections.

Existing topography at the CIIDF Site

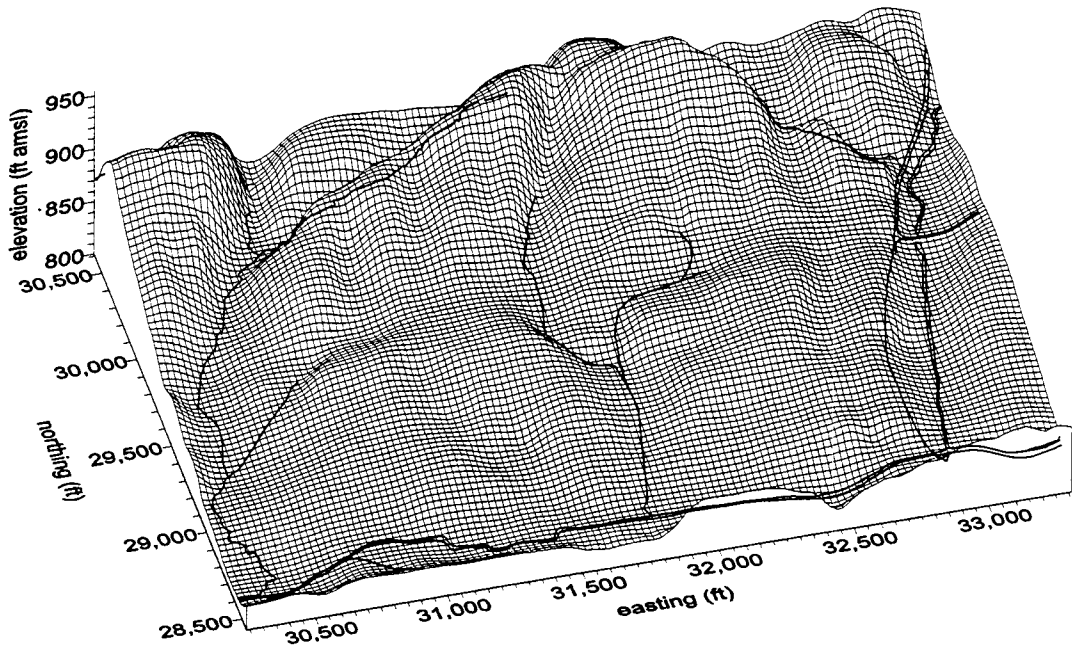

Modified topography proposed for the CIIDF Site

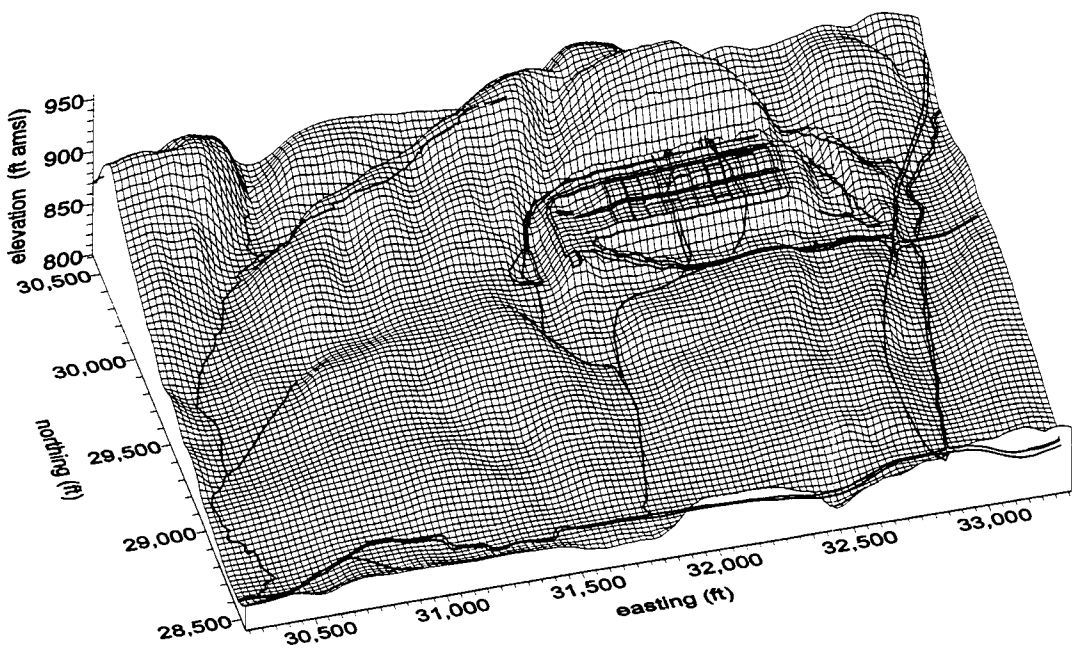

Fig. 2.2. Pre- and postconstruction topography in the vicinity of CIIDF.

2.1.4.1 Water Budget

The water budget for the CIIDF site is determined by precipitation inputs, liquid and vapor outflows, and soil water storage changes. Precipitation records for the Oak Ridge area show the 40-year mean annual precipitation for 1950–1990 to be 1370 mm/year (Kornegay and West 1991). This input of water to the landscape is partitioned into two main components on an annual basis. The evapotranspiration process returns an average of 730 mm of water to the atmosphere as vapor (Luxmoore and Huff 1989). The difference of 640 mm/year (1370 - 730) drains through the root zone and vadose zone to produce stream flow and groundwater recharge. On an annual basis there is little or no significant change in soil water storage. The annual water budget is composed of many storm events and diurnal changes in weather that contribute to dynamic changes in water status and water flow in the landscape. On average about 50% of annual precipitation drains through soil as lateral flow to streams or as recharge to groundwater. Smaller streams are often intermittent, flowing only when fed by lateral inflow or discharge from a high water. In effect, they act as drains, providing an outlet for discharging subsurface waters but, unlike perennial streams, not contributing enough recharge to maintain a constant water table elevation.

On a monthly basis, precipitation is received somewhat uniformly through the year. In contrast, evapotranspiration is highly seasonal, increasing with leaf out of vegetation in spring to a maximum in summer, then declining in autumn with leaf fall. The combination of rather uniform monthly precipitation and seasonal evapotranspiration results in soil water drainage being dominant during winter and early spring. In autumn, precipitation preferentially recharges soil water to field capacity before significant drainage occurs. The seasonal pattern of soil water drainage has an important influence on chemical transport in the landscape.

2.1.4.2 Bear Creek Watershed

The Bear Creek watershed, identified in Fig. 2.3, covers about 20 km^2 and is entirely within ORR. While the western portion of Bear Creek Valley is drained by Grassy Creek to the Clinch River, the part of the valley lying between the divide located about 2 km west of the Pine Ridge gap and the western edge of the Y-12 Plant is drained by Bear Creek. The bulk of Y-12 is drained to the northeast by East Fork Poplar Creek, which also cuts to the northwest through Pine Ridge at the City of Oak Ridge and turns to the southwest, draining East Fork Valley. The headwaters of Bear Creek, 10 km upstream of its mouth, originate in the western end of the Y-12 Plant. Flowing southwest down Bear Creek Valley, it picks up several regularly spaced northern tributaries (numbered consecutively) from between the knobs along the edge of Pine Ridge and several other tributaries and springs from the south. The CIIDF site lies about 100 m from northern tributary NT-14 (Gum Hollow Branch), which enters Bear Creek at about km 6. About 1 km downstream of CIIDF, Bear Creek turns abruptly to the northwest, picks up several tributaries draining the western part of Bear Creek Valley, and cuts through a water gap in Pine Ridge. After flowing through the Pine Ridge gap alongside Highway 95,

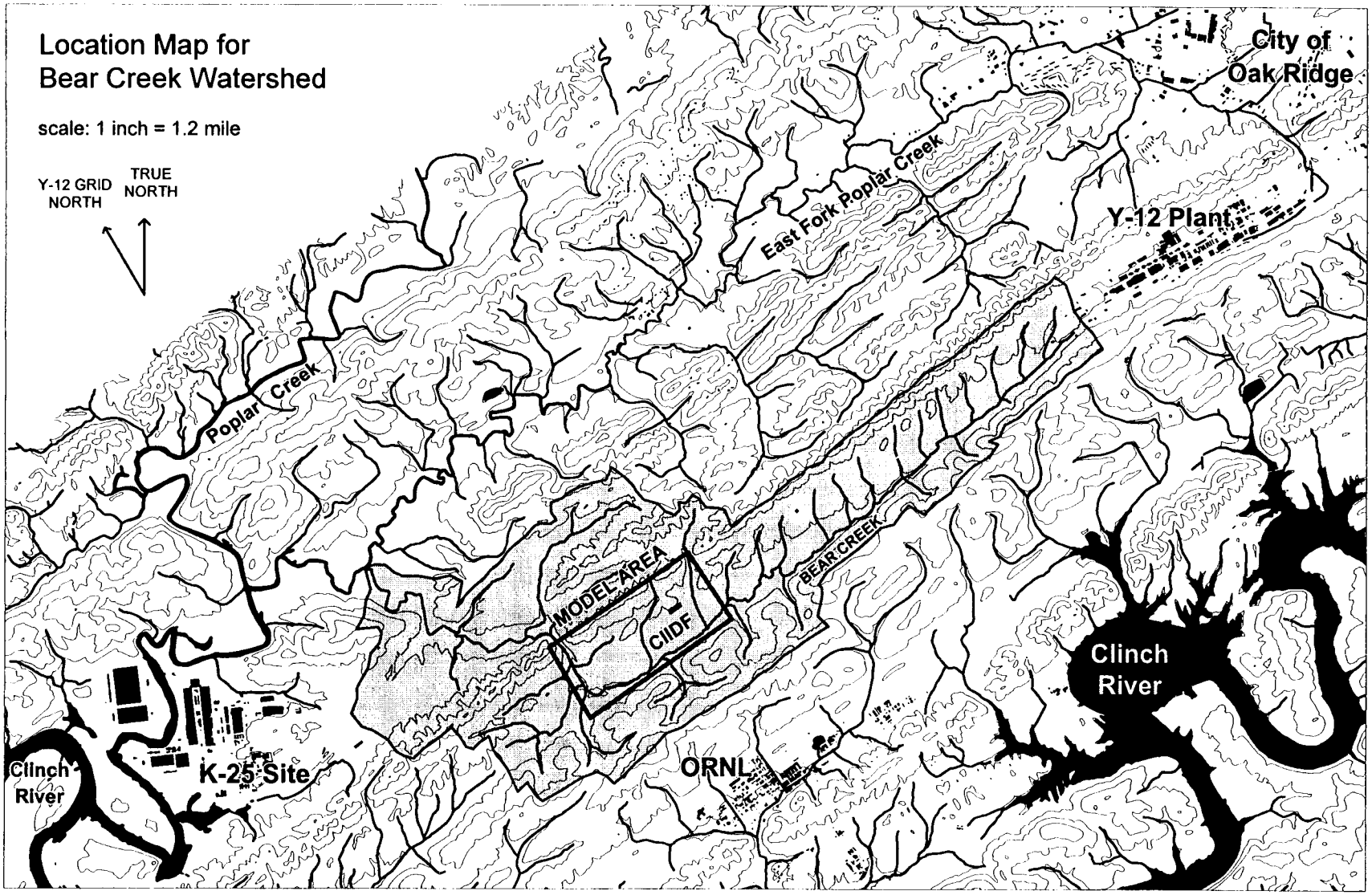

Fig. 2.3. Location of Bear Creek watershed on the Oak Ridge Reservation.

Bear Creek enters East Fork Valley and joins East Fork Poplar Creek, which in 2 km joins Poplar Creek 8 km above its mouth (and the boundary of ORR) at the Clinch River. The last 7 km of Poplar Creek flows through the K-25 Site.

2.1.4.3 Surface Waters

Bear Creek is the primary drainage for Bear Creek Valley in the vicinity of CIIDF. Surface runoff from CIIDF drains east to northern tributary NT-14, and to a small tributary to the southwest, which is fed by two smaller tributaries that transect the site. All surface runoff pathways soon merge with the main stem of Bear Creek about 1 km upstream of U.S. Geological Survey (USGS) gauging station 03538270. Discharge data from this station are used in estimating radionuclide concentrations, as discussed in Sect. 3.3.4.3. Surface water flow in the region is highly dependent on precipitation and soil water conditions, and runoff is heaviest in the winter and spring. During the summer and autumn, most tributaries run dry, and parts of the main stem of Bear Creek may be dry as well, with flow only in the subsurface. Subsurface flow in the Maynardville Limestone is intimately connected with the surface channel, the location of which is largely controlled by dissolution along fractures in the limestone (Geraghty & Miller 1987). Drilling in the vicinity of Bear Creek has revealed an active hydraulic communication between the surface and groundwaters (Shevnell, Dreier, and Jago 1993).

Although there are currently no sources of radionuclides at the proposed CIIDF site, there is contamination in the Bear Creek watershed and in the waters of Bear Creek southeast of CIIDF. Major sources of contamination are the variety of disposal sites at the west end of the Y-12 Plant. Several sites there witnessed undocumented disposals of liquids and solids contaminated with uranium, plutonium, neptunium, radium, iodine, americium, technetium, strontium, and tritium. All of these radionuclides are currently found in Bear Creek (Kornegay et al. 1994) and in neighboring wells (HSW 1995) in concentrations which decrease downstream (see Table 2.1). In the vicinity of the CIIDF site and at current concentrations, these radiological contaminants constitute a significant fraction of the allowable dose from drinking water.

This pre-existing contamination and potential contamination from other planned disposal sites will be the subject of the composite analysis for the Bear Creek and Poplar Creek watershed portion of ORR. The composite analysis will be prepared as a separate document following guidance issued by DOE headquarters (DOE 1996a) according to the schedule presented in the Implementation Plan for Defense Nuclear Facilities Safety Board Recommendation 94-2 (DOE 1996b). The composite analysis will estimate the potential cumulative impacts to a hypothetical future member of the public from CIIDF and any other planned disposal facilities (including those for environmental restoration activities), as well as other sources of radioactive material in the ground that may interact with CIIDF. In contrast, this draft PA considers only those wastes to be disposed of in CIIDF.

Table 2.1. Surface water radionuclide measurements in Bear Creek

Measured parameter	Median measured concentrations at location in km upstream from East Fork Poplar Creek (pCi/L)		
	km 0.63[a]	km 4.55[b,c]	km 9.40[a]
^{3}H	370	170	510
^{60}Co	1.8		2.2
^{90}Sr	1.4[d]	0.77	1.4[d]
^{99}Tc	13	20	110
^{226}Ra		0.05	
^{230}Th		0.31	
^{232}Th		0.088	
^{234}U	3.6	5	26
^{235}U	0.29	0.3	2.9
^{238}U	5.4	8.8	51
Gross α	10	16	59
Gross β	13	13	77

[a] Data source: Kornegay et al. 1994, Table 5.30; 4 or 5 samples.
[b] Data source: Kornegay et al. 1994, Table 4.34; over 50 samples.
[c] Bear Creek km 4.55 corresponds to Y-12 NPDES Discharge Point 304, USGS Station 03538720, and to the surface water compliance point for the CIIDF PA.
[d] Strontium reported as "Total radionuclide Sr."

2.1.5 Geology and Soils

This section discusses the regional geologic setting within the Valley and Ridge Province in east Tennessee, as well as the local geology and soils in the vicinity of Bear Creek Valley and CIIDF.

2.1.5.1 Geologic Setting

ORR is underlain by sedimentary bedrock of the Paleozoic Age that generally dips to the southeast in an imbricate pattern due to the regional geologic structure that formed during the Appalachian Orogeny some 300 million years ago. The stratigraphic column in Table 2.2 includes descriptions and local thicknesses of bedrock formations recognized on ORR (Lee and Ketelle 1989). A geologic map of ORR is shown in Fig. 2.4. Geologic structures present on ORR include regional-scale thrust faults, local faults having various orientations, local folds, and numerous sets of local joints and fractures. Bedrock fracturing is ubiquitous on ORR with variation in the degree of fracturing based on local bedrock type and proximity to local or regional-scale folds and faults. Two regionally

Table 2.2. Stratigraphic column of Cambro-Ordovician Rocks, White Oak Mountain Thrust Block, Oak Ridge, Tennessee

Age	Group	Formation/unit	Description	Thickness (m)
Middle Ordovician	Chickamauga (Och)[a]	Unit H[b]	Thin interbedded limestone and calcareous siltstone. Gray, olive, buff, and maroon. [Moccasin Fm][c]	>82
		Unit G	Limestone and siltstone in thick beds. Limestone fine to medium grained, nodular. [Witten Fm]	88
		Unit F	Laminated to thin-bedded calcareous and shaly siltstone. Maroon and olive gray. [Bowen Fm]	6
		Unit E	Limestone and siltstone in thick beds. Limestone fine to medium grained, nodular, and amorphous. Siltstone dark gray with limestone laminae. [Benbolt/Wardell Fm]	91
		Unit D	Limestone. Medium grained and stylolitic. Nodular chert. [Rockdell Fm]	43
		Unit C	Limestone and siltstone in thick beds. Limestone nodular and micritic. Siltstone calcareous and dark gray. Nodular chert. [Fleanor Shale Member, Lincolnshire Fm]	29
		Unit B	Siltstone. Massive maroon and gray with limestone in thin, even beds. [Eidson Member, Lincolnshire Fm]	76
		Unit A	Limestone and siltstone in thick beds. Dark to light gray, purplish to maroon. Nodular and bedded chert. [Blackford Fm]	91
Lower Ordovician	Knox (Œk)	Newala	Medium-bedded dolostones and limestones with variable chert content, scattered chert matrix limestones. Abundant maroon mottling. [Mascot Dolomite / Kingsport Fm]	274[d]
		Longview	Dense, massive chert, bedded chert, and dolomoldic chert observed in residuum.	15–30[d]
		Chepultepec	Dolostone, fine to medium grained, light to medium gray, medium to thick bedded, sandy near base.	150–300[d]
Upper Cambrian		Copper Ridge	Dolostone, medium to thick bedded, fine to coarse crystalline, medium to dark gray. Chert varieties include massive, cryptopoan, and oolitic.	274–396[d]

See footnotes at end of table.

Table 2.2 (continued)

Age	Group	Formation/unit	Description	Thickness (m)
Middle Cambrian	Conasauga (Єc)	Maynardville (Єmn)	Upper (Chances Branch Mbr.)—limestone and dolomitic limestone in thick massive beds.	43
			Lower (Low Hollow Mbr.)—dolomotic limestone in thick massive beds. Light gray to buff.	61
		Nolichucky (Єn)	Upper—shale and limestone in thin to thick beds. Shale dark gray or maroon. Limestone light gray, oolitic, wavy bedded, or massive.	18–43
			Lower—shale and limestone in medium to thick beds. Shale dark gray, olive gray, or maroon. Limestone light gray, oolitic, glauconitic, wavy bedded, and intraclastic.	131–137
		Maryville (Єm)	Limestone and shale or siltstone in medium beds. Limestone light gray, intraclastic, or wavy bedded. Shale or siltstone dark gray. [Dismal Gap Fm]	98–125
		Rogersville (Єrg)	Shale and argillaceous limestone. Laminated to thin bedded, maroon, dark gray, and light gray.	24–34
		Rutledge (Єrt)	Limestone and shale in thin beds. Limestone light to olive gray. Shale gray or maroon. [Friendship Fm]	30–37
		Pumpkin Valley (Єpv)	Upper—shale and calcareous siltstone. Laminated to very thin bedded. Shale reddish brown, reddish gray, or gray. Calcareous siltstone light gray or glauconitic.	40–46
			Lower—shale and siltstone or silty sandstone. Thin bedded. Shale reddish brown or gray to greenish gray. Siltstone and silty sandstone light gray.	53
Lower Cambrian		Rome (Єr)	Sandstone and thin shale interbeds. Sandstone fine grained, light gray or pale maroon. Shale maroon or olive gray.	Unknown

[a] Group name abbreviations are those commonly used on geologic maps and cross sections in the region.

[b] Chickamauga Group stratigraphic subdivisions reflect those identified at the ORNL site, since a standardized nomenclature for these units has not been published. Other formation names are consistent with regional stratigraphic nomenclature, though some more recent workers have introduced new names.

[c] Nonstandard formation names which may be found in some documents are indicated in square brackets (Hatcher et al. 1992).

[d] Estimated value.

Source: after Lee and Ketelle 1989.

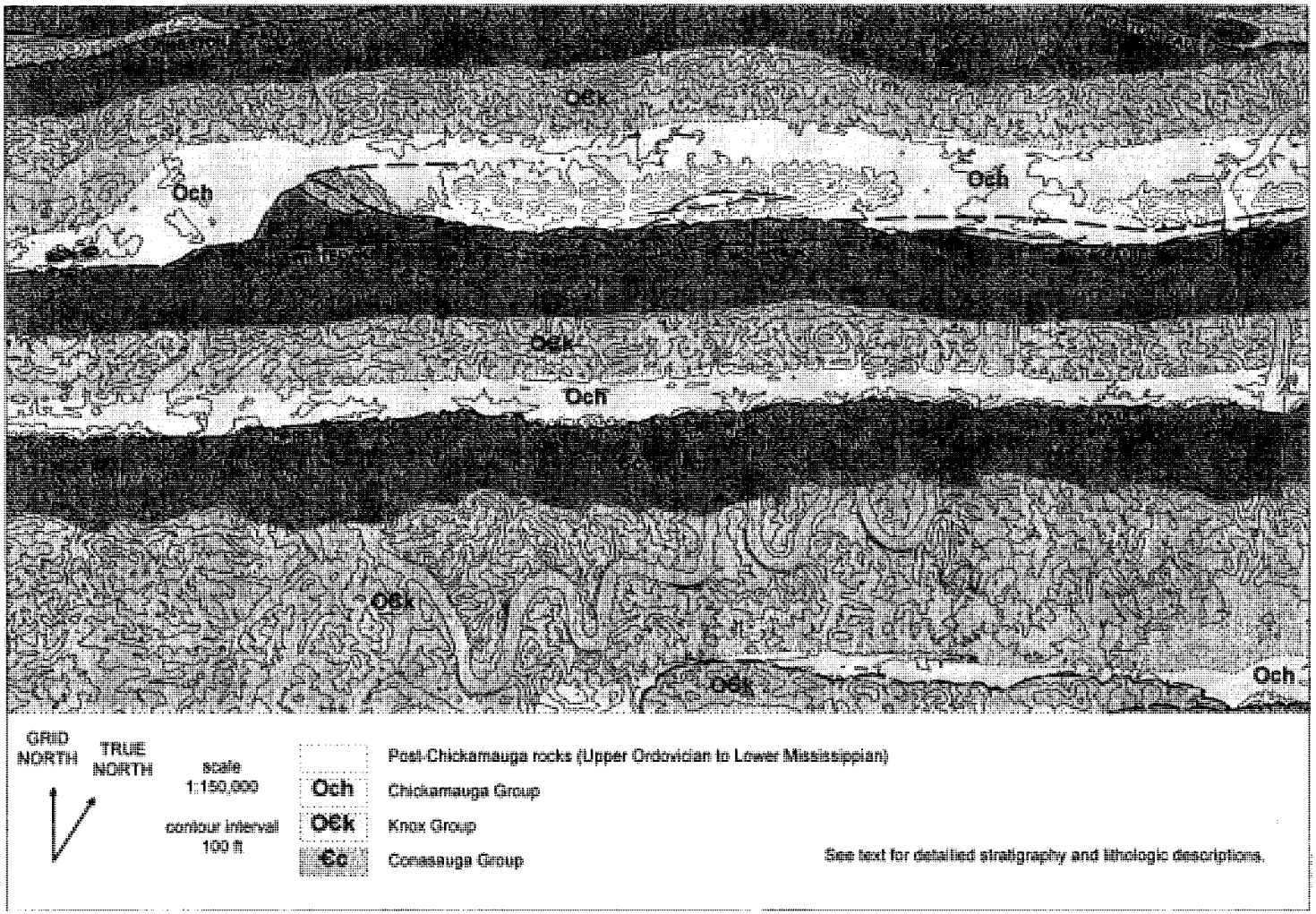

Fig. 2.4. Geologic map of the Oak Ridge Reservation.

important thrust faults cross ORR in a northeast-southwest direction. These faults are the White Oak Mountain Fault Zone, which outcrops on the northwest slope of Pine Ridge about 1 km northwest of CIIDF, and the Copper Creek Fault, which lies several kilometers to the southwest under Haw Ridge.

The White Oak Mountain Fault underlies CIIDF site at a depth of about a kilometer below the land surface. Motion of bedrock above this now inactive thrust fault during the Appalachian Orogeny carried the Upper Rome Formation, the Conasauga Group, and the overlying Knox Group strata to their present orientation. At the end of the Paleozoic Age, the rocks that outcrop at the land surface were buried deeply beneath a mountainous deformation belt. The present regional terrain is the result of weathering and erosion of bedrock and soils over the millennia since the Appalachian Orogeny.

Variable resistance to weathering and erosion of the dipping strata causes the parallel alignment of ridges and valleys characteristic of the region. Locally, ridges are underlain by weathering- or erosion-resistant rock types, while valleys are underlain by the easily weathered or erodible rock types. Pine Ridge, northwest of CIIDF, is underlain by the hard sandstones of the Upper Rome Formation. Bear Creek Valley is underlain by interbedded shale, calcareous siltstone, and limestone bedrock of the Cambrian Age Conasauga Group. The Conasauga Group is divided into six geologic formations on ORR (Table 2.2). Conasauga bedrock is fairly weatherable because of the dominance of calcium-carbonate-cemented rock and the high silt content. Variations in the weathering and erosion patterns of the Conasauga formations result in the presence of a line of knobs underlain by the Maryville Limestone on the southern slopes of Pine Ridge.

2.1.5.2 Site Geology

The geology of the CIIDF site has been well investigated by Lee and Ketelle (1989). The site is located on southern slopes of a midvalley knoll, on the contact between the Maryville Limestone and the Nolichucky Shale, as seen on the CIIDF geologic map (Fig. 2.5) and cross section (Fig. 2.6). In general, the local bedrock dips to the southeast at an attitude of about 45°. However, at any specific location within the site, strike and dip of bedding are variable and are affected by local tight, plunging folds that are typically several meters wide and of undetermined length. Localized faulting typical of the upper Maryville and lower Nolichucky occurs within the site.

The upper several meters of subsurface materials consist of a gradationally weathered regolith, similar in character to saprolite, although the source rocks are sedimentary in origin. Borings at the CIIDF site contain soils derived from strongly weathered rock near the surface and essentially unweathered bedrock at depth (boring refusal). Between these extremes is a smooth progression through highly fractured shales and limestones (with subangular fragments on the order of 1 cm^3 in size with weathered surfaces) and moderately fractured, friable rocks (several centimeters in dimension) with minor weathering.

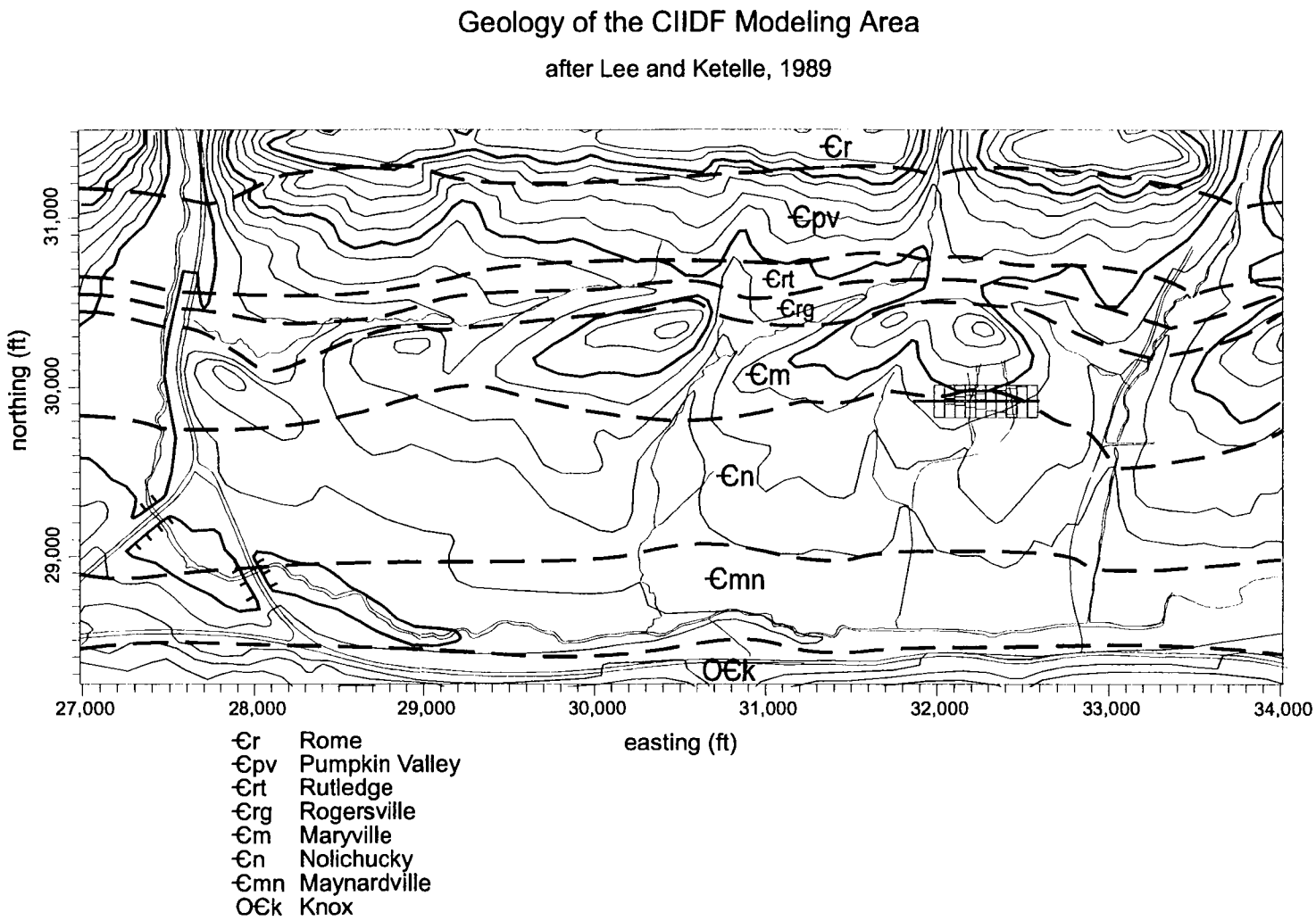

Fig. 2.5. Geologic map of the CIIDF modeling area.

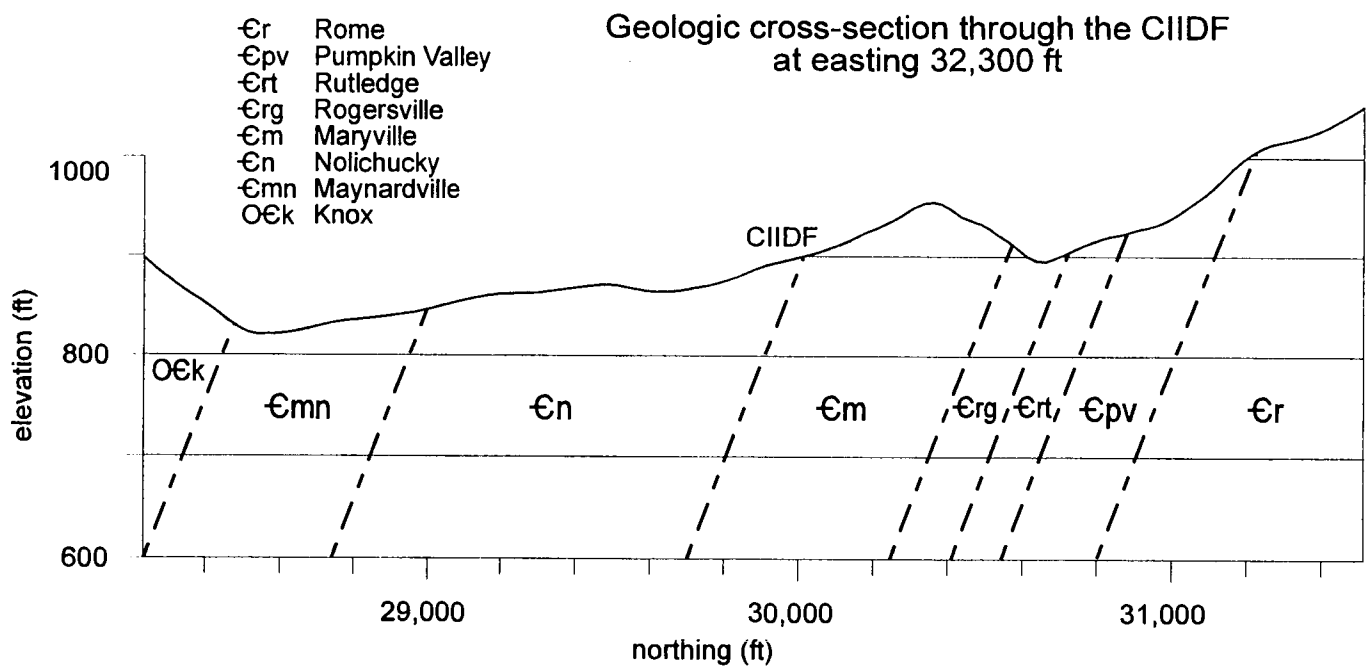

Fig. 2.6. Geologic cross section through the CIIDF modeling area.

2.1.5.3 Soils

The soil survey report for the Low-Level Waste Disposal Development and Demonstration (LLWDDD) site in Bear Creek Valley was prepared by Lietzke, Lee, and Lambert (1988). This site includes the proposed CIIDF. Individual soils and map units were identified for the LLWDDD area. The soil mapping was based on soil morphology, which is largely controlled by geology, hydrology, and geomorphic processes. Mapping units were established according to landform configuration, slope, wetness, and erosion class. A computer file of the digitized soil map was obtained. The digitized soil map was overlain onto the topographic file providing accurate identification of soil types with the terrain.

The soils of the CIIDF site are predominantly derived from Nolichucky residuum. A transect through the CIIDF site, described by Lietzke, Lee, and Lambert (1988), provides detailed soil type identification of the CIIDF site. The dominant soil type at the CIIDF site has three forms of Ruptic Ultic Dystrochrept: clayey (Bt argillic horizon), loamy-skeletal (Bw cambic horizon), or saprolite (Cr ruptic horizon) subsoil, mixed, thermic. High proportions of argillaceous limestone in the parent material leads to the argillic member. These soils occupy the summits and upper, middle, and lower side slopes. The favorable topography suggests that the area was probably intensively cultivated prior to becoming ORR in the early 1940s. Evidence of severe erosion is found even on gentle slopes.

The three members of the Ruptic Ultic Dystrochrept (ruptic, cambic, argillic) encompass the variability of the pedon determined by variability in limestone layer thicknesses in the parent material. The ruptic member, with little or no limestone in the parent material, is described by Lietzke, Lee, and Lambert (1988) as follows:

Horizon: depth; description.

Ap: 0 to 18 cm; dark yellowish brown shaley silt loam; weak fine granular structure; very friable; many fine and medium roots between peds; many fine pores; pH 4.7; abrupt wavy boundary.

Cr: 18 to 30 cm; oxidized and leached saprolite from siltstone and claystone; fragment interiors are yellowish brown or strong brown; rock-controlled structure; very firm; fragments are coated with either brown clay or black manganese coatings; few fine roots in cracks; pH 4.8; abrupt inclined boundary.

2Bt: 30 to 66 cm; yellowish brown silty clay loam; moderate coarse subangular blocky structure; firm; common fine prominent gray mottles in ped interiors; ped exteriors are coated with continuous brown clay; common fine and medium roots between peds; common fine and medium pores; pH 4.8; abrupt inclined boundary.

3Cr: 66 to 117 cm; oxidized and leached saprolite from siltstone and claystone; rock-controlled structure; very firm; many discontinuous prominent red iron stains on some fragment faces; other fragments are partially coated with black manganese oxides; no clay films were noted on fragments; water seems to flow in an unsaturated mode in this material; pH 4.9.

In comparison, the argillic member has subangular blocky clay for the second horizon (Bt), and the cambic member has a shaley silty clay loam for the second horizon (Bw) with weak subangular blocky structure.

The relatively impermeable saprolite of the C horizons can cause the soils to generate high amounts of lateral subsurface flow during storm events. This shallow subsurface flow can rise to the surface and become surface runoff in lower landscape positions. Lietzke, Lee, and Lambert (1988) noted that the soils of the area have morphological similarities with the soils of SWSA 6. The soil hydraulic properties developed for the SWSA 6 PA (ORNL 1994) are the most suitable data available for the PA of the CIIDF site.

The vegetation at the CIIDF site is dominated by pine stands and poorly growing deciduous species. The forest is tolerant of the low nutrient status and high acidity of the root zone. The vegetation attributes used in water budget modeling are available from simulations conducted for similar areas within ORR (Luxmoore and Huff 1989).

2.1.6 Hydrogeology

The hydrologic framework for ORR has been described by Solomon et al. (1992) in terms of the following four zones (see Fig. 2.7):

- A *storm-flow zone* constitutes the upper 1–2 m of the soil profile, in which precipitation-driven lateral flow generates up to 90% of stream flow. This zone is a major pathway for laterally transporting contaminants from the subsurface to surface waters.
- A *vadose zone* is predominantly unsaturated and consists of weathered saprolite 1–15 m thick, with a fluctuating water table as the lower boundary. This zone has (exponentially) decreasing hydraulic conductivity with depth.
- A *groundwater zone* contributes the remaining 10% of stream flow, and this occurs through a permeable saprolite layer called the water table interval. This flow zone has a thickness of 1–5 m (Clapp 1992, pp. 123–26). Intermediate and deep intervals of the aquifer have thicknesses of up to 100 m and contribute very little to stream flow due to low hydraulic conductivity and disconnected fractures.
- An *aquiclude* beyond a depth of 200 m has extremely slow water flow rates that are estimated to change on geological time scales.

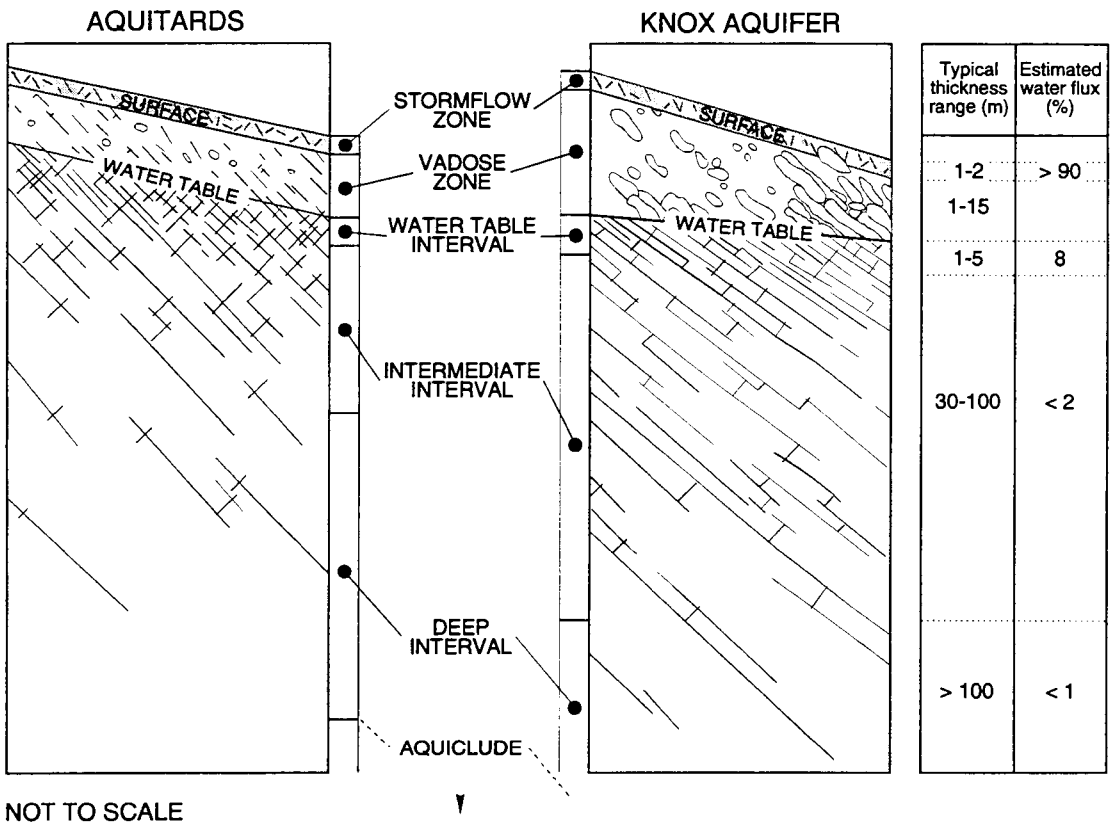

Fig. 2.7. Schematic profile showing subsurface flow zones and intervals, general thickness ranges, estimated relative water flux, and change in water type with depth for the aquitard of the CIIDF site in comparison to the aquifer of the Knox geological formation. *Source:* after Solomon et al. 1992.

These four zones occupy the upper 30 m or less of the landscape. The hydrologically active features of the upper three zones are responsible for essentially all radionuclide transport from waste sites.

The shallow lateral flow and groundwater proportions contributing to stream flow of 90% and 10%, respectively, (Fig. 2.7) were not supported by a recent hydrologic analysis of Clapp, Scanlon, and Timmins (N.d.). They used topographic indices of convergent flow to model the hydrologic responses of Center Seven Creek in Melton Valley. The soils and subsoils of this area are similar to those of the proposed CIIDF site. Clapp, Scanlon, and Timmins (N.d.) estimated the proportions of shallow flow and groundwater contributing to stream flow to be 53% and 47%, respectively, for seven annual simulations. The shallow flow proportion is likely to be a lower bound since the study was conducted for 7 years with a mean annual precipitation that was 25% less than the average for the area. The shallow flow contribution to stream flow is estimated to rise to 70% in an average year on the assumption that the majority of additional flow generated with additional rainfall would be contributed largely by shallow flow rather than by groundwater flow. It is more conservative for PA to favor the recharge path than the shallow flow path for the analysis of water quality at 100 m from the disposal site, and an approximate 70:30 ratio for the shallow flow and groundwater contributions to stream flow was adopted (Appendix D.2). The hydrologic modeling of Clapp, Scanlon, and Timmins (N.d.) also suggested, from comparisons of simulation results with groundwater elevation data, that recharge is not spatially uniform across the landscape.

Solomon et al. (1992) concluded that groundwater flow volumes decrease and solute residence times increase sharply with depth. They further estimate that the chemical transport rate in the storm-flow zone is on the order of meters per hour, decreasing exponentially with depth to flow rates of a few centimeters per year. Their review showed no evidence for contaminant migration along deep subsurface flow paths of the intermediate and deep intervals of the groundwater. The residence times for solutes in the water table interval range from a few days to a few years. Deeper flow rates of solutes have been estimated from ^{14}C measurements to be in the order of hundreds to tens of thousands of years (Solomon et al. 1992). Chemical adsorption and matrix diffusion have been identified as important geochemical and physical processes that retard chemical transport in burial ground soils creating secondary contaminant sources that may persist for many decades.

The water table at CIIDF, as in other areas on ORR, is a subdued replica of the land surface. In areas underlain by the shales and silty limestones of the Conasauga Group, groundwater occurs in a continuous, unconfined, saturated zone. Porosity of weathered and unweathered bedrock in the Conasauga Group is quite low (<5%). In turn, groundwater storage is low and groundwater flow velocities are rapid through the fracture network (flow velocities >0.1 m/d have been documented) (Moore 1989). The most prominent fracture orientations are parallel to local geologic strike and include bedding planes and strike-parallel fractures and joints. Less prominent and less penetrative fractures are perpendicular and oblique to local strike. The combined influences of bedrock dip and fracture control of groundwater flow result in anisotropy of the aquifer hydraulic conductivity. Maximum hydraulic conductivity in this regime predominantly occurs parallel to local geologic strike.

Saturated hydraulic conductivity at the CIIDF site, as elsewhere in the Conasauga, generally decreases with increasing depth below the land surface, and at any discrete depth the conductivity may vary within two to three orders of magnitude. The decline in conductivity with depth is roughly exponential (Moore 1988), leading to some uncertainty as to the thickness of the active groundwater circulation zone. The degree of anisotropy of hydraulic conductivity is variable and depends upon local conditions and the analytical method used in data interpretation. Anisotropy values determined from Conasauga Group aquifer pump tests on ORR range from 3:1 to >30:1 with maximum conductivity parallel to strike (Geraghty & Miller 1990; Davis et al. 1984; Lozier, Spiers, and Pearson 1987; Lee and Ketelle 1989). Tracer tests performed near the CIIDF site confirm that groundwater flow is strata-bound, moving in a direction parallel to strike rather than to the local head gradient, and that this behavior can be effectively emulated in computer models by employing an anisotropic hydraulic conductivity tensor (Lee et al. 1992).

While the flow behavior at depth is not well understood, flow in the regolith near the surface tends to follow geologic strike and discharge at the ephemeral creeks which transect the midvalley knolls. The main stem of Bear Creek follows the Maynardville Limestone and is considered to be the surface expression of a larger subsurface flow system which drains the valley. Throughout the valley, flow converges into the Maynardville and Bear Creek, which gains and loses along various parts of its reach (Geraghty & Miller 1989). Contaminant plumes from the Y-12 burial grounds are focussed into the channels of the Maynardville (Kornegay et al. 1994) and are not expected to diverge to the northwest into the Nolichucky and Maryville underlying the CIIDF site.

As previously mentioned, groundwater flow velocities tend to be relatively high in aquifers in Oak Ridge because flow occurs through fractures in otherwise low-porosity rock. Solute transport in such systems can also be quite rapid, depending on the ion exchange and adsorption characteristics of the soil or rock through which the solute migrates. Laboratory adsorption tests for various radionuclides have been performed on some soil and bedrock materials typical of those present at SWSA 6 in Melton Valley (Friedman and Kelmers 1990), which are also typical of the CIIDF site. Most of these tests were performed under batch-type test conditions using materials with much higher surface-area-to-volume ratios than are actually present along groundwater flow paths. For some radionuclides, the resulting distribution coefficients are substantially different from field measurements of contaminant movement at waste disposal facilities.

2.2 WASTE CHARACTERISTICS

LLW is radioactive waste generated on ORR but not mixed with hazardous constituents. It is waste not classified as high-level radioactive waste, transuranic (TRU) waste, spent nuclear fuel, or by-product material specified as uranium or thorium mill tailings and waste, as defined by DOE Order 5820.2A.

Approximately 10,000 m^3/year of LLW is routinely handled on ORR. LLW generated at the Y-12 Plant and K-25 Site are primarily uranium-contaminated materials. LLW generated at ORNL consists primarily of mixed fission and activation products. Small quantities of naturally occurring and

accelerator-produced radioactive material are generated and managed as LLW at ORNL. Test specimens of fissionable material, irradiated for research and development only, are also generated and managed as LLW at ORNL, provided the concentration of TRU radionuclides is <100 nCi/g. ORR manages some special categories of LLW, such as fissionable, asbestos, and biological waste. Table 2.3 describes the physical characteristics of DOE LLW, and Table 2.4 provides a breakdown of LLW generated by ORR sites during 1994.

The wastes to be disposed of in CIIDF are expected to include a large number of radionuclides. The radionuclides chosen for evaluation include those with half-lives >5 years that have been disposed of previously on ORR during the past 50 years, as well as other long-half-life radionuclides that potentially might be present in ORR waste streams. Radionuclides with half-lives <5 years were eliminated from consideration because these wastes will decay to levels which present an acceptable hazard to an intruder or public health and safety.

2.3 WASTE TREATMENT, CERTIFICATION, STORAGE, AND DISPOSAL

The shipment of solidified liquid LLW from ORNL to the Nevada Test Site for disposal remains under consideration by the DOE Nevada Operations Office. The approval process focuses on 117 solidified waste forms produced during the two most recent solidification campaigns. However, shipment of these wastes has been delayed indefinitely because of a lawsuit. An effort has been initiated to ship additional waste to the Envirocare facility in Utah, and the additional shipments are expected to begin by the end of fiscal year 1996.

A significant amount of containerized LLW continues to be stored outside at the K-25 Site and at the Y-12 Plant. The Y-12 Plant also continues to store containerized LLW in the Above-Grade Storage Facility. Each of six units can store more than 400 boxes of LLW, and 3100 m^3 (111,000 ft^3) of waste is currently in storage. ORNL continues to store most of its containerized LLW in fabric membrane structures, and the K-25 Site continues to store LLW in a combination of indoor facilities (e.g., the K-25 Building) and outside storage units. The K-25 Site received permission in 1995 from DOE Oak Ridge Operations (DOE-ORO) to begin using the K-33 Building for LLW storage, including containerized LLW from all ORR sites. However, due to uncertainties about the final disposition of the K-33 Building, plans for its use to store LLW were temporarily put on hold. In January 1996, however, DOE-ORO decided to move forward with the plans for storage.

The K-33 Building will accommodate at least 7800 m^3 (274,000 ft^3) of waste. However, this facility may not be suitable for storage of some LLW wastes, including remotely handled LLW from ORNL.

Table 2.3. Physical forms of low-level waste on the Oak Ridge Reservation

Form	Description
Debris—combustible	Examples of combustible waste are personnel protective clothing, laboratory coats, face masks, rags, coveralls, paper suits, shoe covers, mops, tape, brooms, plastic bags, rubber gloves, and wood.
Debris—noncombustible and compactible	Noncombustible, compactible waste consists of dry materials such as light-gauge metal and glassware that can be compacted by conventional compaction equipment. Supercompactors are capable of reducing many items such as motors, pumps, and piping to almost their theoretical maximum density.
Debris—noncombustible and combustible mixed	Waste composed of a mixture of combustible and noncombustible materials.
Activated metal	Waste materials contaminated with radionuclides generated through neutron activation of metal, equipment, and hardware.
Contaminated metal	Contaminated metals include tools, motors, pumps, piping, glove boxes, small tanks and furnaces, and other metal objects.
Filter media	Mechanical filters, cartridge-type filters, air-filtration filters.
Biological waste	Contaminated plants and animals on ORR such as trees, shrubs, grass, deer, groundhogs, geese, ducks, and fish; research animal carcasses, tissues, animal bedding, and litter.
Asbestos waste	Asbestos and asbestos-based materials in ovens, floor tile, insulation, furnaces, transite pipe, and gloves.
Soil, sediment, and rubble	Soil, asphalt, tar, sand, silt, rock, and gravel; sediment from drainage ponds and basins; concrete rubble and roofing materials from building demolition and decontamination and decommissioning activities.
Solidified liquids, chelates, and oils	Liquids and oils immobilized or stabilized by cement, polymers, or bitumen into a solid form.
Solidified/dewatered sludge	Any solid, semisolid, or liquid waste generated from air- or water-treatment processes with a total suspended/settled solids >30%.
Radiation sources	Waste material composed of encapsulated or unencapsulated radioactive material used for its known amounts and type of radiation.
Paint waste	Dried paint chips and dried paint in buckets.
Salt waste	Chloride salt, sulfate salt, and nitrate salt wastes.
Incinerator ash	An inorganic particulate waste that is primarily bottom or fly ash resulting from incineration.
Activated carbon	An inorganic particulate waste that is primarily spent or unused activated carbon.
Resin	Spent inorganic or organic ion-exchange resins used in wastewater treatment.
Other	Other solid wastes not meeting the criteria in one of the above categories.

Source: adapted from DOE 1995.

Table 2.4. Volume (m^3) of low-level waste generated on the Oak Ridge Reservation during 1994

Physical form	K-25	X-10	Y-12
Debris			
Combustible	1848	79	912
Noncombustible and compactible	11	3	6
Noncombustible and combustible mixed	793	1	1013
Activated metal	0	0	0
Contaminated metal	4186	9	0
Filter media	17	0	61
Biological waste	0	1	0
Asbestos waste	143	3	122
Soil, sediment, rubble	462	27	58
Solidified liquids/chelates/oils	0	183	0
Solidified sludge/resin	0	33	0
Radiation sources	0	<<1	0
Paint waste	0	0	<1
Salt waste	0	136	1
Incinerator ash	38	0	0
Activated carbon	<1	35	1
Other inorganic pariculates	197	1	14
Other	440	811	139
Totals	8135	1322	3131

Source: DOE 1995.

The disposal of high-range, suspect, and some biological waste contaminated with radioactive material was suspended in ORNL's SWSA 6 on December 11, 1992, because of results of the draft SWSA 6 PA and concerns expressed by Tennessee Oversight Agreement personnel. All biological shallow land disposal operations were suspended on April 1, 1993. Efforts are continuing to retrievably store the high-range waste in high-range wells in SWSA 6 until closure of SWSA 6 prohibits further storage. Storage of some of this waste at an above-grade storage site will be investigated if needed. The use of above-grade storage should provide enough space until the Class III/IV retrievable waste storage facilities are available in SWSA 7. The earliest projected availability of a SWSA 7 Class III/IV facility is June 1998, although this date may be extended because of continued delays in the approval of National Environmental Policy Act (NEPA) documentation.

Similarly, completion of the Bulk Contaminated Soil Facility at ORNL, or storage at the K-25 Site, will also relieve the projected shortage of available storage space. However, progress on this

project also continues to be delayed pending the approval of NEPA documentation and evaluation of storage of this waste at the K-25 Site, with the schedule for construction completion now undetermined.

2.3.1 Waste Treatment Facilities

Treatment of wastes prior to disposal is accomplished by a combination of techniques with the purpose of meeting the waste acceptance criteria and maximizing the disposal capacity of CIIDF. ORNL has a 1750-psi compactor for treating solid contact-handled LLW (CH-LLW). This facility is to be used for the treatment of some wastes to be disposed of at CIIDF, in conjnction with commercial waste treatment services. Commercial services used to treat wastes include supercompaction, incineration, and metal melting. The selection of waste treatment facilities to be used for wastes to be disposed of at the CIIDF facility is dependent on the specific waste streams and waste forms. CIIDF does not include waste treatment facilities.

2.3.2 Low-Level Waste Characterization and Certification

Requirements for managing LLW are established in DOE Order 5820.2A. Heads of DOE field organizations are assigned the authority to establish waste management requirements for treatment, storage, and disposal (TSD) facilities under their jurisdiction. One of the requirements for appropriate management of wastes generated by DOE operations specified by the order is the development of Waste Acceptance Criteria (WAC) for each TSD facility. The order also specifies that generators of LLW shall implement a certification program to ensure that the WAC for the receiving TSD are met. Generators of the waste and the TSD facility operators receiving the waste are jointly responsible for ensuring compliance with the TSD facility WAC.

2.3.2.1 Waste Certification

The Energy Systems Waste Acceptance Program is published in ES/WM-6, *Waste Certification Program Plan for the Oak Ridge Reservation.* This document, in effect, is an agreement between Energy Systems and the DOE-ORO Waste Management and Technology Division Director on the approach and methods that shall be implemented to certify wastes sent for treatment, storage, or disposal at the K-25 Site, the Y-12 Plant, and ORNL.

The Energy Systems Waste Acceptance Program has been designed to (1) provide a high degree of confidence that the WAC for the receiving TSD facility have been met, (2) designate responsibilities of the various organizations involved, (3) minimize the risks associated with the generation and management of wastes, and (4) improve efficiency and effectiveness of use of on- and off-reservation TSD facilities.

The requirement for generators to establish a waste certification program, the programmatic requirements that the generator waste certification program must meet, as well as the roles and

responsibilities of the organizations involved in the certification process are all found in ES/WM-6. The other two documents that identify the requirements for generator waste certification and waste characterization activities are EP-710, *Waste Certification Requirements for Energy Systems Waste Management Organization*, and ES/WM-10, *Waste Acceptance Criteria for the Oak Ridge Reservation* (MMES 1994).

2.3.2.2 Waste Characterization

Characterization requirements for wastes being sent to CIIDF will be documented in ES/WM-10, *Waste Acceptance Criteria for the Oak Ridge Reservation.* Information regarding the radiological, physical, and chemical characteristics of the waste that must be provided and certified by the waste generator on a per-package basis will be detailed in this document. Additional information related to packaging, labelling, documentation, and prohibited items will also be found in ES/WM-10. Radiological characterization reporting requirements will incorporate the results of the facility PA such that compliance with radioisotope concentration limits for wastes being disposed within the facility can be ensured.

2.4 CLASS L-II DISPOSAL FACILITY

CIIDF will reside on a 10-ha (24-acre) site in west Bear Creek Valley and will be designed to provide a facility for the disposal of solid LLW. A plan view of the facility is provided in Fig. 2.8. CIIDF will be utilized for solid LLW that contains primarily fission product radionuclides with half-lives that are less than 30 years. The waste will be received at CIIDF in metal containers. The waste boxes will be placed in interim storage in the Disposal Operations Building. Empty concrete vaults and lids will be stored outside in the staging area. When a sufficient quantity of waste boxes are in interim storage, the vault loading operation will be conducted in the staging area outside of the Disposal Operations Building. As each concrete vault is loaded with a waste container, the annular space (between the vault and the box) will be filled with a grout material. The lid to the concrete vault will then be placed on the vault and sealed with a butyl rope seal material. Grouted vaults will then be placed on the above-grade concrete pads (tumulus pads). When a tumulus pad has reached its disposal capacity (330 vaults), it will be covered for weather protection until such time as operations on adjacent pads allow for the final engineered cap to be put in place. Each pad will be designed to hold about 850 m^3 (30,000 ft^3) of waste.

Access to CIIDF shall be a gravel road from Bear Creek Road east of the intersection of SR95 and Bear Creek Road. The initial project will construct two tumulus disposal pads and provide the rough grading for four additional pads. The initial two pads will be located on either side of a central drainage gallery. The pads shall be sloped to a drain channel adjacent to the drainage gallery and connected to the drain piping by penetration through the gallery wall. The pads shall be constructed of epoxy-coated, steel-reinforced concrete and shall be curbed on the three lower sides. The high side of the pad is uncurbed to provide access for loading from the adjacent gravel road.

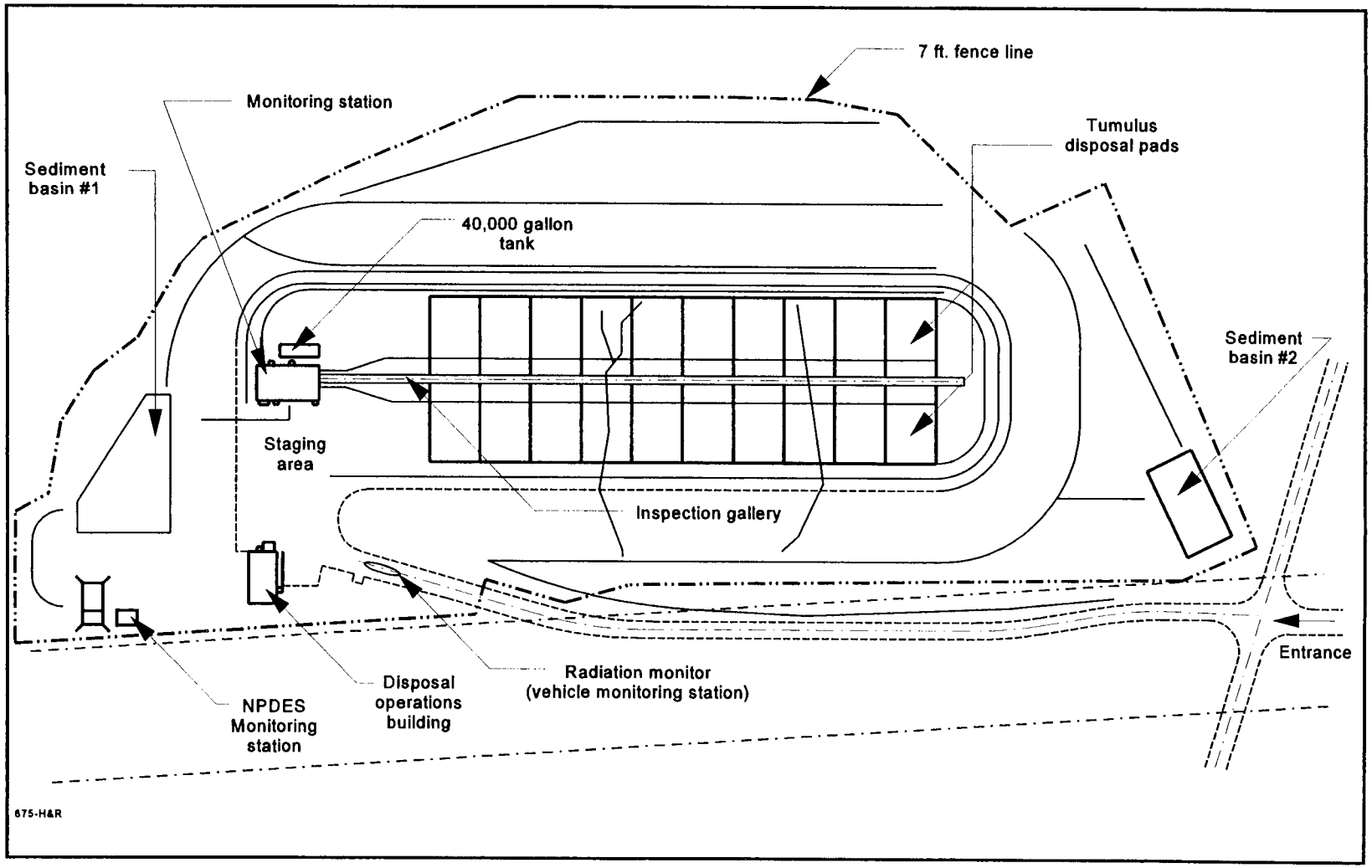

Fig. 2.8. Plan view of the CIIDF site.

The base for the pad shall consist of an underpad drain composed of perforated piping bedded in aggregate. The underpad drain shall provide a means to monitor for leakage through the pad and an avenue for the drainage of near surface water.

A drainage collection system composed of a drainage gallery shall be required to transport liquids collected from the pad surface to the monitoring station. Discharge from the monitoring station shall be piped to the NPDES discharge point. The concrete drainage gallery shall house the drain piping for the system and will extend past the two initial tumulus pads and beyond the area graded for the next four pads. The gallery will allow for long-term access to the drain piping for inspection, maintenance, and sampling.

3. ANALYSIS OF PERFORMANCE

This section describes the methods used to analyze the performance of CIIDF and provides an overview of the data used in the analysis. The wastes to be disposed of in CIIDF are expected to include a broad range of radionuclides. In order for the analysis to be comprehensive, a list of radionuclides was developed that includes radionuclides with half-lives >5 years that might be present in wastes generated on ORR (see Table 3.1.) Radionuclides with half-lives <5 were eliminated from consideration because the performance of the engineered barriers in conjunction with the radionuclide travel times in the environment ensures these radionuclides will decay to innocuous levels before exposures to individuals or the public could reasonably occur. Additional radionuclides not identified in Table 3.1 that may be present in CIIDF wastes with half lives >5 years include ^{227}Ac, ^{133}Ba, ^{247}Bk, ^{194}Hg, ^{166m}Ho, ^{144}Nd, ^{209}Po, ^{228}Ra, ^{186}Re, and ^{123m}Te. These isotopes are expected only to be present in wastes in small concentrations, and associated with small contributions to dose. However, they will be analyzed fully in the next version of the CIIDF PA, which will be prepared once the facility construction begins.

The analysis in this PA determines a limiting average concentration in waste and inventory for each radionuclide that satisfies each performance objective of DOE Order 5820.2A. The approach used to calculate the limiting average concentrations is to identify scenarios for analysis that bound the performance of the facility. With these bounding scenarios, the dose-based performance objectives in DOE Order 5820.2A are converted to inventories for each scenario selected for analysis. The models used for analyzing the scenarios are then used to calculate the limiting average concentrations in waste which correspond to the allowable doses. For potential exposures associated with environmental transport, where the transport phenomena are in general nonlinear, iterative calculations are performed to determine the limiting average concentrations. The limiting inventories for each radionuclide and scenario are examined to determine the most restrictive inventory, termed the "allowable concentration and inventory", for each radionuclide in waste that satisfies the performance objectives in DOE Order 5820.2A. Fig. 3.1 illustrates the iterative analysis method used for analyzing the release and transport of contamination, as described in this section.

This section provides the justification for selecting the bounding scenarios considered in detail in the PA. The data used in the analysis are identified and the sources documented. Any interpretation of these data is presented. The assumptions used for analyzing the scenarios are explicitly identified. Following the discussion of scenarios, data, and assumptions, the conceptual models for analyzing the scenarios are described in detail. The verification and validation of the models used in the analysis are also discussed.

Table 3.1. Radionuclide-specific physical data used throughout the CIIDF performance assessment

Nuclide	Half-life[a] (year)	Decay coefficient (1/year)	Specific activity[a] (Ci/g)
^{3}H	1.23×10^{1}	5.64×10^{-2}	9.65×10^{3}
^{10}Be	1.60×10^{6}	4.33×10^{-7}	2.23×10^{2}
^{14}C	5.73×10^{3}	1.21×10^{-4}	4.46×10^{0}
^{26}Al	7.20×10^{5}	9.63×10^{-7}	1.91×10^{-2}
^{36}Cl	3.01×10^{5}	2.30×10^{-6}	3.30×10^{-2}
^{40}K	1.28×10^{9}	5.42×10^{-10}	6.98×10^{-6}
^{41}Ca	1.03×10^{5}	6.73×10^{-6}	8.46×10^{-2}
^{60}Co	5.27×10^{0}	1.32×10^{-1}	1.13×10^{3}
^{59}Ni	7.50×10^{4}	9.24×10^{-6}	8.08×10^{-2}
^{63}Ni	1.00×10^{2}	6.93×10^{-3}	6.17×10^{1}
^{79}Se	6.50×10^{4}	1.07×10^{-5}	6.97×10^{-2}
^{87}Rb	4.80×10^{10}	1.44×10^{-11}	8.59×10^{-8}
^{90}Sr	2.85×10^{1}	2.43×10^{-2}	1.36×10^{2}
^{93}Zr	1.53×10^{6}	4.53×10^{-7}	2.51×10^{-3}
^{93m}Nb	1.36×10^{1}	5.10×10^{-2}	2.83×10^{2}
^{94}Nb	2.03×10^{4}	3.41×10^{-5}	1.87×10^{-1}
^{99}Tc	2.13×10^{5}	3.25×10^{-6}	1.70×10^{-2}
^{107}Pd	6.50×10^{6}	1.07×10^{-7}	5.14×10^{-4}
^{113m}Cd	1.37×10^{1}	5.06×10^{-2}	2.17×10^{2}
^{121m}Sn	5.50×10^{1}	1.26×10^{-2}	5.91×10^{1}
^{126}Sn	1.00×10^{5}	6.93×10^{-6}	2.84×10^{-2}
^{129}I	1.57×10^{7}	4.41×10^{-8}	1.77×10^{-4}
^{135}Cs	3.00×10^{6}	2.31×10^{-7}	1.15×10^{-3}
^{137}Cs	3.00×10^{1}	2.31×10^{-2}	8.70×10^{1}
^{151}Sm	9.00×10^{1}	7.70×10^{-3}	2.63×10^{1}
^{152}Eu	1.33×10^{1}	5.21×10^{-2}	1.73×10^{2}
^{154}Eu	8.80×10^{0}	7.88×10^{-2}	2.70×10^{2}
^{155}Eu	4.96×10^{0}	1.40×10^{-1}	4.65×10^{2}
^{207}Bi	3.22×10^{1}	2.15×10^{-2}	5.36×10^{1}
^{210}Pb	2.23×10^{1}	3.11×10^{-2}	7.63×10^{1}
^{226}Ra	1.60×10^{3}	4.33×10^{-4}	9.89×10^{-1}
^{229}Th	7.34×10^{3}	9.44×10^{-5}	2.13×10^{-1}
^{230}Th	7.54×10^{4}	9.19×10^{-6}	2.11×10^{-2}
^{232}Th	1.41×10^{10}	4.92×10^{-11}	1.10×10^{-7}
^{231}Pa	3.28×10^{4}	2.11×10^{-5}	4.72×10^{-2}
^{232}U	6.89×10^{1}	1.01×10^{-2}	2.14×10^{1}
^{233}U	1.59×10^{5}	4.36×10^{-6}	9.68×10^{-3}
^{234}U	2.45×10^{5}	2.83×10^{-6}	6.25×10^{-3}

Table 3.1 (continued)

Nuclide	Half-life[a] (year)	Decay coefficient (1/year)	Specific activity[a] (Ci/g)
^{235}U	7.04×10^{8}	9.85×10^{-10}	2.16×10^{-6}
^{236}U	2.34×10^{7}	2.96×10^{-8}	6.47×10^{-5}
^{238}U	4.47×10^{9}	1.55×10^{-10}	3.36×10^{-7}
^{237}Np	2.14×10^{6}	3.24×10^{-7}	7.05×10^{-4}
^{238}Pu	8.77×10^{1}	7.90×10^{-3}	1.71×10^{1}
^{239}Pu	2.41×10^{4}	2.88×10^{-5}	6.22×10^{-2}
^{240}Pu	6.56×10^{3}	1.06×10^{-4}	2.28×10^{-1}
^{241}Pu	1.44×10^{1}	4.81×10^{-2}	1.03×10^{2}
^{242}Pu	3.76×10^{5}	1.84×10^{-6}	3.82×10^{-3}
^{244}Pu	8.26×10^{7}	8.39×10^{-9}	1.77×10^{-5}
^{241}Am	4.33×10^{2}	1.60×10^{-3}	3.43×10^{0}
^{242m}Am	1.41×10^{2}	4.92×10^{-3}	9.72×10^{0}
^{243}Am	7.37×10^{3}	9.40×10^{-5}	1.99×10^{-1}
^{243}Cm	2.85×10^{1}	2.43×10^{-2}	5.16×10^{1}
^{244}Cm	1.81×10^{1}	3.83×10^{-2}	8.09×10^{1}
^{245}Cm	8.50×10^{3}	8.15×10^{-5}	1.72×10^{-1}
^{246}Cm	4.73×10^{3}	1.47×10^{-4}	3.97×10^{-1}
^{247}Cm	1.56×10^{7}	4.44×10^{-8}	9.28×10^{-5}
^{248}Cm	3.40×10^{5}	2.04×10^{-6}	4.25×10^{-3}
^{249}Cf	3.51×10^{2}	1.97×10^{-3}	4.09×10^{0}
^{250}Cf	1.31×10^{1}	5.29×10^{-2}	1.09×10^{2}
^{251}Cf	9.00×10^{2}	7.70×10^{-4}	1.58×10^{0}

[a] *Source*: Brown and Firestone 1986.

3.1 SCENARIO DEVELOPMENT AND SELECTION

This section describes the scenarios used in the analysis of the performance of CIIDF and the rationale for their selection. The scenarios identified for detailed analysis represent reasonable, yet conservative, representations of the transport of radionuclides in the environment and potential exposures that could arise from operation of the disposal facilities. The selected scenarios are not intended to include all of the possible transport mechanisms or exposure pathways that could occur in the future, but are intended to include all of those transport mechanisms and exposure pathways that are needed to provide reasonable assurance that the facility meets the performance objectives of DOE Order 5820.2A. The selected scenarios are considered to have a reasonable probability of occurrence and are analyzed deterministically to provide limiting average concentrations and inventories for radionuclides in wastes to be disposed of in CIIDF. Environmental transport scenarios are used for addressing the performance objectives for exposures to the general public and the protection of groundwater resources, and direct intrusion scenarios are used to address the performance objective for

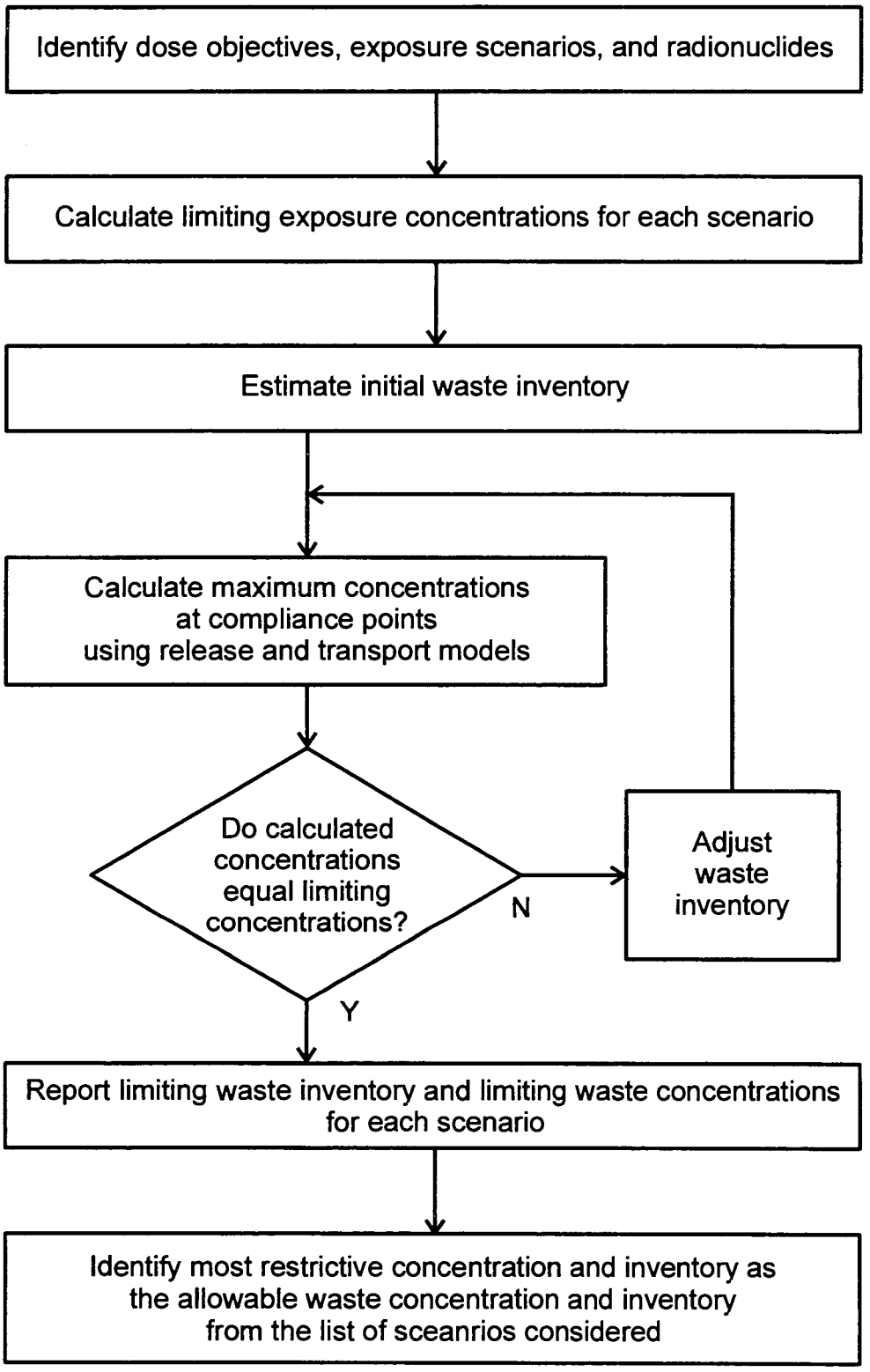

Fig. 3.1. Iterative analysis method for releases to the environment for the CIIDF performance assessment.

the protection of inadvertent intruders. The description of each scenario includes the features, events, and mechanisms that lead to the transport of and exposure to radionuclides disposed of in the facility.

The scenarios for analyzing the performance of CIIDF consider three different time periods: (1) the operational period, (2) the institutional control period, and (3) the period after institutional control. The operational period is the time during which waste is actively emplaced and the facility is closed. During this period of 22 years, access to the facility by individuals is denied, and the facility is actively maintained. The institutional control period is prescribed to be the 100 years following the completion of facility closure, during which the site is maintained and access by the public is denied. The post-institutional control period begins with the presumed loss of institutional control and extends for an indefinite period of time. Access to the facility by the public is assumed to occur, and no maintenance of the facility is assumed to occur during this time period.

3.1.1 Release and Environmental Transport Scenarios

This section provides the description and rationale for the selection of the release and environmental transport scenarios. Radionuclides in waste can be released from the facility as contaminated solid, liquid, vapor, or gas. These releases can occur once the capability of the disposal facility to isolate the wastes has been diminished by natural processes such as diffusion or by degradation of the disposal facility features (e.g., cover, pad, vaults, leachate collection system). The subsequent transport of contamination from the disposal facility to a point of exposure is influenced by physical, chemical, and biological processes. A comprehensive understanding of all of the natural processes likely to influence the transport of contamination from CIIDF to a point of exposure at some time in the future is not available. Nevertheless, as discussed in Sect. 2.1, the abundance of precipitation, presence of shallow groundwater conditions, and abundant surface water resources are primary environmental factors influencing the transport of contaminants from waste disposal facilities. Consequently, the importance of any pathway of environmental transport can be established by comparison to the water transport pathway.

3.1.1.1 Closure Scenario

The timetable of CIIDF site activities involves three main periods of operation, maintenance, and postmaintenance (a, b, and c) with differing time periods and differing influences on site hydrology. The period of the initial site preparation and landscape modification for construction of the facility was not specifically considered in the modeling analysis. The first time period (a1) assessed in this analysis accounts for the sequential construction of a 20-pad facility loaded with concrete vaults at a rate of one pad per year. For reference purposes, the year 2000 is taken as the first year of operation of CIIDF. Pad filling is followed by the construction of a compacted soil cap over the tumulus pads. The various components of the closure scenario are:

- Operation
  a1. Pad filling operations, 20 years (2000–2019)
  a2. Construction of cap, 2 years (2020–2021)
- Maintenance
  b1. Effective cap with grass cover, 10 years (2022–2031)
  b2. Linear increase in cap leakage, 10 years (2032–2041)
  b3. Leaking cap with mown grass, 80 years (2042–2121)
- Postmaintenance
  c1. Succession from grass to forest, 30 years (2122–2151)
  c2. Deciduous forest cover over site (2152+)

A 100-year maintenance period consists of a 10-year period with effective cap operation, followed by a 10-year period of progressive cap failure represented by a linear increase in drainage through the cap. The final cap condition is complete hydrologic failure associated with the development of preferential flow paths in the soil and seam separation in the geotextile layers, allowing soil water drainage to interact freely with the concrete vaults (b3). The site is abandoned during the postmaintenance period, and the grass vegetation is gradually replaced by naturally invading forest vegetation.

3.1.1.2 Releases from Disposal Units to Environmental Pathways

The disposal technology for CIIDF is described in Sect. 2.3. The highly engineered disposal technology utilizes large quantities of concrete to isolate the wastes from the environment. The durability of concrete, the bulk movement of water through the concrete, and the flow of water within the disposal facility are significant elements in the performance model for the release of contamination from the disposal facility. Leachate generated after water reaches the waste in the disposal vaults may be released through leaks in containment and by advection and diffusion through the walls of the concrete vaults. When concrete degrades and cracks are assumed to form, advection becomes the dominant mechanism for the release of radionuclides. The performance of the disposal vaults and the assumptions used in source term modeling are discussed in Sects. 3.3.3 and 3.2.2, respectively.

Once contamination has been released from the vaults in the form of leachate, the most likely pathways for the transport of contamination are surface water and groundwater. Transport of contamination as a gas or vapor could occur from volatilization [e.g., tritium (^{3}H) or ^{14}C] or evaporation of leachate. Observations at radioactive waste disposal facilities over the last few decades suggest that emission of radionuclides to the atmosphere in gas or vapor is not an important release mechanism on ORR (ORNL 1994, Bechtel 1991). Routine monitoring of gaseous emissions at SWSA 6, the operating radioactive waste disposal facility at ORNL, is not performed. However, an ambient air monitoring station is located at White Oak Dam, just south of SWSA 6. The ambient air monitoring station takes biweekly samples of both airborne particulates and gases. Remote air monitoring stations at Norris Dam and Fort Loudon Dam collect the same data. Table 3.2 summarizes the data collected in

Table 3.2. Mean radionuclide concentrations in air, 1994

Nuclide	Concentration (10^{-15} μCi/mL)	
	White Oak Dam	Remote network
^{7}Be	2.85×10^{1}	8.31×10^{1}
^{60}Co	3.93×10^{-2}	2.08×10^{-2}
Total Sr	3.14×10^{-2}	2.31×10^{-2}
^{137}Cs	4.91×10^{-2}	1.68×10^{-2}
^{238}Pu	0.00×10^{0}	2.85×10^{-4}
^{239}Pu	0.00×10^{0}	2.85×10^{-4}
^{228}Th	4.32×10^{-3}	1.96×10^{-3}
^{230}Th	7.50×10^{-3}	2.17×10^{-3}
^{232}Th	5.30×10^{-3}	2.07×10^{-3}
^{234}U	4.32×10^{-2}	1.32×10^{-2}
^{235}U	1.77×10^{-3}	2.04×10^{-3}
^{238}U	2.26×10^{-2}	6.09×10^{-3}
^{241}Am	0.00×10^{0}	6.89×10^{-4}
^{244}Cm	0.00×10^{0}	1.88×10^{-4}

1994 (Frazier et al. 1995). These data indicate little difference in the radionuclide concentrations in air adjacent to a radioactive waste disposal facility on the ORR as compared with the radionuclide concentrations at significant distances from the reservation.

Suspension of particulates by natural processes has not been identified as an important pathway for the transport of contamination. Observations in Oak Ridge and nearby areas clearly show that extensive vegetative ground cover is quickly established on any cleared lands and that reforestation of unattended lands naturally occurs within a few decades. Extensive vegetation and forestation at the disposal units, combined with the high annual rainfall and low average wind speeds in Oak Ridge, provide conditions that minimize the suspension of radionuclides in particulate form by natural processes. Even if some waste should become exposed due to natural erosion at the site, the amount of waste that could be suspended into the atmosphere by natural processes would be small. Assuming the airborne activity measured at the White Oak Dam Monitoring Station is indicative of releases from SWSA 6, the annual effectve dose to an individual would be <0.10 mrem. In reality, these data represent activity from all operations at ORNL, the Y-12 Plant, and K-25 Site, including stack releases and releases from 50 years of operations. Over the period of historical operations in Oak Ridge, millions of curies have been disposed of in nearby disposal facilities and discharged directly to surface water. The data in Table 3.2 suggest that the release of radioactivity as gases and particulate matter in the atmosphere is not significant. Consequently, nonvolatile airborne releases of contamination are not considered in detail in this PA. Volatiles are not measured at the ambient air monitoring station and need to be considered separately. Appendix C provides a conservative analysis

of the volatilization of radioactivity from the CIIDF. This analysis demonstrates that volatiles do not need to be considered in detail in this PA.

ORR is in full compliance with the requirements of 40 CFR 61. Total EDEs for 1994 have been determined for ORR and are well below the 10-mrem National Emission Standards for Hazardous Air Pollutants limit (Frazier et al. 1995). For CIIDF to exceed the 40 CFR 61 limit, atmospheric releases from the disposal facility would need to increase by more than two orders of magnitude above the levels currently observed at SWSA 6. With the highly engineered disposal system used for CIIDF, such an increase in emissions is not plausible, and reasonable scenarios for analysis are difficult to construct. Consequently, atmospheric releases from CIIDF are given no further consideration in this PA.

Release of radionuclides from CIIDF is considered to occur primarily to surface water or to the soil surface. Leachate generated within the vaults is considered to move out of the vaults by diffusion or advection through cracks in the concrete. Leachate not captured by the concrete pad and collection system is available for transport to surface water or groundwater. The disposal facility includes engineered features to suppress the groundwater table in the vicinity of the disposal facility and minimize vertical transport of leachate. Nevertheless, mixing of leachate with groundwater beneath the disposal facility is considered in the analysis, both from infiltration of leachate runoff from the concrete pad and of leachate passing through the concrete pad.

Releases due to biotic intrusion

Radionuclides could be released from disposal units into the environment as a result of biotic intrusion into the waste (e.g., by burrowing animals or plant roots). Although biotic intrusion and its consequences have been studied using largely generic models (e.g., see McKenzie et al. 1982a, 1982b, 1983, 1984, 1985, 1986 and Kennedy, Caldwell, and McKenzie 1985), the magnitude of releases due to biotic intrusion into near-surface waste disposal facilities relative to releases due to infiltrating water or inadvertent human intrusion and the importance of these releases for exposures of humans have not been firmly established, especially for facilities constructed with engineered barriers. However, the following arguments can be made to indicate that radionuclide releases due to biotic intrusion probably would be relatively unimportant for CIIDF and, thus, need not be considered explicitly in the PA.

First, biotic intrusion could redistribute radionuclides throughout the soil column between the disposal facility and the ground surface, and the redistributed radionuclides in the soil column could be readily transported in water. However, during the time after disposal when the concrete barriers in the disposal facility remain intact, only a small fraction of the waste should be transportable into the soil column by biotic intrusion, primarily because extensive penetration of the intact barriers by burrowing animals and plant roots should not occur. Rather than modeling this phenomenon explicitly, the possibility that a small amount of waste could be transported in water as a result of biotic intrusion is taken into account implicitly by using pessimistic assumptions about the lifetime of the concrete barriers. Furthermore, in the absence of concrete barriers, transport of radionuclides that have been moved into the soil column by biotic intrusion would essentially be the same as transport of

radionuclides that have remained in the disposal facility. Therefore, once the concrete barriers are assumed to have failed, biotic intrusion should not significantly enhance transport in water.

Second, biotic intrusion also could transport some radioactive waste to the ground surface. However, it is inconceivable that the amount of waste that could be brought to the surface would be more than a small fraction of the inventory in the disposal facility. Furthermore, the amount of waste deposited on the ground surface that could be suspended into the atmosphere and transported to off-site locations by the wind should be insignificant due to the extensive vegetative ground cover that would be established naturally at the disposal site and the generally high levels of soil moisture and low wind speeds on ORR.

Finally, biotic transport of radioactive waste from the disposal facility into surface soil at the site could, under some circumstances, enhance exposures of inadvertent intruders. However, the scenarios for inadvertent intrusion evaluated in the PA for CIIDF (see Sect. 3.1.2.2) assume either that undisturbed waste in the disposal facility is accessed directly or that the concrete barriers are intact. An assumption that waste is accessed directly maximizes the assumed concentrations of radionuclides to which an inadvertent intruder would be exposed. If transport of waste into the overlying soil column or to the ground surface by biotic intrusion were taken into account, the primary effect would be to dilute the concentrations of radionuclides to which an intruder would be exposed when solid waste in the disposal facility is accessed directly. If the concrete barriers are assumed to be intact, the amount of waste that could be transported from the facility by biotic intrusion should be unimportant, as noted above. Therefore, it does not seem reasonable that biotic intrusion could increase radiation exposures by significant amounts for the scenarios for inadvertent intrusion evaluated in the PA.

Based on these arguments, the effects of biotic intrusion on the mobilization and transport of radionuclides are not considered in the PA for CIIDF. Additional discussions indicating the expected lack of significance of biotic intrusion and transport are presented in Sects. 3.1.1.3 and 3.1.2.3.

3.1.1.3 Environmental Transport via Biotic Pathways

Transport of radionuclides to off-site locations by biotic pathways could occur, particularly when the contamination has been transported to the ground surface or surface water on the disposal site. However, based on available information described below, transport of radionuclides by biotic pathways does not appear to be an important concern for waste disposal on ORR.

Routine monitoring has indicated that contamination of wildlife, particularly deer and waterfowl, has occurred on ORR, presumably as a result of past discharges of contaminated water or ongoing discharges to the land surface or surface streams from old radioactive waste disposal sites. However, the observed levels of contamination in wildlife have been low. For example, less than 2% of the deer killed on ORR during 1991 contained measureable levels of radionuclides, and the estimated maximum annual dose equivalent to an individual from consumption of contaminated deer meat was only about 1 mrem (Kornegay et al. 1992). A similar dose estimate was obtained for consumption of contaminated geese or ducks.

The data from monitoring of wildlife on ORR described above and the likelihood that present-day levels of contamination in the environment from past or ongoing discharges from a variety of sources are greater than levels that might result from future discharges from CIIDF indicate that contamination of wildlife is not likely to be an important mechanism for transport of radionuclides beyond the boundary of the disposal site. Therefore, transport of radionuclides in contaminated wildlife is not considered in the PA for CIIDF.

Transport of radionuclides from the disposal site also could occur as a result of root uptake by plants and subsequent migration of vegetation by natural processes. However, in contrast to arid sites with high average wind speeds and sparse vegetation, migration of plant matter by natural processes over substantial distances should not occur to any significant extent on ORR, due primarily to the extensive vegetation that should be reestablished at the disposal site (which provides a physical barrier to migration), high average rainfall, and low average wind speed. Therefore, transport of radionuclides in vegetation also is not considered in the PA for CIIDF. Biotic recycling of leaves and other plant litter as a means of enhancing exposures of humans is considered in Sect. 3.1.2.3.

3.1.2 Human Exposure Scenarios

This section describes the exposure scenarios and exposure pathways assumed in evaluating doses to off-site individuals and inadvertent intruders resulting from disposal of LLW in CIIDF. The assumed scenarios and pathways are described qualitatively, and justifications for the choice of the scenarios and pathways are provided. The models and parameter values used in implementing the assumed exposure scenarios and exposure pathways are summarized in Sect. 4.4 and described in detail in Appendix G.

3.1.2.1 Exposure Scenarios for Off-Site Members of the Public

Exposures of off-site members of the public due to releases of radionuclides from CIIDF may occur at any time after disposal operations commence at the site. However, only those releases which are projected to occur after waste emplacement is completed and the disposal facility closed are of concern to this PA. During the preclosure operating period, a facility and environmental monitoring program will be used to evaluate compliance with the applicable performance objectives for off-site releases, which include the performance objectives for off-site individuals and protection of groundwater and surface water resources.

The models for assessing dose to off-site members of the public at any time after facility closure provide estimates of dose per unit concentration of radionuclides in contaminated environmental media for individuals who are assumed to reside outside the 100-m buffer zone around the disposal facility, discussed in greater detail in Sect. 3.3.4. Estimates of collective dose in the exposed population beyond the site boundary are not considered, in part because the size and location of future populations that could be affected by disposals at CIIDF cannot be predicted. An additional consideration is that the present off-site population which could be exposed to releases from CIIDF is

located a considerable distance from the disposal site, and the most important pathway for exposure of this population is transport of radionuclides into the Clinch River, which provides a large dilution factor for releases from CIIDF. Therefore, the dose received by average individuals in population groups outside the present boundary of ORR is expected to be far less than the dose to a hypothetical individual residing near the disposal facility.

The PA for CIIDF assumes that radionuclides released from the disposal facility are transported to off-site locations primarily by water pathways. As described in Sect. 1, two performance objectives are applied in limiting allowable releases by water pathways and exposures of individuals at off-site locations: (1) an annual EDE of 25 mrem from all exposure pathways combined and (2) an annual EDE of 4 mrem from the drinking water pathway only. The latter performance objective is used to define protection of groundwater and surface water resources at any locations outside the 100-m buffer zone around the disposal facility. The useable surface water resource outside the buffer zone is assumed to be Bear Creek.

Given the performance objectives for off-site releases by water pathways listed above, the models for assessing dose to off-site individuals are used to establish limits on the concentrations of radionuclides in groundwater or surface water that would provide reasonable assurance of compliance with the performance objectives. These results then are combined with the results of the source-term and environmental-transport modeling to provide limits on inventories of radionuclides for disposal that would provide reasonable assurance of compliance with the performance objectives.

For releases by water pathways, the dose-assessment modeling is based on the assumption that an individual residing outside the boundary of the buffer zone around CIIDF uses contaminated water, either groundwater or surface water from Bear Creek, for domestic purposes, and the following exposure pathways are considered:

- direct ingestion of contaminated drinking water,
- ingestion of milk and meat obtained from dairy and beef cattle that drink contaminated water and consume pasture grass irrigated with contaminated water,
- ingestion of vegetables obtained from a garden irrigated with contaminated water,
- direct ingestion of contaminated soil from the vegetable garden in conjunction with vegetable intakes,
- external exposure to contaminated soil while working in the vegetable garden, and
- inhalation of radionuclides suspended into air while working in the vegetable garden.

However, based on the following considerations, only the dose from the drinking water pathway is evaluated in the PA for off-site releases from the CIIDF.

First, a previous analysis for the SWSA 6 disposal facility on ORR (ORNL 1994) showed that the dose from ingestion of milk and meat from dairy and beef cattle that drink contaminated water generally is less than the dose from direct ingestion of contaminated drinking water.

Second, irrigation is not commonly practiced near Oak Ridge, due to the normally abundant rainfall. Furthermore, even if irrigation were practiced to an extent reasonable for normal rainfall

conditions, a previous analysis for a disposal facility at the Savannah River Site (MMES, EG&G, and WSRC 1994), where rainfall conditions are similar to those in Oak Ridge, indicated that the dose from all of the exposure pathways resulting from use of contaminated water for irrigation of a vegetable garden and pasture grass would be less than the dose from direct ingestion of contaminated drinking water.

Finally, the assumed performance objective of 4 mrem per year EDE for the drinking water pathway only is considerably less than the performance objective of 25 mrem per year for all exposure pathways combined.

Taking all of these factors into account, all of the exposure pathways involving use of contaminated water for purposes other than drinking water listed above can be neglected in the dose analysis for off-site individuals for purposes of demonstrating compliance with the applicable performance objectives for off-site releases.

Off-site individuals also could receive exposures from ingestion of fish obtained from contaminated surface water and from external exposure to contaminated surface water while engaged in recreational activities, such as swimming or boating. However, given the small size and flow rate of Bear Creek, the nearest location where these exposure pathways reasonably could occur is near the point of discharge into the Clinch River. However, the concentrations of radionuclides released from CIIDF into Bear Creek and thence into the Clinch River would be diluted by a large amount compared with the concentrations in groundwater or Bear Creek near the boundary of the buffer zone around the disposal facility. Therefore, exposure pathways involving consumption of contaminated fish and use of contaminated surface water for recreational purposes also can be neglected in the dose analysis for off-site individuals.

In summary, as indicated in Table 3.3, direct consumption of drinking water from a contaminated source, either groundwater or surface water from Bear Creek, is the only exposure pathway evaluated in the PA for off-site releases from CIIDF by water pathways. If the assumed performance objective of 4 mrem per year EDE for the drinking water pathway only is met, then the performance objective of 25 mrem per year for all exposure pathways combined also would be met without the need to evaluate doses from any other pathways.

3.1.2.2 Exposure Scenarios for Inadvertent Intruders

Following loss of active institutional control over CIIDF, which is assumed to occur at 100 years after facility closure, inadvertent intruders are assumed to come onto the site and establish a permanent homestead, including sources of water and foodstuffs, with no prior knowledge of waste disposal activities at the site. Inadvertent intruders are assumed to receive exposures from use of contaminated groundwater obtained from an on-site well and from direct intrusion into solid waste in the disposal facility. There are no useable surface waters on the disposal site. As described in Sect. 1, the following two performance objectives are applied to inadvertent intruders: (1) an annual EDE of 100 mrem from all exposure pathways combined for scenarios involving chronic exposure and (2) an

Table 3.3. Summary of exposure pathways for off-site individuals due to releases by water pathways[a]

Assumed pathways	Status	Discussion
Drinking water	Evaluated	Applicable performance objective is assumed to be annual EDE of 4 mrem.
Ingestion of milk and meat from dairy and beef cattle that drink contaminated water; internal and external exposure pathways resulting from irrigation of vegetable garden and pasture grass	Considered but not evaluated	Pathways can be neglected because (1) total dose would be comparable to or less than dose from drinking water pathway and (2) applicable performance objective for all exposure pathways of 25 mrem per year EDE is higher than performance objective for drinking water pathway only.
Ingestion of contaminated fish; external exposure to contaminated surface water during recreational activities	Considered but not evaluated	Pathways can be neglected because concentrations of radionuclides in surface water at locations where pathways are credible would be much less than concentrations in groundwater or surface water near disposal facility.

[a]Airborne releases and releases due to biotic intrusion are assumed to be negligible compared with releases due to infiltrating water.

EDE of 500 mrem from all exposure pathways combined for scenarios involving a single, acute exposure.

The models for assessing dose to inadvertent intruders provide estimates of dose per unit concentration of radionuclides in contaminated environmental media on the disposal site. Given the performance objectives for inadvertent intruders listed above, the models for assessing dose then are used to establish limits on the concentrations and inventories of radionuclides in disposed waste that would provide reasonable assurance of compliance with the performance objectives.

For inadvertent intruders, the assumed exposure pathways involving use of contaminated water obtained from an on-site well are the same as those for off-site individuals listed in the previous section. However, based on the following considerations, these exposure pathways can be neglected for inadvertent intruders.

First, as discussed in the previous section, the dose from all exposure pathways involving use of contaminated water other than direct consumption of drinking water would be less than the dose from the drinking water pathway itself.

Second, compliance with the performance objective of 4 mrem per year EDE for the drinking water pathway at any locations beyond the boundary of the 100-m buffer zone around the disposal facility would ensure that the dose from the drinking water pathway at on-site locations would be only a small fraction of the performance objective of 100 mrem per year for chronic exposure of inadvertent intruders from all exposure pathways combined.

Finally, the maximum concentrations of radionuclides in groundwater at on-site locations at any time after loss of active institutional control, and thus the maximum doses to an inadvertent intruder from use of contaminated groundwater, would not occur at the same time as the maximum

doses from direct intrusion into solid waste in the disposal facility. Furthermore, for some mobile radionuclides (e.g., ^{3}H), the maximum concentrations in groundwater at on-site locations would occur during the 100-year period of active institutional control, when exposures of inadvertent intruders would be precluded, but the concentrations thereafter would be considerably less.

Taking all of these factors into account, exposures of inadvertent intruders to contaminated groundwater obtained from an on-site well need not be considered in demonstrating compliance with the applicable performance objectives for chronic and acute exposure from all exposure pathways combined. Therefore, the dose analysis for inadvertent intruders can focus on exposure scenarios involving direct intrusion into solid waste in the disposal facility.

In the PA for CIIDF, direct intrusion into solid waste in the disposal facility by an inadvertent intruder is assumed to occur according to one of three scenarios: the agriculture, resident, and post-drilling scenarios. Each of these scenarios involves chronic exposure for which the performance objective is an annual EDE of 100 mrem. The following paragraphs provide a brief description of these three scenarios.

Agriculture scenario

In the agriculture scenario, an inadvertent intruder is assumed to construct a home directly on top of the disposal facility, with the foundation extending into the waste itself. Some of the waste exhumed during construction of the foundation, which is assumed to be indistinguishable from native soil, is assumed to be mixed with native soil in the intruder's vegetable garden. The agriculture scenario then occurs after construction of the home is completed and the vegetable garden established, and the following pathways involving chronic exposure are assumed to occur:

- ingestion of vegetables grown in the contaminated garden soil,
- direct ingestion of contaminated soil from the garden in conjunction with vegetable intakes,
- external exposure to contaminated soil while working in the garden or residing in the home on top of exposed waste in the disposal facility, and
- inhalation of radionuclides suspended into air from contaminated soil while working in the garden or while residing in the home.

Resident scenario

As in the agriculture scenario described above, the resident scenario assumes that an inadvertent intruder excavates a foundation for a home on top of the disposal facility. However, during excavation the intruder is assumed to encounter an intact engineered barrier on top of the disposal facility which cannot be penetrated by the types of excavation equipment normally used on ORR, and the intruder is assumed to construct a home directly on top of the intact barrier. The resident scenario then occurs after construction of the home is completed, and the only assumed exposure pathway is chronic external exposure to photon-emitting radionuclides in the waste while residing in the home on

top of the disposal facility. The presence of intact engineered barriers, which are assumed not to be penetrated during excavation, would preclude any ingestion or inhalation exposures.

The external exposure pathway assumed in the resident scenario is conceptually the same as one of the pathways in the agriculture scenario listed above. However, the external dose per unit concentration of radionuclides while residing in the home will be considerably less in the resident scenario than in the agriculture scenario, because the resident scenario assumes the presence of an intact engineered barrier between the waste and the receptor location, but the agriculture scenario assumes exposure to unshielded waste. On the other hand, as described later in this section, the agriculture scenario is assumed not to occur for a substantial period of time after the resident scenario, because the agriculture scenario requires that the engineered barriers be physically degraded and penetrated by normal excavation procedures, whereas the barriers presumably will remain intact for substantially longer than the 100-year period of active institutional control over the disposal site. Therefore, for any photon-emitting radionuclide, the resident scenario is potentially important (i.e., could result in doses comparable to or greater than the dose for the agriculture scenario) only if the inventory in the disposal facility would be depleted significantly over time prior to failure of the engineered barriers, either by radioactive decay or by mobilization and transport in infiltrating water. For relatively long-lived and immobile radionuclides, the resident scenario would result in considerably lower estimates of dose than the agriculture scenario and, thus, would not be important in demonstrating compliance with the applicable performance objective.

Post-drilling scenario

In the post-drilling scenario, an inadvertent intruder is assumed to drill through the disposal facility for the purpose of constructing a well for a domestic water supply, but no other means of accessing solid waste is assumed to occur (e.g., construction of a home on top of the disposal facility). The contaminated drilling waste is assumed to be indistinguishable from native soil, and all of the drilling waste is assumed to be mixed with native soil in the intruder's vegetable garden. The post-drilling scenario then occurs after the vegetable garden is established, and the following pathways involving chronic exposure are assumed to occur:

- ingestion of vegetables grown in the contaminated garden soil,
- direct ingestion of contaminated soil from the garden in conjunction with vegetable intakes,
- external exposure to contaminated soil while working in the garden, and
- inhalation of radionuclides suspended into air from contaminated soil while working in the garden.

The exposure pathways assumed in the post-drilling scenario are conceptually the same as the corresponding pathways in the agriculture scenario listed previously. In the post-drilling scenario, external and inhalation exposures while residing in the home on the disposal site are not relevant because all waste exhumed by drilling is assumed to be mixed with native soil in the intruder's

vegetable garden and the intruder's home is assumed not to be located directly on top of the disposal facility or contaminated soil.

However, the dose per unit concentration of radionuclides in the disposal facility should be considerably less in the post-drilling scenario than for the corresponding exposure pathways in the agriculture scenario, because the volume of drilling waste that could be mixed with native soil in the intruder's vegetable garden presumably is considerably less than the volume of waste that could be mixed with garden soil following excavation of a foundation for a home. Therefore, as is the case for the resident scenario described above, the post-drilling scenario is potentially important for any radionuclide compared with the agriculture scenario only if the post-drilling scenario could occur considerably earlier and the inventory in the disposal facility would be depleted significantly over time prior to occurrence of the agriculture scenario, either by radioactive decay or by mobilization and transport in infiltrating water. For relatively long-lived and immobile radionuclides, the post-drilling scenario would result in considerably lower estimates of dose than the agriculture scenario and, thus, would not be important in demonstrating compliance with the applicable performance objective.

Time of occurrence of intrusion scenarios

For the exposure scenarios involving direct intrusion or attempts at direct intrusion into solid waste in the disposal facility described above, an important assumption is the time after disposal at which the scenarios first occur, because the dose from many radionuclides is reduced significantly over time due to radioactive decay or mobilization and transport from the disposal facility into the environment. The earliest time after disposal at which the scenarios can occur depends on the time period for active institutional control over the disposal site, which is assumed to be 100 years after disposal. In addition, for the agriculture and post-drilling scenarios, the earliest time of occurrence would depend on the length of time the engineered barriers in the disposal facility are assumed to maintain their integrity and preclude direct intrusion into waste by excavation or drilling, provided the barrier lifetime is longer than 100 years. The lifetime of the engineered barriers is not relevant for the resident scenario, because this scenario assumes that the barriers are intact.

The agriculture scenario cannot occur unless the disposal facility is penetrable by the types of excavation equipment normally used in digging a foundation for a home. Therefore, based on an assumption that normal excavation procedures cannot readily penetrate an intact concrete barrier, the agriculture scenario is assumed not to occur until the concrete barriers in the disposal facility have lost their structural and physical integrity.

A detailed analysis of the degradation of concrete barriers has not been performed in the PA for CIIDF. Rather, the presence of concrete barriers is assumed to preclude the agriculture scenario for 300 years after disposal. Although the expected lifetime of the concrete barriers is not known, this assumption is intended to be somewhat pessimistic for the thicknesses of concrete to be used in the disposal facility. The concrete barriers could maintain their integrity and preclude intrusion by excavation for longer than 300 years, but a technical justification for a longer barrier lifetime cannot be provided. On the other hand, the assumed lifetime of the concrete barriers affects the estimated dose in

the agriculture scenario only for shorter-lived or relatively mobile radionuclides. For long-lived and immobile radionuclides, the dose essentially is independent of the lifetime of the concrete barriers, because the concentration in the disposal facility would change only very slowly over time periods much longer than can reasonably be assumed for the barrier lifetime.

For most radionuclides, the dose for the agriculture scenario decreases with time after the assumed failure of the engineered barriers at 300 years after disposal, due to radioactive decay or mobilization and transport from the disposal facility in infiltrating water, and the scenario is evaluated only at that time. However, the dose can increase with time for long-lived radionuclides, such as uranium, which are relatively immobile and decay to long-lived decay products which are radiologically more significant than the parent isotope, and the maximum dose may occur long after the concrete barriers are assumed to have failed, even when mobilization and transport from the disposal facility in infiltrating water is taken into account. For radionuclides with radiologically significant long-lived decay products which build up in the waste only over long periods of time, the agriculture scenario is evaluated at the time during the assumed 10,000-year time period for compliance with the performance objective for inadvertent intruders when the maximum dose from the parent isotope and its decay products would occur.

The resident scenario is based on an assumption that the disposal facility is not penetrable by normal excavation procedures used in digging a foundation for a home. Therefore, this scenario is assumed to occur immediately upon loss of active institutional control at 100 years after disposal. The resident scenario also could occur between 100 and 300 years, when the engineered barriers are assumed to have failed and the agriculture scenario would occur instead. However, for all of the radionuclides for which the resident scenario could be important compared with the agriculture scenario, the dose decreases with time after disposal. Therefore, the scenario is evaluated only at 100 years.

The post-drilling scenario cannot occur unless the disposal facility is penetrable by the types of equipment normally used in drilling a well. However, since drilling through hard rock is commonplace on ORR, normal drilling procedures should easily penetrate any intact concrete barriers in the disposal facility. Therefore, no credit is taken for the ability of engineered barriers to preclude the post-drilling scenario, and the scenario is assumed to occur at 100 years after disposal. The post-drilling scenario also could occur at any time after 100 years. However, as in the case of the resident scenario described above, the maximum dose would occur at 100 years for all radionuclides for which the post-drilling scenario is potentially important, and the scenario is evaluated only at this time.

Other intrusion scenarios

Three other scenarios for inadvertent intrusion—the construction, discovery, and drilling scenarios—were considered in the PA for CIIDF but were not evaluated. Each of these scenarios involves a single, short-term exposure for which the performance objective is an EDE of 500 mrem. These scenarios and the justifications for neglecting them from the PA are as follows.

The construction scenario considers doses that would be received while excavating a foundation for a home on the disposal site that extends into the waste itself. The construction scenario thus can be viewed as the initiator of the agriculture scenario, which considers chronic exposures after construction of the home is completed. The potential importance of the construction scenario arises primarily from an assumption that excavation activities would result in airborne concentrations of radionuclides substantially higher than those experienced during normal residence on top of exposed waste, which are considered in the agriculture scenario. Ingestion exposure also could be important during excavation activities. However, external exposure during excavation should be considerably less than external exposure while residing in the home after construction is completed, due to the much shorter exposure time involved.

Since the construction scenario would occur at the same time as the agriculture scenario, the dose analysis for each scenario would be based on the same concentrations of radionuclides. Previous calculations (Kennedy and Peloquin 1988) provide a direct comparison of doses for the two scenarios. For a few radionuclides, the dose per unit concentration could be slightly higher in the construction scenario, but for most radionuclides the dose per unit concentration is expected to be higher in the agriculture scenario. This result is based on a reasonable exposure time in the construction scenario and the use of reasonably consistent assumptions for the exposure pathways in the two scenarios. Therefore, since the performance objective for the construction scenario is five times higher than the performance objective for the agriculture scenario, the construction scenario should be relatively unimportant for all radionuclides and can be neglected in the PA for inadvertent intruders.

In the discovery scenario, an intruder attempts to excavate a foundation for a home at the location of the disposal facility, but is assumed to encounter an intact and impenetrable engineered barrier used in constructing the facility. Thus, the discovery scenario is based on the same assumption about the integrity of engineered barriers as the resident scenario described previously. However, the discovery scenario differs in that, shortly after encountering an intact engineered barrier, the intruder decides to abandon excavating at that location and moves elsewhere, thus resulting in a short-term, rather than a chronic, exposure. As in the case of the resident scenario, the only assumed exposure pathway for the discovery scenario is external exposure to photon-emitting radionuclides in the waste during the time the intruder excavates at the site. The presence of intact barriers would preclude any ingestion or inhalation exposures.

The discovery scenario would occur at the same time as the resident scenario. Furthermore, the assumed external exposure pathway is the same for the two scenarios, as is the thickness of the engineered barriers which provide shielding between the waste and the receptor location. Thus, the dose analyses for the discovery and resident scenarios would differ only in regard to (1) the assumed exposure time and (2) the shielding factor during indoor residence, which applies only in the resident scenario and reduces the external dose rate per unit concentration of radionuclides in the waste compared with the dose rate outdoors in the discovery scenario. The exposure time should be much less in the discovery scenario, but the shielding factor in the resident scenario should be no more than a factor of two (NRC 1977). Based on these considerations and also taking into account the higher performance objective for the discovery scenario, it is evident that the discovery scenario would be

relatively unimportant for all radionuclides and, thus, can be neglected in the PA for inadvertent intruders.

The drilling scenario considers doses that would be received while drilling through waste and constructing a well. The drilling scenario thus can be viewed as the initiator of the post-drilling scenario, which considers chronic exposures after well drilling is completed. The potential importance of the drilling scenario arises primarily from an assumption that the intruder would be located near an unshielded pile of drilling waste for a substantial period of time and, thus, would receive a significant external exposure. Ingestion and inhalation exposures during drilling activities also could be important.

Since the drilling scenario would occur at the same time as the post-drilling scenario, the dose analysis for each scenario would be based on the same concentrations of radionuclides. Previous calculations (Kennedy and Peloquin 1988) provide a direct comparison of doses for the two scenarios. For all radionuclides, the dose per unit concentration in the drilling scenario is expected to be at least an order of magnitude less than the dose in the post-drilling scenario. This result is based on a reasonable exposure time in the drilling scenario and the use of reasonably consistent assumptions for the exposure pathways in the two scenarios. Therefore, the drilling scenario should be relatively unimportant for all radionuclides and can be neglected in the PA for inadvertent intruders.

Summary of intrusion scenarios

As summarized in Table 3.4, three scenarios involving direct intrusion into solid waste in the disposal facility and chronic exposure of inadverent intruders are assumed in the PA for CIIDF. Three scenarios involving a single, short-term exposure of inadvertent intruders—the construction, discovery, and drilling scenarios—also were considered. However, these scenarios are not evaluated in the PA because (1) the dose per unit concentration of radionuclides in the construction, discovery, or drilling scenario should be comparable to or less than the values in the agriculture, resident, or post-drilling scenario, respectively, and (2) the performance objective for a single, short-term exposure is five times higher than the performance objective for chronic exposure.

3.1.2.3 Exposure Pathways Resulting from Biotic Recycling

Release of radionuclides due to biotic intrusion into the disposal facility and biotic transport of radionuclides from the disposal site to off-site locations in contaminated wildlife and vegetation were considered in Sects. 3.1.1.2 and 3.1.1.3, respectively. These release and transport mechanisms were judged to be unimportant on ORR compared with release and transport of radionuclides in water and, thus, are not considered in the PA for CIIDF.

An additional possibility that should be considered is biotic recycling of radionuclides in contaminated areas, which could result in enhanced exposures of off-site individuals or inadvertent intruders at the same locations. Biotic recycling of radionuclides has been observed on ORR; for

Table 3.4. Summary of exposure scenarios for inadvertent intrusion into solid waste in disposal facility[a]

Assumed scenarios	Status	Discussion
Agriculture[b]	Evaluated	Assumed to occur between 300 and 10,000 years after disposal as result of excavation into disposal facility and mixing of exhumed waste with garden soil. Assumed exposure pathways include ingestion of vegetables grown in contaminated garden soil, ingestion of contaminated garden soil, external and inhalation exposure while working in garden, and external and inhalation exposure while residing in home on top of exposed waste.
Resident[b]	Evaluated	Assumed to occur at 100 years after disposal as result of attempted excavation into disposal facility in presence of intact engineered barriers. Assumed exposure pathway is external exposure while residing in home on top of intact barriers.
Post-drilling[b]	Evaluated	Assumed to occur at 100 years after disposal as result of drilling through disposal facility and mixing of drilling waste with garden soil. Assumed exposure pathways include ingestion of vegetables grown in contaminated garden soil, ingestion of contaminated garden soil, and external and inhalation exposure while working in garden.
Construction, discovery, and drilling[c]	Considered but not evaluated	Scenarios can be neglected because doses for any radionuclide should be comparable to or less than doses in agriculture, resident, or post-drilling scenario, respectively, and performance objective for short-term exposure scenarios is higher than that for chronic exposure scenarios.

[a]Scenario for exposure of inadvertent intruders to contaminated groundwater obtained from on-site well also was considered but was not evaluated because doses should be negligible compared to allowable doses from direct intrusion into solid waste in disposal facility.

[b]Scenario involves chronic exposure of inadvertent intruders, for which performance objective is annual EDE of 100 mrem.

[c]Scenarios involve single, short-term exposure of inadvertent intruders, for which performance objective is EDE of 500 mrem.

example, see Garten, Gardner, and Dahlman (1980); Garten, Trabalka, and Bogle (1982); and Trabalka and Garten (1983).

A plausible scenario for biotic recycling on the disposal site or at off-site locations is the following. Plants, including vegetables consumed by individuals as well as trees, could absorb water from the surface or shallow subsurface environment which has been contaminated by radionuclides released from the disposal facility. Enhanced exposures then could occur as a result of consumption of vegetables which absorb radionuclides from the contaminated water or external exposure to contaminated leaves and other plant litter which are deposited on the ground surface. However, simple bounding analyses can be used to show that the vegetable and external exposure pathways resulting from root uptake of contaminated water from a particular source should not be important relative to direct consumption by humans of drinking water from a source at the same location.

For consumption of contaminated vegetables, consider a simple model which assumes that (1) all of the water in vegetables consumed by an individual comes from the contaminated source,

(2) the concentrations of radionuclides in vegetable water are the same as the concentrations in the source, and (3) the vegetables consist entirely of water. All of these assumptions are conservative for any radionuclide and, thus, would bound actual exposures from consumption of contaminated vegetables. If an individual then is assumed to consume 90 kg/year of contaminated vegetables (see Sect. G.5.2.1 of Appendix G) and, as described above, the vegetables are assumed to consist entirely of water with a density of 1000 kg/m^3, the volume of contaminated water consumed in the contaminated vegetables would be 90 L. However, the same individual is assumed to consume 730 L/year of drinking water (see Sect. G.5.1 of Appendix G) from the same location, an amount which is nearly an order of magnitude greater than the consumption in contaminated vegetables. Therefore, given the conservative assumptions in the model for intakes in vegetables, it is evident that uptake of radionuclides by vegetables from contaminated water should result in ingestion intakes which are only a small fraction of the ingestion intakes in drinking water itself.

For external exposure to contaminated leaves and other plant litter deposited on the ground surface, the conditions described above for contaminated vegetables, which again are conservative, are assumed. In addition, it is assumed that 2 kg/m^2 of vegetation, which is a typical areal density of vegetation consumed by humans (NRC 1977), is deposited on the ground surface annually. It then is easy to show that even if the concentrations of radionuclides in the contaminated litter deposited on the ground surface are depleted only by radioactive decay, the external dose from continuous exposure to the contaminated ground surface would be only a small fraction of the dose from ingestion of the contaminated water itself. It also should be noted that the assumption of continuous external exposure at the location of the deposited litter is itself quite conservative.

The discussions in this section on biotic recycling of radionuclides in contaminated water and the previous discussions on biotic intrusion into waste disposal facilities in Sect. 3.1.1.2 and environmental transport in biota in Sect. 3.1.1.3 illustrate a general conclusion about the importance of these processes in PAs for disposal of LLW. Under some circumstances, biointrusion, transport of biota in the environment, and biotic recycling can be important processes for transporting radionuclides in disposed waste or the environment to the ground surface, into vegetation and animals, and to other locations in the environment, and radiation exposures could result from these processes. However, if exposures of humans to radionuclides in the particular source media which are impacted by biointrusion, biotic transport, or biotic recycling (i.e., contaminated water, contaminated soil, or disposed waste itself) are presumed to occur, which usually is the case in PAs, exposures to radionuclides in the source media themselves should always be considerably greater than exposures that would result from biointrusion, biotic transport, or biotic recycling. In other words, biotic processes normally would be of concern for LLW disposal only if exposure to the source media for the biotic processes were presumed not to occur, which is usually not the case in PAs.

3.1.3 Scenarios Analyzed

This section summarizes the scenarios to be considered in detail in the PA of CIIDF. The scenarios to be considered in detail are derived from the consideration of satisfying the performance

objectives of DOE Order 5820.2A. For the purposes of satisfying the performance objective for protection of a member of the public of 25 mrem per year, the discussion in Sect. 3.1.2 provides the justification for considering the consumption of contaminated drinking water with a performance objective of 4 mrem per year as the bounding scenario to be considered in detail. Protection of drinking water resources to <4 mrem per year will ensure that members of the public will receive doses of <25 mrem per year from all pathways. The discussion presented in Sect. 3.1.1.2 demonstrates that any releases to the atmosphere will be in compliance with the requirements of 40 CFR 61 and do not warrant detailed analysis. For the purposes of satisfying the performance objective for the protection of an inadvertent intruder, three scenarios are considered in detail: the agriculture, resident, and post-drilling scenarios. All three of these scenarios are chronic-exposure scenarios. Postulated scenarios for acute exposure are certain to be less than the chronic-exposure scenarios selected for detailed analysis. The performance objective for protecting groundwater resources is addressed by the consideration of the environmental transport of contamination from CIIDF to groundwater. Compliance with this performance objective is demonstrated using a 4-mrem per year dose standard applied at the edge of a 100-m buffer zone surrounding the disposal facility. The point of maximum concentration over time is used to determine the limiting concentrations for radionuclides in waste that are acceptable for disposal in the CIIDF.

3.2 ASSUMPTIONS

The PA analyses made use of a variety of assumptions, particular to the models used. This section enumerates the assumptions made for the analysis of the waste form, the release of radionuclides from a degrading facility, and the transport of radionuclides through the environment.

3.2.1 Wastes

The waste disposed of in a tumulus-type facility is placed inside a metal box which, in turn, is placed inside a concrete disposal vault. The annular space between the inner wall of the vault and the outside of the metal box is filled with grout before placing the lid on the vault. To develop waste transport parameters, each disposal vault was assumed to contain a uniform composition of waste and concrete. The waste radionuclides were assumed to be uniformly distributed throughout each of the vaults on a disposal pad (i.e., each vault is assumed to have the same radionuclide composition). The density of the waste-concrete mixture was assumed to be 1.76 g/cm^3 with a porosity of 0.35. The concrete used in the construction of the vaults was assumed to have a density of 2.34 g/cm^3 with a porosity of 0.15. Radionuclide transport parameters (e.g., distribution and diffusion coefficients) were developed for the assumed composition of the waste and concrete and are described in Appendix B. The concrete used in filling the annular space in the vaults was assumed to contain no special additives for retarding specific radionuclides. Finally, the release of radionuclides is influenced by the amount of water saturation of the disposal facility (i.e., the waste and concrete containment). The relative saturation of the waste (i.e., volume of water/volume of waste) can range from zero up to the porosity

of the waste. In this assessment, the relative saturation of waste is taken to be equal to the porosity of the waste (0.35). In other words, the pores in the waste are full of water or saturated. The assumption that a disposal facility is saturated represents conservatism in that it gives the largest release by advection and diffusion with all other parameters being fixed.

3.2.2 Source Term Assumptions

This section describes the assumptions used in calculation source terms for the CIIDF PA. Section 3.2.2.1 describes assumptions related to radionuclide release; Sect. 3.2.2.2 presents assumptions about CIIDF degradation and performance.

3.2.2.1 Radionuclide Release

The total radionuclide release from the disposal vaults is assumed to be the sum of the advective and diffusive releases. This total release is limited by the solubility limit for the assumed chemical form of the waste radionuclide. Complex forms of waste and barriers are approximated as simpler forms (e.g., slabs). As a result, both the advection and diffusion models are one-dimensional.

Advective transport of radionuclides is modeled as a first-order leaching process that accounts for both sorption and decay. A linear isotherm model [e.g., distribution coefficient (K_d)] is used to mimic sorption processes in the waste.

Diffusive transport of radionuclides is modeled as diffusion through a two-layered system. The inner layer (i.e., the waste) is initially uniformly contaminated. The outer layer (i.e., the vault wall) is initially uncontaminated. Diffusion calculations also account for radionuclide decay and sorption. Retarded diffusion coefficients incorporate the sorption behavior of the radionuclide.

Distribution and diffusion coefficients are estimated based on appropriate literature values and using the methodology outlined by Godbee (1996) and in Appendix B. This method adjusts the literature values to system-specific values for CIIDF. Additionally, in the absence of data for a given radionuclide, Godbee (1996) provides a methodology for transport parameter estimation.

The water flow rate through the disposal vaults is assumed to be the minimum of the input seepage rate and either the saturated hydraulic conductivity of concrete (for intact vaults) or the saturated hydraulic conductivity of the soil backfill (for cracked vaults). Water seepage values are provided for each month of the year to reflect seasonal variations. Additionally, the water seepage values are updated as required to reflect environmental changes (e.g., growth of vegetation on top of the disposal facility and degradation of the cap on the disposal facility).

The release of radionuclides is calculated in monthly time steps. Based on knowledge of the site hydrology, the total release is partitioned into two components: a vertical component available for recharge to groundwater and a lateral component available for shallow subsurface transport. The total release is partitioned first to the vertical component because drainage from the disposal facility is assumed to move vertically at a low recharge rate throughout a simulation. Any excess water (i.e., the seepage rate in the disposal facility is greater that the recharge rate under the pad) will move laterally

away from the facility. The fraction of the radionuclide release partitioned to the vertical component is determined by the ratio of the saturated hydraulic conductivity for the soil under the disposal pad to the water seepage rate in the disposal facility. The saturated hydraulic conductivity under the pad is assumed to be 5.8×10^{-7} cm/s (see Appendix D, Table D.2, soil layer = 400 to 500 cm). The remainder of the radionuclide release, if any, is partitioned to the lateral component.

3.2.2.2 Facility Degradation and Performance

The degradation of concrete is assumed to be caused by sulfate attack of the concrete, calcium hydroxide leaching from the concrete, and corrosion of reinforcing steel. Metal barriers (e.g., metal waste containers) are assumed to degrade linearly as a function of time.

The effect of concrete cracking on the leaching of radionuclides is delayed until structural degradation (i.e., the formation of through-wall cracks) of the disposal vault occurs. Hydraulic failure (i.e., through-wall cracking) of one component (e.g., roof, wall, or floor) in a vault results in a step change in the hydraulic conductivity of the vault. The resulting increased flow rate of water through the vault leads to advection becoming the dominant transport mechanism.

Metal barriers are assumed to attenuate the radionuclide release from the disposal vaults. As these barriers degrade (linearly), the allowed radionuclide release is increased proportionately.

The degradation of the concrete pad and leachate collection system is represented by a linear failure model. The functionality of the pad and collection system determines how much of the calculated release from the disposal vaults is available for transport in the environment. The pad and collection system are assumed to be initially 80% functional, degrading linearly to 0% functional at the end of the institutional control period (100 years). The degradation of the pad is also calculated using the sulfate attack and calcium hydroxide leaching concrete degradation models. Pad failure is estimated based on the reinforcement ratio, which is primarily a function of the concrete cover thickness on the steel reinforcement and the concrete strength. The sulfate attack model updates the cover thickness while the concrete strength is updated with the calcium hydroxide leaching model. If failure of the pad (as determined by comparison of the calculated reinforcement ratio with the limiting reinforcement ratio) occurs before the end of the institutional control period, the functionality of the pad and collection system is set to zero.

3.2.3 Site Assumptions

Modeling the behavior of natural systems requires the use of simplifying assumptions. The following sections discuss in detail the assumptions made for the PA analyses, including hydrologic and hydrogeologic analysis, and credit taken for engineered features.

3.2.3.1 Runoff/Recharge Factors

Terrain modification undertaken during site preparation was incorportated into a contour map and used in terrain analysis (Appendix D.1) of site hydrology. The general topography present during loading of the pads was assumed to be preserved in the CIIDF assessment.

The monthly water flow contacting vaults on a tumulus pad was determined from hourly water budget simulations obtained for the average environmental conditions in the area. The nuclides released from concrete vaults were dissolved in the monthly water volumes and the solution was partitioned into vertical and lateral subsurface flow. Groundwater was preferentially recharged each month up to a maximum rate with the nuclide leachate, and monthly values were summed to give annual recharge values used in the groundwater modeling. The remainder of monthly leachate fluxes, if any, were summed to an annual total and used in lateral subsurface transport calculations.

In subsurface transport, chemicals passed through the soils of the stormflow and vadose zones, and chemical adsorption was calculated during transport. The soil volume associated with the recharge pathway to groundwater was determined from the pad area multiplied by the average depth to the water table (8.1 m) obtained from groundwater simulations (Appendix E). In the case of lateral flow, the average path length from the pads to the nearest surface drainage channel (50.0 m) was determined from a contour map. This value was multiplied by one quarter of the pad area to give the soil volume interacting with chemicals moving laterally in shallow subsurface flow. This is an arbitrary estimate of the relevant soil volume for chemical adsorption during lateral subsurface flow.

The calculations of lateral subsurface transport through the storm-flow zone did not specifically account for the effects of matrix diffusion. This effect can cause a difference between the time of first arrival of chemical during a transport event and the time of peak concentration in the flow paths (Solomon et al. 1992). Matrix diffusion acts as a buffer that "smears out" the transport of chemicals by diffusive uptake of solutes from flow paths into the microporosity of the matrix. These solutes are later released as a secondary source from the matrix after decline in the chemical concentration from the primary source (e.g., leaking vaults). Annual time steps were adopted for chemical transport in the storm-flow zone, and a quasi-matrix diffusion effect was provided by mixing (numerical dispersion) the new input of chemical in a given year with the soil solution that was retained by capillary forces in the flow path (field capacity) in the previous time step.

There was allowance for bypass (macropore or preferential) flow in calculation of chemical transport to surface water through the lateral storm-flow zone but not for the vertical recharge path. This resulted in proportions of the leachate bypassing the soil matrix during lateral subsurface transport. These calculations depended on the length of the lateral transport path and the K_d of the nuclide (Appendix D.3). Nuclides with higher adsorption had less bypass flow. These bypass proportions provide conservative approximations for an important transport mechanism applicable to the CIIDF site. Preferential flow below 3 m depth in the soil profile was not shown in the field study of Wilson et al. (1993). This result combined with the rapid decline in hydraulic conductivity with depth (Sect. 2.1.5) was the rationale for not including preferential flow through the vadose zone to the water table. These approximations provide simulation results that were consistent with field observations and

avoided the need for the application of a three-dimensional finite-element transport model, which was viewed as unjustified given the uncertainties in parameter values used in waste containment degradation and environmental transport.

3.2.3.2 Areal Recharge Estimates for Groundwater Modeling

Recharge to groundwater has been estimated from water budget and modeling methods, providing values in the range of 10 to 70 mm/year (Tucci 1986, Bailey and Lee 1991, Solomon et al. 1992). These estimates were used as a guide for comparison with simulations obtained with the Unified Transport Model (UTM) hydrologic model. Terrain analysis was used to identify areas with enhanced recharge along ephemeral stream channels and wetland areas.

3.2.3.3 Assumptions in Surface Water Analyses

The most significant assumptions made in calculating the concentrations in surface water concern the characterization of flow in Bear Creek. Since the PA analyses were performed on an annual time step, an annual average flow was used, based on measured daily maximum values.

3.2.3.4 Hydrogeology Assumptions

For purposes of PA groundwater modeling, the following assumptions were made concerning properties of the saturated zone:

- Porous medium—The groundwater flow and transport model constructed for this analysis assumes that movement of contaminants through the subsurface under CIIDF can be adequately modeled by solving the advection-dispersion equation (see Appendix E) in a porous medium. Properties of this medium and the transported constituents follow.
- Saturated thickness—The thickness of the saturated zone was variable, extending from the water table down to an elevation of 700 ft above mean sea level.
- Bulk density—The bulk density of all geologic materials was set at 1.35 g/mL, consistent with the shallow subsurface modeling.
- Porosity—A value of 0.05 (5%) effective porosity was used. This value is based on aquifer tests performed at the Engineered Test Facility, located in a similar geologic setting in Melton Valley (Davis et al. 1984).
- Hydraulic conductivity—The spatially varying saturated hydraulic conductivity (K) field was derived from a geostatistical analysis of the logarithm of point hydraulic conductivity data derived from hydraulic tests performed at wells in the modeling area. The hydraulic conductivity tensor was assigned a constant anisotropy of K_x:K_y:K_z::3:1:1, based on results at the Engineered Test Facility site (Davis et al. 1984). The hydraulic conductivity of the lowermost layer (Layer 3) was reduced by one order of magnitude in order to simulate the tighter materials found at depth.

- Dispersivity—The following constant values of dispersivity were used: $\alpha_L = 0.15$ m (0.5 ft), $\alpha_T = 0.08$ m (0.25 ft), and $\alpha_V = 0.08$ m. These values are consistent with those reported by Lee et al. (1989).

One of the primary goals of the contaminant transport analysis was to determine the maximum groundwater concentrations for each nuclide at any point greater than 100 m from the disposal facility, in accordance with the guidance presented in Sect. 1. For modeling purposes, this determination was made by recording concentrations at grid cells located approximately 100 m from the edge of the finished CIIDF closure cap (see Sect. 2.3) for all vertical layers of the model. This "ring" of monitoring points will capture the highest groundwater concentrations, under the assumption that concentrations will decrease with distance from the source. Fig. 3.2 shows the location of these model cells. More detailed information concerning the implementation of the groundwater model can be found in Sect. 3.3.4.2 and Appendix E.

3.2.3.5 Retardation in the Subsurface

Values for chemical adsorption (K_d) of radionuclides to the subsoil materials at the CIIDF site are presented in Table 3.5. The nuclides fall into three broad groups of K_d values:

Low	0–30 range	H, C, Cl, K, Ca, Se, Rb, Sr, Tc, I
Medium	40–300	Zr, Nb, Cd, Sn, Eu, Pb, U, Np, Pu, Am, Cm, Cf
High	400–3000	Be, Al, Co, Ni, Pd, Cs, Sm, Bi, Ra, Th, Pa

The K_d value of zero for H, C, Cl, Se, Tc, and I was selected because the soluble anion forms of these nuclides were not expected to adsorb onto soil. The K_d for cadmium was obtained from Turner and Steele (1988), and the value for nickel is from the investigation of Swanson (1983). The K_ds for the remainder of the nuclides are based on the recommendations from several sources, including Friedman and Kelmers (1990). In all cases the K_d values were obtained with equilibrium methods using soil material from the waste site or soil values that were available.

These K_d values were used in transport calculations through the shallow subsurface zone to surface water and in the transport of nuclides into the groundwater through the vadose zone. The K_d values were applied to a soil volume estimated to occur between the pads and the nearest surface drainage channel or water table as appropriate for lateral flow and recharge calculations. Jardine, Jacobs, and Wilson (1993) have shown that K_ds obtained by equilibrium methods are suitable for representing adsorption during unsaturated flow, even if the flow is close to saturation. The specific K_d values for soil were estimated or obtained from the following sources: Baes and Sharp (1981); Davis et al. (1984); Friedman and Kelmers (1990); Ketelle et al. (1995); Johnson and Gillham (1980); Rothschild et al. (1984); Sheppard et al. (1984); Sheppard and Thibault (1990); Solomon et al. (1992); Swanson (1983); and Turner and Steele (1988).

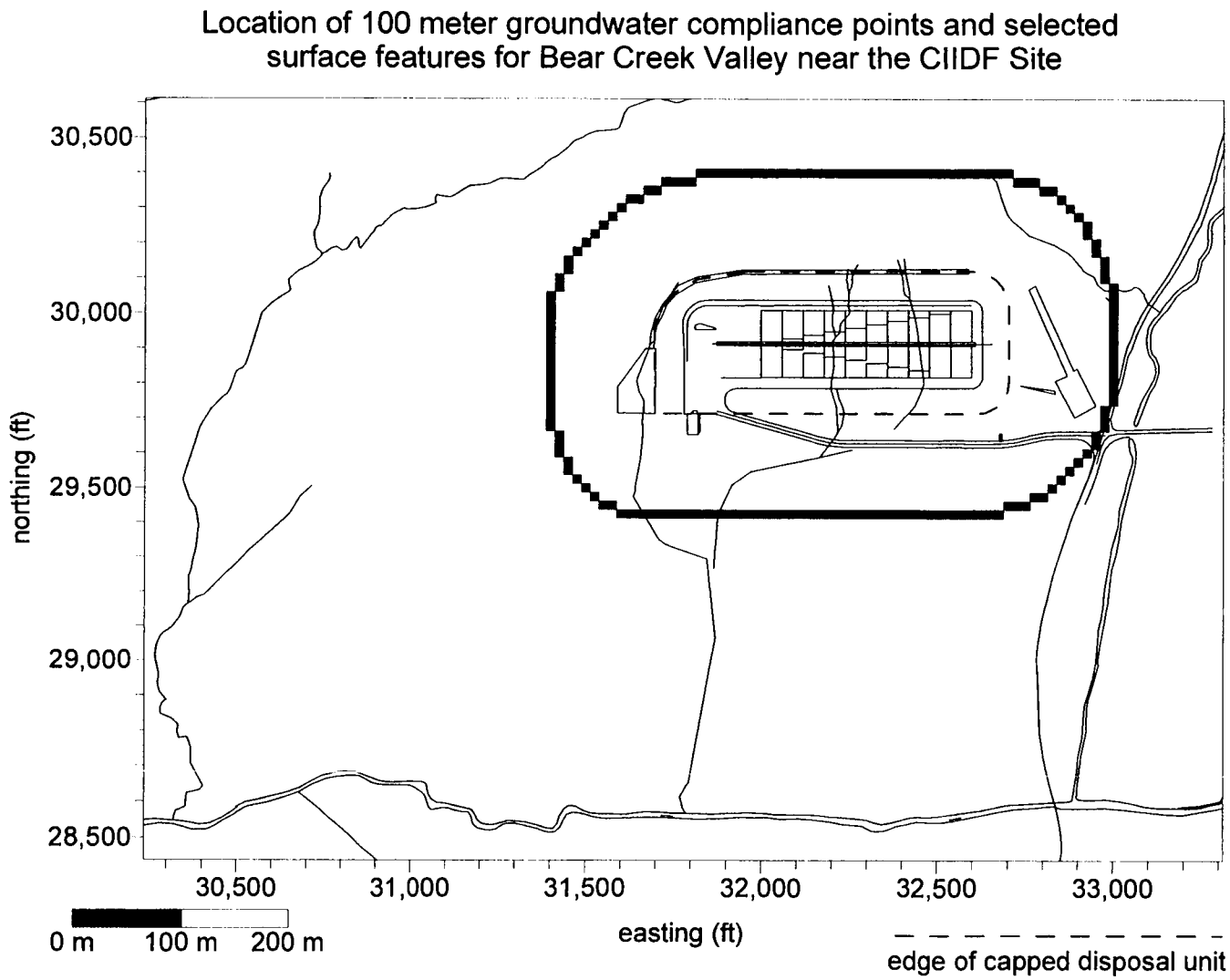

Fig. 3.2. Grid cells representing the CIIDF 100-m compliance boundary.

Table 3.5. Radionuclide-specific soil/water partition coefficients used for environmental transport analyses

Nuclide	Soil/water K_d[a] (mL/g)	Nuclide	Soil/water K_d[a] (mL/g)
^{3}H	0	^{226}Ra	3000
^{10}Be	1000	^{229}Th	3000
^{14}C	0	^{230}Th	3000
^{26}Al	3000	^{232}Th	3000
^{36}Cl	0	^{231}Pa	400
^{40}K	30	^{232}U	40
^{41}Ca	30	^{233}U	40
^{60}Co	800	^{234}U	40
^{59}Ni	2000	^{235}U	40
^{63}Ni	2000	^{236}U	40
^{79}Se	0	^{238}U	40
^{87}Rb	30	^{237}Np	40
^{90}Sr	30	^{238}Pu	40
^{93}Zr	50	^{239}Pu	40
^{93m}Nb	100	^{240}Pu	40
^{94}Nb	100	^{241}Pu	40
^{99}Tc	0	^{242}Pu	40
^{107}Pd	2000	^{244}Pu	40
^{113m}Cd	200	^{241}Am	40
^{121m}Sn	100	^{242m}Am	40
^{126}Sn	100	^{243}Am	40
^{129}I	0	^{243}Cm	40
^{135}Cs	3000	^{244}Cm	40
^{137}Cs	3000	^{245}Cm	40
^{151}Sm	1000	^{246}Cm	40
^{152}Eu	40	^{247}Cm	40
^{154}Eu	40	^{248}Cm	40
^{155}Eu	40	^{249}Cf	40
^{207}Bi	500	^{250}Cf	40
^{210}Pb	100	^{251}Cf	40

[a] *Sources:* see Sect. 3.2.3.5.

Retardation R is a function of K_d and the soil bulk density ρ_b and total porosity n, defined as

$$R = 1 + \frac{\rho_b K_d}{n} \quad . \tag{3.1}$$

Retardation factors have a major influence on all components of the transport analysis. For the groundwater component, larger values of K_d effectively slowed the advective transport so that diffusion became an important factor for very large values for time.

3.2.3.6 Credit for Engineered Features

In addition to the engineered barriers discussed in Sect. 3.2.2.2, several geotechnical designs were incorporated to enhance the performance of the CIIDF site, including excavated drainage trenches (see Fig. 2.2 and Sects. 2.1.2 and 2.3) and an assumed closure cap. The drainages alter the local water table elevation and groundwater flow field and serve both to reduce the risk of inundation of the pads by groundwater and to provide an interception of groundwater-borne contaminants before reaching the 100-m compliance boundary.

The attributes of the engineered cover for the site following closure are based on the capping plan developed and implemented for Tumulus I and II at SWSA 6 (Map No. C3E020016A046). The same cap specifications are expected for the CIIDF site with the following layers:

45 cm (minimum) top soil with grass vegetation
composite drainage net
flexible membrane liner
60 cm (minimum) compacted subsoil
geomembrane
15 cm (minimum) variable fill layer
composite drainage net

These layers will be placed over each tumulus pad loaded with vaults. The soil hydraulic properties selected to represent the cap (Appendix D.2, Table D.1) did not have the identical features of the tumulus cap; however, these properties significantly restricted seepage to the vaults. The hydrologic effect of the stacked concrete vaults was ignored in all water budget simulations. The cap was assigned an effective life of 10 years (years 2022–2031, based on initiation of CIIDF operations in 2000) with a low drainage rate. During the following 10 years (2032–2041), percolation through the cap was linearly ramped up to values simulated for a leaking cap with macropores. The integrity of the geomembrane was expected to diminish during this period, and root penetration into the compacted soil layer was also expected to occur. These changes would lead to shrinkage and swelling of clay materials and the gradual formation of cracks and channels that allow drainage to bypass through the compacted clay/soil matrix (Bass, Lyman, and Trantnyek 1985; Goldman et al. 1988). For the remaining 80 years (2042–2121) of the 100-year maintenance period, the burial site was simulated with a mown grass cover and a leaking cap. The 100-year period of institutional control ends in 2121.

Any additional seepage resulting from cap failure is collected and treated during the institutional control period (see Section 3.2.2.2).

The site is considered to revert to forest vegetation through species succession after the grass cover is no longer actively maintained. Natural succession proceeds by invasion of early succession tree species such as eastern red cedar, shortleaf pine, and sweet gum; and these are followed by oak-hickory forest species at a later stage (Suter, Luxmoore, and Smith 1993). The successional process takes about 30 years. The hydrologic consequence of these temporal changes in vegetation was not considered significant, and one set of soil hydraulic properties (Appendix D.2, Table D.2) was used for water budget simulations during the period following termination of institutional control.

3.3 CONCEPTUAL MODELS

This section describes the conceptual models used in the PA and the approach used to model CIIDF. The models are developed using the scenarios described in Sect. 3.1, and the assumptions concerning the facility discussed in Sect. 3.2. Following conceptual model development is the development of analytical models to quantitatively determine the limiting concentrations and allowable concentrations in wastes suitable for disposal in CIIDF. The data used in model development are discussed and any interpretations of these data are presented.

Four models are used for representation of nuclide transport at the CIIDF site. Each model is outlined below. Results from these models (UTM, SOURCE1, PADSIM, FTWORK) are linked in the simulation of various components of chemical transport at the site (Fig. 3.3). The UTM is used to determine the water budget of the CIIDF site. This hydrologic modeling is supplemented with terrain analysis for estimation of spatial variation in recharge to groundwater. The SOURCE1 simulator describes diffusive and advective fluxes of nuclides from concrete vaults. Seepage of soil water into cracks that develop in the vaults is used in advective calculations. Output from SOURCE1 gives the vertical and lateral component fluxes of nuclides into the vadose zone. PADSIM takes these results and estimates the recharge flux of nuclides to the groundwater model, FTWORK, and the flux of nuclides to surface waters through shallow subsurface transport. FTWORK determines nuclide concentrations at compliance points in the landscape and the flux of nuclides to surface water. The shallow subsurface and groundwater sources of surface discharge are added for dose assessment calculations.

3.3.1 Waste Characteristics

This PA will be used to generate disposal limits for a master list of radionuclides that reasonably could be present in waste from ORR. (see Table 3.1.) Two primary assumptions were used in developing the master list of radionuclides to be analyzed. First, the half-life of each radionuclide must be about 5 years or greater. The rationale for this assumption is that, given the expected

Linkage of Contaminant Transport Models for Performance Assessment of CIIDF

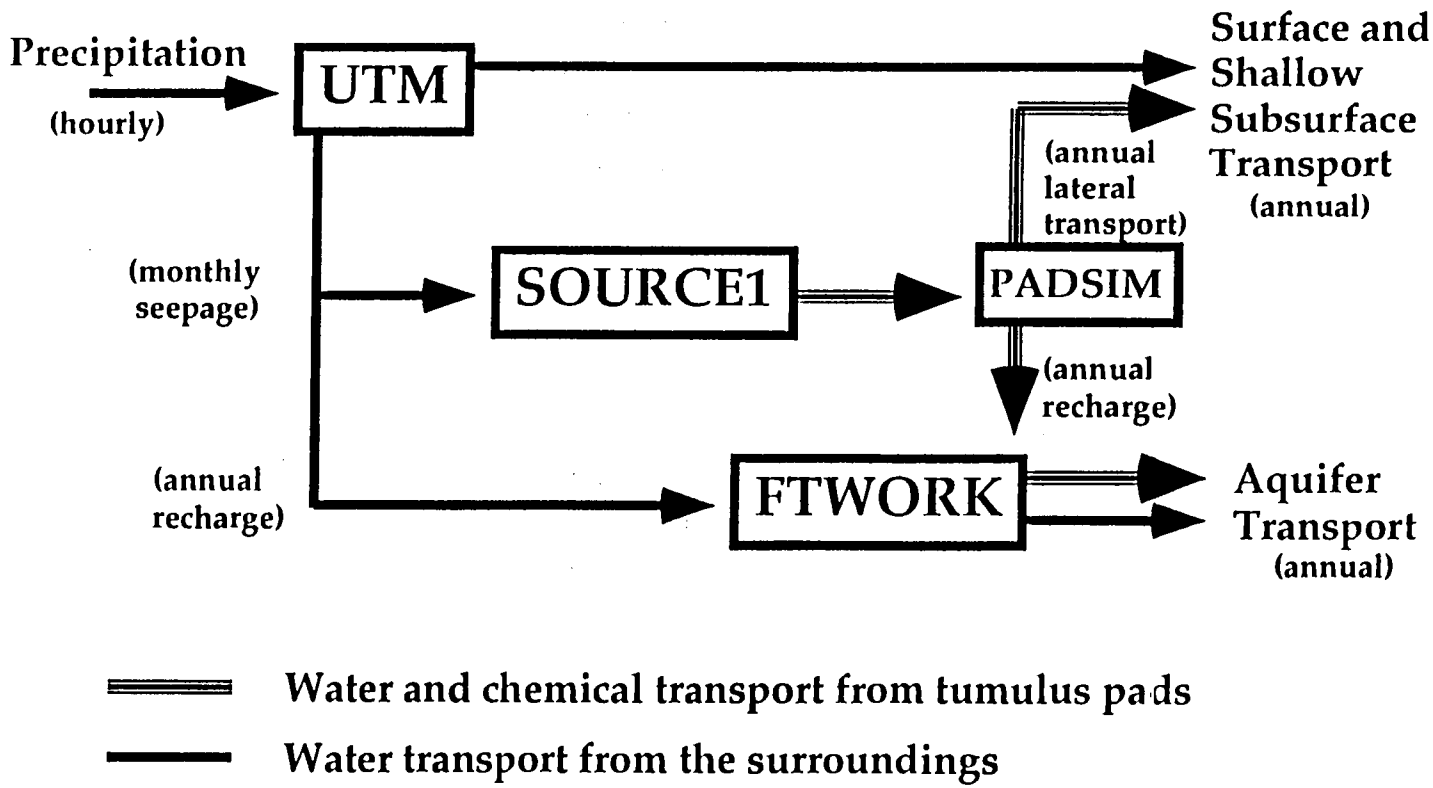

Fig. 3.3. Linkage of simulation results from four simulation models for quantifying nuclide transport in the environment and surroundings of the CIIDF.

performance of engineered barriers in the disposal facility and the expected use of active institutional controls for 100 years after closure of the facility, radionuclides with shorter half-lives should decay to innocuous levels before significant transport into the environment or access by inadvertent intruders could occur. Second, the radionuclide must be produced to a significant extent in fission reactors or by neutron activation of materials that reasonably could be present in or near reactors, because fission and activation are likely to be the most important sources of radionuclides in waste in the foreseeable future. However, a few additional radionuclides have been included based on past disposals in Oak Ridge.

Given the eclectic nature of waste generation in Oak Ridge in the past and the unpredictability of future generations, other radionuclides not included in Table 3.1 may come to the fore. The methodology developed for evaluating disposal limits for this PA can be applied to any radionuclide. Hence, future revisions to this document can incorporate other radionuclides as they are identified.

The inventory limits evaluated for this PA are based on the assumption that the radionuclides are homogeneously mixed throughout the waste. These analyses result in a total radionuclide inventory (or waste concentration) limit for a disposal pad. Localized "hot spots" are not analyzed because the source term for environmental transport provides the total release rate from the entire waste disposal pad, not just a portion of it. Therefore, the homogeneous distribution of the radionuclides for the analyses provides an appropriate representation of the total radionuclide release rate from a disposal pad. Similarly, for the direct intrusion analyses, homogeneous (or average) radionuclide concentrations are used because the intruder is assumed to access the facility at random locations.

3.3.2 Site Hydrology

The hydrology of the CIIDF site was characterized with terrain analysis and water budget modeling. Terrain analysis was conducted independently of the linkage of models (Fig. 3.3) and was used to determine spatial variation in recharge to the water table. These recharge values were used in calibration of the groundwater simulation results to water table observations for the area. Results from water budget modeling were used in environmental transport calculations of nuclide migration from concrete vaults.

3.3.2.1 Terrain Analysis

Surface and subsurface movement of water can be inferred from the dominant influence of topography on gravitational and convergent flow processes. The significance of topography for modeling surface hydrology has been described by Dawes and Short (1994). Soil wetness of any location is affected by the degree of convergence of flow, with convergent places (valleys) being wetter than divergent places (ridges). Terrain analysis methods have been verified in previous investigations of Walker Branch watershed and Center 7 Creek in Melton Valley on ORR (Timmins, Huston, and Clapp 1989).

The steps involved in terrain analysis are (1) preparation of a suitable contour map for the proposed waste site and surroundings, (2) conversion of this vector map into a fine digital grid of elevation cells each representing the local topography [a digital elevation model (DEM) (Schwartz et al. 1995)], and (3) determination of the spatial distribution of a topographic index which represents surface water flow convergence over the landform using slope and topography (Appendix D.1).

Site contours were modified to account for landscape grading planned for construction of tumulus pads (Fig. 2.2). Drainage from the pads is expected to flow to the north, west, and south, with very little to the east. A narrow, concrete-lined surface drain is modelled along the eastern and southern boundaries of the site preventing runoff to the east and south. A roadway along the southern side diverts drainage to a pond immediately southwest of the pads. The road is artificially breached to model the under-road culvert which connects the drainway and the pond. Modifications of the contour map were made to conform to the CIIDF site plan.

A DEM with 0.1-ft vertical resolution and 10-ft horizontal resolution was derived. The nominal 0.1-ft vertical resolution is needed for slope calculations. Spurious features (dams in streams and ponds in the landscape) were removed from the raw DEM as appropriate, and the terrain model was smoothed through adjustment of about 3.3% of the digital elevations (Fig. 3.4).

Hydrologic analysis of the DEM produced a map and frequency distribution of the Beven and Kirkby (1979) topographic index, $\ln(a/\tan\beta)$, where a is the upslope area above a unit length of contour with average slope angle β (Fig. 3.5). The histogram for the CIIDF site shows a characteristic log normal distribution indicating large areas with low soil wetness (uplands, ridges) and relatively few areas of wetlands. The results of the analysis show that the DEM was created with sufficient information to capture the flow pathways present in the terrain map (Fig. 3.4). This analysis was used to derive spatially varying estimates of recharge for use in groundwater modeling. Areas with greater wetness were given higher recharge values.

3.3.2.2 Water Budget Modeling

The UTM (Appendix D.2) was used to determine monthly water budget values for the CIIDF site. The flow diagram for the model shows the input of precipitation passing through a series of hydrologic processes generating outflow and vapor loss (Fig. 3.6). The basic concepts of the UTM involve four equations and four unknowns that are solved at each time step (Fig. 3.7). The Penman-Monteith equation is used for calculation of water vapor loss from the vegetated surface ("big-leaf" approach). The vapor flux is a function of surface resistance. A relationship between surface resistance and surface water potential is provided as input for the vegetation of interest. The flux of water from the soil to the evaporating surface is a function of the water potential of the vegetated surface. This flux is calculated with Darcy flow (conductivity-water potential gradient) equations for the soil and plant components. The fourth equation is the assumption that the flux of vapor from the evaporating surface is equal to the flux of liquid water to the surface (steady-state assumption). The four unknowns—vapor flux, surface resistance, surface water potential, and liquid flux—are determined for

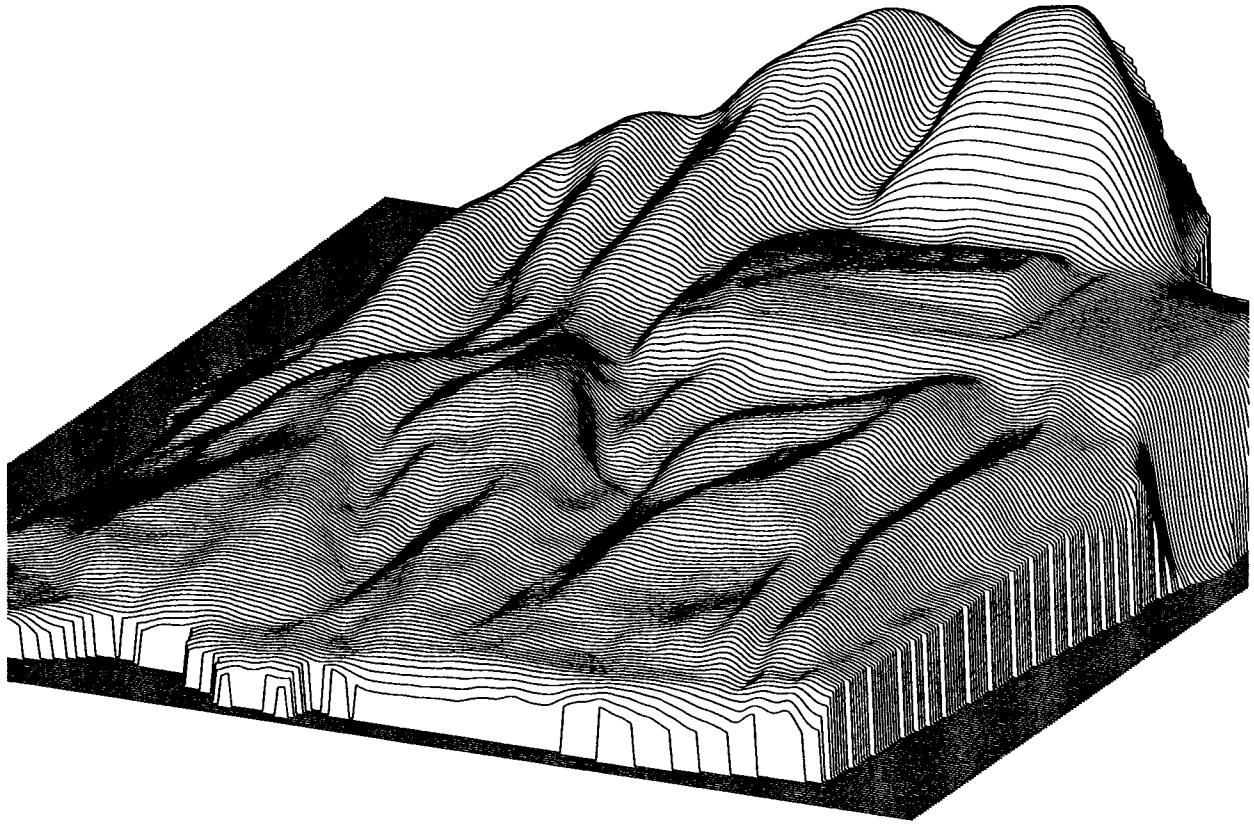

Fig. 3.4. The landscape surface generated from the digital elevation model of the CIIDF site as modified for facility construction. Vertical exaggeration is 10:1.

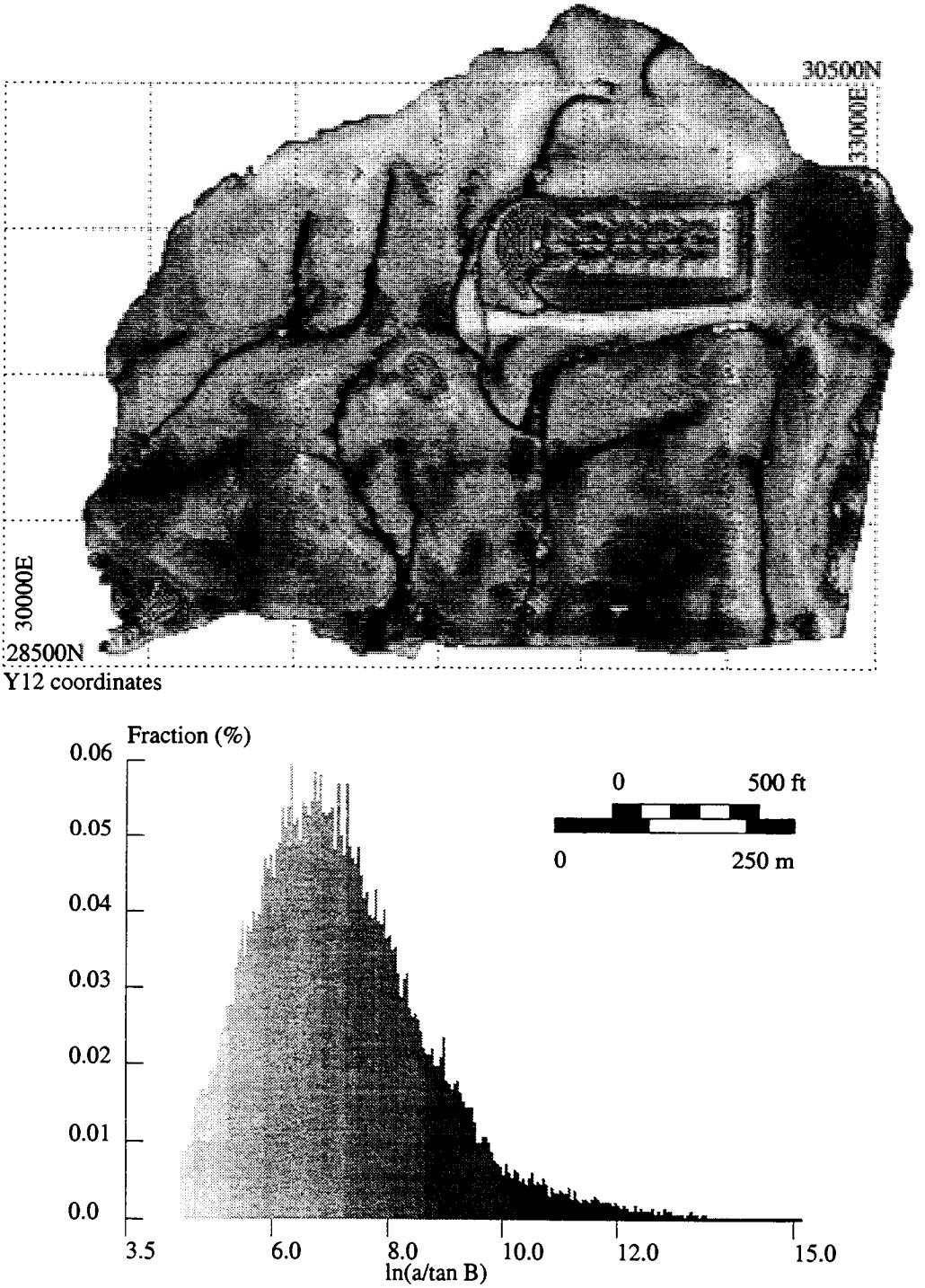

Fig. 3.5. Map and frequency distribution of topographic index for the CIIDF site used for estimation of spatial variation in groundwater recharge.

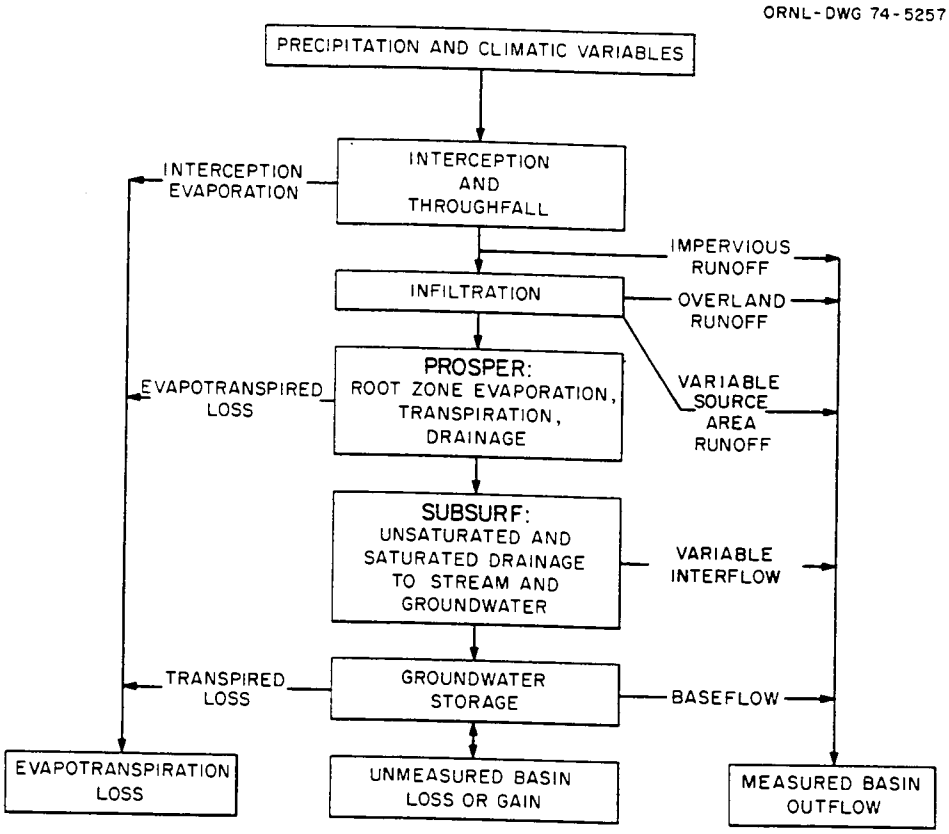

Fig. 3.6. Flow chart of the major components of hydrologic simulation with the Unified Transport Model. The PROSPER component estimated the seepage used by the SOURCE1 model.

Location	Properties	Structural Equations
Atmosphere	Environmental conditions Solar radiation Precipitation Dew point temperature Max. and min. Air temperature Average wind speed	Vapor flux from surface $F_v = f(R_x)$ Calculation uses combined energy balance-aerodynamic method
Boundary Layer	Resistance to vapor and heat flow	
Evaporating Surface	Resistance to vapor flow (R_x) Surface water potential (ψ)	Surface characteristic $R_x = f(\psi)$
Plant and Soil System	Plant and root resistances Root distribution in upper two soil layers Soil water characteristic for each soil layer Hydraulic conductivity vs water content for each soil layer Soil layer thicknesses	Liquid flux to surface $F_w = f(\psi)$ Calculation uses electrical network equations
Whole System	Steady state	Vapor flux = Liquid flux $F_v = F_w$

Fig. 3.7. The properties and structural equations of the PROSPER component of the Unified Transport Model used for calculation of evapotranspiration and soil water drainage.

a given set of hourly weather conditions. After completion of these calculations, drainage through the soil profile layers is calculated with one-dimensional Darcy flow calculations.

Precipitation occurs throughout the year, and soil water drainage is typically pulsing through the landscape in nonlinear unsaturated flow events. Monthly totals of drainage and evapotranspiration fluxes determined from hourly calculations provide more realistic water budget results due to self-correction in water budget modeling with longer periods of temporal integration (Luxmoore 1983b). The UTM simulations provided surface runoff, drainage, and lateral flow of water in response to hourly inputs of precipitation. The model accounted for the nonlinear flow dynamics using variable time steps (0.5–60 min.) as needed. These flow values were summed to give monthly totals that were used in the simulation of chemical leaching from vaults with the SOURCE1 model and in the groundwater transport simulations with FTWORK (Fig. 3.3).

The PA calculations were carried out for a minimum of 1000 years for each nuclide. Each simulation was divided into three main periods to reflect differing conditions at the CIIDF site. These time periods consisted of the active use of the site for loading of vaults onto pads, a monitored closure period of 100 years, and a postmonitoring period that extended for 1000 years or until a maximum annual radionuclide flux was obtained in both the vertical and lateral flow calculations. Water budget calculations were not conducted for the first 22 years (20 years of pad loading and 2 years of cap construction). The vaults were considered to be exposed to precipitation, and the monthly rainfall was used as seepage values for SOURCE1 calculations. The vegetation for the monitored period was mown grass with a leaf area index of 4.9 and high infiltration rates for the top soil. The same leaf area index and infiltration properties were used for the following postmonitoring period even though the vegetation is projected to change from grass to deciduous forest by natural succession.

3.3.3 Source Term

The source term for environmental transport is the release rate of the radionuclide as a function of time, while the source term for direct intrusion is the remaining radionuclide inventory at a specific time. These two source terms cannot both be conservatively evaluated by a single calculational method. Consider a conservative source term calculation for environmental transport. In this sense, conservative means that the calculated source term is believed to be a reasonable upper-bound release rate. Hence, a conservative calculated-release rate will result in a rapid depletion of the radionuclide inventory. However, from the standpoint of direct intrusion, the remaining inventory at a specific time could not be considered conservative. For direct intrusion, conservative means that the remaining inventory is believed to be a reasonable upper-bound estimate. Therefore, to evaluate conservative source terms for environmental transport and direct intrusion, two calculational approaches are used. The SOURCE1 computer code (Icenhour and Tharp 1996) is used in both of these approaches. An overview of SOURCE1 is presented in Sect. 3.3.3.1. The calculational approaches for environmental transport source terms and for direct-intrusion source terms are described in Sects. 3.3.3.2 and 3.3.3.3, respectively.

3.3.3.1 SOURCE1 Computer Code

Source terms for environmental transport and direct intrusion were calculated using Version 2.0 of the SOURCE1 computer code (Icenhour and Tharp 1996). This code (1) simulates the degradation and failure of engineered barriers (e.g., concrete and metal) used in tumulus-type disposal facilities and (2) calculates releases of radionuclides as a result of advection and diffusion. The following two sections provide an overview of the conceptual model summary and a brief description of major revisions that were incorporated into Version 2.0 of SOURCE1. Appendix A presents a description of the SOURCE1 conceptual model. A detailed description of SOURCE1, including algorithms, input requirements, and output options, can be found in the user's manual (Icenhour and Tharp 1996).

Conceptual model summary

The routines of the SOURCE1 code have four primary functions: structural analysis, simulation of concrete- and metal-barrier degradation, cracking analysis, and nuclide-leaching calculations. The structural analysis routine establishes initial bending moments and shear forces. The concrete- and metal-barrier degradation routines simulate the deterioration of engineered barriers with time. The cracking analyses routines calculate moments and shears required for concrete cracking and compare these values with the moments and shears evaluated in the structural analysis. Moments and shears required for cracking vary as the engineered facility degrades. The leaching routines calculate the release rate of nuclides to the environment. A detailed illustration of the logic flow used in the SOURCE1 computer code to model the aforementioned processes is provided in Fig. 3.8. The structural analysis is performed once at the beginning of a simulation. The concrete- and metal-barrier degradation and cracking analyses are performed using annual time steps. Nuclide release rates are calculated using monthly time steps.

Before the annual simulation begins, structural analyses of the disposal facility are conducted to establish the moments and forces placed on the various structural components. For the roof, walls, and floor, the SOURCE1 code calculates the uniform load, bending moments resulting from uniform loading, and shear and compressive forces. The walls are subjected also to hydrostatic pressures caused by the backfill and waste. Bending moments and shear forces are calculated for the walls based on these hydrostatic pressures. The bending moments and shear forces attributed to hydrostatic pressures are added to the bending moments and shear forces for the uniform load to give total bending moments and shear forces for the walls.

Following the structural analysis, the computer code enters an annual loop in which chemical and physical deterioration of the concrete and steel barriers used in the disposal facility is modeled. Properties of the structural members of the facility are updated to reflect degradation and are used in cracking analyses of the roof, walls, and floor of the disposal facility to assess the ability of the structure to bear the loads placed upon it. The deterioration of the concrete barriers is simulated with respect to the (1) removal of calcium hydroxide from the cement matrix, (2) sulfate attack of the

ORNL DWG 93A-738

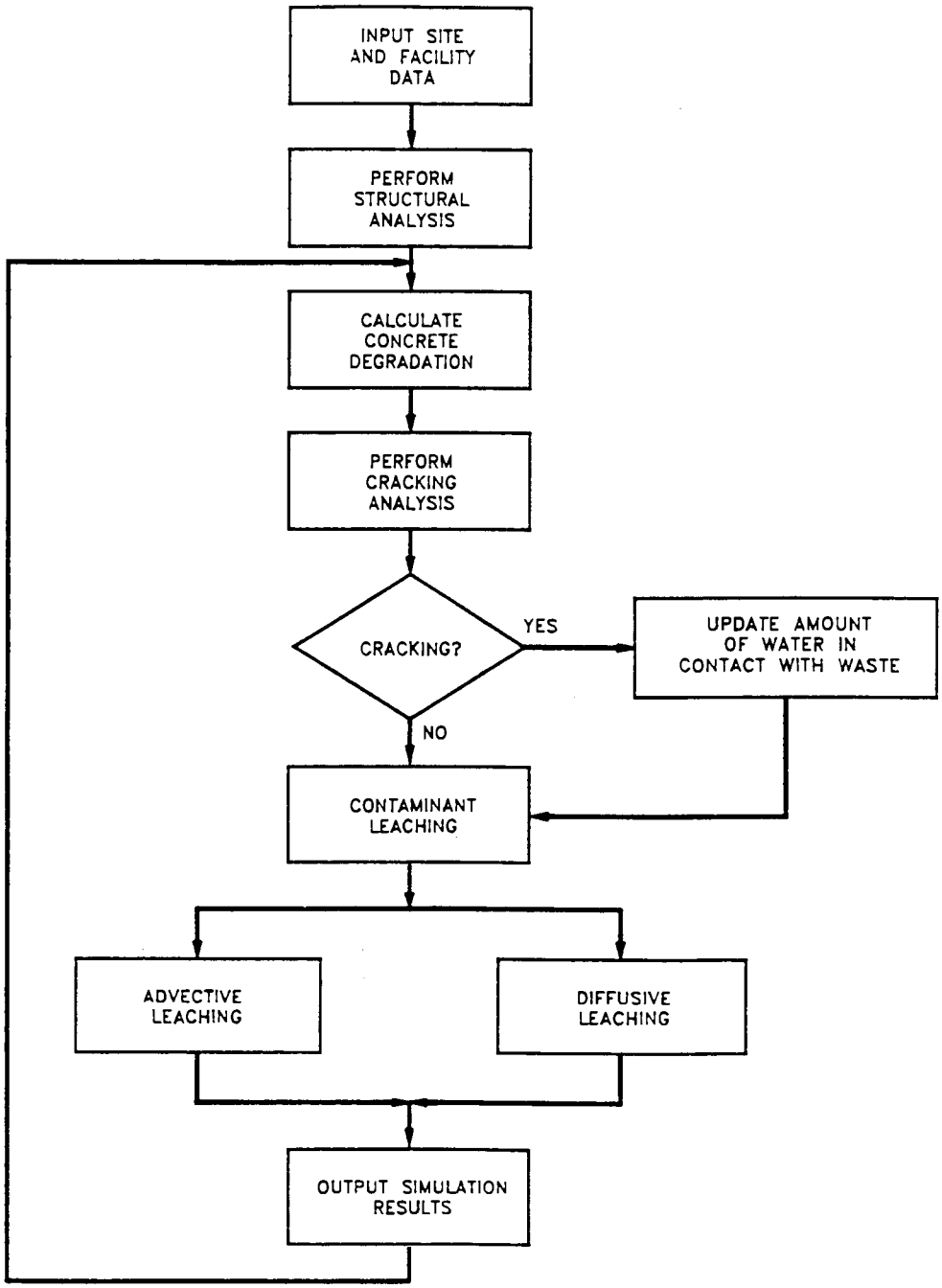

Fig. 3.8. Logic flow of the SOURCE1 computer code.

concrete, and (3) corrosion of steel reinforcement. Concrete component properties (strength, thickness, and pH) are updated for each year of the simulation to reflect projected rates of deterioration. Failure rates of steel containers and the epoxy coating on reinforcing steel are determined by using a linear failure model.

As the engineered structure is weakened by chemical and physical attack, a point is reached at which time the structure is no longer able to bear the loads placed upon it. Under these conditions, the engineered barriers will crack or otherwise fail. Failure is judged in terms of the capability of the facility to isolate the waste from water percolating through the disposal site. When the disposal facility is no longer hydraulically intact, the engineered barriers are assumed to offer no benefit. The cracking analysis is performed if hydraulic failure of the disposal facility has not occurred. The cracking moment, cracking shear, and ultimate strength are each calculated for the roof, walls, and floor and compared to the moments and forces calculated in the structural analysis. If the calculated moments or shears exceed the cracking moments or shear forces, the structural member is projected to crack. Fracture characteristics (depth, spacing, and width) are calculated with the onset of cracking. Cracking or spalling of concrete members of the disposal facility may result from corrosion of the steel reinforcement. In the event of the former, fracture characteristics are calculated. Concrete-member thicknesses are updated in the event that spalling of the concrete surface occurs. Fig. 3.9 demonstrates the logic flow of the structural and cracking analyses that are performed to estimate the time of failure of the disposal facility.

Radionuclide release rates from waste disposal facilities are a function of the integrity of the waste (or waste form) and the engineered barriers used in construction of the facility (e.g., concrete and metal containers). When intact, these barriers minimize the contact of water with the waste, thereby minimizing releases of radionuclides. As the barriers deteriorate over time, water can more readily contact the waste and mobilize radionuclides, thus accelerating releases to the environment. The SOURCE1 computer code considers two mechanisms through which waste radionuclides are released into the environment: advection (bulk flow driven by hydraulic pressure differences) and diffusion (nuclide movement driven by concentration differences). The calculated total release rate resulting from advection and diffusion is compared with the rate of release dictated by the solubility limit of the nuclide in water. If the solubility limit is exceeded, the release rate is adjusted to the solubility-limited rate. As a disposal facility degrades, the percolation rate of water through the waste increases. Thus, except for cases constrained by solubility, advective releases will increase with degradation and, in general, dominate the total release. The total release is divided into two components: one that flows vertically for recharge to groundwater and a second that flows laterally in the shallow-subsurface flow region of the site.

The CIIDF design includes a steel-reinforced concrete pad under the disposal vaults and a leachate collection system. The SOURCE1 code simulates the degradation and failure of the pad and the collection system. While the pad and the collection system are functional, releases to the environment are attenuated. Increased degradation results in increased releases to the environment until the pad and collection system are no longer functional. At this point, calculated releases from the disposal vaults are no longer attenuated.

ORNL DWG 93A-737

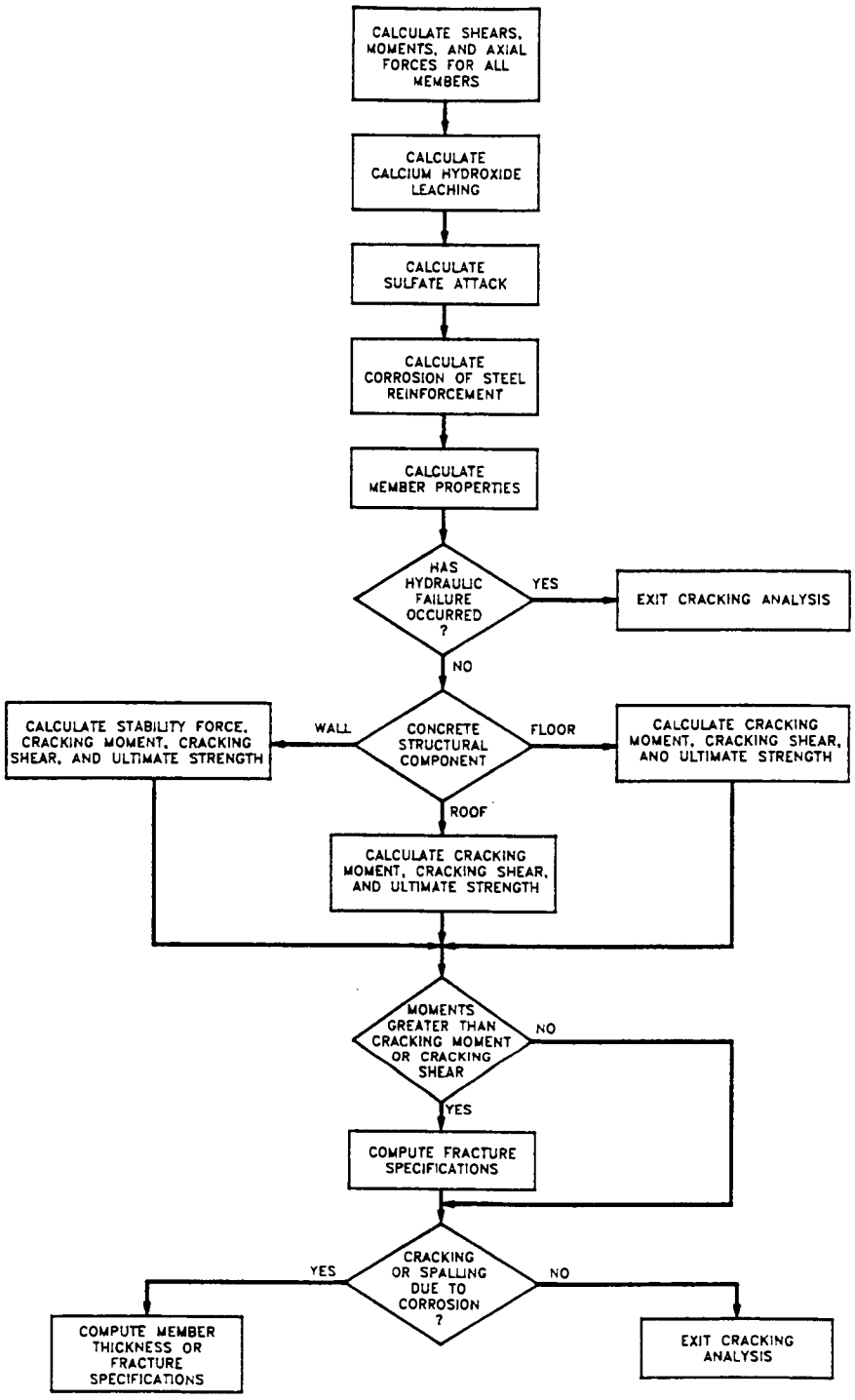

Fig. 3.9. Logic flow of the concrete-degradation and -cracking subroutines.

Revision of SOURCE1

Several revisions have been incorporated into SOURCE1 Version 2.0. These revisions include the incorporation of a new advective transport model, development of a new model that calculates the degradation and failure of a tumulus-type pad and leachate collection system, improvement of routines for controlling water seepage and radionuclide inventory inputs, and expansion of options for obtaining output summaries. A detailed description of each of these changes can be found in the SOURCE1 user's manual (Icenhour and Tharp 1996).

3.3.3.2 Source Terms for Environmental Transport

For environmental-transport calculations, SOURCE1 provides the radionuclide release rate as a function of time. These releases, which are divided into two components, are used in subsequent calculations of radionuclide transport to the aquifer and shallow-subsurface transport of the radionuclide.

The SOURCE1 input parameters for the environmental-transport calculation can be divided into four general categories: disposal facility physicochemical parameters, radionuclide transport parameters, radionuclide inventory, and water seepage rates. Values for the first two categories are obtained from the literature and are presented in this section. Values for the third and fourth categories are calculated and are presented in Sect. 4.

The disposal facility physicochemical parameters describe the dimensions and construction of the facility and the chemical composition of the media interacting with the facility. Table 3.6 provides the SOURCE1 physicochemical parameters used for the environmental transport calculations.

Radionuclide-transport parameters (e.g., distribution coefficient, diffusion coefficients, and solubility) are used in the calculation of the release rates of the radionuclides from the waste. Radionuclide-specific transport parameters for the environmental transport source term calculations are summarized in Table 3.7. Appendix B outlines the methodology used in developing the radionuclide-specific input parameters.

The radionuclide inventory is input to the SOURCE1 code as the number of grams per vault. The environmental transport calculations were performed iteratively to determine the initial radionuclide inventory that resulted in a surface-water or groundwater concentration equal to the limit established by dose considerations. The limiting inventories used in the calculations are presented in Sect. 4.2.1. The water seepage rates are calculated using the UTM model as described in Sects. 3.3.2.2 and 4.1. The results of these calculations are presented in Sect. 4.2.

3.3.3.3 Source Terms for Direct Intrusion

The source term for direct intrusion is evaluated also by using the SOURCE1 computer code and is defined as the remaining radionuclide inventory at the time of intrusion. Hence, the SOURCE1

Table 3.6. Physicochemical parameters used in the SOURCE1 simulation of CIIDF[a]

Parameter	Value
Disposal facility area for one pad, m^2	4.99×10^2
Groundwater total dissolved solids, ppm	3.49×10^2
Groundwater temperature, °C	1.50×10^1
Groundwater pH	6.75×10^0
Saturated hydraulic conductivity, cm/s	
Recharge	5.80×10^{-7}
Soil backfill	3.50×10^{-3}
Concrete	1.00×10^{-10}
Groundwater constituent concentrations, mol/L	
Ca^{2+}	2.10×10^{-3}
Cl^-	2.04×10^{-4}
CO_3^{2-}	1.00×10^{-3}
Mg^{2+}	5.21×10^{-4}
SO_4^{2-}	2.62×10^{-4}
O_2	3.44×10^{-4}
CO_2	8.81×10^{-6}
Constituent solubilities, mol/L	
$Ca(OH)_2$	2.00×10^{-2}
CO_3^{2-}	1.20×10^{-3}
Mg^{2+}	1.20×10^{-3}
Concrete constituent concentrations, mol/L	
Calcium concentration in C-S-H[b] system	1.75×10^0
Calcium concentration in pore fluid	2.00×10^{-2}
CaO content in cement	2.11×10^0
Free Cl^-	1.00×10^{-2}
Silica concentration in C-S-H[b] system	7.10×10^{-1}
Vault-concrete design specifications	
Compressive strength at 28 d, Pa	3.45×10^7
Poisson's ratio of concrete	1.50×10^{-1}
Modulus of elasticity of steel reinforcement, Pa	2.00×10^{11}
Yield strength of steel, Pa	4.14×10^8
Modulus of subgrade reaction, Pa	1.38×10^7
Young's modulus of elasticity (concrete), Pa	2.00×10^{10}
Water:cement ratio	4.00×10^{-1}
Density, g/cm^3	2.40×10^0
Porosity	1.50×10^{-1}
Cement content, kg/m^3	4.03×10^2
Initial pH	1.25×10^1
Concrete pad failure model parameters	
Radius of pad steel reinforcement, cm	1.11×10^0
Modulus of elasticity of steel reinforcement, Pa	2.00×10^{11}
Yield strength of steel reinforcement, Pa	4.14×10^8

Table 3.6 (continued)

Parameter	Value
Compressive strength of pad concrete, Pa	2.76×10^{7}
Spacing between steel reinforcing rods, cm	1.52×10^{1}
Concrete cover thickness from the center of the bottom row of steel reinforcing rods to the bottom of the pad, cm	1.52×10^{1}
Diffusion coefficients in concrete, m^2/s	
NaOH, KOH	2.12×10^{-11}
$Ca(OH)_2$	1.82×10^{-11}
Cl^-	5.08×10^{-11}
CO_2	1.92×10^{-10}
O_2	2.10×10^{-10}
SO_4^{2-}	1.06×10^{-11}
Tumulus design specifications	
Layers of vaults	3
Number of vaults wide	10
Number of vaults long	11
Vault dimensions, m	
Width	1.52×10^{0}
Length	2.21×10^{0}
Height	1.65×10^{0}
Concrete member thickness, cm	
Roof	1.78×10^{1}
Walls	1.78×10^{1}
Floor	1.78×10^{1}
Pad	3.81×10^{1}
Steel reinforcement radius, cm	
Roof	7.94×10^{-1}
Walls	6.35×10^{-1}
Floor	6.35×10^{-1}
Spacing of steel reinforcement, cm	
Roof	2.54×10^{1}
Walls	3.05×10^{1}
Floor	3.05×10^{1}
Concrete cover thickness on tension face, cm	
Roof:	
X-direction	7.77×10^{0}
Y-direction	9.37×10^{0}
Walls:	
Horizontal direction	8.26×10^{0}
Vertical direction	9.52×10^{0}
Floor:	
X-direction	5.08×10^{0}
Y-direction	6.35×10^{0}
Soil and waste properties	

Table 3.6 (continued)

Parameter	Value
Earthen cover thickness, m	1.83×10^0
Earthen cover density, g/cm^3	1.76×10^0
Friction angle of waste backfill, degrees	4.00×10^1
Friction angle of soil backfill, degrees	3.00×10^1
Density of soil backfill, g/cm^3	1.76×10^0
Waste density, g/cm^3	1.76×10^0
Relative saturation of waste	3.50×10^{-1}
Waste container and epoxy coating failure times, years	
Waste container:	
Start of failure	0.00×10^0
Time to complete failure	6.00×10^1
Epoxy coating:	
Start of failure	0.00×10^0
Time to complete failure	2.00×10^1

[a] Actual values of input parameters for SOURCE1 may be different because of unit conversions.
[b] C-S-H = calcium-silicate-hydrate.

code is used to calculate the depletion of the radionuclide inventory during the time period from disposition to intrusion.

As stated previously, it would not be conservative to use the same computer code input parameters for both the environmental transport and direct-intrusion calculations. Parameters that result in a conservative release-rate calculation would result in a rapid depletion of the radionuclide inventory and, thus, result in a nonconservative estimate of the remaining radionuclide inventory.

To provide a conservative estimate of the remaining radionuclide inventory, code input parameters were adjusted to lower the calculated rate of degradation of the disposal facility and the calculated radionuclide release rate. For disposal facility degradation, parameter adjustments were made on the basis of sensitivity analyses and environmental data. For radionuclide release, no credit was taken for the diffusion-transport pathways, and advective transport was lowered by increasing distribution coefficients. Graphs of the fraction of original radionuclide inventory remaining (without decay) as a function of distribution coefficient were prepared to use in the direct-intrusion calculations. Concentration limits evaluated at the time of intrusion can then be adjusted back to the initial time of disposal by using the mobilization and transport factors obtained from these graphs. The details of the input parameter changes and the results of the source-term analysis for direct intrusion are presented in Sect. 4.2.2.

3.3.4 Environmental Transport

Estimation of leachage migration from concrete vaults to compliance points in the landscape involves a linked series of simulators for the major components of nuclide containment and transport

Table 3.7 Radionuclide-specific input data to SOURCE1 for the CIIDF performance assessment[a]

Nuclide	Half-life (years)	Solubility (mol/L)	Waste K_d (mL/g)	Diffusion coefficient (m^2/s)	
				Waste	Concrete
^{3}H	1.23×10^{1}	1.11×10^{2}	1.99×10^{-1}	3.88×10^{-9}	1.86×10^{-9}
^{10}Be	1.60×10^{6}	2.88×10^{-6}	3.12×10^{6}	3.46×10^{-17}	6.55×10^{-11}
^{14}C	5.73×10^{3}	1.11×10^{-4}	1.09×10^{0}	1.44×10^{-11}	2.18×10^{-12}
^{26}Al	7.20×10^{5}	5.24×10^{0}	1.99×10^{5}	1.24×10^{-16}	7.23×10^{-13}
^{36}Cl	3.01×10^{5}	4.61×10^{0}	1.99×10^{-1}	3.38×10^{-10}	5.08×10^{-11}
^{40}K	1.28×10^{9}	4.61×10^{0}	3.98×10^{0}	1.26×10^{-11}	9.66×10^{-13}
^{41}Ca	1.03×10^{5}	1.40×10^{-4}	4.61×10^{0}	3.12×10^{-11}	3.38×10^{-12}
^{60}Co	5.27×10^{0}	3.46×10^{0}	3.97×10^{6}	1.66×10^{-17}	6.77×10^{-13}
^{59}Ni	7.50×10^{4}	7.83×10^{-4}	6.36×10^{0}	1.01×10^{-11}	1.21×10^{-12}
^{63}Ni	1.00×10^{2}	7.83×10^{-4}	6.36×10^{0}	1.01×10^{-11}	1.21×10^{-12}
^{79}Se	6.50×10^{4}	2.88×10^{0}	1.99×10^{-1}	6.88×10^{-11}	1.02×10^{-11}
^{87}Rb	4.80×10^{10}	1.44×10^{1}	1.33×10^{1}	1.12×10^{-11}	8.46×10^{-13}
^{90}Sr	2.85×10^{1}	7.45×10^{-5}	8.74×10^{0}	1.17×10^{-11}	1.34×10^{-12}
^{93}Zr	1.53×10^{6}	1.26×10^{-3}	4.97×10^{1}	4.71×10^{-13}	5.42×10^{-14}
^{93m}Nb	1.36×10^{1}	2.60×10^{-1}	2.38×10^{1}	6.90×10^{-14}	7.71×10^{-15}
^{94}Nb	2.03×10^{4}	2.60×10^{-1}	2.38×10^{1}	6.90×10^{-14}	7.71×10^{-15}
^{99}Tc	2.13×10^{5}	9.11×10^{-2}	1.29×10^{0}	1.25×10^{-11}	1.82×10^{-12}
^{107}Pd	6.50×10^{6}	8.69×10^{-8}	1.43×10^{6}	3.25×10^{-17}	3.44×10^{-13}
^{113m}Cd	1.37×10^{1}	7.64×10^{0}	3.97×10^{5}	2.33×10^{-16}	9.09×10^{-13}
^{121m}Sn	5.50×10^{1}	1.37×10^{1}	1.15×10^{1}	5.43×10^{-12}	6.54×10^{-13}
^{126}Sn	1.00×10^{5}	1.37×10^{1}	1.15×10^{1}	5.43×10^{-12}	6.54×10^{-13}
^{129}I	1.57×10^{7}	7.68×10^{0}	1.99×10^{-1}	3.42×10^{-10}	5.13×10^{-11}
^{135}Cs	3.00×10^{6}	1.60×10^{1}	1.99×10^{1}	6.80×10^{-12}	5.12×10^{-13}
^{137}Cs	3.00×10^{1}	1.60×10^{1}	1.99×10^{1}	6.80×10^{-12}	5.12×10^{-13}
^{151}Sm	9.00×10^{1}	7.25×10^{-7}	3.78×10^{0}	7.95×10^{-13}	9.17×10^{-14}
^{152}Eu	1.33×10^{1}	2.84×10^{-6}	3.78×10^{0}	7.95×10^{-13}	9.17×10^{-14}
^{154}Eu	8.80×10^{0}	2.84×10^{-6}	3.78×10^{0}	7.95×10^{-13}	9.17×10^{-14}
^{155}Eu	4.96×10^{0}	2.84×10^{-6}	3.78×10^{0}	7.95×10^{-13}	9.17×10^{-14}
^{207}Bi	3.22×10^{1}	5.40×10^{-6}	4.79×10^{0}	2.12×10^{-12}	2.30×10^{-13}
^{210}Pb	2.23×10^{1}	1.46×10^{-4}	4.55×10^{1}	6.63×10^{-14}	7.76×10^{-15}
^{226}Ra	1.60×10^{3}	6.21×10^{-8}	1.99×10^{1}	4.10×10^{-13}	4.74×10^{-14}
^{229}Th	7.34×10^{3}	7.57×10^{-8}	5.36×10^{1}	3.24×10^{-14}	3.73×10^{-15}
^{230}Th	7.54×10^{4}	7.57×10^{-8}	5.36×10^{1}	3.24×10^{-14}	3.73×10^{-15}
^{232}Th	1.41×10^{10}	7.57×10^{-8}	5.36×10^{1}	3.24×10^{-14}	3.73×10^{-15}
^{231}Pa	3.28×10^{4}	5.34×10^{-4}	5.47×10^{1}	3.19×10^{-14}	3.63×10^{-15}
^{232}U	6.89×10^{1}	1.46×10^{-6}	5.56×10^{1}	3.11×10^{-14}	3.50×10^{-15}
^{233}U	1.59×10^{5}	1.46×10^{-6}	5.56×10^{1}	3.11×10^{-14}	3.50×10^{-15}
^{234}U	2.45×10^{5}	1.46×10^{-6}	5.56×10^{1}	3.11×10^{-14}	3.50×10^{-15}
^{235}U	7.04×10^{8}	1.46×10^{-6}	5.56×10^{1}	3.11×10^{-14}	3.50×10^{-15}
^{236}U	2.34×10^{7}	1.46×10^{-6}	5.56×10^{1}	3.11×10^{-14}	3.50×10^{-15}
^{238}U	4.47×10^{9}	1.46×10^{-6}	5.56×10^{1}	3.11×10^{-14}	3.50×10^{-15}

Table 3.7 (continued)

Nuclide	Half-life (years)	Solubility (mol/L)	Waste K_d (mL/g)	Diffusion coefficient (m^2/s)	
				Waste	Concrete
^{237}Np	2.14×10^6	4.05×10^{-5}	5.56×10^1	3.11×10^{-14}	3.50×10^{-15}
^{238}Pu	8.77×10^1	1.71×10^{-8}	5.76×10^1	3.00×10^{-14}	3.41×10^{-15}
^{239}Pu	2.41×10^4	1.71×10^{-8}	5.76×10^1	3.00×10^{-14}	3.41×10^{-15}
^{240}Pu	6.56×10^3	1.71×10^{-8}	5.76×10^1	3.00×10^{-14}	3.41×10^{-15}
^{241}Pu	1.44×10^1	1.71×10^{-8}	5.76×10^1	3.00×10^{-14}	3.41×10^{-15}
^{242}Pu	3.76×10^5	1.71×10^{-8}	5.76×10^1	3.00×10^{-14}	3.41×10^{-15}
^{244}Pu	8.26×10^7	1.71×10^{-8}	5.76×10^1	3.00×10^{-14}	3.41×10^{-15}
^{241}Am	4.33×10^2	3.27×10^{-6}	5.76×10^1	5.46×10^{-14}	6.26×10^{-15}
^{242m}Am	1.41×10^2	3.27×10^{-6}	5.76×10^1	5.46×10^{-14}	6.26×10^{-15}
^{243}Am	7.37×10^3	3.27×10^{-6}	5.76×10^1	5.46×10^{-14}	6.26×10^{-15}
^{243}Cm	2.85×10^1	2.84×10^{-6}	5.76×10^1	5.46×10^{-14}	6.26×10^{-15}
^{244}Cm	1.81×10^1	2.84×10^{-6}	5.76×10^1	5.46×10^{-14}	6.26×10^{-15}
^{245}Cm	8.50×10^3	2.84×10^{-6}	5.76×10^1	5.46×10^{-14}	6.26×10^{-15}
^{246}Cm	4.73×10^3	2.84×10^{-6}	5.76×10^1	5.46×10^{-14}	6.26×10^{-15}
^{247}Cm	1.56×10^7	2.84×10^{-6}	5.76×10^1	5.46×10^{-14}	6.26×10^{-15}
^{248}Cm	3.40×10^5	2.84×10^{-6}	5.76×10^1	5.46×10^{-14}	6.26×10^{-15}
^{249}Cf	3.51×10^2	3.49×10^0	5.96×10^1	5.28×10^{-14}	6.10×10^{-15}
^{250}Cf	1.31×10^1	3.49×10^0	5.96×10^1	5.28×10^{-14}	6.10×10^{-15}
^{251}Cf	9.00×10^2	3.49×10^0	5.96×10^1	5.28×10^{-14}	6.10×10^{-15}

[a] The methodology for estimation of the values in this table and sources are presented in Appendix B.

(Fig. 3.10). Soil water drainage rates from water budget calculations were provided by the UTM and used by the SOURCE1 model as seepage to determine diffusive and advective release of nuclides from concrete vaults into the unsaturated vadose zone. The SOURCE1 simulations partitioned nuclide release into vertical and lateral subsurface flow components. These two flow components were input to transport through the vadose zone using the PADSIM code. This code calculated chemical adsorption in the unsaturated zone as well as preferential flow in lateral subsurface transport to the surface. Results of nuclide transport to the water table were taken as input by a groundwater model, FTWORK, to calculate groundwater nuclide concentrations at 100 m from the waste site as well as transport to surface water at seeps in lower landscape positions. Outlines of the PADSIM and FTWORK transport models are given below.

3.3.4.1 Shallow Subsurface Transport

The PADSIM code calculates nuclide flux in recharge to groundwater and in lateral subsurface transport to receiving surface drainage channels (Fig. 3.10). The features of the unsaturated zone calculations applicable to the shallow subsurface flow paths are given in Appendix D.3 and are outlined as follows:

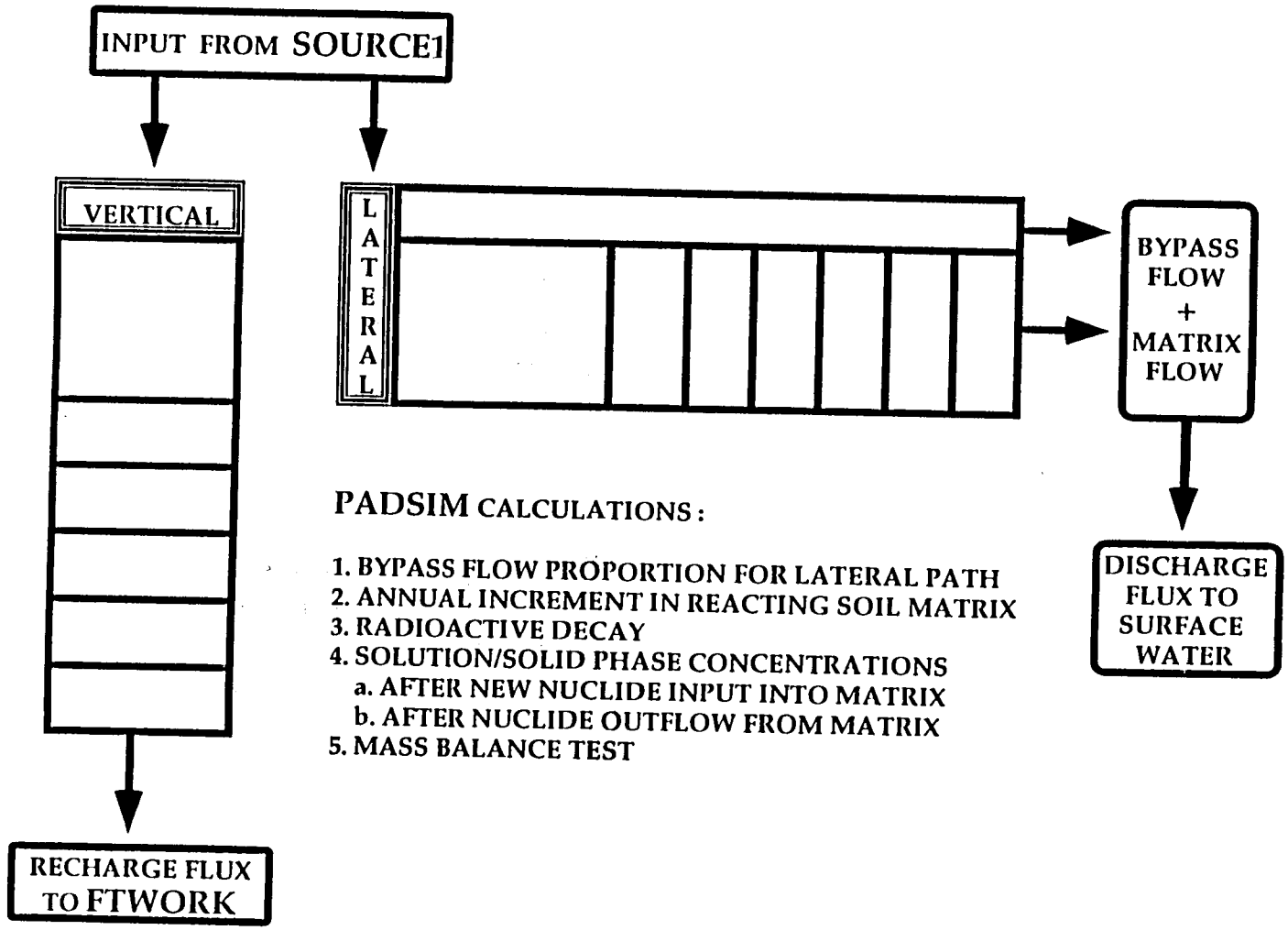

Fig. 3.10. Essential features of PADSIM in the linkage between SOURCE1 and FTWORK for nuclide transport to groundwater and for lateral subsurface transport to surface water.

- Bypass flow—Soils to 3.5-m depth have considerable capability for transporting chemicals through preferential flow paths, and these tend to follow the dip of saprolite structure (Wilson et al. 1993). An algorithm representing bypass flow resulted in decreasing proportions of bypass flow with increase in K_d (Table 3.8). There was no bypass flow for the vertical path due to the 8-m thickness of this zone, which is not expected to show a continuous network of preferential flow paths to the water table.

- Interaction soil volume—Nuclide movement through the unsaturated soil matrix is represented by an expanding soil volume according to an algorithm that depends on the K_d. The volumes of soil matrix were incremented annually after the first arrival of nuclide resulting in increasing times for full soil matrix exposure to nuclides with increasing K_d (Table 3.9). Nuclides with a $K_d \geq 100$ mL/g took 0 and 48 years to migrate through the soil matrix of the vertical (8.1-m) and lateral (50.0-m) flow paths, respectively.

- Half-life—Each year the nuclide mass in the shallow subsurface is reduced to account for decay according to the applicable half-life for each nuclide (Table 3.1).

- Chemical adsorption—The nuclide leachate entering the soil matrix is assumed to come to equilibrium between the solution phase and the adsorbed phase on soil surfaces according to the K_d values and the current interacting soil volume. This revised solute concentration is used to determine nuclide outflow from the matrix. Following removal of the nuclide outflow, solution phase/solid phase calculations are conducted to determine a new nuclide equilibrium between the solid and solution phases of the soil matrix.

- Matrix diffusion—This mechanism was not specifically represented in PADSIM; however, the annual averaging of added nuclide into the reacting volume of soil matrix provided numerical dispersion that results in an equivalent effect of "diffusing" nuclide through the soil matrix. Matrix diffusion is considered an important mechanism (Solomon et al. 1992), and this is facilitated by small-scale preferential flow paths which distribute nuclides through the soil, allowing solute diffusion into the microporosity of the soil matrix.

3.3.4.2 Contaminant Transport in Groundwater

Groundwater flow and transport of contaminants from CIIDF was modeled using the FTWORK computer program and is examined in detail in Appendix E. The validation and verification of the model are discussed in Sect. 3.3.6.4. Given the basic hydrogeological data for geologic material properties, water table elevations, spatially variable recharge values, and types and locations of boundaries, a groundwater flow model was constructed and calibrated to existing conditions. Since CIIDF will be hydrologically isolated, water inflow occurs from infiltration of precipitation through overlying soils and subsurface strata, seepage of leachate through the disposal facility, or recharge

Table 3.8. The proportion of bypass flow for vertical and lateral flow paths and the maximum first-year transport through the soil matrix as a function of chemical adsorption

K_d (mL/g)	Vertical path	Lateral path	Maximum matrix transport (m)
0	0.00	0.38	80.0
30	0.00	0.17	60.5
40	0.00	0.07	54.0
50	0.00	0.00	47.5
≥100	0.00	0.00	15.0

Table 3.9. Annual increment in soil matrix path length and times to full matrix exposure to nuclides as a function of K_d for the vertical and lateral flow paths

K_d (mL/g)	Nuclide path increment through soil matrix (cm/year)	Time to full vertical path exposure (year)	Time to full lateral path exposure (year)
0	400.0	0	0
30	302.5	0	0
40	270.0	0	0
50	237.5	0	2
≥100	75.0	0	48

from losing streams. Water exits the groundwater model as discharge to surface streams, and ultimately via Bear Creek.

In order to model contaminant transport, a flow model was derived to account for changes in the topography, water table elevation, and boundary conditions due to construction of CIIDF. The underlying material properties such as hydraulic conductivity were not changed due to construction. A postconstruction flow model was created based on the new conditions, and this model was used for the contaminant transport calculations. Radionuclides enter the groundwater model as part of the recharge in cells which underly the CIIDF pads, as calculated by the PADSIM model.

The 20 pads were assumed to be filled at the rate of one per year, so it would be possible for some pads to release contamination before others are loaded. For short-lived, highly mobile nuclides, it is conceivable that this loading pattern could have considerable effect on the time, location, and magnitude of ground and surface water concentrations. For nuclides that were long lived or readily adsorbed onto the soil media, the effects of this variable loading pattern were assumed to be much less critical, and all 20 pads were assumed to be loaded in the first time step.

The radionuclide fluxes from the pads to the shallow subsurface and to groundwater were allowed to vary with time, and to undergo retarded advection and dispersion through the two pathways. Concentrations in the groundwater were examined over time at a ring of points located 100 m from the disposal unit, which is considered to be the edge of the graded site after construction (see Sect. 2.3). Groundwater discharged to surface water features was accounted for by summing all discharges for surface water calculations.

3.3.4.3 Transport of Contaminants to Surface Water

The principal goal of this analysis is to determine limiting disposal inventories for all radionuclides based on exposure to contaminated drinking water obtained from either groundwater or surface water supplies. In determining the surface water limiting inventory, it was necessary to define a location which could be used for a reliable, perennial surface water supply. This surface water compliance point is presumed to be in the main stem of Bear Creek at USGS Station 03538270, about 1 km downstream of CIIDF (see Fig. 3.11). Changes in discharge in the reach between CIIDF and the gauge would be due to minor bank inflow and interactions with the underlying Maynardville formation. The differences are not quantified but are presumed to be insignificant compared to other contributions to the creek. For example, discharges at Station 03538273 are about 20% higher than those at 03538270 (see Table 3.10) since there are several more tributaries from the western part of Bear Creek Valley which contribute to flow.

The flow rate used to calculate concentrations of radionuclides in surface water is the mean annual flow rate for the period of record of the gauge at station 03538720: 18,500 m^3/d (USGS 1994). While there is a strong seasonal variation in the flow of Bear Creek (Fig. 3.12), the frequency of these variations could not be captured in the time frame of the analysis, which is on the order of 1000 years.

As with calculation of disposal limits based on groundwater concentration, determination of the limiting inventory of each isotope based on surface water concentrations required several iterations to solve for the inventory corresponding to the drinking water exposure limit. This process involved choosing an initial estimate of the inventory limit (based on the drinking water pathways) and running the environmental transport calculations to produce a concentration in Bear Creek (Fig. 3.1). This initial result was compared to the concentration limit corresponding to the allowable dose, and a new inventory limit was estimated, assuming (temporarily) a linear relationship between inventory and surface water calculations. In most cases, the linear assumption was valid, and the new estimate was accurate. In some cases, however, the relationship became nonlinear, due principally to solubility limitations in the waste form or the environment. These cases required several iterations to arrive at a limiting inventory which corresponded to the drinking water limit.

Location of USGS Stream Gauges in the CIIDF Model

Scale 1" = 1000'

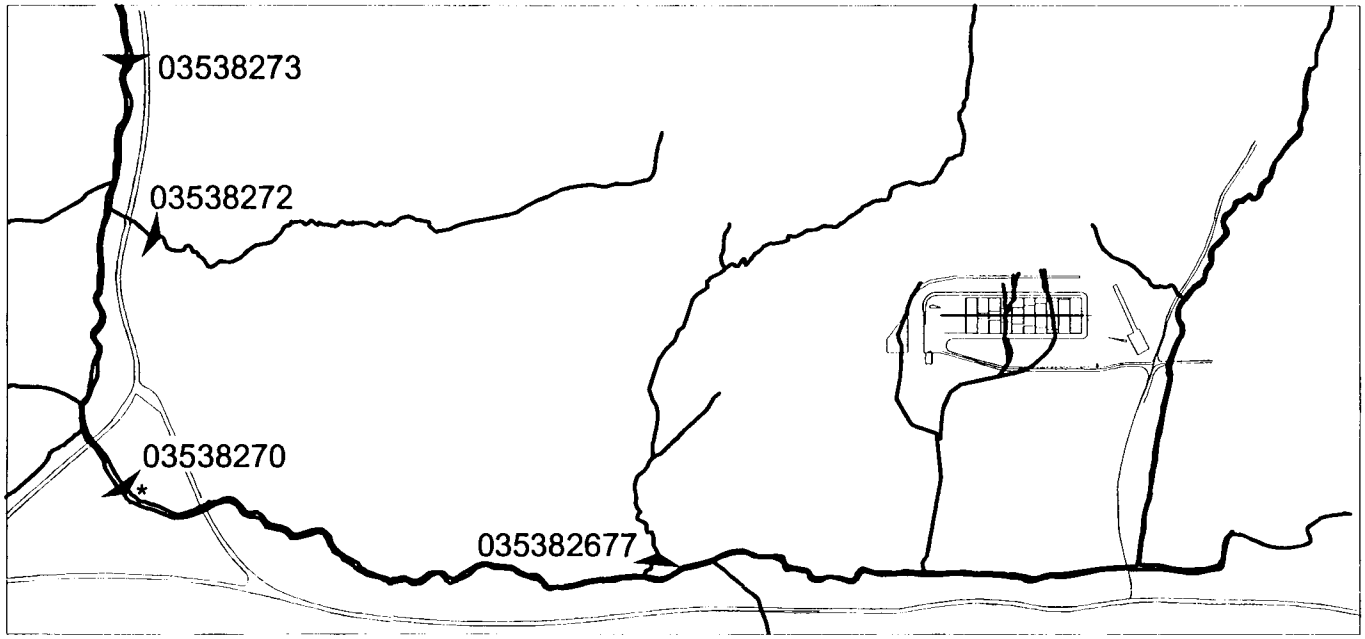

* Surface water compliance point

Fig. 3.11. Locations of USGS stream gauging stations in the vicinity of CIIDF.

Table 3.10. Bear Creek discharges measured at USGS gauging stations

Station number	Period of record	Drainage area [km^2 (mi^2)]	Number of records	Annual mean discharge [m^3/d (cfs)]
03538270[a]	1985.03.01–1994.09.30	11.2 (4.34)	3501	18,500 (7.54)
03538273[b]	1986.09.25–1991.09.30	13.0 (5.0)	1832	22,000 (8.97)

[a] *Source*: USGS 1994.
[b] *Source*: USGS 1991.

3.3.5 Exposure Pathway Modeling and Dose Estimation

The models used in estimating releases of radionuclides from CIIDF and transport by water pathways provide estimates of concentrations in groundwater and surface water as a function of time after disposal at those locations beyond the boundary of the 100-m buffer zone around the disposal facility where the highest concentrations are predicted to occur. These concentrations provide input to a simple multiplicative-chain model for estimating maximum annual EDEs to off-site individuals from the drinking water pathway. The model, which is described in Sect. G.5.1 of Appendix G, takes into account the assumed yearly consumption of drinking water and the dose per unit activity intake of radionuclides by ingestion.

Only the drinking water pathway is considered in the dose analysis for off-site individuals. All other exposure pathways involving use of contaminated water are neglected, essentially because achieving compliance with the assumed performance objective of 4-mrem per year EDE for the drinking water pathway only would ensure compliance with the performance objective of 25-mrem per year EDE for all exposure pathways combined. In addition, doses to off-site individuals resulting from airborne releases from the disposal facility or from biotic intrusion and transport are assumed to be negligible compared with doses from the drinking water pathway and thus are not evaluated.

Estimates of dose to inadvertent intruders resulting from direct intrusion or attempts at direct intrusion into solid waste in the disposal facility are based on assumptions for the agriculture, resident, and post-drilling scenarios, each of which involves chronic exposure. The models for each scenario provide estimates of annual EDEs per unit concentration of radionuclides in the disposal facility at the time intrusion is assumed to occur. For each of the assumed scenarios, the doses from the assumed exposure pathways are estimated using simple multiplicative-chain models described in Sect. G.5.2 of Appendix G.

Chronic exposures of inadvertent intruders to contaminated groundwater obtained from a well on the disposal site and exposures resulting from direct intrusion or attempts at direct intrusion into solid waste in the disposal facility based on assumptions for the construction, discovery, and drilling scenarios, each of which involves a single, short-term exposure, also were considered. However, these

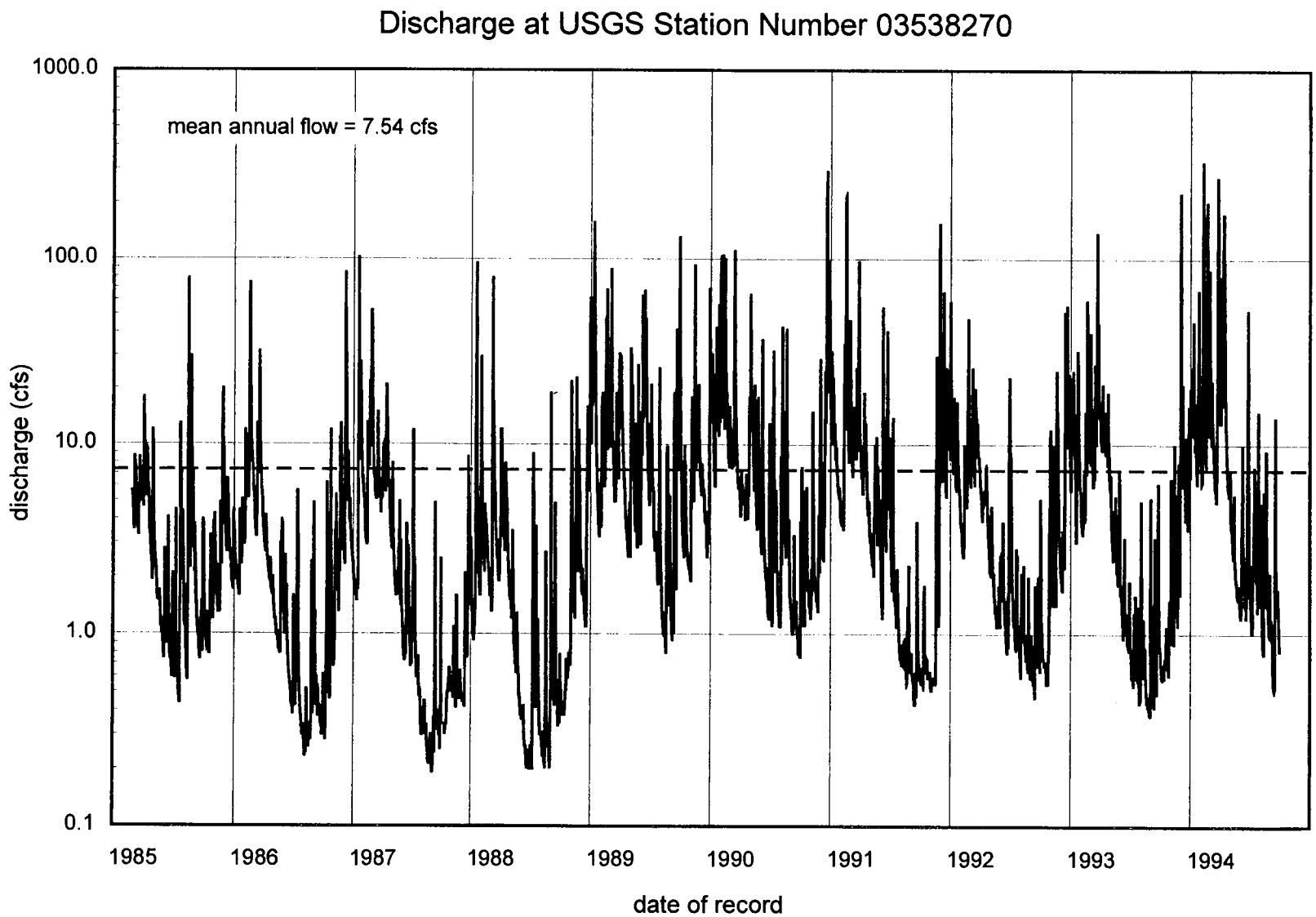

Fig. 3.12. Record of stream discharge at USGS Station 03538270.

exposure scenarios should result in doses that are insignificant compared to doses resulting from the chronic exposure scenarios considered in the analysis and thus are not evaluated.

The dose analysis for inadvertent intruders takes into account changes in the concentrations of radionuclides in the disposal facility due to radioactive decay between the time of disposal and the time exposures are assumed to occur, which is either at 100 years for the resident and post-drilling scenarios or at 300 years and beyond for the agriculture scenario. A model for estimating releases of radionuclides from the disposal facility in infiltrating water also is used in estimating the concentrations of radionuclides remaining in the facility as a function of time after disposal. However, the source-term models used in the PA to estimate radionuclide concentrations in groundwater and surface water are not appropriate for an intruder dose analysis because these models are intended to overestimate actual releases and, thus, should underestimate radionuclide concentrations remaining in the facility. Therefore, the source-term models are modified for the intruder dose analysis with the intent of providing conservative estimates of radionuclide concentrations remaining in the disposal facility.

3.3.6 Verification and Validation of Methodology

Verification and validation of the codes used in the PA for CIIDF are necessary to ensure that the results presented are meaningful. These efforts are discussed in this section. Verification is considered to mean that the codes are correct in a mathematical and numerical sense and that the theory incorporated into the codes is correct. Validation is considered to mean that the application of the code to CIIDF is a reasonable representation of the site. The verification and validation efforts to date are not complete; however, providing unequivocal assurance that the codes used for this performance assessment are verified and validated is not reasonable because data characterizing long-term performance of engineered disposal facilities such as CIIDF in a humid environment are not available.

3.3.6.1 Verification and Validation of UTM

UTM has been under development for over two decades and has been applied in a range of locations, including North Carolina, Missouri, Oklahoma, and Tennessee. Water budget simulations involve algorithms for various components of the hydrologic cycle that are based on well-established physical and physiological relationships. UTM is used in the PA for simulation of water budgets for various conditions of the CIIDF site during operations, closure, and postclosure. The paragraphs that follow outline the components of the water budget calculations in UTM.

Interception

A defined volume for water caught in the canopy and litter that varies for the winter and summer seasons and is filled with rainfall before throughfall enters the soil. Water in this storage has

priority in evaporation calculations. The storage volumes were adjusted for deciduous forests so that simulated interception matched the empirical observations of Helvey and Patric (1965). This model development and testing are described in Huff et al. (1977). Input values for simulations with grass cover were obtained from a previous application (Luxmoore and Sharma 1980).

Infiltration

The time-compression method of Reeves and Miller (1975) has been implemented in UTM to partition throughfall into infiltration and surface runoff at the soil surface. Reeves and Miller describe the algorithm and have tested the method. This algorithm is not often invoked in forest simulations due to the high infiltration rates of forest soils. Runoff in forested watersheds is generally the result of exfiltration of subsurface flow in lower slope positions. Huff et al. (1977) describe the method for the UTM hydrologic module.

Evapotranspiration

The complex of evaporative surfaces (foliage, litter, and soil) in a vegetated landscape is viewed as one surface in a "big-leaf" approach for which the Penman-Montieth equation determines evapotranspiration. Sinclair, Murphy, and Knoerr (1976) demonstrated the utility of this approach for calculation of evapotranspiration. A number of meteorological variables (air temperature, vapor pressure, solar radiation, and wind speed) are needed along with an empirical surface resistance to vapor loss from the surface. The resistance was obtained from experimental observations for the vegetation of interest (Luxmoore et al. 1978, Luxmoore and Sharma 1980). The algorithms are described in Huff et al. (1977). Luxmoore and Huff (1989) showed that the calculations of forest evapotranspiration are in agreement with independent estimates for the Oak Ridge area.

Recharge and subsurface lateral flow

The Darcy flow equation was used in soil water-flow calculations between soil layers. (The parameters for the layers of soil in question are specified by the user.) The equation uses a hydraulic gradient and hydraulic conductivity that are determined from soil hydraulic properties. These properties (water pressure–water content and hydraulic conductivity–water content relationships) are based on input values chosen by the user for the site of interest. Huff et al. (1977) describes the flow equations and the uses of soil hydraulic properties. The calculation of recharge to groundwater uses a hydraulic gradient of unity and a hydraulic conductivity appropriate to the water content of the lowest layer of the soil profile being simulated. Lateral flow is calculated as the excess of soil water above the saturation value flowing into a soil layer from above. Algorithms for bypass flow, due to macropores, are an option in the soil water-flow calculations. The basis for the macropore flow option is described in Hetrick, Holdeman, and Luxmoore (1982).

Water budgets for soil-plant systems

UTM has been applied to a range of sites, and reasonable agreement has been obtained for the components of the water budgets at the sites as follows:

- Grassland watersheds in Oklahoma—Results are published in open literature in Sharma and Luxmoore (1979), Luxmoore and Sharma (1980), and Luxmoore (1983a). These results show the utility of UTM for grassland conditions, which are part of the CIIDF closure scenario.

- Forested watershed on the ORR—Open literature publication of UTM applications to the forest stand of ORR are given in Luxmoore et al. (1978), Luxmoore, Stolzy, and Holdeman (1981), and Luxmoore (1983b).

- Scenarios of landfill barrier designs—The hydrologic behavior of four alternative cap designs simulated with UTM is described in Luxmoore and Tharp (1993).

- Forested watershed in southeastern Missouri—Simulation of water budgets and heavy metal transport in a watershed adjacent to a lead mining and smelter operation is reported in Luxmoore and Begovich (1979).

The experience gained from these studies provides a sound basis for analysis of the CIIDF water budgets and closure scenarios. Several sensitivity studies have also been conducted and are reported in Luxmoore, Stolzy, and Holdeman (1976); Begovich and Luxmoore (1979); Luxmoore, Stolzy, and Holdeman (1981); and Sharma et al. (1987). These studies have provided a thorough appreciation for the important vegetation and soil variables in water budget modeling for CIIDF and provide the basis for concluding that UTM is both verified and validated to an extent that is reasonable for this PA.

3.3.6.2 Verification and Validation of SOURCE1

The SOURCE1 computer code consists of a collection of models that, taken together, simulate the performance of a tumulus-type disposal facility. These models, which include structural analysis, cracking analyses, concrete- and metal-barrier degradation, and radionuclide release calculations, were developed separately based on established theory and, in some cases, empiricism. The individual models were then combined to form the overall conceptual model for the disposal facility performance.

To verify the SOURCE1 computer code, quality assurance (Icenhour 1994) and verification plans (Icenhour and Tharp 1994) were developed and implemented. The verification plan consisted of a detailed review of the algorithms used in the SOURCE1 code, a review of code structure and programming, and a comparison of different advective transport models. In addition, tools such as sensitivity analyses and graphical representation of output were used to evaluate the performance of

the SOURCE1 code (Icenhour 1995). Verification of SOURCE1 was completed according to the verification plan; the user's manual reflects the changes that were made during the verification process. Supporting data are available in the literature for validation of many of the individual models. However, the limited performance data available for the tumulus-type disposal facility and the length of the performance simulations (≥1000 years) make the overall validation of SOURCE1 a complex task that cannot currently be addressed.

3.3.6.3 Verification and Validation of PADSIM

PADSIM is a custom-written FORTRAN code prepared for this PA. The code calculates two well-accepted phenomena, chemical adsorption (K_d) and radionuclide decay, using annual time steps. The chemical adsorption calculation with K_d is an appropriate representation of adsorption according to Jardine, Jacobs, and Wilson (1993), who demonstrated its utility for unsaturated flow in saprolite material. The half-life calculations are based on the precise half-life equation and the well-established half-life values for the various nuclides (Table 3.1).

Additional mechanisms have been added in PADSIM to account for (1) preferential flow of solutes during storm events and (2) expanding volume of soil matrix interacting with solutes with increase in time. PADSIM uses an annual time step for the long-term simulations required for this assessment. Incorporation of bypass flow and changing soil matrix volumes has been undertaken with a quantitative implementation of qualitative information. The algorithms for bypass flow and soil matrix volume were made a function of K_d such that nuclides with a low K_d had greater proportion of bypass flow and a more rapid expansion of soil matrix volume (Appendix D.3). These algorithms have not been verified or validated, but they capture the behavior of nuclide migration known to occur in ORR.

3.3.6.4 Verification and Validation of FTWORK

The documentation supplied with the FTWORK computer code (Faust et al. 1990) lists results for a number of test problems in which numerical solutions generated by FTWORK were compared with the corresponding analytical solution. These test problems include "Flow to Parallel Drains in an Unconfined Aquifer Subjected to Vertical Recharge" (analytical solution by Bear 1979), "Transient Flow to a Drain in a Semi-Infinite Aquifer Due to a Step Change in Head" (analytical solution by Venetis 1968), and "Unsteady Flow in a Confined Aquifer Near a Recharge Boundary" (analytical solution by Theis 1935). In all cases, the numerical solutions generated by FTWORK were nearly identical to the corresponding analytical solution, verifying the accuracy of the model's numerical formulation.

Prior to 1989, a tracer study was performed in West Bear Creek Valley in which a conservative tracer (a nonretarded, nondecaying dye called Rhodamine-WT) was injected into the ground at a test site located about 1 km west of the proposed CIIDF site. Comparison of the results from this study (Lee et al. 1989) to those generated numerically using the porous-medium modeling

program FTWORK was used to validate its use in simulating groundwater flow and contaminant transport in Bear Creek Valley. A description of the model grid and input parameters associated with the FTWORK model follows.

Numerical simulation of the development of the Rhodamine plume by FTWORK was accomplished by constructing a uniform model grid (20 × 20 × 1 cells) to represent the tracer study site. Model gridblock dimensions in the X and Y directions were 12 and 3 ft, respectively, and a uniform thickness of 15 ft was also assumed. Constant head (i.e., Dirichlet) boundary conditions corresponding to measured head values (Lee et al. 1989) were imposed on the outermost grid cells. The longitudinal component of the hydraulic conductivity tensor was set equal to 3.0 ft/d, and no recharge, retardation, or decay were assumed. The injection of dye was modeled by setting the initial concentration at the location of the injection point to 1×10^5 ppb. Initial contaminant concentrations at all other grid locations were identically zero. The remaining flow and transport parameters were set equal to those used in the analysis of the CIIDF facility (see Appendix E). These input values were used by FTWORK to generate a steady-state flow field. Once this was accomplished, a 180-d contaminant transport simulation was performed.

The results from the analysis are shown in Fig. 3.13, which depicts calculated concentrations at 30 and 180 d, respectively. Contour plots of the measured concentrations at 26 and 182 d (Lee et al. 1989) are also shown. Based on a comparison of the measured versus calculated concentrations at 30 and 180 d, FTWORK adequately reproduces the results of the tracer study. Hence, use of FTWORK in simulating groundwater flow contaminant transport in Bear Creek Valley is justified.

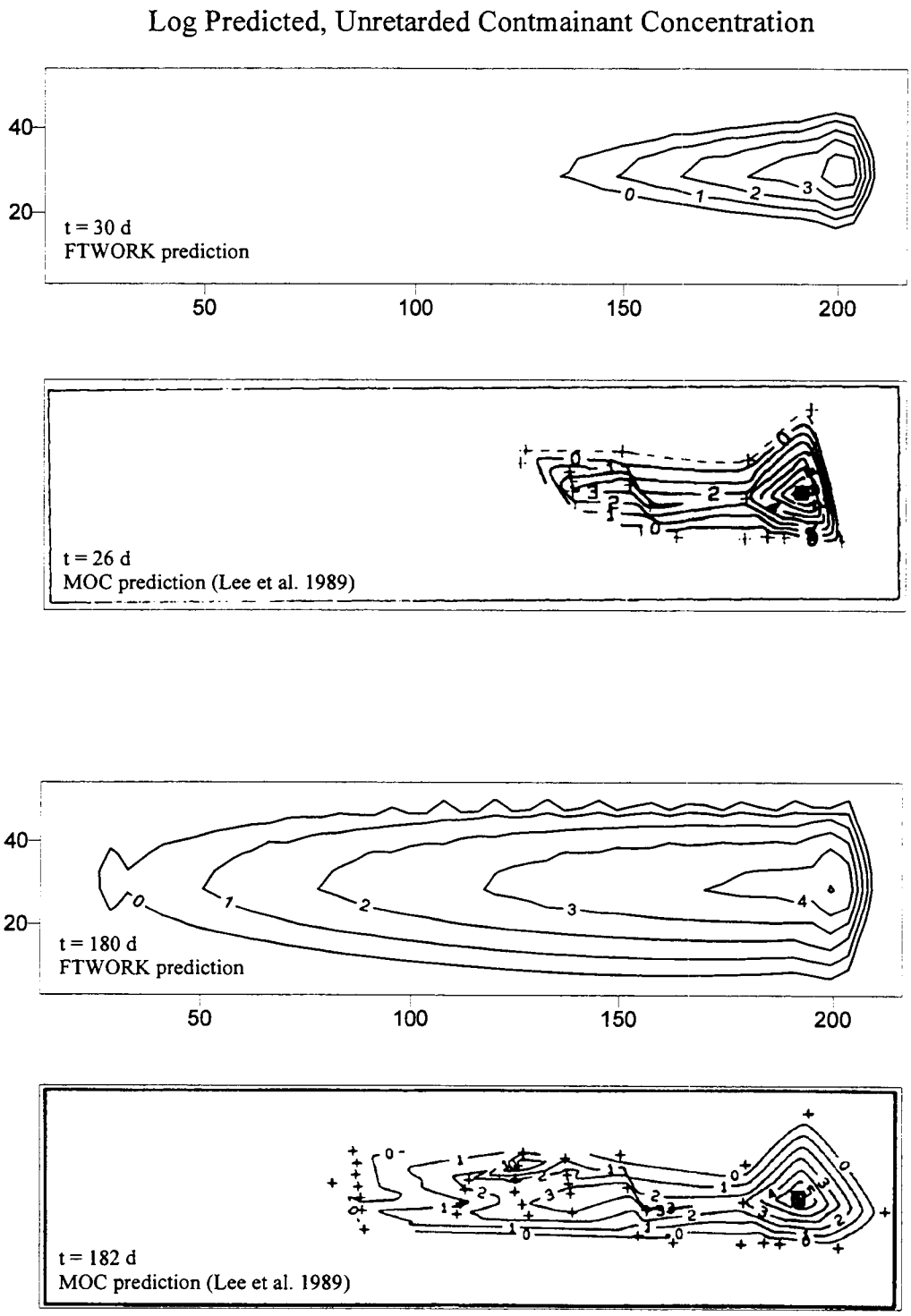

Fig. 3.13. Validation of FTWORK using study at the West Bear Creek site.

4. RESULTS OF ANALYSIS

This section presents the results of the analysis of the PA, a qualitative discussion of the sensitivity and uncertainty of the results, an interpretation of the results, and a discussion of continued work to be performed on this PA. The results from the analysis of the scenario for release and environmental transport, described in Sects. 3.1.1 and 3.1.2 and presented in Sects. 4.3 and 4.4.1, represent a reasonably conservative estimate of the long-term performance of the facility. The results from this scenario are applied to the performance objective for protection of the public and groundwater resources. The results from the analysis of the scenarios for direct intrusion, described in Sect. 3.1.2 and presented in Sect. 4.4.2, represent a reasonably conservative estimate of potential exposures to inadvertent intruders who could gain access to the facility in the future.

The results of these analyses have been prepared to define the limiting average concentration and inventory for each radionuclide that could be present in wastes generated on ORR for each scenario considered. The most restrictive of these limiting average concentrations for each radionuclide becomes the allowable average concentration and inventory for that radionuclide in wastes. The application of these allowable concentrations and inventories for assessment of wastes with mixtures of radionuclides is also presented. To calculate the limiting inventories for each radionuclide for each scenario, the calculations were done by iteration for linear processes. In other words, the dose objective was converted to a concentration at the point of exposure, the model for that particular scenario was used to back-calculate the concentration of the radionuclide in soil or water, and then the source term model was used to determine the corresponding limiting inventory in waste. For the environmental transport scenario with a nonlinear model, the calculations were performed iteratively to establish the limiting inventory in waste. The results in this section are presented beginning with the limiting inventory of radionuclides in waste calculated in the analysis to the point of exposure. Consequently, these results represent the final iteration of the many calculations made for this PA and provide waste inventories that are consistent with the performance objectives of DOE Order 5820.2A.

For the purposes of illustration of transport behavior throughout the analyses, a subset of radionuclides was selected. These species, listed in Table 4.1, cover ranges of half-lives and distribution coefficients (K_ds) which are representative of the full suite of 60 presented in Table 3.1.

4.1 SITE HYDROLOGY

Results from terrain analysis and site water budget modeling provided the hydrologic basis needed for site-specific nuclide transport calculations applicable to the CIIDF site. Terrain analysis gave the basis for determining elevated recharge in zones with greater durations of elevated soil water status. The spatially varying groundwater recharge results were input for calibration of the FTWORK groundwater model. Additionally, water budget simulations provided monthly seepage values used in

Table 4.1. Subset of representative radionuclides used to illustrate transport behavior

Nuclide	Half-life	Waste K_d
^{3}H	Short	Low
^{14}C	Medium	Low
^{60}Co	Short	High
^{90}Sr	Short	Medium
^{99}Tc	Long	Low
^{137}Cs	Short	Medium
$^{238}U^{a}$	Long	High

[a]Release rate was limited by solubility for the inventory analyzed.

nuclide transport from the tumulus pads simulated with the SOURCE1 model. Results from these hydrologic calculations are presented in the next two subsections.

4.1.1 Terrain Analysis and Site Recharge

The topographic index results from the digital terrain analysis were grouped arbitrarily (Fig. 4.1) to identify stream channels with ephemeral flow (shown in black) and some light grey areas where water flow through ephemeral wetlands is expected. The majority (87%) of the CIIDF site and surroundings (dark grey areas) contribute water flow to ephemeral wetlands and stream channels. Recharge estimates for the three differing wetness conditions were estimated from UTM simulations and recharge values determined from hydrologic modeling for ORR (Sect. 3.2.3.2). Locations with greater ephemeral wetness were given higher recharge values. The annual recharge estimates below were provided as input for groundwater modeling of the CIIDF site with the FTWORK model:

	Recharge (mm/year)	**Proportional area (%)**	**ln(a/tanβ)**
Stream channels	180	2.4	>11.0
Ephemeral wetlands	140	10.6	9.0–11.0
Remaining landscape	90	87.0	<9.0

The ln(a/tanβ) values are the topographic index ranges from Fig. 3.4 associated with the three landscape components, as discussed in Sect. 3.3.2.1.

Channel (black) : 2.4%

Wetlands (light grey) : 10.6%

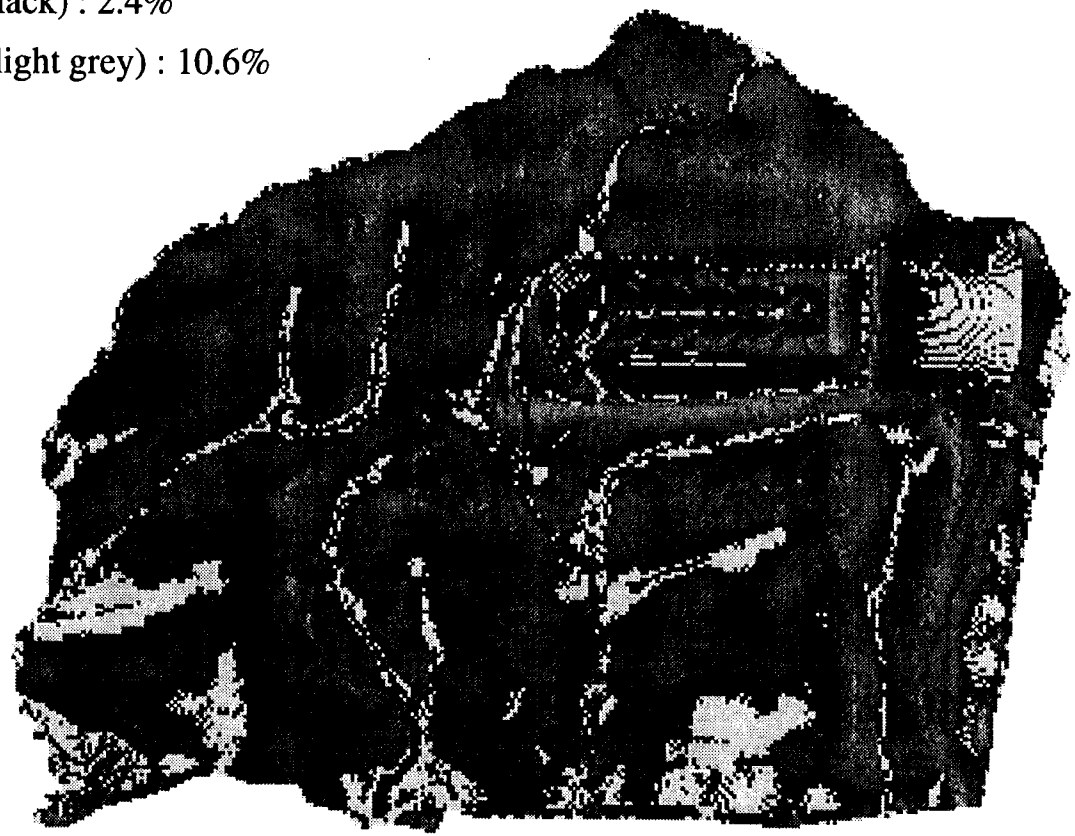

Fig. 4.1. Areas of stream channels (black), ephemeral wetlands (light grey), and remaining areas identified with differing rates of recharge from terrain analysis.

4.1.2 Site Water Budgets

The site water budgets were used to estimate the quantity of water interacting with concrete vaults during all phases of site assessment.

UTM provided hydrologic simulations of surface runoff, lateral flow, and soil water drainage using inputs of hourly precipitation and daily weather conditions for three selected years. Data from the ORR for three years having high (1895-mm), average (1372-mm), and low (933-mm) annual precipitation were used to compare a range of simulated hydrologic conditions. During the period of pad construction and the loading of pads with concrete vaults, the conservative assumption was made that the vaults were exposed to precipitation. Monthly precipitation values for the average year were used as seepage values for the SOURCE1 model during the period 2000–2021. This period included two years for construction of a compacted soil cap over the tumulus pads at the end of pad loading.

The monthly sums of surface runoff, lateral flow, and drainage were obtained from UTM simulations for the monitored and postmonitoring periods. These results (Table 4.2) showed seasonal differences, particularly during and after development of a leaking cap (after year 2042). Reduced drainage and lateral flow occurred in the July–November period, when evapotranspiration was high. Lateral flow increased as annual precipitation increased from a dry to a wet year. Lateral flow was excluded from interaction with vaults during the period of effective cap operation. A low hydraulic conductivity value was used for the geotextile and compacted soil layer (saturated conductivity of 1.2×10^{-7} m/s) in water budgets simulated for the functional cap period (2022–2031). During this period, some drainage entered each tumulus as seepage through leaks in seams of the flexible geomembrane within the cap. In the following 10 years (2032–2041), a linear ramp function was used to estimate drainage entering the stacked vaults. In the remaining 80 years of the monitoring period, drainage was high as a result of failure of the cap, represented by macropore flow algorithms in UTM. The simulation results for the period 2042–2121 (cap failure) and for the postmonitoring period (forest) were the same (Table 4.2). Strong seasonality was shown with high lateral flow during the late winter and spring months of this period.

The monthly water flow values in Table 4.2 are shown on a per unit area basis (mm^3/mm^2). After 2021, the UTM drainage and lateral flow results for the average year were summed and used as seepage estimates for use in the SOURCE1 model (Table 4.3). The conditions selected for the dry, average, and wet years were made on the basis of annual precipitation. In some cases monthly precipitation values for a wetter case were less than for the drier case. The use of actual weather data in the water budget simulations preserved the natural relationships between meteorological variables needed for calculation of evapotranspiration.

Table 4.2. Monthly precipitation, soil water drainage, lateral subsurface flow, and surface runoff results from the Unified Transport Model for three sets of weather conditions and various periods at the CIIDF site

Operation period	Precipitation (mm/month)			Month[b]
	Dry	Average[a]	Wet	
2000–2021 Pad loading and cap construction; gravel surface; exposed vaults	106.2	124.2	111.3	Jan
	17.5	124.2	98.3	Feb
	117.1	116.8	284.2	Mar
	113.5	109.2	126.5	Apr
	93.5	157.5	268.0	May
	104.9	84.8	140.5	Jun
	53.1	234.4	151.4	Jul
	49.3	62.0	39.9	Aug
	55.6	80.0	73.2	Sep
	56.6	63.8	86.6	Oct
	56.9	55.4	274.1	Nov
	108.7	159.8	241.3	Dec

	Drainage (mm/month)			Lateral flow (mm/month)			Runoff (mm/month)		
	Dry	Average	Wet	Dry	Average	Wet	Dry	Average	Wet
2022–2031 Monitored closure; grass cover; cap functional; LAI[c] = 4.9	0.1	0.3	2.9	0.0	0.0	0.0	0.0	0.0	0.0
	0.7	3.8	7.8	0.0	0.0	0.0	0.0	0.0	0.0
	2.6	11.2	20.1	0.0	0.0	0.0	0.0	0.0	0.0
	8.0	11.2	18.3	0.0	0.0	0.0	0.0	0.0	0.0
	7.8	7.7	9.0	0.0	0.0	0.0	0.0	0.0	0.0
	2.9	3.4	4.6	0.0	0.0	0.0	0.0	0.0	0.0
	1.5	1.6	2.4	0.0	0.0	0.0	0.0	0.0	0.0
	0.7	0.8	1.1	0.0	0.0	0.0	0.0	0.0	0.0
	0.4	0.4	0.6	0.0	0.0	0.0	0.0	0.0	0.0
	0.2	0.2	0.3	0.0	0.0	0.0	0.0	0.0	0.0
	0.1	0.1	0.2	0.0	0.0	0.0	0.0	0.0	0.0
	0.1	0.1	0.2	0.0	0.0	0.0	0.0	0.0	0.0
2032–2041 Monitored closure; 10-year linear ramp in drainage with cap failure									

Table 4.2 (continued)

	Drainage (mm/month)			Lateral flow (mm/month)			Runoff (mm/month)		
	Dry	Average	Wet	Dry	Average	Wet	Dry	Average	Wet
2042–2121 Monitored closure; grass cover; leaking cap	3.3	15.5	15.5	0.0	81.9	84.0	0.0	0.0	0.0
	13.3	14.0	14.0	0.0	84.5	94.5	0.0	0.0	0.0
	15.5	15.5	15.5	24.9	97.0	215.6	0.0	0.0	0.0
	15.0	15.0	15.0	73.1	60.9	84.7	0.0	0.0	0.0
2122+ Postmonitoring; Forest cover; LAI[c] = 4.9	15.5	15.5	15.5	24.9	108.9	139.4	0.0	0.0	0.0
	15.0	15.0	15.0	5.6	17.1	35.1	0.0	0.0	0.0
	15.5	15.5	15.5	0.0	0.3	12.5	0.0	0.0	0.0
	14.7	15.5	15.5	0.0	1.6	0.0	0.0	0.0	0.0
	6.3	15.0	15.0	0.0	1.5	0.0	0.0	0.0	0.0
	4.6	15.5	15.5	0.0	0.0	0.0	0.0	0.0	0.0
	3.8	13.6	9.6	0.0	0.0	105.2	0.0	0.0	0.0
	3.4	8.5	15.5	0.0	0.0	166.7	0.0	0.0	0.0

[a] The values for the average case were used to determine seepage for simulation with SOURCE1 (see Table 4.3).
[b] Each column shows twelve monthly values, beginning with January.
[c] LAI = leaf area index (m^2/m^2)

4.2 SOURCE TERM

The SOURCE1 computer code was used to calculate source terms for CIIDF. Input parameters for SOURCE1 are listed in Sect. 3.3.3.2. Additional input parameters to the code were water seepage rates and the initial radionuclide inventory. The calculation of water seepage rates is described in Sect. 4.1. The water seepage rates used in all source term simulations are listed in Table 4.3. For environmental transport calculations, radionuclide inventories were determined iteratively by calculating peak groundwater and surface water concentrations and comparing these calculated values with concentration limits. The inventory was varied until either the groundwater or surface water concentration equaled the concentration limits developed in Sect. 4.4 (see Table 4.12). For environmental transport, the results of the final iteration are presented in Sect. 4.2.1. Source term results for direct intrusion are presented in Sect. 4.2.2.

4.2.1 Source Terms for Environmental Transport

SOURCE1 provides the release rate of a radionuclide (grams of nuclide released per year) from all of the disposal vaults on a disposal pad. This release is then divided into two components based on knowledge of site hydrology: a vertical component which is available for recharge to groundwater and a lateral component which is available for shallow subsurface transport. Table 4.4 provides an abridged illustration of SOURCE1 output for a simulation for ^{137}Cs release from one CIIDF disposal pad. This table presents, as a function of time, (1) the total ^{137}Cs inventory remaining

Table 4.3. Simulated monthly seepage results used in source term calculations for CIIDF

Year of simulation	Monthly seepage (cm)											
	Jan	Feb	Mar	Apr	May	Jun	Jul	Aug	Sep	Oct	Nov	Dec
1–22	12.42	12.42	11.68	10.92	15.75	8.48	23.44	6.20	8.00	6.38	5.54	15.98
23–32	0.03	0.38	1.12	1.12	0.77	0.34	0.16	0.08	0.04	0.02	0.01	0.01
33	0.91	1.24	2.04	1.71	1.83	0.60	0.29	0.23	0.19	0.16	0.13	0.09
34	1.80	2.10	2.96	2.30	2.89	0.86	0.42	0.38	0.33	0.30	0.26	0.16
35	2.68	2.96	3.88	2.88	3.95	1.12	0.55	0.52	0.48	0.44	0.38	0.24
36	3.56	3.82	4.80	3.47	5.01	1.38	0.68	0.67	0.63	0.58	0.50	0.32
37	4.44	4.68	5.72	4.06	6.07	1.64	0.81	0.82	0.77	0.72	0.62	0.39
38	5.33	5.55	6.65	4.65	7.14	1.91	0.93	0.97	0.92	0.85	0.75	0.47
39	6.21	6.41	7.57	5.24	8.20	2.17	1.06	1.12	1.06	0.99	0.87	0.54
40	7.09	7.27	8.49	5.83	9.26	2.43	1.19	1.27	1.21	1.13	0.99	0.62
41	7.97	8.13	9.41	6.41	10.32	2.69	1.32	1.41	1.36	1.27	1.11	0.70
42	8.86	8.99	10.33	7.00	11.38	2.95	1.45	1.56	1.50	1.41	1.24	0.77
43–99999	9.74	9.85	11.25	7.59	12.44	3.21	1.58	1.71	1.65	1.55	1.36	0.85

Table 4.4. Abridged[a] SOURCE1 output for ^{137}Cs[b]

Year	Inventory remaining[c] (g)	Calculated release from a disposal pad[d]				Calculated release to environment[d]	
		Advection (g/year)	Diffusion (g/year)	Total (g/year)	Cumulative (g)	Vertical (g/year)	Lateral (g/year)
1	4.14×10^{3}	4.01×10^{-5}	0.00×10^{0}	4.01×10^{-5}	4.01×10^{-5}	1.32×10^{-6}	7.01×10^{-6}
2	4.05×10^{3}	7.83×10^{-5}	0.00×10^{0}	7.83×10^{-5}	1.18×10^{-4}	2.68×10^{-6}	1.42×10^{-5}
3	3.96×10^{3}	1.15×10^{-4}	0.00×10^{0}	1.15×10^{-4}	2.33×10^{-4}	4.07×10^{-6}	2.16×10^{-5}
4	3.87×10^{3}	1.50×10^{-4}	0.00×10^{0}	1.50×10^{-4}	3.83×10^{-4}	5.49×10^{-6}	2.92×10^{-5}
5	3.78×10^{3}	1.83×10^{-4}	0.00×10^{0}	1.83×10^{-4}	5.65×10^{-4}	6.94×10^{-6}	3.69×10^{-5}
6	3.69×10^{3}	2.14×10^{-4}	0.00×10^{0}	2.14×10^{-4}	7.79×10^{-4}	8.41×10^{-6}	4.47×10^{-5}
7	3.61×10^{3}	2.44×10^{-4}	3.71×10^{-32}	2.44×10^{-4}	1.02×10^{-3}	9.89×10^{-6}	5.26×10^{-5}
8	3.52×10^{3}	2.73×10^{-4}	3.14×10^{-28}	2.73×10^{-4}	1.30×10^{-3}	1.14×10^{-5}	6.06×10^{-5}
9	3.44×10^{3}	3.00×10^{-4}	3.66×10^{-25}	3.00×10^{-4}	1.60×10^{-3}	1.29×10^{-5}	6.86×10^{-5}
10	3.37×10^{3}	3.25×10^{-4}	1.06×10^{-22}	3.25×10^{-4}	1.92×10^{-3}	1.44×10^{-5}	7.67×10^{-5}
11	3.29×10^{3}	3.50×10^{-4}	1.12×10^{-20}	3.50×10^{-4}	2.27×10^{-3}	1.59×10^{-5}	8.48×10^{-5}
12	3.21×10^{3}	3.73×10^{-4}	5.53×10^{-19}	3.73×10^{-4}	2.64×10^{-3}	1.75×10^{-5}	9.29×10^{-5}
13	3.14×10^{3}	3.95×10^{-4}	1.51×10^{-17}	3.95×10^{-4}	3.04×10^{-3}	1.90×10^{-5}	1.01×10^{-4}
14	3.07×10^{3}	4.15×10^{-4}	2.61×10^{-16}	4.15×10^{-4}	3.45×10^{-3}	2.05×10^{-5}	1.09×10^{-4}
15	3.00×10^{3}	4.35×10^{-4}	3.10×10^{-15}	4.35×10^{-4}	3.89×10^{-3}	2.20×10^{-5}	1.17×10^{-4}
16	2.93×10^{3}	4.53×10^{-4}	2.73×10^{-14}	4.53×10^{-4}	4.34×10^{-3}	2.35×10^{-5}	1.25×10^{-4}
17	2.86×10^{3}	4.71×10^{-4}	1.87×10^{-13}	4.71×10^{-4}	4.81×10^{-3}	2.50×10^{-5}	1.33×10^{-4}
18	2.80×10^{3}	4.87×10^{-4}	1.04×10^{-12}	4.87×10^{-4}	5.30×10^{-3}	2.65×10^{-5}	1.41×10^{-4}
19	2.73×10^{3}	5.02×10^{-4}	4.84×10^{-12}	5.02×10^{-4}	5.80×10^{-3}	2.80×10^{-5}	1.49×10^{-4}
20	2.67×10^{3}	5.17×10^{-4}	1.94×10^{-11}	5.17×10^{-4}	6.32×10^{-3}	2.94×10^{-5}	1.57×10^{-4}
21	2.61×10^{3}	5.30×10^{-4}	6.86×10^{-11}	5.30×10^{-4}	6.85×10^{-3}	3.09×10^{-5}	1.64×10^{-4}
22	2.55×10^{3}	5.42×10^{-4}	2.16×10^{-10}	5.42×10^{-4}	7.39×10^{-3}	3.23×10^{-5}	1.72×10^{-4}
23	2.49×10^{3}	5.54×10^{-4}	6.20×10^{-10}	5.54×10^{-4}	7.94×10^{-3}	2.13×10^{-4}	0.00×10^{0}
24	2.44×10^{3}	5.65×10^{-4}	1.63×10^{-9}	5.65×10^{-4}	8.51×10^{-3}	2.22×10^{-4}	0.00×10^{0}
25	2.38×10^{3}	5.75×10^{-4}	3.97×10^{-9}	5.75×10^{-4}	9.08×10^{-3}	2.30×10^{-4}	0.00×10^{0}
26	2.33×10^{3}	5.85×10^{-4}	9.07×10^{-9}	5.85×10^{-4}	9.67×10^{-3}	2.38×10^{-4}	0.00×10^{0}
27	2.27×10^{3}	5.93×10^{-4}	1.95×10^{-8}	5.93×10^{-4}	1.03×10^{-2}	2.47×10^{-4}	0.00×10^{0}
28	2.22×10^{3}	6.01×10^{-4}	3.97×10^{-8}	6.01×10^{-4}	1.09×10^{-2}	2.55×10^{-4}	0.00×10^{0}
29	2.17×10^{3}	6.08×10^{-4}	7.72×10^{-8}	6.08×10^{-4}	1.15×10^{-2}	2.63×10^{-4}	0.00×10^{0}
30	2.12×10^{3}	6.15×10^{-4}	1.44×10^{-7}	6.15×10^{-4}	1.21×10^{-2}	2.71×10^{-4}	0.00×10^{0}
31	2.07×10^{3}	6.21×10^{-4}	2.57×10^{-7}	6.21×10^{-4}	1.27×10^{-2}	2.78×10^{-4}	0.00×10^{0}
32	2.02×10^{3}	6.26×10^{-4}	4.45×10^{-7}	6.27×10^{-4}	1.33×10^{-2}	2.86×10^{-4}	0.00×10^{0}
33	1.98×10^{3}	6.31×10^{-4}	7.44×10^{-7}	6.32×10^{-4}	1.40×10^{-2}	2.81×10^{-4}	1.27×10^{-5}
34	1.93×10^{3}	6.35×10^{-4}	1.21×10^{-6}	6.37×10^{-4}	1.46×10^{-2}	2.57×10^{-4}	4.38×10^{-5}
35	1.89×10^{3}	6.39×10^{-4}	1.91×10^{-6}	6.41×10^{-4}	1.52×10^{-2}	2.40×10^{-4}	6.75×10^{-5}
36	1.85×10^{3}	6.42×10^{-4}	2.94×10^{-6}	6.45×10^{-4}	1.59×10^{-2}	2.33×10^{-4}	8.24×10^{-5}
37	1.80×10^{3}	6.45×10^{-4}	4.44×10^{-6}	6.50×10^{-4}	1.65×10^{-2}	2.27×10^{-4}	9.54×10^{-5}
38	1.76×10^{3}	6.47×10^{-4}	6.55×10^{-6}	6.54×10^{-4}	1.72×10^{-2}	2.22×10^{-4}	1.08×10^{-4}
39	1.72×10^{3}	6.49×10^{-4}	9.47×10^{-6}	6.59×10^{-4}	1.79×10^{-2}	2.19×10^{-4}	1.18×10^{-4}
40	1.68×10^{3}	6.51×10^{-4}	1.35×10^{-5}	6.64×10^{-4}	1.85×10^{-2}	2.18×10^{-4}	1.27×10^{-4}
41	1.64×10^{3}	6.52×10^{-4}	1.88×10^{-5}	6.71×10^{-4}	1.92×10^{-2}	2.18×10^{-4}	1.36×10^{-4}

Table 4.4 (continued)

Year	Inventory remaining[c] (g)	Calculated release from a disposal pad[d]				Calculated release to environment[d]	
		Advection (g/year)	Diffusion (g/year)	Total (g/year)	Cumulative (g)	Vertical (g/year)	Lateral (g/year)
42	1.60×10^{3}	3.95×10^{0}	2.59×10^{-5}	3.95×10^{0}	3.97×10^{0}	6.24×10^{-1}	1.49×10^{0}
43	1.56×10^{3}	4.28×10^{0}	3.50×10^{-5}	4.28×10^{0}	8.25×10^{0}	6.44×10^{-1}	1.68×10^{0}
44	1.52×10^{3}	4.24×10^{0}	4.66×10^{-5}	4.24×10^{0}	1.25×10^{1}	6.48×10^{-1}	1.69×10^{0}
45	1.48×10^{3}	4.21×10^{0}	6.14×10^{-5}	4.21×10^{0}	1.67×10^{1}	6.52×10^{-1}	1.70×10^{0}
46	1.45×10^{3}	4.16×10^{0}	7.99×10^{-5}	4.16×10^{0}	2.09×10^{1}	6.54×10^{-1}	1.71×10^{0}
47	1.41×10^{3}	4.12×10^{0}	1.03×10^{-4}	4.12×10^{0}	2.50×10^{1}	6.57×10^{-1}	1.72×10^{0}
48	1.37×10^{3}	4.08×10^{0}	1.31×10^{-4}	4.08×10^{0}	2.91×10^{1}	6.58×10^{-1}	1.72×10^{0}
49	1.34×10^{3}	4.03×10^{0}	1.65×10^{-4}	4.03×10^{0}	3.31×10^{1}	6.60×10^{-1}	1.72×10^{0}
50	1.30×10^{3}	3.98×10^{0}	2.06×10^{-4}	3.98×10^{0}	3.71×10^{1}	6.60×10^{-1}	1.73×10^{0}
51	1.27×10^{3}	3.93×10^{0}	2.54×10^{-4}	3.93×10^{0}	4.10×10^{1}	6.60×10^{-1}	1.73×10^{0}
52	1.24×10^{3}	3.87×10^{0}	3.12×10^{-4}	3.87×10^{0}	4.49×10^{1}	6.60×10^{-1}	1.73×10^{0}
53	1.20×10^{3}	3.82×10^{0}	3.80×10^{-4}	3.82×10^{0}	4.87×10^{1}	6.59×10^{-1}	1.72×10^{0}
54	1.17×10^{3}	3.76×10^{0}	4.59×10^{-4}	3.76×10^{0}	5.24×10^{1}	6.58×10^{-1}	1.72×10^{0}
55	1.14×10^{3}	3.71×10^{0}	5.50×10^{-4}	3.71×10^{0}	5.62×10^{1}	6.56×10^{-1}	1.72×10^{0}
56	1.11×10^{3}	3.65×10^{0}	6.56×10^{-4}	3.65×10^{0}	5.98×10^{1}	6.54×10^{-1}	1.71×10^{0}
57	1.08×10^{3}	3.59×10^{0}	7.76×10^{-4}	3.59×10^{0}	6.34×10^{1}	6.51×10^{-1}	1.70×10^{0}
58	1.05×10^{3}	3.53×10^{0}	9.14×10^{-4}	3.53×10^{0}	6.69×10^{1}	6.48×10^{-1}	1.70×10^{0}
59	1.03×10^{3}	3.47×10^{0}	1.07×10^{-3}	3.47×10^{0}	7.04×10^{1}	6.45×10^{-1}	1.69×10^{0}
60	1.00×10^{3}	3.41×10^{0}	1.24×10^{-3}	3.41×10^{0}	7.38×10^{1}	6.41×10^{-1}	1.68×10^{0}
61	9.74×10^{2}	3.29×10^{0}	1.42×10^{-3}	3.29×10^{0}	7.71×10^{1}	6.27×10^{-1}	1.64×10^{0}
62	9.49×10^{2}	3.18×10^{0}	1.60×10^{-3}	3.18×10^{0}	8.03×10^{1}	6.12×10^{-1}	1.60×10^{0}
63	9.24×10^{2}	3.07×10^{0}	1.81×10^{-3}	3.07×10^{0}	8.34×10^{1}	5.98×10^{-1}	1.57×10^{0}
64	9.00×10^{2}	2.97×10^{0}	2.03×10^{-3}	2.97×10^{0}	8.63×10^{1}	5.85×10^{-1}	1.53×10^{0}
65	8.76×10^{2}	2.87×10^{0}	2.28×10^{-3}	2.87×10^{0}	8.92×10^{1}	5.71×10^{-1}	1.49×10^{0}
66	8.54×10^{2}	2.77×10^{0}	2.54×10^{-3}	2.77×10^{0}	9.20×10^{1}	5.58×10^{-1}	1.46×10^{0}
67	8.31×10^{2}	2.67×10^{0}	2.82×10^{-3}	2.68×10^{0}	9.46×10^{1}	5.45×10^{-1}	1.43×10^{0}
68	8.10×10^{2}	2.58×10^{0}	3.12×10^{-3}	2.59×10^{0}	9.72×10^{1}	5.32×10^{-1}	1.39×10^{0}
69	7.89×10^{2}	2.50×10^{0}	3.44×10^{-3}	2.50×10^{0}	9.97×10^{1}	5.19×10^{-1}	1.36×10^{0}
70	7.68×10^{2}	2.41×10^{0}	3.78×10^{-3}	2.41×10^{0}	1.02×10^{2}	5.07×10^{-1}	1.33×10^{0}
71	7.49×10^{2}	2.33×10^{0}	4.14×10^{-3}	2.33×10^{0}	1.04×10^{2}	4.95×10^{-1}	1.30×10^{0}
72	7.29×10^{2}	2.25×10^{0}	4.52×10^{-3}	2.25×10^{0}	1.07×10^{2}	4.83×10^{-1}	1.27×10^{0}
73	7.10×10^{2}	2.17×10^{0}	4.92×10^{-3}	2.18×10^{0}	1.09×10^{2}	4.72×10^{-1}	1.24×10^{0}
74	6.92×10^{2}	2.10×10^{0}	5.35×10^{-3}	2.10×10^{0}	1.11×10^{2}	4.60×10^{-1}	1.21×10^{0}
75	6.74×10^{2}	2.03×10^{0}	5.79×10^{-3}	2.03×10^{0}	1.13×10^{2}	4.49×10^{-1}	1.18×10^{0}
76	6.57×10^{2}	1.96×10^{0}	6.26×10^{-3}	1.96×10^{0}	1.15×10^{2}	4.38×10^{-1}	1.15×10^{0}
77	6.40×10^{2}	1.89×10^{0}	6.75×10^{-3}	1.90×10^{0}	1.17×10^{2}	4.28×10^{-1}	1.12×10^{0}
78	6.23×10^{2}	1.83×10^{0}	7.25×10^{-3}	1.83×10^{0}	1.19×10^{2}	4.17×10^{-1}	1.09×10^{0}
79	6.07×10^{2}	1.76×10^{0}	7.78×10^{-3}	1.77×10^{0}	1.21×10^{2}	4.07×10^{-1}	1.07×10^{0}
80	5.92×10^{2}	1.70×10^{0}	8.33×10^{-3}	1.71×10^{0}	1.22×10^{2}	3.97×10^{-1}	1.04×10^{0}
81	5.77×10^{2}	1.65×10^{0}	8.90×10^{-3}	1.66×10^{0}	1.24×10^{2}	3.88×10^{-1}	1.02×10^{0}
82	5.62×10^{2}	1.59×10^{0}	9.49×10^{-3}	1.60×10^{0}	1.25×10^{2}	3.78×10^{-1}	9.91×10^{-1}
83	5.48×10^{2}	1.54×10^{0}	1.01×10^{-2}	1.55×10^{0}	1.27×10^{2}	3.69×10^{-1}	9.67×10^{-1}
84	5.34×10^{2}	1.48×10^{0}	1.07×10^{-2}	1.49×10^{0}	1.29×10^{2}	3.60×10^{-1}	9.43×10^{-1}

Table 4.4 (continued)

Year	Inventory remaining[c] (g)	Calculated release from a disposal pad[d]				Calculated release to environment[d]	
		Advection (g/year)	Diffusion (g/year)	Total (g/year)	Cumulative (g)	Vertical (g/year)	Lateral (g/year)
85	5.20×10^{2}	1.43×10^{0}	1.14×10^{-2}	1.44×10^{0}	1.30×10^{2}	3.51×10^{-1}	9.20×10^{-1}
86	5.07×10^{2}	1.38×10^{0}	1.20×10^{-2}	1.40×10^{0}	1.31×10^{2}	3.42×10^{-1}	8.98×10^{-1}
87	4.94×10^{2}	1.34×10^{0}	1.27×10^{-2}	1.35×10^{0}	1.33×10^{2}	3.33×10^{-1}	8.76×10^{-1}
88	4.81×10^{2}	1.29×10^{0}	1.34×10^{-2}	1.30×10^{0}	1.34×10^{2}	3.25×10^{-1}	8.54×10^{-1}
89	4.69×10^{2}	1.25×10^{0}	1.41×10^{-2}	1.26×10^{0}	1.35×10^{2}	3.17×10^{-1}	8.33×10^{-1}
90	4.57×10^{2}	1.20×10^{0}	1.48×10^{-2}	1.22×10^{0}	1.36×10^{2}	3.09×10^{-1}	8.13×10^{-1}
91	4.45×10^{2}	1.16×10^{0}	1.56×10^{-2}	1.18×10^{0}	1.38×10^{2}	3.01×10^{-1}	7.93×10^{-1}
92	4.34×10^{2}	1.12×10^{0}	1.63×10^{-2}	1.14×10^{0}	1.39×10^{2}	2.94×10^{-1}	7.74×10^{-1}
93	4.23×10^{2}	1.09×10^{0}	1.71×10^{-2}	1.10×10^{0}	1.40×10^{2}	2.87×10^{-1}	7.55×10^{-1}
94	4.10×10^{2}	2.90×10^{0}	1.79×10^{-2}	2.91×10^{0}	1.43×10^{2}	7.66×10^{-1}	2.01×10^{0}
95	3.98×10^{2}	2.80×10^{0}	1.86×10^{-2}	2.82×10^{0}	1.46×10^{2}	7.46×10^{-1}	1.96×10^{0}
96	3.86×10^{2}	2.70×10^{0}	1.93×10^{-2}	2.72×10^{0}	1.48×10^{2}	7.27×10^{-1}	1.91×10^{0}
97	3.75×10^{2}	2.61×10^{0}	2.00×10^{-2}	2.63×10^{0}	1.51×10^{2}	7.08×10^{-1}	1.86×10^{0}
98	3.64×10^{2}	2.52×10^{0}	2.07×10^{-2}	2.54×10^{0}	1.54×10^{2}	6.90×10^{-1}	1.81×10^{0}
99	3.53×10^{2}	2.44×10^{0}	2.14×10^{-2}	2.46×10^{0}	1.56×10^{2}	6.72×10^{-1}	1.77×10^{0}
100	3.43×10^{2}	2.35×10^{0}	2.21×10^{-2}	2.37×10^{0}	1.58×10^{2}	6.55×10^{-1}	1.72×10^{0}
101	3.33×10^{2}	2.27×10^{0}	2.28×10^{-2}	2.30×10^{0}	1.61×10^{2}	6.32×10^{-1}	1.66×10^{0}
102	3.23×10^{2}	2.19×10^{0}	2.35×10^{-2}	2.22×10^{0}	1.63×10^{2}	6.11×10^{-1}	1.61×10^{0}
103	3.13×10^{2}	2.12×10^{0}	2.42×10^{-2}	2.14×10^{0}	1.65×10^{2}	5.91×10^{-1}	1.55×10^{0}
104	3.04×10^{2}	2.05×10^{0}	2.49×10^{-2}	2.07×10^{0}	1.67×10^{2}	5.71×10^{-1}	1.50×10^{0}
105	2.95×10^{2}	1.98×10^{0}	2.56×10^{-2}	2.00×10^{0}	1.69×10^{2}	5.51×10^{-1}	1.45×10^{0}
106	2.86×10^{2}	1.91×10^{0}	2.63×10^{-2}	1.94×10^{0}	1.71×10^{2}	5.33×10^{-1}	1.40×10^{0}
107	2.78×10^{2}	1.84×10^{0}	2.70×10^{-2}	1.87×10^{0}	1.73×10^{2}	5.15×10^{-1}	1.36×10^{0}
108	2.70×10^{2}	1.78×10^{0}	2.76×10^{-2}	1.81×10^{0}	1.75×10^{2}	4.98×10^{-1}	1.31×10^{0}
109	2.62×10^{2}	1.72×10^{0}	2.83×10^{-2}	1.75×10^{0}	1.76×10^{2}	4.81×10^{-1}	1.27×10^{0}
110	2.54×10^{2}	1.66×10^{0}	2.90×10^{-2}	1.69×10^{0}	1.78×10^{2}	4.65×10^{-1}	1.23×10^{0}
111	2.47×10^{2}	1.61×10^{0}	2.96×10^{-2}	1.63×10^{0}	1.80×10^{2}	4.49×10^{-1}	1.19×10^{0}
112	2.40×10^{2}	1.55×10^{0}	3.02×10^{-2}	1.58×10^{0}	1.81×10^{2}	4.34×10^{-1}	1.15×10^{0}
113	2.33×10^{2}	1.50×10^{0}	3.09×10^{-2}	1.53×10^{0}	1.83×10^{2}	4.20×10^{-1}	1.11×10^{0}
114	2.26×10^{2}	1.45×10^{0}	3.15×10^{-2}	1.48×10^{0}	1.84×10^{2}	4.06×10^{-1}	1.07×10^{0}
115	2.19×10^{2}	1.40×10^{0}	3.21×10^{-2}	1.43×10^{0}	1.86×10^{2}	3.92×10^{-1}	1.04×10^{0}
116	2.13×10^{2}	1.35×10^{0}	3.27×10^{-2}	1.38×10^{0}	1.87×10^{2}	3.79×10^{-1}	1.00×10^{0}
117	2.07×10^{2}	1.30×10^{0}	3.32×10^{-2}	1.34×10^{0}	1.89×10^{2}	3.66×10^{-1}	9.70×10^{-1}
118	2.01×10^{2}	1.26×10^{0}	3.38×10^{-2}	1.29×10^{0}	1.90×10^{2}	3.54×10^{-1}	9.38×10^{-1}
119	1.95×10^{2}	1.22×10^{0}	3.44×10^{-2}	1.25×10^{0}	1.91×10^{2}	3.42×10^{-1}	9.07×10^{-1}
120	1.89×10^{2}	1.17×10^{0}	3.49×10^{-2}	1.21×10^{0}	1.92×10^{2}	3.31×10^{-1}	8.78×10^{-1}
121	1.84×10^{2}	1.13×10^{0}	3.54×10^{-2}	1.17×10^{0}	1.93×10^{2}	3.20×10^{-1}	8.49×10^{-1}
122	1.78×10^{2}	1.09×10^{0}	3.59×10^{-2}	1.13×10^{0}	1.95×10^{2}	3.09×10^{-1}	8.21×10^{-1}
123	1.73×10^{2}	1.06×10^{0}	3.64×10^{-2}	1.09×10^{0}	1.96×10^{2}	2.99×10^{-1}	7.95×10^{-1}
124	1.68×10^{2}	1.02×10^{0}	3.69×10^{-2}	1.06×10^{0}	1.97×10^{2}	2.89×10^{-1}	7.69×10^{-1}
125	1.63×10^{2}	9.86×10^{-1}	3.74×10^{-2}	1.02×10^{0}	1.98×10^{2}	2.79×10^{-1}	7.44×10^{-1}
126	1.59×10^{2}	9.52×10^{-1}	3.78×10^{-2}	9.90×10^{-1}	1.99×10^{2}	2.70×10^{-1}	7.20×10^{-1}
127	1.54×10^{2}	9.19×10^{-1}	3.82×10^{-2}	9.58×10^{-1}	2.00×10^{2}	2.61×10^{-1}	6.97×10^{-1}

Table 4.4 (continued)

Year	Inventory remaining[c] (g)	Calculated release from a disposal pad[d]				Calculated release to environment[d]	
		Advection (g/year)	Diffusion (g/year)	Total (g/year)	Cumulative (g)	Vertical (g/year)	Lateral (g/year)
128	1.50×10^{2}	8.88×10^{-1}	3.87×10^{-2}	9.27×10^{-1}	2.01×10^{2}	2.52×10^{-1}	6.74×10^{-1}
129	1.45×10^{2}	8.57×10^{-1}	3.91×10^{-2}	8.96×10^{-1}	2.02×10^{2}	2.44×10^{-1}	6.53×10^{-1}
130	1.41×10^{2}	8.28×10^{-1}	3.94×10^{-2}	8.67×10^{-1}	2.02×10^{2}	2.36×10^{-1}	6.32×10^{-1}
131	1.37×10^{2}	8.00×10^{-1}	3.98×10^{-2}	8.39×10^{-1}	2.03×10^{2}	2.28×10^{-1}	6.11×10^{-1}
132	1.33×10^{2}	7.72×10^{-1}	4.02×10^{-2}	8.12×10^{-1}	2.04×10^{2}	2.21×10^{-1}	5.92×10^{-1}
133	1.29×10^{2}	7.46×10^{-1}	4.05×10^{-2}	7.86×10^{-1}	2.05×10^{2}	2.13×10^{-1}	5.73×10^{-1}
134	1.25×10^{2}	7.20×10^{-1}	4.08×10^{-2}	7.61×10^{-1}	2.06×10^{2}	2.06×10^{-1}	5.55×10^{-1}
135	1.22×10^{2}	6.95×10^{-1}	4.11×10^{-2}	7.36×10^{-1}	2.06×10^{2}	1.99×10^{-1}	5.37×10^{-1}
136	1.18×10^{2}	6.71×10^{-1}	4.14×10^{-2}	7.13×10^{-1}	2.07×10^{2}	1.93×10^{-1}	5.20×10^{-1}
137	1.15×10^{2}	6.48×10^{-1}	4.17×10^{-2}	6.90×10^{-1}	2.08×10^{2}	1.86×10^{-1}	5.03×10^{-1}
138	1.12×10^{2}	6.26×10^{-1}	4.19×10^{-2}	6.68×10^{-1}	2.08×10^{2}	1.80×10^{-1}	4.87×10^{-1}
139	1.08×10^{2}	6.04×10^{-1}	4.21×10^{-2}	6.46×10^{-1}	2.09×10^{2}	1.74×10^{-1}	4.72×10^{-1}
140	1.05×10^{2}	5.84×10^{-1}	4.24×10^{-2}	6.26×10^{-1}	2.10×10^{2}	1.69×10^{-1}	4.57×10^{-1}
141	1.02×10^{2}	5.63×10^{-1}	4.26×10^{-2}	6.06×10^{-1}	2.10×10^{2}	1.63×10^{-1}	4.43×10^{-1}
142	9.95×10^{1}	5.44×10^{-1}	4.27×10^{-2}	5.87×10^{-1}	2.11×10^{2}	1.58×10^{-1}	4.29×10^{-1}
143	9.66×10^{1}	5.25×10^{-1}	4.29×10^{-2}	5.68×10^{-1}	2.11×10^{2}	1.53×10^{-1}	4.15×10^{-1}
144	9.39×10^{1}	5.07×10^{-1}	4.31×10^{-2}	5.50×10^{-1}	2.12×10^{2}	1.48×10^{-1}	4.03×10^{-1}
145	9.12×10^{1}	4.90×10^{-1}	4.32×10^{-2}	5.33×10^{-1}	2.13×10^{2}	1.43×10^{-1}	3.90×10^{-1}
146	8.86×10^{1}	4.73×10^{-1}	4.33×10^{-2}	5.16×10^{-1}	2.13×10^{2}	1.38×10^{-1}	3.78×10^{-1}
147	8.61×10^{1}	4.56×10^{-1}	4.34×10^{-2}	5.00×10^{-1}	2.14×10^{2}	1.34×10^{-1}	3.66×10^{-1}
148	8.36×10^{1}	4.41×10^{-1}	4.35×10^{-2}	4.84×10^{-1}	2.14×10^{2}	1.29×10^{-1}	3.55×10^{-1}
149	8.12×10^{1}	4.25×10^{-1}	4.36×10^{-2}	4.69×10^{-1}	2.14×10^{2}	1.25×10^{-1}	3.44×10^{-1}
150	7.89×10^{1}	4.11×10^{-1}	4.37×10^{-2}	4.54×10^{-1}	2.15×10^{2}	1.21×10^{-1}	3.33×10^{-1}
151	7.67×10^{1}	3.96×10^{-1}	4.37×10^{-2}	4.40×10^{-1}	2.15×10^{2}	1.17×10^{-1}	3.23×10^{-1}
152	7.45×10^{1}	3.83×10^{-1}	4.37×10^{-2}	4.26×10^{-1}	2.16×10^{2}	1.13×10^{-1}	3.13×10^{-1}
153	7.24×10^{1}	3.69×10^{-1}	4.38×10^{-2}	4.13×10^{-1}	2.16×10^{2}	1.10×10^{-1}	3.04×10^{-1}
154	7.03×10^{1}	3.57×10^{-1}	4.38×10^{-2}	4.00×10^{-1}	2.17×10^{2}	1.06×10^{-1}	2.94×10^{-1}
155	6.83×10^{1}	3.44×10^{-1}	4.38×10^{-2}	3.88×10^{-1}	2.17×10^{2}	1.03×10^{-1}	2.85×10^{-1}
156	6.64×10^{1}	3.32×10^{-1}	4.37×10^{-2}	3.76×10^{-1}	2.17×10^{2}	9.94×10^{-2}	2.77×10^{-1}
157	6.45×10^{1}	3.21×10^{-1}	4.37×10^{-2}	3.65×10^{-1}	2.18×10^{2}	9.62×10^{-2}	2.68×10^{-1}
158	6.27×10^{1}	3.10×10^{-1}	4.37×10^{-2}	3.53×10^{-1}	2.18×10^{2}	9.31×10^{-2}	2.60×10^{-1}
159	6.09×10^{1}	2.99×10^{-1}	4.36×10^{-2}	3.43×10^{-1}	2.18×10^{2}	9.01×10^{-2}	2.52×10^{-1}
160	5.92×10^{1}	2.89×10^{-1}	4.35×10^{-2}	3.32×10^{-1}	2.19×10^{2}	8.72×10^{-2}	2.45×10^{-1}
161	5.75×10^{1}	2.79×10^{-1}	4.34×10^{-2}	3.22×10^{-1}	2.19×10^{2}	8.44×10^{-2}	2.38×10^{-1}
162	5.55×10^{1}	6.45×10^{-1}	4.33×10^{-2}	6.88×10^{-1}	2.20×10^{2}	1.86×10^{-1}	5.02×10^{-1}
163	5.36×10^{1}	6.22×10^{-1}	4.29×10^{-2}	6.65×10^{-1}	2.20×10^{2}	1.79×10^{-1}	4.86×10^{-1}
164	5.17×10^{1}	6.01×10^{-1}	4.25×10^{-2}	6.43×10^{-1}	2.21×10^{2}	1.73×10^{-1}	4.70×10^{-1}
165	4.99×10^{1}	5.80×10^{-1}	4.21×10^{-2}	6.22×10^{-1}	2.22×10^{2}	1.67×10^{-1}	4.54×10^{-1}
166	4.82×10^{1}	5.60×10^{-1}	4.17×10^{-2}	6.01×10^{-1}	2.22×10^{2}	1.62×10^{-1}	4.39×10^{-1}
167	4.65×10^{1}	5.40×10^{-1}	4.13×10^{-2}	5.81×10^{-1}	2.23×10^{2}	1.56×10^{-1}	4.25×10^{-1}
168	4.49×10^{1}	5.21×10^{-1}	4.08×10^{-2}	5.62×10^{-1}	2.23×10^{2}	1.51×10^{-1}	4.11×10^{-1}
169	4.33×10^{1}	5.03×10^{-1}	4.04×10^{-2}	5.43×10^{-1}	2.24×10^{2}	1.46×10^{-1}	3.97×10^{-1}
170	4.18×10^{1}	4.85×10^{-1}	3.99×10^{-2}	5.25×10^{-1}	2.25×10^{2}	1.41×10^{-1}	3.84×10^{-1}

Table 4.4 (continued)

Year	Inventory remaining[c] (g)	Calculated release from a disposal pad[d]				Calculated release to environment[d]	
		Advection (g/year)	Diffusion (g/year)	Total (g/year)	Cumulative (g)	Vertical (g/year)	Lateral (g/year)
180	2.92×10^{1}	3.40×10^{-1}	3.52×10^{-2}	3.75×10^{-1}	2.29×10^{2}	9.98×10^{-2}	2.75×10^{-1}
190	2.04×10^{1}	2.37×10^{-1}	3.03×10^{-2}	2.67×10^{-1}	2.32×10^{2}	7.06×10^{-2}	1.97×10^{-1}
200	1.42×10^{1}	1.65×10^{-1}	2.55×10^{-2}	1.90×10^{-1}	2.34×10^{2}	4.98×10^{-2}	1.40×10^{-1}
210	9.84×10^{0}	1.14×10^{-1}	2.11×10^{-2}	1.35×10^{-1}	2.36×10^{2}	3.51×10^{-2}	1.00×10^{-1}
220	6.80×10^{0}	7.90×10^{-2}	1.71×10^{-2}	9.61×10^{-2}	2.37×10^{2}	2.47×10^{-2}	7.14×10^{-2}
230	4.68×10^{0}	5.44×10^{-2}	1.37×10^{-2}	6.80×10^{-2}	2.38×10^{2}	1.73×10^{-2}	5.08×10^{-2}
240	3.21×10^{0}	3.73×10^{-2}	1.08×10^{-2}	4.80×10^{-2}	2.38×10^{2}	1.21×10^{-2}	3.60×10^{-2}
250	2.19×10^{0}	2.54×10^{-2}	8.38×10^{-3}	3.38×10^{-2}	2.39×10^{2}	8.41×10^{-3}	2.54×10^{-2}
260	1.49×10^{0}	1.73×10^{-2}	6.43×10^{-3}	2.37×10^{-2}	2.39×10^{2}	5.83×10^{-3}	1.79×10^{-2}
270	1.00×10^{0}	1.17×10^{-2}	4.87×10^{-3}	1.65×10^{-2}	2.39×10^{2}	4.02×10^{-3}	1.25×10^{-2}
280	6.75×10^{-1}	7.84×10^{-3}	3.64×10^{-3}	1.15×10^{-2}	2.39×10^{2}	2.76×10^{-3}	8.72×10^{-3}
290	4.51×10^{-1}	5.24×10^{-3}	2.69×10^{-3}	7.94×10^{-3}	2.39×10^{2}	1.89×10^{-3}	6.05×10^{-3}
300	3.00×10^{-1}	3.48×10^{-3}	1.97×10^{-3}	5.45×10^{-3}	2.40×10^{2}	1.28×10^{-3}	4.17×10^{-3}

[a] Actual simulation length was 1000 years.

[b] Results presented are for one CIIDF disposal pad. The output presented in this table is a composite of four SOURCE1 output files (^{137}Cs output files with file name extensions *.sum*, *.lch*, *.lat*, and *.rch* were used).

[c] Initial ^{137}Cs inventory was 1.285×10^{1} g/vault for 330 vaults (= 4.241×10^{3} g total). The inventory remaining is the total ^{137}Cs inventory in the 330 vaults at the year indicated.

[d] During the institutional control period (i.e., years 1–100), the total calculated release rate from the disposal pad does not equal the total calculated release rate to the environment (i.e., sum of vertical and lateral components) because the concrete pad and leachate collection system attenuate releases to the environment.

on the disposal pad, (2) the calculated release rates by advection and diffusion, and (3) the calculated release to the environment for the lateral and recharge components. The total calculated release is greater than the calculated release to the environment during the institutional control period (0–100 years) because the concrete pad and leachate collection system attenuate releases. Note that there is a step increase in the advective release rate at years 42, 94, and 162. This is a result of the hydraulic failure of the lower layer of vaults, then the middle layer of vaults, and finally, the top layer of vaults. Hydraulic failure leads to increased water flow through the failed vaults and hence, increased advective transport. Finally, note that the lateral release component is zero in years 23–32. This time period corresponds to that during which it is assumed that there is an intact cap on top of the disposal facility (see Table 4.3). During this time period, the seepage rates of water through the disposal facility are very low, and as a result all of the releases are partitioned to the vertical component. The partitioning of the total release to the environment between the vertical and lateral components varies during the simulation as a result of variation in water seepage rates in the facility.

To illustrate the calculated release rates from a CIIDF disposal pad, graphs (Fig. 4.2 through Fig. 4.8) were prepared for seven radionuclides. These radionuclides, which are listed along with property summaries in Table 4.1, are representative of the range of radionuclides (i.e., based on half-life, K_d, and solubility limitation) analyzed for this PA. Two figures are presented for each of the seven

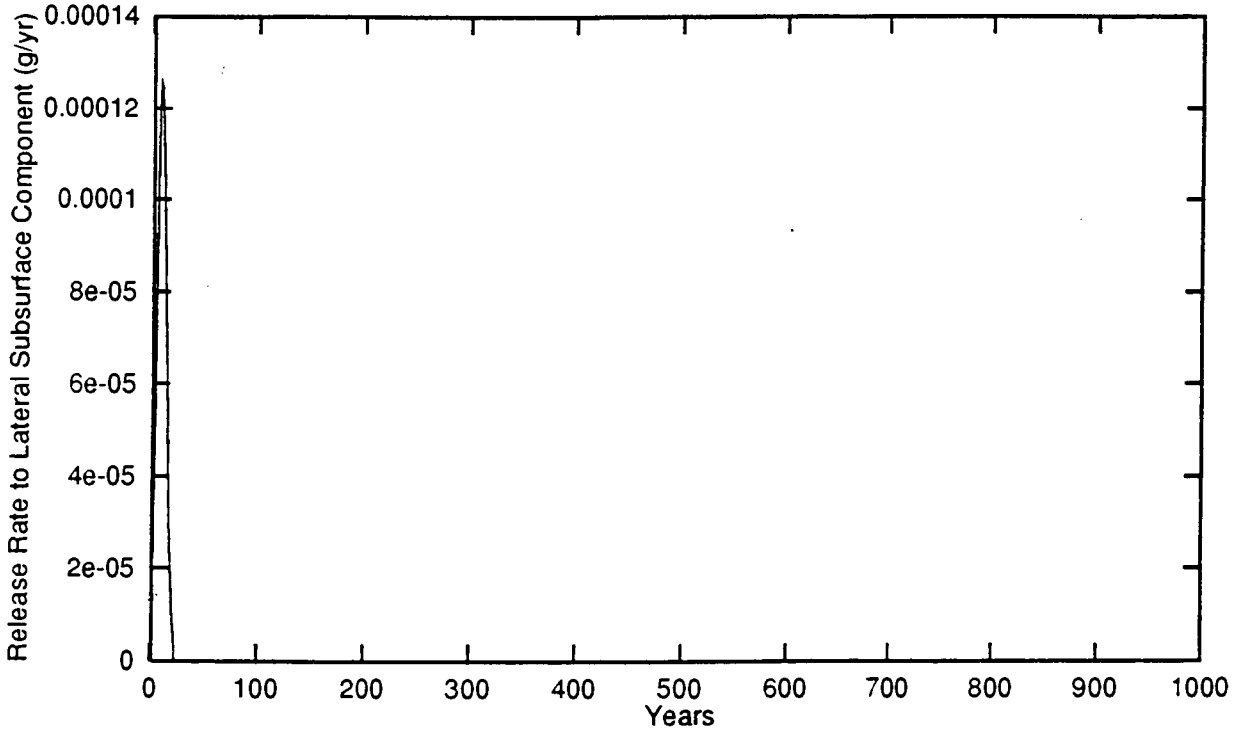

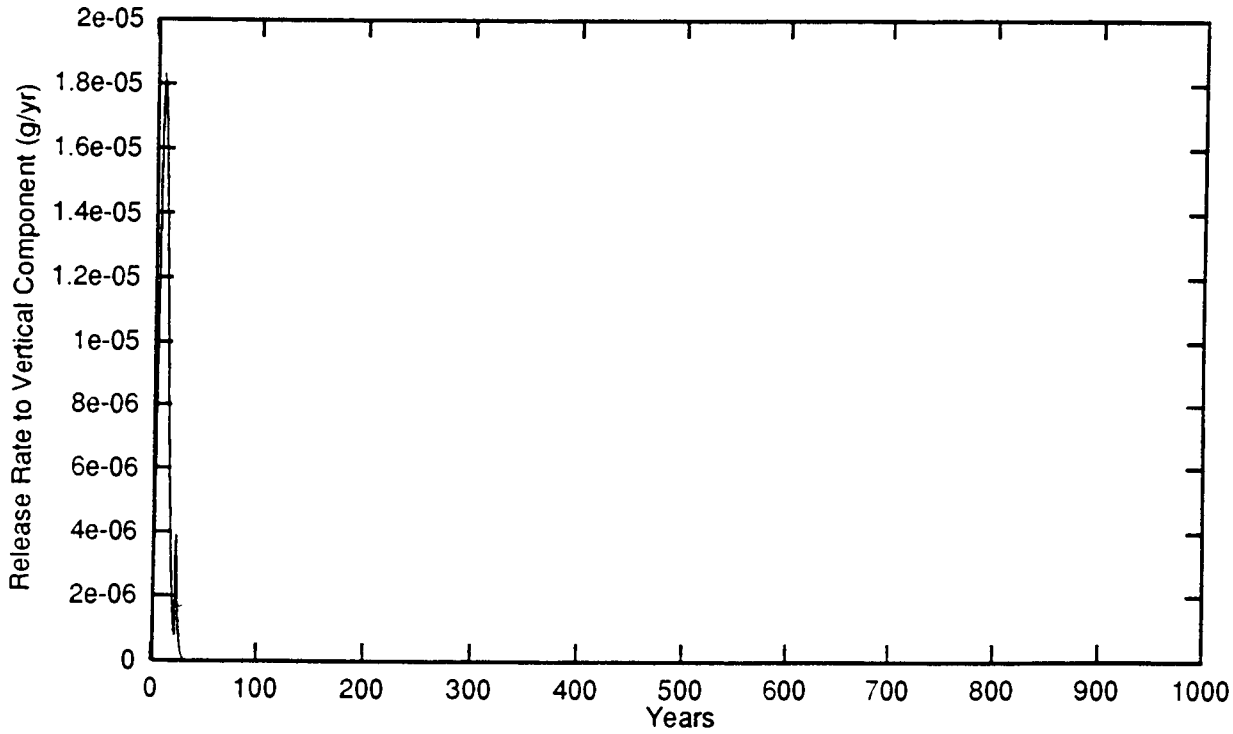

Fig. 4.2 Calculated release rates of ^{3}H from a CIIDF pad as a function of time.

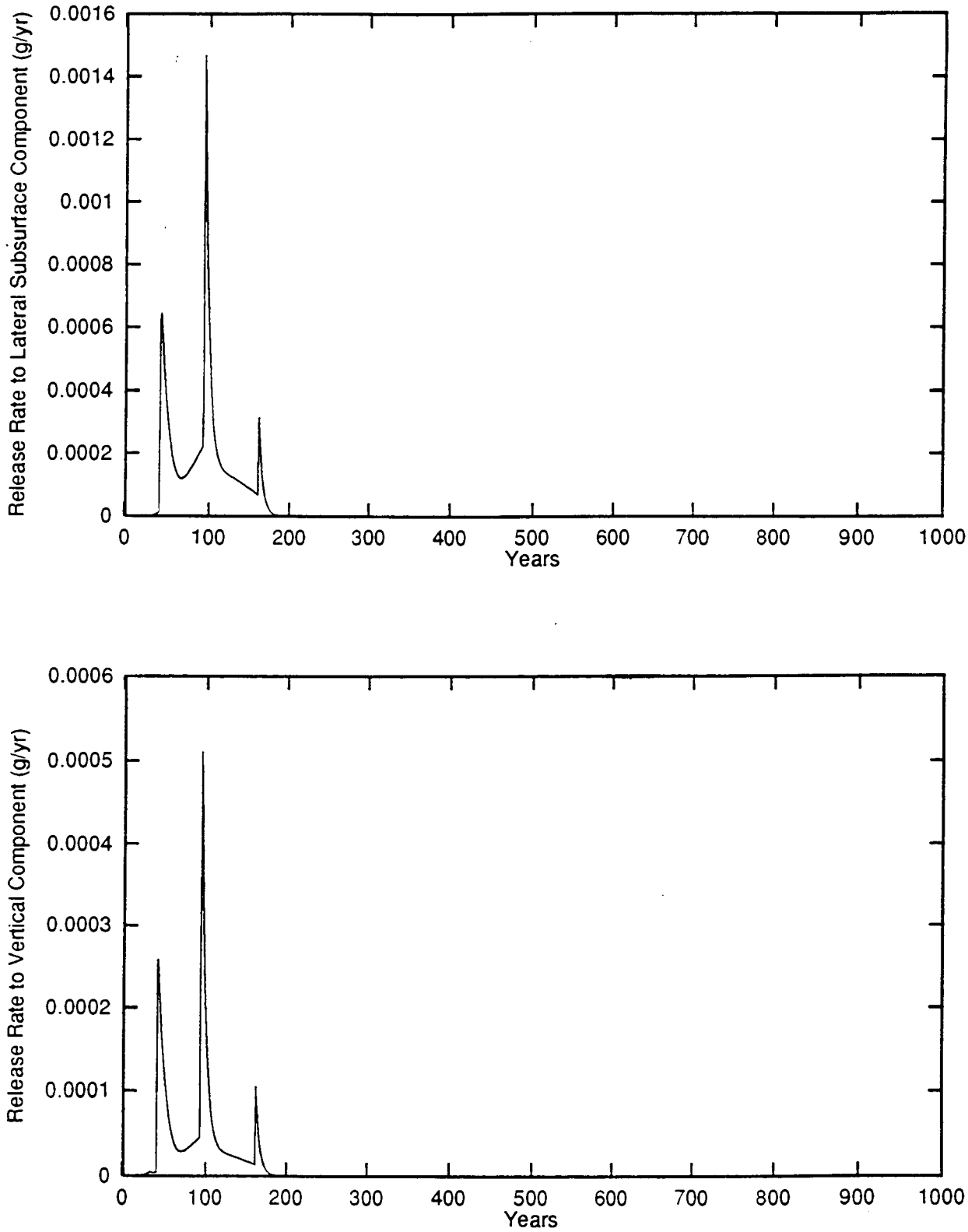

Fig. 4.3 Calculated release rates of ^{14}C from a CIIDF pad as a function of time.

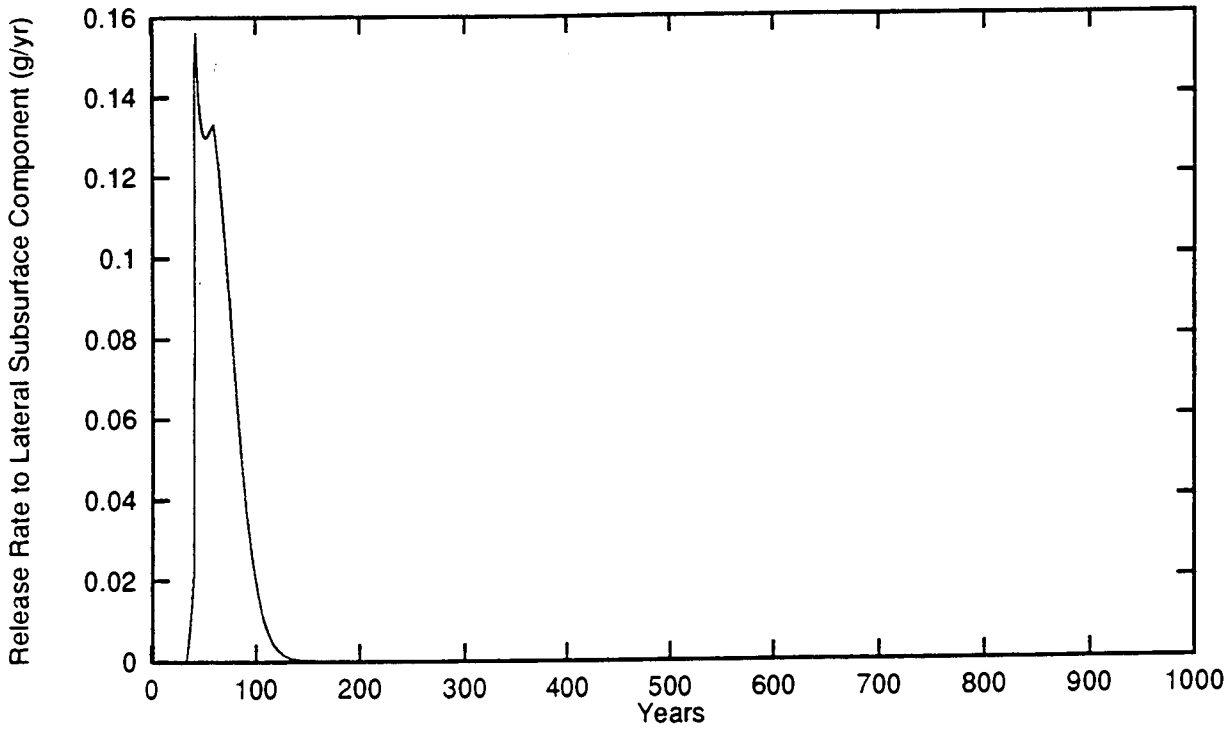

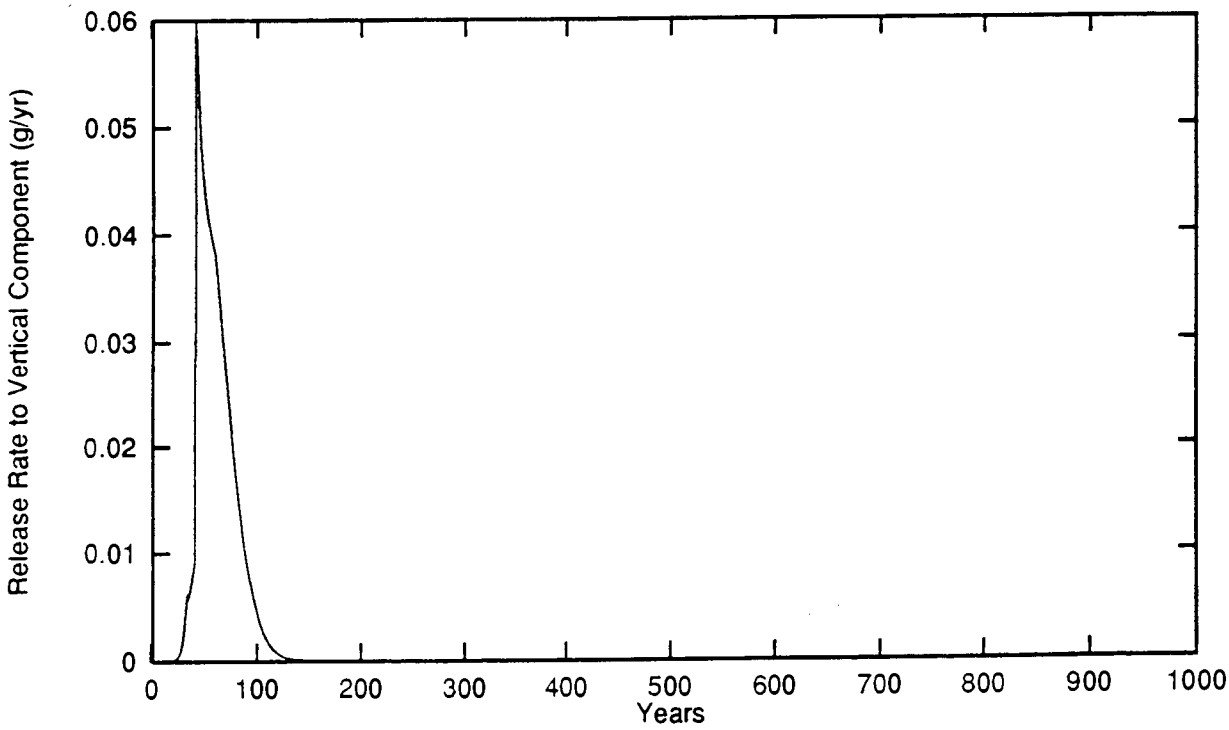

Fig. 4.4 Calculated release rates of ^{60}Co from a CIIDF pad as a function of time.

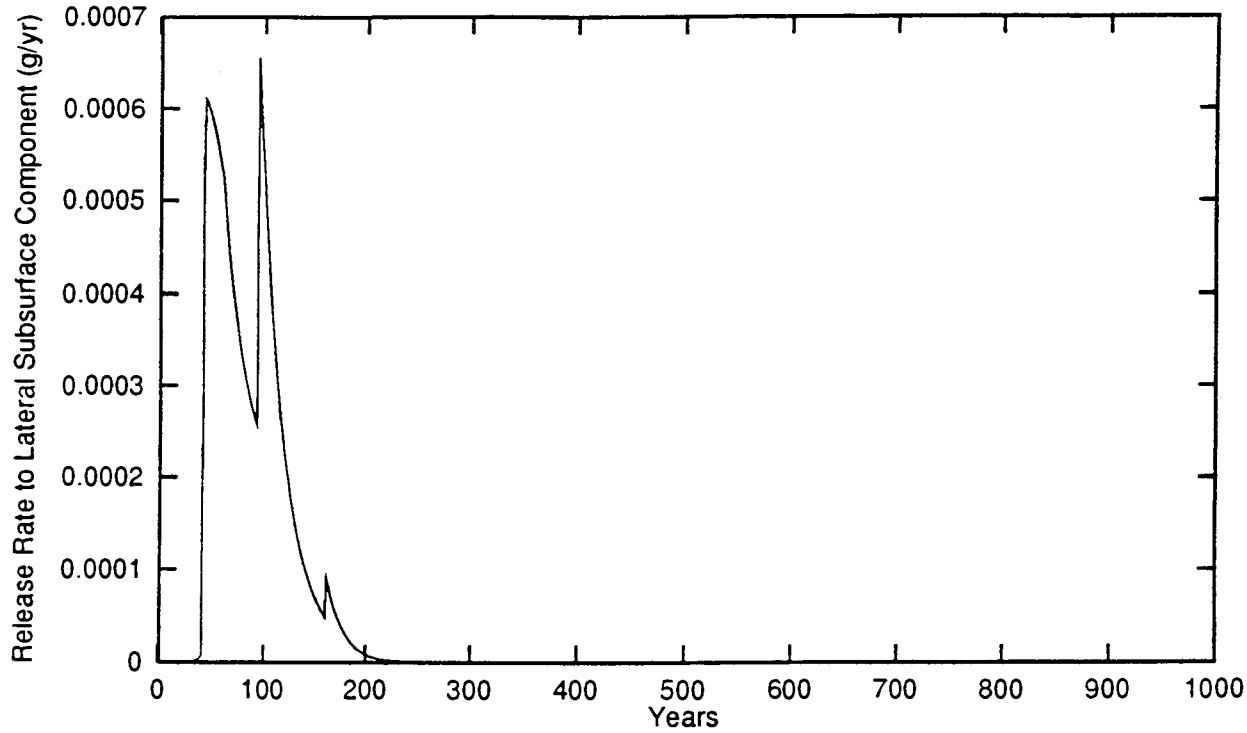

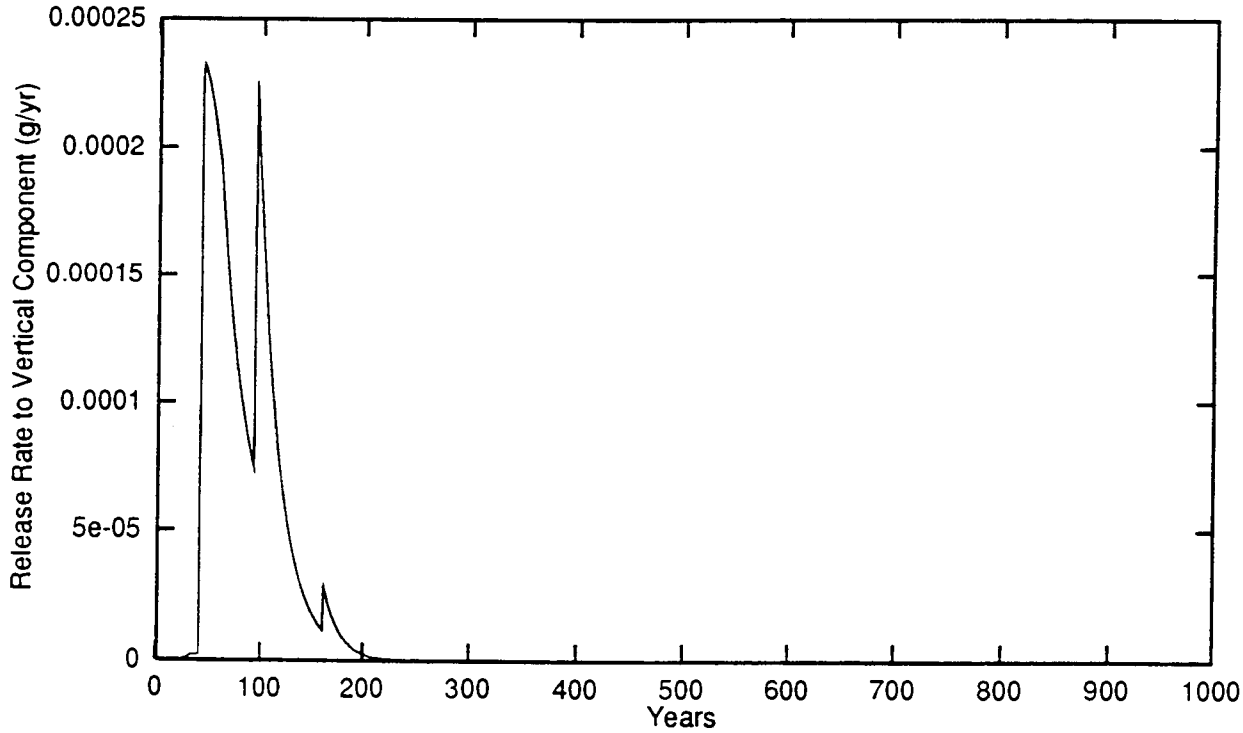

Fig. 4.5 Calculated release rates of ^{90}Sr from a CIIDF pad as a function of time.

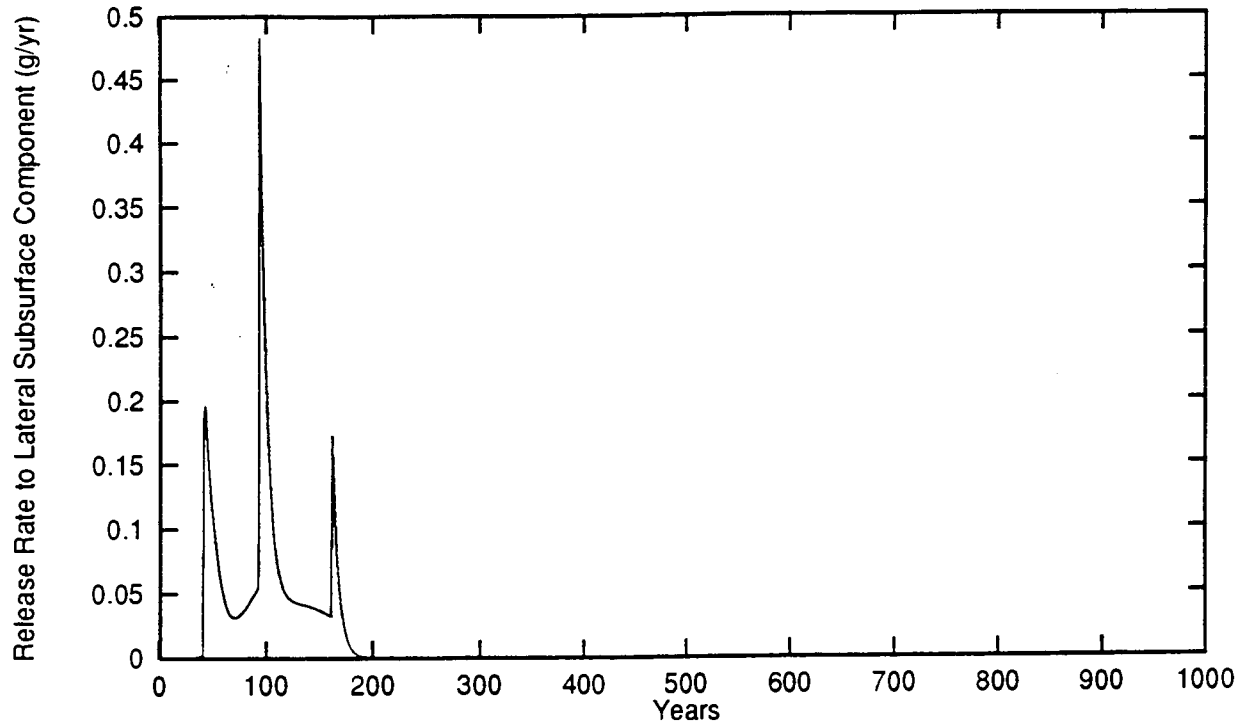

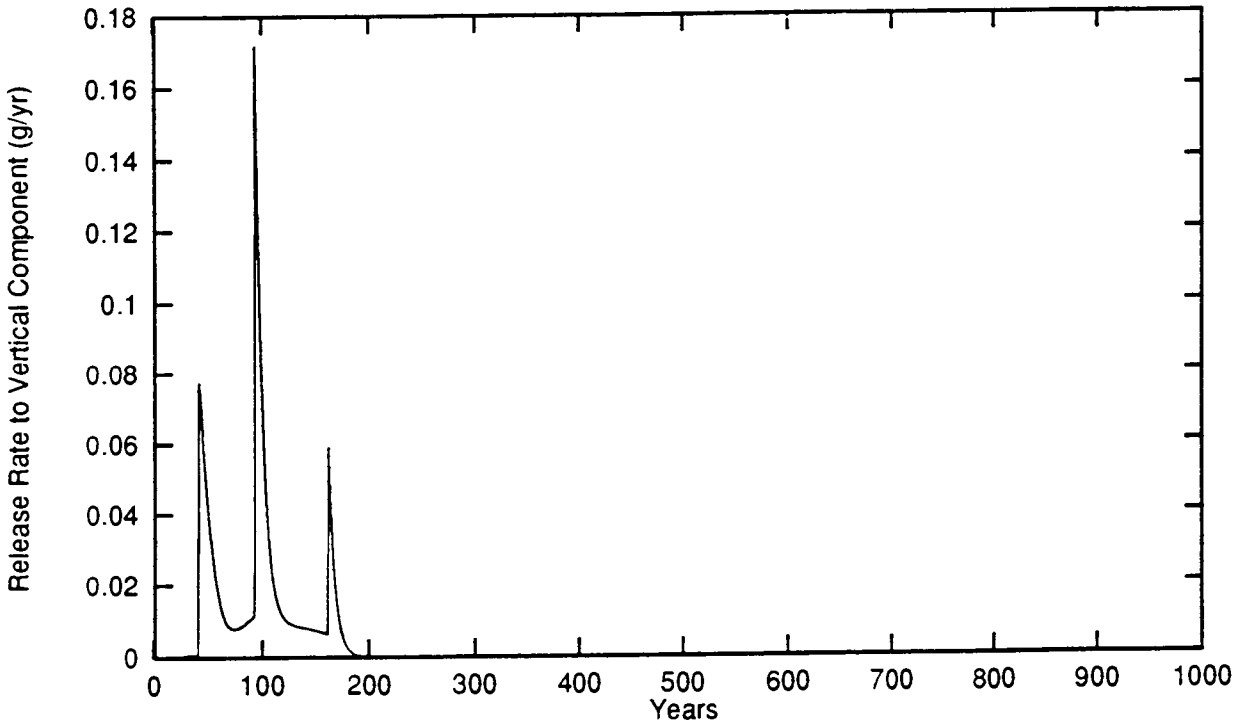

Fig. 4.6 Calculated release rates of ^{99}Tc from a CIIDF pad as a function of time.

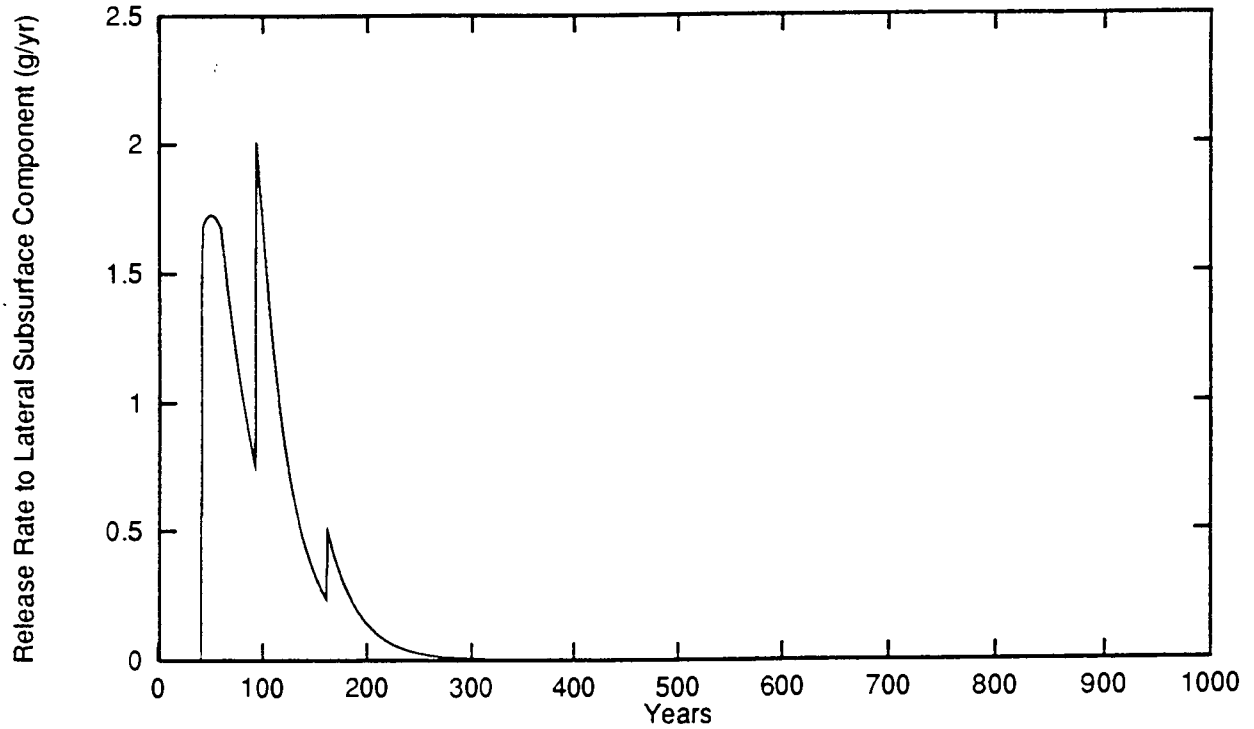

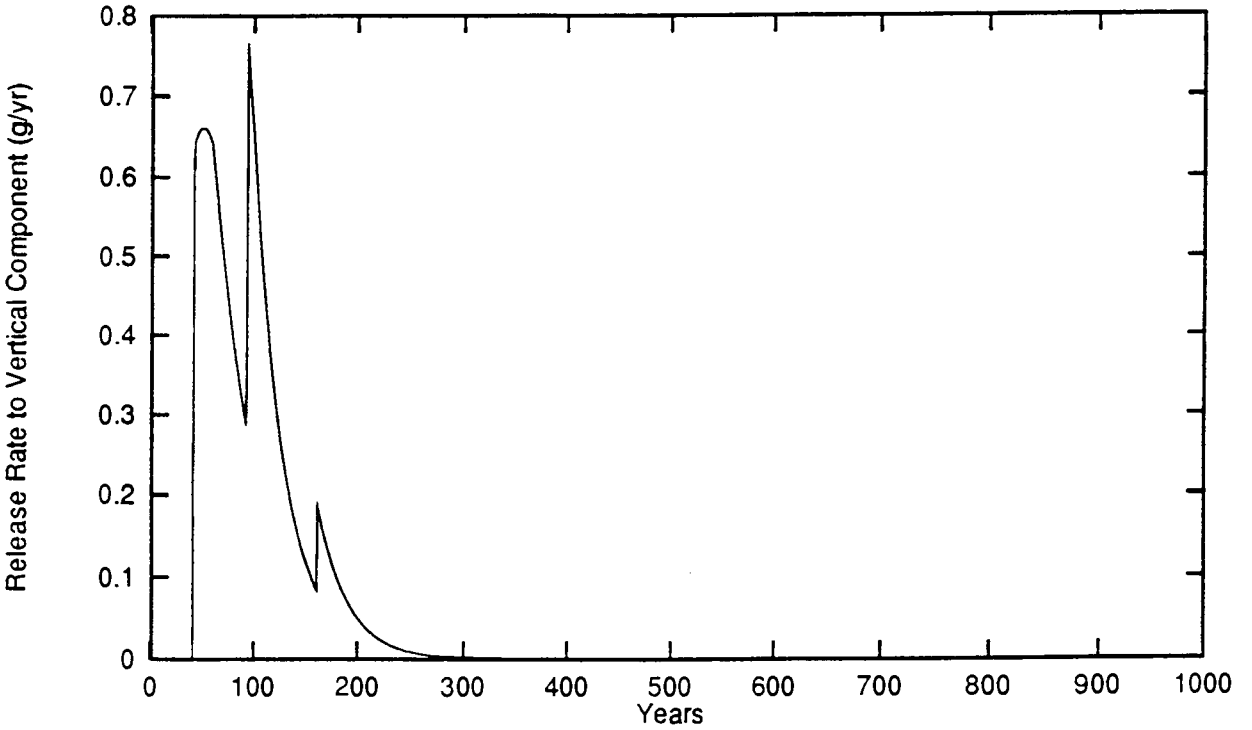

Fig. 4.7 Calculated release rates of ^{137}Cs from a CIIDF pad as a function of time.

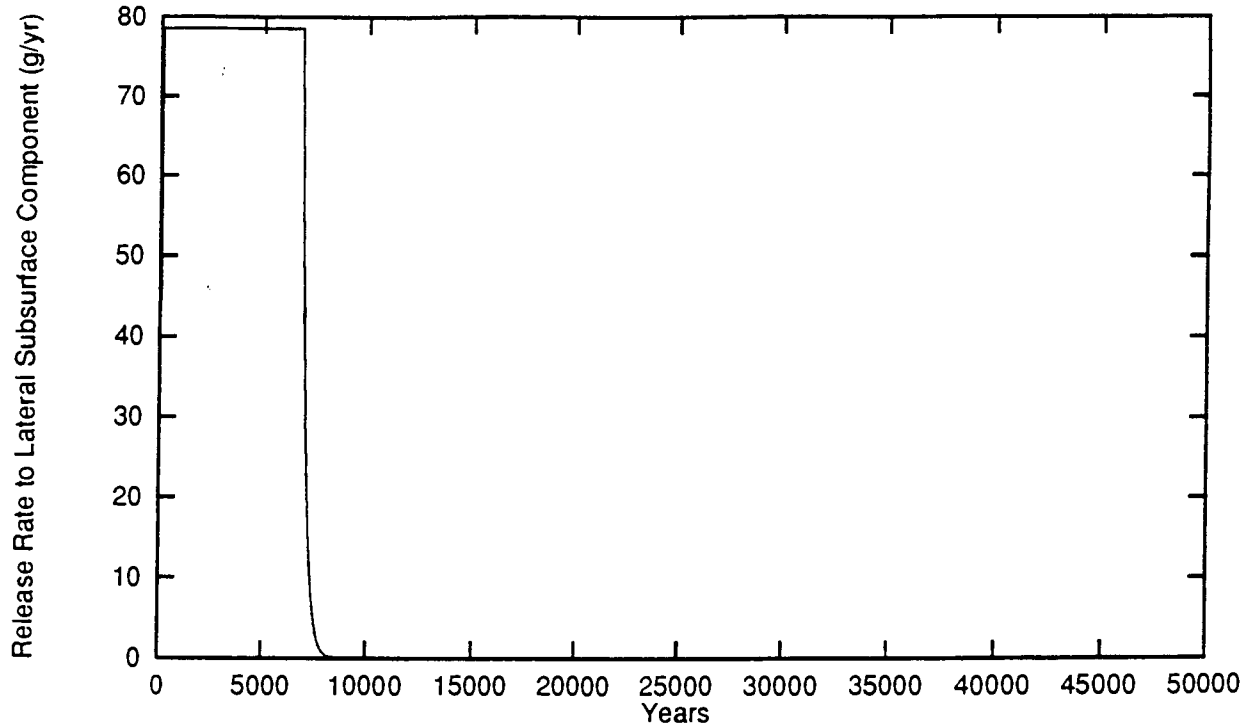

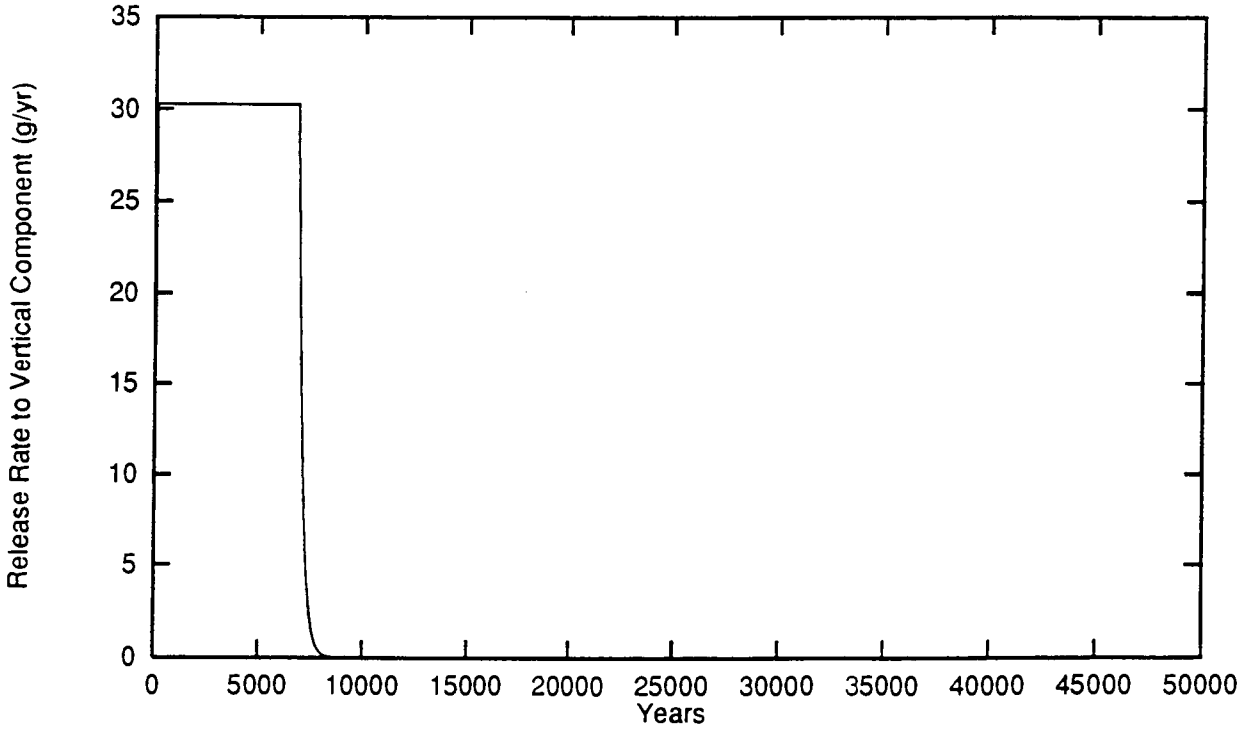

Fig. 4.8 Calculated release rates of ^{238}U from a CIIDF pad as a function of time.

radionuclides: one illustrates releases to the lateral component, whereas the second illustrates releases to the vertical component. Fig. 4.2 depicts the release of ^{3}H, which has a low K_d, a high diffusion coefficient in waste, and a short half-life. As a result, ^{3}H is released early in the simulation. The figures for ^{14}C, ^{90}Sr, ^{99}Tc, and ^{137}Cs (Fig. 4.3, Fig. 4.5, Fig. 4.6, and Fig. 4.7, respectively) all show three distinct peaks at the times of failure of the three vault layers. Again, as vaults fail hydraulically, the advective release rate increases. The height and width of the peaks are functions of the K_d and half-life for the radionuclide. Note that the first release peak, which occurs before 100 years, is attenuated by the concrete pad and leachate collection system. The second peak, which occurs at year 94, is only slightly attenuated. Fig. 4.4 for ^{60}Co, which has a relatively short half-life and a high K_d, does not exhibit the three distinct advective release peaks primarily as a result of the slow advective release rate. This slow rate results in one large release peak. Finally, Fig. 4.8 illustrates the solubility-limited release of ^{238}U from a CIIDF disposal pad. The release rate is constant for both the lateral and vertical components until about year 6800, at which point the inventory has been depleted such that solubility is no longer exceeded.

For each radionuclide, Table 4.5 provides a summary of (1) the radionuclide inventory analyzed, (2) the maximum annual release rate calculated, and (3) the time of occurrence of the maximum. The inventory presented in Table 4.5 is the inventory at which either the groundwater or surface water concentration limit was reached (see Table 4.12). Radionuclides that exceeded solubility limits during a simulation for the indicated inventory are annotated with a footnote. For some radionuclides, the solubility limit may have been exceeded only briefly (e.g., during one month) for a time period with a low seepage rate through the facility. As more water became available (with facility deterioration), solubility was not exceeded, and the maximum release rate was determined by the K_d of the radionuclide. However, other radionuclides exceeded solubility during a number of years, and the maximum release rate presented in Table 4.5 is for a range of years and is determined by the solubility limit.

4.2.2 Source Terms for Direct Instrusion

The SOURCE1 computer code was also used in generating source terms for intruder scenario calculations. However, in order to be conservative for the intruder scenarios, several of the input parameters for SOURCE1 were adjusted. The methodology for estimating radionuclide inventories for intruder scenarios is described in the following paragraphs.

To support the estimation of radionuclide inventory depletion for intruder scenarios, Fig. 4.9 through Fig. 4.11 were prepared. These figures portray the fraction of initial inventory remaining at specific times (i.e., 100, 300, 500, 1000, 2000, 5000, and 10,000 years) as a function of waste K_d. These figures were generated as a result of SOURCE1 calculations. Basic assumptions in these calculations were that (1) there was no transport by diffusion, (2) there was no radioactive decay, (3) the release of the radionuclide was not limited by solubility, and (4) the rate of degradation of the disposal vaults was reduced as compared to the degradation rate used in the environmental transport calculations. In summary, these assumptions imply that the release of radionuclides is only by

Table 4.5. Maximum annual radionuclide release rate from a CIIDF pad and year of occurrence for vertical and lateral release components of SOURCE1 calculations

Nuclide	Initial inventory[a] (g/pad)	Vertical component		Lateral component	
		Maximum rate (g/year)	Year of occurrence	Maximum rate (g/year)	Year of occurrence
^{3}H	9.87×10^{-3}	1.77×10^{-5}	8	1.23×10^{-4}	8
$^{3}H^{b}$	1.07×10^{0}	1.92×10^{-3}	8	1.33×10^{-2}	8
$^{10}Be^{c}$	3.63×10^{4}	2.70×10^{-1}	162	1.21×10^{0}	162
^{14}C	4.72×10^{-2}	5.11×10^{-4}	94	1.47×10^{-3}	94
^{26}Al	9.24×10^{4}	1.35×10^{1}	852	7.09×10^{1}	854
^{36}Cl	1.56×10^{0}	2.81×10^{-2}	27	2.17×10^{-2}	22
$^{36}Cl^{b}$	4.85×10^{0}	8.72×10^{-2}	27	6.74×10^{-2}	22
$^{40}K^{c}$	4.19×10^{5}	2.11×10^{3}	94	5.64×10^{3}	94
$^{41}Ca^{c}$	6.30×10^{2}	4.89×10^{0}	162	1.91×10^{1}	162
^{60}Co	6.60×10^{9}	5.99×10^{-2}	42	1.56×10^{-1}	43
$^{59}Ni^{c}$	1.20×10^{7}	4.02×10^{3}	100–838	1.05×10^{4}	100–838
$^{63}Ni^{c}$	2.37×10^{4}	4.58×10^{1}	94	1.24×10^{2}	94
^{79}Se	4.75×10^{-1}	5.57×10^{-3}	42	1.57×10^{-2}	42
$^{79}Se^{b}$	7.52×10^{-1}	8.83×10^{-3}	42	2.50×10^{-2}	42
$^{87}Rb^{c}$	1.26×10^{8}	3.17×10^{5}	162	9.31×10^{5}	162
^{90}Sr	7.23×10^{-1}	2.32×10^{-4}	43	6.55×10^{-4}	94
^{93}Zr	1.46×10^{4}	1.46×10^{1}	162	3.78×10^{1}	162
^{93m}Nb	7.69×10^{4}	2.93×10^{0}	43	7.71×10^{0}	43
^{94}Nb	4.59×10^{2}	7.49×10^{-1}	162	1.95×10^{0}	162
^{99}Tc	1.61×10^{1}	1.72×10^{-1}	94	4.83×10^{-1}	94
$^{107}Pd^{c}$	2.34×10^{7}	8.10×10^{-1}	159–1,000,000	2.10×10^{0}	159–1,000,000
^{113m}Cd	1.86×10^{5}	4.94×10^{-3}	94	2.25×10^{-2}	96
^{121m}Sn	1.28×10^{3}	9.35×10^{-1}	94	2.46×10^{0}	94
^{126}Sn	4.52×10^{2}	1.11×10^{0}	162	3.02×10^{0}	162
^{129}I	3.24×10^{0}	5.83×10^{-2}	27	4.53×10^{-2}	22
$^{129}I^{b}$	1.01×10^{1}	1.81×10^{-1}	27	1.41×10^{-1}	22
^{135}Cs	1.14×10^{6}	2.12×10^{3}	162	5.70×10^{3}	162
^{137}Cs	4.26×10^{3}	7.66×10^{-1}	94	2.01×10^{0}	94
$^{151}Sm^{c}$	6.60×10^{9}	9.50×10^{0}	100–1829	2.46×10^{1}	100–1829
^{152}Eu	1.26×10^{2}	2.64×10^{-2}	42	6.79×10^{-2}	43
^{154}Eu	2.05×10^{2}	1.39×10^{-2}	42	3.50×10^{-2}	43
^{155}Eu	1.39×10^{4}	7.14×10^{-2}	42	1.76×10^{-1}	42
^{207}Bi	4.32×10^{3}	2.71×10^{0}	43	7.09×10^{0}	43
^{210}Pb	5.15×10^{0}	2.47×10^{-4}	47	6.46×10^{-4}	47
^{226}Ra	4.29×10^{1}	7.28×10^{-2}	162	1.90×10^{-1}	162
^{229}Th	3.93×10^{2}	3.65×10^{-1}	162	9.48×10^{-1}	162
$^{230}Th^{c}$	2.67×10^{4}	1.52×10^{0}	100–4609	3.94×10^{0}	100–4609
$^{232}Th^{c}$	5.54×10^{5}	1.53×10^{0}	100–100,585	3.97×10^{0}	100–100,585
^{231}Pa	9.74×10^{0}	8.99×10^{-3}	162	2.34×10^{-2}	162
^{232}U	7.62×10^{-1}	1.98×10^{-4}	94	5.15×10^{-4}	94
^{233}U	2.46×10^{1}	2.25×10^{-2}	162	5.86×10^{-2}	162

Table 4.5 (continued)

Nuclide	Initial inventory[a] (g/pad)	Vertical component		Lateral component	
		Maximum rate (g/year)	Year of occurrence	Maximum rate (g/year)	Year of occurrence
^{234}U	3.89×10^{1}	3.58×10^{-2}	162	9.29×10^{-2}	162
^{235}U[c]	1.07×10^{5}	2.99×10^{1}	100–808	7.76×10^{1}	100–808
^{236}U	3.60×10^{3}	3.28×10^{0}	162	8.53×10^{0}	162
^{238}U[c]	7.66×10^{5}	3.03×10^{1}	100–6843	7.86×10^{1}	100–6843
^{237}Np	2.15×10^{1}	1.97×10^{-2}	162	5.11×10^{-2}	162
^{238}Pu	4.95×10^{-1}	1.52×10^{-4}	94	3.97×10^{-4}	94
^{239}Pu	4.69×10^{-1}	4.16×10^{-4}	162	1.08×10^{-3}	162
^{240}Pu	3.92×10^{-1}	3.44×10^{-4}	162	8.93×10^{-4}	162
^{241}Pu	1.63×10^{2}	2.93×10^{-3}	43	7.71×10^{-3}	43
^{242}Pu	5.02×10^{0}	4.47×10^{-3}	162	1.16×10^{-2}	162
^{244}Pu[c]	1.11×10^{3}	3.63×10^{-1}	100–654	9.44×10^{-1}	100–654
^{241}Am	7.56×10^{-1}	5.19×10^{-4}	162	1.35×10^{-3}	162
^{242m}Am	2.60×10^{-1}	1.06×10^{-4}	94	2.76×10^{-4}	94
^{243}Am	3.83×10^{-1}	3.35×10^{-4}	162	8.70×10^{-4}	162
^{243}Cm	1.16×10^{0}	7.56×10^{-5}	94	1.98×10^{-4}	94
^{244}Cm	3.80×10^{0}	1.05×10^{-4}	43	2.76×10^{-4}	43
^{245}Cm	3.70×10^{-1}	3.26×10^{-4}	162	8.46×10^{-4}	162
^{246}Cm	4.98×10^{-1}	4.34×10^{-4}	162	1.13×10^{-3}	162
^{247}Cm	2.00×10^{2}	1.78×10^{-1}	162	4.63×10^{-1}	162
^{248}Cm	1.13×10^{0}	1.01×10^{-3}	162	2.62×10^{-3}	162
^{249}Cf	5.58×10^{-1}	3.52×10^{-4}	162	9.15×10^{-4}	162
^{250}Cf	6.83×10^{0}	9.70×10^{-5}	43	2.55×10^{-4}	43
^{251}Cf	9.93×10^{-1}	7.60×10^{-4}	162	1.98×10^{-3}	162

[a] The inventory reported for each radionuclide is that at which the concentration limit was reached for either groundwater or surface water. The inventory is assumed to be initially uniformly distributed within the 330 vaults on the disposal pad.

[b] The inventory for this radionuclide corresponds to a groundwater or surface water concentration (whichever is most limiting) at 100 years that equals the drinking water concentration limit. For all other radionuclides (including additional listings for this particular radionuclide), the inventory corresponds to the peak groundwater or surface water concentration (whichever is most limiting) that equals the drinking water concentration limit at any time.

[c] At some point during the simulation for this radionuclide, the release rate was solubility limited.

advection and that this release is delayed when compared to releases used in the environmental transport calculations.

Parameters used in the concrete degradation calculations in SOURCE1 were adjusted to delay disposal vault failure. Based on sensitivity analyses of the SOURCE1 computer code, for the expected environmental conditions at the CIIDF site, sulfate attack has been identified as the primary degradation mechanism for the disposal vaults (Icenhour and Tharp 1995). Hence, sulfate attack input parameters (i.e., sulfate diffusion coefficient and sulfate concentration in groundwater) were adjusted within reasonable bounds to cause reduced, simulated degradation of the vaults. Groundwater data for the CIIDF site were used to evaluate a mean and standard deviation (assuming a normal distribution)

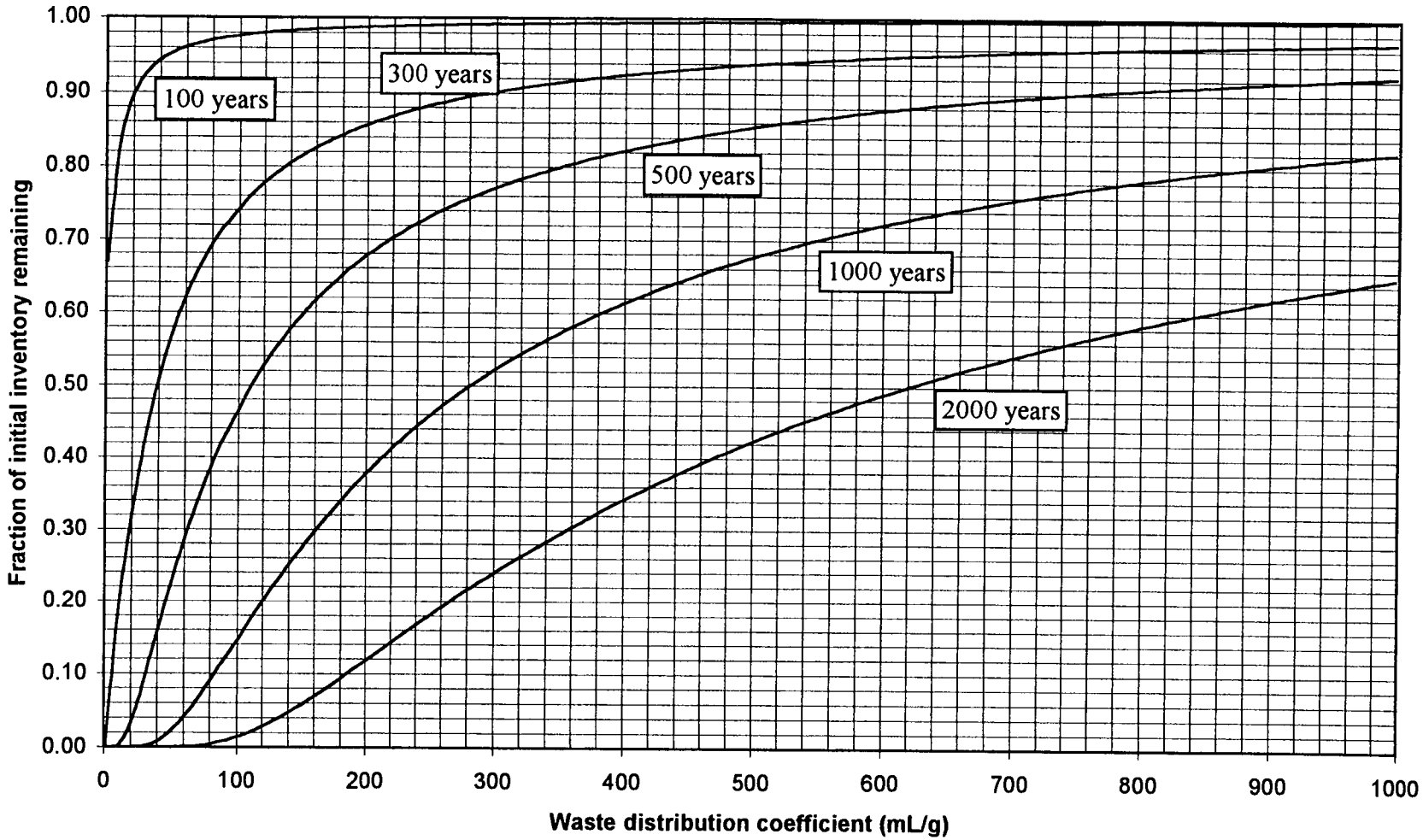

Fig. 4.9. Fraction of initial radionuclide inventory remaining in CIIDF as a function of K_d for years 100, 300, 500, 1000, and 2000. (Assumes no diffusive transport, no radioactive decay, transport not solubility-limited, and reduced degradation of the facility.)

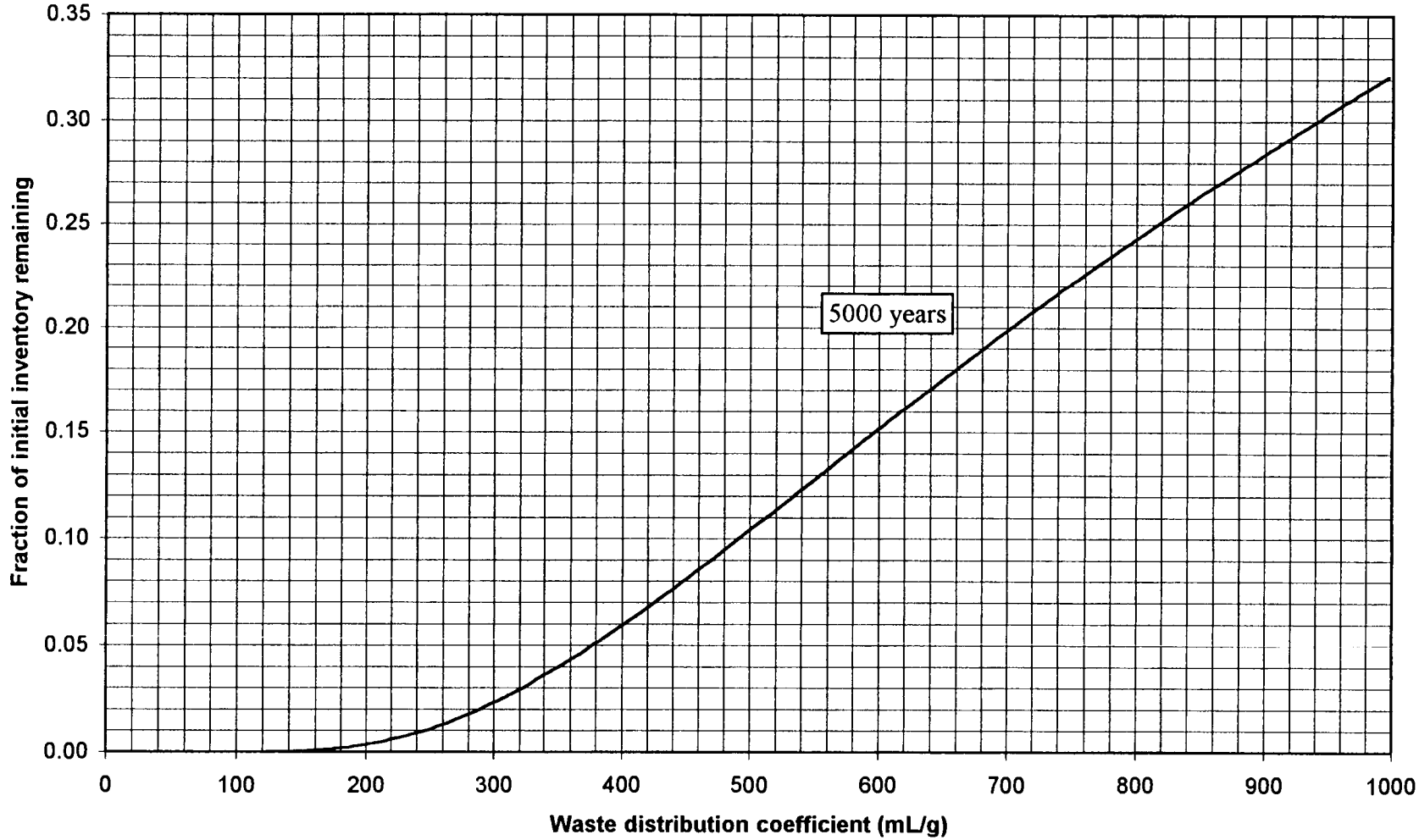

Fig. 4.10. Fraction of initial radionuclide inventory remaining in CIIDF as a function of K_d for year 5000. (Assumes no diffusive transport, no radioactive decay, transport not solubility-limited, and reduced degradation of the facility.)

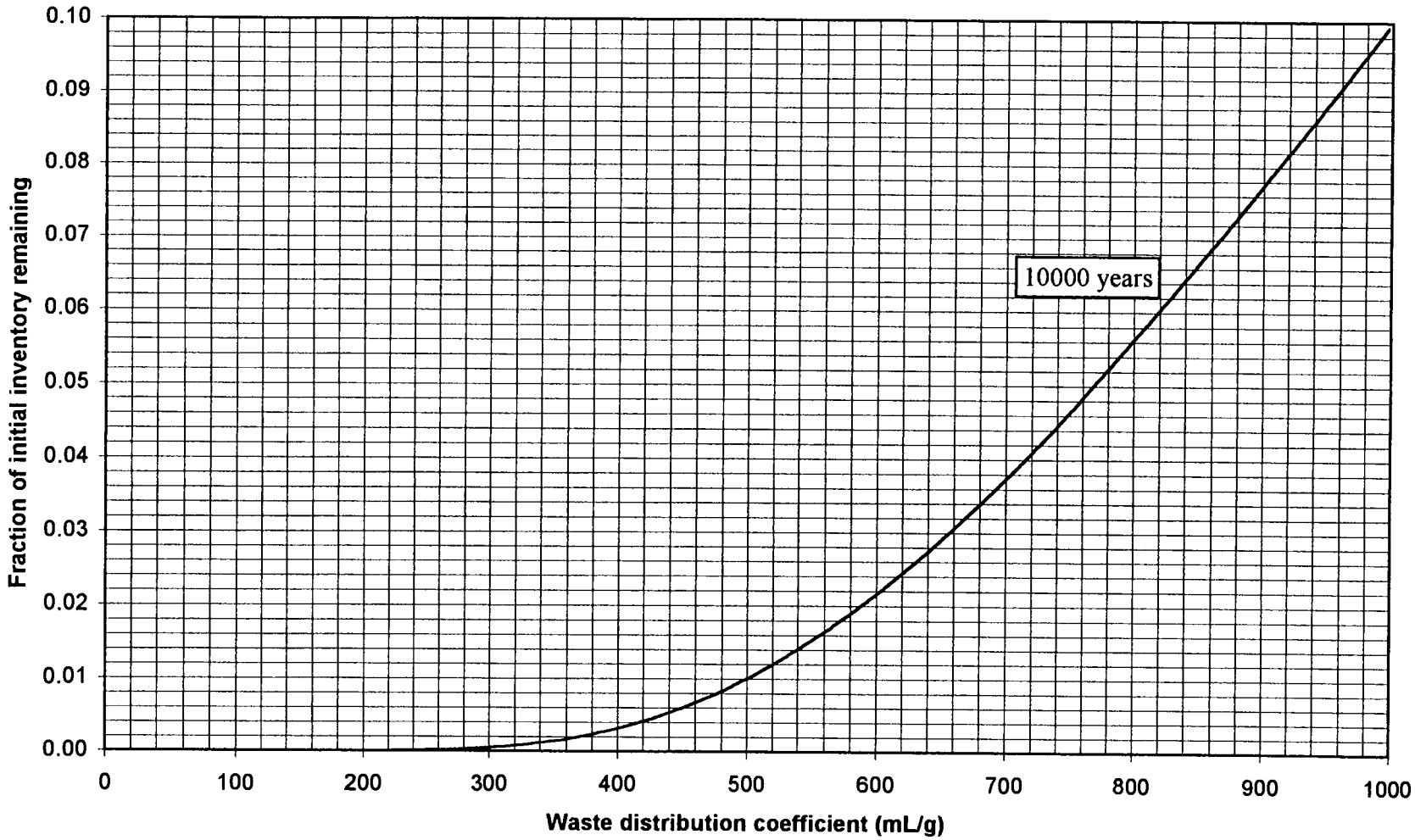

Fig. 4.11. Fraction of initial radionuclide inventory remaining in CIIDF as a function of K_d for year 10,000. (Assumes no diffusive transport, no radioactive decay, transport not solubility-limited, and reduced degradation of the facility.)

for the sulfate concentration.* The concentration selected for the intruder inventory calculations was two standard deviations below the mean value. Additionally, the concentration used was 23% lower than the value used for the environmental transport calculations. The sulfate diffusion coefficient was reduced by 25% from the value used for environmental transport calculations. With the exception of the sulfate parameters, all other input parameters that describe CIIDF are the same as those presented in Table 3.5 and Table 4.3. For the radionuclide-specific parameters, half-life was set to a large value (10^{20} years), and the diffusion coefficients were set to small values (10^{-20} m^2/s). A unit inventory (1 g/vault) was assumed, and it was verified that solubility was not exceeded. The combined effect of the adjustments in the sulfate attack parameters was that the lifetime of each of the disposal vaults was extended by about 65%. The change in the simulated lifetimes of the disposal vaults is presented in Table 4.6.

Table 4.6. Vault failure times from environmental transport calculations and from direct intrusion calculations

Vault layer	Year of vault failure	
	Environmental transport	Direct intrusion
Lower	42	69
Middle	94	156
Upper	162	270

Table 4.7 provides K_d values for use in conjunction with Fig. 4.9 through Fig. 4.11. The values reported in this table are at the high end of the expected range of K_d values for a given element. The K_d values used for the environmental transport calculations are lower than those in Table 4.7 (see Table 3.6), and were selected to provide a conservative release rate. Also shown in Table 4.7 are those radionuclides which reached solubility limits in the calculations for releases to groundwater and surface water. Therefore, even considering the conservative nature of Fig. 4.9 through Fig. 4.11 and Table 4.7, for nuclides limited by solubility, the fraction of initial inventory obtained from the figures may be an underestimate. Table 4.8 lists solubility-limited concentrations for radionuclides that reached solubility limits in the environmental transport calculations. If a concentration being evaluated for intruder calculations is below the value in Table 4.8, then Fig. 4.9 through Fig. 4.11 are applicable.

To estimate disposal limits based on direct intrusion, concentration limits (as described in Sect. 4.4.2) are determined for the time of intrusion. Table 4.7, Table 4.8, and Fig. 4.9 through Fig. 4.11 are used to estimate the inventory depletion during the period from disposal to intrusion. The factor obtained from the figures (which is also called the mobilization and transport factor), along with

* R. J. Luxmoore, "Pore Water Chemistry of the East Hill Slope of the Site," personal communication to A. S. Icenhour, Oak Ridge Natl. Lab., Apr. 15, 1994.

Table 4.7. Waste distribution coefficient (K_d) values for intruder scenario inventory estimation

Element	Waste K_d (mL/g)	Element	Waste K_d (mL/g)
Al[a]	1,990,000	Ni[c]	63.6
Am	576	Np	556
Be[b,c]	31,200,000	Pa	547
Bi	47.9	Pb	455
C	10.9	Pd[b,c]	14,300,000
Ca[c]	46.1	Pu[c]	576
Cd[a]	3,970,000	Ra	199
Cf	596	Rb[c]	133
Cl	1.99	Se	1.99
Cm	576	Sm[c]	37.8
Co[a]	39,700,000	Sn	115
Cs	199	Sr	87.4
Eu	37.8	Tc	12.9
H	1.99	Th[c]	536
I	1.99	U[c]	556
K[c]	39.8	Zr	497
Nb	238		

[a] A pseudo-K_d calculated from a diffusion coefficient estimated from corrosion data for a metal (see Appendix B).
[b] A quasi K_d calculated from a diffusion coefficient estimated from solubility data for a species (see Appendix B).
[c] Some radioisotopes of this element were solubility-limited in calculations of releases to groundwater and surface water. See Table 4.8 for solubility-limited concentrations.

any radioactive decay and waste dilution adjustments, are then used to convert the concentration limit at the time of intrusion to a concentration limit at the time of disposal. Section 4.4.2 provides a detailed description of the application of the mobilization and transport factors and tables of the factors used in the intruder calculations.

4.3 Environmental Transport

The results of the SOURCE1 model leaching calculations discussed in Sect. 4.2.1 provide radionuclide flux rates over time from the disposal pad into the subsurface environment. These fluxes are used as input into the PADSIM model, which accepts vertical and lateral radionuclide flux components from the pad and determines nuclide flux through the recharge and lateral subsurface paths of the vadose zone. Transport through the lateral subsurface path involves retarded migration of nuclides through an expanding soil volume and discharge into the surface water system. This produces a time-dependent radionuclide flux into surface waters, contributing one component to the surface

Table 4.8. Solubility-limited concentration for selected radionuclides[a]

Nuclide	Solubility-limited concentration[b]	
	g/vault	μCi/L of waste[c]
^{10}Be	3.530×10^{-4}	3.037×10^{-3}
^{40}K	4.400×10^{2}	1.185×10^{0}
^{41}Ca	2.545×10^{-3}	8.307×10^{-2}
^{59}Ni	8.100×10^{-2}	2.525×10^{0}
^{63}Ni	2.578×10^{-1}	6.135×10^{3}
^{87}Rb	3.990×10^{3}	1.318×10^{-1}
^{107}Pd	9.300×10^{-2}	1.845×10^{-2}
^{151}Sm	3.404×10^{0}	3.455×10^{4}
^{230}Th	4.750×10^{0}	3.865×10^{1}
^{232}Th	4.745×10^{0}	2.008×10^{-4}
^{235}U	9.535×10^{1}	7.949×10^{-2}
^{238}U	9.700×10^{1}	1.258×10^{-2}
^{244}Pu	1.192×10^{0}	8.158×10^{-3}

[a] The radionuclides listed in this table exceeded solubility limits (at some point in the simulation) in the environmental transport calculations for the CIIDF PA.

[b] The solubility-limited concentration is that concentration (using assumed seepage rates for the CIIDF site) at which the calculated release of a radionuclide exceeds the solubility limit in water at some time during the simulation.

[c] Waste volume is considered to be the volume of the metal container placed in the vault (1.2 × 1.2 × 1.8 m = 2592 L).

water exposure analysis. Contaminants transported with groundwater recharge are used as input to the FTWORK groundwater model, which calculates transport through the aquifer system. Groundwater calculations are evaluated as contaminants migrate passed the 100-m boundary, and the peak concentration is recorded for comparison to compliance limits. Groundwater discharges to surface waters are also simulated and added to fluxes from the lateral subsurface model to produce the total radionuclide flux to surface water. Surface water concentrations are calculated from these fluxes and the flow rate of Bear Creek, and are compared to drinking water compliance limits. Results from these calculations are presented in the following sections.

4.3.1 Transport in Shallow Subsurface and to Groundwater

Extensive sets of computer results were obtained with PADSIM for vadose zone transport of 60 nuclides that were each simulated for 1000 or more years. The model output files of chemical transport to groundwater and lateral flow were each scanned to identify the maximum annual nuclide flux in the vertical and lateral flow paths along with the years of occurrence. These values (Table 4.9) show that nuclide transport in the lateral path was approximately an order of magnitude larger than transport to groundwater. The lateral flux results were added with the surface water outflow results

Table 4.9. Maximum annual flux and concentration of nuclides, and year of occurrence for the recharge and lateral subsurface flow paths

Nuclide	Recharge				Lateral flow			
	Flux (g/year)	Time (year)	Conc'n (g/mL)	Time (year)	Flux (g/year)	Time (year)	Conc'n (g/mL)	Time (year)
^{3}H	5.7×10^{-6}	13	6.3×10^{-14}	13	8.5×10^{-5}	10	1.5×10^{-13}	10
$^{3}H^{a}$	6.2×10^{-4}	13	6.7×10^{-12}	13	9.3×10^{-3}	10	1.6×10^{-11}	10
^{10}Be	7.5×10^{-2}	25,461	8.6×10^{-10}	25,459	5.8×10^{-1}	25,406	2.6×10^{-9}	25,390
^{14}C	1.4×10^{-4}	102	1.6×10^{-12}	102	7.1×10^{-4}	94	3.1×10^{-12}	94
^{26}Al	7.8×10^{-2}	2,669	8.9×10^{-10}	2,675	6.8×10^{-1}	2,589	3.0×10^{-9}	2,618
^{36}Cl	1.3×10^{-2}	40	2.0×10^{-10}	34	1.7×10^{-2}	22	8.2×10^{-11}	35
$^{36}Cl^{a}$	4.1×10^{-2}	40	6.2×10^{-10}	34	5.2×10^{-2}	22	2.6×10^{-10}	35
^{40}K	4.9×10^{1}	217	5.6×10^{-7}	218	1.1×10^{3}	162	4.7×10^{-6}	162
^{41}Ca	6.5×10^{-2}	193	7.5×10^{-10}	193	3.5×10^{0}	162	1.5×10^{-8}	162
^{60}Co	2.6×10^{1}	895	3.0×10^{-7}	898	1.1×10^{2}	898	5.0×10^{-7}	900
^{59}Ni	6.3×10^{-6}	58	7.2×10^{-14}	58	3.4×10^{-5}	63	1.5×10^{-13}	63
^{63}Ni	1.1×10^{-2}	183	1.3×10^{-10}	183	5.2×10^{-2}	185	2.3×10^{-10}	185
^{79}Se	2.1×10^{-3}	45	2.4×10^{-11}	45	7.2×10^{-3}	42	3.6×10^{-11}	42
$^{79}Se^{a}$	3.4×10^{-3}	45	3.9×10^{-11}	45	1.1×10^{-2}	42	5.7×10^{-11}	42
^{87}Rb	1.5×10^{4}	276	1.7×10^{-4}	274	1.9×10^{5}	162	8.3×10^{-4}	162
^{90}Sr	2.6×10^{-6}	108	3.0×10^{-14}	108	1.2×10^{-4}	94	5.3×10^{-13}	94
^{93}Zr	4.7×10^{-3}	64	5.5×10^{-11}	64	2.1×10^{-2}	64	9.3×10^{-11}	64
^{93m}Nb	1.0×10^{0}	708	1.2×10^{-8}	717	4.2×10^{0}	626	1.8×10^{-8}	617
^{94}Nb	1.8×10^{-2}	501	2.1×10^{-10}	518	7.6×10^{-2}	475	3.3×10^{-10}	476
^{99}Tc	4.8×10^{-2}	103	5.5×10^{-10}	103	2.3×10^{-1}	94	1.0×10^{-9}	94
^{107}Pd	8.0×10^{-1}	1,158,161	9.2×10^{-9}	1,345,531	2.1×10^{0}	821,006	9.2×10^{-9}	719,871
^{113m}Cd	6.8×10^{-6}	108	7.9×10^{-14}	108	5.2×10^{-5}	110	2.3×10^{-13}	110
^{121m}Sn	4.3×10^{-3}	127	4.9×10^{-11}	127	1.9×10^{-2}	127	8.4×10^{-11}	128
^{126}Sn	1.7×10^{-2}	312	2.0×10^{-10}	315	7.9×10^{-2}	313	3.5×10^{-10}	307
^{129}I	2.7×10^{-2}	40	4.1×10^{-10}	34	3.5×10^{-2}	22	1.7×10^{-10}	35
$^{129}I^{a}$	8.4×10^{-2}	40	1.3×10^{-9}	34	1.1×10^{-1}	22	5.3×10^{-10}	35
^{135}Cs	1.5×10^{0}	472	1.8×10^{-8}	469	7.2×10^{0}	505	3.2×10^{-8}	485
^{137}Cs	9.8×10^{-5}	112	1.1×10^{-12}	112	4.3×10^{-4}	112	1.9×10^{-12}	112
^{151}Sm	2.0×10^{-2}	1,406	2.3×10^{-10}	1,217	8.6×10^{-2}	1,362	3.8×10^{-10}	1,244
^{152}Eu	7.3×10^{-5}	57	8.4×10^{-13}	57	5.1×10^{-3}	43	2.4×10^{-11}	42
^{154}Eu	2.7×10^{-5}	53	3.1×10^{-13}	53	2.6×10^{-3}	43	1.3×10^{-11}	42
^{155}Eu	8.6×10^{-5}	48	9.9×10^{-13}	48	1.3×10^{-2}	42	6.5×10^{-11}	42
^{207}Bi	1.4×10^{-3}	108	1.6×10^{-11}	108	6.3×10^{-3}	108	2.8×10^{-11}	108
^{210}Pb	7.7×10^{-7}	106	8.8×10^{-15}	106	3.4×10^{-6}	105	1.5×10^{-14}	105
^{226}Ra	4.9×10^{-5}	401	5.6×10^{-13}	394	2.1×10^{-4}	389	9.5×10^{-13}	400
^{229}Th	5.1×10^{-4}	967	5.8×10^{-12}	961	2.2×10^{-3}	939	9.8×10^{-12}	970
^{230}Th	3.7×10^{-2}	5,143	4.2×10^{-10}	5,154	1.6×10^{-1}	5,138	7.1×10^{-10}	5,138
^{232}Th	6.3×10^{-1}	100,762	7.3×10^{-9}	100,703	2.4×10^{0}	100,602	1.0×10^{-8}	100,653
^{231}Pa	5.3×10^{-1}	79,139	6.0×10^{-9}	79,134	2.0×10^{0}	79,038	8.9×10^{-9}	79,100
^{232}U	3.5×10^{-6}	190	4.0×10^{-14}	189	4.4×10^{-5}	95	1.9×10^{-13}	94
^{233}U	2.1×10^{-3}	724	2.4×10^{-11}	710	8.0×10^{-3}	466	3.5×10^{-11}	460

Table 4.9 (continued)

Nuclide	Recharge				Lateral flow			
	Flux (g/year)	Time (year)	Conc'n (g/mL)	Time (year)	Flux (g/year)	Time (year)	Conc'n (g/mL)	Time (year)
^{234}U	3.3×10^{-3}	711	3.8×10^{-11}	717	1.3×10^{-2}	448	5.6×10^{-11}	464
^{235}U	8.7×10^{0}	1,085	1.0×10^{-7}	1,094	3.2×10^{1}	808	1.4×10^{-7}	808
^{236}U	3.0×10^{-1}	720	3.5×10^{-9}	720	1.2×10^{0}	450	5.1×10^{-9}	463
^{238}U	1.8×10^{-3}	727	2.1×10^{-11}	718	7.0×10^{-3}	460	3.1×10^{-11}	457
^{237}Np	3.4×10^{-6}	208	3.9×10^{-14}	207	3.4×10^{-5}	100	1.5×10^{-13}	100
^{238}Pu	2.8×10^{1}	6,839	3.2×10^{-7}	6,838	7.7×10^{1}	6,831	3.4×10^{-7}	6,822
^{239}Pu	3.9×10^{-5}	717	4.4×10^{-13}	717	1.5×10^{-4}	465	6.6×10^{-13}	465
^{240}Pu	3.1×10^{-5}	671	3.5×10^{-13}	677	1.2×10^{-4}	432	5.3×10^{-13}	439
^{241}Pu	2.8×10^{-5}	387	3.2×10^{-13}	387	1.5×10^{-4}	202	6.5×10^{-13}	206
^{242}Pu	1.3×10^{-5}	67	1.5×10^{-13}	67	5.8×10^{-4}	43	2.6×10^{-12}	42
^{244}Pu	6.4×10^{-6}	251	7.3×10^{-14}	251	5.3×10^{-5}	162	2.4×10^{-13}	162
^{241}Am	4.2×10^{-4}	737	4.8×10^{-12}	729	1.6×10^{-3}	475	7.1×10^{-12}	476
^{242m}Am	1.6×10^{-5}	678	1.9×10^{-13}	686	6.6×10^{-5}	443	2.8×10^{-13}	440
^{243}Am	7.3×10^{-7}	113	8.4×10^{-15}	113	1.7×10^{-5}	94	7.5×10^{-14}	94
^{243}Cm	6.2×10^{-7}	73	7.1×10^{-15}	73	2.1×10^{-5}	47	9.2×10^{-14}	47
^{244}Cm	9.1×10^{-2}	980	1.0×10^{-9}	978	3.4×10^{-1}	728	1.5×10^{-9}	717
^{245}Cm	2.9×10^{-5}	690	3.4×10^{-13}	689	1.1×10^{-4}	445	5.1×10^{-13}	449
^{246}Cm	3.8×10^{-5}	659	4.3×10^{-13}	658	1.5×10^{-4}	428	6.6×10^{-13}	429
^{247}Cm	1.7×10^{-2}	723	1.9×10^{-10}	723	6.4×10^{-2}	477	2.8×10^{-10}	480
^{248}Cm	9.5×10^{-5}	739	1.1×10^{-12}	723	3.6×10^{-4}	474	1.6×10^{-12}	465
^{249}Cf	1.8×10^{-5}	361	2.0×10^{-13}	366	9.9×10^{-5}	185	4.4×10^{-13}	184
^{250}Cf	4.0×10^{-7}	64	4.5×10^{-15}	64	1.9×10^{-5}	43	8.6×10^{-14}	42
^{251}Cf	5.2×10^{-5}	500	6.0×10^{-13}	497	2.3×10^{-4}	303	1.0×10^{-12}	295

[a] Values are based on that inventory which corresponds to the drinking water concentration limit in groundwater or surface water (whichever is most limiting) at the end of the 100-year institutional control period.

from groundwater modeling for surface water dose calculations. The recharge flux results were provided as input to the FTWORK groundwater model.

Four nuclides with no chemical adsorption—^{3}H, ^{36}Cl, ^{79}Se, and ^{129}I—were simulated twice for an inventory meeting drinking water standards during the institutional control period with and without water collection and recycling. Lower flux values were simulated for the latter case (Table 4.9). Several of the 60 nuclides showed peak transport rates before the end of the institutional control period for the lateral and recharge paths (22 and 20 nuclides, respectively). The years of peak transport rates were often similar for both the recharge and lateral flow paths.

Changes in nuclide flux with time were plotted for seven selected nuclides with differing half-life and chemical adsorption properties (Table 4.1). Results for the lateral path calculations included a proportion of bypass flow that varied with K_d (Table 3.8). A large part of tritium [half-life ($T_{½}$) = 12.3 years, $K_d = 0$] transport occurred during the first few decades (Fig. 4.12) due to its rapid release rate from the concrete vaults and zero K_d in the vadose zone. Carbon-14 ($T_{½}$ = 5730 years, $K_d = 0$) showed three peaks in total flux (Fig. 4.13) that are associated with releases during major

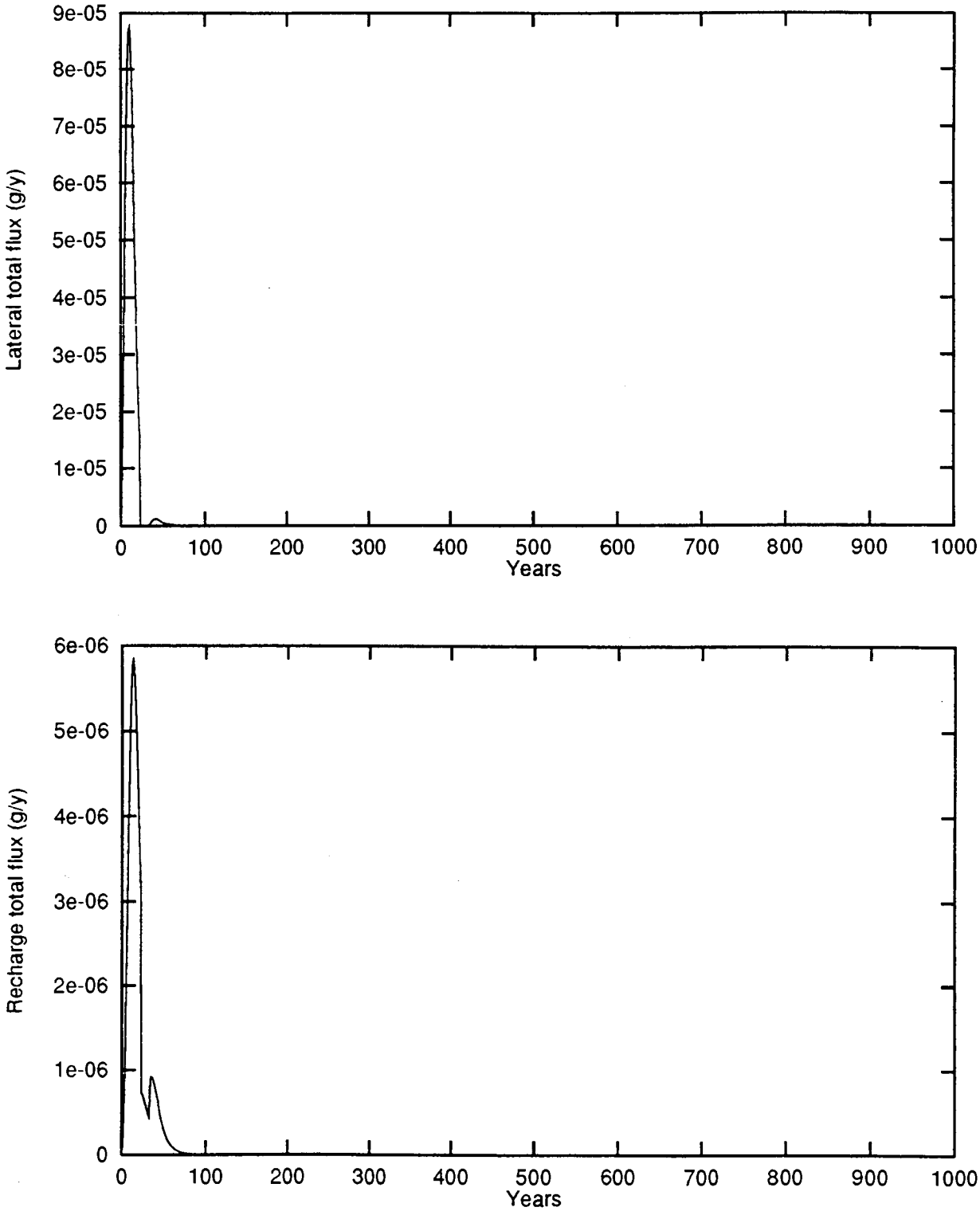

Fig. 4.12. Simulated ^3H release rates for the lateral subsurface and recharge paths from PADSIM as a function of time.

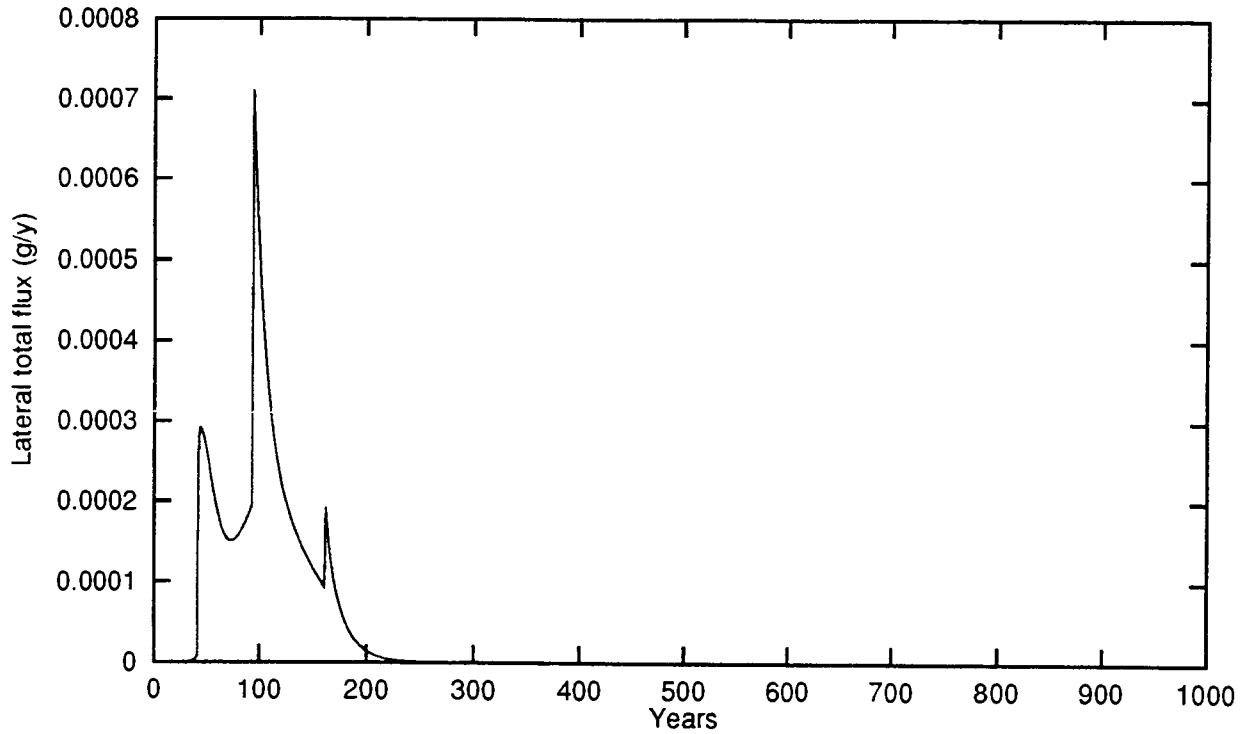

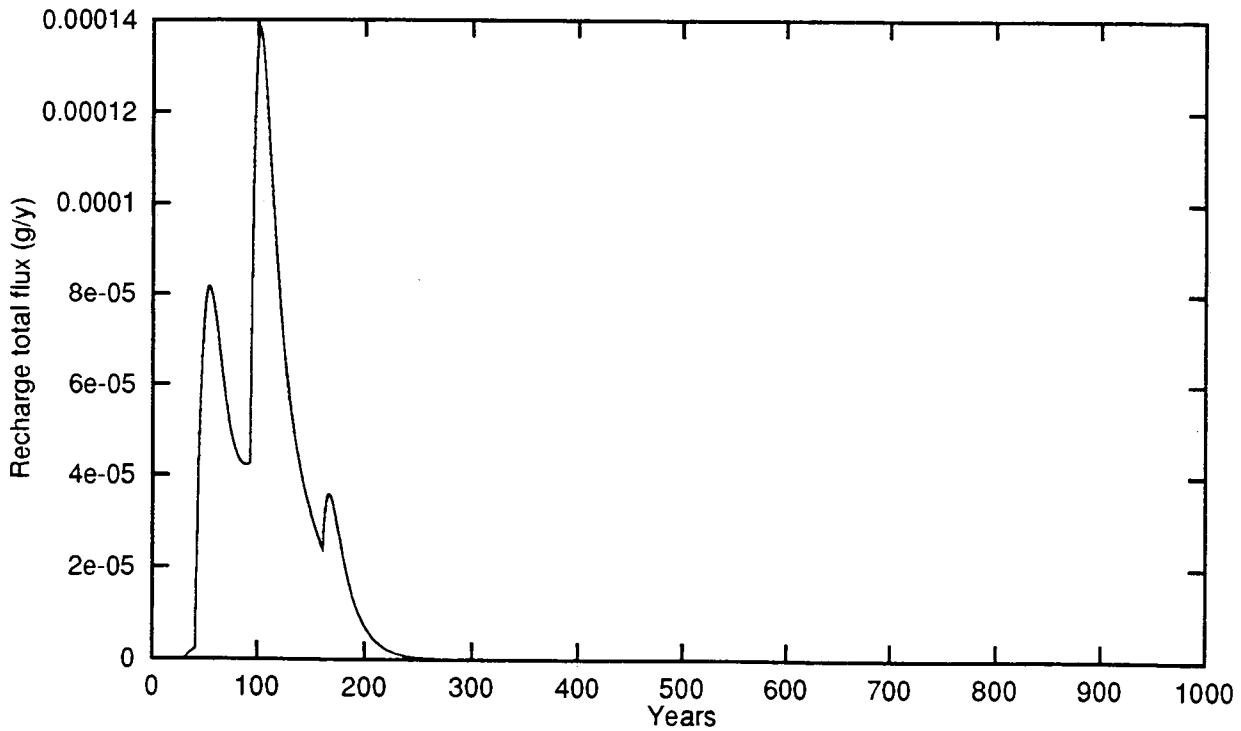

Fig. 4.13. Simulated ^{14}C release rates for the lateral subsurface and recharge paths from PADSIM as a function of time.

vault cracking events in SOURCE1 simulations (Fig. 4.3). The influence of chemical adsorption can be seen in the comparison of results for ^{14}C and ^{60}Co (Fig. 4.14), which show much smoother fluxes with time for ^{60}Co ($T_{½}$ = 5.27 years, K_d = 800) due to adsorption. The fluxes of ^{90}Sr ($T_{½}$ = 28.5 years, K_d = 30, Fig. 4.15) reflect greater peaks in the lateral flow path from the contributions of bypass flow (no chemical retention) than those obtained for the recharge path, where all nuclides interacted with the soil matrix. The results obtained for ^{99}Tc ($T_{½} = 2.13 \times 10^5$ years, K_d = 0, Fig. 4.16) were similar to those of ^{14}C, which also has no chemical adsorption in the flow paths. The higher K_d for cesium than strontium resulted in smoother fluxes with time for ^{137}Cs ($T_{½}$ = 30 years, K_d = 3000, Fig. 4.17). The long half-life for ^{238}U ($T_{½} = 4.47 \times 10^9$ years, K_d = 40) resulted in nuclide fluxes (Fig. 4.18) persisting for a much longer time than for the other nuclides.

The subsurface transport results show some movement of all nuclides to surface water. Field monitoring at ORNL waste areas has shown nuclide movement to surface water. The annual discharge of radionuclides at White Oak Dam in 1994 included 3.4 Ci of ^{90}Sr, 2800 Ci of ^{3}H, and 0.62 Ci of ^{137}Cs. These discharges were higher than in 1993 in association with greater precipitation in 1994 (Clapp and Watts 1995). The dominant sources of these discharges were from seepage areas from subsurface flow and groundwater outflow. Wickliff et al. (1989) have shown releases of ^{3}H, ^{90}Sr, and ^{137}Cs in association with bathtubbing trenches in SWSA 5 during storm events. Some transport of cesium could be occurring through adsorption on migrating clay colloids. Solomon et al. (1989) reported significant storm-driven migration of tritium from burial grounds on ORR. Actinide movement has also been observed (Ketelle et al. 1995). This was a surprising observation since actinides were thought to be essentially immobile in natural hydrologic systems. Natural organic colloids have been suggested as a means for enhancing actinide migration between a well and a seep situated 60 m downslope. We deliberately selected relatively low K_d values for uranium and transuranic radionuclides (K_d of 40) to allow for the effects of colloid transport in field soils.

4.3.2 Groundwater Transport

Radionuclides are introduced to the groundwater system as contaminated recharge beneath the disposal facility, with fluxes calculated by PADSIM as presented in the previous section. The groundwater flow and transport model, discussed in detail in Appendix E, calculates the fate of these radionuclides, which ultimately either discharge to surface waters or decay to insignificance on the way.

Groundwater concentrations were continuously "monitored" at a collection of compliance points making a ring 100 m from the edge of the grading used to support the disposal pad, which is presumed to be the edge of the closed and capped disposal facility (see Fig. 3.2). As contaminants migrated across this boundary during the simulation, the concentration of radionuclides was noted, and a peak concentration identified in time. This peak value was compared to the drinking water limit for the radionuclide in question. Results of the groundwater contaminant transport calculations were combined with those of the surface water transport as discussed in Sect. 4.3.4.

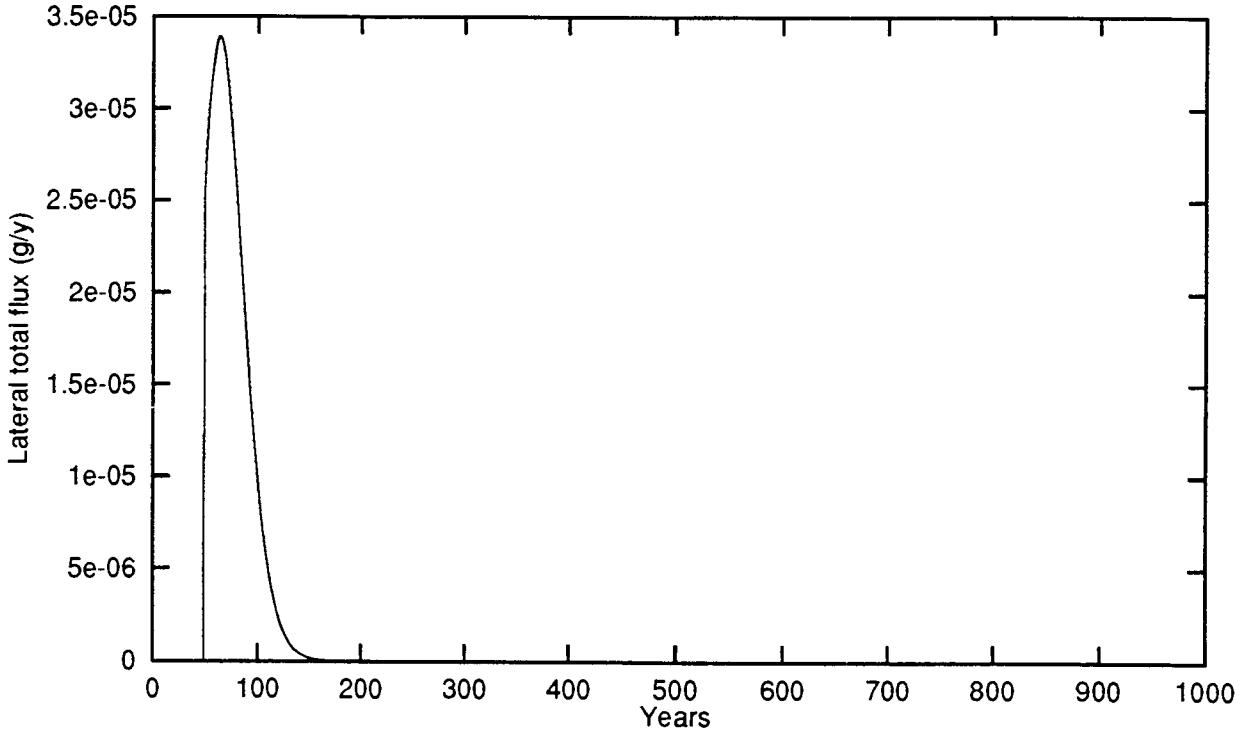

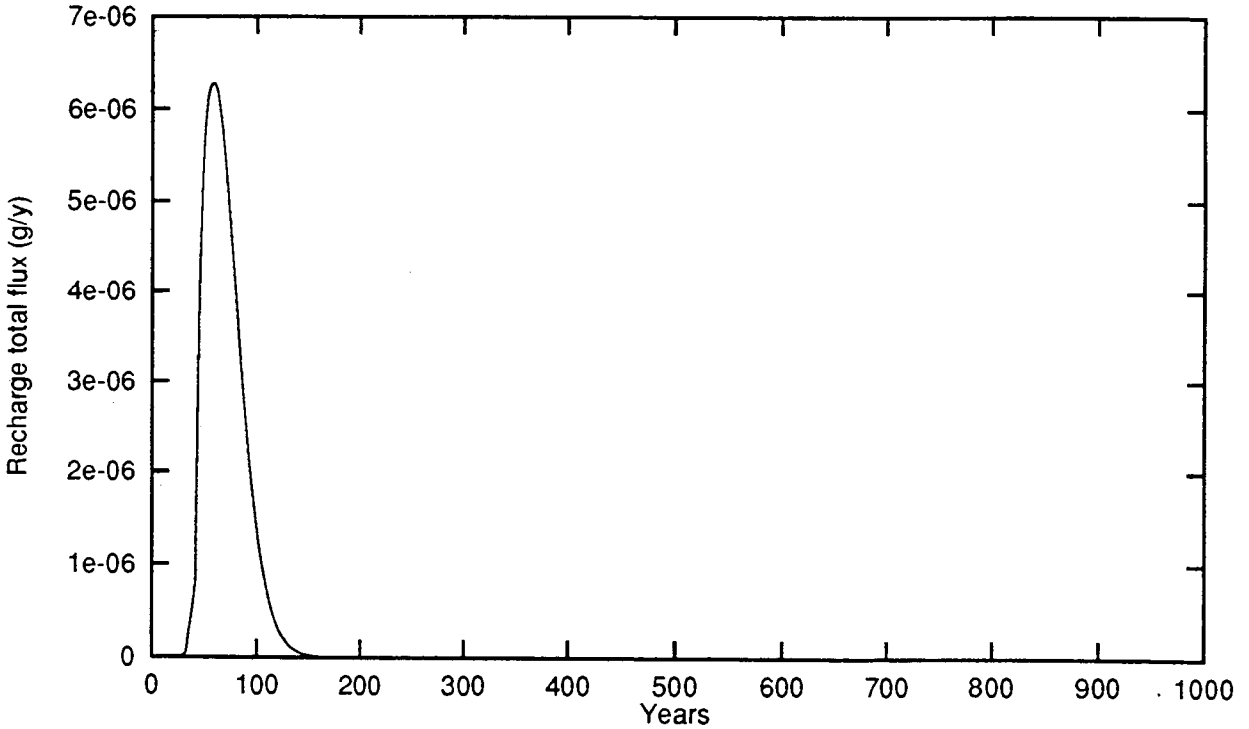

Fig. 4.14. Simulated ^{60}Co release rates for the lateral subsurface and recharge paths from PADSIM as a function of time.

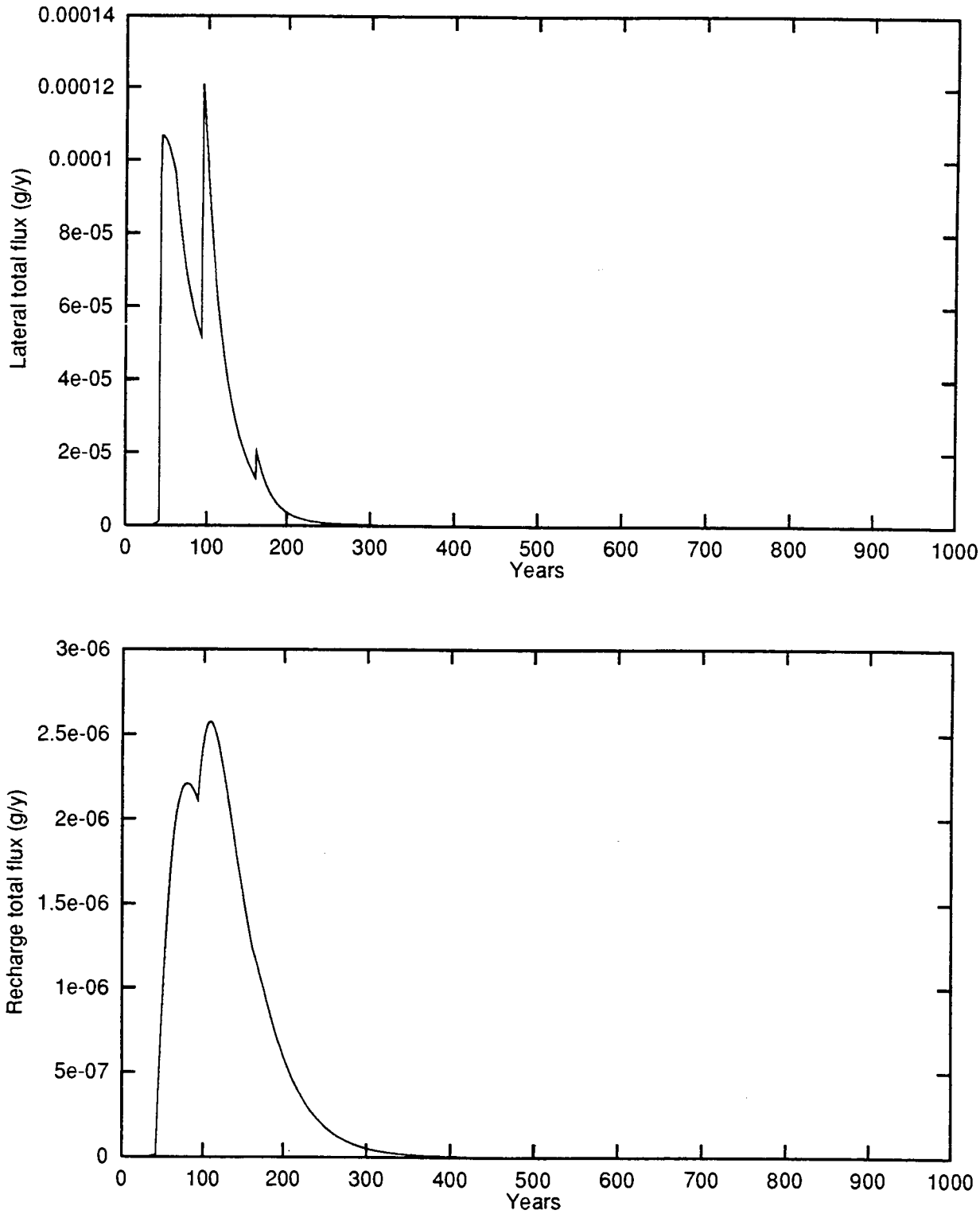

Fig. 4.15. Simulated ^{90}Sr release rates for the lateral subsurface and recharge paths from PADSIM as a function of time.

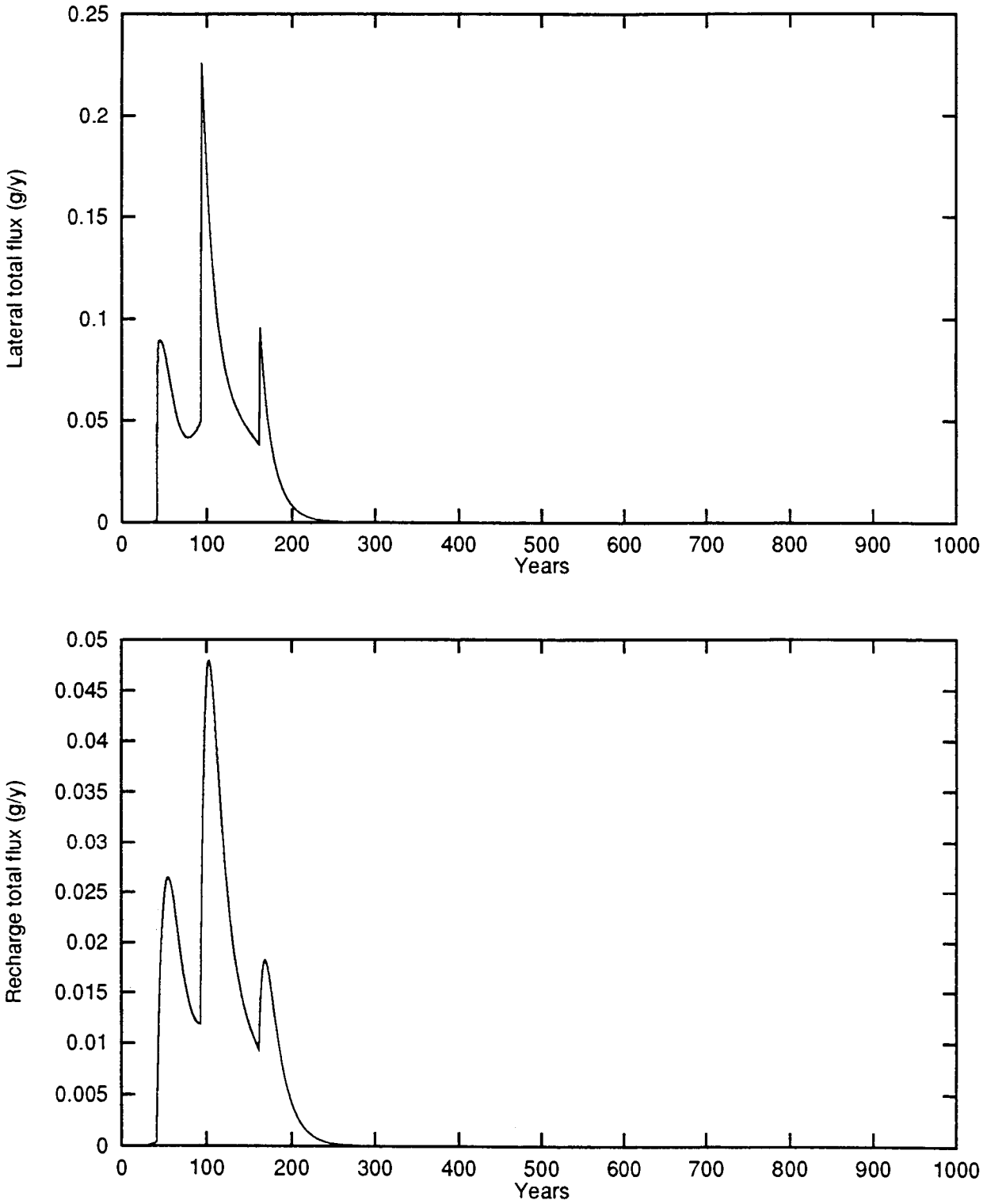

Fig. 4.16. Simulated ^{99}Tc release rates for the lateral subsurface and recharge paths from PADSIM as a function of time.

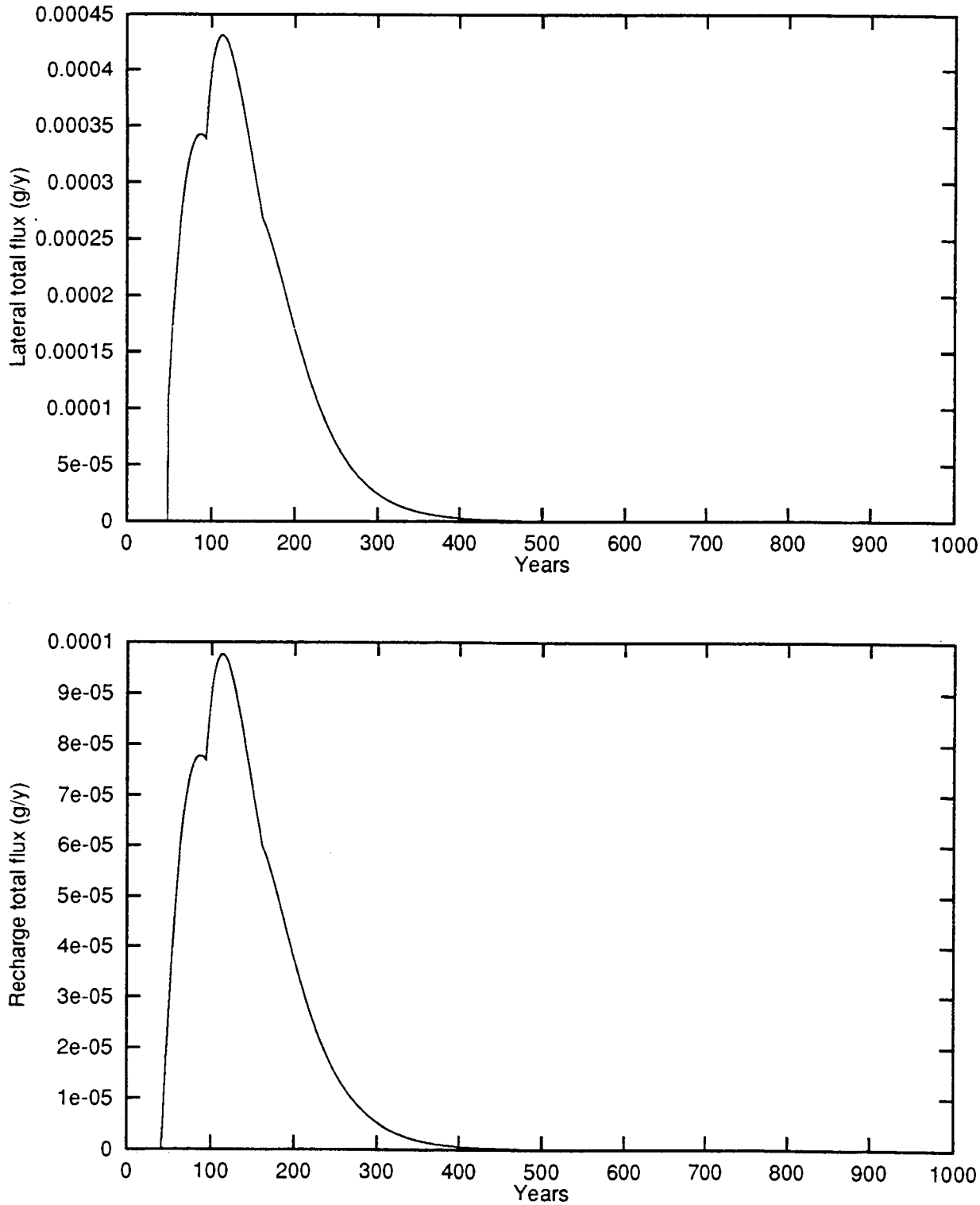

Fig. 4.17. Simulated ^{137}Cs release rates for the lateral subsurface and recharge paths from PADSIM as a function of time.

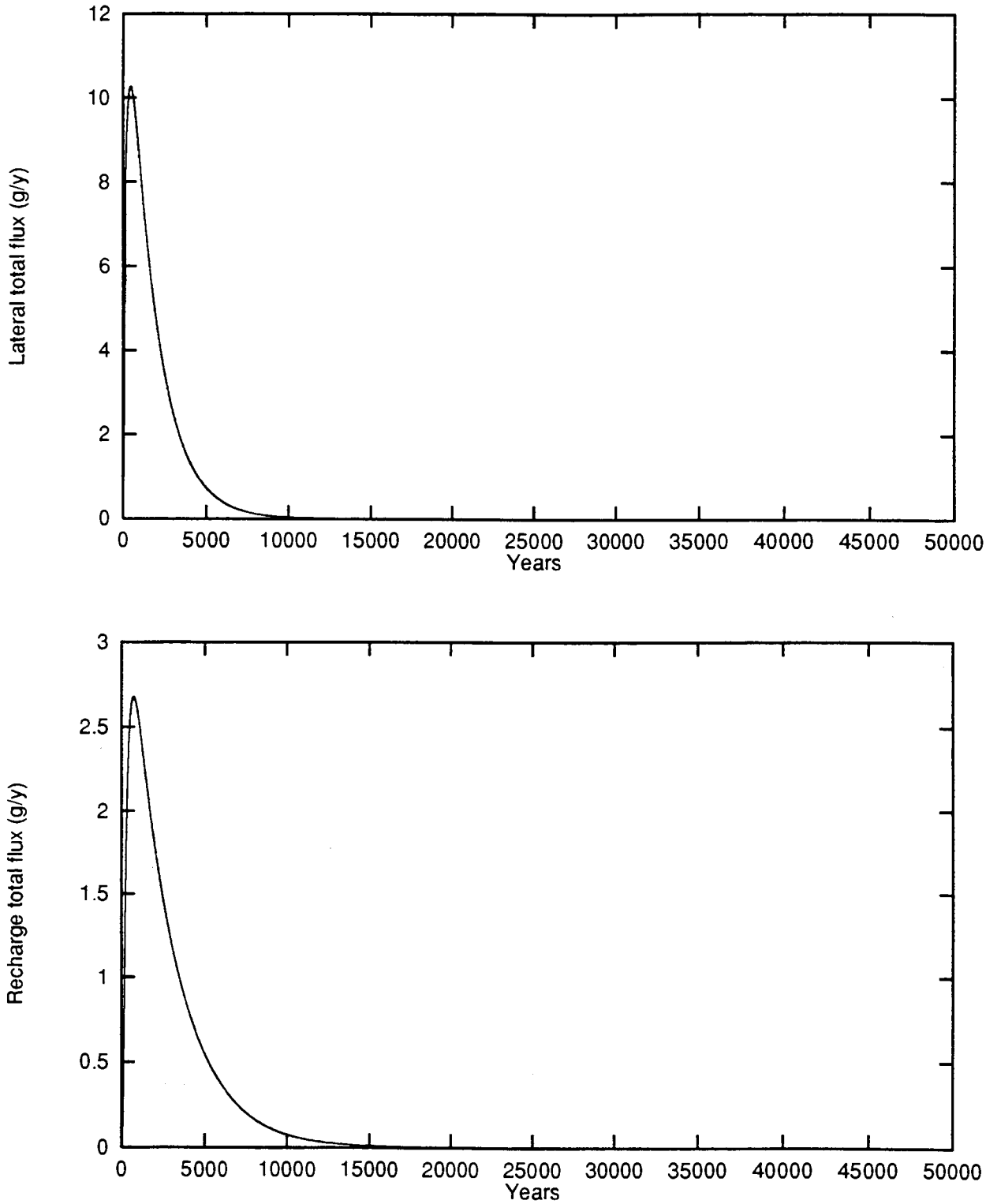

Fig. 4.18. Simulated ^{238}U release rates for the lateral subsurface and recharge paths from PADSIM as a function of time.

4.3.3 Surface Water Transport

Surface waters near CIIDF may be contaminated by either groundwater discharge to streams or by discharge of shallow subsurface transport. Both of these sources are aggregated on an annual time step to produce a drinking water concentration in Bear Creek, the region's only consistently available surface water source. For each radionuclide, the concentration in Bear Creek was noted over time, and a peak was identified. As for the groundwater source, this peak value was compared to the drinking water limit for the radionuclide in question. Results of the surface water contaminant transport calculations were combined with those of the groundwater transport as discussed in the following section.

4.3.4 Calculation of Contaminant Concentrations in Groundwater and Surface Water

The objective of the groundwater/surface water contaminant transport analysis was to determine the maximum allowable disposal limits for the CIIDF facility, based on an individual's exposure to contaminated drinking water (groundwater or surface water), for each of the 60 radionuclides listed in Table 3.1. As previously described, for each radionuclide, a series of iterations was performed in which time-dependent values for groundwater concentration at 100-m compliance points and surface water concentration in Bear Creek were calculated for various initial inventories. The limiting inventory for the drinking water pathway was determined to be that inventory of a given radionuclide which resulted in either a maximum groundwater* or maximum surface water concentration† which was equal to the allowable drinking water limit‡ for that radionuclide.

These limiting inventories and the corresponding concentrations in groundwater and surface water (and the times at which these values occur) are presented in Table 4.10. In most cases, either the groundwater or surface water concentration reached the drinking water limit and is identified in bold type along with the corresponding concentration in the other water source. For example, for the limiting inventory of ^{14}C presented in Table 4.5 and in Fig. 4.19, the corresponding peak concentrations in groundwater and surface water are in Table 4.10. The limiting pathway in this case is groundwater (values in bold type), which shows a peak concentration of 2.7×10^{-3} μCi/L at 140 years. This concentration of ^{14}C corresponds to the 4-mrem/year dose limit for drinking water, introduced in

* The maximum groundwater concentration for a given inventory is defined as the maximum concentration value that occurred at any point in time at any of the 100-m compliance points defined in Sect. 3.3.4.

† The maximum, combined surface water concentration for a given inventory is defined as the maximum concentration value that occurred at any point in time at a surface water receptor located in Bear Creek (see Sect. 3.3.4).

‡ These values are based on a dose limit for drinking water pathway of 4-mrem/year EDE, and the assumption that an individual would consume 2 L/d of contaminated water, as described in Sect. 4.4.1. Values are presented in Table 4.12.

Table 4.10. Maximum groundwater and surface water concentrations resulting from water pathway limiting inventories[a]

Nuclide	Groundwater		Surface water	
	Peak concentration (μCi/L)	Time of peak (year)	Peak concentration (μCi/L)	Time of peak (year)
^{3}H	**8.5×10^{-2}**	**45**	7.8×10^{-4}	22
^{3}H[b]	**8.5×10^{-2}**	**100**	8.5×10^{-2}	22
^{10}Be	**1.2×10^{-3}**	**440,000**	3.8×10^{-5}	26,000
^{14}C	**2.7×10^{-3}**	**140**	6.7×10^{-6}	110
^{26}Al	**3.6×10^{-4}**	**1,000,000**	3.9×10^{-5}	2,500
^{36}Cl	**1.8×10^{-3}**	**74**	4.4×10^{-7}	56
^{36}Cl[b]	**1.8×10^{-3}**	**100**	1.4×10^{-6}	56
^{40}K	**2.9×10^{-4}**	**14,000**	1.5×10^{-5}	110
^{41}Ca	**4.2×10^{-3}**	**14,000**	3.8×10^{-4}	180
^{60}Co[c]	No limit		**5.5×10^{-5}**	**73**
^{59}Ni	5.7×10^{-3}	500,000	**2.7×10^{-2}**	**920**
^{63}Ni	3.2×10^{-43}	2,700	**9.5×10^{-3}**	**200**
^{79}Se	**6.3×10^{-4}**	**80**	5.8×10^{-7}	61
^{79}Se[b]	**6.3×10^{-4}**	**100**	9.2×10^{-7}	61
^{87}Rb	**1.1×10^{-3}**	**14,000**	4.3×10^{-5}	180
^{90}Sr	4.6×10^{-24}	780	**3.6×10^{-5}**	**110**
^{93}Zr	**2.5×10^{-3}**	**23,000**	3.1×10^{-5}	640
^{93m}Nb	1.8×10^{-34}	460	**1.1×10^{-2}**	**100**
^{94}Nb	**7.7×10^{-4}**	**35,000**	4.2×10^{-5}	490
^{99}Tc	**3.6×10^{-3}**	**140**	8.7×10^{-6}	110
^{107}Pd[d]	2.1×10^{-3}	19,000,000	4.0×10^{-6}	1,600,000
^{113m}Cd	4.8×10^{-43}	480	**3.3×10^{-5}**	**120**
^{121m}Sn	3.2×10^{-25}	1,500	**3.3×10^{-3}**	**140**
^{126}Sn	**2.7×10^{-4}**	**43,000**	6.7×10^{-6}	330
^{129}I	**2.0×10^{-5}**	**100**	1.5×10^{-8}	56
^{129}I[b]	**2.0×10^{-5}**	**74**	4.9×10^{-9}	56
^{135}Cs	**7.7×10^{-4}**	**1,100,000**	2.5×10^{-5}	540
^{137}Cs[c]	No limit		**1.1×10^{-4}**	**120**
^{151}Sm[e]	4.8×10^{-38}	3,400	6.7×10^{-3}	1,800
^{152}Eu	4.3×10^{-43}	140	**8.5×10^{-4}**	**61**
^{154}Eu	1.2×10^{-33}	290	**5.8×10^{-4}**	**61**
^{155}Eu	2.9×10^{-37}	190	**3.6×10^{-3}**	**61**
^{207}Bi[c]	No limit		**9.8×10^{-4}**	**120**
^{210}Pb	1.8×10^{-35}	670	**7.5×10^{-7}**	**120**
^{226}Ra	1.9×10^{-29}	40,000	**6.3×10^{-7}**	**410**
^{229}Th	1.3×10^{-18}	160,000	**1.4×10^{-6}**	**970**
^{230}Th	1.2×10^{-7}	610,000	**1.0×10^{-5}**	**5,200**
^{232}Th[d]	7.2×10^{-8}	1,500,000	6.7×10^{-10}	79,000
^{231}Pa	**2.1×10^{-7}**	**120,000**	5.9×10^{-8}	1,000
^{232}U	2.2×10^{-20}	1,700	**2.7×10^{-6}**	**110**

Table 4.10 (continued)

Nuclide	Groundwater		Surface water	
	Peak concentration (μCi/L)	Time of peak (year)	Peak concentration (μCi/L)	Time of peak (year)
^{233}U	**1.9×10^{-5}**	**18,000**	2.3×10^{-7}	470
^{234}U	**2.0×10^{-5}**	**18,000**	2.4×10^{-7}	480
^{235}U	**2.0×10^{-5}**	**19,000**	2.1×10^{-7}	850
^{236}U	**2.0×10^{-5}**	**18,000**	2.2×10^{-7}	480
^{238}U	**2.1×10^{-5}**	**23,000**	7.8×10^{-8}	6,800
^{237}Np	**1.3×10^{-6}**	**18,000**	1.5×10^{-8}	480
^{238}Pu	3.1×10^{-19}	2,000	**1.7×10^{-6}**	**110**
^{239}Pu	**1.5×10^{-6}**	**18,000**	2.8×10^{-8}	480
^{240}Pu	**1.5×10^{-6}**	**13,500**	8.1×10^{-8}	450
^{241}Pu	1.6×10^{-30}	450	**8.0×10^{-5}**	**61**
^{242}Pu	**1.6×10^{-6}**	**18,000**	1.8×10^{-8}	490
^{244}Pu	**1.7×10^{-6}**	**19,000**	1.8×10^{-8}	740
^{241}Am	8.1×10^{-11}	6,200	**1.5×10^{-6}**	**220**
^{242m}Am	8.3×10^{-16}	3,300	**8.2×10^{-7}**	**180**
^{243}Am	**1.5×10^{-6}**	**14,000**	6.9×10^{-8}	470
^{243}Cm	4.8×10^{-27}	800	**2.2×10^{-6}**	**110**
^{244}Cm	3.2×10^{-30}	550	**2.7×10^{-6}**	**110**
^{245}Cm	**1.5×10^{-6}**	**14,000**	5.8×10^{-8}	460
^{246}Cm	**1.5×10^{-6}**	**13,000**	1.4×10^{-7}	440
^{247}Cm	**1.6×10^{-6}**	**18,000**	1.8×10^{-8}	500
^{248}Cm	**4.0×10^{-7}**	**18,000**	4.6×10^{-9}	480
^{249}Cf	7.5×10^{-12}	5,000	**1.2×10^{-6}**	**200**
^{250}Cf	9.9×10^{-33}	410	**2.7×10^{-6}**	**61**
^{251}Cf	2.1×10^{-8}	8,800	**1.1×10^{-6}**	**320**

[a] Limiting inventories are presented in Table 4.5, and drinking water concentration limits are presented in Table 4.12.

[b] Inventory limit was based on allowing the maximum concentration to occur at the end of the 100-year institutional control period, rather than at any earlier time.

[c] Groundwater concentration corresponding to surface water limited inventory was incalculably low.

[d] Intruder limit was used, since the drinking water limit was extremely high and no peak could be defined.

[e] Limited by physical disposal considerations, since allowable drinking water concentration could not be reached in either groundwater or surface water.

Sect. 3.3.5. The peak surface water concentration results from the same limiting inventory. It should be restated that the limiting inventory was reached only after iterating on the concentration values, until one of the values reached the maximum allowable drinking water concentration for each radionuclide.

All but two radionuclides (^{151}Sm and ^{107}Pd) displayed a substantially linear relationship between concentration in the waste and concentration in the drinking water, at both the groundwater compliance well "ring" and at the surface water point. This linear behavior can be used to estimate the allowable waste concentrations which would correspond to other concentrations in the drinking water, as in the case of assessing compound doses from various contributing radionuclides. Fig. 4.19

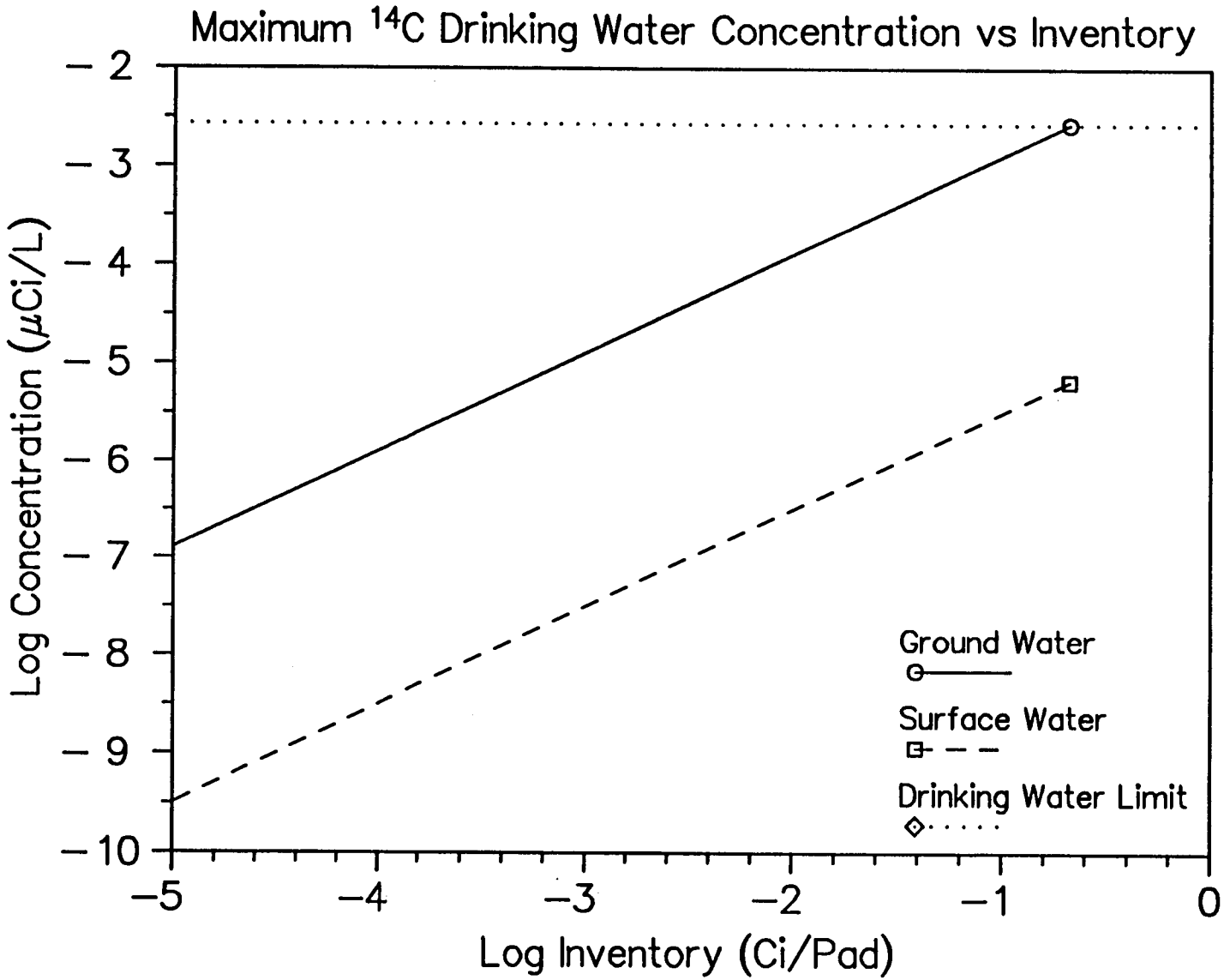

Fig. 4.19. Drinking water concentration as a function of CIIDF inventory for ^{14}C.

illustrates this standard linear behavior with ^{14}C. A complete set of graphs illustrating the relationship between source (inventory) concentration and drinking water concentration is given in Appendix F.

Several radionuclides encountered solubility limitations at some point during the analysis, as shown in Table 4.8. While most of these displayed a nearly linear relationship between inventory and drinking water concentrations, a few are worthy of further discussion. The effect of solubility limitation in the environmental transport pathway was to truncate the concentration vs time curve (either in the facility or in the environment) at the chemical's solubility concentration and to increase the duration of that peak concentration until the source became exhausted. This resulted in a nonlinear relation between the source concentration and the drinking water concentration, with some interesting effects.

For four radionuclides either with long half-lives and high K_d or with low solubilities it was necessary to use completely unrealistic inventories in order to calculate a "peak" groundwater or surface water concentration equal to allowable limits. For ^{60}Co and ^{151}Sm, groundwater and surface water calculations were made using the inventory corresponding to a maximum physical disposal limit (disposal of pure material) and are illustrated by ^{60}Co in Fig. 4.20.

For ^{107}Pd and ^{232}Th, even with the use of physical disposal limits, it was impossible to obtain groundwater or surface water concentrations which reached a peak value in time. Although these radionuclides did not lend themselves well to water transport analysis, they are clearly not limited by the water pathway. So for practical reasons, the maximum groundwater and surface water concentrations were calculated using inventories corresponding to intruder limits.

For a few radionuclides (^{3}H, ^{36}Cl, ^{79}Se, and ^{129}I) peak concentrations in groundwater occurred before the end of the institutional control period at 100 years. For these species, additional simulations were conducted to determine what the limiting inventory would be if concentrations before 100 years were ignored. In other words, a higher limiting inventory is acheived if the maximum allowable concentration is not considered before 100 years. Since these values are not protective of the groundwater resource, however, these values are presented for informational purposes only, and are not considered to constitute a limiting or allowable inventory.

Complete concentration vs time curves for seven radionuclides of particular interest (^{3}H, ^{14}C, ^{60}Co, ^{90}Sr, ^{99}Tc, ^{137}Cs, and ^{238}U) are given in Fig. 4.21 through Fig. 4.27.

4.4 DOSE ANALYSIS

This section presents the results of the dose analyses for off-site individuals and inadvertent intruders in the PA for CIIDF. The results are given in the form of annual EDEs per unit concentration of radionuclides in a particular medium of concern, which is assumed to be groundwater or surface water for exposures of off-site individuals and the disposal facility itself for exposures of inadvertent intruders.

In Sect. 4.5.1, the results of the dose analysis for off-site individuals are combined with the calculated maximum concentrations of radionuclides in groundwater or surface water per unit initial inventory in the disposal facility to derive allowable limits on the inventory of radionuclides that would

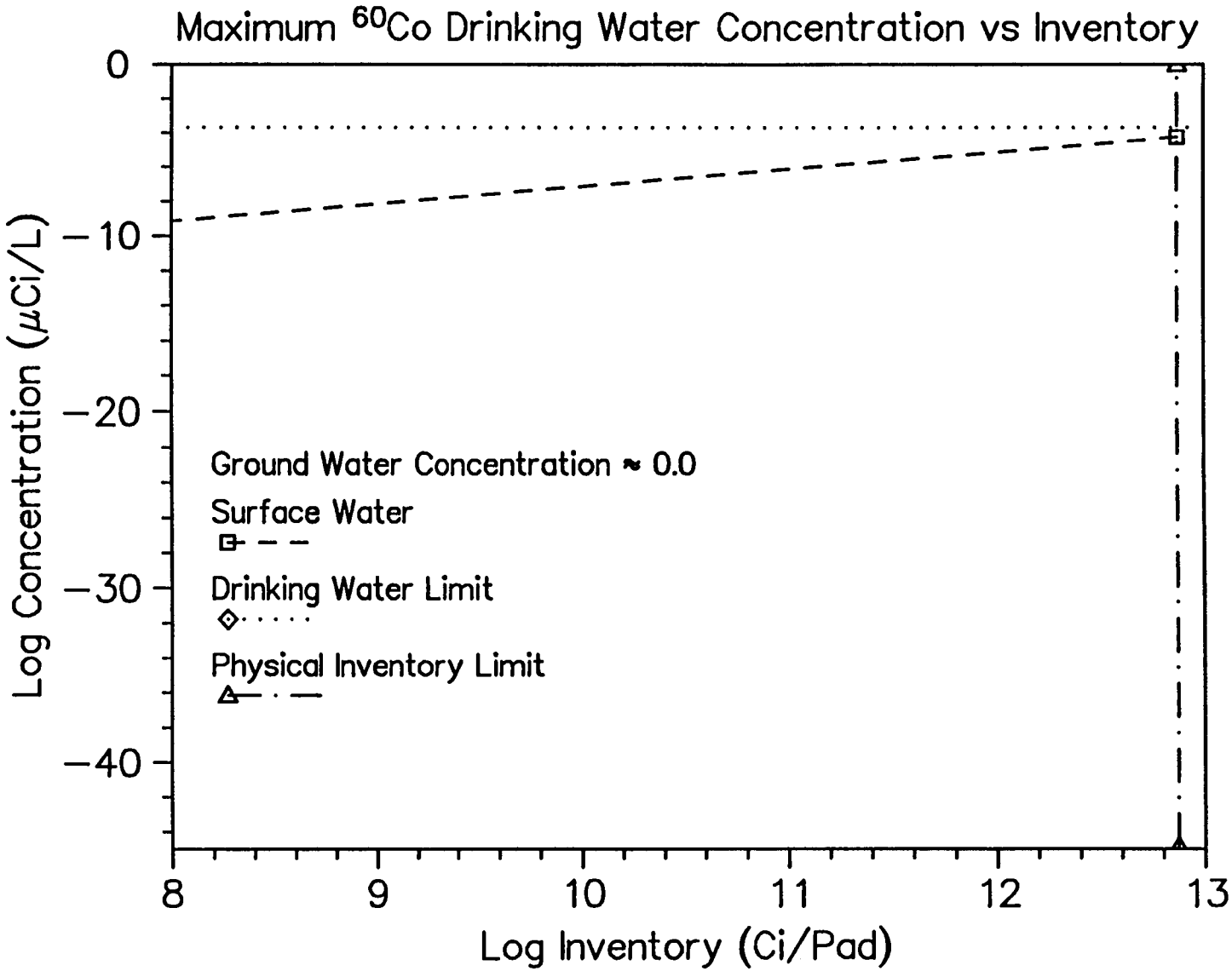

Fig. 4.20. Drinking water concentration as a function of CIIDF inventory for ^{60}Co.

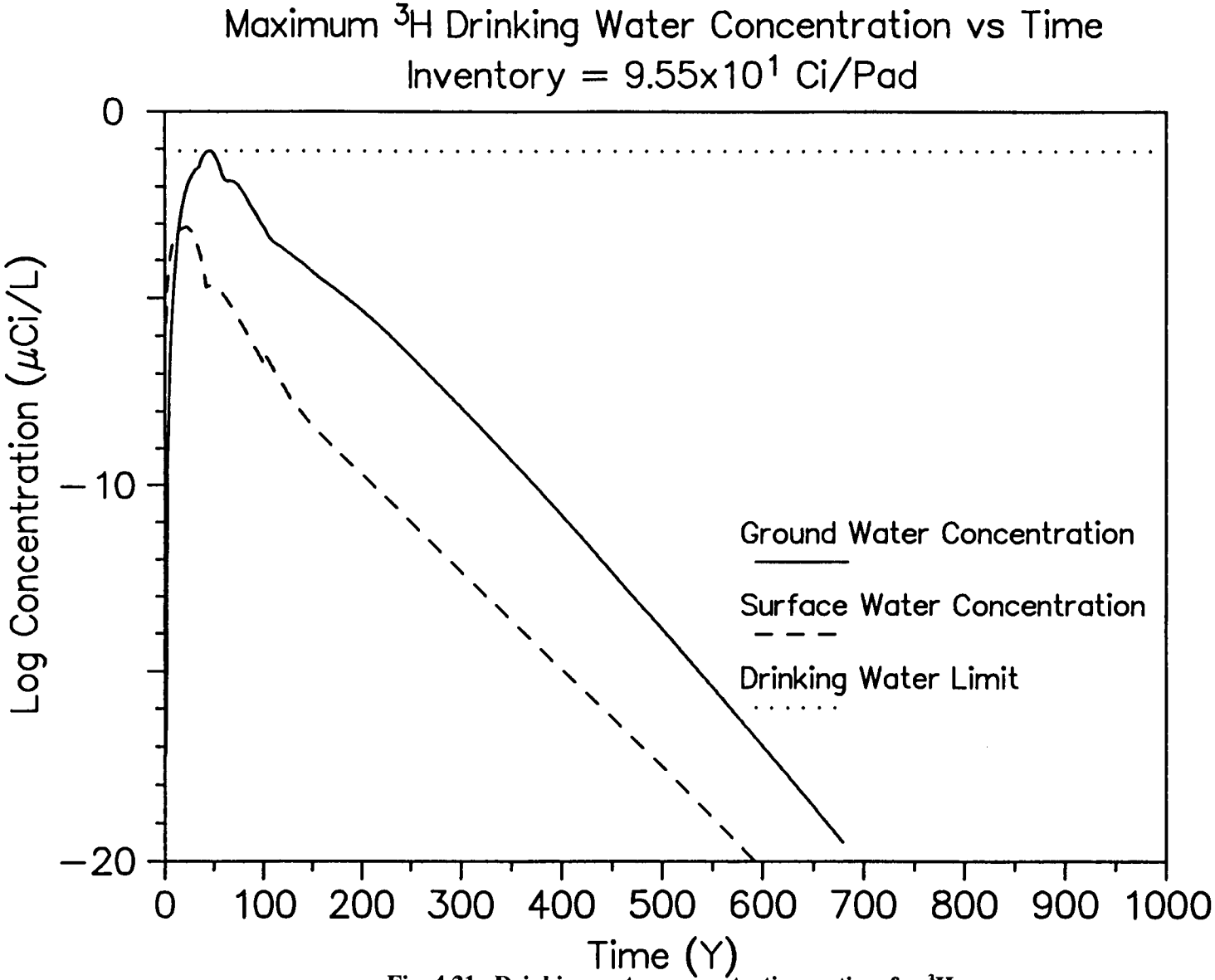

Fig. 4.21. Drinking water concentration vs time for ^{3}H.

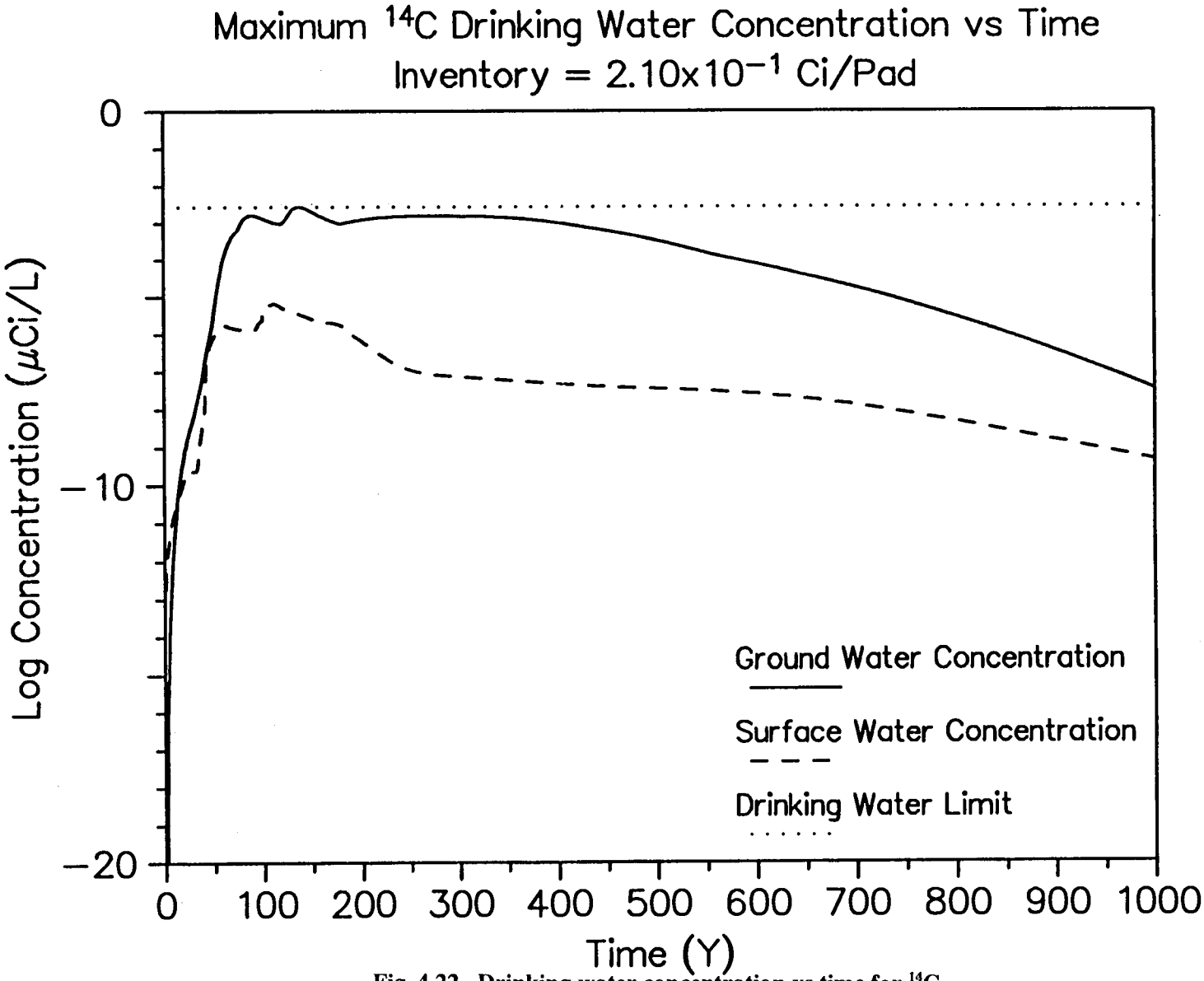

Fig. 4.22. Drinking water concentration vs time for ^{14}C.

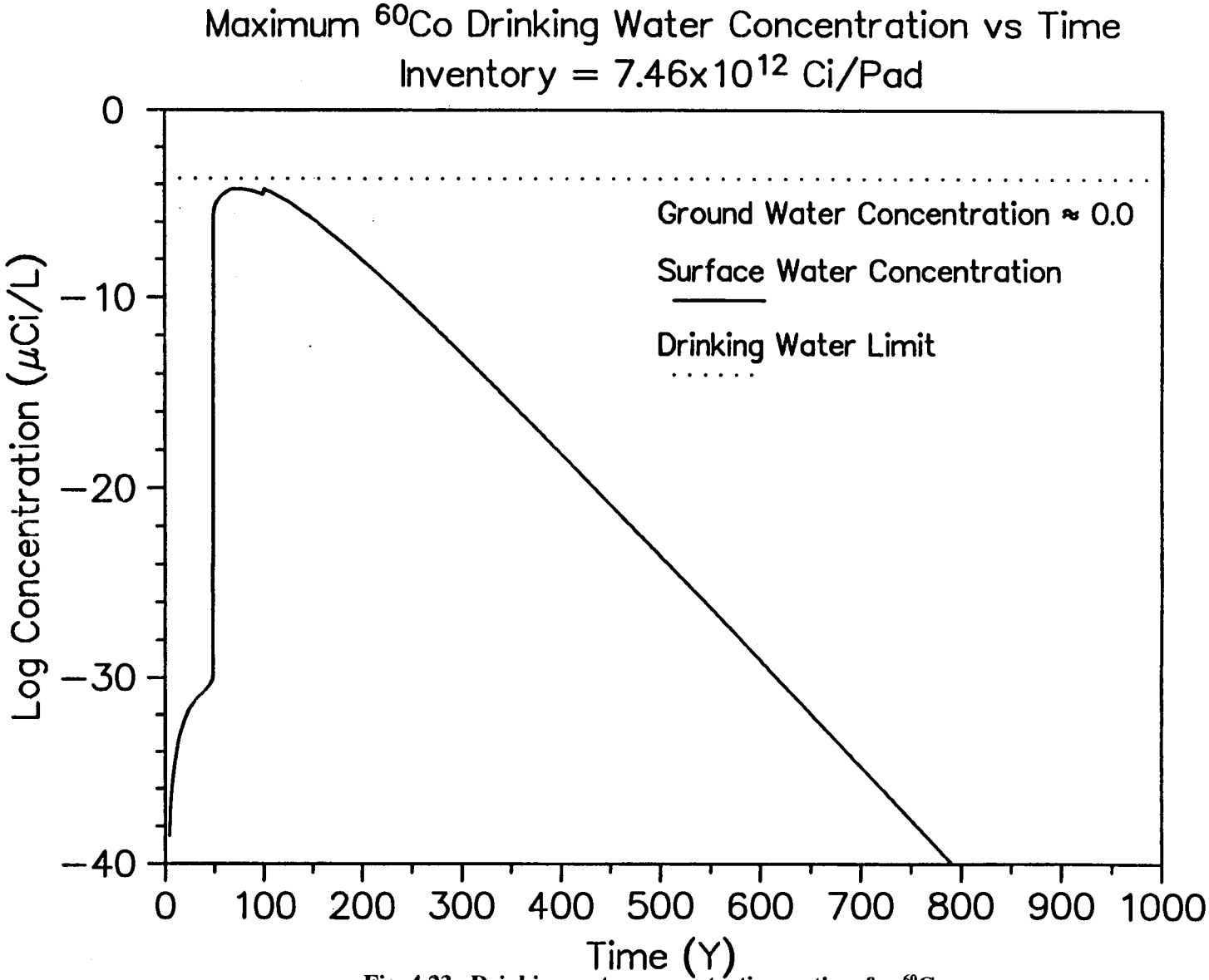

Fig. 4.23. Drinking water concentration vs time for ^{60}Co.

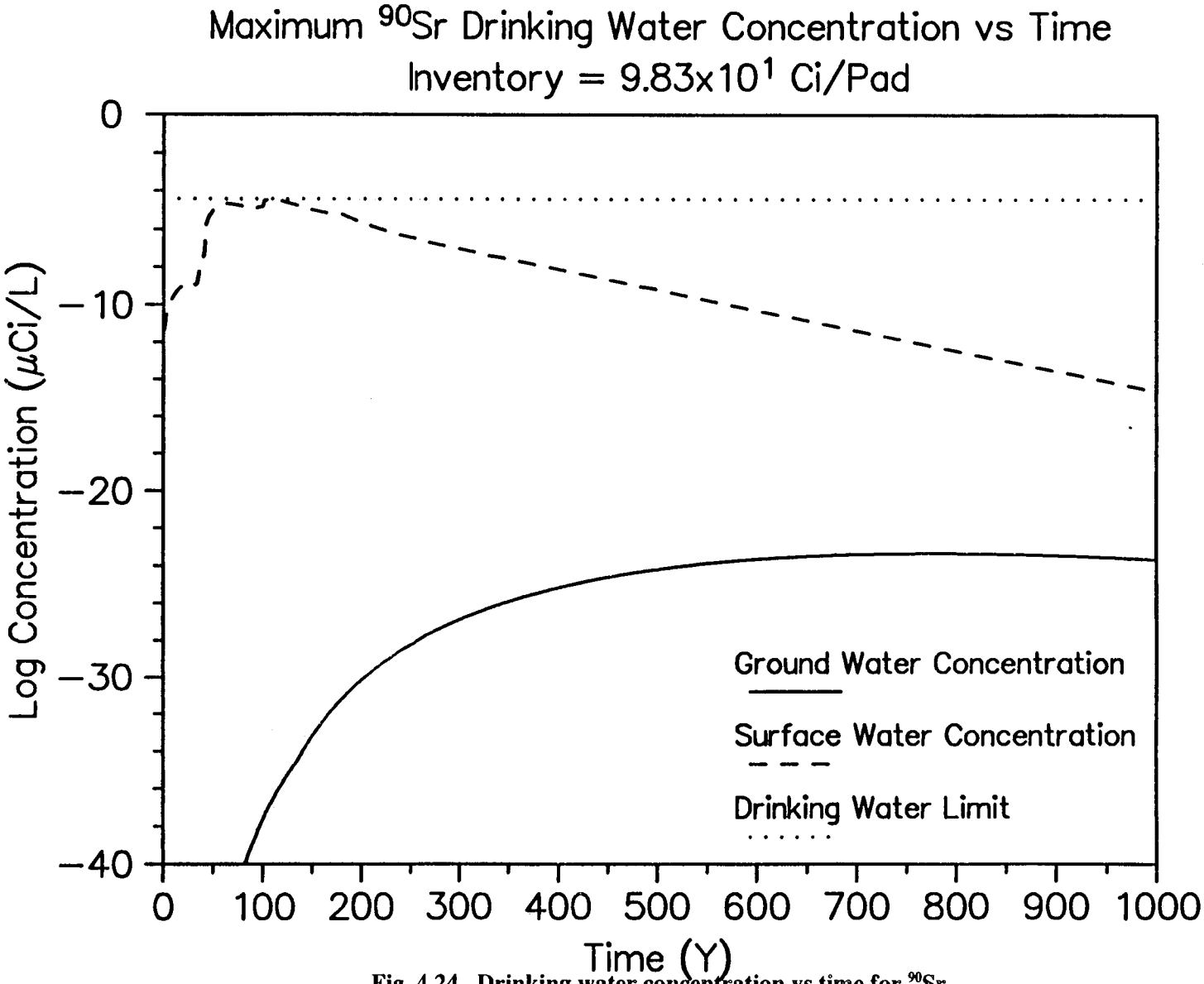

Fig. 4.24. Drinking water concentration vs time for ^{90}Sr.

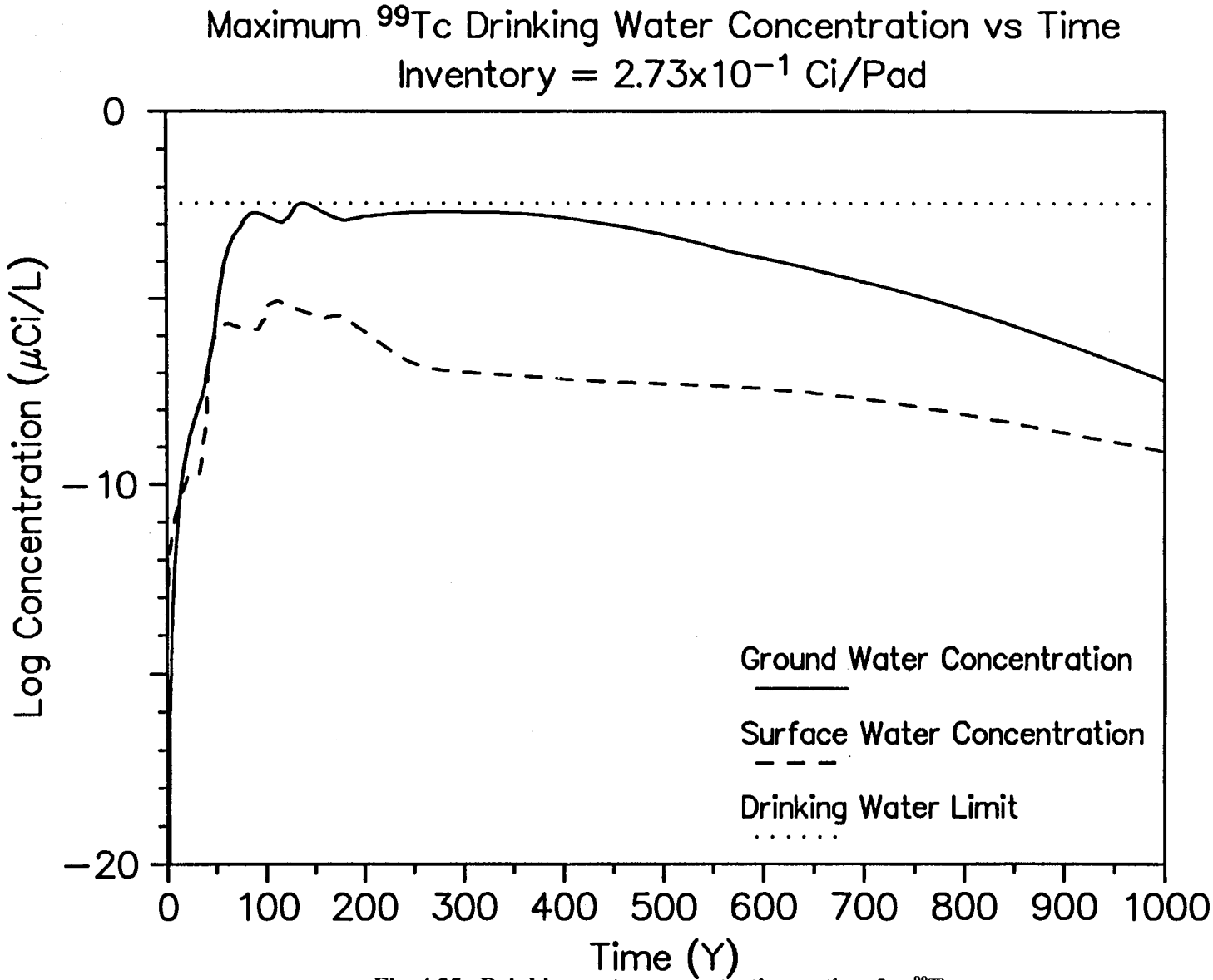

Fig. 4.25. Drinking water concentration vs time for ^{99}Tc.

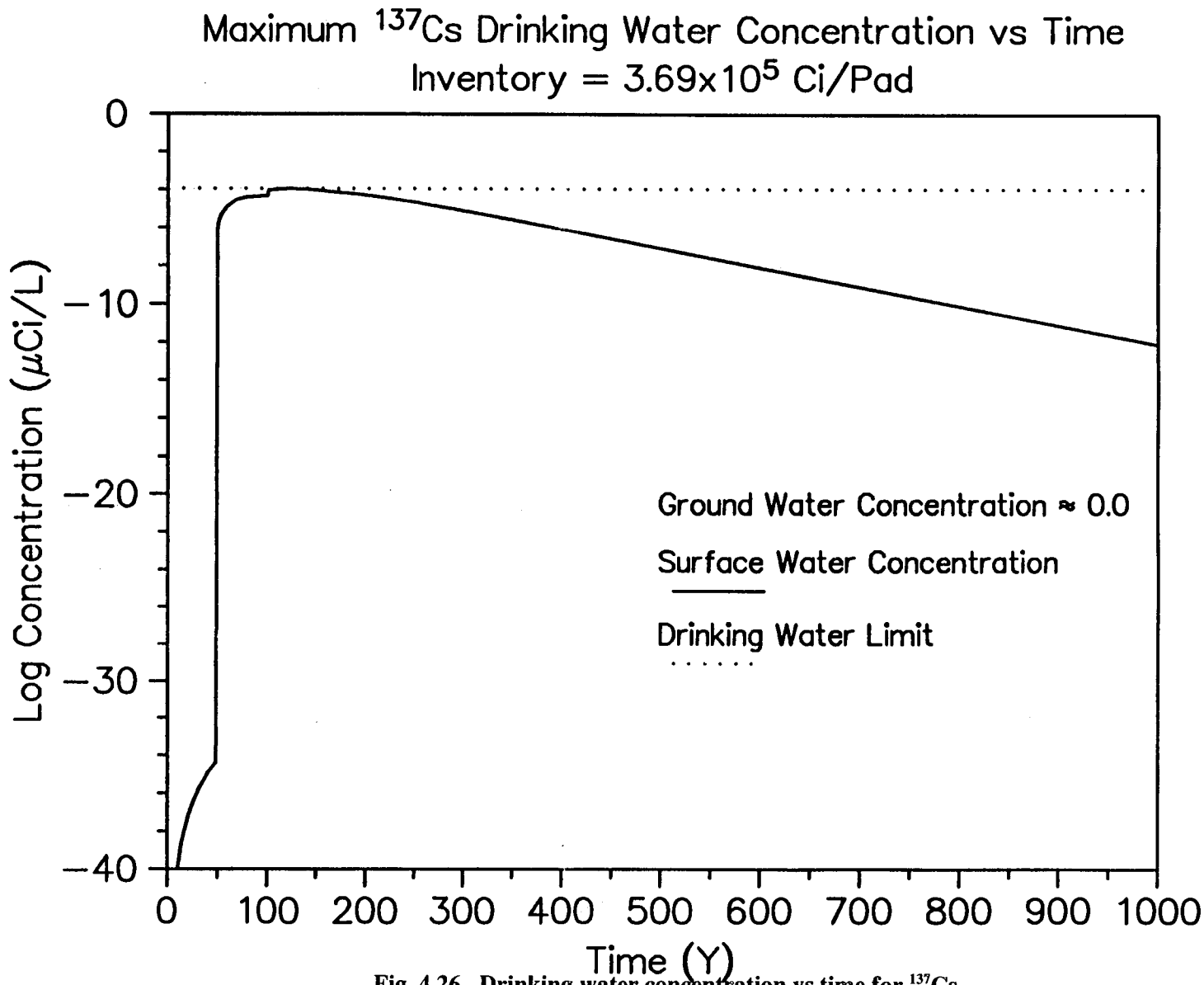

Fig. 4.26. Drinking water concentration vs time for ^{137}Cs.

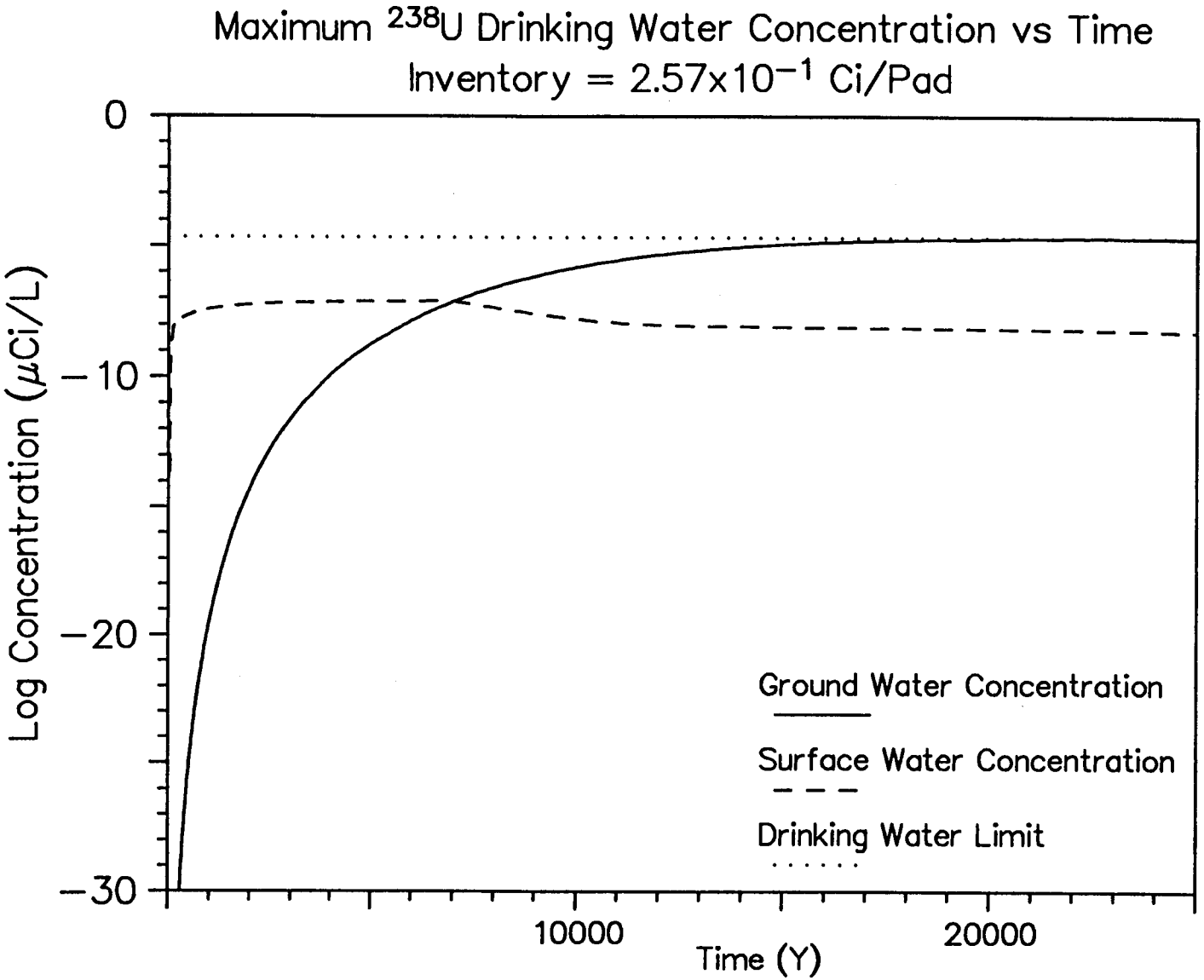

Fig. 4.27. Drinking water concentration vs time for ^{238}U.

provide reasonable assurance of compliance with the applicable performance objectives for off-site releases by water pathways. Similarly, in this section and in Sect. 4.5.2, the results of the dose analysis for inadvertent intruders are combined with calculated concentrations of radionuclides in the disposal facility at the time intrusion is assumed to occur per unit concentration in waste prior to disposal to derive allowable limits on inventory that would provide reasonable assurance of compliance with the performance objectives for inadvertent intruders. The allowable limit on inventory for any radionuclide then would be based on the more restrictive of the estimated limits for off-site releases and protection of inadvertent intruders.

4.4.1 Off-Site Exposure

As discussed in Sect. 3.1, releases of radionuclides to groundwater or surface water are the only transport pathways evaluated in the PA for CIIDF for the purpose of demonstrating compliance with the applicable performance objectives for off-site individuals. Potential releases to the atmosphere and potential releases due to biotic intrusion are believed to be negligible compared with the estimated releases by water pathways.

Furthermore, as discussed in Sect. 3.1.2.1, the only exposure pathway evaluated in the PA for off-site releases by water pathways is direct consumption of drinking water obtained from contaminated groundwater or surface water. If the dose to an off-site individual from the drinking water pathway only would be in compliance with the assumed performance objective for this pathway of 4-mrem/year EDE, then the total dose from all exposure pathways involving use of contaminated water would not exceed the applicable performance objective of 25-mrem/year EDE.

The results of the dose analysis for the drinking water pathway are given in Table 4.11. The annual EDE from the drinking water pathway per unit concentration of radionuclides in water is based on the model and parameter values described in Sect. G.5.1 of Appendix G, and the results in Table 4.11 are obtained from Table G.6 of Appendix G.

The results in Table 4.11 can be combined with the assumed performance objective for the drinking water pathway to obtain the allowable limits on concentrations of radionuclides in groundwater or surface water at off-site locations. The allowable limit on concentration in water (C_w) for a radionuclide is given by

$$C_w\,(\mu\text{Ci/L}) = \frac{(0.004\ \text{rem/year})}{\text{PDCF}_w(\text{rem/year per }\mu\text{Ci/L})}\ , \qquad \textbf{(4.1)}$$

where the numerator is the performance objective for the groundwater pathway and PDCF_w is the so-called pathway dose conversion factor for the drinking water pathway given in Table 4.11. The resulting allowable limits on concentrations of radionuclides in groundwater or surface water at off-site locations are given in Table 4.12.

Table 4.11. Annual effective dose equivalents from drinking water pathway per unit concentration of radionuclides in water[a]

Nuclide[b]	Annual dose (rem/year per μCi/L)	Nuclide[b]	Annual dose (rem/year per μCi/L)
^{3}H	4.7×10^{-2}	^{226}Ra[d]	9.5×10^{2}
^{10}Be	3.4	$^{229}Th + d$	2.9×10^{3}
^{14}C	1.5	^{230}Th	4.0×10^{2}
^{26}Al	1.1×10^{1}	$^{232}Th + d$	3.6×10^{3}
^{36}Cl	2.2	$^{231}Pa + d$	1.9×10^{4}
^{40}K	1.4×10^{1}	$^{232}U + d$	1.5×10^{3}
^{41}Ca	9.5×10^{-1}	^{233}U	2.1×10^{2}
^{60}Co	2.0×10^{1}	^{234}U	2.0×10^{2}
^{59}Ni	1.5×10^{-1}	^{235}U	2.0×10^{2}
^{63}Ni	4.2×10^{-1}	^{236}U	2.0×10^{2}
^{79}Se	6.4	$^{238}U + d$	1.9×10^{2}
^{87}Rb	3.6	^{237}Np	3.2×10^{3}
$^{90}Sr + d$	1.1×10^{2}	^{238}Pu	2.3×10^{3}
^{93}Zr[c]	1.2	^{239}Pu	2.6×10^{3}
^{93m}Nb	3.8×10^{-1}	^{240}Pu	2.6×10^{3}
^{94}Nb	5.2	^{241}Pu	5.0×10^{1}
^{99}Tc	1.1	^{242}Pu	2.5×10^{3}
^{107}Pd	1.1×10^{-1}	^{244}Pu	2.4×10^{3}
^{113m}Cd	1.2×10^{2}	^{241}Am	2.6×10^{3}
^{121m}Sn	1.2	$^{242m}Am + d$[e]	2.6×10^{3}
$^{126}Sn + d$	1.5×10^{1}	^{243}Am	2.6×10^{3}
^{129}I	2.0×10^{2}	^{243}Cm	1.8×10^{3}
^{135}Cs	5.2	^{244}Cm	1.5×10^{3}
^{137}Cs	3.7×10^{1}	^{245}Cm	2.7×10^{3}
^{151}Sm	2.8×10^{-1}	^{246}Cm	2.7×10^{3}
^{152}Eu	4.7	^{247}Cm	2.5×10^{3}
^{154}Eu	6.9	^{248}Cm	1.0×10^{4}
^{155}Eu	1.1	^{249}Cf	3.4×10^{3}
^{207}Bi	4.0	^{250}Cf	1.5×10^{3}
$^{210}Pb + d$	5.3×10^{3}	^{251}Cf	3.5×10^{3}

[a] Results obtained from Table G.6 of Appendix G give 50-year committed EDEs from one year's intake of drinking water and apply to concentrations of radionuclides in groundwater or surface water at point of use.

[b] The notation "+ d" in some entries denotes short-lived decay products that are assumed to be in secular equilibrium with parent radionuclide; see Table G.1 of Appendix G for decay products and branching fractions.

[c] Possible contributions to dose from ^{93m}Nb decay product are not included.

[d] Possible contributions to dose from ^{210}Pb decay product are not included.

[e] Possible contributions to dose from ^{238}Pu decay product are not included.

Table 4.12. Allowable limits on concentrations of radionuclides in groundwater or surface water at off-site locations[a]

Nuclide	Concentration (μCi/L)	Nuclide	Concentration (μCi/L)
^{3}H	8.5×10^{-2}	^{226}Ra[c]	6.3×10^{-7}
^{10}Be	1.2×10^{-3}	^{229}Th	1.4×10^{-6}
^{14}C	2.7×10^{-3}	^{230}Th	1.0×10^{-5}
^{26}Al	3.6×10^{-4}	^{232}Th	1.1×10^{-6}
^{36}Cl	1.8×10^{-3}	^{231}Pa	2.1×10^{-7}
^{40}K	2.9×10^{-4}	^{232}U	2.7×10^{-6}
^{41}Ca	4.2×10^{-3}	^{233}U	1.9×10^{-5}
^{60}Co	2.0×10^{-4}	^{234}U	2.0×10^{-5}
^{59}Ni	2.7×10^{-2}	^{235}U	2.0×10^{-5}
^{63}Ni	9.5×10^{-3}	^{236}U	2.0×10^{-5}
^{79}Se	6.3×10^{-4}	^{238}U	2.1×10^{-5}
^{87}Rb	1.1×10^{-3}	^{237}Np	1.3×10^{-6}
^{90}Sr	3.6×10^{-5}	^{238}Pu	1.7×10^{-6}
^{93}Zr[b]	2.5×10^{-3}	^{239}Pu	1.5×10^{-6}
^{93m}Nb	1.1×10^{-2}	^{240}Pu	1.5×10^{-6}
^{94}Nb	7.7×10^{-4}	^{241}Pu	8.0×10^{-5}
^{99}Tc	3.6×10^{-3}	^{242}Pu	1.6×10^{-6}
^{107}Pd	3.6×10^{-2}	^{244}Pu	1.7×10^{-6}
^{113m}Cd	3.3×10^{-5}	^{241}Am	1.5×10^{-6}
^{121m}Sn	3.3×10^{-3}	^{242m}Am[d]	8.2×10^{-7}
^{126}Sn	2.7×10^{-4}	^{243}Am	1.5×10^{-6}
^{129}I	2.0×10^{-5}	^{243}Cm	2.2×10^{-6}
^{135}Cs	7.7×10^{-4}	^{244}Cm	2.7×10^{-6}
^{137}Cs	1.1×10^{-4}	^{245}Cm	1.5×10^{-6}
^{151}Sm	1.4×10^{-2}	^{246}Cm	1.5×10^{-6}
^{152}Eu	8.5×10^{-4}	^{247}Cm	1.6×10^{-6}
^{154}Eu	5.8×10^{-4}	^{248}Cm	4.0×10^{-7}
^{155}Eu	3.6×10^{-3}	^{249}Cf	1.2×10^{-6}
^{207}Bi	1.0×10^{-3}	^{250}Cf	2.7×10^{-6}
^{210}Pb	7.5×10^{-7}	^{251}Cf	1.1×10^{-6}

[a]Allowable limits are calculated from Eq. (4.1) using annual doses per unit concentration in water in Table 4.11.

[b]Decay product ^{93m}Nb is assumed to be in activity equilibrium in water.

[c]Decay product ^{210}Pb is assumed to be in activity equilibrium in water.

[d]Decay product ^{238}Pu is assumed to be in activity equilibrium in water.

4.4.2 Analysis for Inadvertent Intruders

As described in Sect. 3.1.2.2, exposures of inadvertent intruders are assumed to occur according to one of three scenarios, called the agriculture, resident, and post-drilling scenarios. Each of these scenarios involves chronic exposure to solid waste in the disposal facility, and the applicable performance objective is an annual EDE of 100 mrem. This section presents the results of the dose analysis for each exposure scenario for inadvertent intruders and the derivation of limits on allowable inventories of radionuclides for disposal in CIIDF based on the results for each scenario.

4.4.2.1 Analysis for Agriculture Scenario

In the agriculture scenario, inadvertent intruders are assumed to be exposed to garden soil which has been contaminated with waste exhumed from the disposal facility while digging a foundation for a home and to unshielded waste in the disposal facility during indoor residence on the disposal site. The assumed pathways involving exposure to contaminated garden soil include

- ingestion of vegetables which have been contaminated by root uptake,
- direct ingestion of contaminated garden soil in conjunction with vegetable intakes,
- external exposure to contaminated soil while working in the garden, and
- inhalation of radionuclides suspended into air from contaminated soil while working in the garden.

The assumed pathways involving exposure during indoor residence on the disposal site include

- external exposure while residing in a home on top of unshielded waste in the disposal facility and
- inhalation exposure while residing in the home.

The results of the dose analysis for the agriculture scenario are given in Table 4.13. For each of the assumed exposure pathways, the dose per unit concentration of radionuclides in waste in the disposal facility at the time intrusion is assumed to occur is based on the models and parameter values described in Sect. G.5.2.1 of Appendix G. Separate results are given for the pathways involving exposure to contaminated garden soil and the pathways involving exposure during indoor residence at the disposal site because, as described below, the radionuclide concentrations in exhumed waste which is mixed with garden soil should be considerably less than the concentrations remaining in the disposal facility itself when the thickness of the cover used in constructing the disposal facility is taken into account. The total dose would be the sum of the doses from the garden and residence pathways given in Table 4.13 only if the concentrations of radionuclides in exhumed waste are assumed to be the same as the concentrations in the disposal facility itself. Application of these results to the calculation of limits on allowable inventories of radionuclides for disposal in CIIDF is described as follows.

Table 4.13. Annual effective dose equivalents from agriculture scenario for inadvertent intruders per unit concentration of radionuclides in disposal facility[a]

Nuclide[b]	Annual dose (rem/year per μCi/m³)		Nuclide[b]	Annual dose (rem/year per μCi/m³)	
	Garden pathways	Residence pathways		Garden pathways	Residence pathways
^{3}H	4.0×10^{-6}	1.9×10^{-12}	$^{229}Th + d$	3.0×10^{-5}	4.0×10^{-4}
^{10}Be	6.5×10^{-8}	1.0×10^{-8}	^{230}Th	3.5×10^{-6}	7.5×10^{-6}
^{14}C	1.5×10^{-5}	6.1×10^{-11}	$^{232}Th + d$[e]	6.4×10^{-5}	3.5×10^{-3}
^{26}Al	1.8×10^{-5}	3.9×10^{-3}	^{220}Rn	2.1×10^{-5}	1.0×10^{-2}
^{36}Cl	1.2×10^{-3}	6.4×10^{-10}	$^{231}Pa + d$	2.0×10^{-4}	6.5×10^{-4}
^{40}K	6.0×10^{-5}	2.3×10^{-4}	$^{232}U + d$[e]	5.7×10^{-5}	2.2×10^{-3}
^{41}Ca	2.5×10^{-6}	3.8×10^{-11}	^{220}Rn	2.1×10^{-5}	1.0×10^{-2}
^{60}Co	1.8×10^{-5}	3.5×10^{-3}	^{233}U	8.1×10^{-6}	4.1×10^{-6}
^{59}Ni	7.2×10^{-8}	3.8×10^{-11}	^{234}U	7.8×10^{-6}	3.8×10^{-6}
^{63}Ni	2.0×10^{-7}	9.0×10^{-11}	$^{235}U + d$	8.5×10^{-6}	1.6×10^{-4}
^{79}Se	1.2×10^{-6}	1.9×10^{-10}	^{236}U	7.5×10^{-6}	3.8×10^{-6}
^{87}Rb	1.9×10^{-6}	9.3×10^{-11}	$^{238}U + d$	7.2×10^{-6}	3.3×10^{-5}
$^{90}Sr + d$	2.0×10^{-4}	7.3×10^{-9}	$^{237}Np + d$	2.7×10^{-4}	2.6×10^{-4}
^{93}Zr[c]	1.4×10^{-8}	9.3×10^{-9}	^{238}Pu	1.8×10^{-5}	1.1×10^{-5}
^{93m}Nb	1.8×10^{-8}	8.4×10^{-10}	^{239}Pu	2.0×10^{-5}	1.2×10^{-5}
^{94}Nb	1.1×10^{-5}	2.1×10^{-3}	^{240}Pu	2.0×10^{-5}	1.2×10^{-5}
^{99}Tc	1.3×10^{-5}	2.9×10^{-11}	^{241}Pu	3.9×10^{-7}	2.4×10^{-7}
^{107}Pd	3.4×10^{-8}	3.5×10^{-10}	^{242}Pu	1.9×10^{-5}	1.2×10^{-5}
^{113m}Cd	1.4×10^{-4}	4.4×10^{-8}	$^{244}Pu + d$	2.0×10^{-5}	4.7×10^{-4}
^{121m}Sn	6.5×10^{-8}	4.2×10^{-7}	^{241}Am	2.5×10^{-5}	2.3×10^{-5}
$^{126}Sn + d$	1.4×10^{-5}	2.6×10^{-3}	$^{242m}Am + d$[f]	2.5×10^{-5}	2.8×10^{-5}
^{129}I	8.2×10^{-5}	2.8×10^{-6}	$^{243}Am + d$	2.6×10^{-5}	2.1×10^{-4}
^{135}Cs	1.2×10^{-6}	1.3×10^{-10}	^{243}Cm	1.4×10^{-5}	1.4×10^{-4}
$^{137}Cs + d$	1.3×10^{-5}	7.4×10^{-4}	^{244}Cm	1.1×10^{-5}	7.3×10^{-6}
^{151}Sm	1.1×10^{-8}	8.7×10^{-10}	^{245}Cm	2.1×10^{-5}	8.7×10^{-5}
^{152}Eu	7.8×10^{-6}	1.5×10^{-3}	^{246}Cm	2.1×10^{-5}	1.3×10^{-5}
^{154}Eu	8.5×10^{-6}	1.7×10^{-3}	$^{247}Cm + d$	2.1×10^{-5}	4.1×10^{-4}
^{155}Eu	2.6×10^{-7}	3.9×10^{-5}	^{248}Cm	7.7×10^{-5}	4.9×10^{-5}
^{207}Bi	1.0×10^{-5}	2.1×10^{-3}	^{249}Cf	2.8×10^{-5}	4.4×10^{-4}
$^{210}Pb + d$	3.1×10^{-4}	6.7×10^{-7}	^{250}Cf	1.1×10^{-5}	7.5×10^{-6}
$^{226}Ra + d$[d,e]	3.0×10^{-5}	2.4×10^{-3}	^{251}Cf	2.7×10^{-5}	1.4×10^{-4}
^{222}Rn	1.3×10^{-4}	1.2×10^{-1}			

[a] Results obtained from Table G.15 of Appendix G give sum of EDEs from one year's external exposure and 50-year EDEs from one year's intake by ingestion and inhalation.

[b] The notation "+ d" with some entries denotes short-lived decay products that are assumed to be in secular equilibrium with parent radionuclide. Indented entries are radiologically significant decay products of parent radionuclides. See Table G.1 of Appendix G for decay products and branching fractions.

[c] Possible contributions to dose from ^{93m}Nb decay product are not included.

[d] Possible contributions to dose from ^{210}Pb decay product are not included.

[e] Contribution to dose from radon decay product is listed separately.

[f] Possible contributions to dose from ^{238}Pu decay product are not included.

For a particular exposure scenario for inadvertent intruders, the total annual EDE from all exposure pathways per unit concentration of radionuclides in the disposal facility at the time intrusion is assumed to occur is a quantity referred to as the scenario dose conversion factor (SDCF). For example, the results in Table 4.13 give the SDCFs for the garden and residence pathways for the agriculture scenario. Then the limit on allowable average concentration of a radionuclide in the disposal facility ($\overline{C}_F$) in μCi/m^3 at this time is given by

$$\overline{C}_F(t) = \frac{(0.1 \text{ rem/year})}{\text{SDCF}_{ag}(\text{rem/year per } \mu\text{Ci/m}^3)} , \tag{4.2}$$

where the numerator is the applicable performance objective for inadvertent intruders and SDCF_{ag} is the scenario dose conversion factor for the agriculture scenario. The radionuclide concentration obtained from Eq. (4.2) is the average over the disposal facility. The performance objective for inadvertent intruders is applied to the average concentrations of radionuclides in the disposal facility, rather than to the concentration in any waste vault, essentially because an inadvertent intruder is assumed to access the disposal facility at random locations.

In establishing allowable limits on inventories of radionuclides for disposal, the desired quantity is the limit on the average concentration of a radionuclide in waste prior to disposal, rather than the average concentration in the disposal facility at the time intrusion is assumed to occur, as obtained from Eq. (4.2). These two concentrations are related by the following three factors: (1) the so-called waste dilution factor, which takes into account the dilution of waste following disposal due to the presence of uncontaminated material in the disposal facility and the presence of a cap on top of the facility; (2) changes in inventory due to radioactive decay between the time of disposal and the time the scenario is assumed to occur; and (3) reductions in inventory due to mobilization and transport in infiltrating water during this time. Thus, the limit on the allowable average concentration of a radionuclide in waste prior to disposal, $\overline{C}_W$, can be represented conceptually by

$$\overline{C}_W(t) = \frac{\overline{C}_F(t)}{G \times f_D(t) \times f_w(t)} , \tag{4.3}$$

where G denotes the waste dilution factor described below, f_D denotes the change in inventory due to radioactive decay, and f_w denotes the reduction in inventory due to mobilization and transport in infiltrating water.

As discussed in Sect. 3.1.2.2, the agriculture scenario is assumed to occur at 300 years after disposal or thereafter. For most radionuclides, the maximum dose would occur at 300 years. However, for radionuclides with radiologically significant long-lived decay products which build up in the waste only slowly over time, the maximum dose could occur at times beyond 300 years. On

the other hand, as discussed in Sect. 1.1, the performance objectives for inadvertent intruders are assumed to apply for only 10,000 years after disposal, rather than indefinitely. The various terms in the denominator of Eq. (4.3) are described below.

Waste dilution factor

The waste dilution factor (G) in Eq. (4.3) takes into account that the average concentration of a radionuclide to which an inadvertent intruder would be exposed would be less than the average concentration in waste prior to disposal, because the latter does not take into account the volume of uncontaminated material in the disposal facility (i.e., the volume of the waste vaults which is not occupied by waste) as well as the thickness of the cap on the disposal facility. When the thickness of the cap is taken into account, separate waste dilution factors are needed for the pathways in the agriculture scenario involving exposure to contaminated garden soil and exposure during residence in a home on top of unshielded waste.

For the exposure pathways during indoor residence on top of unshielded waste, the waste dilution factor is given by the fraction of the volume of a waste vault that contains radioactive waste. This result assumes that the vaults are stacked next to one another in the disposal facility without significant spacing. Based on the dimensions of a waste vault and the waste container which is placed inside a vault given in Sect. 2.3, the waste dilution factor that would be applied to the exposure pathways during indoor residence is assumed to be 0.4.

The waste dilution factor of 0.4 described above also would apply to the pathways involving exposure to contaminated garden soil, because waste exhumed from the disposal facility by excavation would include the uncontaminated material in the waste vaults. However, an additional waste dilution factor, given by the thickness of the layer of waste that would be exhumed during excavation of the foundation relative to the total depth of the excavation below the ground surface, applies to these exposure pathways, because the excavated material that is mixed with garden soil would contain uncontaminated material from the cap on the disposal facility as well as material from the waste vaults themselves. In this analysis, the depth of an excavation below the ground surface is assumed to be 3 m (Oztunali and Roles 1986), which is the maximum depth that normally would occur in digging a foundation for a home. The depth of the cover material that will be placed on top of the waste vaults in CIIDF has not been determined at this time. Therefore, in this analysis, the cover design for the Interim Waste Management Facility (IWMF) in the SWSA 6 disposal facility (ORNL 1994) is assumed. In the IWMF, the region between the top of the waste vaults and the ground surface is expected to include about 1.2 m of material. In addition, in the waste vaults themselves, the thickness of the vault cap and grout above the waste boxes is 0.3 m. With these assumptions, the total thickness of uncontaminated material between the ground surface and the top layer of waste is 1.5 m. Therefore, the fraction of the total depth of an excavation of 3 m that would be occupied by waste would be $1.5/3 = 0.5$, and the resulting waste dilution factor for the garden pathways is $0.4 \times 0.5 = 0.2$.

Thus, as summarized in Table 4.14, two waste dilution factors are assumed in the dose analysis for the agriculture scenario: (1) a waste dilution factor for the exposure pathways during indoor residence on the disposal site (G_r) of 0.4 and (2) a waste dilution factor for the pathways involving exposure to contaminated garden soil (G_g) of 0.2.

Combining Eqs. (4.2) and (4.3) and taking into account the different SDCFs in Table 4.13 and waste dilution factors in Table 4.14 for the garden (g) and residence (r) pathways give the limit on the allowable average concentration of a radionuclide in waste prior to disposal, based on the dose analysis for the agriculture scenario, as

$$\overline{C}_W(\mu\text{Ci/m}^3) = \frac{0.1 \text{ rem/year}}{(\text{SDCF}_{ag,g}\, G_g + \text{SDCF}_{ag,r}\, G_r) \times f_D(t) \times f_w(t)} \quad . \tag{4.4}$$

Again, t is the time after disposal when exposures of inadvertent intruders are assumed to occur.

Table 4.14 Waste dilution factors applied to dose analysis for agriculture scenario[a]

Waste dilution factor	Value	Applicable exposure pathways
G_r	0.4[b]	Pathways during indoor residence on top of unshielded waste in disposal facility[c]
G_g	0.2[d]	Pathways involving mixing of waste exhumed from disposal facility in garden soil[e]

[a]Waste dilution factors take into account that average concentrations of radionuclides in exhumed waste and in disposal facility would be less than average concentrations in waste prior to disposal, due to volume of uncontaminated material in waste vaults and thickness of cover material on top of disposal facility (see Sect. 4.4.2.1).

[b]Value takes into account fraction of total volume of waste vaults occupied by radioactive waste.

[c]Waste dilution factor during indoor residence also is applied to dose analysis for resident scenario described in Sect. 4.4.2.2.

[d]Value takes into account fraction of total volume of waste vaults occupied by radioactive waste and fraction of depth of excavation below ground surface occupied by radioactive waste.

[e]Waste dilution factor for exposure pathways involving mixing of exhumed waste with garden soil is not applied to dose analysis for post-drilling scenario described in Sect. 4.4.2.3.

Radioactive decay factor

For radionuclides without radiologically significant decay products or radionuclides with short-lived decay products (e.g., ^{90}Sr) which were taken into account in calculating the SCDFs in Table 4.13, the correction for radioactive decay in Eq. (4.4) is given by

$$f_D(t) = \exp(-0.693\, t/T_{1/2}) \quad , \tag{4.5}$$

where $T_{1/2}$ is the radionuclide half-life. However, when buildup of radiologically significant decay products occurs prior to the assumed time for intrusion (e.g., for ^{234}U, which decays to ^{230}Th and ^{226}Ra), the limit on the average concentration of the parent radionuclide in waste at the time of disposal is obtained by replacing the terms of the form SDCF $\times f_D(t)$ in Eq. (4.4) by a sum of products of the SDCFs and decay factors for all radiologically significant members of the decay chain, including the parent, which can be represented by

$$\sum \left[\mathrm{SDCF}_i \times f_{D,i} \right] \ , \quad i = \text{radionuclide index} \ , \tag{4.6}$$

where the decay factor $f_{D,i}$ is the activity of the ith radionuclide in the decay chain at time (t) relative to the initial activity of the parent radionuclide ($i = 1$), as obtained from the Bateman equations for radioactive decay (Evans 1955).

Mobilization and transport factor

The factor f_w in Eq. (4.4) represents the reduction in the inventory of a radionuclide in the disposal facility prior to the time intrusion is assumed to occur due to mobilization and transport in infiltrating water. This factor is based on a model, described in Sects. 3.3.3.3 and 4.2.2, which is intended to be conservative in describing retention of radionuclides in the disposal facility, in order not to underestimate exposures of inadvertent intruders. The model assumes (1) no transport from the disposal facility by diffusion, (2) a reduced rate of degradation of the disposal vaults compared with the degradation rate assumed in the PA for releases by water pathways, (3) the release of the radionuclide not to be limited by solubility, and (4) values of the distribution coefficient (K_d) for each element in the disposal facility which are at the upper end of the expected range of values. In addition, the model is not applied when the release of a radionuclide is solubility limited, because the fraction of the inventory remaining at any time is a function of the initial inventory but is independent of K_d and, furthermore, the correction for mobilization and transport would be very small (i.e., the factor f_w would be essentially unity). Thus, the model for estimating inventories of radionuclides in the disposal facility over time for use in the dose analysis for inadvertent intruders gives estimated releases of radionuclides which are substantially less than the model used in the PA for releases by water pathways.

The correction factor for mobilization and transport in infiltrating water is applied to the dose analysis for inadvertent intruders only when a radionuclide could be removed sufficiently rapidly from the disposal facility that application of the correction factor would result in a significant reduction in estimated dose at the time intrusion is assumed to occur. In this analysis, separate considerations of this correction factor are applied in two cases, as described below.

The first case applies to those radionuclides which do not decay to radiologically significant long-lived decay products which build up on the waste only slowly over time. This case applies to

most of the radionuclides evaluated in this analysis. For these radionuclides, the maximum dose to an inadvertent intruder would be obtained at the earliest time that intrusion could occur, because the concentrations decrease monotonically with time after disposal.

The values of the correction factor (f_w) assumed in this analysis for the isotopes of elements which do not decay to radiologically significant long-lived decay products are summarized in Table 4.15. This correction factor is applied only if two conditions are met. First, the concentration limit in waste prior to disposal that would be calculated from Eq. (4.4) without applying the correction factor must not be substantially greater than the solubility limit in the waste given in Table 4.8, because the source term model assumes solubility is not exceeded. Second, the correction factor is applied only when the assumed upper-bound value of K_d for an element in the waste is less than 250 mL/g. For higher assumed values of K_d, the correction factor would be greater than 0.9 and thus would not be significant (see Fig. 4.9).

Table 4.15. Reductions in inventory of elements in disposal facility due to mobilization and transport in infiltrating water—Part I[a]

Element[b]	Time after disposal		Element[b]	Time after disposal	
	100 years[c]	300 years[d]		100 years[c]	300 years[d]
H	0.68	0.002	Tc	0.86	0.23
C	0.84	0.20	Sn	*e*	0.77
Cl	0.68	0.002	I	0.68	0.002
K	*e*	0.51	Cs	*e*	0.86
Ni	*e*	0.64	Sm	*e*	0.49
Se	0.68	0.002	Eu	*e*	0.49
Rb	*e*	0.80	Bi	*e*	0.56
Sr	*e*	0.71	Ra	*e*	0.86
Nb	*e*	0.88			

[a]Values are factor f_w in denominator of Eq. (4.4) and give fraction of initial inventory in waste remaining in disposal facility at specified times.

[b]For elements not listed, reduction factor is assumed to be unity at either time.

[c]Assumed time of occurrence for residence and post-drilling scenarios for inadvertent intruders discussed in Sects. 4.4.2.2 and 4.4.2.3, respectively.

[d]Assumed time of first occurrence for agriculture scenario for inadvertent intruders discussed in Sect. 4.4.2.1.

[e]Reduction factor is greater than 0.9 and thus is assumed to be unity.

Values of the correction factor f_w are given in Table 4.15 for two times after disposal. As noted above, 300 years is the assumed time when the agriculture scenario first occurs. The time of 100 years is when the resident and post-drilling scenarios discussed in Sects. 4.5.2.2 and 4.5.2.3, respectively, are assumed to occur.

The second case applies to those long-lived radionuclides which decay to other long-lived radionuclides that become radiologically significant beyond the time when the agriculture scenario first could occur. The radionuclides of concern in this case include ^{230}Th, ^{233}U, ^{234}U, ^{235}U, ^{238}U,

^{237}Np, ^{242m}Am, ^{245}Cm, and ^{247}Cm. For these elements, the values of the correction factor f_w at various times after disposal are given in Table 4.16. The values at 300 years for all of these elements are greater than 0.9 and thus are assumed to be unity. Values are not given for times beyond 10,000 years, because this is the assumed time for compliance with the performance objective for protection of inadvertent intruders. As in the first case described above, this correction factor is not applied if the concentration limit in waste prior to disposal that would be calculated from Eq. (4.4) without applying the correction factor substantially exceeds the solubility limit. This condition applies only to ^{235}U and ^{238}U, and the maximum dose for the agriculture scenario during the time for compliance occurs at 10,000 years.

Table 4.16. Reductions in inventory of elements in disposal facility due to mobilization and transport in infiltrating water—Part II[a]

Element	Time after disposal[b]				
	500 years	1000 years	2000 years	5000 years	10,000 years
Th	8.7×10^{-1}	7.0×10^{-1}	4.5×10^{-1}	1.2×10^{-1}	1.4×10^{-2}
U	8.7×10^{-1}	7.0×10^{-1}	4.5×10^{-1}	1.2×10^{-1}	1.4×10^{-2}
Np	8.7×10^{-1}	7.1×10^{-1}	4.7×10^{-1}	1.3×10^{-1}	1.6×10^{-2}
Am	8.7×10^{-1}	7.1×10^{-1}	4.8×10^{-1}	1.4×10^{-1}	1.9×10^{-2}
Cm	8.7×10^{-1}	7.1×10^{-1}	4.8×10^{-1}	1.4×10^{-1}	1.9×10^{-2}

[a]Values are factors f_w in denominator of Eq. (4.4) and give fraction of initial inventory in waste remaining in disposal facility at specified times. Values are applied only to agriculture scenario for inadvertent intruders discussed in Sect. 4.4.2.1 and only for radionuclides with radiologically significant long-lived decay products.

[b]Factor is assumed to be unity for all elements at 300 years after disposal and is not evaluated beyond 10,000 years.

Estimated inventory limits

Finally, the limit on allowable average concentration of a radionuclide in waste prior to disposal calculated from Eq. (4.4) is converted to a limit on allowable inventory by multiplying by the total volume of waste that would be placed in the facility. In this analysis, each pad in CIIDF is treated as a separate disposal facility for purposes of developing inventory limits of radionuclides in waste prior to disposal. Each pad is assumed to contain 330 disposal vaults, each of which has a waste volume of 2.6 m^3. Therefore, the total volume of disposed waste per pad is 860 m^3, and the limit on allowable inventory for a radionuclide per pad is given by

$$I_W\ (\mathrm{Ci}) = \overline{C}_W\,(\mu\mathrm{Ci/m^3}) \times (10^{-6}\ \mathrm{Ci}/\mu\mathrm{Ci}) \times 860\ \mathrm{m^3} = (8.6 \times 10^{-4})\ \overline{C}_W\,(\mu\mathrm{Ci/m^3}) \quad . \qquad (4.7)$$

Results for agriculture scenario

The limits on allowable average concentrations and inventories of radionuclides in waste prior to disposal based on the dose analysis for the agriculture scenario described above are given in Table 4.17. Some of these results are described further as follows.

First, for the radionuclides ^{60}Co, ^{87}Rb, and ^{155}Eu, the calculated limit on allowable concentration exceeds the specific activity of the radionuclide. Therefore, in these cases, there is no limit based on the analysis for the agriculture scenario. The half-lives of ^{60}Co and ^{155}Eu are very short compared to the assumed time of first occurrence for the scenario, and ^{87}Rb has a long half-life (i.e., low specific activity) and low annual dose per unit concentration.

Second, for the radionuclides ^{93}Zr and ^{226}Ra, the shorter-lived decay products ^{93m}Nb and ^{210}Pb, respectively, are assumed to be in activity equilibrium with the parent isotope. Therefore, the SDCF for these radionuclides is the sum of the values for the parent and its decay product. The radionuclide ^{242m}Am also decays to the shorter-lived radionuclide ^{238}Pu, but the activity of the decay product at 300 years after disposal is somewhat greater than the activity of the parent, and this difference is taken into account in the calculations.

Third, for the radionuclides ^{226}Ra, ^{230}Th, ^{232}Th, ^{232}U, ^{234}U, and ^{238}U, calculations are performed both excluding and including the contribution to dose from radon decay products. In this analysis, the performance objective for inadvertent intruders is assumed to exclude any contributions from radon.

Fourth, for the radionuclides ^{230}Th, ^{233}U, ^{234}U, ^{235}U, ^{238}U, ^{237}Np, ^{245}Cm, and ^{247}Cm, the buildup of long-lived decay products in the waste after disposal is taken into account in estimating the dose for the agriculture scenario. For each radionuclide, the maximum dose during the 10,000-year time for compliance with the performance objective for inadvertent intruders is estimated by taking into account (1) the activity of the decay products as a function of time after disposal and their SCDFs and waste dilution factors (G) and (2) the mobilization and transport factor for the parent radionuclide (f_w) as a function of time given in Table 4.16. However, as noted previously, the mobilization and transport factor is not applied to ^{235}U and ^{238}U, because the calculated limit on allowable concentration without taking this factor into account greatly exceeds the solubility limit of uranium in water. Therefore, for these radionuclides, the maximum dose during the compliance period occurs at 10,000 years, and the dose continues to increase thereafter until activity equilibrium in the decay chain is achieved, provided the mobilization and transport factor is not significant beyond 10,000 years. It also should be noted that the maximum dose from ^{245}Cm and ^{247}Cm occurs at 300 years, even though the respective decay products ^{241}Am and ^{243}Am have not achieved activity equilibrium with the parent radionuclide, because the later increase in activity of the decay product is more than compensated by the decrease in activity of the parent due to mobilization and transport in infiltrating water. Similarly, for the radionuclide ^{237}Np, the buildup of the ^{233}U decay product is not significant at any time after disposal when mobilization and transport of the parent in infiltrating water is taken into account.

Table 4.17. Allowable limits on concentrations and inventories of radionuclides for CIIDF based on agriculture scenario for inadvertent intruders

Nuclide[a]	SDCF × G (rem/year per μCi/m^3)[b]	f_D [c]	f_w [d]	$\bar{C}_w$ (μCi/m^3)[e]	Inventory limit (Ci/pad)[f]
^{3}H	8.0×10^{-7}	4.5×10^{-8}	2.0×10^{-3}	1.4×10^{15}	1.2×10^{12}
^{10}Be	1.7×10^{-8}	1.0	1.0	5.9×10^{6}	5.1×10^{3}
^{14}C	3.0×10^{-6}	9.6×10^{-1}	2.0×10^{-1}	1.7×10^{5}	1.5×10^{2}
^{26}Al	1.6×10^{-3}	1.0	1.0	6.4×10^{1}	5.5×10^{-2}
^{36}Cl	2.4×10^{-4}	1.0	2.0×10^{-3}	2.1×10^{5}	1.8×10^{2}
^{40}K	1.0×10^{-4}	1.0	5.1×10^{-1}	2.0×10^{3}	1.7
^{41}Ca	5.0×10^{-7}	1.0	1.0[g]	2.0×10^{5}	1.7×10^{2}
^{60}Co	1.4×10^{-3}	6.3×10^{-18}	1.0	No limit[h]	No limit
^{59}Ni	1.4×10^{-8}	1.0	1.0[g]	6.9×10^{6}	6.0×10^{3}
^{63}Ni	4.0×10^{-8}	1.3×10^{-1}	1.0[g]	1.9×10^{7}	1.6×10^{4}
^{79}Se	2.4×10^{-7}	1.0	2.0×10^{-3}	2.1×10^{8}	1.8×10^{5}
^{87}Rb	3.8×10^{-7}	1.0	1.0[g]	No limit[h]	No limit
^{90}Sr	4.0×10^{-5}	6.8×10^{-4}	7.1×10^{-1}	5.2×10^{6}	4.5×10^{3}
^{93}Zr[i]	1.0×10^{-8}	1.0	1.0	1.0×10^{7}	8.6×10^{3}
^{93m}Nb	3.9×10^{-9}	2.3×10^{-7}	8.8×10^{-1}	1.3×10^{14}	1.1×10^{11}
^{94}Nb	8.4×10^{-4}	1.0	8.8×10^{-1}	1.4×10^{2}	1.1×10^{-1}
^{99}Tc	2.6×10^{-6}	1.0	2.3×10^{-1}	1.7×10^{5}	1.4×10^{2}
^{107}Pd	6.9×10^{-9}	1.0	1.0	1.4×10^{7}	1.2×10^{4}
^{113m}Cd	2.8×10^{-5}	2.6×10^{-7}	1.0	1.4×10^{10}	1.2×10^{7}
^{121m}Sn	1.8×10^{-7}	2.3×10^{-2}	7.7×10^{-1}	3.1×10^{7}	2.7×10^{4}
^{126}Sn	1.0×10^{-3}	1.0	7.7×10^{-1}	1.2×10^{2}	1.1×10^{-1}
^{129}I	1.8×10^{-5}	1.0	2.0×10^{-3}	2.8×10^{6}	2.4×10^{3}
^{135}Cs	2.4×10^{-7}	1.0	8.6×10^{-1}	4.8×10^{5}	4.2×10^{2}
^{137}Cs	3.0×10^{-4}	9.8×10^{-4}	8.6×10^{-1}	4.0×10^{5}	3.4×10^{2}
^{151}Sm	5.7×10^{-9}	9.9×10^{-2}	4.9×10^{-1}	3.6×10^{8}	3.1×10^{5}
^{152}Eu	6.0×10^{-4}	1.6×10^{-7}	4.9×10^{-1}	2.1×10^{9}	1.8×10^{6}
^{154}Eu	6.8×10^{-4}	5.4×10^{-11}	4.9×10^{-1}	5.6×10^{12}	4.8×10^{9}
^{155}Eu	1.6×10^{-5}	5.7×10^{-19}	4.9×10^{-1}	No limit[h]	No limit
^{207}Bi	8.4×10^{-4}	1.6×10^{-3}	1.0	7.4×10^{4}	6.4×10^{1}
^{210}Pb	6.2×10^{-5}	8.9×10^{-5}	1.0	1.8×10^{7}	1.6×10^{4}
^{226}Ra[j]	1.0×10^{-3}[k] 4.8×10^{-2}[m]	8.8×10^{-1}	8.6×10^{-1}	1.3×10^{2}[k] 2.8[m]	1.1×10^{-1}[k] 2.4×10^{-3}[m]
^{229}Th	1.7×10^{-4}	9.7×10^{-1}	1.0	6.1×10^{2}	5.2×10^{-1}
^{230}Th[n,o] ^{226}Ra[j]	3.7×10^{-6} 1.0×10^{-3}[k] 4.8×10^{-2}[m]	9.8×10^{-1} 5.7×10^{-1}	4.5×10^{-1}	3.9×10^{2}[k] 7.9[m]	3.4×10^{-1}[k] 6.8×10^{-3}[m]
^{232}Th	1.4×10^{-3}[k] 5.6×10^{-3}[m]	1.0	1.0	7.1×10^{1}[k] 1.8×10^{1}[m]	6.1×10^{-2}[k] 1.5×10^{-2}[m]

Table 4.17 (continued)

Nuclide[a]	SDCF × G (rem/year per μCi/m^3)[b]	f_D [c]	f_w [d]	$\bar{C}_w$ (μCi/m^3)[e]	Inventory limit (Ci/pad)[f]
^{231}Pa	3.0×10^{-4}	1.0	1.0	3.3×10^{2}	2.9×10^{-1}
^{232}U	8.9×10^{-4}[k]	4.8×10^{-2}	1.0	2.3×10^{3}[k]	2.0[k]
	4.8×10^{-3}[m]			4.3×10^{2}[m]	3.7×10^{-1}[m]
^{233}U[n,o]	3.2×10^{-6}	9.9×10^{-1}	4.5×10^{-1}	6.9×10^{3}	6.0
^{229}Th	1.7×10^{-4}	1.7×10^{-1}			
^{234}U[n,p]	3.1×10^{-6}	9.9×10^{-1}	4.5×10^{-1}	2.4×10^{4}[k]	2.1×10^{1}[k]
^{230}Th	3.7×10^{-6}	1.8×10^{-2}			
^{226}Ra[j]	1.0×10^{-3}[k]	5.9×10^{-3}			
^{234}U[n,p]	3.1×10^{-6}	9.9×10^{-1}	1.2×10^{-1}	7.6×10^{2}[m]	6.5×10^{-1}[m]
^{230}Th	3.7×10^{-6}	4.4×10^{-2}			
^{226}Ra[j]	4.8×10^{-2}[m]	2.3×10^{-2}			
^{235}U[n,q]	6.6×10^{-5}	1.0	1.0[g]	8.3×10^{2}	7.2×10^{-1}
^{231}Pa	3.0×10^{-4}	1.9×10^{-1}			
^{236}U	3.0×10^{-6}	1.0	1.0	3.3×10^{4}	2.9×10^{1}
^{238}U[n,q]	1.4×10^{-5}	1.0	1.0[g]	6.7×10^{3}[k]	5.7[k]
^{234}U	3.1×10^{-6}			1.9×10^{3}[m]	1.7[m]
^{230}Th	3.7×10^{-6}				
^{226}Ra[j]	1.0×10^{-3}[k]				
	4.8×10^{-2}[m]				
^{237}Np[r]	1.6×10^{-4}	1.0	1.0	6.3×10^{2}	5.4×10^{-1}
^{238}Pu	8.0×10^{-6}	9.3×10^{-2}	1.0	1.3×10^{5}	1.2×10^{2}
^{239}Pu	8.8×10^{-6}	9.9×10^{-1}	1.0	1.1×10^{4}	9.9
^{240}Pu	8.8×10^{-6}	9.7×10^{-1}	1.0	1.2×10^{4}	1.0×10^{1}
^{241}Pu	1.7×10^{-7}	5.4×10^{-7}	1.0	1.1×10^{12}	9.4×10^{8}
				3.5×10^{5}[s]	3.0×10^{2}[s]
^{242}Pu	8.6×10^{-6}	1.0	1.0	1.2×10^{4}	1.0×10^{1}
^{244}Pu	1.9×10^{-4}	1.0	1.0	5.3×10^{2}	4.6×10^{-1}
^{241}Am	1.4×10^{-5}	6.2×10^{-1}	1.0	1.2×10^{4}	9.9
^{242m}Am[n]	1.6×10^{-5}	2.3×10^{-1}	1.0	1.5×10^{4}	1.3×10^{1}
^{238}Pu	8.0×10^{-6}	3.6×10^{-1}			
^{243}Am	8.9×10^{-5}	9.7×10^{-1}	1.0	1.2×10^{3}	1.0
^{243}Cm	5.9×10^{-5}	6.8×10^{-4}	1.0	2.5×10^{6}[t]	2.1×10^{3}[t]
^{244}Cm	5.1×10^{-6}	1.0×10^{-5}	1.0	2.0×10^{9}	1.7×10^{6}
				4.2×10^{6}[u]	3.6×10^{3}[u]
^{245}Cm[n,v]	3.9×10^{-5}	9.8×10^{-1}	1.0	2.3×10^{3}	2.0
^{241}Am	1.4×10^{-5}	3.6×10^{-1}			
^{246}Cm	9.4×10^{-6}	9.6×10^{-1}	1.0	1.1×10^{4}	9.5
^{247}Cm[n,v]	1.6×10^{-4}	1.0	1.0	6.3×10^{2}	5.4×10^{-1}
^{243}Am	8.9×10^{-5}	2.8×10^{-2}			
^{248}Cm	3.5×10^{-5}	1.0	1.0	2.9×10^{3}	2.5
^{249}Cf	1.8×10^{-4}	5.5×10^{-1}	1.0	1.0×10^{3}	8.7×10^{-1}

Table 4.17 (continued)

Nuclide[a]	SDCF × G (rem/year per μCi/m^3)[b]	f_D [c]	f_w [d]	$\bar{C}_w$ (μCi/m^3)[e]	Inventory limit (Ci/pad)[f]
^{250}Cf	5.2×10^{-6}	1.3×10^{-7}	1.0	1.5×10^{11} 4.0×10^{6}[w]	1.3×10^{8} 3.4×10^{3}[w]
^{251}Cf	6.1×10^{-5}	7.9×10^{-1}	1.0	2.1×10^{3}	1.8

Note: Allowable limits are calculated from Eqs. (4.4) through (4.7); unless otherwise noted, time of occurrence for agriculture scenario is assumed to be 300 years after disposal.

[a]Indented entries are radiologically significant decay products of parent radionuclides.

[b]Calculated as $SDCF_{ag,g}G_g + SDCF_{ag,r}G_r$, where scenario dose conversion factors (SDCF) for garden (g) and residence (r) exposure pathways for agriculture scenario are obtained from Table 4.13 and corresponding waste dilution factors (G) are obtained from Table 4.14.

[c]Radionuclide inventory at time agriculture scenario is assumed to occur relative to inventory at time of disposal due to radioactive decay. For long-lived decay products listed with some radionuclides, factor gives inventory of decay product relative to initial inventory of parent radionuclide.

[d]Radionuclide inventory at time agriculture scenario is assumed to occur relative to inventory at time of disposal due to mobilization and transport in infiltrating water obtained from Table 4.15 or Table 4.16.

[e]Limit on allowable average concentration of radionuclide in waste prior to disposal.

[f]Limit on allowable inventory of radionuclide in waste prior to disposal for individual disposal pads in CIIDF, based on assumption of 330 vaults per pad and waste volume per vault of 2.6 m^3.

[g]Correction factor for mobilization and transport in infiltrating water is not applied because calculated concentration limit without correction factor greatly exceeds assumed solubility limit in water.

[h]Calculated limit exceeds specific activity of radionuclide.

[i]Calculated limits include contribution from ^{93m}Nb decay product, which is assumed to be in activity equilibrium with parent radionuclide.

[j]Calculated limits include contribution from ^{210}Pb decay product, which is assumed to be in activity equilibrium with parent radionuclide.

[k]Contribution from radon decay product is excluded.

[m]Contribution from radon decay product is included.

[n]Indented entries are radiologically significant long-lived decay products of parent radionuclide.

[o]Maximum dose occurs at 2000 years after disposal, taking into account reductions in inventory due to mobilization and transport in water, and all results are based on calculations at this time.

[p]Maximum dose occurs at 2000 years after disposal if contribution from radon decay product is excluded but at 5000 years if radon is included, taking into account reductions in inventory due to mobilization and transport in water, and all results are based on calculations at these times.

[q]Results are based on calculations at 10,000 years after disposal, which is time for compliance with performance objective for inadvertent intruders. If reductions in inventory due to mobilization and transport in infiltrating water are not significant, dose continues to increase beyond 10,000 years.

[r]Buildup of long-lived ^{233}U and ^{229}Th decay products is not significant at any time after disposal if reductions in inventory due to mobilization and transport in infiltrating water are taken into account.

[s]Value is 30 times limit for ^{241}Am decay product, based on ratio of half-lives of decay product and parent radionuclide.

[t]Limit based on exposure to parent radionuclide is more restrictive than 850 times limit for exposure to ^{239}Pu decay product, based on ratio of half-lives of decay product and parent radionuclide.

[u]Value is 360 times limit for ^{240}Pu decay product, based on ratio of half-lives of decay product and parent radionuclide.

[v]Dose decreases after 300 years, even with buildup of decay product, if reductions in inventory due to mobilization and transport in infiltrating water are taken into account.

[w]Value is 360 times limit for ^{246}Cm decay product, based on ratio of half-lives of decay product and parent radionuclide.

Finally, for the relatively short-lived radionuclides ^{241}Pu, ^{244}Cm, and ^{250}Cf, the allowable limits are determined by the limits for the longer-lived decay products ^{241}Am, ^{240}Pu, and ^{246}Cm, respectively. That is, taking into account the assumption that the agriculture scenario first occurs at 300 years after disposal and the half-lives of these parent radionuclides and their longer-lived decay products, the dose from the decay product is greater than the dose from the parent itself. For the relatively short-lived radionuclide ^{243}Cm, the dose from the longer-lived decay product ^{239}Pu also was considered. However, the half-life of the parent radionuclide is sufficiently long in this case that the dose from the parent is greater than the dose from the decay product.

4.4.2.2 Analysis for Resident Scenario

In the resident scenario, inadvertent intruders are assumed to be exposed to waste in the disposal facility during indoor residence in a home located on top of intact engineered barriers used in constructing the facility. Because the engineered barriers are assumed to be intact and impenetrable, external exposure to photon-emitting radionuclides in the waste during indoor residence is the only pathway of concern. A similar pathway occurs in the agriculture scenario.

The results of the dose analysis for the resident scenario are given in Table 4.18. The dose per unit concentration of radionuclides in waste in the disposal facility at the time intrusion is assumed to occur (the SCDF) is based on the model and parameter values described in Sect. G.5.2.2 of Appendix G. Application of these results to the calculation of limits on allowable inventories of radionuclides for disposal in CIIDF is described as follows.

Similar to Eq. (4.4) developed for the agriculture scenario, the limit on allowable average concentration of a radionuclide in waste prior to disposal, $\bar{C}_w$, based on the dose analysis for the resident (*re*) scenario, is given by

$$\bar{C}_W\,(\mu\text{Ci/m}^3) = \frac{0.1\ \text{rem/year}}{\text{SDCF}_{re}\,G_r \times f_D(t) \times f_w(t)}\ , \qquad \textbf{(4.8)}$$

where SDCF_{re} is the SDCF given in Table 4.18, G_r is the waste dilution factor for exposure pathways during indoor residence on top of the disposal facility given in Table 4.14, f_D is the radioactive decay factor given in Eq. (4.5) or (4.6), f_w is the mobilization and transport factor given in Table 4.15, and t is the time after disposal when exposures of inadvertent intruders are assumed to occur. The resident scenario is assumed to occur at 100 years after disposal, when active institutional controls over the disposal site are relinquished and inadvertent intrusion onto the site first could occur. The limit on allowable inventory for a radionuclide in waste prior to disposal per disposal pad in CIIDF, based on the dose analysis for the resident scenario, then is obtained from Eq. (4.7).

The limits on allowable average concentrations and inventories of radionuclides in waste prior to disposal based on the dose analysis for the resident scenario are given in Table 4.19. Calculated limits are given in this table only for radionuclides with relatively short half-lives or with a

Table 4.18. Annual effective dose equivalents from resident scenario for inadvertent intruders per unit concentration of radionuclides in disposal facility[a]

Nuclide[b]	Annual dose (rem/year per μCi/m³)	Nuclide[b]	Annual dose (rem/year per μCi/m³)
^{26}Al	3.3×10^{-4}	$^{231}Pa + d$	7.0×10^{-6}
^{40}K	2.1×10^{-5}	$^{232}U + d$	2.3×10^{-4}
^{60}Co	2.9×10^{-4}	$^{235}U + d$	5.6×10^{-7}
^{94}Nb	1.1×10^{-4}	$^{238}U + d$	1.2×10^{-6}
$^{126}Sn + d$	1.1×10^{-4}	$^{237}Np + d$	3.5×10^{-6}
$^{137}Cs + d$	3.2×10^{-5}	$^{244}Pu + d$	2.1×10^{-5}
^{152}Eu	9.8×10^{-5}	$^{242m}Am + d$	2.5×10^{-7}
^{154}Eu	1.1×10^{-4}	$^{243}Am + d$	1.1×10^{-6}
^{155}Eu	2.0×10^{-8}	^{243}Cm	7.7×10^{-7}
^{207}Bi	1.2×10^{-4}	^{245}Cm	9.8×10^{-8}
$^{226}Ra + d$	1.9×10^{-4}	$^{247}Cm + d$	8.4×10^{-6}
$^{229}Th + d$	1.1×10^{-5}	^{249}Cf	8.1×10^{-6}
$^{232}Th + d$	3.0×10^{-4}	^{251}Cf	3.9×10^{-7}

[a] Results obtained from Table G.16 of Appendix G give effective dose equivalents from one year's external exposure. Dose is negligible for radionuclides which are not high-energy photon emitters.

[b] The notation "+ d" with some entries denotes short-lived decay products that are assumed to be in secular equilibrium with parent radionuclide; see Table G.1 of Appendix G for decay products and branching fractions.

mobilization and transport factor (f_w) substantially less than unity. For longer-lived radionuclides or radionuclides with a mobilization and transport factor near unity, it is evident from a comparison of the SDCFs for the resident scenario in Table 4.18 to those for the agriculture scenario in Table 4.13 that the agriculture scenario gives a much higher dose per unit concentration in the disposal facility and thus is more restrictive in determining allowable limits for disposal. The much higher dose per unit concentration for the agriculture scenario results from (1) the presence of shielding provided by the intact engineered barriers in the analysis for the resident scenario, but not in the dose analysis for the same exposure pathway in the agriculture scenario, and (2) the presence of additional exposure pathways in the agriculture scenario that are not relevant for the resident scenario. Because the concentrations of relatively long-lived and immobile radionuclides that would apply in the agriculture and resident scenarios would be nearly the same, the resident scenario can be neglected and allowable limits need not be given in Table 4.19.

4.4.2.3 Analysis for Post-drilling Scenario

In the post-drilling scenario, inadvertent intruders are assumed to be exposed to garden soil which has been contaminated with waste exhumed from the disposal facility while drilling a well on

Table 4.19. Allowable limits on concentrations and inventories of radionuclides for CIIDF based on resident scenario for inadvertent intruders[a]

Nuclide[b]	SDCF × G (rem/year per μCi/m^3)[c]	f_D[d]	f_w[e]	$\bar{C}_w$ (μCi/m^3)[f]	Inventory limit (Ci/pad)[g]
^{40}K	8.4×10^{-6}	1.0	1.0	1.2×10^{4}	1.0×10^{1}
^{60}Co	1.2×10^{-4}	1.9×10^{-6}	1.0	4.5×10^{8}	3.9×10^{5}
^{137}Cs	1.3×10^{-5}	9.9×10^{-2}	1.0	7.9×10^{4}	6.8×10^{1}
^{152}Eu	3.9×10^{-5}	5.5×10^{-3}	1.0	4.6×10^{5}	4.0×10^{2}
^{154}Eu	4.4×10^{-5}	3.8×10^{-4}	1.0	6.0×10^{6}	5.1×10^{3}
^{155}Eu	8.0×10^{-9}	8.3×10^{-7}	1.0	1.5×10^{13}	1.3×10^{10}
^{207}Bi	4.8×10^{-5}	1.2×10^{-1}	1.0	1.7×10^{4}	1.5×10^{1}
^{232}U	9.2×10^{-5}	3.6×10^{-1}	1.0	3.0×10^{3}	2.6
^{242m}Am	1.0×10^{-7}	6.1×10^{-1}	1.0	1.6×10^{6}	1.4×10^{3}
^{243}Cm	3.1×10^{-7}	8.8×10^{-2}	1.0	3.7×10^{6}	3.2×10^{3}
^{249}Cf	3.2×10^{-6}	8.2×10^{-1}	1.0	3.8×10^{4}	3.2×10^{1}

[a]Allowable limits are calculated from Eqs. (4.8), (4.5), and (4.7). Time for occurrence of resident scenario is assumed to be 100 years after disposal.

[b]For radionuclides listed in Table 4.18 which are omitted from this table, allowable limits are much less than limits based on analysis for agriculture scenario given in Table 4.17.

[c]Product of SDCF for resident scenario given in Table 4.18 and waste dilution factor for exposure pathways during indoor residence (G_r) given in Table 4.14.

[d]Radionuclide inventory at time resident scenario is assumed to occur relative to inventory at time of disposal due to radioactive decay.

[e]Radionuclide inventory at time resident scenario is assumed to occur relative to inventory at time of disposal due to mobilization and transport in infiltrating water obtained from Table 4.15.

[f]Limit on allowable average concentration of radionuclide in waste prior to disposal.

[g]Limit on allowable inventory of radionuclide in waste prior to disposal for individual disposal pads in CIIDF, based on assumption of 330 vaults per pad and waste volume per vault of 2.6 m^3.

the site. All of the drilling waste is assumed to be mixed with garden soil, and the assumed pathways involving exposure to contaminated garden soil include

- ingestion of vegetables which have been contaminated by root uptake,
- direct ingestion of contaminated garden soil in conjunction with vegetable intakes,
- external exposure to contaminated soil while working in the garden, and
- inhalation of radionuclides suspended into air from contaminated soil while working in the garden.

Similar pathways occur in the agriculture scenario.

The results of the dose analysis for the post-drilling scenario are given in Table 4.20. The dose per unit concentration of radionuclides in waste in the disposal facility at the time intrusion is assumed to occur (the SCDF) is based on the model and parameter values described in Sect. G.5.2.3 of

Table 4.20. Annual effective dose equivalents from post-drilling scenario for inadvertent intruders per unit concentration of radionuclides in disposal facility[a]

Nuclide[b]	Annual dose (rem/year per μCi/m³)	Nuclide[b]	Annual dose (rem/year per μCi/m³)
^{3}H	4.0×10^{-8}	$^{229}Th + d$	3.0×10^{-7}
^{10}Be	6.5×10^{-10}	^{230}Th	3.5×10^{-8}
^{14}C	1.5×10^{-7}	$^{232}Th + d$[c]	6.4×10^{-7}
^{26}Al	1.8×10^{-7}	^{220}Rn	2.1×10^{-7}
^{36}Cl	1.2×10^{-5}	$^{231}Pa + d$	2.0×10^{-6}
^{40}K	6.0×10^{-7}	$^{232}U + d$[c]	5.7×10^{-7}
^{41}Ca	2.5×10^{-8}	^{220}Rn	2.1×10^{-7}
^{60}Co	1.8×10^{-7}	^{233}U	8.1×10^{-8}
^{59}Ni	7.2×10^{-10}	^{234}U	7.8×10^{-8}
^{63}Ni	2.0×10^{-9}	$^{235}U + d$	8.5×10^{-8}
^{79}Se	1.2×10^{-8}	^{236}U	7.5×10^{-8}
^{87}Rb	1.9×10^{-8}	$^{238}U + d$	7.2×10^{-8}
$^{90}Sr + d$	2.0×10^{-6}	$^{237}Np + d$	2.7×10^{-6}
^{93}Zr[c]	1.4×10^{-10}	^{238}Pu	1.8×10^{-7}
^{93m}Nb	1.8×10^{-10}	^{239}Pu	2.0×10^{-7}
^{94}Nb	1.1×10^{-7}	^{240}Pu	2.0×10^{-7}
^{99}Tc	1.3×10^{-7}	^{241}Pu	3.9×10^{-9}
^{107}Pd	3.4×10^{-10}	^{242}Pu	1.9×10^{-7}
^{113m}Cd	1.4×10^{-6}	$^{244}Pu + d$	2.0×10^{-7}
^{121m}Sn	6.5×10^{-10}	^{241}Am	2.5×10^{-7}
$^{126}Sn + d$	1.4×10^{-7}	$^{242m}Am + d$[f]	2.5×10^{-7}
^{129}I	8.2×10^{-7}	$^{243}Am + d$	2.6×10^{-7}
^{135}Cs	1.2×10^{-8}	^{243}Cm	1.4×10^{-7}
^{137}Cs	1.3×10^{-7}	^{244}Cm	1.1×10^{-7}
^{151}Sm	1.1×10^{-10}	^{245}Cm	2.1×10^{-7}
^{152}Eu	7.8×10^{-8}	^{246}Cm	2.1×10^{-7}
^{154}Eu	8.5×10^{-8}	$^{247}Cm + d$	2.1×10^{-7}
^{155}Eu	2.6×10^{-9}	^{248}Cm	7.7×10^{-7}
^{207}Bi	1.0×10^{-7}	^{249}Cf	2.8×10^{-7}
$^{210}Pb + d$	3.1×10^{-6}	^{250}Cf	1.1×10^{-7}
^{226}Ra[d,e]	3.0×10^{-7}	^{251}Cf	2.7×10^{-7}
^{222}Rn	1.3×10^{-6}		

[a]Results obtained from Table G.17 of Appendix G give sum of EDEs from one year's external exposure and 50-year committed EDEs from one year's intake by ingestion and inhalation.

[b]The notation "+ d" with some entries denotes short-lived decay products that are assumed to be in secular equilibrium with parent radionuclide. Indented entries are radiologically significant decay products of parent radionuclides. See Table G.1 of Appendix G for decay products and branching fractions.

[c]Possible contributions to dose from ^{93m}Nb decay product are not included.

[d]Possible contributions to dose from ^{210}Pb decay product are not included.

[e]Contribution to dose from radon decay product is listed separately.

[f]Possible contributions to dose from ^{238}Pu decay product are not included.

Appendix G. Application of these results to the calculation of limits on allowable inventories of radionuclides for disposal in CIIDF is described as follows.

Similar to Eq. (4.4) developed for the agriculture scenario, the limit on allowable average concentration of a radionuclide in waste prior to disposal, $\bar{C}_w$, based on the dose analysis for the post-drilling (*pd*) scenario, is given by

$$\bar{C}_W\,(\mu\text{Ci/m}^3) = \frac{0.1\ \text{rem/year}}{\text{SDCF}_{pd}\,G_r \times f_D(t) \times f_w(t)}\ , \qquad \textbf{(4.9)}$$

where SDCF_{pd} is the SDCF given in Table 4.20, f_D is the radioactive decay factor given in Eq. (4.5) or (4.6), f_w is the mobilization and transport factor given in Table 4.15, and t is the time after disposal when exposures of inadvertent intruders are assumed to occur. The waste dilution factor (G) in Eq. (4.4) and also in Eq. (4.8) for the resident scenario is not used in the dose analysis for the post-drilling scenario because the dilution factor for mixing of exhumed waste with native soil in the vegetable garden which is used in calculating the SDCFs, as described in Sect. G.5.2.3 of Appendix G, is based on the total thickness of waste in the disposal facility, and thus, the amount of uncontaminated material that also would be exhumed by drilling is not relevant in estimating dose. The post-drilling scenario is assumed to occur at 100 years after disposal, when active institutional controls over the disposal site are relinquished and inadvertent intrusion onto the site first could occur. The limit on allowable inventory for a radionuclide in waste prior to disposal per disposal pad in CIIDF, based on the dose analysis for the post-drilling scenario, then is obtained from Eq. (4.7).

The limits on allowable average concentrations and inventories of radionuclides in waste prior to disposal based on the dose analysis for the post-drilling scenario are given in Table 4.21. Calculated limits are given in this table only for radionuclides with relatively short half-lives or with a mobilization and transport factor (f_w) substantially less than unity. For longer-lived radionuclides or radionuclides with a mobilization and transport factor near unity, it is evident from a comparison of the SDCFs for the post-drilling scenario in Table 4.20 with those for the agriculture scenario in Table 4.13 that the agriculture scenario gives a much higher dose per unit concentration in the disposal facility and, thus, is more restrictive in determining allowable limits for disposal. The much higher dose per unit concentration for the agriculture scenario results from (1) the assumption of a much larger volume of waste exhumed from the disposal facility which is mixed with native soil in the vegetable garden in agriculture scenario compared to the post-drilling scenario, and (2) the presence of additional exposure pathways during indoor residence on top of the disposal facility in the agriculture scenario that are not relevant for the post-drilling scenario. Because the concentrations of relatively long-lived and immobile radionuclides that would apply in the agriculture and post-drilling scenarios would be nearly the same, the post-drilling scenario can be neglected and allowable limits need not be given in Table 4.21. Some of the results in the table are described further as follows.

Table 4.21. Allowable limits on concentrations and inventories of radionuclides for CIIDF based on post-drilling scenario for inadvertent intruders[a]

Nuclide[b]	SDCF (rem/year per μCi/m³)[c]	f_D [d]	f_w [e]	$\bar{C}_w$ (μCi/m³)[f]	Inventory limit (Ci/pad)[g]
^{3}H	4.0×10^{-8}	3.6×10^{-3}	6.8×10^{-1}	1.0×10^{9}	8.8×10^{5}
^{14}C	1.5×10^{-7}	9.9×10^{-1}	8.4×10^{-1}	8.0×10^{5}	6.9×10^{2}
^{36}Cl	1.2×10^{-5}	1.0	6.8×10^{-1}	1.2×10^{4}	1.1×10^{1}
^{40}K	6.0×10^{-7}	1.0	1.0	1.7×10^{5}	1.4×10^{2}
^{60}Co	1.8×10^{-7}	1.9×10^{-6}	1.0	2.9×10^{11}	2.5×10^{8}
^{63}Ni	2.0×10^{-9}	5.0×10^{-1}	1.0	1.0×10^{8}	8.6×10^{4}
^{79}Se	1.2×10^{-8}	1.0	6.8×10^{-1}	1.2×10^{7}	1.1×10^{4}
^{90}Sr	2.0×10^{-6}	8.8×10^{-2}	1.0	5.7×10^{5}	4.9×10^{2}
^{93m}Nb	1.8×10^{-10}	6.1×10^{-3}	1.0	9.1×10^{10}	7.8×10^{7}
^{99}Tc	1.3×10^{-7}	1.0	8.6×10^{-1}	8.9×10^{5}	7.7×10^{2}
^{113m}Cd	1.4×10^{-6}	6.3×10^{-3}	1.0	1.1×10^{7}	9.8×10^{3}
^{121m}Sn	6.5×10^{-10}	2.8×10^{-1}	1.0	5.5×10^{8}	4.7×10^{5}
^{129}I	8.2×10^{-7}	1.0	6.8×10^{-1}	1.8×10^{5}	1.5×10^{2}
^{137}Cs	1.3×10^{-7}	9.9×10^{-2}	1.0	7.8×10^{6}	6.7×10^{3}
^{151}Sm	1.1×10^{-10}	4.6×10^{-1}	1.0	2.0×10^{9}	1.7×10^{6}
^{152}Eu	7.8×10^{-8}	5.5×10^{-3}	1.0	2.3×10^{8}	2.0×10^{5}
^{154}Eu	8.5×10^{-8}	3.8×10^{-4}	1.0	3.1×10^{9}	2.7×10^{6}
^{155}Eu	2.6×10^{-9}	8.3×10^{-7}	1.0	4.6×10^{13}	4.0×10^{10}
^{207}Bi	1.0×10^{-7}	1.2×10^{-1}	1.0	8.3×10^{6}	7.2×10^{3}
^{210}Pb	3.1×10^{-6}	4.5×10^{-2}	1.0	7.2×10^{5}	6.2×10^{2}
^{232}U	5.7×10^{-7}[h] 7.8×10^{-7}[i]	3.6×10^{-1}	1.0	4.9×10^{5}[h] 3.6×10^{5}[i]	4.2×10^{2}[h] 3.1×10^{2}[i]
^{238}Pu	1.8×10^{-7}	4.5×10^{-1}	1.0	1.2×10^{6}	1.1×10^{3}
^{241}Pu	3.9×10^{-9}	8.1×10^{-3}	1.0	3.2×10^{9} 1.4×10^{7}[j]	2.7×10^{6} 1.2×10^{4}[j]
^{241}Am	2.5×10^{-7}	8.5×10^{-1}	1.0	4.7×10^{5}	4.0×10^{2}
^{242m}Am ^{238}Pu[k]	2.5×10^{-7} 1.8×10^{-7}	6.1×10^{-1} 4.2×10^{-1}	1.0	4.3×10^{5}	3.7×10^{2}
^{243}Cm	1.4×10^{-7}	8.8×10^{-2}	1.0	8.1×10^{6}	7.0×10^{3}
^{244}Cm	1.1×10^{-7}	2.2×10^{-2}	1.0	4.1×10^{7}	3.6×10^{4}
^{246}Cm	2.1×10^{-7}	9.9×10^{-1}	1.0	4.8×10^{5}	4.1×10^{2}

Table 4.21 (continued)

Nuclide[b]	SDCF (rem/year per μCi/m³)[c]	f_D [d]	f_w [e]	$\bar{C}_w$ (μCi/m³)[f]	Inventory limit (Ci/pad)[g]
^{249}Cf	2.8×10^{-7}	8.2×10^{-1}	1.0	4.4×10^{5}	3.7×10^{2}
^{250}Cf	1.1×10^{-7}	5.0×10^{-3}	1.0	1.8×10^{8} 1.7×10^{8}[m]	1.6×10^{5} 1.5×10^{5}[m]
^{251}Cf	2.7×10^{-7}	9.3×10^{-1}	1.0	4.0×10^{5}	3.4×10^{2}

[a]Allowable limits are calculated from Eqs. (4.9), (4.5) or (4.6), and (4.7). Time for occurrence of post-drilling scenario is assumed to be 100 years after disposal.

[b]For radionuclides listed in Table 4.20 which are omitted from this table, allowable limits are much less than limits based on analysis for agriculture scenario given in Table 4.17.

[c]SDCF for post-drilling scenario obtained from Table 4.20.

[d]Radionuclide inventory at time post-drilling scenario is assumed to occur relative to inventory at time of disposal due to radioactive decay.

[e]Radionuclide inventory at time post-drilling scenario is assumed to occur relative to inventory at time of disposal due to mobilization and transport in infiltrating water obtained from Table 4.15.

[f]Limit on allowable average concentration of radionuclide in waste prior to disposal.

[g]Limit on allowable inventory of radionuclide in waste prior to disposal for individual disposal pads in CIIDF, based on assumption of 330 vaults per pad and waste volume per vault of 2.6 m³.

[h]Contribution from radon decay product is excluded.

[i]Contribution from radon decay product is included.

[j]Value is 30 times limit for ^{241}Am decay product, based on ratio of half-lives of decay product and parent radionuclide.

[k]Indented entry is radiologically significant decay product of parent radionuclide.

[m]Value is 360 times limit for ^{246}Cm decay product, based on ratio of half-lives of decay product and parent radionuclide.

First, for the radionuclide ^{232}U, calculations are performed both excluding and including the contribution to dose from the ^{220}Rn decay product. In this analysis, the performance objective for inadvertent intruders is assumed to exclude any contributions from radon.

Second, for the relatively short-lived radionuclides ^{241}Pu and ^{250}Cf, the allowable limits are determined by the limits for the longer-lived decay products ^{241}Am and ^{246}Cm, respectively. That is, taking into account the assumption that the post-drilling scenario occurs at 100 years after disposal and the half-lives of the parent radionuclides and their longer-lived decay products, the dose from the decay product is greater than the dose from the parent itself. For the relatively short-lived radionuclides ^{243}Cm and ^{244}Cm, the dose from the longer-lived decay products ^{239}Pu and ^{240}Pu, respectively, also was considered. However, the half-life of the parent radionuclide is sufficiently long in these cases that the dose from the parent is greater than the dose from the decay product.

Finally, for the radionuclide ^{242m}Am, the buildup of the decay product ^{238}Pu in the waste after disposal is taken into account in estimating the dose for the post-drilling scenario. At 100 years after disposal, the activity of the decay product has not achieved equilibrium with the activity of the parent radionuclide, and separate decay factors are applied to the parent and decay product. The dose from ^{242m}Am and its decay product decreases with time after 100 years.

4.5 SUMMARY OF DISPOSAL LIMITS

This section summarizes the results of the PA for CIIDF in the form of allowable limits on inventories of radionuclides that would be acceptable for disposal. The disposal limits are based either on the analysis for off-site releases via water pathways or on the analysis for exposures of inadvertent intruders.

4.5.1 Disposal Limits Based on Analyses for Off-Site Releases

The PA for releases by water pathways provides estimates of the maximum concentrations of radionuclides in groundwater and surface water per unit initial activity in the disposal facility (see Sect. 4.3.4). For each radionuclide, the allowable limit on inventory for disposal based on the dose analysis for the drinking water pathway (I_w) then is given by

$$I_w\,(\text{Ci}) = \frac{(0.004\ \text{rem/year})}{\text{PDCF}_w\,(\text{rem/year per }\mu\text{Ci/L}) \times C_w\,(\mu\text{Ci/L per Ci})}\ , \qquad \textbf{(4.10)}$$

where the numerator is the performance objective for the drinking water pathway, PDCF_w is the so-called pathway dose conversion factor for the drinking water pathway, which is given in Table 4.11, and C_w is the maximum concentration of the radionuclide in groundwater or surface water, whichever is lower, per unit initial activity of the radionuclide in the disposal facility, as obtained from Table 4.10. In this analysis, the inventory limit is calculated per pad; that is, each pad in CIIDF is treated as a separate disposal facility for purposes of determining disposal limits of radionuclides. Some of the results in Table 4.22 are described further as follows.

First, for the relatively mobile radionuclides ^{3}H, ^{36}Cl, ^{79}Se, and ^{129}I, the maximum concentration in water at off-site locations occurs during the 100-year period of active institutional control over the disposal facility. Although the performance objective for protection of groundwater or surface water resources is assumed to apply at off-site locations at any time after disposal, exposures of individuals are unlikely to occur at the locations of maximum concentrations during the active institutional control period, especially if controls are maintained over a sizeable portion of ORR near the disposal site. Therefore, for these radionuclides, an inventory limit also is calculated based on the maximum concentration in water at any time after loss of active institutional controls at 100 years after disposal. For the radionuclides ^{152}Eu, ^{154}Eu, ^{155}Eu, ^{241}Pu, and ^{250}Cf, the maximum concentrations also occur within 100 years, but these radionuclides are sufficiently short-lived that significant releases to off-site locations do not occur beyond 100 years. In addition, as described below, the inventory limits for ^{241}Pu and ^{250}Cf are based on the limits for their longer-lived decay products ^{241}Am and ^{246}Cm, respectively.

Table 4.22. Allowable limits on inventories of radionuclides for CIIDF based on allowable off-site releases in groundwater or surface water[a]

Nuclide	PDCF[b] (rem/year per μCi/L)	C_w [c] (μCi/L per Ci/pad)	Time[d] (years)	Inventory limit[e] (Ci/pad)
^{3}H	4.7×10^{-2}	8.7×10^{-4} (g) 7.7×10^{-6} (g)[g]	4.5×10^{1}[f] 1.0×10^{2}	9.6×10^{1} 1.1×10^{4}
^{10}Be	3.4	1.5×10^{-7} (g) 4.7×10^{-9} (s)	4.4×10^{5}[h] 2.6×10^{4}[h]	8.1×10^{3} 2.6×10^{5}
^{14}C	1.5	1.3×10^{-2} (g)	1.4×10^{2}	2.1×10^{-1}
^{26}Al	1.1×10^{1}	2.0×10^{-7} (g) 2.2×10^{-8} (s)	1.0×10^{6}[h] 2.5×10^{3}	1.8×10^{3} 1.7×10^{4}
^{36}Cl	2.2	3.5×10^{-2} (g) 1.1×10^{-2} (g)[g]	7.4×10^{1}[f] 1.0×10^{2}	5.2×10^{-2} 1.6×10^{-1}
^{40}K	1.4×10^{1}	1.0×10^{-4} (g) 5.2×10^{-6} (s)	1.4×10^{4}[h] 1.1×10^{2}	2.9 5.6×10^{1}
^{41}Ca	9.5×10^{-1}	7.9×10^{-5} (g) 7.2×10^{-6} (s)	1.4×10^{4}[h] 1.8×10^{2}	5.3×10^{1} 5.9×10^{2}
^{60}Co	2.0×10^{1}			No limit[i]
^{59}Ni	1.5×10^{-1}	2.8×10^{-8} (s)	9.2×10^{2}	9.7×10^{5}
^{63}Ni	4.2×10^{-1}	6.3×10^{-9} (s)	2.0×10^{2}	1.5×10^{6}
^{79}Se	6.4	1.9×10^{-2} (g) 1.2×10^{-2} (g)[g]	8.0×10^{1}[f] 1.0×10^{2}	3.3×10^{-2} 5.3×10^{-2}
^{87}Rb	3.6			No limit[j]
^{90}Sr	1.1×10^{2}	3.7×10^{-7} (s)	1.1×10^{2}	9.8×10^{1}
^{93}Zr[k]	1.6	6.8×10^{-5} (g) 8.4×10^{-7} (s)	2.3×10^{4}[h] 6.4×10^{2}	3.7×10^{1} 3.0×10^{3}
^{93m}Nb	3.8×10^{-1}	5.0×10^{-10} (s)	1.0×10^{2}	2.2×10^{7}
^{94}Nb	5.2	9.0×10^{-6} (g) 4.9×10^{-7} (s)	3.5×10^{4}[h] 4.9×10^{2}	8.6×10^{1} 1.6×10^{3}
^{99}Tc	1.1	1.3×10^{-2} (g)	1.4×10^{2}	2.7×10^{-1}
^{107}Pd	1.1×10^{-1}			1.2×10^{4}[m]
^{113m}Cd	1.2×10^{2}	8.0×10^{-13} (s)	1.2×10^{2}	4.1×10^{7}
^{121m}Sn	1.2	4.3×10^{-8} (s)	1.4×10^{2}	7.6×10^{4}
^{126}Sn	1.5×10^{1}	2.1×10^{-5} (g) 5.2×10^{-7} (s)	4.3×10^{4}[h] 3.3×10^{2}	1.3×10^{1} 5.2×10^{2}
^{129}I	2.0×10^{2}	3.5×10^{-2} (g) 1.1×10^{-2} (g)[g]	7.4×10^{1}[f] 1.0×10^{2}	5.7×10^{-4} 1.8×10^{-3}
^{135}Cs	5.2	5.9×10^{-7} (g) 1.9×10^{-8} (s)	1.1×10^{6}[h] 5.4×10^{2}	1.3×10^{3} 4.0×10^{4}
^{137}Cs	3.7×10^{1}	3.0×10^{-10} (s)	1.2×10^{2}	3.7×10^{5}
^{151}Sm	2.8×10^{-1}			No limit[i]
^{152}Eu	4.7	3.9×10^{-8} (s)	6.1×10^{1}[f]	2.2×10^{4}
^{154}Eu	6.9	1.1×10^{-8} (s)	6.1×10^{1}[f]	5.5×10^{4}
^{155}Eu	1.1	5.5×10^{-10} (s)	6.1×10^{1}[f]	6.5×10^{6}

Table 4.22 (continued)

Nuclide	PDCF[b] (rem/year per μCi/L)	C_w [c] (μCi/L per Ci/pad)	Time[d] (years)	Inventory limit[e] (Ci/pad)
^{207}Bi	4.0	4.3×10^{-9} (s)	1.2×10^{2}	2.3×10^{5}
^{210}Pb	5.3×10^{3}	1.9×10^{-9} (s)	1.2×10^{2}	3.9×10^{2}
^{226}Ra[n]	6.3×10^{3}	1.5×10^{-8} (s)	4.1×10^{2}	4.2×10^{1}
^{229}Th	2.9×10^{3}	1.7×10^{-8} (s)	9.7×10^{2}	8.4×10^{1}
^{230}Th	4.0×10^{2}	1.8×10^{-8} (s)	5.2×10^{3}	5.6×10^{2}
^{232}Th	3.6×10^{3}			6.1×10^{-2}[m]
^{231}Pa	1.9×10^{4}	4.6×10^{-7} (g) 1.3×10^{-7} (s)	1.2×10^{5}[h] 1.0×10^{3}	4.6×10^{-1} 1.6
^{232}U	1.5×10^{3}	1.7×10^{-7} (s)	1.1×10^{2}	1.6×10^{1}
^{233}U	2.1×10^{2}	7.9×10^{-5} (g) 9.6×10^{-7} (s)	1.8×10^{4}[h] 4.7×10^{2}	2.4×10^{-1} 2.0×10^{1}
^{234}U	2.0×10^{2}	8.3×10^{-5} (g) 1.0×10^{-6} (s)	1.8×10^{4}[h] 4.8×10^{2}	2.4×10^{-1} 2.0×10^{1}
^{235}U	2.0×10^{2}	8.7×10^{-5} (g) 9.1×10^{-7} (s)	1.9×10^{4}[h] 8.5×10^{2}	2.3×10^{-1} 2.2×10^{1}
^{236}U	2.0×10^{2}	8.3×10^{-5} (g) 9.2×10^{-7} (s)	1.8×10^{4}[h] 4.8×10^{2}	2.4×10^{-1} 2.2×10^{1}
^{238}U	1.9×10^{2}	8.1×10^{-5} (g) 3.0×10^{-7} (s)	2.3×10^{4}[h] 6.8×10^{3}	2.6×10^{-1} 7.0×10^{1}
^{237}Np	3.2×10^{3}	8.7×10^{-5} (g) 1.0×10^{-6} (s)	1.8×10^{4}[h] 4.8×10^{2}	1.5×10^{-2} 1.3
^{238}Pu	2.3×10^{3}	2.0×10^{-7} (s)	1.1×10^{2}	8.5
^{239}Pu	2.6×10^{3}	5.2×10^{-5} (g) 9.7×10^{-7} (s)	1.8×10^{4}[h] 4.8×10^{2}	2.9×10^{-2} 1.6
^{240}Pu	2.6×10^{3}	5.8×10^{-5} (g) 9.2×10^{-7} (s)	1.8×10^{4}[h] 4.5×10^{2}	2.6×10^{-2} 1.6
^{241}Pu	5.0×10^{1}	4.7×10^{-9} (s)	6.1×10^{1}[f] 2.2×10^{2}[o]	1.7×10^{4} 7.8×10^{1}[p]
^{242}Pu	2.5×10^{3}	8.4×10^{-5} (g) 9.5×10^{-7} (s)	1.8×10^{4}[h] 4.9×10^{2}	1.9×10^{-2} 1.7
^{244}Pu	2.4×10^{3}	8.5×10^{-5} (g) 9.0×10^{-7} (s)	1.9×10^{4}[h] 7.4×10^{2}	2.0×10^{-2} 1.9
^{241}Am	2.6×10^{3}	5.8×10^{-7} (s)	2.2×10^{2}	2.6
^{242m}Am[q]	4.9×10^{3}	9.9×10^{-8} (s)	1.8×10^{2}	1.4
^{243}Am	2.6×10^{3}	1.9×10^{-5} (g) 9.1×10^{-7} (s)	1.4×10^{4}[h] 4.7×10^{2}	7.6×10^{-2} 1.7
^{243}Cm	1.8×10^{3}	3.7×10^{-8} (s)	1.1×10^{2} 1.8×10^{4}[o]	6.0×10^{1} 2.5×10^{1}[r]
^{244}Cm	1.5×10^{3}	8.7×10^{-9} (s)	1.1×10^{2} 1.8×10^{4}[o]	3.1×10^{2} 9.4[s]
^{245}Cm	2.7×10^{3}	2.3×10^{-5} (g) 9.1×10^{-7} (s)	1.4×10^{4}[h] 4.6×10^{2}	6.4×10^{-2} 1.7
^{246}Cm	2.7×10^{3}	1.0×10^{-5} (g) 9.3×10^{-7} (s)	1.3×10^{4}[h] 4.4×10^{2}	1.5×10^{-1} 1.6

Table 4.22 (continued)

Nuclide	PDCF[b] (rem/year per μCi/L)	C_w [c] (μCi/L per Ci/pad)	Time[d] (years)	Inventory limit[e] (Ci/pad)
^{247}Cm	2.5×10^3	8.4×10^{-5} (g) 9.5×10^{-7} (s)	1.8×10^{4}[h] 5.0×10^2	1.9×10^{-2} 1.7
^{248}Cm	1.0×10^4	8.3×10^{-5} (g) 9.6×10^{-7} (s)	1.8×10^{4}[h] 4.8×10^2	4.8×10^{-3} 4.2×10^{-1}
^{249}Cf	3.4×10^3	5.2×10^{-7} (s)	2.0×10^2 1.4×10^{4}[o]	2.3 1.5[f]
^{250}Cf	1.5×10^3	3.6×10^{-9} (s)	6.1×10^{1}[f] 1.3×10^{4}[o]	7.5×10^2 5.4×10^{1}[u]
^{251}Cf	3.5×10^3	6.9×10^{-7} (s)	3.2×10^2	1.6

[a]Allowable limits are calculated from Eq. (4.10).

[b]Annual EDE from drinking water pathway per unit concentration in water obtained from Table 4.11.

[c]Estimated maximum concentration in groundwater (*g*) or surface water (*s*) beyond 100-m buffer zone around disposal facility per unit activity in waste at time of disposal obtained from Table 4.10.

[d]Time after disposal when maximum concentration in groundwater or surface water beyond 100-m buffer zone is estimated to occur.

[e]Limit on allowable inventory of radionuclide in waste prior to disposal for individual disposal pads in CIIDF, based on assumption of 330 vaults per pad.

[f]Maximum concentration occurs during 100-year period of active institutional control.

[g]Estimated maximum concentration after loss of active institutional control.

[h]Maximum concentration occurs beyond assumed 10,000-year time for compliance with performance objective for protection of groundwater or surface water resources.

[i]Estimated maximum concentration within assumed 10,000-year time for compliance with performance objective for protection of groundwater or surface water resources.

[j]Half-life of radionuclide is much less than estimated travel time beyond 100-m buffer zone.

[k]Decay product ^{93m}Nb is assumed to be in activity equilibrium in water.

[m]Significant releases to groundwater or surface water beyond 100-m buffer zone are not estimated to occur after loss of active institutional control, due to short half-life of radionuclide.

[n]Decay product ^{210}Pb is assumed to be in activity equilibrium in water.

[o]Time after disposal when maximum concentration of longer-lived decay product in groundwater or surface water beyond 100-m buffer zone is estimated to occur.

[p]Value is 30 times inventory limit for ^{241}Am decay product, based on ratio of half-lives of decay product and parent radionuclide.

[q]Decay product ^{238}Pu is assumed to be in activity equilibrium in water.

[r]Value is 850 times inventory limit for ^{239}Pu decay product, based on ratio of half-lives of decay product and parent radionuclide.

[s]Value is 360 times inventory limit for ^{240}Pu decay product, based on ratio of half-lives of decay product and parent radionuclide.

[t]Value is 24 times inventory limit for ^{245}Cm decay product, based on ratio of half-lives of decay product and parent radionuclide.

[u]Value is 360 times inventory limit for ^{246}Cm decay product, based on ratio of half-lives of decay product and parent radionuclide.

Second, many of the radionuclides are sufficiently immobile that the maximum concentration in groundwater at off-site locations occurs after the assumed 10,000-year time period for compliance with the performance objective for protection of groundwater or surface water resources. Therefore, for these radionuclides, an inventory limit also is calculated based on the maximum concentration in surface water, which occurs during the assumed time period for compliance. However, it also should be emphasized that the maximum concentrations of these radionuclides in groundwater during the assumed 10,000-year time period for compliance could exceed the maximum concentrations in surface water (e.g., see Fig. 4.27 for ^{238}U).

Third, the radionuclides ^{60}Co and ^{151}Sm are sufficiently short-lived and immobile that significant releases to off-site locations in either groundwater or surface water do not occur at any time after disposal. Therefore, there essentially is no inventory limit for these radionuclides based on the analysis for off-site releases by water pathways.

Fourth, for the long-lived radionuclides ^{107}Pd and ^{232}Th, the maximum concentrations in both groundwater and surface water occur well after 10,000 years, and the predicted concentrations per unit activity in the disposal facility are very low. Therefore, it is evident that the inventory limit based on an analysis of releases to water would be much higher than the limit based on the dose analysis for inadvertent intruders summarized in Sect. 4.5.2. Therefore, results for releases to water are not given in Table 4.22 for these radionuclides.

Fifth, for the radionuclides ^{93}Zr, ^{226}Ra, and ^{242m}Am, the shorter-lived decay products ^{93m}Nb, ^{210}Pb, and ^{238}Pu, respectively, are assumed to be in activity equilibrium in water with the parent radionuclide at the location of its maximum concentration (see Sect. 4.4.1).

Finally, for the relatively short-lived radionuclides ^{241}Pu, ^{243}Cm, ^{244}Cm, ^{249}Cf, and ^{250}Cf, the inventory limit is based on the limit for the longer-lived decay product ^{241}Am, ^{239}Pu, ^{240}Pu, ^{245}Cm, and ^{246}Cf, respectively. Specifically, by making the conservative assumption that the inventory of parent radionuclide at the time of disposal is converted instantly to the equivalent inventory of its decay product, the inventory limit for the parent is given by the limit for the decay product multiplied by the the ratio of the half-life of the decay product to the half-life of the parent. This procedure results in a considerably lower inventory limit than the value estimated from consideration of transport of the parent isotope to off-site locations.

4.5.2 Disposal Limits Based on Analysis for Inadvertent Intruders

In the dose analysis for inadvertent intruders, limits on allowable average concentrations and inventories of radionuclides in waste prior to disposal were developed based on the agriculture, resident, and post-drilling scenarios, and the results for these scenarios are given in Table 4.17, Table 4.19, and Table 4.21, respectively. The allowable limits based on the dose analysis for inadvertent intruders then are the most restrictive of the allowable limits for each scenario. The allowable limits based on the analyses for the three scenarios are summarized in Table 4.23.

For most of the radionuclides, the allowable limits are based on the dose analysis for the agriculture scenario. The exceptions occur for shorter-lived, photon-emitting radionuclides, for

Table 4.23. Allowable limits on concentrations and inventories of radionuclides in CIIDF based on analyses of scenarios for inadvertent intruders[a]

Nuclide	Limiting scenario[b]	Concentration limit[c] (μCi/m^3)	Inventory limit[d] (Ci/pad)
^{3}H	Post-drilling	1.0×10^{9}	8.8×10^{5}
^{10}Be	Agriculture	5.9×10^{6}	5.1×10^{3}
^{14}C	Agriculture	1.7×10^{5}	1.5×10^{2}
^{26}Al	Agriculture	6.4×10^{1}	5.5×10^{-2}
^{36}Cl	Post-drilling	1.2×10^{4}	1.1×10^{1}
^{40}K	Agriculture	2.0×10^{3}	1.7
^{41}Ca	Agriculture	2.0×10^{5}	1.7×10^{2}
^{60}Co	Resident	4.5×10^{8}	3.9×10^{5}
^{59}Ni	Agriculture	6.9×10^{6}	6.0×10^{3}
^{63}Ni	Agriculture	1.9×10^{7}	1.6×10^{4}
^{79}Se	Post-drilling	1.2×10^{7}	1.1×10^{4}
^{87}Rb	None	No limit[e]	No limit[e]
^{90}Sr	Post-drilling	5.7×10^{5}	4.9×10^{2}
^{93}Zr	Agriculture	1.0×10^{7}	8.6×10^{3}
^{93m}Nb	Post-drilling	9.1×10^{10}	7.8×10^{7}
^{94}Nb	Agriculture	1.4×10^{2}	1.1×10^{-1}
^{99}Tc	Agriculture	1.7×10^{5}	1.4×10^{2}
^{107}Pd	Agriculture	1.4×10^{7}	1.2×10^{4}
^{113m}Cd	Post-drilling	1.1×10^{7}	9.8×10^{3}
^{121m}Sn	Agriculture	3.1×10^{7}	2.7×10^{4}
^{126}Sn	Agriculture	1.2×10^{2}	1.1×10^{-1}
^{129}I	Post-drilling	1.8×10^{5}	1.5×10^{2}
^{135}Cs	Agriculture	4.8×10^{5}	4.2×10^{2}
^{137}Cs	Resident	7.9×10^{4}	6.8×10^{1}
^{151}Sm	Agriculture	3.6×10^{8}	3.1×10^{5}
^{152}Eu	Resident	4.6×10^{5}	4.0×10^{2}
^{154}Eu	Resident	6.0×10^{6}	5.1×10^{3}
^{155}Eu	Resident	1.5×10^{13}	1.3×10^{10}
^{207}Bi	Resident	1.7×10^{4}	1.5×10^{1}
^{210}Pb	Post-drilling	7.2×10^{5}	6.2×10^{2}
^{226}Ra[f]	Agriculture	1.3×10^{2}	1.1×10^{-1}
^{229}Th	Agriculture	6.1×10^{2}	5.2×10^{-1}
^{230}Th[f]	Agriculture[g]	3.9×10^{2}	3.4×10^{-1}
^{232}Th[f]	Agriculture	7.1×10^{1}	6.1×10^{-2}
^{231}Pa	Agriculture	3.3×10^{2}	2.9×10^{-1}
^{232}U[f]	Agriculture	2.3×10^{3}	2.0
^{233}U	Agriculture[g]	6.9×10^{3}	6.0
^{234}U[f]	Agriculture[g]	2.4×10^{4}	2.1×10^{1}
^{235}U	Agriculture[h]	8.3×10^{2}	7.2×10^{-1}

Table 4.23 (continued)

Nuclide	Limiting scenario[b]	Concentration limit[c] (μCi/m^3)	Inventory limit[d] (Ci/pad)
^{236}U	Agriculture	3.3×10^4	2.9×10^1
^{238}U[f]	Agriculture[h]	6.7×10^3	5.7
^{237}Np	Agriculture	6.3×10^2	5.4×10^{-1}
^{238}Pu	Agriculture	1.3×10^5	1.2×10^2
^{239}Pu	Agriculture	1.1×10^4	9.9
^{240}Pu	Agriculture	1.2×10^4	1.0×10^1
^{241}Pu	Agriculture	3.5×10^5[i]	3.0×10^2[i]
^{242}Pu	Agriculture	1.2×10^4	1.0×10^1
^{244}Pu	Agriculture	5.3×10^2	4.6×10^{-1}
^{241}Am	Agriculture	1.2×10^4	9.9
^{242m}Am	Agriculture	1.5×10^4	1.3×10^1
^{243}Am	Agriculture	1.2×10^3	1.0
^{243}Cm	Agriculture	2.5×10^6	2.1×10^3
^{244}Cm	Agriculture	4.2×10^6[j]	3.6×10^3[j]
^{245}Cm	Agriculture	2.3×10^3	2.0
^{246}Cm	Agriculture	1.1×10^4	9.5
^{247}Cm	Agriculture	6.3×10^2	5.4×10^{-1}
^{248}Cm	Agriculture	2.9×10^3	2.5
^{249}Cf	Agriculture	1.0×10^3	8.7×10^{-1}
^{250}Cf	Agriculture	4.0×10^6[k]	3.4×10^3[k]
^{251}Cf	Agriculture	2.1×10^3	1.8

[a]Allowable limits based on analyses for agriculture, resident, and post-drilling scenarios are obtained from Table 4.17, Table 4.19, and Table 4.21, respectively.

[b]Agriculture scenario is assumed to occur at 300 years after disposal, unless otherwise noted; resident and post-drilling scenarios are assumed to occur at 100 years after disposal.

[c]Limit on allowable average concentration of radionuclide in waste prior to disposal.

[d]Limit on allowable inventory of radionuclide in waste prior to disposal for individual disposal pads in CIIDF, based on assumption of 330 vaults per pad and waste volume per vault of 2.6 m^3.

[e]Calculated limits for all scenarios exceed specific activity of radionuclide.

[f]Calculated limits exclude contribution from radon decay product.

[g]Scenario is evaluated at 2000 years after disposal when maximum dose from radionuclide and its decay products occurs.

[h]Scenario is evaluated at 10,000 years after disposal when maximum dose from radionuclide and its decay products during assumed 10,000-year time for compliance with performance objective for inadvertent intruders occurs. If reductions in inventory due to mobilization and transport in infiltrating water are not significant, dose continues to increase beyond 10,000 years.

[i]Value is 30 times limit for longer-lived ^{241}Am decay product, based on ratio of half-lives of decay product and parent radionuclide; limit due to activity of parent radionuclide at time scenario is assumed to occur is less restrictive.

[j]Value is 360 times limit for longer-lived ^{240}Pu decay product, based on ratio of half-lives of decay product and parent radionuclide; limit due to activity of parent radionuclide at time scenario is assumed to occur is less restrictive.

[k]Value is 360 times limit for longer-lived ^{246}Cm decay product, based on ratio of half-lives of decay product and parent radionuclide; limit due to activity of parent radionuclide at time scenario is assumed to occur is less restrictive.

which the allowable limits are based on the dose analysis for the resident scenario, and for shorter-lived radionuclides which are not photon emitters or longer-lived radionuclides which are removed from the disposal facility relatively rapidly by mobilization and transport in infiltrating water, for which the allowable limits are based on the dose analysis for the post-drilling scenario. Since the agriculture scenario generally results in the lowest dose per unit concentration of radionuclides in the disposal facility at the time intrusion occurs, the allowable limits are based on the dose analysis for the other scenarios only when the inventory of a radionuclide is depleted significantly by radioactive decay or by mobilization and transport in infiltrating water between 100 years after disposal, when the resident and post-drilling scenarios are assumed to occur, and 300 years, when the agriculture scenario is assumed to occur.

4.5.3 Estimated Disposal Limits

The limits on allowable inventories of radionuclides in waste prior to disposal for individual disposal pads in CIIDF based on the dose analysis for off-site releases to groundwater or surface water are given in Table 4.22, and the limits on allowable average concentrations and inventories based on the dose analysis for inadvertent intruders are given in Table 4.23. The allowable limits for CIIDF based on compliance with all applicable performance objectives then are the more restrictive of the allowable limits in the two cases, and the limit for each radionuclide is summarized in Table 4.24. When the allowable limit is based on the dose analysis for off-site releases, the inventories in Table 4.22 are converted to average concentrations in waste using Eq. (4.7).

The allowable limits in Table 4.24 are based on the following assumptions about the applicability of performance objectives for CIIDF.

First, the performance objective for protection of groundwater and surface water resources, which provides the basis for the allowable limits for off-site releases, is assumed to apply beyond the 100-m buffer zone around the disposal facility at any time after disposal. Therefore, for some mobile radionuclides, the maximum dose from off-site releases, which occurs during the 100-year period for active institutional control over the disposal site, is used in obtaining the allowable limits for disposal, even though exposures to contaminated water near the boundary of the disposal facility during this time are unlikely. This approach is based on the interpretation of the performance objective as applying to resource protection, rather than protection of individuals who might be exposed to contaminated water.

Second, the performance objective for inadvertent intruders is assumed to exclude any contributions to dose from inhalation of radon and its short-lived decay products. For some isotopes of thorium and uranium, the maximum dose for the intruder/agriculture scenario would be increased if the dose from radon were included, but these results are not used in obtaining the allowable limits for disposal.

Third, the performance objectives for off-site releases and inadvertent intruders are assumed to apply for 10,000 years after disposal. However, the results in Table 4.24 take into account the 10,000-year time of compliance only in estimating inventory limits based on the intruder/agriculture

Table 4.24. Allowable limits on concentrations and inventories of radionuclides in CIIDF based on analyses of off-site releases and scenarios for inadvertent intruders[a]

Nuclide	Limiting scenario[b]	Concentration limit[c] (μCi/m^3)	Inventory limit[d] (Ci/pad)
^{3}H	Off-site/groundwater	1.1×10^{5}	9.6×10^{1}
^{10}Be	Intruder/agriculture	5.9×10^{6}	5.1×10^{3}
^{14}C	Off-site/groundwater	2.4×10^{2}	2.1×10^{-1}
^{26}Al	Intruder/agriculture	6.4×10^{1}	5.5×10^{-2}
^{36}Cl	Off-site/groundwater	6.1×10^{1}	5.2×10^{-2}
^{40}K	Intruder/agriculture	2.0×10^{3}	1.7
^{41}Ca	Off-site/groundwater	6.2×10^{4}	5.3×10^{1}[e]
^{60}Co	Intruder/resident	4.5×10^{8}	3.9×10^{5}
^{59}Ni	Intruder/agriculture	6.9×10^{6}	6.0×10^{3}
^{63}Ni	Intruder/agriculture	1.9×10^{7}	1.6×10^{4}
^{79}Se	Off-site/groundwater	3.8×10^{1}	3.3×10^{-2}
^{87}Rb	None	No limit[f]	No limit[f]
^{90}Sr	Off-site/surface water	1.1×10^{5}	9.8×10^{1}
^{93}Zr	Off-site/groundwater	4.3×10^{4}	3.7×10^{1}[e]
^{93m}Nb	Off-site/surface water	2.6×10^{10}	2.2×10^{7}
^{94}Nb	Intruder/agriculture	1.4×10^{2}	1.1×10^{-1}
^{99}Tc	Off-site/groundwater	3.1×10^{2}	2.7×10^{-1}
^{107}Pd	Intruder/agriculture	1.4×10^{7}	1.2×10^{4}
^{113m}Cd	Intruder/post-drilling	1.1×10^{7}	9.8×10^{3}
^{121m}Sn	Intruder/agriculture	3.1×10^{7}	2.7×10^{4}
^{126}Sn	Intruder/agriculture	1.2×10^{2}	1.1×10^{-1}
^{129}I	Off-site/groundwater	6.6×10^{-1}	5.7×10^{-4}
^{135}Cs	Intruder/agriculture	4.8×10^{5}	4.2×10^{2}
^{137}Cs	Intruder/resident	7.9×10^{4}	6.8×10^{1}
^{151}Sm	Intruder/agriculture	3.6×10^{8}	3.1×10^{5}
^{152}Eu	Intruder/resident	4.6×10^{5}	4.0×10^{2}
^{154}Eu	Intruder/resident	6.0×10^{6}	5.1×10^{3}
^{155}Eu	Off-site/surface water	7.6×10^{9}	6.5×10^{6}
^{207}Bi	Intruder/resident	1.7×10^{4}	1.5×10^{1}
^{210}Pb	Off-site/surface water	4.5×10^{5}	3.9×10^{2}
^{226}Ra	Intruder/agriculture	1.3×10^{2}	1.1×10^{-1}
^{229}Th	Intruder/agriculture	6.1×10^{2}	5.2×10^{-1}
^{230}Th	Intruder/agriculture	3.9×10^{2}	3.4×10^{-1}
^{232}Th	Intruder/agriculture	7.1×10^{1}	6.1×10^{-2}
^{231}Pa	Intruder/agriculture	3.3×10^{2}	2.9×10^{-1}
^{232}U	Intruder/agriculture	2.3×10^{3}	2.0
^{233}U	Off-site/groundwater	2.8×10^{2}	2.4×10^{-1}[e]
^{234}U	Off-site/groundwater	2.8×10^{2}	2.4×10^{-1}[e]

Table 4.24 (continued)

Nuclide	Limiting scenario[b]	Concentration limit[c] ($\mu Ci/m^3$)	Inventory limit[d] (Ci/pad)
^{235}U	Off-site/groundwater	2.7×10^2	2.3×10^{-1}[e]
^{236}U	Off-site/groundwater	2.8×10^2	2.4×10^{-1}[e]
^{238}U	Off-site/groundwater	3.0×10^2	2.6×10^{-1}[e]
^{237}Np	Off-site/groundwater	1.7×10^1	1.5×10^{-2}[e]
^{238}Pu	Off-site/surface water	9.9×10^3	8.5
^{239}Pu	Off-site/groundwater	3.4×10^1	2.9×10^{-2}[e]
^{240}Pu	Off-site/groundwater	3.0×10^1	2.6×10^{-2}[e]
^{241}Pu	Off-site/surface water	9.1×10^4	7.8×10^1
^{242}Pu	Off-site/groundwater	2.2×10^1	1.9×10^{-2}[e]
^{244}Pu	Off-site/groundwater	2.3×10^1	2.0×10^{-2}[e]
^{241}Am	Off-site/surface water	3.0×10^3	2.6
^{242m}Am	Off-site/surface water	1.6×10^3	1.4
^{243}Am	Off-site/groundwater	8.9×10^1	7.6×10^{-2}[e]
^{243}Cm	Off-site/groundwater	2.9×10^4	2.5×10^1[e]
^{244}Cm	Off-site/groundwater	1.1×10^4	9.4[e]
^{245}Cm	Off-site/groundwater	7.5×10^1	6.4×10^{-2}[e]
^{246}Cm	Off-site/groundwater	1.7×10^2	1.5×10^{-1}[e]
^{247}Cm	Off-site/groundwater	2.2×10^1	1.9×10^{-2}[e]
^{248}Cm	Off-site/groundwater	5.6	4.8×10^{-3}[e]
^{249}Cf	Intruder/agriculture	1.0×10^3	8.7×10^{-1}
^{250}Cf	Off-site/groundwater	6.3×10^4	5.4×10^1[e]
^{251}Cf	Off-site/surface water	1.9×10^3	1.6

[a]Allowable limits based on analyses for off-site releases and scenarios for inadvertent intruders are obtained from Table 4.22 and Table 4.23, respectively.

[b]Times at which maximum doses for off-site releases and scenarios for inadvertent intruders occur are given in Table 4.22 and Table 4.23, respectively.

[c]Limit on allowable average concentration of radionuclide in waste prior to disposal.

[d]Limit on allowable inventory of radionuclide in waste prior to disposal for individual disposal pads in CIIDF, based on assumption of 330 vaults per pad and waste volume per vault of 2.6 m^3.

[e]Limit is based on estimated maximum concentration in groundwater at time beyond 10,000 years and, thus, is conservative representation of inventory limit based on analyses during assumed 10,000-year time of compliance with performance objectives.

[f]Estimated limits based on analyses for releases to water or exposures of inadvertent intruders exceed values that reasonably could occur in waste, due to the very long half-life (very low specific activity) of radionuclide.

scenario for those actinide radionuclides which decay to radiologically significant long-lived decay products. For many long-lived and relatively immobile radionuclides, the results in Table 4.24 are based on the maximum concentrations in groundwater which occur between 13,000 and 23,000 years after disposal (see Table 4.10), and the results in Table 4.24 do not yet take into account that the concentrations at 10,000 years would be less than the maximum concentrations at later times. Therefore, the inventory limits based on the groundwater calculations in these cases provide conservative values for the development of WAC for the disposal facility.

The results in Table 4.24 may be summarized as follows.

1. Of the 60 radionuclides evaluated, the allowable limits for 35 are determined by the dose analysis for off-site releases. Of these, most of the allowable limits are determined by the dose analysis for releases to groundwater, but the allowable limits for nine shorter-lived radionuclides are determined by the dose analysis for releases to surface water.

2. Of the 24 radionuclides for which the allowable limits are determined by the dose analysis for inadvertent intruders, the limits for 18 radionuclides are determined by the analysis for the agriculture scenario, the limits for five shorter-lived, photon-emitting radionuclides are determined by the analysis for the resident scenario, and the limits for a single radionuclide are determined by the analysis for the post-drilling scenario.

3. For ^{87}Rb, the analyses for off-site releases and exposures of inadvertent intruders do not provide practical inventory limits for disposal. This radionuclide is so long-lived (and thus has such a low specific activity) that the calculated limits in either case exceed those that could occur in the waste.

4. For most of the radionuclides evaluated, the difference between the allowable limits based on the analysis for off-site releases and the allowable limits based on the analysis for inadvertent intruders differs by more than an order of magnitude. However, for a few radionuclides, there is relatively little difference between the allowable limits in the two cases. For example, the limits differ by only about a factor of 3 or less for ^{10}Be, ^{40}K, ^{41}Ca, ^{93m}Nb, ^{121m}Sn, ^{135}Cs, ^{210}Pb, ^{231}Pa, ^{235}U, ^{241}Am, ^{249}Cf, and ^{251}Cf, although, in some cases, this comparison is based on results for the groundwater release pathway at times beyond the 10,000-year time of compliance.

Application of the allowable limits in Table 4.24 to LLW intended for disposal in CIIDF is discussed in the following section.

4.5.4 Application of Disposal Limits to Mixtures of Radionuclides

In practice, the allowable limits on inventory of radionuclides given in Table 4.24, rather than the allowable limits on average concentration, will be used to determine acceptable disposals in the CIIDF. The allowable limits on inventory apply when only a single radionuclide is present in the waste. However, LLW in CIIDF generally should consist of mixtures of radionuclides, and a sum-of-fractions rule would need to be applied in determining allowable limits on inventory for actual disposals (e.g., using Table 4.24). This rule states that the ratio of the inventory of each radionuclide to its inventory limit, summed over all radionuclides, should not exceed unity.

The sum-of-fractions rule can be applied in several different ways. The simplest approach would be to apply the rule to all radionuclides in the waste, without regard for whether the limit on

inventory for any radionuclide is based on the analysis for off-site releases or the analysis for inadvertent intruders. This approach would be the most conservative in ensuring compliance with the performance objectives for off-site releases and inadvertent intruders, essentially because the doses from off-site releases and exposures of inadvertent intruders generally are not additive.

A second approach would be to apply the sum-of-fractions rule separately to those radionuclides for which the inventory limit is determined by the analysis for off-site releases and those radionuclides for which the limit is determined by the analysis for inadvertent intruders, but without regard for the time at which the maximum doses in the two cases occur. This approach is particularly valid when the inventory limits based on the analyses for off-site releases and inadvertent intruders differ by large amounts (e.g., by substantially more than an order of magnitude), because the dose from the scenario which is less restrictive would not be significant. This approach also is conservative in that the maximum doses from off-site releases of radionuclides usually do not occur at the same time (see Table 4.22) and the maximum doses for inadvertent intruders do not occur at the same time for all radionuclides (see Table 4.23). However, in applying this approach, special consideration would be needed when the allowable limits on inventory of a radionuclide based on the analyses for off-site releases and inadvertent intruders do not differ by large amounts, because ignoring the scenario which is not the more restrictive would be nonconservative.

Finally, the second approach could be modified to take into account the time history of doses from off-site releases and doses for inadvertent intruders. The basis for this approach would be the requirement that the performance objectives in either case should not be exceeded at any time. This approach would be the least conservative and, thus, would allow the highest inventories of radionuclides for disposal. However, application of this approach would be more complicated because (1) time histories of the dose per unit inventory of each radionuclide would need to be developed for off-site releases and inadvertent intruders and (2) the total dose from all radionuclides for off-site releases and inadvertent intruders over time would need to be recalculated as new waste is received. On the other hand, these calculations would be required only when the sum-of-fractions rules described in the second approach would be violated.

The particular approach that should be taken in applying the sum-of-fractions rule depends on the actual inventories of radionuclides for disposal compared with the allowable limits in Table 4.24. For example, if the most conservative application described in the first approach would not disqualify significant amounts of waste for disposal, then there would be no harm in taking this approach. The more complicated approaches then could be applied only if significant amounts of waste would otherwise be disqualified.

4.6 SENSITIVITY AND UNCERTAINTY

The Latin hypercube sampling method (Iman and Helton 1985) was used to analyze the effects of input variable sensitivites on the simulation models used in the SWSA 6 PA (ORNL 1994). PRISM (Gardner, Rojder, and Berstrom 1983) was the program used to implement the Latin hypercube sampling technique for sensitivity and uncertainty analyses of the model predictions. A statistical

summary of the model results produced indices of sensitivity that related the effects of heterogeneity of input variables to model predictions. The use of Latin hypercube sampling for systematic uncertainty analysis has not been undertaken for the CIIDF assessment at this stage, but the results of the analysis performed for the SWSA 6 PA provide some insight into the CIIDF results.

4.6.1 Source Terms

The SOURCE1 computer code requires more than 100 input parameters for a performance simulation. Sensitivity analyses can be used to reduce the number of parameters to be considered in uncertainty analyses. For conditions expected at Oak Ridge, previous studies (Icenhour and Tharp 1995) have summarized the SOURCE1 sensitive parameters. Several parameters related to the waste (or waste form) were identified as sensitive, including waste density, K_d, moisture content, radionuclide diffusion coefficient in concrete, and radionuclide inventory. For the mechanism of sulfate attack, the sulfate diffusion coefficient and sulfate concentrations were identified as sensitive parameters. The water seepage parameters of soil hydraulic conductivity, concrete hydraulic conductivity, and containment area per unit were also sensitive. Finally, soil density, metal container corrosion time, and the initial functionality of the concrete pad and leachate collection system were sensitive parameters.

Quantitative uncertainty analyses were not conducted for this PA. However, from a qualitative standpoint, the majority of the uncertainty is judged to be in the sensitive waste parameters listed previously. Uncertainty about the chemical and physical form of the waste radionuclide translates into uncertainty about waste properties. Such uncertainty cannot be totally avoided because the calculations are for future, not historical, disposals. However, knowledge of past operational and disposal practices can be used to postulate reasonable chemical and physical forms for the disposed radionuclide.

Even if the chemical and physical forms of the radionuclide can be established, there still will be uncertainty about the properties for such forms. This uncertainty is largely a result of either a lack of experimental data or the inapplicability of the experimental data to the situation being modeled. Additionally, a wide variability often exists in the experimental data for a given waste parameter (e.g., K_d, radionuclide diffusion coefficient). The methods described in Appendix B are used to address the problems just discussed. These methods illustrate how to extrapolate experimental data from one chemical to another and from one set of experimental conditions to another. The parameters calculated in Appendix B are considered to be conservative for environmental transport calculations because it is expected that they will result in an overestimation of the radionuclide release rate. For the direct intrusion calculations, the sulfate attack parameters and waste K_ds are adjusted to lower the release rate to provide a conservative estimate of the remaining radionuclide inventory.

4.6.2 Shallow Subsurface Transport

4.6.2.1 UTM and Shallow Subsurface Transport—Sensitivity Analysis

A number of sensitivity simulations were conducted with the UTM during model development (Luxmoore, Stolzy, and Holdeman 1976; Begovich and Luxmoore 1979; Sharma and Luxmoore 1979) to evaluate the sensitivity of water budget components of soil-plant systems to variation of input variables. The heterogeneity of plant physiological variables and of soil physical properties have complex interacting effects that need not be reevaluated for this PA. Such heterogeneity causes the quantity of water interacting with waste units to vary. This effect was previously examined in the SWSA 6 PA (ORNL 1994) by directly varying the water interacting with waste units. This was done by multiplying the water flux value used in each simulation by the SOURCE1 model by ±50%. In addition, the sensitivity of chemical leaching to water flux in the SOURCE1 model was combined with the uncertainty analysis of subsurface chemical transport as calculated with shallow subsurface transport codes similar to PADSIM. There was no effect of the water flow on the total transport of nuclides since all nuclides were transported by high or low water fluxes. Nuclide concentrations were influenced by water flow, being higher with lower water fluxes. All nuclides transported to surface water were diluted by perrenial stream flow in the assessment, and this large water source negated any sensitivity influence of soil and plant properties in the assessment.

4.6.2.2 Uncertainty of Shallow Subsurface Chemical Transport

No quantitative evaluation has been undertaken for uncertainty analysis of shallow subsurface transport at the CIIDF site. However, five variables in the PADSIM code have been examined by uncertainty analysis in the SWSA 6 PA (ORNL 1994) as follows:

- bulk density of soil,
- chemical adsorption (K_d),
- waste site area,
- distance from the waste site to groundwater, and
- distance from the waste site to nearest stream channel.

The saprolite of the transport pathway to groundwater and in the lateral flow path were given the same mean bulk density of 1.35 Mg/m^3 based on saprolite measurements (Luxmoore 1982). A normal frequency distribution was assumed for bulk density with a standard deviation of 0.15, and the maximum and minimum values for the distribution were set at 1.8 and 0.9, respectively. The frequency distributions for the nuclide K_d values were normal for all K_d values that were greater than 10; otherwise, they were lognormal. The frequency distributions for the area and distance variables of the waste sites were all assumed to be normal. Variation in the distance variables reflects tortuosity of flow in porous media. The distance to groundwater also represents variability in mean annual water table elevation. This uncertainty analysis has relevance to the CIIDF site; however, additional algorithms

have been added to PADSIM (K_d effects on bypass flow and reactive soil path length) that also need to be examined.

4.6.3 Groundwater

Although no uncertainty analyses were performed, major sources of uncertainty for the groundwater pathway are expected to be the nature of the spatially varying hydrogeologic properties (including hydraulic conductivity, porosity, bulk density, and dispersivity) as well as the value of recharge to groundwater, and the nature of chemical adsorption.

Of these parameters, exposure concentrations resulting from radionuclide transport in groundwater are expected to be most sensitive to velocity and dispersivity of the flow field and to retardation. The flow field is a function of the physical properties of the hydrogeologic medium and the occurrence of recharge—all values of high uncertainty. Although no formal sensitivity analysis was performed, a minor investigation into the effects of changes in the anisotropy of the hydraulic conductivity tensor $\boldsymbol{K}$ was done. The results showed that using a conductivity tensor anisotropy of K_x:K_y:K_z = 30:1:1, rather than 3:1:1, reduced the allowable inventory of those radionuclides limited by the groundwater pathway by a factor of about 2.

Retardation is a function of the porous medium's porosity and bulk density and the distribution coefficient of each chemical species to the porous medium. This distribution coefficient, K_d, is easily the value to which transport behavior is most sensitive. It is also highly uncertain, and reliable data on in situ retardation of radionuclides at the CIIDF site is not obtainable.

4.6.4 Surface Water Transport

The conceptual model behind transport via surface water is so simple that it has few parameters about which to be uncertain. It was assumed that any water entering any stream or drain near the CIIDF was instantly transported to Bear Creek and mixed with its waters to generate an annual average concentration at the weir. What is uncertain here is the applicability of that model to a site which sees strong seasonal variation in surface water generation and flow in a karstic terrain. In times of less rain, the base flow of the creeks will be maintained by groundwater discharge. Under these conditions, however, the concentration in the creeks will not exceed that in the groundwater.

4.6.5 Human Exposure Scenarios

This section discusses the sensitivity and uncertainty analysis for the models used to estimate the annual dose to off-site individuals per unit concentration of radionuclides in water or the annual dose to inadvertent intruders per unit concentration of radionuclides in waste in the disposal facility. The analysis focuses on the release and exposure scenarios which are the most important in determining limits on allowable inventories of radionuclides for disposal, as listed in Table 4.24 for each radionuclide considered in the PA.

The uncertainties in the dose assessment models are evaluated only semiquantitatively. This approach can be justified on the grounds that these uncertainties should be considerably less than the uncertainties in predicting concentrations of radionuclides in water at off-site locations or concentrations in the disposal facility at times far in the future. Therefore, a rigorous, quantitative analysis of uncertainty in the dose assessment models is not needed.

4.6.5.1 Exposure of Off-Site Individuals to Radionuclides in Water

In the PA for CIIDF, radionuclides are assumed to be transported from the disposal facility into the environment primarily by the groundwater and surface water pathways. Possible releases to the atmosphere and transport by biotic pathways are assumed to be negligible.

Furthermore, only a single exposure pathway—namely, direct consumption of drinking water from a contaminated source—is considered in the dose analysis for releases by water pathways. As discussed in Sect. 3.1.2.1, if the dose from the drinking water pathway complies with the assumed performance objective for protection of groundwater and surface water resources of 4 mrem/year, the performance objective of 25 mrem/year for off-site individuals from all exposure pathways involving use of contaminated water combined also should be met, without the need for an evaluation of the dose from the other exposure pathways.

As shown in Eq. (G.1) of Appendix G, the annual dose from the drinking water pathway per unit concentration of a radionuclide in groundwater or surface water is proportional to the intake of contaminated water and the ingestion dose conversion factor for the radionuclide. Although both of these parameters are variable quantities in any real population, they are assumed in this analysis to be fixed quantities which are prescribed by regulatory authorities and radiation protection experts. That is, consistent with current approaches to radiation protection and application of drinking water standards, the dose analysis for the drinking water pathway is based on calculations for hypothetical reference individuals with prescribed intakes of water and prescribed ingestion dose conversion factors, to which no uncertainty is ascribed. Therefore, given estimates of the concentrations of radionuclides in groundwater or surface water, the estimated annual dose from the drinking water pathway per unit concentration essentially has no uncertainty, and the uncertainty in the estimated dose from the drinking water pathway is due entirely to the uncertainty in the estimated concentration of the radionuclide in water.

As indicated in Table 4.24, off-site releases to groundwater or surface water are the limiting scenario for determining allowable limits on inventory for disposal for more than 60% of the radionuclides considered in this analysis. Therefore, based on the foregoing discussion, the uncertainty in the estimated allowable limits on inventory for these radionuclides would be due entirely to the uncertainty in the estimated maximum concentrations in groundwater or surface water beyond the boundary of the 100-m buffer zone around the disposal facility.

An additional consideration in the uncertainty analysis for doses from the water pathways is the possibility that the dose from the exposure pathways other than direct consumption of drinking water, which are listed in Sect. 3.1.2.1, could be underestimated by an extent sufficient that the dose

from all exposure pathways combined could exceed 25 mrem/year even when the dose from the drinking water pathway would not exceed 4 mrem/year. However, based on previous analyses (ORNL 1994; MMES, EG&G, and WSRC 1994), the dose from the other exposure pathways usually should be much less (i.e., by at least an order of magnitude) than the dose from the drinking water pathway. Therefore, the dose from the exposure pathways other than direct consumption of drinking water usually would be of concern only if the parameters in the dose assessment models for these pathways were underestimated by factors of at least an order of magnitude or more. Based on the available data, however, it appears unlikely that such underestimates would be experienced on ORR. Therefore, it is a reasonable conclusion that uncertainties in the dose assessment models for the exposure pathways other than direct consumption of drinking water are not important in determining allowable limits on inventory for disposal when the limits are based on the analysis for releases to water.

4.6.5.2 Exposure of Inadvertent Intruders

As indicated in Table 4.24, scenarios for exposure of inadvertent intruders to waste in the disposal facility determine the allowable limits on inventory for disposal for slightly less than 40% of the radionuclides considered. All three of the exposure scenarios for inadvertent intruders considered in this analysis—the agriculture, resident, and post-drilling scenarios—are important in determining the allowable limits for at least one of these radionuclides.

As listed in Sect. 3.1.2.2 and presented in detail in Sect. G.5.2 of Appendix G, the agriculture and post-drilling scenarios take into account several exposure pathways. However, the relative importance of the different exposure pathways for these scenarios and the importance of uncertainties in the parameter values for these pathways depend on the particular radionuclide. The resident scenario considers only a single external exposure pathway. The following paragraphs discuss the uncertainty analysis for the important exposure scenarios and exposure pathways in cases where the allowable limits on inventory in Table 4.24 are based on the dose analysis for inadvertent intruders.

Uncertainties for photon-emitting radionuclides

For the radionuclides ^{26}Al, ^{60}Co, ^{94}Nb, ^{121m}Sn, ^{126}Sn, ^{137}Cs, ^{152}Eu, ^{154}Eu, ^{207}Bi, ^{226}Ra, ^{229}Th, ^{230}Th, ^{232}Th, ^{231}Pa, ^{232}U, and ^{249}Cf, the allowable limits on inventory in Table 4.24 are based mostly or entirely on the dose analysis for the pathway involving external exposure during indoor residence in a home on top of the disposal facility. That is, when the agriculture scenario is limiting, the doses from the other exposure pathways considered in the scenario are relatively insignificant, and this is the only pathway considered in the resident scenario. These radionuclides emit significant intensities of high-energy photons, or they have decay products which are high-energy photon emitters.

As indicated in Eq. (G.8) of Appendix G, the external dose per unit concentration of a radionuclide in the disposal facility during indoor residence on top of the facility is proportional to the exposure time, the external dose rate conversion factor, and the shielding factor during indoor residence. As in the case of the ingestion dose conversion factor for the drinking water pathway

discussed in the previous section, the external dose rate conversion factor is treated as a fixed parameter for reference individuals and, thus, essentially has no uncertainty.

The exposure time is subject to uncertainty, but the value of 50% assumed in this analysis is intended to be reasonably conservative, and the assumed exposure time cannot underestimate the actual value by more than a factor of 2. The shielding factor during indoor residence also is subject to uncertainty, but the assumed shielding factor of 0.7 cannot underestimate the actual value by more than 50% and probably does not overestimate actual values for typical homes on ORR by more than a factor of 2 (Kocher 1980).

Based on these considerations, the uncertainties in the dose assessment models for inadvertent intruders and the effect of these uncertainties on the resulting estimates of allowable limits on inventory should not be significant for the photon-emitting radionuclides listed above compared with the uncertainties in predicting concentrations remaining in the disposal facility at times far in the future, including the uncertainties in estimated inventories of radionuclides in waste prior to disposal.

Uncertainties for other radionuclides

For the radionuclides ^{10}Be, ^{59}Ni, ^{63}Ni, ^{107}Pd, ^{113m}Cd, ^{135}Cs, ^{151}Sm, which are the remaining radionuclides considered in this analysis, the allowable limits on inventory in Table 4.24 are based mostly or entirely on the dose analysis for the exposure pathway involving consumption of vegetables grown in contaminated garden soil. All other exposure pathways considered in the agriculture or post-drilling scenarios generally result in lower estimates of dose than the vegetable pathway.

As indicated in Eqs. (G.2) and (G.3) of Appendix G, the dose from the vegetable pathway per unit concentration of a radionuclide in the disposal facility is proportional to the intake of contaminated vegetables, the plant-to-soil concentration ratio for the radionuclide, and the ingestion dose conversion factor for the radionuclide. In addition, for the agriculture scenario, which is the limiting scenario for all radionuclides listed above except for ^{113m}Cd, the dose from the vegetable pathway is proportional to the dilution factor for mixing of material exhumed from the disposal facility with native soil in the vegetable garden. As in the dose analyses for other exposure scenarios, the ingestion dose conversion factor is treated as a fixed parameter for reference individuals and, thus, essentially has no uncertainty.

The dilution factor for mixing of exhumed material in the vegetable garden essentially is a nonmeasureable parameter used in defining the agriculture scenario, and the value 0.2 assumed in this analysis was based on a previous definition of this scenario developed by the Nuclear Regulatory Commission (NRC 1982). This parameter could be underestimated by as much as a factor of 5. On the other hand, as discussed in Sect. G.5.2.1 of Appendix G, such an underestimation seems unlikely, because it is unlikely that a fertile vegetable garden would consist of soil containing nothing but materials exhumed from the disposal facility.

The assumed intake rate of vegetables from a garden of 90 kg/year was selected to be somewhat conservative for an average site resident. Available data (Hamby 1992) indicate that, for a

resident homesteader, the assumed intake rate probably would underestimate actual values by no more than a factor of 2.

The plant-to-soil concentration ratio could be highly uncertain (i.e., by an order of magnitude or more) for the radionuclides listed above, due to the variability in the available measurements and the uncertainty in the factor for converting concentration ratios reported on a dry-weight basis to wet weight (Baes et al. 1984). In addition, the available data are numerous for some of the elements (i.e., Ni, Cs, and Cd) but sparse or nonexistent for others (i.e., Be, Pd, and Sm), and the variability in the available measurements in the latter cases may not be indicative of the uncertainty. Furthermore, an important source of uncertainty which cannot be quantified is the applicability of generic data obtained for a variety of plant and soil types to garden crops grown in the type of soil found near the disposal site on ORR.

Considering all of these factors together, the uncertainty in the dose assessment models for inadvertent intruders for the radionuclides which are not photon-emitters listed above appears to be significant, i.e., at least an order of magnitude or more. The most important source of uncertainty in the dose assessment models for these radionuclides appears to be the uncertainty in the plant-to-soil concentration ratio. In the absence of site-specific data for this parameter, there is little that can be done to reduce these uncertainties.

Importance of uncertainties in dose assessment models for inadvertent intruders

In evaluating the importance of the different sources of uncertainty in the dose assessment models for inadvertent intruders considered in this section, it should be recognized that the most important source of uncertainty probably is the definitions of the exposure scenarios themselves, notwithstanding any parameter uncertainties that could be quantified and regardless of whether the results would represent the variability in doses that could be experienced on ORR. The dose analyses for the different exposure scenarios for inadvertent intruders are based on assumptions that the scenarios will occur as postulated, but many of the assumptions used in defining the scenarios are questionable and, furthermore, are likely to be conservative.

In defining exposure scenarios for inadvertent intruders, it seems reasonable to assume that individuals will establish a homestead within the boundary of the disposal facility at some time after loss of active institutional control over the site, because such activities commonly occurred on ORR prior to 1942. However, several of the assumptions used in developing the exposure scenarios are less certain and probably pessimistic. For example, all scenarios assume that individuals will have no knowledge of prior waste disposal activities at the site, but this assumption seems unreasonable for times soon after loss of active institutional control. Furthermore, even if knowledge of the disposal facility were lost, all exposure scenarios assume that an inadvertent intruder will build a home or drill a well at the location of disposed waste, rather than in uncontaminated areas on the disposal site, and that exhumed waste from excavation or drilling activities will be mixed with uncontaminated soil in a vegetable garden.

By their very definitions, the exposure scenarios for inadvertent intruders assume conditions that tend to maximize estimates of dose that reasonably could be experienced by individuals who might come onto the disposal site after loss of active institutional control. Therefore, it is not the purpose of a dose analysis for inadvertent intruders to provide best estimates of dose that likely would be received and a quantification of the uncertainties in these dose estimates. Rather, the primary purpose of the analysis is to indicate whether the assumed disposal practices would be adequately protective of future inadvertent intruders, and this is done by establishing WAC in the form of limits on average concentrations or inventories of radionuclides in waste prior to disposal. If the WAC are met, then future inadvertent intruders may be assumed to be protected, without undue concern for the magnitude of doses that any such individuals might actually experience. Furthermore, quantitative estimates of uncertainties in calculated doses based on parameter uncertainty analysis may not be particularly meaningful, because the results are conditional on the occurrence of the assumed exposure scenarios. Therefore, the most important factor in determining whether the WAC derived from the dose analysis for inadvertent intruders are reasonable is the credibility of the assumed exposure scenarios—i.e., whether the assumed scenarios reasonably could occur at the disposal site—rather than any estimates of uncertainties in the results due to uncertainties in the parameters contained in the dose assessment models.

4.7 INTERPRETATION OF RESULTS

The results presented in Sect. 4.5 provide allowable limits on inventory for each radionuclide potentially present in wastes and the application of these results to mixtures of radionuclides in wastes. These results are consistent with the performance objectives in DOE Order 5820.2A. Disposal operations performed within the allowable limits ensure compliance with the performance objectives subject to the uncertainties in the analysis. An understanding of the assumptions and the uncertainty of the results gives some insight into needed improvements in the PA for subsequent revisions of this draft PA and the conservatism incorporated into the analysis.

The present analysis includes limited credit for closure and the cover system for CIIDF, since existing plans for closure and maintenance of the installed cover are incomplete. Consequently, a basis for establishing credits for closure and the cover system is not available. Ongoing efforts toward the developing a closure system that will provide long-term performance have been initiated. Once a cover system is developed, the PA will be revised to reflect the presence of an effective closure scheme. The eventual development of a cover system for the CIIDF provides additional assurance that the existing results are conservative for the entire facility because some portion of the facility is likely to be loaded with waste prior to the development of the closure system.

The results of the analysis summarized in Table 4.24 show the importance of the transport of contamination in groundwater and surface water for establishing WAC for CIIDF. Of the 60 radionuclides considered in this analysis, 35 were limited by the surface water or groundwater pathway. The water-pathway-limited radionuclides were all associated with off-site exposure, with 26 of these radionuclides limited by groundwater transport. The point of compliance for the

consumption of groundwater was 100 m from the disposal facility cover. This provides additional assurance that the public is likely to be protected from CIIDF operations because the release of the facility from institutional control for ready access by the public could be extended into the indefinite future and is likely to extend beyond 100 years.

Surface water limits were determined by a long-term projection of contaminant transport through the shallow subsurface and groundwater pathways with the combined transport discharged to surface water. This analysis required the temporal behavior of groundwater and especially surface water to be represented in annual time steps, with the full understanding that water transport on ORR is the consequence of individual storm events. Since the largest transport of contamination is associated with storm events, when surface water discharges and therefore dilutions are the highest, a reasonable interpretation of the results would be that the surface water limits determined by this analysis may be considered conservative estimates of actual concentrations to be measured in Bear Creek.

The time of compliance for the performance objectives to be met for CIIDF was selected to be 10,000 years, as discussed in Sect. 1. The results of the analysis show that only four of the radionuclides considered had the allowable limits on inventory determined by transport of contamination that extended beyond 1000 years. These four radionuclides—^{10}Be, ^{26}Al, ^{230}Th, and ^{238}U—reached their peak concentrations at 26,000, 2500, 5200, and 6800 years, respectively. The rapid transport of contamination on ORR, as compared to other DOE sites, is a consequence of the abundant precipitation, resulting in the shallow groundwater system and the highly developed surface water system. Reductions in the time of compliance to less than 10,000 years have little effect on disposals at CIIDF.

The allowable limits on inventory determined by the actions of an inadvertent intruder in this analysis presume aggressive behavior by an individual to realize exposures. Of the 25 radionuclides with allowable limits on inventory determined from inadvertent intrusion, 9 radionuclides had half-lives of less than 100 years. Extended institutional control periods of several hundred years could result in an increase in the allowable limits on inventory for these radionuclides; however, for most of the radionuclides limited by inadvertent intrusion, only the assumption of perpetual institutional control, which would effectively preclude consideration of inadvertent intruders, would have a significant effect on the results.

Sensitivity and uncertainty in the results is discussed in Sect. 4.6 in a qualitative manner. Based on the results from the SWSA 6 PA, the greatest source of uncertainty is expected to be associated with the characterization and certification of wastes. Improvements in waste characterization and certification of LLW discussed in Sect. 2.3.2 reduce some of the uncertainty present in the SWSA 6 PA. Continued improvements in waste characterization are anticipated. The experience gained to date with respect to the improved procedures for waste characterization indicates that the approach taken in the CIIDF PA is conservative. As additional experience is gained and further improvements are realized, the allowable limits on inventory can reasonably be expected to increase. Any changes to the allowable limits on inventory would be documented in a revision to the CIIDF PA.

The CIIDF PA has been prepared without consideration of other sources of contamination on ORR. These include contamination sources in Bear Creek Valley upstream of CIIDF that are the result of historical waste disposal activities and operations of the Y-12 Plant. Downstream of CIIDF are sources of contamination at the K-25 Site and contributions from East Fork Poplar Creek, which receives discharges from the Y-12 Plant. The consideration of these other sources of contamination and the combined effect on members of the public will be addressed in a composite analysis prior to the disposal of wastes at CIIDF.

The results presented in this PA provide a reasonable basis for evaluating the performance of CIIDF and provide reasonable assurance that the performance objectives of DOE Order 5820.2A will be met for the disposal of radioactive waste. Continued work to reduce uncertainties and improve the methodology used to analyze the performance of CIIDF is likely to relax the allowable limits on inventory determined by the analysis.

4.8 CONTINUED WORK

The present PA provides a comprehensive analysis of the performance of CIIDF for the disposal of newly generated wastes from ORR. The analysis provides a qualitative review of the uncertainties associated with the results. The results provide conservative estimates of limiting concentrations and inventories of radionuclides that could be disposed of, such that the facility would operate in compliance with the performance objectives of DOE Order 5820.2A. Recognizing the development of the PA as a process, further improvements can be expected and are appropriate for reducing uncertainty and conservatism and improving the accuracy of the assessment.

The draft PA was prepared with a qualitative assessment of sensitivity and uncertainty. As part of the continuing work on the PA, a quantitative analysis of the sensitivity and uncertainty is necessary. Such an analysis allows for an improved understanding of the overall assessment and provides a meaningful method for identifying areas requiring further investigation.

The closure plan used in the PA is a conservative approximation of how closure is expected to occur. Plans for the closure of CIIDF are not finalized. Continued work to identify more effective closure methods is warranted. Development and approval of a more effective closure plan can be expected to reduce exposures from potential intrusion into wastes and reduce the potential for the generation and transport of leachate from the disposal facility. A more effective closure plan for the facility could be expected to increase concentration limits and inventories in the disposal facility.

The arbitrary algorithms in the PADSIM model that determine the proportion of bypass flow and reactive soil path length as functions of chemical adsorption need to be revised as suitable new information becomes available.

To execute calculations predicting the environmental transport of radionuclides in the distant future, it was necessary to assume a steady-state flow field through which transport would occur. The steady state was applied to groundwater flow, shallow subsurface flow, and surface water flows; and the validity of results based on this simplifying assumption becomes more questionable in that progression of media. Continued work is necessary either to find ways to permit a relaxation of the

steady-state assumption while not incurring substantially greater computational expense or to improve our understanding of what effects the assumption may have on the results. It is not known, for example, whether using the average annual flow in Bear Creek for dilution of surface water contamination is more or less conservative than performing a more involved integral calculation using daily fluctuations of creek flow combined with varying subsurface flows and their discharges.

4.9 QUALITY ASSURANCE

This draft PA has been prepared in accordance with the Quality Assurance Program of ORNL (ORNL 1993). The program is based on the requirements set forward in the American National Standards Institute/American Society of Mechanical Engineers Quality Assurance Standards for Nuclear Facilities (ANSI/ASME NQA-1) program requirements. Software developed for this draft PA has been prepared in accordance with Lockheed Martin Energy Systems Policy, Standards, and Procedures for software quality assurance (Mynatt 1992). The requirements set forward in software quality assurance have been adhered to; however, full documentation requirements specified for all of the software used in this draft PA have not been completed. Completion of the documentation requirements for software is part of the continued work for this PA.

5. PERFORMANCE EVALUATION

This draft PA provides a systematic, site-specific analysis of the long-term performance of the proposed CIIDF. The PA has been prepared to provide allowable concentrations and inventories of radionuclides that can be disposed of in the facility while maintaining compliance with the performance objectives of DOE Order 5820.2A. This section summarizes the results presented in the previous sections and discusses the implications of these results on operations at the facility and future efforts to finalize the PA.

5.1 COMPARISON OF THE PERFORMANCE ASSESSMENT RESULTS WITH THE PERFORMANCE OBJECTIVES

This PA provides a comprehensive assessment of potential doses to the public, potential doses to an inadvertent intruder, and the protection of groundwater resources from the disposal of radioactive wastes in CIIDF. The PA has been conducted using what is considered to be a conservative representation of the likely mechanisms that would result in the transport of contamination in the environment and to a member of the general public. The performance objective for protection of an individual member of the general public from all pathways of exposure is 25 mrem/year, but the protection of drinking water resources to a maximum dose of 4 mrem/year was shown to be more restrictive for the protection of a member of the public. The 4-mrem/year dose objective was used to iteratively calculate the limiting concentration of radionuclides in wastes that would satisfy this performance objective. The performance objective for protection against inadvertent intrusion into the waste at some future time of 100-mrem/year chronic exposure and 500-mrem/year acute exposure was used to calculate the maximum concentration of radionuclides in waste that would satisfy the performance objective. The performance objective of 100 mrem/year for chronic exposure was shown to be a more restrictive performance objective than the 500 mrem/year for acute exposure performance objective. Consequently, only chronic exposure scenarios were used to determine limiting concentrations from direct intrusion. Limiting concentrations from the transport of contamination to groundwater beyond a 100-m buffer zone with a 4-mrem/year dose objective from the consumption of 2 L/d of contaminated water were calculated to demonstrate compliance with the performance objective for the protection of groundwater resources.

The limiting concentrations of radionuclides in waste that would protect the general public were based on potential doses from the use of contaminated groundwater 100 m from the disposal facility or surface waters of Bear Creek as a drinking water supply. Using a 4-mrem/year dose standard, the performance objective for the protection of the general public to a dose less than 25 mrem/year from all pathways is ensured. The calculated limiting concentrations also serve to provide reasonable assurance for the protection of groundwater resources. Limiting concentrations of radionuclides in waste that would provide reasonable assurance from excessive exposures from

inadvertent intrusion into the waste facility were determined with consideration of the agriculture, resident, and post-drilling scenarios. For CIIDF, these scenarios were shown to be the most restrictive scenarios of the widely used scenarios for addressing inadvertent intrusion. The most restrictive limiting concentration for each radionuclide from the consideration of these three intrusion scenarios was used to define the limiting concentration for direct intrusion. The most restrictive of the limiting concentrations from direct intrusion and environmental transport was used to determine the allowable concentration limit for each radionuclide and the allowable inventory of each radionuclide for the disposal facility.

Since the allowable concentrations and inventories of radionuclides were calculated to satisfy the performance objectives, the PA, by definition, demonstrates compliance with the performance objectives of DOE Order 5820.2A. The allowable concentrations and inventories represent the most restrictive concentrations for protection of the public, an inadvertent intruder, and groundwater resources. Application of these allowable concentrations and inventories to mixtures of radionuclides present in wastes is discussed to ensure compliance with DOE Order 5820.2A.

5.2 APPLICATION OF THE RESULTS TO WASTE ACCEPTANCE CRITERIA

The WAC for the disposal of wastes on ORR are documented in ES/WM 10 (MMES 1994). These criteria specify the specific requirements for waste characterization and categorization for wastes managed by ESWMO. Certification of wastes is conducted according to documented procedures, in accordance with the Waste Certification Program. Once wastes have been certified, specific WAC for each ESWMO radioactive waste management facility on ORR are used to select the appropriate management options for generated wastes. For disposal facilities, these facility-specific WAC are used to ensure that waste packages are within the concentration and inventory limits set by the PA.

Facility-specific WAC have not yet been developed for the CIIDF. The results of this draft PA along with the results from the associated composite analysis of impacted watersheds provide the basis for developing these criteria, which are required for DOE approval and form the operating basis for disposal operations at CIIDF.

5.3 IMPROVEMENT AND MAINTENANCE OF THE PERFORMANCE ASSESSMENT

This draft PA was prepared using the proposed design and operating conditions for CIIDF. Construction may result in changes to the facility design, as well as the assumptions related to the site conditions and the facility itself. Furthermore, the changing missions and programs on ORR may result in changes to the waste streams anticipated to be generated for CIIDF. Any of these changes may have

an effect on the validity of the results presented in this draft PA. Changes to the facility, site, and wastes that would affect the performance of the facility require a revision to the PA, as outlined in DOE Order 5820.2A.

Revisions to this draft PA will be initiated once the commitment is made to construct CIIDF. The revision will include any changes that have occurred in the process of design review and safety analysis documentation, as well as comments provided by DOE Headquarters. The revision will also include the consideration of additional radionuclides that are likely to be present in wastes to be disposed of in CIIDF. The revision will be submitted to DOE Headquarters for approval along with the composite analysis required by the implementation plan for Defense Nuclear Facilities Safety Board recommendation 94-2 (DOE 1996b) for the required disposal authorization statement prior to operation of CIIDF.

Future revisions of the PA will be performed as part of the PA maintenance program. This program is directed to ensure that PAs for waste management on ORR are representative of the performance of the respective facilities. Improvements in the PA may be initiated as a result of changes in operations, improvements in the understanding of site behavior, or in response to reviews and audits by DOE.

6. PREPARERS

The following individuals were responsible for the preparation of this PA for CIIDF. Unless otherwise noted, these individuals are associated with ORNL.

J. Robert Forgy, Jr.; M.S., radiological health; waste characteristics, treatment, and certification

Alan S. Icenhour; M.S., nuclear engineering; source term analysis

David C. Kocher; Ph.D., nuclear physics; dose analysis

Donald W. Lee; Ph.D., applied mechanics; task group leader

Steve L. Loghry; B.S., chemical engineering; source term analysis

Douglas A. Lombardi; M.S., environmental engineering; atmospheric emissions analysis

Herschel W. Godbee; Ph.D., chemical engineering; transport parameter development for source term models (retired)

Robert J. Luxmoore; Ph.D., soil science; water budget and shallow subsurface analyses

Maria L. Socolof; M.S., environmental health management; dose analysis

John D. Tauxe; Ph.D., civil engineering; site characterization, groundwater transport analysis

M. Lynn Tharp; M.S., computer science; source term and shallow subsurface analyses

Sidey Timmins; B.S., geological engineering; terrain analysis (Science Applications International Corporation)

Martin W. Tull; B.A., physics; waste characterization and certification (Lockheed Martin Energy Systems)

Mark W. Yambert; B.S., engineering mechanics; groundwater analysis

7. REFERENCES

Baes, C. F. III, and R. D. Sharp 1981. "Predicting Radionuclide Leaching from Root Zone Soil for Assessment Applications," *Trans. Am. Nucl. Soc.* **38**, 111–12.

Baes, C. F. III et al. 1984. *A Review and Analysis of Parameters for Assessing Transport of Environmentally Released Radionuclides Through Agriculture*, ORNL-5786, Martin Marietta Energy Systems, Inc., Oak Ridge Natl. Lab.

Bailey, Z. C., and R. W. Lee 1991. *Hydrogeology and Geochemistry in Bear Creek and Union Valleys, near Oak Ridge, Tennessee*, Water Resources Investigation Report 90-4088, U. S. Geological Survey, Nashville, Tenn.

Bass, J. M., W. J. Lyman, and J. P. Trantnyek 1985. *Assessment of Synthetic Membrane Successes and Failures at Waste Storage and Disposal Sites*, EPA/S2-85/100, U.S. Environmental Protection Agency, Washington, D.C.

Bear, J. 1979. *Hydraulics of Groundwater*, McGraw-Hill, New York.

Bechtel (Bechtel National, Inc.) 1991. *RCRA Facility Investigation Report for Waste Area Grouping 6 at Oak Ridge National Laboratory, Oak Ridge, Tennessee*, ES/ER-22/V1 & D1, ORNL/ER/Sub-87/99053/5/V3, Vol. 1, Oak Ridge, Tenn.

Begovich, C. L., and R. J. Luxmoore 1979. *Some Sensitivity Studies of Chemical Transport Simulated in Models of the Soil-Plant-Litter System*, ORNL/TM-6791, Union Carbide Corp., Oak Ridge Natl. Lab.

Bevan, K. J., and M. J. Kirkby 1979. "A Physically-Based Variable Contributing Area Model of Basin Hydrology," *Hydrol. Sci. Bull.* **24**, 43–69.

Brown, E., and R. B. Firestone 1986. *Table of Radioactive Isotopes*, ed. V. S. Shirley, Wiley, New York.

Clapp, R. B., ed. 1992. *Annual Report of the Environmental Restoration Monitoring and Assessment Program at Oak Ridge National Laboratory for FY 1992*, ORNL/ER-124, Martin Marietta Energy Systems, Inc., Oak Ridge Natl. Lab.

Clapp, R. B., T. M. Scanlon, and S. Timmins N.d. *Modifying TOPMODEL to Simulate the Separate Processes of Shallow Subsurface and Groundwater Discharge*, Oak Ridge Natl. Lab. Forthcoming.

Clapp, R. B., and J. A. Watts, eds. 1995. *Fourth Annual Environmental Monitoring and Assessment Report (FY 1995)*, DOE/OR/01-1413&D1, Lockheed Martin Energy Systems, Inc., Oak Ridge Natl. Lab.

Davis, E. C. et al. 1984, *Site Characterization Techniques Used at a Low-Level Waste Shallow Land Burial Field Demonstration Facility,* ORNL/TM-9146, Martin Marietta Energy Systems, Inc., Oak Ridge Natl. Lab.

Dawes, W. R., and D. Short 1994. "The Significance of Topology for Modeling the Surface Hydrology of Fluvial Landscapes," *Water Resour. Res.* **30**, 1681–92.

DOE (U.S. Department of Energy) 1989. *Recommended Format and Content for DOE Low-Level Waste Disposal Facility Radiological Performance Assessment Reports*, DOE/LLW-81, Washington, D.C.

DOE (U.S. Department of Energy) 1991. *Performance Assessment Review Guide for DOE Low-Level Waste Disposal Facilities*, DOE/LLW-93, Washington, D.C.

DOE (U.S. Department of Energy) 1995. *Integrated Data Base Report—1994: U.S. Spent Nuclear Fuel and Radioactive Waste Inventories, Projections, and Characteristics*, DOE/RW-0006, Rev. 11, Oak Ridge Natl. Lab. [Internet URL: http://www.em.doe.gov/idb95/]

DOE (U.S. Department of Energy) 1996a. *Guidance for a Composite Analysis of the Impact of Interacting Source Terms on the Radiological Protection of the Public from Department of Energy Low-Level Waste Disposal Facilities*, Washington, D.C.

DOE (U.S. Department of Energy) 1996b. *Implementation Plan—Defense Nuclear Facilities Safety Board Recommendation 94-2*, Rev. 1, Washington, D.C.

Evans, R. D. 1955. "Radioactive-Series Decay," Chap. 15 in *The Atomic Nucleus*, McGraw-Hill, New York.

Faust, C. R. et al. 1990. *FTWORK: Groundwater Flow and Solute Transport in Three Dimensions, Version 2.4* [computer code documentation], GeoTrans, Inc., Herndon, Va.

Foster-Wheeler Environmental Corporation / Parsons Engineering Science, Inc. 1995. *Class L-II LLW Disposal Facility,* engineering drawings C3E017096A004 and C3E017096A005, Oak Ridge, Tenn.

Frazier, D. W. et al. 1995. *Oak Ridge Reservation Annual Site Environmental Report for 1994*, ES/ESH-57, Lockheed Martin Energy Systems, Inc., Oak Ridge, Tenn.

Friedman, H. A., and A. D. Kelmers 1990. *Laboratory Measurement of Radionuclide Sorption in Solid Waste Storage Area 6 Soil/Groundwater Systems*, ORNL/TM-10561, Martin Marietta Energy Systems, Inc., Oak Ridge Natl. Lab.

Gardner, R. H., B. Rojder, and U. Berstrom 1983. *PRISM: A Systematic Method for Determining the Effect of Parameter Uncertainties on Model Predictions*, Report NW-83-555, Studsvik Energiteknik AB, Nykoping, Sweden.

Garten, C. T., Jr., R. H. Gardner, and R. C. Dahlman 1980. "A Model of Plutonium Dynamics in a Deciduous Forest Ecosystem," p. 513 in *Transuranic Elements in the Environment*, ed. W. C. Hanson, DOE/TIC-22800, U.S. Department of Energy, Washington, D.C.

Garten, C. T., Jr., J. R. Trabalka, and M. A. Bogle 1982. "Comparative Food Chain Behavior and Distribution of Actinide Elements in and Around a Contaminated Fresh-Water Pond," p. 299 in *Environmental Migration of Long-Lived Radionuclides*, International Atomic Energy Agency, Vienna.

Geraghty & Miller, Inc. 1987. *Hydrogeologic Investigations of the S-3 Ponds Area at the Y-12 Plant*, Y/SUB/87-00206C/18, prepared for Martin Marietta Energy Systems, Oak Ridge, Tenn.

Geraghty & Miller, Inc. 1989. *Tracer Study of the Hydrologic System of Upper Bear Creek, Y-12 Plant, Oak Ridge, Tennessee,* Y/SUB/89-00206C/4, prepared for Martin Marietta Energy Systems, Oak Ridge, Tenn.

Geraghty & Miller, Inc. 1990. *Development of Groundwater Flow Models for the S-3 Waste Management Area, Y-12 Plant, Oak Ridge, Tennessee*, Y/SUB/89-00206C/1, prepared for Martin Marietta Energy Systems, Oak Ridge, Tenn.

Godbee, H. W. 1996. *Estimated Transport Parameters for Selected Radionuclides in Low-Level Waste and Concrete Containment*, D21-A20005-01-95, Delta-21 Resources, Inc., Knoxville, Tenn.

Golder Associates 1988. *Task 2, Well Logging and Geohydrologic Testing, Site Characterization and Groundwater Flow Computer Model Application*, Vol. 1, ORNL/Sub/30X-SA706C, Martin Marietta Energy Systems, Inc. Oak Ridge Natl. Lab.

Goldman, L. J. et al. 1988. *Design, Construction, and Evaluation of Clay Liners for Waste Management Facilities*, EPA/530-SW-86-007-F, Risk Reduction Engineering Laboratory, U.S. Environmental Protection Agency, Cincinnati, Ohio.

Hamby, D. M. 1992. "Site-Specific Parameter Values for the Nuclear Regulatory Commission's Food Pathway Dose Model," *Health Phys.* **62**, 136.

Hatcher, R. D., Jr. et al. 1992, *Status Report on the Geology of the Oak Ridge Reservation*, ORNL/TM-12074, Martin Marietta Energy Systems, Inc., Oak Ridge Natl. Lab.

Helvey, J. D., and J. H. Patric 1965. "Canopy and Litter Interception of Rainfall by Hardwoods of Eastern United States," *Water Resour. Res.* **1**, 193–206.

Hetrick, D. M., J. T. Holdeman, and R. J. Luxmoore 1982. *AGTEHM: Documentation of Modifications to the Terrestrial Ecosystem Hydrology Model (TEHM) for Agricultural Applications*, ORNL/TM-7856, Union Carbide Corp., Oak Ridge Natl. Lab.

HSW Environmental Consultants, Inc. 1995. *Calendar Year 1994 Groundwater Quality Report for the Bear Creek Hydrogeologic Regime, Y-12 Plant, Oak Ridge, Tennessee*, Y/SUB/95-EAQ10C/1/P1, Martin Marietta Energy Systems, Inc., Oak Ridge, Tenn.

Huff, D. D. et al. 1977. *TEHM: A Terrestrial Ecosystem Hydrology Model*, ORNL/NSF/EATC-27, Union Carbide Corp., Oak Ridge Natl. Lab.

Icenhour, A. S. 1994. "Addendum to QAP-X-88-CT-011 for the SOURCE1 Computer Code," Martin Marietta Energy Systems, Inc., Oak Ridge Natl. Lab.

Icenhour, A. S. 1995. *Analysis of Source Term Modeling for Low-Level Radioactive Waste Performance Assessments*, ORNL/TM-12908, Lockheed Martin Energy Systems, Inc., Oak Ridge Natl. Lab.

Icenhour, A. S., and M. L. Tharp 1994. *SOURCE1 Verification Plan*, Martin Marietta Energy Systems, Inc., Oak Ridge Natl. Lab.

Icenhour, A. S., and M. L. Tharp 1995. "Recent Improvements to the SOURCE1 and SOURCE2 Computer Codes," in *Proc. U.S. Department of Energy 17th Annual Low-Level Radioactive Waste Management Conference, Phoenix, Arizona, December 12–14, 1995*, Idaho National Engineering Laboratory, Idaho Falls, Idaho.

Icenhour, A. S., and M. L. Tharp 1996. *User's Manual for the SOURCE1 and SOURCE2 Computer Codes: Models for Evaluating Low-Level Radioactive Waste Disposal Facility Source Terms (Version 2.0)*, ORNL/TM-13035, Lockheed Martin Energy Systems, Inc., Oak Ridge Natl. Lab.

Iman, R. L., and J. C. Helton 1985. *A Comparison of Uncertainty and Sensitivity Analysis Techniques for Computer Models*, NUREG/CR-3904 SAND84-1461, Sandia National Laboratory, Albuquerque, N.M.

Jardine, P. M., G. K. Jacobs, and G. V. Wilson 1993. "Unsaturated Transport Processes in Undisturbed Heterogeneous Media: I. Inorganic Contaminants," *Soil Sci. Soc. Am. J.* **57**, 945–53.

Johnston, H. M., and R. W. Gillham 1980. *A Review of Selected Radionuclide Distribution Coefficients of Geologic Materials*, TR-90, Waterloo Research Institute, University of Waterloo, Canada.

Kennedy, W. E., Jr., L. L. Cadwell, and D. H. McKenzie 1985. "Biotic Transport of Radionuclides from a Low-Level Radioactive Waste Site," *Health Phys.* **49**, 11.

Kennedy, W. E., Jr., and R. A. Peloquin 1988. *Intruder Scenarios for Site-Specific Low-Level Waste Classification*, DOE/LLW-71T, Idaho Operations Office, U.S. Department of Energy, Idaho Falls, Idaho.

Ketelle, R. H. et al. 1995. "Groundwater," pp. 4.1–4.38 in *Fourth Annual Environmental Restoration Monitoring and Assessment Report (FY 1995)*, DOE/OR/01-1413&D1, ed. R. B. Clapp and J. A. Watts, Lockheed Martin Energy Systems, Inc., Oak Ridge Natl. Lab.

Kocher, D. C. 1980. "Effects of Indoor Residence on Radiation Doses from Routine Releases of Radionuclides to the Atmosphere," *Nucl. Technol.* **48**, 171.

Kornegay, F. C., and D. C. West 1991. *Oak Ridge Reservation Environmental Report for 1990, Volume 1: Narrative, Summary, and Conclusions*, ES/ESH-18/V1, Martin Marietta Energy Systems, Inc., Oak Ridge, Tenn.

Kornegay, F. C. et al. 1992. *Oak Ridge Reservation Environmental Report for 1991*, ES/ESH-31/V1, Martin Marietta Energy Systems, Inc., Oak Ridge, Tenn.

Kornegay, F. C. et al. 1994. *Environmental Monitoring and Surveillance on the Oak Ridge Reservation: 1993 Data*, ES/ESH-48, Martin Marietta Energy Systems, Inc., Oak Ridge, Tenn.

Lee, R. R. and R. H. Ketelle 1989, *Geology of the West Bear Creek Site*, ORNL/TM-10887, Martin Marietta Energy Systems, Inc., Oak Ridge Natl. Lab.

Lee, R. R. et al. 1989. *Calibration of a Groundwater Flow and Contaminant Transport Model: Progress Toward Model Validation*, ORNL/TM-11294, Martin Marietta Energy Systems, Inc., Oak Ridge Natl. Lab.

Lee, R. R. et al. 1992. "Aquifer Analysis and Modeling in a Fractured, Heterogeneous Medium," *Ground Water* **30**, 4.

Lietzke, D. A., S. Y. Lee, and R. E. Lambert 1988. *Soils, Surficial Geology, and Geomorphology of the Bear Creek Valley Low-Level Waste Disposal Development and Demonstration Program Site*, ORNL/TM-10573, Martin Marietta Energy Systems, Inc., Oak Ridge Natl. Lab.

Lozier, W. B., C. A. Spiers, and R. Pearson 1986. *Aquifer Pump Test with Tracers*, ORNL/Sub/86-32136/2, Martin Marietta Energy Systems, Inc., Oak Ridge Natl. Lab.

Luxmoore, R. J. 1982. *Physical Characteristics of Soils of the Southern Region*, Fullerton and Sequoia series, ORNL-5868, Union Carbide Corp., Oak Ridge Natl. Lab.

Luxmoore, R. J. 1983a. "Infiltration and Runoff Predictions for a Grassland Watershed," *J. Hydrol.* **65**, 271–78.

Luxmoore, R. J. 1983b. "Water Budget of an Eastern Deciduous Forest Stand," *Soil Sci. Soc. Am. J.* **47**, 785–91.

Luxmoore, R. J., and C. L. Begovich 1979. "Simulated Heavy Metal Fluxes in Tree Microcosms and a Deciduous Forest," *Int. Soc. Ecol. Model. J.* **1**, 48–60.

Luxmoore, R. J., and D. D. Huff 1989. "Water," pp. 164–96 in *Analysis of Biogeochemical Cycling Processes in Walker Branch Watershed*, ed. D. W. Johnson and R. I. Van Hook, Springer-Verlag, New York.

Luxmoore, R. J., and M. L. Sharma 1980. "Runoff Responses to Soil Heterogeneity: Experimental and Simulation Comparisons for Two Contrasting Watersheds," *Water Resour. Res.* **16**, 675–84.

Luxmoore, R. J., J. L. Stolzy, and J. T. Holdeman 1976. *Some Sensitivity Analyses of an Hourly Soil-Plant-Water Relations Model*, ORNL/TM-5343, Union Carbide Corp., Oak Ridge Natl. Lab.

Luxmoore, R. J., J. L. Stolzy, and J. T. Holdeman 1981. "Sensitivity of a Soil-Plant-Atmosphere Model to Changes in Air Temperature, Dewpoint Temperature, and Solar Radiation," *Agric. Meteorol.* **23**, 115–29.

Luxmoore, R. J. and M. L. Tharp 1993. *Simulation of Barrier Heterogeneity and Preferential Flow Effects on the Performance of Shallow Land Burial Facilities*, ORNL/TM-12058, Martin Marietta Energy Systems, Inc., Oak Ridge Natl. Lab.

Luxmoore, R. J. et al. 1978. "Some Measured and Simulated Plant Water Relations of Yellow Poplar," *For. Sci.* **24**, 327–41.

McKenzie, D. H. et al. 1982a. *Relevance of Biotic Pathways to the Long-Term Regulation of Nuclear Waste Disposal: A Report on Tasks 1 and 2*, NUREG/CR-2675, Vol. 1, Pacific Northwest Laboratory, Richland, Wash.

McKenzie, D. H. et al. 1982b. *Relevance of Biotic Pathways to the Long-Term Regulation of Nuclear Waste Disposal: Topical Report on Reference Western Arid Low-Level Sites*, NUREG/CR-2675, Vol. 2, Pacific Northwest Laboratory, Richland, Wash.

McKenzie, D. H. et al. 1983. *Relevance of Biotic Pathways to the Long-Term Regulation of Nuclear Waste Disposal: Topical Report on Reference Eastern Humid Low-Level Sites*, NUREG/CR-2675, Vol. 3, Pacific Northwest Laboratory, Richland, Wash.

McKenzie, D. H. et al. 1984. *Relevance of Biotic Pathways to the Long-Term Regulation of Nuclear Waste Disposal: Phase I—Final Report*, NUREG/CR-2675, Vol. 4, Pacific Northwest Laboratory, Richland, Wash.

McKenzie, D. H. et al. 1985. *Relevance of Biotic Pathways to the Long-Term Regulation of Nuclear Waste Disposal: Estimation of Radiation Dose to Man Resulting from Biotic Transport: The BIOPORT/MAXI1 Software Package*, NUREG/CR-2675, Vol. 5, Pacific Northwest Laboratory, Richland, Wash.

McKenzie, D. H. et al. 1986. *Relevance of Biotic Pathways to the Long-Term Regulation of Nuclear Waste Disposal: Phase 2—Final Report*, NUREG/CR-2675, Vol. 6, Pacific Northwest Laboratory, Richland, Wash.

MMES (Martin Marietta Energy Systems, Inc.) 1994. *Waste Acceptance Criteria for the Oak Ridge Reservation*, ES/WM-10, Rev. 1, Oak Ridge, Tenn.

MMES, EG&G, and WSRC (Martin Marietta Energy Systems, Inc.; EG&G Idaho, Inc.; and Westinghouse Savannah River Company) 1994. *Radiological Performance Assessment for the E-Area Vaults Disposal Facility*, WSRC-RP-94-218, Westinghouse Savannah River Company, Aiken, S.C.

Moore, G. K. 1988. *Concepts of Groundwater Occurrence and Flow near Oak Ridge National Laboratory, Tennessee*, ORNL/TM-10969, Martin Marietta Energy Systems, Inc., Oak Ridge Natl. Lab.

Moore, G. K. 1989. *Groundwater Parameters and Flow Systems Near Oak Ridge National Laboratory*, ORNL/TM-11368, Martin Marietta Energy Systems, Inc., Oak Ridge Natl. Lab.

Mynatt, F. R. 1992. *Software Quality Assurance*, ESS-QA-19.0, Martin Marietta Energy Systems, Inc., Oak Ridge, Tenn.

NRC (U.S. Nuclear Regulatory Commission) 1977. "Calculation of Annual Doses to Man from Routine Releases of Reactor Effluents for the Purpose of Evaluating Compliance with 10 CFR Part 50, Appendix I," Regulatory Guide 1.109, Washington, D.C.

NRC (U.S. Nuclear Regulatory Commission) 1982. *Final Environmental Impact Statement on 10 CFR Part 61 "Licensing Requirements for Land Disposal of Radioactive Waste,"* NUREG-0945, Vol. 1, Washington, D.C.

Ogden Environmental and Energy Services Co., Inc. 1995. *Hydrogeologic and Geotechnical Study—Low-Level Waste Disposal Facility CIIDF, K-25, Oak Ridge, Tennessee*, Ogden File No. 1-4636-004C, Oak Ridge, Tenn.

ORNL (Oak Ridge National Laboratory) 1993. *Quality Assurance Manual*, Martin Marietta Energy Systems, Inc., Oak Ridge, Tenn.

ORNL (Oak Ridge National Laboratory) 1994. *Performance Assessment for Continuing and Future Operations at Solid Waste Storage Area 6*, ORNL-6783, Martin Marietta Energy Systems, Inc., Oak Ridge, Tenn.

Oztunali, O. I., and G. W. Roles 1986. *Update of Part 61 Impacts Analysis Methodology*, NUREG/CR-4370, Vol. 1, Envirosphere Co. and U.S. Nuclear Regulatory Commission, Washington, D.C.

Reeves, M., and E. E. Miller 1975. "Estimating Infiltration for Erratic Rainfall," *Water Resour. Res.* **11**, 102–10.

Rothschild, E. R. et al. 1984. *Characterization of Soils at Proposed Solid Waste Storage Area (SWSA) 7*, ORNL/TM-9326, Martin Marietta Energy Systems, Inc., Oak Ridge Natl. Lab.

Schwartz, P. M. et al. 1995. *TERRAIN: A Computer Program to Process Digital Elevation Models for Modeling Surface Flow*, ORNL/TM-13071, Lockheed Martin Energy Systems, Inc., Oak Ridge Natl. Lab.

Sharma, M. L., and R. J. Luxmoore 1979. "Soil Spatial Variability and Its Consequence on Simulated Water Balance," *Water Resour. Res.* **15**, 1567–73.

Sharma, M. L. et al. 1987. "Subsurface Water Flow Simulated for Hillslopes with Spatially Dependent Soil Hydraulic Characteristics," *Water Resour. Res.* **23**, 1523–30.

Sheppard, M. I., and D. H. Thibault 1990. "Default Soil Solid/Liquid Partition Coefficients, K_ds for Four Major Soil Types: A Compendium," *Health Phys.* **59**, 471–82.

Sheppard, M. I. et al. 1984. *Soil Nuclide Distribution Coefficients and Their Statistical Distributions*, AECL-8364, Whiteshell Nuclear Research Establishment, Pinawa, Manitoba, Canada.

Shevnell, L. A., R. B. Dreier, and W. K. Jago 1993. *1992 Summary of Fiscal Years 1991 and 1992 Construction, Hydrologic, and Geologic Data Obtained from the Maynardville Limestone Exit-Pathway Monitoring Program*, Y/TS-814, Martin Marietta Energy Systems, Inc., Oak Ridge, Tenn.

Sinclair, T. R., C. E. Murphy, Jr., and K. R. Knoerr 1976. "Development and Evaluation of Simplified Models for Simulating Canopy Photosynthesis and Transpiration," *J. Appl. Ecol.* **13**, 813–29.

Solomon, D. K. et al. 1989. *The Transport of Contaminants During Storms in the White Oak Creek and Melton Branch Watersheds*, ORNL/RAP/LTR-89/8, Martin Marietta Energy Systems, Inc., Oak Ridge Natl. Lab.

Solomon, D. K. et al. 1992. *Status Report: A Hydrologic Framework for the Oak Ridge Reservation*, ORNL/TM-12026, Martin Marietta Energy Systems, Inc., Oak Ridge Natl. Lab.

Suter, G. W., R. J. Luxmoore, and E. D. Smith 1993. "Compacted Soil Barriers at Abandoned Landfill Sites Are Likely to Fail in the Long Term," *J. Environ. Qual.* **22**, 217–26.

Swanson, J. L. 1983. *Mobility of Organic Complexes of Nickel and Cobalt in Soils*, Report PNL-4796, Pacific Northwest Laboratory, Richland, Wash.

Theis, C. V. 1935. "The Relation Between the Lowering of the Piezometric Surface and the Rate and Duration of Discharge of a Well Using Groundwater Storage," *Trans. Am. Geophys. Union* **2**, 519–524.

Timmins, S. P., M. A. Huston, and R. B. Clapp 1989. "Generation of Digital Elevation Models from Contours and Comparison of Topographic Indices," *Eos, Trans. Am. Geophys. Union* **70**, 1094.

Trabalka, J. R., and C. T. Garten, Jr. 1983. "Behavior of the Long-Lived Synthetic Elements and Their Natural Analogs in Food Chains," *Adv. Radiat. Biol.* **10**, 39.

Tucci, P. 1986. *Groundwater Flow in Melton Valley, Oak Ridge Reservation, Roane County, Tennessee—Preliminary Model Analysis*, Water Resources Investigation Report 85-4221, U.S. Geological Survey, Nashville, Tenn.

Turner, R. R. and K. F. Steele 1988. "Cadmium and Manganese Sorption by Soil Macropore Linings and Fillings," *Soil Sci.* **145**, 79–86.

USGS (U.S. Geological Survey) 1991. *Water Resources Data, Tennessee, Water Year 1991*, Report TN-91-1, Reston, Va.

USGS (U.S. Geological Survey) 1994. *Water Resources Data, Tennessee, Water Year 1994,* Report TN-94-1, Reston, Va.

Venetis, C. 1968. "On the Impulse Response of an Aquifer," *Bull. Int. Assoc. Sci. Hydrol*, 136.

Wickliff D. S. et al. 1989. *Contaminant Transport During Storms near Solid Waste Areas 4 and 5*, ORNL/RAP/LTR-89/20, Martin Marietta Energy Systems, Inc., Oak Ridge Natl. Lab.

Wilson, G. V. et al. 1993. "Field-Scale Transport from a Buried Line Source in Variably Saturated Soil," *J. Hydrol.* **145**, 83–109.

Appendix A

DESCRIPTION OF THE SOURCE1 COMPUTER PROGRAM

A. S. Icenhour
M. L. Tharp

Appendix A

DESCRIPTION OF THE SOURCE1 COMPUTER PROGRAM

A.1 INTRODUCTION

Version 2.0 of the SOURCE1 computer code (Icenhour and Tharp 1996) was used to calculate source terms for this performance assessment. The original version of this computer code, Version 1.0, was developed by Rogers and Associates Engineering Corporation (Shuman, Chau, and Jennrich 1992). This appendix provides an overview of the SOURCE1 computer code. A more detailed description of the code, including algorithms, input requirements, and output options, can be found in the user's manual (Icenhour and Tharp 1996).

The conceptual and mathematical modeling methodology used in the SOURCE1 computer code is discussed in the following subsections. This discussion considers the approaches taken in (1) modeling concrete degradation, (2) performing the structural and cracking analyses for the disposal structures, (3) partitioning water through the disposal facility, and (4) modeling advective and diffusive releases of radionuclides from waste.

A.2 CONCRETE DEGRADATION MODELING

Modes of concrete degradation are considered in terms of surface- and bulk-attack mechanisms. Surface-attack mechanisms are initiated at the surface of the concrete component and progress inward over time. Bulk-attack mechanisms modify the properties of the entire concrete component uniformly.

Sulfate attack is generally considered the most significant surface-attack mechanism in the context of waste repositories (Atkinson and Hearne 1984). In areas characterized by cold winters, freeze-thaw cycling may also represent a serious threat to concrete in disposal facilities. In terms of bulk-attack processes, the most notable degradation processes are likely to be calcium hydroxide leaching and alkali-aggregate attack.

Corrosion of reinforced steel may also undermine the ability of engineered disposal facilities to isolate waste therein from the environment. This process differs from the surface- and bulk-attack processes noted previously because it does not directly alter the properties of the concrete.

The models used in simulating concrete degradation are discussed in Sects. A.2.1 through A.2.3. The deterioration processes considered in the SOURCE1 computer code include sulfate attack, calcium hydroxide leaching, and corrosion of steel reinforcement.

A.2.1 Sulfate Attack

Sulfate attack generally manifests itself in the form of expansion and, ultimately, cracking of concrete. It may also result in a progressive loss of strength and mass resulting from deterioration in the cohesiveness of the cement hydration products.

Three steps are recognized in the deterioration of concrete as a result of sulfate attack (Atkinson and Hearne 1990):

- Sulfate ions from the environment penetrate into the concrete, usually by diffusion.
- Sulfate ions react expansively with certain aluminum-containing phases in the concrete to form ettringite.
- The resulting internal expansion causes stress, cracking, and exfoliation of the concrete surface.

These aspects of the degradation process are incorporated into the sulfate attack model used in the SOURCE1 computer code.

The sulfate-attack model is based on the work of Atkinson and Hearne (1990). In this model, the reaction zone is assumed to spall out when it reaches a critical thickness given by

$$X_{spall} = \frac{2\alpha\gamma(1 - \mu_c)}{E(\beta C_e)^2} , \qquad (A.1)$$

where

X_{spall} = reaction zone thickness at which spalling occurs (m),
α = roughness factor for fracture path (unitless),
γ = fracture surface energy of concrete (J/m^2),
μ_c = Poisson's ratio for concrete (unitless),
E = Young's modulus (Pa),
β = linear strain caused by a mole of sulfate reacted in 1 m^3 (m^3/mol),
C_e = concentration of sulfate as ettringite at the time at which spalling occurs (mol/m^3).

This critical thickness is achieved at a time

$$t_{spall} = \frac{X_{spall}^2 C_e}{2D_i c_o} , \qquad (A.2)$$

where

t_{spall} = time at which spalling occurs (s),
D_i = "intrinsic" diffusion coefficient of sulfate ions in water-saturated cement (m^2/s), and
c_o = groundwater sulfate concentration (mol/m^3).

The rate of degradation, R_1, is defined as X_{spall}/t_{spall} (m/s). Then, based on Eqs. (A.1) and (A.2), R is given by

$$R = \frac{E\beta^2 c_o C_e D_i}{\alpha\gamma\left(1 - \mu_c\right)} \quad . \tag{A.3}$$

As sulfate attack progresses into the concrete member, it is assumed that the affected layers spall off, thus effectively reducing the thickness of the concrete member.

It is necessary to use an iterative method to determine the concentration of sulfate as ettringite, C_e, and the degradation rate caused by sulfate attack. The starting approximation for C_e is calculated assuming that the alumina has been completely converted to ettringite in the reacted zone (Atkinson and Hearne 1990). Zero-order values of the X_{spall}, t_{spall}, and R are calculated on this basis, and t_{spall} is compared with the time required for the reaction to go to completion. If t_{spall} is not great enough to permit complete reaction, t_{spall} and C_e are iterated to self-consistency using the reaction kinetics expression described in Atkinson and Hearne (1990).

A.2.2 Calcium Hydroxide Leaching

Calcium hydroxide [$Ca(OH)_2$] leaching results in a loss of strength in the concrete as well as a lowering of the pH of the material. A loss of strength will affect the concrete structure's ability to withstand the loads placed upon it. Declines in the pH of the concrete may lead to depassivation of the steel reinforcement, thereby promoting corrosion of the steel.

$Ca(OH)_2$ may be leached from the concrete because of diffusion and advection. The loss of $Ca(OH)_2$ from concrete members from diffusion is calculated by solving the following equation:

$$\frac{df_t}{dt} = - D_y \frac{d^2 f_t}{dy^2} \quad , \tag{A.4}$$

where

f_t	=	fraction of $Ca(OH)_2$ remaining in concrete member as a function of position and time (unitless),
t	=	time (s),
D_y	=	effective diffusion coefficient of $Ca(OH)_2$ in concrete (m^2/s),
y	=	distance from centerline (m).

The boundary conditions that apply are

$$f_t(y,t=0) = \begin{cases} 1 & \text{for } |y| < \frac{\hat{W}}{2} \\ 0 & \text{for } |y| > \frac{\hat{W}}{2} \end{cases} , \tag{A.5}$$

where

$\hat{W}$ = width of concrete member (m).

The equation for f_t is given by

$$f_t = 0.5 \text{ erf } \frac{(y + \hat{W}/2)R_f}{2(D_y t)^{0.5}} - 0.5 \text{ erf } \frac{(y - \hat{W}/2)R_f}{2(D_y t)^{0.5}} , \tag{A.6}$$

where

R_f = retardation factor for $Ca(OH)_2$ in concrete (unitless).

The $Ca(OH)_2$ retardation factor, R_f, is given by

$$R_f = 1 + \frac{Ca_c}{\epsilon_c Ca_p} , \tag{A.7}$$

where

Ca_c = $Ca(OH)_2$ concentration in concrete (mol/L),
ϵ_c = concrete porosity (dimensionless),
Ca_p = $Ca(OH)_2$ concentration in concrete pore solution (mol/L).

The potential for leaching of $Ca(OH)_2$ through advective mechanisms will depend upon the nature of the groundwater. If the groundwater is saturated or supersaturated with calcium carbonate, no dissolution of $Ca(OH)_2$ will occur. Groundwater which is not saturated with calcium carbonate may leach $Ca(OH)_2$ as the groundwater passes through the concrete.

Langelier (1936) developed the calcium carbonate saturation (or Langelier) index as a means of characterizing the degree of calcium carbonate saturation of groundwater. The index takes into account the effects of temperature, total dissolved solids, total alkalinity, pH, and calcium content on the saturation characteristics of the groundwater. A negative value for the Langelier index denotes a groundwater which is not saturated with calcium carbonate [i.e., one capable of leaching $Ca(OH)_2$ from concrete]. Index values equal to or greater than zero indicate calcium carbonate saturation.

Data taken from Langelier (1936) are used in a regression to estimate the saturation index as a function of the total dissolved solids and temperature of the groundwater. When predicted values of the index are positive, losses of $Ca(OH)_2$ are modeled to occur as a result of diffusion only. When the groundwater is not saturated with calcium carbonate (i.e., the Langelier index is negative), advective leaching of $Ca(OH)_2$ is calculated using (Atkinson 1985):

$$Ca_l = I \frac{Ca_p}{C_t Ca_c} , \tag{A.8}$$

where

Ca_l = fractional groundwater release rate of $Ca(OH)_2$ ($year^{-1}$),
I = water percolation rate through vault (m/year),
C_t = concrete-member thickness (m).

The presence of other ions in the groundwater may influence the rate at which $Ca(OH)_2$ is leached from the concrete. Atkinson (1985) reports that magnesium and carbonate are among the species most likely to speed the loss of $Ca(OH)_2$. The effect of these species is modeled using Eq. (A.8), replacing the pore solution concentration of $Ca(OH)_2$, Ca_p, with the sum of this concentration and the groundwater concentrations of magnesium and carbonates.

The quantities of $Ca(OH)_2$ lost from the concrete member by diffusion and advection are summed to determine the total amount of the constituent leached from the concrete. The concentration of $Ca(OH)_2$ in the concrete is adjusted downward to reflect these losses. All $Ca(OH)_2$ leached from the concrete is assumed to be drawn from the calcium-silicate-hydrate (C-S-H) system of the concrete. The calcium incorporated into the relatively less-soluble phases of the concrete is not considered.

Changes in the pH of concrete as a result of the loss of $Ca(OH)_2$ have been well documented (Atkinson 1985). The pH of the concrete is maintained at levels greater than approximately 12.5 in the presence of alkalis, sodium hydroxide (NaOH), and potassium hydroxide (KOH). As these highly soluble species are lost because of leaching, the pH declines until it reaches 12.5, at which point the pH of the concrete is controlled primarily by the $Ca(OH)_2$ content of the concrete.

Changes in the pH of the concrete are modeled as alkalis and $Ca(OH)_2$ are leached from the concrete. Based on the data of Greenberg and Chang (1965), the pH is modeled to decline linearly from the initial pH of the concrete, as specified by the user, to 12.5 in direct proportion to the reduction in NaOH and KOH in the concrete. The rates of loss of these species from leaching by diffusion and advection are calculated using Eqs. (A.6) and (A.8), respectively.

Following the complete loss of NaOH and KOH from the concrete, changes in the pH of the concrete are modeled as a function of the $Ca(OH)_2$ content. Using data from the work of Greenberg and Chang (1965), concrete pH was regressed on the Ca:Si ratio of the material. As $Ca(OH)_2$ is leached from the concrete, the Ca:Si ratio is updated, and the pH of the concrete is estimated using this regression.

In addition to the pH effects noted, the loss of $Ca(OH)_2$ will result also in a reduction in the strength of the concrete. The loss in strength has been estimated to be approximately 1.5% for every 1.0% of the $Ca(OH)_2$ leached from the concrete (Lea 1970). Based on this relationship, the compressive strengths of the concrete members are updated to reflect losses of $Ca(OH)_2$.

A.2.3 Corrosion of Steel Reinforcement

The damage to concrete resulting from the corrosion of steel reinforcement manifests itself in expansion, cracking, and spalling of the concrete member. The reinforced concrete member may suffer structural damage because of (1) the loss of the bond between the steel and concrete and (2) the loss of reinforcement cross-sectional area.

Steel reinforcement is generally passivated because of the alkaline nature of the liquid phase in the concrete pores and, hence, does not undergo corrosion. The passive layer on the steel may be destroyed through a direct lowering of the pH of the concrete via carbonation or because of chloride ion penetration to the steel. Both mechanisms of depassivation are considered in the SOURCE computer codes.

Carbonation of the concrete occurs as a result of the diffusion of carbon dioxide (CO_2) into the material. The depth of carbonation is given by (Tuutti 1982) as

$$X = kt^{0.5} \quad , \tag{A.9}$$

where

X = depth of carbonation (m),
k = carbonation coefficient ($m/s^{0.5}$).

Given the value of k, the depth of penetration of the carbonation front into the concrete can be determined for any specified time.

The carbonation coefficient is calculated using (Tuutti 1982)

$$\frac{C_x - C_s}{g\left(k/2D_{CO2}^{0.5}\right)} + C_x - C_f = 0 \quad , \tag{A.10}$$

where

C_x = concentration of CO_2 bound in concrete (mol/L),
C_s = CO_2 concentration at surface of concrete (mol/L),
C_f = CO_2 concentration ahead of carbonation front (mol/L),
$g\left(k/2D_{CO2}^{0.5}\right)$ = function, where
D_{CO2} = diffusion coefficient of CO_2 in concrete (m^2/s).

The function $g\left(k/2D_{CO2}^{0.5}\right)$ is given by

$$g\left(k/2D_{CO2}^{0.5}\right) = \pi^{0.5}\frac{k}{2D_{CO2}^{0.5}}\exp\left(\frac{k^2}{4D_{CO2}}\right)\mathrm{erf}\left(\frac{k}{2D_{CO2}^{0.5}}\right) \quad . \tag{A.11}$$

Equations (A.10) and (A.11) are combined to arrive at a solution for k, the carbonation coefficient. Assuming that the concentration of CO_2 ahead of the carbonation front is zero (i.e., that the carbonation front is discontinuous), this solution can be simplified to yield

$$k^2 = \frac{4D_{CO2}}{\pi^{0.5}}\left(\frac{C_s}{C_x} - 1\right) \quad . \tag{A.12}$$

When using Eq. (A.12) to evaluate k, the model takes into account that a portion of the CO_2 diffusing into the concrete is bound by concrete constituents and does not penetrate to the steel reinforcement. This bound CO_2 plays no role in depassivation. The amount of CO_2 bound in the concrete is set equal to amount of hydrated lime in the concrete (Tuutti 1982). The quantity of hydrated lime is calculated as the product of the calcium oxide (CaO) content in the concrete and the degree of hydration. The degree of hydration, estimated based on the water/cement ratio for Portland cements (Tuutti 1982), is given by

$$H_f = 0.4 + 0.5(\mathrm{WCR}) \quad , \tag{A.13}$$

where

H_f = fraction of hydrated CaO (unitless),
WCR = water-cement ratio (unitless).

Given the carbonation coefficient, k, the depth of carbonation is calculated using Eq. (A.9). As stated previously, this solution assumes that the carbonation front is discontinuous. At that time when the front has penetrated to the depth of the steel reinforcement, depassivation of the steel is assumed to occur, and corrosion is thus initiated.

Steel reinforcement may also be depassivated as a result of the penetration of chloride ions to the steel surface. Using a standard solution to Fick's first law of diffusion, the chloride ion concentration at the steel is calculated as

$$CL_s = CL_i + \left(CL_{gw} - CL_i\right)\left[1 - \mathrm{erf}\left(\frac{C_c}{2\left(D_{Cl}t\right)^{0.5}}\right)\right] \quad , \tag{A.14}$$

where

CL_s = chloride ion concentration at steel reinforcement (mol/L),
CL_i = initial chloride ion concentration in concrete (mol/L),
CL_{gw} = chloride ion concentration in groundwater (mol/L),
C_c = concrete cover thickness (m),
D_{Cl} = effective diffusivity of chloride in concrete (m^2/s).

The concentration of chloride ions at the steel reinforcement required to depassivate the steel has been considered by numerous investigators. Hausmann (1967) found that the pH of the concrete had an effect on the level of chloride ions required to initiate corrosion. In studies carried out using NaOH and $Ca(OH)_2$ solutions, it was found that a chloride-ion-to-hydroxide-ion concentration ratio of 0.61 was sufficient to depassivate the steel.

Using the results of Hausmann (1967), a chloride-ion-to-hydroxide-ion ratio of 0.61 is assumed to result in depassivation of the steel. The hydroxide ion concentration used in calculating this ratio is determined using the modeled concrete pH. As discussed in Sect. A.2.2, the pH of the concrete changes with time as NaOH, KOH, and $Ca(OH)_2$ are leached from the material.

Upon depassivation of the steel reinforcement by either carbonation or chloride penetration, corrosion is modeled to occur at a rate determined by the rate of diffusion of oxygen to the steel. The molar flow of oxygen to the surface of the steel reinforcement is modeled using Fick's first law of diffusion:

$$J_o = - D_o A \frac{d[O_2]}{dx} , \qquad (A.15)$$

where

J_o = oxygen flux at the steel reinforcement (g/s),
D_o = effective diffusivity of oxygen through concrete (cm^2/s),
A = surface area over which oxygen diffuses to the reinforcement (cm^2),
$\frac{d[O_2]}{dx}$ = dissolved oxygen concentration gradient (g/cm^4).

The rate of oxygen consumption by the corrosion reaction is assumed to be greater than the rate of oxygen diffusion to the reaction surface. Under these conditions, the corrosion rate is limited by the flux of oxygen at the steel reinforcement.

The use of epoxy-coated steel reinforcement may delay the onset of corrosion by isolating the steel from aggressive ions and oxygen. The use of epoxy coating is not assumed to delay the time of depassivation of the reinforcement. However, upon depassivation, the coating is assumed to prevent corrosion as long as it remains intact.

The effectiveness of epoxy coating on steel reinforcement is modeled using a linear failure function. Using the time at which failure of the coating begins and the time required for all epoxy

coating to fail, a fraction of the reinforcement coating which has failed is calculated. This failure fraction is used to linearly adjust the projected rate of corrosion downward.

Corrosion of components other than steel reinforcement will also affect the long-term performance of low-level waste (LLW) disposal facilities. For example, the metal boxes placed inside tumulus vaults will all eventually fail as a result of corrosion.

Corrosion of steel barriers used in the tumulus technology is considered in the SOURCE1 computer code. Failure rates of these barriers are modeled using linear failure functions. The user specifies the time at which corrosion of the metal component begins and the number of years required, following this time, for the member to fail completely. Using these input data, a failure fraction is calculated for each year of the simulation.

A.3 CONCRETE STRUCTURAL AND CRACKING ANALYSES

The structural and cracking analyses serve two distinct purposes in modeling the long-term performance of LLW facilities. The structural analysis considers the loads placed on the disposal facility to determine the bending moments, shears, axial tension, and compressive forces placed on the various structural components. Because these loads vary with the structural component under consideration, this analysis is carried out for the roof, walls, and floor of each disposal facility.

The cracking analyses are concerned with the ability of the disposal facility to bear the loads placed upon it. Bending moments, shears, axial tensions, and compressive forces calculated as part of the structural analysis are compared with loads and forces at which structural failure will occur to determine the structural integrity of the disposal facility. The cracking analyses must account for the changes in concrete properties projected to occur because of physical and chemical attack. As such, it is conducted for each year of the simulation, or until hydraulic failure of the disposal facility is complete.

The long-term performance of a tumulus disposal facility is a function of the performance of the individual vaults of which it is composed. The structural and cracking analyses performed to model the behavior of these vaults are discussed in Sects. A.3.1 and A.3.2, respectively. Additionally, models for the degradation and failure of the tumulus pad and leachate collection system are presented in Sects. A.3.3 and A.3.4.

A.3.1 Structural Analysis

Each structural component of the vaults has unique loading conditions placed upon it. As such, separate structural analyses are conducted for the roof or lid, walls, and floor of the vaults. A description of these analyses follows.

A.3.1.1 Vault Roof

The roof is analyzed structurally as a simply supported, or hinged, slab. The uniform load on the roof of a vault in layer i of the tumulus disposal facility is calculated as

$$q_r = s\rho_s + ih_r\rho_c + (i-1)\left[h_w\rho_w + \left(h_f + h_r\right)\rho_c\right] , \tag{A.16}$$

where

q_r = uniform load on vault roof in layer i (lb/in.^{2}),
s = soil cover thickness (in.),
ρ_s = density of soil cover (lb/in.^{3}),
i = layer number (unitless),
h_r = roof thickness (in.),
ρ_c = density of reinforced concrete (lb/in.^{3}),
h_w = waste thickness (in.),
ρ_w = density of waste (lb/in.^{3}),
h_f = floor thickness (in.).

Thermal loads on the vaults are not considered because the insulating properties of the cover material minimize thermal gradients across the concrete structural components.

The deflection of the simply supported rectangular roof resulting from the uniform load is given by

$$W(x, y) = \frac{16 q_r w_r}{\pi^6 D_r} \sum_{m=1}^{\infty} \sum_{n=1}^{\infty} \frac{\sin\frac{m\pi x}{a} \sin\frac{n\pi y}{b}}{mn\left(\frac{m^2}{a^2} + \frac{n^2}{b^2}\right)^2} , \tag{A.17}$$

where

$W(x, y)$ = deflection of roof at location (x, y) (in.),
w_r = width of roof in (x, y) direction (in.),
m, n = 1,3,5, . . .,
a = width of waste cell (in.),
b = length of waste cell (in.),
D_r = flexural rigidity of the roof (lb-in.^{2}).

The flexural rigidity of the roof is calculated using

$$D_r = \frac{E_c h_r^3 w_r}{12\left(1 - \mu_c^2\right)} \quad , \tag{A.18}$$

where

E_c = modulus of elasticity of concrete (lb/in.^{2}).

Based on Eqs. (A.17) and (A.18), the bending moments resulting from uniform loading as a function of location on the roof are calculated as

$$M_x = q_r a^2 \left[\frac{16}{\pi^4} \sum_{m=1}^{\infty} \sum_{n=1}^{\infty} \frac{\sin \frac{m\pi x}{a} \sin \frac{n\pi y}{b}}{\frac{n}{m}\left(m^2 + \frac{n^2}{\left(\frac{b}{a}\right)^2}\right)^2} + \mu_c \frac{\sin \frac{m\pi x}{a} \sin \frac{n\pi y}{b}}{\left(\frac{b}{a}\right)^2 \left(\frac{m}{n}\right)\left(m^2 + \frac{n^2}{\left(\frac{b}{a}\right)^2}\right)^2} \right] \quad , \tag{A.19}$$

and

$$M_y = q_r b^2 \left[\frac{16}{\pi^4} \sum_{m=1}^{\infty} \sum_{n=1}^{\infty} \frac{\sin \frac{m\pi x}{a} \sin \frac{n\pi y}{b}}{\frac{m}{n}\left(\frac{m^2}{\left(\frac{a}{b}\right)^2} + n^2\right)^2} + \mu_c \frac{\sin \frac{m\pi x}{a} \sin \frac{n\pi y}{b}}{\left(\frac{a}{b}\right)^2 \left(\frac{n}{m}\right)\left(\frac{m^2}{\left(\frac{a}{b}\right)^2} + n^2\right)^2} \right] \quad , \tag{A.20}$$

where

M_x = bending moment resulting from uniform loading in the x-direction parallel to width of roof (lb-in./in.) and

M_y = bending moment resulting from uniform loading in the y-direction parallel to length of roof (lb-in./in.).

Uniform loads on the vault roof result in shear forces upon that component as well. These forces are calculated as

$$Q_x = q_r a \left\{ \frac{16}{\pi^3} \sum_{m=1}^{\infty} \sum_{n=1}^{\infty} \cos \frac{m\pi x}{a} \cdot \sin \frac{n\pi y}{b} \left[\frac{m^2}{n\left(m^2 + n^2\left(\frac{a}{b}\right)^2\right)^2} + \frac{n}{\left(m^2\left(\frac{b}{a}\right) + n^2\left(\frac{a}{b}\right)\right)^2} \right] \right\}, \tag{A.21}$$

and

$$Q_y = q_r b \left\{ \frac{16}{\pi^3} \sum_{m=1}^{\infty} \sum_{n=1}^{\infty} \sin \frac{m\pi x}{a} \cos \frac{n\pi y}{b} \left[\frac{m}{\left(m^2\left(\frac{b}{a}\right) + n^2\left(\frac{a}{b}\right)\right)^2} + \frac{n^2}{m\left(m^2\left(\frac{b}{a}\right)^2 + n^2\right)^2} \right] \right\}, \tag{A.22}$$

where

Q_x = shear force resulting from uniform loading in the x-direction (lb/in.),

Q_y = shear force resulting from uniform loading in the y-direction (lb/in.).

A.3.1.2 Vault Walls

The vault walls are subject to vertical, or uniform, loads and hydrostatic pressures. The uniform loads are calculated for a vault in layer i of the tumulus disposal facility using

$$q_w = \rho_s\left(\frac{h_r}{2}i + (h_f + h_w)(i - 1) + s\right)(1 - \sin f_s) \quad , \tag{A.23}$$

where

q_w = uniform load on vault wall in layer i (lb/in.^{2}) and

f_s = friction angle of soil backfill around tumulus (deg).

Hydrostatic pressures on the vault walls are a result of lateral soil pressures from the soil backfill and from the waste and grout inside the vault. This pressure is calculated as

$$P = \rho_s\left(h_w + \frac{h_r + h_f}{2}\right)(h - \sin f_s) - \rho_w\left(h_w + \frac{h_r + h_f}{2}\right)(1 - \sin f_w) \quad , \tag{A.24}$$

where

P = maximum hydrostatic pressure (lb/in.^{2}),

f_w = friction angle of waste (deg).

Bending moment calculations for the vault walls must account for the uniform loads and hydrostatic pressures on the structural components. Bending moments resulting from the uniform load are calculated using Eqs. (A.19) and (A.20), substituting the uniform load on the wall for the uniform load on the roof and changing roof dimensions to those of the wall. Bending moments caused by hydrostatic pressures are calculated using

$$M_{xh} = Pa^2 \sum_{m=1}^{\infty} (m\pi)^2 \left[\frac{2(-1)^{m+1}}{\pi^5 m^5} + \left[(1-\mu_c)A_m - 2\mu_c B_m\right]\cosh\left(\frac{m\pi y}{a}\right)\right.$$
$$\left. + (1-\mu_c)B_m\left(\frac{m\pi}{a}\right) y\sinh\left(\frac{m\pi y}{a}\right)\right]\sin\frac{m\pi x}{a} \quad , \tag{A.25}$$

and

$$M_{yh} = Pa^2 \sum_{m=1}^{\infty} (m\pi)^2 \left[\frac{2(-1)^{m+1}}{\pi^5 m^5} \mu_c + \left[(\mu_c - 1) A_m - 2B_m \right] \cosh\left(\frac{m\pi y}{a} \right) \right.$$

$$\left. + (\mu_c - 1) B_m \left(\frac{m\pi}{a} \right) y \sinh\left(\frac{m\pi y}{a} \right) \right] \sin \frac{m\pi x}{a} \quad , \tag{A.26}$$

where

M_{xh} = bending moment resulting from hydrostatic pressures in the x-direction parallel to the width of the wall (lb-in./in.),

M_{yh} = bending moment resulting from hydrostatic pressures in the y-direction parallel to the length of the wall (lb-in./in.).

The quantities A_m and B_m are given, respectively, by

$$A_m = - \frac{(2 + \alpha_m \tanh \alpha_m)(-1)^{m+1}}{\pi^5 m^5 \cosh \alpha_m} \quad , \tag{A.27}$$

and

$$B_m = \frac{(-1)^{m+1}}{\pi^5 m^5 \cosh \alpha_m} \quad , \tag{A.28}$$

where

$$\alpha_m = \frac{m\pi b}{2a} \quad . \tag{A.29}$$

Bending moments calculated for the uniform load and hydrostatic pressure on the wall are summed to arrive at the final bending moments for the wall as a function of location. The calculations of the bending moments are repeated for each wall geometry composing the disposal vault.

Shear forces caused by hydrostatic pressures on the vault walls are calculated as

$$Q_{xh} = 2Pa \sum_{m=1}^{\infty} (m\pi)^3 \left[\frac{(-1)^{m+1}}{\pi^5 m^5} - B_m \cosh\left(\frac{m\pi y}{a} \right) \right] \cos\left(\frac{m\pi x}{a} \right) \quad , \tag{A.30}$$

and

$$Q_{yh} = -2Pa \sum_{m=1}^{\infty} (m\pi)^3 B_m \sinh\left(\frac{m\pi y}{a}\right) \sin\left(\frac{m\pi x}{a}\right) \quad , \tag{A.31}$$

where

Q_{xh} = shear force resulting from hydrostatic loading in the x-direction (lb/in.),
Q_{yh} = shear force resulting from hydrostatic loading in the y-direction (lb/in.).

The shear forces on vault walls resulting from uniform loads are calculated using Eqs. (A.21) and (A.22) and substituting appropriate parameters for the wall. Shear forces caused by uniform and hydrostatic loads are summed for each wall location. Calculations of shear forces are performed for each wall geometry composing the vault.

The walls of the vaults are subject to compressive forces from the roof reaction and the weight of the walls. The compressive force, calculated as a function of height on the wall, is given by

$$F_w = R_{ry} + h_{wl} z \rho_c \quad , \tag{A.32}$$

where

F_w = compressive force on wall at height z (lb/in.),
R_{ry} = roof reaction in y direction at height z (lb/in.),
h_{wl} = thickness of wall (in.),
z = wall height (in.)

A.3.1.3 Vault Floor

The floor of a given vault must bear loads from the walls, including the wall weight and loads transmitted to the walls from the roof, and loads from the waste within the vault. Based on the floor geometry illustrated in Fig. A.1, the bending moments in the region x (or y) $\leq$ a of the beam subjected to a concentrated force and moment are calculated as

$$M_x = \frac{P_x I_{1px}}{2\lambda_x\left[\sinh^2(\lambda_x w_f) - \sin^2(\lambda_x w_f)\right]} \quad , \tag{A.33}$$

ORNL-DWG 94-5975

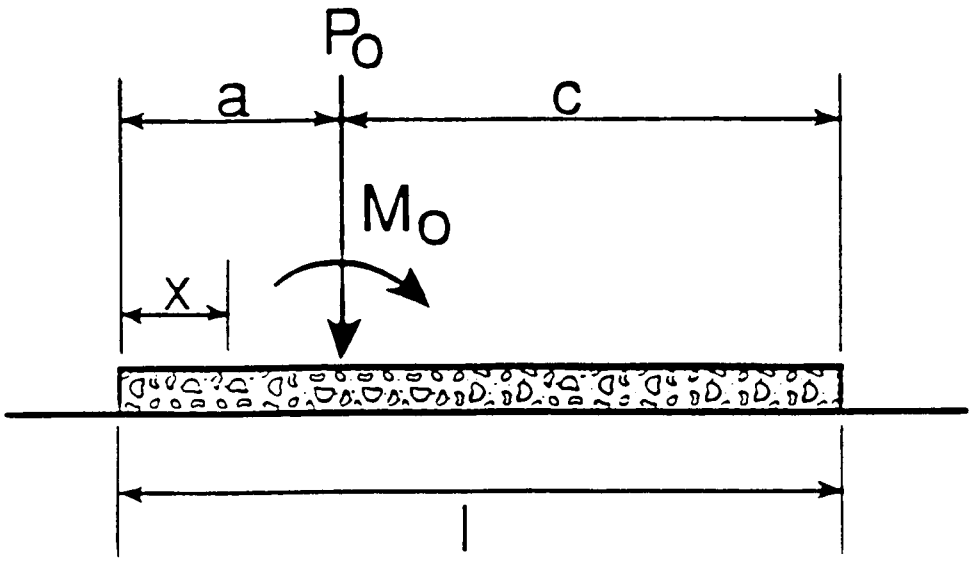

Fig. A.1. Schematic diagram of floor geometry used in the calculation of bending moments.

and

$$M_y = \frac{P_y I_{1py}}{2\lambda_y\left[\sinh^2(\lambda_y l_f) - \sin^2(\lambda_y l_f)\right]} \quad , \tag{A.34}$$

where

M_x = bending moment in x-direction parallel to width of floor (lb-in./in.),
P_x = applied concentrated load caused by wall in x-direction (lb/in.),
I_{1px} = trigonometric function (unitless),
λ_x = $\left[\frac{\tilde{k} l_f}{4D_{fx}}\right]^{0.25} \left(\text{in.}^{-1}\right)$,
$\tilde{k}$ = modulus of the subgrade reaction (lb/in.^{3}),
l_f = length of floor (in.),
D_{fx} = flexural rigidity of floor in the x-direction (lb-in.^{2}),
w_f = width of floor (in.),
M_y = bending moment in y-direction parallel to length of floor (lb-in./in.),
P_y = applied concentrated load caused by wall in y-direction (lb/in.),
I_{1py} = trigonometric function (unitless),
λ_y = $\left[\frac{\tilde{k} w_f}{4D_{fy}}\right]^{0.25} \left(in.^{-1}\right)$ and
D_{fy} = flexural rigidity of floor in the y-direction (lb-in.^{2}).

Applied moments caused by the wall are not considered in the bending moment calculations because it is assumed that the floor and walls are hinged.

The concentrated load on the floor, P_x or P_y, is calculated as a function of location using

$$P_x = R_{rx} + h_{wl}\left(h_w + \frac{h_r + h_f}{2}\right)(\rho_c - \rho_w) \quad , \tag{A.35}$$

and

$$P_y = R_{ry} + h_{wl}\left(h_w + \frac{h_r + h_f}{2}\right)(\rho_c - \rho_w) \quad , \tag{A.36}$$

where

R_{rx} = roof reaction in x-direction (lb/in.).

The flexural rigidity of the floor is calculated using Eq. (A.18). To calculate the quantity D_{fx} the thickness and width of the floor are substituted for h_r and w_r, respectively. The thickness and length of the floor are substituted for h_r and w_r, respectively, to calculate D_{fy}.

The parameters I_{1px} and I_{1py} are complex trigonometric functions of λ_x, λ_y, and the geometry of the structural member and are given by

$$\begin{aligned} I_{1px} = {} & 2\sinh(\lambda_x x)\sin(\lambda_x x)\left[\sinh(\lambda_x w_f)\cos(\lambda_x a)\cosh(\lambda_x c)\right. \\ & - \sin(\lambda_x w_f)\cosh(\lambda_x a)\cos(\lambda_x c)\Big] - \Big[\sinh(\lambda_x x)\cos(\lambda_x x) \\ & - \cosh(\lambda_x x)\sin(\lambda_x x)\Big]\Big[\sinh(\lambda_x w_f)\{\sin(\lambda_x a)\cosh(\lambda_x c) \\ & - \cos(\lambda_x a)\sinh(\lambda_x c)\} + \sin(\lambda_x w_f)\{\sinh(\lambda_x a)\cos(\lambda_x c) \\ & - \cosh(\lambda_x a)\sin(\lambda_x c)\}\Big] \quad , \end{aligned} \tag{A.37}$$

and

$$\begin{aligned} I_{1py} = {} & 2\sinh(\lambda_y y)\sin(\lambda_y y)\left[\sinh(\lambda_y l_f)\cos(\lambda_y a)\cosh(\lambda_y c)\right. \\ & - \sin(\lambda_y l_f)\cosh(\lambda_y a)\cos(\lambda_y c)\Big] - \Big[\sinh(\lambda_y y)\cos(\lambda_y y) \\ & - \cosh(\lambda_y y)\sin(\lambda_y y)\Big]\Big[\sinh(\lambda_y l_f)\{\sin(\lambda_y a)\cosh(\lambda_y c) \\ & - \cos(\lambda_y a)\sinh(\lambda_y c)\} + \sin(\lambda_y l_f)\{\sinh(\lambda_y a)\cos(\lambda_y c) \\ & - \cosh(\lambda_y a)\sin(\lambda_y c)\}\Big] \quad , \end{aligned} \tag{A.38}$$

where the parameters a and c are indicated in Fig. A.1.

Shear forces on the floor of the vault are calculated as a function of location using

$$Q_x = \frac{P_x I_{2px}}{\left[\sinh^2(\lambda_x w_f) - \sin^2(\lambda_x w_f)\right]} \quad , \tag{A.39}$$

and

$$Q_y = \frac{P_y I_{2py}}{\left[\sinh^2(\lambda_y l_f) - \sin^2(\lambda_y l_f)\right]} \quad , \tag{A.40}$$

where

I_{2px} = trigonometric function (unitless),
I_{2py} = trigonometric function (unitless).

The parameters I_{2px} and I_{2py} are functions of λ_x, λ_y, and the geometry of the structural member and are given by

$$\begin{aligned} I_{2px} = {} & \left[\cosh(\lambda_x x)\sin(\lambda_x x) + \sinh(\lambda_x x)\cos(\lambda_x x)\right]\left[\sinh(\lambda_x w_f)\right. \\ & \left.\cos(\lambda_x a)\cosh(\lambda_x c)\sin(\lambda_x w_f)\cosh(\lambda_x a)\cos(\lambda_x c)\right] \\ & + \sinh(\lambda_x x)\sin(\lambda_x s)\left[\sinh(\lambda_x w_f)\left\{\sin(\lambda_x a)\cosh(\lambda_x c)\right.\right. \\ & \left.\left. - \cos(\lambda_x a)\sinh(\lambda_x c)\right\} + \sin(\lambda_x w_f)\left\{\sinh(\lambda_x a)\cos(\lambda_x c)\right.\right. \\ & \left.\left. - \cosh(\lambda_x a)\sin(\lambda_x c)\right\}\right] \quad , \end{aligned} \tag{A.41}$$

and

$$\begin{aligned} I_{2py} = {} & \left[\cosh(\lambda_s y)\sin(\lambda_y y) + \sinh(\lambda_y y)\cos(\lambda_y y)\right]\left[\sinh(\lambda_y w_f)\right. \\ & \left.\cos(\lambda_y a)\cosh(\lambda_y c)\sin(\lambda_y l_f)\cosh(\lambda_y a)\cos(\lambda_y c)\right] \\ & + \sinh(\lambda_y y)\sin(\lambda_y s)\left[\sinh(\lambda_y l_f)\left\{\sin(\lambda_y a)\cosh(\lambda_y c)\right.\right. \\ & \left.\left. - \cos(\lambda_y a)\sinh(\lambda_y c)\right\} + \sin(\lambda_y l_f)\left\{\sinh(\lambda_y a)\cos(\lambda_y c)\right.\right. \\ & \left.\left. - \cosh(\lambda_y a)\sin(\lambda_y c)\right\}\right] \quad . \end{aligned} \tag{A.42}$$

A.3.2 Cracking Analyses

The cracking analyses are performed to assess the ability of the structural components of each vault to bear the loads placed upon it. In the event that the roof, wall(s), or floor of a vault cannot bear these loads, cracking will occur. Cracking of these components may occur as a result of shear forces or bending; cracking of the vault walls may also result from compressive loads on the structure. The manner in which these modes of cracking are modeled is discussed in the following.

Shear cracking will occur if the shear force on a concrete member exceeds the cracking shear of the member. The cracking shears for the roof, floor, and wall in the horizontal direction are calculated as the minimum of

$$V_{cr} = d_t\left(1.9\, C_{str}^{0.5} + 2500 S_{tn} Q_x / M_x\right) \quad , \tag{A.43}$$

or

$$V_{cr} = 3.5\, C_{str}^{0.5}\, d_t \quad , \tag{A.44}$$

where

V_{cr} = shear force at which cracking occurs (lb/in.),
d_t = distance from steel reinforcement in tension to compression face of concrete (in.),
C_{str} = compressive strength of concrete (lb/in.^{2}),
S_{tn} = area of steel reinforcement in tension per unit width (in.^{2}/in.).

The cracking shear for the wall in the vertical direction is the minimum of Eqs. (A.43) and (A.45).

$$V_{cr} = 3.5\, C_{str}^{0.5} d_t\left(1.0 + F_w / \left(500\, h_{wl}\right)\right)^{0.5} \quad . \tag{A.45}$$

In the event of cracking caused by shear failure, crack characteristics are determined. The depth of the single crack is the thickness of the concrete member, and the crack width is 0.013 in.

Cracking caused by bending will be initiated if the bending moments calculated for a given concrete member exceed the cracking moment for that structural component. The cracking moment is given by

$$M_{cr} = \frac{I_g f_r}{y_t a_u} \quad , \tag{A.46}$$

where

M_{cr} = cracking moment per unit width (lb-in./in.),
I_g = moment of inertia of concrete section (in.^{4}),

f_r = modulus of rupture (lb/in.^{2}),
y_t = distance from the centroidal axis to the tensile face of the concrete (in.),
a_u = unit width of concrete member.

For a rectangular slab

$$I_g = \frac{a_u h_m^3}{12} \quad , \tag{A.47}$$

where

h_m = concrete member thickness (in.).

The value of y_t is given by

$$y_t = \frac{h_m}{2} \quad . \tag{A.48}$$

Axial compression force is conservatively neglected in the roof and floor.

If the bending moments exceed the cracking moment but do not exceed the ultimate strength of the concrete member, cracks will not propagate through the entire member. If, however, the bending moments exceed the ultimate strength of the structural component, cracks will span the thickness of the member. The ultimate flexural strength of a member without compressive steel is approximated using

$$M_u = \phi S_{tn} f_y \left(d_t - \frac{C_d}{2} \right) \quad , \tag{A.49}$$

where

M_u = ultimate flexural strength (lb-in./in.),
ϕ = strength reduction factor (unitless),
f_y = yield strength of steel reinforcement (lb/in.^{2}), and
C_d = depth of the compression block (in.).

The depth of the compression block is calculated using

$$C_d = \frac{S_{tn} f_y}{0.85\, C_{str}} \quad . \tag{A.50}$$

If all reinforcement has been lost because of corrosion, the ultimate strength is equal to the cracking moment.

Crack characteristics are calculated as fractures due to loading and propagate through a given structural component. The depth of cracking caused by bending is calculated as the distance from the surface of the concrete to the neutral axis. Crack depth is computed using the strain compatibility relation wherein the tensile crack depth is given by

$$d_{cr} = \frac{d_t}{\frac{St_n}{E_s} + \frac{St_m}{E_c}} \left[\frac{St_n}{E_s} + \epsilon_{sh} \right] + d_c \quad , \tag{A.51}$$

where

d_{cr} = crack depth (in.),
ϵ_{sh} = shrinkage strain of concrete (in./in.),
d_c = concrete cover thickness on tension face (in.),
St_n = tensile stress in steel reinforcement (lb/in.^{2}),
St_m = maximum concrete compressive stress (lb/in.^{2}),
E_s = modulus of elasticity of steel reinforcement (MPa) (for this application, taken as 200,000 MPa).

The tensile stress in steel reinforcement is calculated using

$$St_n = \left(\frac{E_s}{E_c} \right) M \left(\frac{d_t - R_t}{I_e} \right) \quad , \tag{A.52}$$

where

M = bending moment due to uniform loading in x or y direction (lb-in./in.) and
I_e = effective moment of inertia per unit width of concrete member (in.^{3}).

The quantity R_t (in.) is given by

$$R_t = \frac{-\left(\hat{\beta}_1 + \hat{\beta}_2\right) + \left[\left(\hat{\beta}_1 + \hat{\beta}_2\right)^2 - 4\alpha\left(C_c\hat{\beta}_1 - d_t\hat{\beta}_2\right)\right]^{0.5}}{2\alpha_1} \quad . \tag{A.53}$$

The quantities α_1 (unitless), $\hat{\beta}_1$ (in.), and $\hat{\beta}_2$ (in.) are calculated by

$$\alpha_1 = 0.5 \quad , \tag{A.54}$$

$$\hat{\beta}_1 = \left(\frac{\pi}{S_{p2}}\right)\left(\frac{S_{d1}}{2}\right)^2\left(\frac{E_s}{E_c} - 1\right) \quad , \tag{A.55}$$

and

$$\hat{\beta}_2 = \left(\frac{\pi}{S_{p2}}\right)\left(\frac{S_{d1}}{2}\right)^2\left(\frac{E_s}{E_c}\right) \quad , \tag{A.56}$$

where

S_{d1} = diameter of steel reinforcement in direction 1, and closest to concrete outer tension face (in.),

S_{p2} = spacing of steel reinforcement in direction 2, perpendicular to direction 1 (in.).

The quantity I_e is given by

$$I_e = \left(\frac{1}{a_u}\right)\left[\left(\frac{M_{cr}}{M}\right)^3 I_g + \left(1 - \left(\frac{M_{cr}}{M}\right)^3\right) I_c\right] \quad , \tag{A.57}$$

where

I_c = cracking moment of inertia in the x or y direction (in.^{4}).

The cracking moment of inertia is calculated using the following equation:

$$I_c = a_u\left[0.333\ R_t^3 + \hat{\beta}_1(R_t - C_c)^2 + \hat{\beta}_2(d_t - R_t)^2\right] \quad . \tag{A.58}$$

The maximum concrete compressive stress is given by

$$St_m = M\left(\frac{R_t}{I_e}\right) \quad . \tag{A.59}$$

In modeling the water flow characteristics of failed concrete, it is assumed that cracks achieving a depth equal to three-fourths of the remaining slab thickness functionally penetrate the slab. Prior to this, flow through the concrete is the same as that through intact concrete. If the bending moment exceeds the ultimate strength of the concrete slab, cracks penetrate immediately through the slab.

Numerous equations have been proposed for the prediction of crack spacing and width in flexural members. Nawy (1966) developed a formula for calculating mean crack spacing for a two-way concrete slab:

$$S_{m1} = 0.5\, K_n \left(\frac{S_{d1} S_{p2}}{Q_d} \right)^{0.5} , \qquad (A.60)$$

where

S_{m1} = mean crack spacing in direction 1 (in.).

The variables K_n and Q_d are given by

$$K_n = \left[1.6 + 2.4 \left(\frac{a}{b} - 0.5 \right) \right] 0.29 , \qquad (A.61)$$

and

$$Q_d = \frac{S_{tn}}{24 d_c} . \qquad (A.62)$$

If the bending moment exceeds the cracking moment but not the ultimate strength of the concrete member, the mean crack width is given by

$$W_m = S_m \left(\beta_r \frac{St_n}{E_s} + \epsilon_{sh} \right) , \qquad (A.63)$$

where

W_m = mean crack width (in.),

S_m = mean crack spacing (in.).

The quantity β_r is given by

$$\beta_r = \frac{d_{cr}}{d_{cr} - d_c} \quad . \tag{A.64}$$

If the bending moment exceeds the ultimate strength of the concrete member, the crack width is calculated as

$$W_m = S_m \left(\frac{f_y}{E_s} + \epsilon_{sh} \right) \quad . \tag{A.65}$$

If the compressive forces on the wall exceed the ultimate strength of the wall in compression, cracking will occur. The ultimate strength of the wall in compression is calculated as

$$M_{uc} = 0.39\, h_{wl} C_{str} \left[1.0 - \left(\frac{h_c}{32 h_{wl}} \right)^2 \right] \quad , \tag{A.66}$$

where

M_{uc} = ultimate strength of the wall in compression (lb/in.) and
h_c = height of vault wall (in.).

Cracking because of compression results in a single crack extending through the concrete member; the crack width is one-tenth of the height of the wall section under consideration.

Cracking of a reinforced concrete member may occur also as a result of corrosion of the steel reinforcement. As the concrete surrounding the reinforcement prevents free expansion, the steel-corrosion products will exert pressure within the concrete. Based on elasticity theory (Saada 1974), the magnitude of this internal pressure is approximated using

$$P_i = \frac{\Delta}{r_o} \frac{1}{\left[\frac{1-\mu_r}{E_r} + \frac{(1-\mu_c) r_o^2 + (1+\mu_c) d_{cv}^2}{E_c \left(d_{cv} - r_o^2 \right)} \right]} \quad , \tag{A.67}$$

where

P_i = internal pressure due to corrosion (lb/in.^{2}),
Δ = thickness of the free expansion layer (in.),
r_o = original radius of steel reinforcement (in.),
μ_r = Poisson's ratio of corrosion product (unitless),

d_{cv} = distance from concrete face to center of steel reinforcement (in.),
E_r = modulus of elasticity of corrosion product (lb/in.^{2}).

The thickness of the free expansion layer is given by

$$\Delta = r_e + C_{tc} - r_o \quad , \tag{A.68}$$

where

r_e = radius of remaining steel reinforcement (in.),
C_{tc} = thickness of corrosion layer under conditions of free expansion (in.).

A general series form of the stress function in bipolar coordinates was given by Jeffrey (1920). This function has been applied to the situation of a semi-infinite region with a circular hole under a uniform radius pressure (Fig. A.2). Based on this work, the stress on the surface of the concrete is given by

$$\sigma_x = -4P_i \frac{r_o^2\left(x^2 - d_{cv}^2 + r_o^2\right)}{\left(x^2 + d_{cv}^2 - r_o^2\right)^2} \quad , \tag{A.69}$$

where

σ_x = stress at surface of concrete (lb/in.^{2}),
x = distance from point A (Fig. A.2) along the surface of the concrete (in.).

The point of maximum stress occurs at point A (Fig. A.2), where x = 0. For this case, Eq. (A.69) reduces to

$$\sigma_{xA} = \frac{4P_i r_0^2}{\left(d_{cv}^2 - r_0^2\right)} \quad . \tag{A.70}$$

The tangent stress at any point, Q or Q′, around the circular hole is given by

$$\sigma_{\theta Q} = P_i\left(1 + 2\tan^2\phi\right) \quad , \tag{A.71}$$

where

$\sigma_{\theta Q}$ = tangent stress at point Q (lb/in.^{2}).

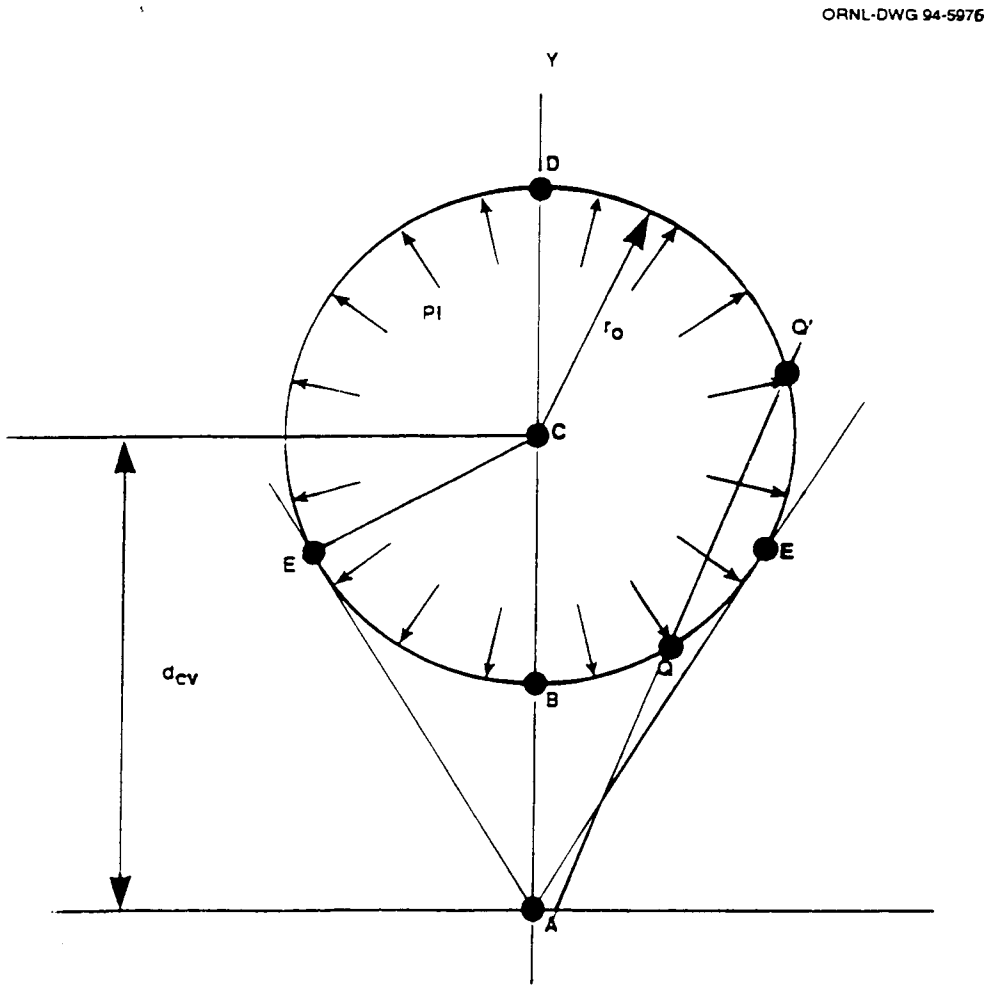

Fig. A.2. Schematic diagram of steel and concrete geometry used in calculating stress resulting from corrosion of steel reinforcement.

This relationship exhibits a maximum tangent stress at point E and is calculated using

$$\sigma_{\theta E} = P_i \frac{d_{cv}^2 + r_o^2}{d_{cv}^2 - r_o^2} \quad , \tag{A.72}$$

where

$\sigma_{\theta E}$ = maximum tangent stress (lb/in.^{2}).

The magnitude of the maximum stress around the circular hole is a function of the ratio of the concrete cover thickness and the radius of the remaining steel reinforcement. The following dependencies are noted:

if $d_{cv} < 1.73r$, $\sigma_{xA} > \sigma_{\theta E} > 2P_i$;
if $d_{cv} = 1.73r$, $\sigma_{xA} = \sigma_{\theta E} = 2P_i$;
if $d_{cv} > 1.73r$, $\sigma_{xA} < \sigma_{\theta E} < 2P_i$.

These relationships provide a simple method for determining where cracking from corrosion will begin.

When the concrete cover thickness is greater than three times the diameter of the reinforcing steel, the tensile stresses around the circular boundary will approach the applied pressure P_i. Plain concrete has minimal tensile strength to resist these stresses—only 6 to 8% of the specified compressive strength of concrete. Consequently, the maximum tension stress can readily exceed the tensile strength of concrete, at which point cracking begins.

Cracking from corrosion is typically initiated internally, along the circular boundary, as the ratio of concrete cover thickness to the original radius of the steel is usually greater than 1.73 (Jeffrey 1920). As corrosion progresses, accompanied by the deterioration of the concrete cover, cracking will propagate towards the surface of the concrete slab. When the tension stress at the concrete surface equals or exceeds the tensile strength of the concrete, the cracking will penetrate the concrete cover. This cracking will occur along the length of the steel reinforcement.

Spalling out of the concrete will occur if the concrete cover over the steel reinforcement is small ($d_{cv} \leq 1.73r_o$). Under these conditions, the stresses at the concrete surface exceed both the stresses at the steel surface and the tensile strength of concrete and spalling along the reinforcement occurs.

A.3.3 Concrete Pad Degradation Model

Tumulus-type disposal facilities may use a steel-reinforced concrete pad upon which disposal vaults are placed. This pad, while intact, should divert water to the leachate collection system. To incorporate the performance of the concrete pad into SOURCE1, a compressive failure model is assumed. Failure is estimated by calculating the reinforcement ratio (Cowan 1982), which is defined by

$$\rho = \left(\frac{A}{b}\right)\frac{1}{d} \quad , \tag{A.73}$$

where

ρ = reinforcement ratio (dimensionless),

$\left(\frac{A}{b}\right)$ = cross-sectional area of steel reinforcement per unit width of slab (m),

d = effective depth of steel (distance from the top of the slab to the center of the steel reinforcement) (m).

The reinforcement ratio at which compressive failure may occur is called the limiting reinforcement ratio and is given by (Cowan 1982):

$$\rho_{lim} = \frac{\epsilon_c'}{\epsilon_c' + \epsilon_y} 0.85\beta_1 \frac{f_c'}{f_y} \quad , \tag{A.74}$$

where

ρ_{lim} = limiting reinforcement ratio (dimensionless),
ϵ_c' = ultimate concrete strain (dimensionless) (for this application, taken as 0.003),
ϵ_y = yield strain of steel (dimensionless),
β_1 = a factor used in the equivalent rectangular stress diagram for concrete at the ultimate load (dimensionless),
f_c' = specified compressive strength of concrete (MPa), and
f_y = specified yield strength of steel reinforcement (MPa).

The yield strain of the steel reinforcement can be calculated by

$$\epsilon_y = \frac{f_y}{E_s} \quad , \tag{A.75}$$

where

E_s = modulus of elasticity of steel reinforcement (MPa) (for this application, taken as 200,000 MPa).

The value of β_1 is determined as follows (Cowan 1982):

$$\beta_1 = 0.85 \text{ for } f_c' \leq 30 \text{ MPa} \quad , \tag{A.76}$$

or

$$\beta_1 = 0.85 - 0.08\left(\frac{f_c' - 30}{10}\right) \text{ for } f_c' > 30 \text{ MPa} \quad . \tag{A.77}$$

The values of the reinforcement ratio and the limiting reinforcement ratio are evaluated at annual time steps in SOURCE1. These two values are compared, and when the reinforcement ratio exceeds the limiting value, the pad is said to have failed hydraulically. Pad failure allows leachate to pass through it. Values of both ρ and ρ_{lim} will change because of the degradation of the concrete. The concrete is simulated to degrade by using the sulfate attack and $Ca(OH)_2$ leaching subroutines in SOURCE1.

Sulfate attack results in the spalling off of the concrete cover on the reinforcing steel. Hence, as the effective depth of the steel decreases, the reinforcement ratio increases. Leaching of $Ca(OH)_2$ from the concrete pad results in reduced concrete strength. Therefore, as the compressive strength of the concrete decreases, the limiting reinforcement ratio decreases. Both of the concrete degradation mechanisms result in a decrease of the margin between the reinforcement ratio and the limiting reinforcement ratio, ultimately resulting in pad failure.

A.3.4 Leachate Collection System Degradation Model

Water that reaches an intact concrete pad of a tumulus-type facility will be diverted to a leachate collection system. This system consists of piping, valves, collection sumps, and monitoring equipment. Ideally, with a properly functioning system, all leachate will be collected, and no release of radionuclides to the environment will occur.

The leachate collection system degradation model describes the functionality fraction of the collection system as a function of time. The functionality fraction is defined as the ratio of the amount of radionuclide in the collected leachate to the total radionuclide release from the disposal vaults and can vary from 0 to 1. With a value of 1, the leachate collection system is fully functional, and no radionuclides are released to the environment. A zero value indicates a fully degraded system that allows all leached radionuclides to be released to the environment.

The initial functionality fraction and the length of the institutional control period are input parameters to the SOURCE1 code. The functionality fraction degrades linearly to zero from the beginning of the simulation until the end of the institutional control period. The degradation of the collection system is assumed to result from piping and valve leaks or failures, flow obstructions within the system, leakage or overflow of collection sumps, degraded monitoring equipment, etc. At the end of the institutional control period, no maintenance of the collection system is assumed to occur. Hence, no credit is taken for the collection system after the end of institutional control. Additionally, if the concrete pad is predicted to fail hydraulically before the end of institutional control, the functionality fraction is set to zero at the time of pad failure.

A.4 FLOW PARTITIONING

A benefit of the concrete engineered barriers used in the tumulus disposal facilities is the material's low hydraulic conductivity. When intact, the concrete largely prevents water from contacting the disposed waste. As the concrete members deteriorate with time, cracks form and greater amounts of water may contact the waste. Eventually, the conductivity of the concrete will be no better than that of the soil backfill around the disposal facility.

To calculate radionuclide releases as a result of advection, it is necessary to estimate the amount of water percolating through the waste. The water entering a disposal area is divided into two components: a component which flows around the disposal facility and a component which contacts the waste.

The flow partitioning scheme used in the SOURCE1 computer code is based on the assumption of a saturated steady-state system under a unit hydraulic gradient. Under these conditions, the amount of water percolating through the intact vaults, silos, and wells is equal to the saturated hydraulic conductivity of the concrete. As the concrete members deteriorate and crack, preferential flow of water through the fractures occurs at much greater rates.

Preliminary analyses conducted with the SOURCE1 computer code have indicated that much of the ability of a disposal facility to exclude water is lost when fractures penetrate through one or more concrete members. Based on these observations, the amount of water percolating through the waste is set equal to the amount of water entering the disposal area when fractures first penetrate the disposal facility. From this point on, the amount of water contacting the waste is solely a function of the hydraulic characteristics of the site soils and soil backfill.

A.5 RADIONUCLIDE RELEASE MODELING

The SOURCE1 code incorporates two mass-transport mechanisms (advection and diffusion) that are modeled in one dimension. The concentration that is calculated to be released by these two mechanisms cannot exceed the solubility limit of the assumed chemical form of a nuclide. Rates of release from disposal facilities which have not undergone significant structural failure will generally be low—that is, below detection limits. These releases are dependent largely on the relative water saturation of the waste and concrete and, for the most part, are the result of diffusion. As a facility deteriorates and undergoes cracking, water may percolate more easily through the waste. Under these conditions, leaching of radionuclides by advection can accelerate and may overshadow leaching by diffusion.

Leaching of radionuclides by advection is directly proportional to the amount of water contacting the waste and inversely proportional to the degree to which radionuclides are sorbed by the waste matrix. An analytical expression in which the radionuclide inventory is updated at preset time steps is used to evaluate advective leaching. Leaching by diffusion is calculated using the FLOTHRU computer program (a subroutine in the SOURCE1 code). A description of these two leaching mechanisms is provided in the following sections.

A.5.1 Advective Transport Model

The analytical model for advective transport is based on work presented in Baes and Sharp (1983). A detailed derivation of the model can be found in Icenhour (1995).

The total radionuclide release during a time step is calculated by the following formula:

$$L = \frac{\lambda_L}{\lambda_L + \lambda_d} Q_o \left[e^{-(\lambda_L + \lambda_d) t_1} - e^{-(\lambda_L + \lambda_d) t_2} \right] , \qquad (A.78)$$

where

L = mass of radionuclide leached because of advection (g),
λ_L = leach rate constant (s^{-1}),
λ_d = radioactive decay constant (s^{-1}),
Q_o = initial mass of radionuclide in the waste (g),
t_1, t_2 = the bounds of the time period of interest (s).

The leach constant, λ_L, is given by

$$\lambda_L = \frac{q}{W\theta R_d} \quad , \tag{A.79}$$

where

q = water infiltration rate (cm/s),
W = waste thickness (cm),
θ = relative saturation (i.e., volume of water in waste/volume of waste) (dimensionless),
R_d = retardation factor (dimensionless).

Finally, the retardation factor, R_d, can be calculated by the following equation:

$$R_d = 1 + \frac{\rho_b}{\theta} K_d \quad , \tag{A.80}$$

where

ρ_b = bulk density of waste (g/cm^3),
K_d = distribution coefficient (mL/g).

A.5.2 Diffusion Transport Model

Consider a two-layer slab representation of a waste disposal unit. The inner layer, which is of half-thickness a, initially contains a contaminant with concentration C_o. The outer layer, which has thickness b – a, is initially uncontaminated. This situation is analogous to the grouted waste initially placed inside an uncontaminated concrete vault (e.g., tumulus-type disposal). If there is little bulk fluid flow through this system, then diffusion will be the dominant transport mechanism. Diffusion equations can then be written for the inner and outer layers of the disposal unit. The concentration of contaminant in the inner layer is denoted by C_1, whereas that in the outer layer is denoted by C_2.

The diffusion equation for the inner layer is

$$\frac{\partial C_1}{\partial t} = D_1 \frac{\partial^2 C_1}{\partial x^2} - \lambda_d C_1 \quad , \tag{A.81}$$

where

C_1 = concentration of contaminant in the inner layer (g/cm^3),
D_1 = effective diffusion coefficient for the contaminant in layer 1 (cm^2/s),
x = spatial position (cm).

Similarly, a diffusion equation can be written for the outer layer:

$$\frac{\partial C_2}{\partial t} = D_2 \frac{\partial^2 C_2}{\partial x^2} - \lambda_d C_2 \quad , \tag{A.82}$$

where

C_2 = concentration of contaminant in the outer layer (g/cm^3),
D_2 = effective diffusion coefficient for the contaminant in layer 2 (cm^2/s).

Equations (A.81) and (A.82) can be solved with appropriate initial and boundary conditions. In this case, the initial conditions are

$$C_1(x, 0) = C_0 \text{ for } 0 \le x < a \quad , \tag{A.83}$$

and

$$C_2(x, 0) = 0 \text{ for } a \le x < b \quad . \tag{A.84}$$

The boundary conditions are

$$\left.\frac{\partial C_1}{\partial x}\right|_{x=0} = 0 \quad , \tag{A.85}$$

$$C_2(b,t) = 0 \quad , \tag{A.86}$$

$$C_1(a,t) = C_2(a,t) \quad , \tag{A.87}$$

and

$$D_1 \left.\frac{\partial C_1}{\partial x}\right|_{x=a} = D_2 \left.\frac{\partial C_2}{\partial x}\right|_{x=a} \quad . \tag{A.88}$$

The solution to Eqs. (A.81) through (A.88) is implemented using the FLOTHRU computer code (ORNL 1994), which is incorporated as a subroutine into the SOURCE1 code.

A.5.3 Calculation of Total Radionuclide Release

To calculate the total amount of radionuclide leaching from a disposal facility using the SOURCE1 code, the advective and diffusive components are determined separately. These two components are then added to calculate the total release. This calculated total is compared with the solubility limit of the radionuclide for the amount of water flowing through the facility. If this limit is exceeded, then the release is limited to the amount determined by solubility.

Radionuclides leached from the waste will be transported away from the disposal facility with the water percolating through the disposal facility. Two flow components are observed on the Oak Ridge Reservation. A vertical component represents recharge to the underlying aquifer at the site, while a lateral subsurface component discharges to surface waters.

Radionuclide releases from the disposal facilities are partitioned between the recharge and lateral flow components in proportion to the vertical and lateral fluxes. The amount of water which flows vertically to the aquifer is calculated as the minimum of the amount of water percolating through the disposal facility and the saturated hydraulic conductivity of the site soils. Water in excess of the saturated hydraulic conductivity is modeled as lateral subsurface flow.

Based on the assumption that radionuclide concentrations are equal in each flow component, the amount of material entering the recharge component in a given month is given as

$$Q_r = Q_t \frac{I_r}{I_m} \quad , \tag{A.89}$$

where

Q_r = radionuclide release entering recharge flow component (g/month),
Q_t = total radionuclide release from disposal facility (g/month),
I_r = vertical water percolation rate (cm/month),
I_m = total water percolation rate (cm/month).

The mass of material entering the lateral flow component is simply the difference of the total release and the mass of material transported to the aquifer. Annual releases for each flow component are calculated by summing the monthly releases.

A.6 REFERENCES

Atkinson, A. 1985. *The Time Dependence of pH Within a Repository for Radioactive Waste Disposal*, AERE-R11777, Harwell Laboratory, Oxfordshire, England.

Atkinson, A., and J. A. Hearne 1984. *An Assessment of the Long-Term Durability of Concrete in Radioactive Waste Repositories*, AERE-R11465, Harwell Laboratory, Oxfordshire, England.

Atkinson, A., and J. A. Hearne 1990. "Mechanistic Model for the Durability of Concrete Barriers Exposed to Sulphate-Bearing Groundwaters," *Mat. Res. Soc. Symp. Proc.* **176**, 149–56.

Baes, C. F. III, and R. D. Sharp 1983. "A Proposal for Estimation of Soil Leaching and Leaching Constants for Use in Assessment Models," *J. Environ. Qual.* **12**(1), 17–28.

Cowan, H. J. 1982. *Design of Reinforced Concrete Structures*, Prentice-Hall, Englewood Cliffs, N.J.

Greenberg, S. A., and T. N. Chang 1965. "Investigation of the Colloidal Hydrated Calcium Silicates. II. Solubility Relationships in the Calcium Oxide-Silica-Water System at 25 D," *J. Phys. Chem.* **69**, 182.

Hausmann, D. A. 1967. "Steel Corrosion in Concrete," *Materials Protection*, November, 19–23.

Icenhour, A. S. 1995. *Analysis of Source Term Modeling for Low-Level Radioactive Waste Performance Assessments*, ORNL/TM-12908, Lockheed Martin Energy Systems, Inc., Oak Ridge Natl. Lab.

Icenhour, A. S., and M. L. Tharp 1996. *User's Manual for the SOURCE1 and SOURCE2 Computer Codes: Models for Evaluating Low-Level Radioactive Waste Disposal Facility Source Terms (Version 2.0)*, ORNL/TM-13035, Lockheed Martin Energy Systems, Inc., Oak Ridge Natl. Lab.

Jeffrey, G. B. 1920. *Plane Stress and Plane Strain in Bipolar Coordinates.*

Langelier, W. F. 1936. "The Analytical Control of Anti-Corrosion Water Treatment," *J. Amer. Water Works Assoc.*, **28**(10), 1500–21.

Lea, F. M. 1970. *The Chemistry of Cement and Concrete*, 3rd ed., Edward Arnold, Ltd., London.

Nawy, E. D. 1966. "Crack Width Control in Welded Fabric Reinforced Centrally Loaded Two-Way Concrete Slabs," presentation at 62nd American Concrete Institute Annual Convention in Philadelphia, March.

ORNL (Oak Ridge National Laboratory) 1994. *Performance Assessment for Continuing and Future Operations at Solid Waste Storage Area 6*, ORNL-6783, Martin Marietta Energy Systems, Inc., Oak Ridge, Tenn.

Saada, A. S. 1974. *Elasticity Theory and Application*, Pergamon, New York.

Shuman, R., N. Chau, and E. A. Jennrich 1992. *The SOURCE Computer Codes: Models for Evaluating the Long-Term Performance of SWSA 6 Disposal Units, Version 1.0: User's Manual*, RAE-9005/8-1, Rogers & Associates Engineering Corporation, Salt Lake City, Utah.

Tuutti, K. 1982. *Corrosion of Steel in Concrete*, Swedish Cement and Concrete Research Institute, Stockholm, Sweden.

Appendix B

TRANSPORT-RELATED PROPERTIES OF RADIONUCLIDES IN WASTE AND CONCRETE USED IN THE PERFORMANCE ASSESSMENT OF THE CLASS L-II DISPOSAL FACILITY

H. W. Godbee
A. S. Icenhour
S. L. Loghry
M. L. Tharp

Appendix B

TRANSPORT-RELATED PROPERTIES OF RADIONUCLIDES IN WASTE AND CONCRETE USED IN THE PERFORMANCE ASSESSMENT OF THE ORNL CLASS L-II DISPOSAL FACILITY

B.1 INTRODUCTION

Modeling radionuclide release rates from a low-level radioactive waste facility involves the use of many parameters, including properties of waste, concrete (the engineered barrier), and pertinent radionuclides. Table B.1 shows many of the necessary transport-related properties used in this performance assessment (PA). While there is a large amount of experimental data in the literature, it is rare to find values for all the properties required in a detailed PA. Further, those found are frequently not at the conditions [e.g., acidity or alkalinity (pH), redox potential (Eh), and concentrations] of interest. If available, data based on accurate inventories, reliable field tests, and carefully controlled laboratory experiments are used in PAs. In the absence of such data, interpolations, extrapolations, and relationships based on experimental results are used. If none of these techniques are available, the procedure used is a correlation based on established theories. A last recourse is empiricism based on established engineering practice. The correlations (based on theories) used in this campaign were selected on the basis of generality and simplicity. The empiricisms used are minor modifications of reliable relationships selected on the basis of overall comprehensiveness.

Table B.1. Transport-related properties of radionuclides in waste and concrete used in the performance assessment of the CIIDF

Constituent	Property	Definition
Waste	Porosity	Volume of voids (air, pore water, etc.) per volume of waste
	Density	Mass of waste per volume of waste
	Chemical type	Inorganic (metal, ceramic, glass, salt, etc.) or organic (cloth, paper, plastic, wood, etc.)
	Nuclide concentration	Amount of nuclide per unit amount of waste
	Ion exchange capacity	Total number of sites available for exchange in the ion exchanger [largely a function of the exchanger (acidic or basic) and the solution pH]

Table B.1 (continued)

Constituent	Property	Definition
Concrete	Porosity	Volume of voids (air, pore water, etc.) per volume of concrete
	Density	Mass of concrete per volume of concrete
	Composition	Portland cement plus additives (e.g., sand, crushed rock, fly ash, clay, etc.)
	Permeability	Amount of a substance which passes through a material under a given hydraulic pressure (head)
Pore water	pH	Negative log of the hydrogen ion activity
	Eh	Measured potential difference between an inert electrode and a reference electrode
	Buffer capacity	Response of a system, in terms of pH change, to the addition of hydrogen (H^+) or hydroxide (OH^-) ions
	Complexation capacity	Formation of a complex from a metal ion with another ion by means of one or more chemical bonds
	Ionic strength	A measure of the concentration of an ion and its charge summed over all ions in the solution
	Dielectric constant	The force of attraction between two charges separated by a fixed distance in a uniform medium
Waste/pore water/concrete	Constrictivity	Choking effect that depends on the shape, size, and size distribution of pore space
	Tortuosity	The ratio of the actual tortuous path length for diffusion to the mathematical (i.e., shortest) diffusion path length
	Geometry factor	Tortuosity squared divided by constrictivity
	Distribution coefficient	The distribution or division of a substance between two layers or materials in a definite constant manner (under given conditions)
	Effective diffusion coefficient	A free diffusion coefficient that may be slowed down or speeded up by physical and chemical effects in a heterogeneous system
Radionuclide	Atomic number	Number of protons in the nucleus of an atom
	Atomic weight	Total number of neutrons and protons making up the nucleus of an atom
	Atomic (or ionic radius)	Closest distance to which an atom or ion will approach another atom or ion of any size under the conditions specified
	Half-life	Time required for half the atoms of identical radioisotopes to undergo radioactive decay

Table B.1 (continued)

Constituent	Property	Definition
	Solubility	Maximum amount of a substance that can dissolve in a solvent under the given conditions
	Limiting equivalent ionic conductivity	Contribution made by each ion species of a salt toward an electrolyte's equivalent conductance in the limit of infinite dilution
	Electronegativity	Relative attraction of an atom for the valence electrons in a covalent bond
	Free diffusion coefficient	Diffusion coefficient of an ion in water, or pore liquid, in the limit of infinite dilution

B.2 BACKGROUND

An understanding of the flux (amount per unit surface area per unit time) from a porous medium requires a knowledge of the properties of the medium that affect transport. The flux of a contaminant is a function of both physical and chemical properties. Physical properties include permeability, porosity, pore distribution, pore geometry, and water content. Chemical properties include those that describe mechanisms for taking contaminants out of or pulling them into the pore solution. These range from weak sorption-desorption (e.g., distribution coefficient) to strong chemical bonds (e.g., solubility product constant). With these properties and computer codes (based on appropriate models), predictions can be made of the flux for a contaminant from various matrices as a function of shape, size, and time. The SOURCE computer codes (SOURCE1 and SOURCE2) used at Oak Ridge National Laboratory (ORNL) (ORNL 1994) for this purpose are examples.

In most cases, values determined by experimentation are not available for the majority of the transport parameters needed to evaluate source terms in the complex systems which most waste disposal facilities represent. In a few cases, values obtained through small-scale experiments and large-scale field tests are available for comparable systems and can be applied with judicious modification. However, in most cases, the needed transport parameters are estimated by the application of equilibrium (e.g., thermodynamic) and kinetic (e.g., diffusion) models to simple heterogeneous systems taken to represent or model the components (e.g., waste and engineered barriers) making up a waste disposal facility. In other words, a transport parameter of a multiphase system is determined from a "mixture law" (relationship or model) that describes its variation with other known or more readily determined properties (measured or estimated from first principles) of the constituents or phases making up the system. This approach to parameter estimation is widely applied to engineering materials that may be considered homogeneously heterogeneous. Examples of such systems include the magnetic properties of composites, the molar heat capacity of solids, and the thermal conductivity of powders.

B.3 TRANSPORT MECHANISMS

In this analysis, the waste and concrete are considered to be unconsolidated and consolidated porous media, respectively. The transport of various species through such media can usually be analyzed and explained in terms of advection and diffusion. In this study, the dominant transport mechanism is assumed to be either advection or diffusion, depending on the leaching time. For example, if there is little to no water movement through the waste (i.e., before vault failure), diffusion dominates the radionuclide transport. However, after the concrete cracks and water can contact the porous, grouted waste, advection dominates the transport process. (Note that the SOURCE1 computer code used in this PA calculates the release rate by advection and diffusion and compares that value to the solubility limit of the particular species. If the calculated release rate exceeds the solubility limit, then the solubility limit is used to determine the release rate.)

B.3.1 Advection

Release of radionuclides resulting from advection can be modeled using a first-order leaching process accounting for both sorption and decay (Icenhour 1995). Advective leaching is proportional to the amount of water contacting the waste and concrete, and it is inversely proportional to the degree to which the radionuclides are retained by the waste and concrete matrices. For this model, the radionuclide inventory is assumed to be homogeneously mixed within a finite waste volume that is contacted by a constant infiltration rate of water. The first-order advection equation is given by (Icenhour 1995).

$$L = \frac{\lambda_L}{\lambda_L + \lambda_d} Q_o \left[e^{-(\lambda_L + \lambda_d)t_1} - e^{-(\lambda_L + \lambda_d)t_2} \right] , \qquad \text{(B.1)}$$

where

L = mass of radionuclide leached because of advection (g),
λ_L = leach rate constant (s^{-1}),
λ_d = radioactive decay constant (s^{-1}),
Q_o = initial mass of radionuclide in the waste (g),
t_1, t_2 = the bounds of the time period of interest (s).

The leach rate constant, λ_L, is given by (Icenhour 1995)

$$\lambda_L = \frac{q}{W\theta R_d} , \qquad \text{(B.2)}$$

where

q = water infiltration rate (cm/s),
W = waste thickness (cm),
θ = relative saturation (i.e., volume of water in waste/volume of waste) (dimensionless),
R_d = retardation factor (dimensionless).

Finally, the retardation factor, R_d, can be calculated by the following equation (Icenhour 1995):

$$R_d = 1 + \frac{\rho_b}{\theta} K_d \quad , \tag{B.3}$$

where

ρ_b = bulk density of waste (g/cm^3),
K_d = distribution coefficient (mL/g).

B.3.2 Diffusion

In addition to advection, the transport of various species through cement-based waste forms can also be analyzed and explained in terms of effective diffusion coefficients (Atkinson, Nelson, and Valentine 1986; Johnston and Wilmot 1992; Godbee et al. 1993). This coefficient for a given species with no solubility constraint can be expressed as (Godbee et al. 1993)

$$D = \frac{D_f}{G(1 + K)H^{-1}} \quad , \tag{B.4}$$

where

D = effective diffusion coefficient for the species in the porous body (cm^2/s),
D_f = diffusion coefficient of the species in an infinite or free volume of pore liquid (cm^2/s),
G = geometry (or matrix) factor (dimensionless),
K = distribution coefficient (dimensionless),
H = relative saturation of pores with liquid (dimensionless).

meaning, and independent methods to determine them are available. Tortuosity is a parameter characterizing the asymmetry of the pore space, whereas constrictivity is a factor which depends on the shape, size, and size distribution of the pore space. Thus, G generally represents a physical containment (retardation) factor of the matrix. The expression (1 + K) can account for phenomena such as sorption/desorption and ion exchange. Thus, (1 + K) represents a chemical containment (retardation) factor. Table B.2 shows the relationship of K to other commonly measured distribution

coefficients which have mixed units. Relative pore saturation is the ratio of the water (liquid) volume actually in the pores to the water (liquid) volume in the pores when full. Thus, H represents a retardation factor reflecting the inventory of the transport medium (liquid).

Table B.2. Relationship of the dimensionless distribution coefficient (K) to some other commonly measured distribution coefficients[a]

Types of distribution coefficient	Units of distribution coefficient	Relationship of K
Mixed,[a] K_{MP}	$\frac{\text{amount of species/mass of pore-free solid}}{\text{amount of species/volume of liquid}}$	$K = \rho_p \left(\frac{1 - \epsilon}{\epsilon} \right) K_{MP}$
Mixed,[b] K_{MB}	$\frac{\text{amount of species/mass of porous body}}{\text{amount of species/volume of liquid}}$	$K = \rho_b \left(\frac{1}{\epsilon} \right) K_{MB}$
Volume, K_{VV}	$\frac{\text{amount of species/volume of pore-free solid}}{\text{amount of species/volume of liquid}}$	$K = \left(\frac{1 - \epsilon}{\epsilon} \right) K_{VV}$
Geometry, K_{GV}	$\frac{\text{amount of species/volume of porous body}}{\text{amount of species/volume of liquid}}$	$K = \left(\frac{1}{\epsilon} \right) K_{GV}$

[a] ρ_p is the density of the pore-free solid (i.e., mass of pore-free solid/volume of pore-free solid). ϵ is the void fraction (i.e., volume of pores/volume of porous body).
[b] ρ_b is the density of the porous body (mass of porous body/volume of porous body).
Source: Godbee et al. 1993.

If there is a solubility constraint for a species (i.e., the pore liquid can be saturated) the expression (1 + K) is replaced by β^{-2}, where β is defined as the relative saturation concentration of that species in the porous body. The diffusion coefficient for a given species with a solubility constraint can be expressed as (Godbee et al. 1993)

$$D = \frac{D_f}{G(\beta^{-2})H^{-1}} \quad . \tag{B.5}$$

The relative solubility constraint is calculated using the relationship (Godbee et al. 1993)

$$\beta = (S_L)(V/A_o)(\epsilon)(\rho)(H) \quad , \tag{B.6}$$

where

S_L = solubility limit of species in pore liquid (g of species/g of pore liquid),
V = volume of waste form (porous body) (cm^3),
A_o = initial amount of radionuclide (g),
ϵ = average open-pore void fraction (dimensionless),
ρ = density of liquid (g/cm^3).

Species treated as solubility constrained were Be (as BeO), Pd (as PdO), and Pb [as $PbCl_2 \cdot Pb(OH)_2$]. When necessary (i.e., data needed for the previous methods are unavailable), corrosion rate data can be used to estimate an effective diffusion coefficient (Godbee 1974) by

$$D = \pi \left[\left(\frac{a_n}{A_0} \right) \left(\frac{V}{S} \right) \left(\frac{1}{t_n} \right) \right]^2 \frac{t_n}{2} \quad , \tag{B.7}$$

where

a_n = amount leached during time interval t_n (g),
t_n = duration of leaching interval (s),
S = surface area of sample in contact with leachant (cm^3).

The term in brackets represents a penetration or corrosion rate (length/time). This corrosion-rate approach for estimating a D was used with the metals Al (2 mil/year), Co (1 mil/year), and Cd (3 mil/year).

Speaking broadly, if possible, the distribution coefficients used in Eqs. (B.3) and (B.4) should be determined from leaching tests that determine both a diffusion coefficient and a distribution coefficient, namely, those that approach equilibrium or steady state. Frequently, tests for distribution coefficients that involve grinding the sample and shaking it in a fixed liquid volume (e.g., conventional batch method) or crushing the sample and flowing liquid over it (e.g., conventional column method) often give results that are different from those obtained in diffusion experiments. Among the reasons for this difference is that batch and column tests (because of crushing, grinding, flow, etc.) may not adequately mimic the surface and pore solution conditions of the porous medium in bulk form.

In this campaign, the distribution coefficients to be used in correlative expressions were obtained from leaching tests carried out at ORNL (Mrochek, Gilliam, and McDaniel 1986) and Pacific Northwest Laboratory (PNL) (Serne et al. 1987). Diffusion (effective) and distribution (dimensionless) coefficients were evaluated from the data using an equation that describes the test configuration (Crank 1993) mathematically (i.e., diffusion into a limited volume of leachant). The expression is of the form (Godbee et al. 1989)

$$\frac{A_t}{A_o - A_f} = 1 - \sum_{n=1}^{\infty} \frac{6\alpha(\alpha + 1)\exp\left[-Dq_n^2 t/9(V/S)^2\right]}{9 + 9\alpha + q_n^2 \alpha^2} , \tag{B.8}$$

where the q_ns are the nonzero positive roots of

$$\tan q_n = \frac{3q_n}{3 + \alpha q_n^2} \tag{B.9}$$

and

A_t = total amount leached in time t, mg (μCi),
A_o = initial amount in specimen, mg (μCi),
A_f = amount in specimen at equilibrium, mg (μCi),
D = effective diffusion coefficient (cm^2/s),
t = time (s),
V = volume of specimen (cm^3),
S = surface area (geometric) of specimen (cm^2),
$\alpha = \frac{V_L}{\epsilon KV} = \frac{A_o - A_f}{A_f}$ (dimensionless),
V_L = volume of leachant (cm^3),
ϵ = void fraction (porosity) (dimensionless),
K = distribution coefficient (dimensionless).

Rearrangement of the expressions given for α above shows that

$$K = \frac{\left(\frac{A_f}{V}\right)}{\epsilon\left(\frac{A_o - A_f}{V_L}\right)} . \tag{B.10}$$

The parameters A_o, V, S, and ϵ are properties of the specimen, whereas V_L is a property of the leachant. All are determined at the beginning of the experiment. The parameter A_t is a property of the system and is generated during the experiment as a function of time t. The specimen properties D and A_f are evaluated by fitting the data [$A_t(t)$] to Eq. (B.8). A value for K is then obtained using Eq. (B.10).

The ORNL and PNL experimental data cited above were fitted to Eq. (B.8) using the computer program NEWBOX (Nestor, Godbee, and Joy forthcoming) developed at ORNL. NEWBOX, which is executable on a personal computer, calculates the fractional release of material from four different geometrical shapes (semi-infinite medium; finite slab; finite, circular cylinder; and sphere) and accounts for several different boundary conditions.

The solution of mass transport equations (e.g., Fick's first and second laws), subject to appropriate initial and boundary conditions, are usually nonlinear in some parameters (diffusion coefficient, reaction rate constants, etc.). Thus, use of a method of parameter adjustment involving first partial derivatives can be complicated and prone to errors in the computation of the derivatives. In addition, the parameters must satisfy certain constraints; for example, the diffusion coefficient must remain positive. For these reasons, a variant of the constrained simplex method (Box, Davies, and Swann 1969) is used in NEWBOX to estimate parameters. It is similar, but not identical, to the downhill simplex method (Nelder and Mead 1965). In general, NEWBOX calculates the fraction of material transferred as a function of time from an expression obtained by the inversion (Abramowitz and Stegun 1964) of the Laplace transform of the fraction transferred, rather than by taking derivatives of a calculated concentration profile.

Under certain conditions, some nuclides (e.g., Pd, Th, and Zr) may have low solubilities such that they are transported (by both advection and diffusion) at a rate which is limited by their solubilities. If the pore liquid concentration of a species is at its solubility limit concentration, the effective diffusion coefficient D is calculated using Eq. (B.5). In this case, the relative solubility constraint β is evaluated with Eq. (B.6) using solubility limit data from the literature.

In many cases, a geometry factor G [e.g., in Eqs. (B.4) and (B.5)] is not available for a nuclide of concern in the environment of interest. In this campaign, a semiempirical expression is used for estimating geometry factors of related (i.e., similar chemical and physical characteristics) nuclides in the same porous medium, namely (Godbee 1996),

$$G_x = G_a \left(\frac{r_x}{r_a} \right)^2 , \qquad \text{(B.11)}$$

where

G_x = geometry (matrix) factor of nuclide to be estimated (dimensionless),

G_a = geometry factor of known similar (e.g., chemical group, oxidation state, etc.) nuclide (dimensionless),

r_x = ionic radius of x (Å),

r_a = ionic radius of a (Å).

The relationship is derived largely from an analysis of the data in Mrochek, Gilliam, and McDaniel (1986) and Serne et al. (1987) when fitted to Eq. (B.8).

An empirical correlation is used for estimating geometry factors of the same nuclide in related (i.e., comparable physical retardation factors) porous media. The expression is based on one of the earliest and simplest concepts to relate geometry factor and porosity (Brown et al. 1950), namely,

$$G_x = G_a \left(\frac{\epsilon_a}{\epsilon_x} \right)^2 \left(\frac{1 - \epsilon_x}{1 - \epsilon_a} \right) , \tag{B.12}$$

where

ϵ_a = porosity of medium a (dimensionless),
ϵ_x = porosity of medium x (dimensionless).

Often a distribution coefficient K is not available for a nuclide of concern in the environment of interest. In a manner similar to that used with G, an unsophisticated semiempirical expression [based on an analysis of the data in Mrochek, Gilliam, and McDaniel (1986) and Serne et al. (1987) coupled with the rules for ionic selectivity summarized in Lin (1973)] is used to estimate the needed distribution coefficient from that of a similar nuclide (i.e., same chemical family or group, oxidation state, etc.). The form of the relationship is

$$K_x = K_a \left(\frac{Z_x}{Z_a} \right) , \tag{B.13}$$

where

K_x = distribution coefficient of nuclide to be estimated (dimensionless),
K_a = distribution coefficient of known similar nuclide (dimensionless),
Z_x = atomic number of nuclide x (dimensionless),
Z_a = atomic number of nuclide a (dimensionless).

A correlation that allows the distribution coefficient of a given nuclide in a porous medium to be transposed to a different (but comparable) porous medium is required. The elementary relationship used in this campaign is

$$K_x = K_a \left(\frac{1 - \epsilon_x}{1 - \epsilon_a} \right) \left(\frac{I_x}{I_a} \right) , \tag{B.14}$$

where

K_x = distribution coefficient of nuclide to be estimated (dimensionless),
K_a = distribution coefficient of nuclide in medium a (dimensionless),
ϵ_x = porosity of medium x (dimensionless),
ϵ_a = porosity of medium a (dimensionless),
I_x = number (n) of ion exchange sites per volume of medium x (n/cm^3),
I_a = number (n) of ion exchange sites per volume of medium a, (n/cm^3).

In this campaign, largely because of the dearth of information, a value of 1.0 for I_x / I_a is considered to be reasonable, except for the alkali metals, in which case it is assumed to be proportional to the average pH of the two media.

The free-diffusion coefficient D_f, sometimes referred to as the self-diffusion coefficient (Godbee 1996), is a property of the nuclide in the pore liquid. In other words, it is the diffusion coefficient of the nuclide in the pore liquid if the nuclide is free of the constraints imposed by surfaces, ionic (molecular) filtration, dead-end pores, etc. The free-diffusion coefficients in this campaign were taken from an embryonic database on mass transport parameters compiled at ORNL (Loghry 1995). The majority of the D_f values in this database were obtained from the literature. However, when not readily available, they are calculated* using the Nernst-Einstein equation (Atkins 1990), namely,

$$D_f = \left(\frac{RT}{F^2}\right)\left(\frac{\lambda}{z}\right) \quad , \tag{B.15}$$

where

R = gas constant (8.3144 J K^{-1} mol^{-1}),
T = absolute temperature (K),
F = Faraday constant (9.6493×10^4 C/mol),
λ = equivalent ionic conductance (cm^2 S mol^{-1}),
z = charge number of the ion.

In Eq. (B.15), note that the elementary entity used in a mole (mol) is an electron. Values for λ are available in handbooks on physical chemistry, the literature on electrochemistry, and the ORNL database previously mentioned (Loghry 1995).

In this campaign, the value of H (relative saturation of the pores) is set equal to 1.0. In other words, the pores are full of liquid. Saturation is usually assumed in PAs so that a predicted release is conservative (i.e., higher than if $H < 1.0$).

*S. L. Loghry, Oak Ridge Natl. Lab., "Property Summary," correspondence to H. W. Godbee, Delta-21 Resources, Inc., Oak Ridge, Tenn., July 7, 1995.

B.4 SUMMARY AND CONCLUSIONS

The direct results of the methodology described in this appendix are estimates of the needed diffusion and distribution coefficients for the radionuclides considered in this PA. Further detail on this step-by-step procedure to estimate mass transport parameters when experimental data are not available can be found in Godbee 1996. In summary, this methodology basically involves the use of three kinds of relationships (arranged in a hierarchy of preference):

1. expressions based on established theories that relate a parameter to more fundamental physicochemical properties of the materials making up the system [e.g., Eq. (B.15) for D_f];
2. correlations based on the statistically meaningful analyses of reliable experimental data on similar systems [e.g., Eq. (B.13) for K]; and
3. empiricisms based on engineering judgment derived from experience with related applications [e.g., Eq. (B.11) for G].

The estimated transport parameters used in the Class L-II Disposal Facility (CIIDF) PA are presented in Table B.3, Table B.4, and Table B.5. Parameters for some elements were previously published in Lee et al. (1994). Additional calculations for other elements are detailed in Godbee (1996). The methodology outlined in this appendix was used in developing all of the parameters presented in Table B.3, Table B.4, and Table B.5. The estimated values in those tables appear to be reasonable and should be applicable to assessment studies in the absence of system-specific experimental results (compare Serne et al. 1993). These conclusions are supported largely by the following:

- The values are within the range of experimental results available in the literature for such (or comparable) species in porous media.
- The values are based on representative and internally consistent ancillary parameters which are combined using relationships that range from those grounded in established theories to those rooted in defensible empiricism.
- The values are recognized as estimates of parameters that have unequivocal meaning only in the system in which they are intended to be surrogates for experimental results.

Table B.3. Distribution coefficients and solubility limits of elements evaluated in the CIIDF performance assessment

Element	Formula	Solubility[a] (mol/L)	Waste distribution coefficient[b]		Concrete distribution coefficient[b]	
			K (dimensionless)	K_d (mL/g)	K (dimensionless)	K_d (mL/g)
H	T_2O	1.11×10^{2}	1.00×10^{0}	1.99×10^{-1}	1.00×10^{0}	6.51×10^{-2}
Be	BeO	2.88×10^{-6}	1.57×10^{7}	3.12×10^{6}	2.70×10^{-1}	1.73×10^{-2}
C	$BaCO_3$	1.11×10^{-4}	5.50×10^{0}	1.09×10^{0}	5.50×10^{0}	3.58×10^{-1}
Al	Al	5.24×10^{0}	1.00×10^{6}	1.99×10^{5}	2.50×10^{1}	1.63×10^{0}
Cl	KCl	4.61×10^{0}	1.00×10^{0}	1.99×10^{-1}	1.00×10^{0}	6.51×10^{-2}
K	KCl	4.61×10^{0}	3.50×10^{1}	3.98×10^{0}	6.90×10^{1}	5.07×10^{0}
Ca	$CaCO_3$	1.40×10^{-4}	2.32×10^{1}	4.61×10^{0}	3.05×10^{1}	1.96×10^{0}
Co	Co	3.46×10^{0}	2.00×10^{7}	3.97×10^{6}	7.60×10^{1}	4.95×10^{0}
Ni	$NiCO_3$	7.83×10^{-4}	3.20×10^{1}	6.36×10^{0}	4.20×10^{1}	2.73×10^{0}
Se	$NaSeO_4$	2.88×10^{0}	1.00×10^{0}	1.99×10^{-1}	1.00×10^{0}	6.51×10^{-2}
Rb	Rb_2CO_3	1.44×10^{1}	6.70×10^{1}	1.33×10^{1}	1.35×10^{2}	8.65×10^{0}
Sr	$SrCO_3$	7.45×10^{-5}	4.40×10^{1}	8.74×10^{0}	5.80×10^{1}	3.78×10^{0}
Zr	$Zr(OH)_4$	1.26×10^{-3}	2.50×10^{2}	4.97×10^{1}	3.25×10^{2}	2.08×10^{1}
Nb	$NbOF_3$-2KF	2.60×10^{-1}	1.20×10^{2}	2.38×10^{1}	1.60×10^{2}	1.04×10^{1}
Tc	NH_4TcO_4	9.11×10^{-2}	6.50×10^{0}	1.29×10^{0}	6.50×10^{0}	4.23×10^{-1}
Pd	PdO	8.69×10^{-8}	7.21×10^{6}	1.43×10^{6}	1.09×10^{2}	6.99×10^{0}
Cd	Cd	7.64×10^{0}	2.00×10^{6}	3.97×10^{5}	7.60×10^{1}	4.95×10^{0}
Sn	$SnCl_2$	1.37×10^{1}	5.80×10^{1}	1.15×10^{1}	7.60×10^{1}	4.95×10^{0}
I	KI	7.68×10^{0}	1.00×10^{0}	1.99×10^{-1}	1.00×10^{0}	6.51×10^{-2}
Cs	Cs_2CO_3	1.60×10^{1}	1.00×10^{2}	1.99×10^{1}	2.00×10^{2}	1.30×10^{1}
Sm	$Sm(C_2O_4)$	7.25×10^{-7}	1.90×10^{1}	3.78×10^{0}	2.50×10^{1}	1.63×10^{0}
Eu	Eu_2O_3	2.84×10^{-6}	1.90×10^{1}	3.78×10^{0}	2.50×10^{1}	1.63×10^{0}
Bi	$Bi(OH)_3$	5.40×10^{-6}	2.41×10^{1}	4.79×10^{0}	3.15×10^{1}	2.02×10^{0}
Pb	$PbCl_2 \bullet Pb(OH)_2$	1.46×10^{-4}	2.29×10^{2}	4.55×10^{1}	2.98×10^{2}	1.91×10^{1}
Ra	$RaSO_4$	6.21×10^{-8}	1.00×10^{2}	1.99×10^{1}	1.30×10^{2}	8.47×10^{0}
Th	ThO_2	7.57×10^{-8}	2.70×10^{2}	5.36×10^{1}	3.50×10^{2}	2.28×10^{1}
Pa	PaO_2	5.34×10^{-4}	2.75×10^{2}	5.47×10^{1}	3.60×10^{2}	2.31×10^{1}
U	UO_2	1.46×10^{-6}	2.80×10^{2}	5.56×10^{1}	3.70×10^{2}	2.41×10^{1}
Np	Np_2O_3	4.05×10^{-5}	2.80×10^{2}	5.56×10^{1}	3.70×10^{2}	2.41×10^{1}
Pu	PuO_2	1.71×10^{-8}	2.90×10^{2}	5.76×10^{1}	3.80×10^{2}	2.47×10^{1}
Am	Am_2O_3	3.27×10^{-6}	2.90×10^{2}	5.76×10^{1}	3.80×10^{2}	2.47×10^{1}
Cm	Cm_2O_3	2.84×10^{-6}	2.90×10^{2}	5.76×10^{1}	3.80×10^{2}	2.47×10^{1}
Cf	$Cf(NO_3)_3$	3.49×10^{0}	3.00×10^{2}	5.96×10^{1}	3.90×10^{2}	2.54×10^{1}

[a]*Sources:* D. R. Lide, ed., *CRC Handbook of Chemistry and Physics*, 73rd ed., CRC Press, Boca Raton, Fla., 1992; Freie Universität Berlin and Institut für Anorganische und Analytische Chemie, *Solubility and Speciation of Actinides in Salt Solutions and Migration Experiments of Intermediate Level Waste in Salt Formations*, FUB/FI 53132-415/85, 1986; M. Schweingruber, *Actinide Solubility in Deep Groundwaters—Estimates for Upper Limits Based on Chemical Equilibrium Calculations*, EIR-Bericht Nr. 507, EIDG Institut für Reaktorforschung, Würenlingen, Switzerland, 1983; Agence Internationale de l'Energie Atomique, *Seminaire sur les Techniques d'Etude et les Methodes d'Evaluation des Sites en vue du Stockage Definitif Souterrain des Dechets Radioactifs*, IAEA-SR-104/25, Vienna, 1984; I. G. McKinley and W. R. Alexander, "A Review of the Use of Natural Analogues to Test Performance Assessment Models of a Cementitious Near Field," *Waste Manage.* **12**, 253–59 (1992).

[b]Sources: H. A. Friedman and A. D. Kelmers, *Laboratory Measurement of Radionuclide Sorption in Solid Waste Storage Area 6 Soil/Groundwater Systems*, ORNL-TM-10561, Martin Marietta Energy Systems, Inc., Oak Ridge Natl. Lab. 1990; I. Neretnieks, "Diffusivities of Some Constituents in Compacted Wet Bentonite Clay and the Impact on Radionuclide Migration in the Buffer," *Nucl. Tech.* **71**, 458–70 (1985).

Table B.4. Transport parameters used to calculate diffusion coefficients for waste (D_w)

Element	Self-diffusion coefficient D_f^b (m^2/s)[b]	Transport parameters (dimensionless) for D_w[a]			Waste diffusion coefficient D_w (m^2/s)
		Geometry factor G	Distribution coefficient K	Retardation factor R	
H	9.31×10^{-9}	1.20×10^{0}	1.00×10^{0}	2.40×10^{0}	3.88×10^{-9}
Be	5.99×10^{-10}	1.10×10^{0}	1.57×10^{7}	1.73×10^{7}	3.46×10^{-17}
C	9.20×10^{-10}	9.80×10^{0}	5.50×10^{0}	6.37×10^{1}	1.44×10^{-11}
Al	6.20×10^{-10}	5.00×10^{0}	1.00×10^{6}	5.00×10^{6}	1.24×10^{-16}
Cl	2.03×10^{-9}	3.00×10^{0}	1.00×10^{0}	6.00×10^{0}	3.38×10^{-10}
K	1.96×10^{-9}	4.30×10^{0}	3.50×10^{1}	1.55×10^{2}	1.26×10^{-11}
Ca	7.93×10^{-10}	1.05×10^{0}	2.32×10^{1}	2.54×10^{1}	3.12×10^{-11}
Co	7.30×10^{-10}	2.20×10^{0}	2.00×10^{7}	4.40×10^{7}	1.66×10^{-17}
Ni	7.30×10^{-10}	2.20×10^{0}	3.20×10^{1}	7.26×10^{1}	1.01×10^{-11}
Se	1.06×10^{-9}	7.70×10^{0}	1.00×10^{0}	1.54×10^{1}	6.88×10^{-11}
Rb	2.07×10^{-9}	2.70×10^{0}	6.70×10^{1}	1.84×10^{2}	1.12×10^{-11}
Sr	7.90×10^{-10}	1.50×10^{0}	4.40×10^{1}	6.75×10^{1}	1.17×10^{-11}
Zr	7.92×10^{-10}	6.70×10^{0}	2.50×10^{2}	1.68×10^{3}	4.71×10^{-13}
Nb	4.84×10^{-10}	5.80×10^{1}	1.20×10^{2}	7.02×10^{3}	6.90×10^{-14}
Tc	1.50×10^{-9}	1.60×10^{1}	6.50×10^{0}	1.20×10^{2}	1.25×10^{-11}
Pd	7.50×10^{-10}	3.20×10^{0}	7.21×10^{6}	2.31×10^{7}	3.25×10^{-17}
Cd	7.00×10^{-10}	1.50×10^{0}	2.00×10^{6}	3.00×10^{6}	2.33×10^{-16}
Sn	7.05×10^{-10}	2.20×10^{0}	5.80×10^{1}	1.30×10^{2}	5.43×10^{-12}
I	2.05×10^{-9}	3.00×10^{0}	1.00×10^{0}	6.00×10^{0}	3.42×10^{-10}
Cs	2.06×10^{-9}	3.00×10^{0}	1.00×10^{2}	3.03×10^{2}	6.80×10^{-12}
Sm	6.20×10^{-10}	3.90×10^{1}	1.90×10^{1}	7.80×10^{2}	7.95×10^{-13}
Eu	6.20×10^{-10}	3.90×10^{1}	1.90×10^{1}	7.80×10^{2}	7.95×10^{-13}
Bi	8.10×10^{-10}	1.53×10^{1}	2.41×10^{1}	3.84×10^{2}	2.12×10^{-12}
Pb	8.05×10^{-10}	5.30×10^{1}	2.29×10^{2}	1.21×10^{4}	6.63×10^{-14}
Ra	8.70×10^{-10}	2.10×10^{1}	1.00×10^{2}	2.12×10^{3}	4.10×10^{-13}
Th	5.10×10^{-10}	5.80×10^{1}	2.70×10^{2}	1.57×10^{4}	3.24×10^{-14}
Pa	5.10×10^{-10}	5.80×10^{1}	2.75×10^{2}	1.60×10^{4}	3.19×10^{-14}
U	5.07×10^{-10}	5.80×10^{1}	2.80×10^{2}	1.63×10^{4}	3.11×10^{-14}
Np	5.07×10^{-10}	5.80×10^{1}	2.80×10^{2}	1.63×10^{4}	3.11×10^{-14}
Pu	5.07×10^{-10}	5.80×10^{1}	2.90×10^{2}	1.69×10^{4}	3.00×10^{-14}
Am	6.20×10^{-10}	3.90×10^{1}	2.90×10^{2}	1.13×10^{4}	5.46×10^{-14}
Cm	6.20×10^{-10}	3.90×10^{1}	2.90×10^{2}	1.13×10^{4}	5.46×10^{-14}
Cf	6.20×10^{-10}	3.90×10^{1}	3.00×10^{2}	1.17×10^{4}	5.28×10^{-14}

[a] $D_w = D_s/R$ where $R = G(1 + K)H^{-1}$. The term H is defined as the relative saturation of the pores with water. The pores are assumed to be full in the calculations shown in this table; that is, H = 1.0.

[b] *Sources*: D. G. Miller, *Estimation of Tracer Diffusion Coefficients of Ions in Aqueous Solution*, UCRL-53319, Lawrence Livermore Laboratory, University of California, Livermore, Calif., 1982; C. J. Geankoplis, *Mass Transport Phenomena*, Holt, Rinehart and Winston, New York, 1972; F. Kepak, "Adsorption and Colloidal Properties of Radioactive Elements in Trace Concentrations," *Chem. Rev.* **71**(4), 1972; E. L. Cussler, *Diffusion—Mass Transfer in Fluid Systems*, Cambridge University Press, New York, 1984; *CRC Handbook of Chemistry and Physics*, ed. D. R. Lide, 74th ed., CRC Press, Boca Raton, Fla., 1993; *Lange's Handbook of Chemistry*, ed. J. A. Dean, 14th ed., McGraw-Hill, New York, 1992.

Table B.5. Transport parameters used to calculate diffusion coefficients for concrete (D_c)

Element	Self-diffusion coefficient D_f (m^2/s)[b]	Transport parameters (dimensionless) for D_c[a]			Concrete diffusion coefficient D_c (m^2/s)
		Geometry factor G	Distribution coefficient K	Retardation factor R	
H	9.31×10^{-9}	2.50×10^{0}	1.00×10^{0}	5.00×10^{0}	1.86×10^{-9}
Be	5.99×10^{-10}	7.20×10^{0}	2.70×10^{-1}	9.14×10^{0}	6.55×10^{-11}
C	9.20×10^{-10}	6.50×10^{1}	5.50×10^{0}	4.23×10^{2}	2.18×10^{-12}
Al	6.20×10^{-10}	3.30×10^{1}	2.50×10^{1}	8.58×10^{2}	7.23×10^{-13}
Cl	2.03×10^{-9}	2.00×10^{1}	1.00×10^{0}	4.00×10^{1}	5.08×10^{-11}
K	1.96×10^{-9}	2.90×10^{1}	6.90×10^{1}	2.03×10^{3}	9.66×10^{-13}
Ca	7.93×10^{-10}	7.44×10^{0}	3.05×10^{1}	2.34×10^{2}	3.38×10^{-12}
Co	7.30×10^{-10}	1.40×10^{1}	7.60×10^{1}	1.08×10^{3}	6.77×10^{-13}
Ni	7.30×10^{-10}	1.40×10^{1}	4.20×10^{1}	6.02×10^{2}	1.21×10^{-12}
Se	1.06×10^{-9}	5.20×10^{1}	1.00×10^{0}	1.04×10^{2}	1.02×10^{-11}
Rb	2.07×10^{-9}	1.80×10^{1}	1.35×10^{2}	2.45×10^{3}	8.46×10^{-13}
Sr	7.90×10^{-10}	1.00×10^{1}	5.80×10^{1}	5.90×10^{2}	1.34×10^{-12}
Zr	7.92×10^{-10}	4.50×10^{1}	3.25×10^{2}	1.46×10^{4}	5.42×10^{-14}
Nb	4.84×10^{-10}	3.90×10^{2}	1.60×10^{2}	6.28×10^{4}	7.71×10^{-15}
Tc	1.50×10^{-9}	1.10×10^{2}	6.50×10^{0}	8.25×10^{2}	1.82×10^{-12}
Pd	7.50×10^{-10}	2.00×10^{1}	1.09×10^{2}	2.18×10^{3}	3.44×10^{-13}
Cd	7.00×10^{-10}	1.00×10^{1}	7.60×10^{1}	7.70×10^{2}	9.09×10^{-13}
Sn	7.05×10^{-10}	1.40×10^{1}	7.60×10^{1}	1.08×10^{3}	6.54×10^{-13}
I	2.05×10^{-9}	2.00×10^{1}	1.00×10^{0}	4.00×10^{1}	5.13×10^{-11}
Cs	2.06×10^{-9}	2.00×10^{1}	2.00×10^{2}	4.02×10^{3}	5.12×10^{-13}
Sm	6.20×10^{-10}	2.60×10^{2}	2.50×10^{1}	6.76×10^{3}	9.17×10^{-14}
Eu	6.20×10^{-10}	2.60×10^{2}	2.50×10^{1}	6.76×10^{3}	9.17×10^{-14}
Bi	8.10×10^{-10}	1.09×10^{2}	3.15×10^{1}	3.54×10^{3}	2.30×10^{-13}
Pb	8.05×10^{-10}	3.48×10^{2}	2.98×10^{2}	1.04×10^{5}	7.76×10^{-15}
Ra	8.70×10^{-10}	1.40×10^{2}	1.30×10^{2}	1.83×10^{4}	4.74×10^{-14}
Th	5.10×10^{-10}	3.90×10^{2}	3.50×10^{2}	1.37×10^{5}	3.73×10^{-15}
Pa	5.10×10^{-10}	3.90×10^{2}	3.60×10^{2}	1.40×10^{5}	3.63×10^{-15}
U	5.07×10^{-10}	3.90×10^{2}	3.70×10^{2}	1.45×10^{5}	3.50×10^{-15}
Np	5.07×10^{-10}	3.90×10^{2}	3.70×10^{2}	1.45×10^{5}	3.50×10^{-15}
Pu	5.07×10^{-10}	3.90×10^{2}	3.80×10^{2}	1.49×10^{5}	3.41×10^{-15}
Am	6.20×10^{-10}	2.60×10^{2}	3.80×10^{2}	9.91×10^{4}	6.26×10^{-15}
Cm	6.20×10^{-10}	2.60×10^{2}	3.80×10^{2}	9.91×10^{4}	6.26×10^{-15}
Cf	6.20×10^{-10}	2.60×10^{2}	3.90×10^{2}	1.02×10^{5}	6.10×10^{-15}

[a] $D_c = D_s/R$ where $R = G(1 + K)H^{-1}$. The term H is defined as the relative saturation of the pores with water. The pores are assumed to be full in the calculations shown in this table; that is, H = 1.0.

[b] *Sources*: D. G. Miller, *Estimation of Tracer Diffusion Coefficients of Ions in Aqueous Solution*, UCRL-53319, Lawrence Livermore Laboratory, University of California, Livermore, Calif., 1982; C. J. Geankoplis, *Mass Transport Phenomena*, Holt, Rinehart and Winston, New York, 1972; F. Kepak, "Adsorption and Colloidal Properties of Radioactive Elements in Trace Concentrations," *Chem. Rev.* **71**(4), 1972; E. L. Cussler, *Diffusion—Mass Transfer in Fluid Systems*, Cambridge University Press, New York, 1984; *CRC Handbook of Chemistry and Physics*, ed. D. R. Lide, 74th ed., CRC Press, Boca Raton, Fla., 1993; *Lange's Handbook of Chemistry*, ed. J. A. Dean, 14th ed., McGraw-Hill, New York, 1992.

B.5 REFERENCES

Abramowitz, M., and I. E. Stegun 1964. *Handbook of Mathematical Functions*, National Bureau of Standards, Bethesda, Md.

Atkins, P. W. 1990. *Physical Chemistry*, 4th ed., W. H. Freeman and Co., New York, p. 765.

Atkinson, A., K. Nelson, and T. M. Valentine 1986. "Leach Test Characterisation of Cement-Based Nuclear Waste Forms," *Nucl. Chem. Waste Manage.* **6**, 241–53.

Box, M. J., D. Davies, and W. H. Swann 1969. *Non-linear Optimization Techniques*, Oliver and Boyd, London.

Brown, G. G., et al. 1950. *Unit Operations*, John Wiley & Sons, New York, pp. 217–18.

Crank, J. 1993. *The Mathematics of Diffusion*, 2nd ed., Oxford University Press, Oxford, pp. 93–96.

Godbee, H. W. 1996. *Estimated Transport Parameters for Selected Radionuclides in Low-Level Waste and Concrete Containment,* D21-A20005-01-95, Delta-21 Resources, Inc., Knoxville, Tenn.

Godbee, H. W., and D. S. Joy, 1974, *Assessment of the Loss of Radioactive Isotopes from Waste Solids to the Environment. Part I: Background and Theory*, ORNL/TM-4333, Union Carbide Corp., Oak Ridge Natl. Lab.

Godbee, H. W. et al. 1989. "Application of the NEWBOX Computer Program to an Analysis of the Leaching Data for Several Alkali Metals and Phenol from Cementitious Waste Forms," pp. 184–188 in preprints of papers presented at the 197th ACS National Meeting, Dallas, Texas, April 9–14.

Godbee, H. W. et al. 1993. "Waste Confinement Systems and Waste-Form Durability," pp. 125–41 in *Effective and Safe Waste Management: Interfacing Sciences and Engineering with Monitoring and Risk Analysis,* ed. R. L. Jolley and R. G. M. Wang, Lewis Publishers, Boca Raton, Fla.

Icenhour, A. S. 1995. *Analysis of Source Term Modeling for Low-Level Radioactive Waste Performance Assessments*, ORNL/TM-12908, Lockheed Martin Energy Systems, Inc., Oak Ridge Natl. Lab.

Johnston, H. M., and D. J. Wilmot 1992. "Sorption and Diffusion Studies in Cementitious Grouts," *Waste Manage.* **12**, 289–97.

Lin, K. H. 1973. *Use of Ion Exchange for the Treatment of Liquids in Nuclear Power Plants*, ORNL-4792, Union Carbide Corp., Oak Ridge Natl. Lab.

Mrochek, J. E., T. M. Gilliam, and E. W. McDaniel 1986. "Grout Formulation for the Immobilization of Mixed Organic Containing Wastes," pp. 55–76 in *American Nuclear Society International Topical Meeting on Waste Management and Decontamination and Decommissioning*, proceedings of SPECTRUM '86, Niagara Falls, N.Y., Sept. 14–18.

Nelder, J. A., and R. Mead 1965. "A Simplex Method for Function Minimization," *Comput. J.* **7**, 308–13.

Nestor, C. W., Jr., H. W. Godbee, and D. S. Joy forthcoming. *NEWBOX: A Computer Program for Parameter Estimation in Diffusion Problems,* ORNL/TM-10910, Lockheed Martin Energy Research Corp., Oak Ridge Natl. Lab.

ORNL (Oak Ridge National Laboratory) 1994. *Performance Assessment for Continuing and Future Operations at Solid Waste Storage Area 6,* ORNL-6783, Martin Marietta Energy Systems, Inc., Oak Ridge Natl. Lab.

Serne, R. J. et al. 1987. *Laboratory Leach Tests of Phosphate/Sulfate Waste Grout and Leachate Adsorption Tests Using Hanford Sediment,* PNL-6019, Pacific Northwest Laboratory Richland, Wash.

Serne, R. J. et al. 1993. *Solid-Waste Leach Characteristics and Contaminant-Sediment Interactions Volume 1: Batch Leach and Adsorption Tests and Sediment Characterization,* PNL-8889 Vol. 1, Pacific Northwest Laboratory, Richland, Wash.

Appendix C

ANALYSIS OF ATMOSPHERIC EMISSIONS FROM THE CLASS L-II DISPOSAL FACILITY

D. A. Lombardi
M. L. Socolof

Appendix C

ANALYSIS OF ATMOSPHERIC EMISSIONS FROM THE CLASS L-II DISPOSAL FACILITY

Volatile radionuclides [tritium (^{3}H) and ^{14}C] may be transported from the waste disposal unit to the soil surface through a variety of mechanisms including (1) diffusion, (2) burrowing animals, (3) plant root uptake, and (4) desiccation cracks. When these volatile radionuclides reach the soil surface, they may become airborne and then transported via atmospheric dispersion to receptors located downwind of the waste disposal unit.

The diffusion mechanism was selected to estimate impacts of volatile radionuclide emissions from the Class L-II Disposal Facility (CIIDF). Assumptions were incorporated into this analysis to provide an upper bound estimate of emissions that may occur due to diffusion and are discussed below.

- For this analysis, the waste is assumed to be completely mixed into the soil. Therefore, no credit is taken for reduced diffusion that would occur due to the various engineered barriers in CIIDF. This assumption particularly bounds ^{3}H because of its relatively short half-life (12.3 years). The amount of ^{3}H in the waste at time of closure would be reduced significantly due to radioactive decay during the time in which the engineered barrier maintained its integrity.

- The radionuclide is assumed to diffuse upward only. Radionuclides would actually diffuse in all directions from the waste. Therefore, approximating the flux as one-dimensional and toward the surface leads to the maximum amount that would be diffused upward.

- Diffusive flux is approximated as first order, linear, and steady state. Since the radionuclide concentration is the primary mechanism responsible for diffusion, the high concentration in the waste would lead to a higher diffusive flux at the source. Near the surface, the radionuclide concentration would approach zero, and therefore flux would be significantly reduced.

- Loss of radionuclide via radioactive decay is ignored for this analysis. This again has the greatest bounding effect for ^{3}H due to its relatively short half-life. Only a small amount of ^{14}C (half-life of 5730 years) would decay during the active institutional control period (100 years after disposal); however, a significant amount of ^{3}H would decay before the end of institutional control.

These assumptions are likely to conservatively bound any combination of subsurface pathway mechanism such as burrowing animals, desiccation cracks, or plant root uptake.

Both ^3H and ^{14}C are assumed to be transported to the soil surface by diffusion in the vapor phase. Assuming that the volatile radionuclide in a disposal facility is completely bound in the pore water and that the soil is completely saturated, the concentration of ^3H or ^{14}C in the waste, C_W (Ci/m^3) is calculated as

$$C_W = \frac{A_t}{V_t n} \quad , \qquad \textbf{(C.1)}$$

where

A_t = total projected activity in the waste disposal facility (350 Ci for ^3H and 1.5 Ci for ^{14}C),
V_t = total projected volume of the waste disposal facility (18,690 m^3),
n = void space of the surficial soil at atmospheric pressure , approximately equal to 0.35 (Luxmoore 1994).

For ^3H, $C_W = 5.4 \times 10^{-2}$ Ci/m^3, and for ^{14}C, $C_W = 2.3 \times 10^{-4}$ Ci/m^3. The total projected activity in the waste was determined by taking the limiting concentrations for ^3H and ^{14}C presented in Sect. 4 from the groundwater analysis and multiplying them by the total projected volume in the waste. This estimate of the activity in CIIDF is unquestionably conservative because the concentration limits for each isotope are associated with the approximation that this would be the isotope present in the waste. Because wastes are composed of mixtures, the actual activity of each isotope in the facility will be substantially less than the limiting concentration.

To calculate the concentration of ^3H vapor in the soil, the ratio between the concentration of ^3H in the water vapor to the ^3H concentration in the liquid water bound in the waste was determined. If the air is saturated with water at 10°C (the assumed annual average soil temperature), then the concentration of water vapor in air, or absolute humidity, is 9.2 g of water vapor per cubic meter of dry air (MMES, EG&G, and WSRC 1994). Assuming the density of liquid water is 1.0×10^6 g/m^3, the ratio (r) of the density of water in the air to that in the liquid phase is

$$r = \frac{9.2 \times 10^{-6} \text{ g/m}^3_{\text{(water vapor)}}}{1 \text{ g/m}^3_{\text{(liquid water)}}} \quad . \qquad \textbf{(C.2)}$$

The relation between the concentration of ^{14}C in the air to the ^{14}C concentration in the liquid water bound in the waste was calculated using Henry's Law. This law is a linear, first-order relationship derived by approximating equilibrium conditions between dissolved gas with a particular concentration in liquid water and the same gas with a particular concentration in the air adjacent to the liquid water.

All of the ^{14}C in the disposal facility is assumed to be in the volatile form of $^{14}CO_2$. It is likely that $^{14}CO_2$ would be a small fraction of the total ^{14}C, most of which would probably exist in a nonvolatile form.

For use in Henry's Law, the unit mole fraction (χ) of $^{14}CO_2$ in the liquid water was determined as

$$\chi = \frac{n_{CO_2} \text{ per g of } CO_2}{n_{H_2O} \text{ per m}^3 \text{ of } H_2O} \quad , \tag{C.3}$$

where

n_{CO2} = number of moles in 1 g of CO_2,
n_{H2O} = number of moles in 1 m^3 of liquid water.

Approximating the density of liquid water as 1.0×10^6 g/m^3, χ is equal to 4.1×10^{-7}. The partial pressure of CO_2 in the air [p (atm)] is calculated using Henry's Law:

$$p = k\chi \quad , \tag{C.4}$$

where k is the Henry's Law constant for CO_2. At 10°C, k is equal to 1040 atm/mol fraction (Foust et al. as cited in Copper and Alley 1986).

Substituting the values for the unit mole fraction and Henry's Law constant for CO_2 at 10°C, p is calculated to be 4.3×10^{-4} atm. If the air is at atmospheric pressure, the concentration of CO_2 in the air is approximately equal to 4.3×10^{-4} g/m^3, and therefore the ratio of CO_2 in the air to that dissolved in the water is

$$r = \frac{4.3 \times 10^{-4} \text{ g/m}^3_{(CO_2 \text{ in air})}}{1 \text{ g/m}^3_{(CO_2 \text{ dissolved in water})}} \quad . \tag{C.5}$$

Because the ^3H is assumed to be completely bound with water and ^{14}C is assumed to be in the form of $^{14}CO_2$, the r values can be used to calculate the vapor concentration [C_{vap} (Ci/m^3)] of ^3H and ^{14}C as

$$C_{vap} = C_W r \quad . \tag{C.6}$$

For ^3H, $C_{vap} = 4.9 \times 10^{-7}$ Ci/m^3, and for ^{14}C, $C_{vap} = 9.9 \times 10^{-8}$ Ci/m^3.

The vapor flux [J (Ci/m^2 · s)] was approximated to be a first-order, linear process, and flux is assumed to occur from the top of the waste disposal unit to the soil surface. Based on these approximations, the vapor flux is calculated as

$$J = \frac{DC_{vap}}{x} \quad , \qquad \textbf{(C.7)}$$

where

D = ^{3}H diffusion coefficient in air reported as 2.39×10^{-5} m^2/s or the $^{14}CO_2$ diffusion coefficient in air reported as 1.40×10^{-5} m^2/s (Weast and Astle 1981 as cited in MMES, EG&G, and WSRC 1994),

x = soil thickness above the waste disposal facility (m), approximately equal to 1.8 m.

The assumption that flux would occur as if the entire concentration of waste is at the top of the facility is an upper-bound approximation. Much of the waste would actually be well below the top of the disposal facility, and diffusion would occur over a greater length. Therefore, the concentration gradient and subsequent diffusive flux would be less. For ^{3}H, $J = 6.5 \times 10^{-12}$ Ci/m^2 · s, and for ^{14}C, $J = 7.7 \times 10^{-13}$ Ci/m^2 · s. These values were input as emissions for air dispersion model calculations.

The Industrial Source Complex—Version 2 Long-Term Air Dispersion Model (ISCLT2) (EPA 1992a) was used to determine ambient ^{3}H concentrations for receptors located downwind of CIIDF. ISCLT2 is a Gaussian dispersion model approved by the U.S. Environmental Protection Agency for refined analyses in which annual average atmospheric concentrations in simple terrain are to be calculated (40 CFR 51, App. W). The following basic assumptions are incorporated into Gaussian models (Turner 1994).

- Pollutant emissions are continuous and do not vary over time.
- The emitted mass of pollutant is conserved from the source to the receptor. Therefore, none of the pollutant is removed from the atmosphere via chemical reaction, gravitational settling, or turbulent impaction.
- Meteorological conditions are assumed to be steady state during the time in which the pollutant is transported from the source to the receptor.
- Concentration profiles in the crosswind (perpendicular to the path of transport) and vertical directions are assumed to be well represented by a Gaussian distribution.

For receptors located within a few hundred meters of the source, the accuracy of Gaussian model estimates of ground-level plume centerline concentrations should be within a factor of 3 (Turner 1994).

For this analysis, each waste disposal facility was treated as an area source. Receptors were located 100 m from CIIDF in all directions at a 10-m spacing interval. On-site meteorological data recorded between 1989 and 1993 were used in the analysis. Hourly data were compiled into stability array (STAR) format for use in ISCLT2.

The maximum annual average ^{3}H concentration calculated using ISCLT2 was about 9.1 pCi/m^3, and for ^{14}C, was about 1.1 pCi/m^3. Maximum annual average concentrations occurred at a receptor located 100 m to the northeast of the facility.

The performance objective for atmospheric releases 10 mrem/year includes doses from all potential exposure pathways associated with the atmospheric releases. The annual doses for the two volatiles of interest (^{3}H and ^{14}C) are calculated from four exposure pathways:

- inhalation of airborne radionuclides,
- ingestion of vegetation exposed to airborne radionuclides (i.e., airborne-contaminated vegetation),
- ingestion of beef from cattle consuming airborne-contaminated vegetation, and
- ingestion of milk from cattle consuming airborne-contaminated vegetation.

No external doses are expected since these beta-emitting radionuclides have external dose conversion factors equal to zero (DOE 1988). The total dose from the atmospheric transport pathway is the sum of the doses from each of the four exposure pathways listed above. The equations used to calculate each exposure pathway dose are described below, and the parameter values used in these equations are listed in Table C.1. This methodology is based on a conservative specific-activity model presented in NRC Regulatory Guide 1.109 (NRC 1977). Note that because this is an upper-bound, screening assessment, radioactive decay is not included in the calculations.

The dose from direct inhalation of volatiles is calculated using the following equation:

$$H_{inh,i} = C_{a,i} \times IR_a \times DCF_{inh,i} \quad , \qquad \textbf{(C.8)}$$

where

$H_{inh,i}$	=	annual dose from inhalation of radionuclide I in air (rem/year),
$C_{a,i}$	=	concentration of radionuclide I in air (µCi/m^3),
Ir_a	=	intake rate of air (adult inhalation rate) (m^3/year),
$DCF_{inh,i}$	=	internal dose conversion factor from inhalation for radionuclide I (rem/µCi).

Table C.1. Parameter values used to determine dose from all potential exposure pathways associated with atmospheric emissions

Parameter	Value	Nuclide-specific value		Source
		^3H	^{14}C	
IR_a (adult average), m^3/year	8000			ICRP 1975
$DCF_{inh,i}$, rem/μCi		6.4×10^{-5}	2.4×10^{-5}[b]	EPA 1988
AH, kg/m^3	0.0092			MMES, EG&G, and WSRC 1994
$R_{wv/wa}$ (dimensionless)	0.5			NRC 1977
f_{wv} (dimensionless)	0.75			NRC 1977
$C_{air,C}$, kg/m^3	0.00016			NRC 1977; Napier et al. 1988
f_{Cv} (dimensionless)	0.11			NRC 1977
IR_v, kg/year	90[a]			MMES, EG&G, and WSRC 1994
$DCF_{ing,i}$, rem/μCi		6.4×10^{-5}	2.1×10^{-3}	EPA 1988
$F_{b,i}$, d/kg		3.3×10^{-5}	8.5×10^{-5}	NRC 1977
$IR_{v(cow)}$, kg/year	5694			EPA 1992b
$F_{m,i}$, d/L		2.7×10^{-5}	3.3×10^{-5}	NRC 1977
IR_b, kg/year	85			EPA 1992b
IR_m, L/year	112			EPA 1992b

[a] Assumes approximately half of an individual's vegetable intake is from locally grown, contaminated vegetation.
[b] Carbon as CO_2.

To calculate the tritium doses from contaminated food, it is assumed that the concentration of ^3H in vegetation is from the air surrounding the vegetation. The concentration in the vegetation is based on the amount of water in the vegetation and the amount of tritium that would be in the plant water. The equation for calculating the concentration of tritium in vegetation is as follows:

$$C_{v,^3H} = \frac{C_{a,^3H}}{AH} \times R_{wv/wa} \times f_{wv} \quad , \qquad \textbf{(C.9)}$$

where

$C_{v,^3H}$ = concentration of ^3H in vegetation (μCi/kg),
$C_{a,^3H}$ = concentration of ^3H in air (μCi/m^3),
AH = absolute humidity of the atmosphere (kg/m^3),
$R_{wv/wa}$ = concentration ratio of ^3H in vegetation water to ^3H in atmospheric water (dimensionless),
f_{wv} = fraction of vegetation that is water (dimensionless).

The concentration of ^3H in air ($C_{a,^3H}$) divided by the absolute humidity (AH) is equivalent to the concentration in water. This, when multiplied by the fraction of water in the vegetation (f_{wv}) and the concentration ratio of tritium in vegetation water to atmospheric water ($R_{wv/wa}$), equals the concentration of tritium in the vegetation.

To calculate the doses from ^{14}C-contaminated food, the concentration of ^{14}C in vegetation is assumed to be from the air surrounding the vegetation. Also, the ratio of ^{14}C to the natural carbon in vegetation is assumed to be the same as the ratio of ^{14}C to natural carbon in the atmosphere surrounding the vegetation. For airborne releases, plants are assumed to obtain all their carbon from airborne CO_2 and animals are assumed to obtain all their carbon through ingestion of plants (NRC 1977 p. 1.109-26; Napier et al. 1988, p. 4.86).

The equation for calculating the concentration of ^{14}C in vegetation from contaminated air is:

$$C_{v,^{14}C} = \frac{C_{air,^{14}C}}{C_{air,C}} \times f_{Cv} \quad , \qquad \textbf{(C.10)}$$

where

$C_{v,^{14}C}$ = concentration of ^{14}C in vegetation (μCi/kg),
$C_{air,^{14}C}$ = concentration of ^{14}C in air (μCi/m^3),
$C_{air,C}$ = concentration of natural carbon in air (kg/m^3),
f_{Cv} = fraction of natural carbon in vegetation (dimensionless).

The concentration in vegetation is then used to calculate the dose from ingestion of contaminated vegetation. As shown in Table C.1, approximately 50% of the exposed person's vegetable intake is assumed to come from the contaminated vegetation (WSRC 1994).

$$H_{v,i} = C_{v,i} \times IR_v \times DCF_{ing,i} \quad , \qquad \textbf{(C.11)}$$

where

$H_{v,i}$ = annual dose from radionuclide I in vegetation (rem/year),
$C_{v,i}$ = concentration of radionuclide I in vegetation (μCi/kg),
Ir_v = adult intake rate of vegetables (kg/year),
$DCF_{ing,i}$ = internal dose conversion factor for ingestion of radionuclide I (rem/μCi).

The concentration in vegetation is also used to determine the concentration in beef and milk that will be consumed by humans. The cow's vegetation consumption is assumed to be totally from grazing on fresh pasture grass contaminated with airborne radionuclides. The concentrations in beef and cow milk are calculated as follows:

$$C_{b,i} = C_{v,i} \times F_{b,i} \times IR_{v(cow)} \quad , \tag{C.12}$$

and

$$C_{m,i} = C_{v,i} \times F_{m,i} \times IR_{v(cow)} \quad , \tag{C.13}$$

where

$C_{(b,m),I}$ = concentration of radionuclide I in beef (b) or dairy (m) cattle that consumed contaminated vegetation (µCi/kg for beef and µCi/L for dairy),

$C_{v,i}$ = concentration of radionuclide I in vegetation (v) consumed by beef or dairy cattle (µCi/kg for beef and µCi/L for dairy),

$F_{(b,m),I}$ = transfer coefficient for beef (b) (d/kg) and milk (m) (d/L) for radionuclide element I,

$Ir_{v(cow)}$ = consumption rate of vegetation by beef or dairy cattle (kg/year).

The annual radiation doses from the ingestion of beef and milk are calculated by multiplying the concentration in each medium by the human intake rate and the radionuclide-specific internal dose conversion factor:

$$H_{b,i} = C_{b,i} \times IR_b \times DCF_{ing,i} \quad , \tag{C.14}$$

and

$$H_{m,i} = C_{m,i} \times IR_m \times DCF_{ing,i} \quad , \tag{C.15}$$

where

$H_{(b,m),I}$ = annual dose from radionuclide I in beef (b) or milk (m) (rem/year),

$C_{(b,m),I}$ = concentration of radionuclide I in beef (b) (µCi/kg) or milk (m) (µCi/L),

$IR_{(b,m)}$ = adult intake rate of beef (b) (kg/year) or milk (m) (kg/L),

$DCF_{ing,i}$ = internal dose conversion factor for ingestion of radionuclide I (rem/µCi).

The annual dose from atmospheric releases of radionuclide $I(H_{T,i})$ is the sum of the annual doses from the four exposure pathways described above (i.e., inhalation of contaminated air and ingestion of contaminated vegetables, beef, and milk):

$$H_{T,i} = H_{inh,i} + H_{v,i} + H_{b,i} + H_{m,i} \quad . \tag{C.16}$$

The annual effective dose equivalents from the atmospheric transport pathway, using C_a values of 9.1×10^{-6} μCi/m^3 (9.1 pCi/m^3) and 1.1×10^{-6} μCi/m^3 (1.1 pCi/m^3) for ^{3}H and ^{14}C, respectively, are presented in Table C.2. The annual doses from all exposure pathways resulting from atmospheric releases (H_T) are 7.6×10^{-3} mrem/year for ^{3}H (about 0.08% of the 10-mrem/year performance objective) and 0.24 mrem/year for ^{14}C (about 2% of the performance objective).

Table C.2. Calculated annual dose per unit concentration values and annual effective dose equivalents (EDEs) from the atmospheric transport pathway[a]

	^{3}H		^{14}C	
	Annual EDE per unit concentration (mrem/year per μCi/m^3)	Annual EDE[a] (mrem/year)	Annual EDE per unit concentration (mrem/year per μCi/m^3)	Annual EDE[a] (mrem/year)
H_{inh}	512	4.68×10^{-3}	188	2.07×10^{-4}
H_v	235	2.15×10^{-3}	130,000	0.14
H_b	41.7	3.81×10^{-4}	59,400	0.07
H_m	44.9	4.10×10^{-4}	30,400	0.03
H_T	833	7.62×10^{-3}	220,000	0.24

[a] The calculations are based on ^{3}H concentration of 9.1×10^{-6} μCi/m^3 and ^{14}C concentration of 1.1×10^{-6} μCi/m^3. See text for equations used to calculate doses.

The approximations and assumptions detailed above were chosen to provide a probable upper-bound estimate of effective dose equivalent that would be received on an annual basis. Comparisons between these results and on-site ambient monitoring data were made to check the analysis. The relationship between emissions and ambient concentration can be described by an atmospheric dispersion term, A_D (Ci/y per pCi/m^3), defined as

$$A_D = \frac{Q}{C} \quad , \tag{C.17}$$

where

Q = annual ^3H point source emission rate (Ci/year),
C = annual ambient ^3H concentration (pCi/m^3).

To calculate the potential CIIDF A_D value, area emission rates for CIIDF were converted to an equivalent point source emission rate. Equivalent point source emissions can be calculated by

$$Q = JA\left(3600\frac{\text{s}}{\text{h}}\right)\left(8760\frac{\text{h}}{\text{year}}\right) \quad , \qquad \textbf{(C.18)}$$

where

J = vapor flux out of a waste disposal facility (Ci/m^2 · s),
A = waste disposal unit surface area (m^2).

If the source is approximated as a single point in the disposal facility, then the total emission rate is equal to 2.1 Ci/year. Knowing that the maximum average annual concentration predicted using the ISCLT2 model is 9.1 pCi/m^3, A_D was calculated using Eq. (C.17) and found to be 0.2 Ci/year per pCi/m^3 (Table C.3).

For on-site calculations, almost all of the ^3H emissions at the Oak Ridge Reservation (ORR) occur from the Building 3039 stack located at Oak Ridge National Laboratory (ORNL) (MMES 1991, MMES 1992, and MMES 1993). The nearest ambient ^3H monitor is located about 1100 m to the southwest of this stack. Table C.3 shows emission rate and monitored ambient concentration values for 1990 through 1992 and the calculated A_D values. The value of A_D ranges between 94 and 364 Ci/year per pCi/m^3 for these years.

The A_D values calculated using on-site data are approximately one order of magnitude higher than the A_D calculated from CIIDF modeling results. A lower A_D value indicates that atmospheric dispersion is less and overall impact from the atmospheric pathway would be higher. Two reasons that the A_D value calculated for CIIDF is less are that the on-site source is elevated and that the distance between the stack and monitor is about 1100 m. For the CIIDF modeling analysis, the source is at ground level and receptors were placed at a distance of 100 m. Accounting for these differences would probably bring the modeled A_D value within about two orders of magnitude (Turner 1994) of the on-site A_D values. This two order of magnitude difference is attributable to the conservatism employed in the analysis. Monitoring for ^{14}C does not occur on ORR; however, results would probably be similar to those discussed above for ^3H. Therefore, the upper-bound assumptions in this analysis support the decision discussed in Sect. 3.2.1 to dismiss further analysis of atmospheric releases. Emissions of volatile radionuclides, as well as nonvolatiles, would lead to maximum off-site doses that are well below the 10 mrem/year performance standard.

Table C.3. Emission rate, ambient concentrations, and calculated atmospheric dispersion term values for CIIDF and the Oak Ridge Reservation

Location	Emission rate Q (Ci/year)	Average annual ambient atmospheric concentrations C (pCi/m^3)	Atmospheric dispersion term A_D (Ci/year per pCi/m^3)[a]
CIIDF	2.1[b]	0.37[c]	0.22
Oak Ridge Reservation, 1990	12,000[d]	33[e]	364
Oak Ridge Reservation, 1991	16,000[d]	4700[e]	94
Oak Ridge Reservation, 1992	2,140[d]	2250[e]	113

[a]The atmospheric dispersion term is calculated as the ratio of the emission rate to the ambient concentration.

[b]The emission rate for CIIDF was calculated as the product of the radionuclide diffusive flux and the surface area of the facility.

[c]Ambient atmospheric concentrations were calculated using the Industrial Source Complex— Version 2 Long-Term Air Dispersion Model (ISCLT2) (EPA 1992). The maximum annual concentration was calculated to occur at a receptor located 100 m to the northeast of the disposal facility.

[d]Almost all of the ^{3}H emissions for ORR occur mainly from the Building 3039 stack located at ORNL (MMES 1991, MMES 1992, and MMES 1993).

[e]Ambient atmospheric ^{3}H concentrations are measured at a monitor located at the perimeter of ORNL. This monitor is located about 1100 m to the southwest of the Building 3039 stack (MMES 1991, MMES 1992, and MMES 1993)

REFERENCES

Copper, C. D., and F. C. Alley 1986. *Air Pollution Control: A Design Approach*, Waveland Press, Inc. Prospect Heights, Ill.

DOE (U.S. Department of Energy) 1988. *Internal Dose Conversion Factors for Calculation of Dose to the Public*, DOE/EH-0071, Washington, D.C.

EPA (U.S. Environmental Protection Agency) 1988. *Limiting Values of Radionuclide Intake and Air Concentration and Dose Conversion Factors for Inhalation, Submersion, and Ingestion*, Federal Guidance Report No. 11, EPA 520/1-88-020, Office of Radiation Programs.

EPA (U.S. Environmental Protection Agency) 1992a. *User's Guide for the Industrial Source Complex (ISC2) Dispersion Models, Volume I: User Instructions*, EPA Publication No. EPA-450/4-92-008a, Research Triangle, N.C.

EPA (U.S. Environmental Protection Agency) 1992b. *User's Guide for CAN-PC Version 1.0, Air and Radiation,* 402-B-92-001, Las Vagas, Nev.

Foust, et al. 1960. *Principles of Unit Operations*, John Wiley and Sons, New York.

ICRP (International Committee on Radiation Protection) 1975. *International Commission on Radiological Protection, Task Group Report on Reference Man,* ICRP Publication No. 23, Pergamon, New York.

Luxmoore, R. J. 1994. "Appendix D: Application of the Unified Transport Model, TUMSIM and WELSIM to the Solid Waste Storage Area 6 Performance Assessment," *Performance Assessment for Continuing and Future Operations at Solid Waste Storage Area 6*, ORNL-6783, Martin Marietta Energy Systems, Inc., Oak Ridge Natl. Lab.

MMES (Martin Marietta Energy Systems, Inc.) 1991. *Oak Ridge Reservation Environmental Report for 1990, Volume 2: Data Presentation,* ES/ESH-18/V2, Oak Ridge, Tenn.

MMES (Martin Marietta Energy Systems, Inc.) 1992. *Oak Ridge Reservation Environmental Report for 1991, Volume 1: Narrative, Summary, and Conclusions,* ES/ESH-22/V1, Oak Ridge, Tenn.

MMES (Martin Marietta Energy Systems, Inc.) 1993. *Oak Ridge Reservation Environmental Report for 1992, Volume 1: Narrative,* ES/ESH-31/V1, Oak Ridge, Tenn.

Napier et al. 1988. *GENII—The Hanford Environmental Radiation Dosimetry Software System, Volume 1: Conceptual Representation*, Battelle, Pacific Northwest Laboratory, Hanford, Wash.

NRC (U. S. Nuclear Regulatory Commission) 1977. *Regulatory Guide 1.109. Calculation of Annual doses to Man from Routine Releases of Reactor Effluents for the Purpose of Evaluating Compliance with 10 CFR Part 50, Appendix I,* Washington, D.C.

Turner, D. B. 1994. *Workbook of Atmospheric Dispersion Estimates: An Introduction to Dispersion Modeling,* 2nd ed., Lewis Publishers, Boca Raton, Fla.

Weast, R. C., and M. J. Astle, eds. 1981. *CRC Handbook of Chemistry and Physics,* CRC Press, Boca Raton, Fla.

WSRC (Martin Marietta Energy Systems, Inc.; EG&G Idaho, Inc., and Westinghouse Savannah River Company) 1994. *Radiological Performance Assessment for the E-Area Vaults Disposal Facility*, WSRC-RP-94-218, Westinghouse Savannah River Company, Aiken, S.C.

Appendix D

HYDROLOGY AND SUBSURFACE TRANSPORT MODELING

R. J. Luxmoore
S. Timmins
M. L. Tharp

Appendix D

HYDROLOGY AND SUBSURFACE TRANSPORT MODELING

This appendix contains subsections describing technical aspects of terrain analysis, the Unified Transport Model, and the PADSIM code.

D.1 TERRAIN ANALYSIS

D.1.1 Introduction

Land surface topography has a large influence on water flow within and through a watershed. Current land surfaces reflect water flow and erosion processes determined by interactions between climate, vegetation, soil profiles, and bedrock. Methods for incorporating the topographic features of watersheds into hydrologic modeling were initiated by Beven and Kirkby (1979) and have been applied extensively in hydrologic research (e.g., Quinn et al. 1991). Application of these methods for hydrologic characterization of the Class L-II Disposal Facility (CIIDF) site in Bear Creek in the Oak Ridge Reservation (ORR) was undertaken.

The movement of water into and over a watershed may lead to discharge in stream flow due to hydrologic processes that are significantly affected by

- the intensity and duration of precipitation,
- the porosity and permeability of soil and bedrock in the watershed,
- the antecedent water storage in the watershed, and
- the shape of the landform which gathers water flow to the stream bed.

Change in soil water storage (wetness) at a particular place is a function of the rates of water arrival and departure. As soil water storage increases toward saturation, overland flow may develop. Surface water will collect or disperse depending upon topography. For example, where contours converge as in a stream valley, water will collect favoring the development of saturated areas, whereas where contours diverge, as on ridges, water will disperse (toward convergent flow zones), reducing the tendency for soil water saturation. The combination of basin convergence or divergence and land slope can be used to derive a spatial distribution of topographic index. This index describes the propensity for each place in a watershed to become saturated. Topographic index is of significant value for its use in modeling the hydrologic behavior of a watershed in response to precipitation. Simulated flow may be calibrated with stream flow measurements, and additional flow measurements may be used for model testing and validation.

Beven and Kirkby (1979) developed a hydrologic model, TOPMODEL, that uses a topographic index to simulate hydrologic processes in hilly basins in humid, temperate climates. They conceived of the idea that the dynamics of land areas which become saturated during storm events (variable source areas) are largely determined by topography. Runoff usually originates from saturated soil (source) areas near stream channels, and these areas expand and contract during rain events. This expansion and contraction reflects the state-of-wetness of the watershed and enables the delivery of high volumes of surface runoff when these source areas are a significant proportion of a watershed. Overland flow generated from source areas contributes to the storm hydrograph, often displaying a quick rise in flow rate during a rain event. Flow rate decays to base flow after the event. The modeling of source area dynamics requires an understanding of three-dimensional water flow over the land surface. Basin convergence or divergence determines how much water from upslope areas arrives at a given point. The rate of water flow from this point is determined by slope and soil transmissivity (subsurface flow rate at a unit gradient).

The topographic index used by Beven and Kirkby for a particular location is given by the upslope area (a) which converges on a unit contour width divided by the tangent of the local slope angle (β), all expressed as a natural logarithm: $\ln(a/\tan \beta)$. Locations with similar index values have similar soil wetness characteristics. Places which drain large upslope areas and have low local slope (e.g., valleys) have high index values and tend to be wet. Other places, like ridge tops, have low index values and tend to be dry due to small upslope areas with divergent slopes.

Application of TOPMODEL to a watershed requires a histogram of $\ln(a/\tan \beta)$ values for the site, and these are used in a semidistributed fashion on the assumption that locations with similar index values have similar hydrologic response. TOPMODEL has been applied on two instrumented watersheds (Walker Branch and Center Seven Creek) in ORR with satisfactory results, except for the first storms after a long dry period. The creation of a histogram of topographic indices for a watershed is the goal of digital terrain analysis.

D.1.2 Digital Terrain Analysis Methods

Digital terrain analysis requires the conversion of a contour (vector) map to a grid cell or raster form to permit discrete cell-by-cell analysis of topographic properties such as slope, flow direction, and topographic index. Each cell represents a small map area and is an approximation of a continuous landform. Thus the accuracy of the result increases with decrease in cell size. The major advantage of using a matrix of elevations is that computer analysis can be much more readily undertaken with digital values than with line segments from a contour map.

Modern workstations are convenient for applying algorithms to digitize a contour map and calculate topographic properties from the digital elevation model (DEM). A view of the land surface can be created by drawing continuous lines through the discrete elevation values of the DEM. Grid cells are typically square and range in size from 3 to 70 m on a side. At the low end of this range

continuous surfaces are closely approximated. Nevertheless, discrete representation alone does not provide the interpolation of water flow direction needed for hydrologic studies. Specific digital terrain analysis algorithms are required to extract topographic properties from DEM-derived matrices.

A DEM must retain the original runoff pathways evident on the contour map. Thus, all stream beds and intermittent flow paths must be characterized without unnatural dams or depressions. This is not a trivial requirement, particularly in landscapes with stream channels smaller than the size of a grid cell. Once this runoff constraint is satisfied, the derived properties of slope, upslope area, and flow direction can be reliably determined. Lines of grid cells with the same elevation (contours) can be viewed as equipotential lines across which flow occurs perpendicularly downgradient.

Current methods for producing digital elevation models use either linear, spline, or minimum curvature algorithms to interpolate values between irregularly spaced contours (Schwartz et al. 1995). The best methods use specifically defined input locations for streambeds and ridge lines and apply runoff constraints such that flow cannot cross a ridge and flow along a stream must occur without artificial dams or depressions. Such dams and depressions (or pools) are undesirable because they introduce artificial surface water storages. This problem is determined in part by cell size resolution and in part by the interpolation method used in the digitizing step. The interpolation method is not as important as the cell size resolution in determining the extent of this problem. A grid size of 3 m was used for development of the DEM for the CIIDF site. The quality of the DEM was checked by generating views to confirm the absence of spurious features and using flow matrices to confirm the positions of flow pathways.

Terrain analysis of the CIIDF site required that the site contours be modified to account for landscape grading needed for construction of tumulus pads to store waste. To begin this characterization, the site plan was altered to include the proposed contours, and new contours were manually drawn to show the expected site grading. This map was modified where necessary to allow drainage to behave in the required manner. The drainage from the pads is expected to flow to the north, west, and south, with very little flow to the east. A narrow, concrete-lined surface drain is modeled along the eastern and southern boundaries of the site preventing runoff to the east and south. A roadway along the southern side diverts drainage to a pond immediately southwest of the pads. The road is artificially breached to model the under-road culvert which connects the drainway and the pond. These modifications conformed to the general CIIDF site plan.

The DEM for the CIIDF site was prepared with the CGRID program (Timmins et al. 1989) which uses linear interpolation between contours and the ridge and channel lines to develop the digital model. Contours at a 2-ft interval and stream and ridge lines were digitized and used to produce a DEM with 0.1-ft vertical resolution and 10-ft horizontal resolution. The nominal 0.1-ft vertical resolution permits differencing for calculation of slopes. The raw DEM was viewed as a three-dimensional model to remove spurious features and smooth any irregularities using a check-and-replace algorithm in the CGRID program. DEM values for which the absolute value of the elevation minus the mean of the surrounding eight values exceeded a tolerance of 0.2 feet were replaced by the mean. About 1600 values (3.3%) were edited to obtain the final DEM for the CIIDF site (Fig. 3.4 in text).

D.1.3 Terrain Analysis of the CIIDF Site

The CIIDF site drains to two subwatersheds, and an overlay mask was made to provide appropriate boundaries for the site. The mask used the Bear Creek stream bank and two tributaries for the southern, eastern, and western boundaries, respectively. For the boundary in the northeast, an intermittent stream (which has its course changed on the site plan) was extended to intersect with the tributary to the west. The resulting mask (completely bounded by valleys) has an approximate pentagon shape with Bear Creek forming the southern boundary (Fig. 3.5 in text). The DEM was clipped to these boundaries and used in calculation of topographic indices for the CIIDF site from upslope area and slope angle properties of the landscape (Schwartz et al. 1995). The frequency distribution (histogram) of topographic index values is used in TOPMODEL for hydrologic modeling. This histogram shows a characteristic lognormal distribution (Fig. 3.5 in text), indicating large areas with low soil wetness and relatively small areas of wetlands and stream channels.

D.1.4 Hydrologic Modeling with TOPMODEL

The next step in terrain analysis is the application of TOPMODEL (Beven and Kirkby 1979) to the CIIDF site using the histogram of topographic index values developed from the DEM. This histogram is used by the TOPMODEL code to process the watershed in a semidistributed fashion. The histogram of topographic index is divided into a number of classes using a binning (class) interval of 0.2 logarithmic units. This step generated about 60 binning intervals over the $\ln(a/\tan\beta)$ range of [4–15]. All areas which have a similar $\ln(a/\tan\beta)$ value are classed together and are then processed by the model as a single entity. The mean of the $\ln(a/\tan\beta)$ distribution was also determined and used in Eq. (D.1) to calculate the saturation deficit for each topographic index class.

$$S_i = S + m\left[\Omega - \ln(a/\tan\beta)_i\right] , \qquad \textbf{(D.1)}$$

where

S_i = soil water saturation deficit at location I,
S = average saturation deficit for the whole watershed,
m = scaling factor for soil properties,
Ω = mean of the $\ln(a/\tan\beta)$ distribution.

The value of S is updated at each time step for the whole watershed to reflect changes in average saturation deficit determined from modeling of the site water budget in response to precipitation and potential evaporation inputs. Areas with similar $\ln(a/\tan\beta)$ values have similar dynamics of soil wetness in TOPMODEL simulations. TOPMODEL calculates simulated stream flow as output along with soil wetness maps.

Streamflow measurements can be used to calibrate several input variables required for simulation with TOPMODEL. The hydrologic simulator needs average values that represent the watershed as a whole. The important variables for model calibration are

- maximum hydraulic conductivity of soil—determines the transmissivity in subsurface flow calculations;
- exponential storage parameter—determines initiation of subsurface flow;
- root zone water storage—determines water available for evapotranspiration; and
- groundwater flow multiplier—determines subsurface flow.

Calibration of TOPMODEL was based on comparisons of stream-flow measurements and values derived from simulations of Center Seven Creek in Melton Valley in ORR. The soils and geology of the Center Seven area are similar to those of the CIIDF site.

D.1.5 TOPMODEL Applications

Dynamic simulations of the CIIDF site were conducted with TOPMODEL using 1991 precipitation data from ORR. Prediction of soil saturation deficit (0 means saturation, i.e., wet soil) were plotted for four occasions to demonstrate hydrologic behavior of the area. The largest precipitation and runoff event in 1991 occurred at 1197 h (Feb. 18 at 9:00 p.m.), and the simulation shows a very large expanded area of wet soil indicated by the dark shading in Fig. D.1. Soil saturation declines significantly by 1209 h (12 h later, Fig. D.1) with the cessation of rainfall. Soil wetness is largely confined to stream channels at 1245 h (Fig. D.2), which is 48 h after the peak runoff at 1197 h. A moderate runoff event shown for 3915 h (June 12 at 3:00 a.m.) has less expansive wet zones than at 1197 h; nevertheless, the drainage networks can be clearly identified (Fig. D.2). Runoff has a very flashy behavior during spring and summer storm events, and the expansive wet areas at 1197 h, for example, do not persist. For a significant proportion of time, the landscape drains at a slow rate, as shown for 1245 h in Fig. D.2. These simulations and analyses of hydrologic performance were used to aid interpretation of water flow at the CIIDF site and estimation of spatially varying recharge.

D.2 UNIFIED TRANSPORT MODEL DETERMINATION OF CIIDF WATER BUDGETS

The Unified Transport Model (UTM) is a water budget simulator that includes algorithms for interception storage, interception evaporation, infiltration, soil water drainage, soil evaporation, transpiration, and subsurface lateral flow (Fig. 3.6 in text). The code is documented in Patterson et al. (1974) and Huff et al. (1977b), and hydrologic, simulations have been tested with data from Walker Branch watershed on ORR (Huff et al. 1977a; Luxmoore and Huff 1989). The code operates with

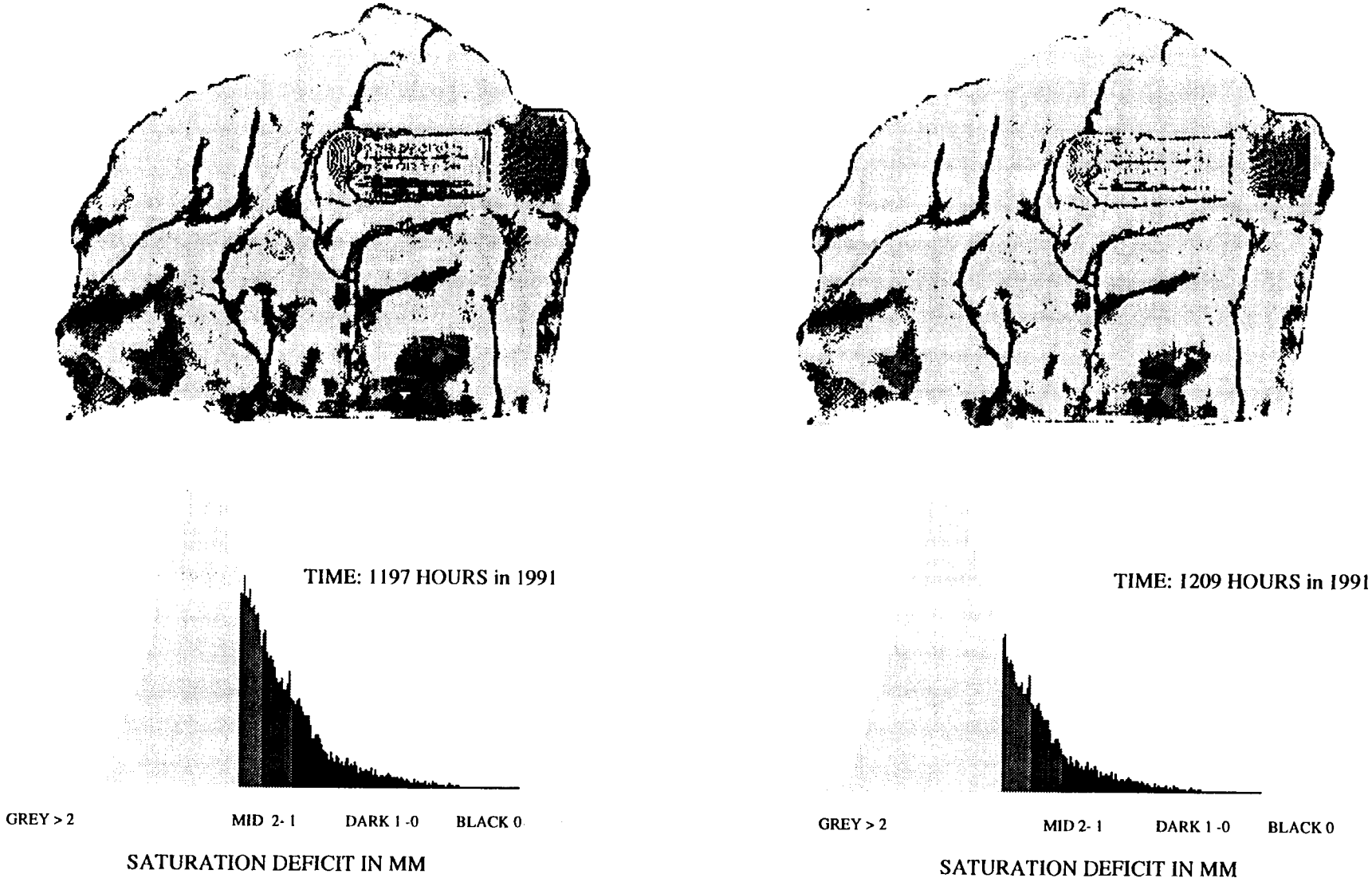

Fig. D.1. Map and frequency distribution of simulated soil water saturation deficit at the CIIDF site for 1197 and 1209 h in 1991. Darker shading indicates greater soil wetness and lower saturation deficit.

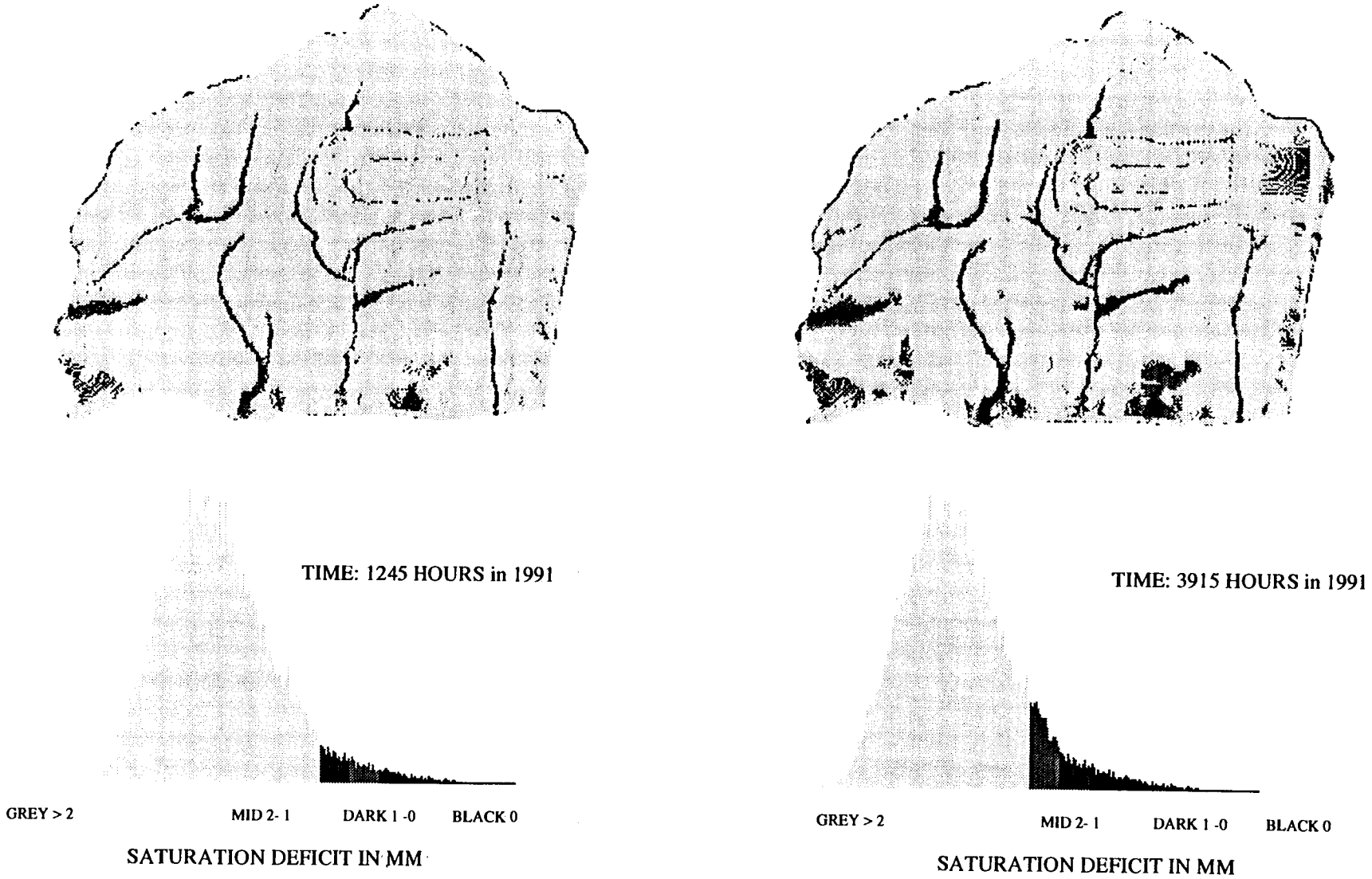

Fig. D.2. Map and frequency distribution of simulated soil water saturation deficit at the CIIDF site for 1245 and 3915 h in 1991. Darker shading indicates greater soil wetness and lower saturation deficit.

15-min. time steps when raining, otherwise hourly, to generate the water dynamics for up to seven soil-plant segments of a watershed. The lateral flow and drainage from each land segment can be assembled to generate stream-flow simulations, but this option was not required for site water budget calculations.

The meteorological data needed for simulation with the UTM are hourly precipitation, daily maximum and minimum air temperature, daily total solar radiation, daily average dew point temperature, and daily average wind speed (Fig. 3.7 in text). Records from Walker Branch Watershed and from the meteorological station at Oak Ridge town site have been compiled into the model format for application at sites in the vicinity of Oak Ridge National Laboratory. An evaluation of the data for 1968–1989 period showed that 1971 was a year with average precipitation (1372 mm/year), with 1968 being a dry year (933 mm/year), and 1973 being a wet year (1895 mm/year). These three contrasting sets of data were selected for simulation to provide a range of hydrologic transport regimes. The data for the average year were used in the CIIDF assessment simulations. Model applications were initialized by repeating simulations with the same weather data for a second year using soil water results at the end of the first year to initiate the repeated simulation. Change in annual soil water storage was close to zero with this initialization procedure, and thus there was little or no influence of initial conditions on the simulated water budgets for the various stages of CIIDF operations.

It is assumed that all chemical leached from waste sites is transported in drainage water, even if the volume is small. Chemical solubility is not a limitation due to the dilution effect of any volume of drainage water mixing with the leachate solution. During the first 22 years of CIIDF operations, water budget simulations were not used for estimation of seepage into concrete vaults. The assumption was made that vaults were exposed to precipitation prior to completion of the compacted soil cap. Monthly precipitation values were used as seepage input for simulations with the SOURCE1 model.

Water budget simulations were conducted for the facility with a compacted soil cap. The soil hydraulic properties used in these simulations (Table D.1) involved 60 cm of top soil in two layers over three layers of compacted soil. The saturated conductivity of the top soil layers was 3.5×10^{-5} m/s. The three compacted soil layers of the cap (60–80, 80–100, and 100–120 cm) were given a saturated hydraulic conductivity of 1.2, or 2.3×10^{-7} m/s (Table D.1). These three layers were effective in reducing drainage and enhancing lateral flow in layer 2. The natural soils of the CIIDF site have been described and classified by Lietzke, Lee, and Lambert (1988), and many of the profiles are shallow, being formed on weathered interbedded shale and limestone (saprolite). The hydraulic properties selected to represent these soils were derived from published sources reporting investigations conducted for the same geologic formation. The hydraulic properties of the subsoil deeper than 120 cm (Table D.1) were based on data from Rothschild et al. (1984). The water retention data were obtained from Luxmoore (1982) and Davis et al. (1987). The CIIDF facility is conceptually placed at the 120-cm depth with no spatial dimensions in the water budget simulations. Each tumulus pad and vaults were assumed to be in a steady-state water flux (flux in = flux out) in simulations conducted with the SOURCE1 model. The water budget calculations were consistent with this assumption.

Table D.1. Volumetric soil water content (m^3/m^3) at selected matric pressures and the saturated hydraulic conductivity for a compacted soil cap with grass vegetation and for soil layers below tumulus pads

Matric pressure (–kPa)	Soil layer (cm)							
	Top soil		Compacted soil cap			Subsoil		
	0–30	30–60	60–80	80–100	100–120	120–130	130–140	140–160
0	0.476	0.476	0.390	0.390	0.390	0.455	0.455	0.455
1	0.472	0.472	0.384	0.384	0.384	0.432	0.432	0.432
2	0.468	0.468	0.378	0.378	0.378	0.418	0.418	0.418
3	0.466	0.466	0.373	0.373	0.373	0.410	0.410	0.410
4	0.463	0.463	0.369	0.369	0.369	0.402	0.402	0.402
5	0.462	0.462	0.366	0.366	0.366	0.396	0.396	0.396
10	0.452	0.452	0.352	0.352	0.352	0.372	0.372	0.372
15	0.439	0.439	0.342	0.342	0.342	0.354	0.354	0.354
18	0.430	0.430	0.336	0.336	0.336	0.347	0.347	0.347
33	0.370	0.370	0.330	0.330	0.330	0.330	0.330	0.330
100	0.355	0.355	0.305	0.305	0.305	0.305	0.305	0.305
200	0.340	0.340	0.295	0.295	0.295	0.295	0.295	0.295
400	0.310	0.310	0.275	0.275	0.275	0.275	0.275	0.275
800	0.250	0.250	0.250	0.250	0.250	0.250	0.250	0.250
1500	0.140	0.140	0.230	0.230	0.230	0.230	0.230	0.230
Saturated hydraulic conductivity, m/s	3.5×10^{-5}	3.5×10^{-5}	1.2×10^{-7}	2.3×10^{-7}	1.2×10^{-7}	9.8×10^{-6}	9.8×10^{-6}	2.3×10^{-7}

At the next stage in the simulations, soil macropores were introduced into the cap to represent the influence of cracks and channels that develop through the matrix material with time. These preferential flow paths progressively negated the hydrologic impedance of the compacted soil matrix during the last 90 years of the institutional control period. The same water retention data were used for simulation of cap failure and for the postmaintenance period with forest vegetation (Table D.2). Total porosity varied from 0.390 to 0.476 m^3/m^3 in the 5-m profile. The water retention data were obtained from Luxmoore (1982) and Davis et al. (1987). Saturated conductivity data for the natural soil layers above 3-m depth (i.e., excluding cap) were obtained from Rothschild et al. (1984). The saturated hydraulic conductivity values for the bottom two layers were decreased from the values given by Rothschild et al. (1984) in an approximately exponential decrease such that the conductivity of the lowest layer was 5.8×10^{-9} m/s (0.5 mm/d). Simulations using these hydraulic properties (Table D.2) gave lateral flow and drainage results that agreed with the hydrologic framework outlined in Sect. 3.2.2. This framework projects about 29% of subsurface flow becoming recharge to aquifers, with the remainder generating lateral subsurface flow through a storm-flow zone located in the upper

Table D.2. Volumetric soil water content (m^3/m^3) at selected matric pressures and the saturated hydraulic conductivity of a failed compacted soil cap and soil layers with grass or forest vegetation

Matric pressure (–kPa)	Soil layer (cm)							
	Top soil	Cap	Subsoil					
	0–60	60–120	120–150	150–200	200–250	250–300	300–400	400–500
0	0.476	0.419	0.455	0.456	0.390	0.390	0.390	0.390
1	0.472	0.410	0.432	0.448	0.384	0.384	0.384	0.384
2	0.468	0.403	0.418	0.440	0.378	0.378	0.378	0.378
3	0.466	0.397	0.410	0.433	0.373	0.373	0.373	0.373
4	0.463	0.392	0.402	0.429	0.369	0.369	0.369	0.369
5	0.462	0.388	0.369	0.425	0.366	0.366	0.366	0.366
10	0.452	0.369	0.372	0.406	0.352	0.352	0.352	0.352
15	0.439	0.352	0.354	0.389	0.342	0.342	0.342	0.342
18	0.430	0.346	0.347	0.380	0.336	0.336	0.336	0.336
33	0.370	0.310	0.330	0.350	0.330	0.330	0.330	0.330
100	0.355	0.300	0.305	0.325	0.305	0.305	0.305	0.305
200	0.340	0.285	0.295	0.315	0.295	0.295	0.295	0.295
400	0.310	0.270	0.275	0.295	0.275	0.275	0.275	0.275
800	0.250	0.250	0.250	0.270	0.250	0.250	0.250	0.250
1500	0.140	0.230	0.230	0.250	0.230	0.230	0.230	0.230
Saturated hydraulic conductivity, m/s	3.5×10^{-5}	2.3×10^{-9} [a]	9.8×10^{-6}	2.3×10^{-6}	5.8×10^{-7}	5.8×10^{-7}	3.5×10^{-8}	5.8×10^{-9}

[a] Conductivity was enhanced by a macropore algorithm.

2–3 m of the soil profile (see Sect. 2.1.6). Saturated hydraulic conductivity measurements show a decrease with depth, and values are about three orders of magnitude smaller at 4–5-m depth than at the surface (Moore 1988).

Spatial variability of hydraulic properties in soil profiles similar to the CIIDF site have been determined for the surface soil (Wilson and Luxmoore 1988) and for subsoil (Luxmoore, Spalding, and Munro 1981; Wilson, Alfonsi, and Jardine 1989). These three studies showed lognormal frequency distributions for soil water flow rates with little or no spatial correlation between measurement sites. Spatial variability of soil properties at the CIIDF site was not included in the present analysis.

D.3 THE PADSIM MODEL

The PADSIM model was developed to simulate vertical and lateral chemical transport through the vadose zone using annual time-step calculations. The choice of annual time steps to represent the dynamics of storm event–driven solute transport was based on the need for assessment simulations for many thousands of years. PADSIM has algorithms for (1) preferential flow as a function of K_d for soil within 3.5 m of the surface, (2) an annual increment in reactive soil path length as a function of K_d, (3) half-life calculations of nuclide decay, (4) chemical partitioning between solution phase concentration and adsorption on soil surfaces, and (5) mass balance calculations. An outline of these algorithms follows.

D.3.1 Preferential Flow Algorithm

Preferential flow was not operational for the 8-m thickness of the vadose zone between the bottom of the tumulus pad and the water table. However, preferential flow has been shown to be a significant component of lateral flow through the shallow subsurface above a depth of 3 m (Wilson et al. 1993). The annual proportion of bypass flow to surface water was made an arbitrary function of K_d such that a smaller proportion of bypass flow resulted with higher K_d.

All nuclides with a K_d (CKD) greater than 100 were allowed to migrate a maximum annual distance (BYLEN) of 15 m. Nuclides with a lower K_d had a linearly greater annual transport distance with decrease in K_d. The following FORTRAN statements calculate BYLEN (m) and determine the proportion of bypass flow, SBYPAS, as a function of STLEN, an input value for the distance (m) of the lateral flow path from the tumulus pads to the nearest surface drainage channel.

```
IF(CKD.GT.100) THEN
BYLEN = 15.0
ELSE
BYLEN = 80.0 – (0.65 * CKD)
ENDIF
SBYPAS = 0.0
IF(STLEN.LT.BYLEN) SBYPAS = 1.0 – (STLEN/BYLEN)
```

Nuclides with a K_d of zero have a BYLEN value of 80 m; thus, with a STLEN value of 50 m for the CIIDF site, the value for SBYPAS is 0.375. SBYPAS decreases to 0.07 for a K_d of 40 and is zero for a K_d of 50 or more (Table 3.8 in text). This simplistic treatment of preferential flow could be refined in continuing work.

D.3.2 Annual Increment in Soil Path Length

An annual increment in the soil path length (ANINC) exposed to nuclide is determined as a proportion of the maximum annual transport distance (BYLEN) obtained in the preferential flow calculations. An arbitrary fraction (FPAINC) of 0.05 was applied to BYLEN to obtain ANINC values that decreased from 4 m for nuclides with a zero K_d to 0.75 m for nuclides with a K_d of ≥ 100 (Table 3.9 in text). The FORTRAN statement is

ANINC = BYLEN * FPAINC .

These calculations resulted in small annual increments in the soil matrix path length that added to the maximum annual transport length given by BYLEN. These increments increased the soil volume interacting with nuclides. Since the recharge path length of 8.1 m is much less than the maximum annual transport distance of 15 m for the strongly adsorbed nuclides ($K_d \geq 100$), the whole of the soil volume in the recharge path interacted with all nuclides in all years. This was not the case for the strongly adsorbed nuclides in the lateral subsurface flow path. In this case it took 48 years for these nuclides to pass through the 50-m path length (Table 3.9 in text). Nuclides with a $K_d \leq 40$ interacted with the whole lateral flow path in all years.

D.3.3 Half-Life Calculations

Nuclide decay is calculated each year for the nuclide mass in the vertical and lateral subsurface flow paths. Nuclide decay for the adsorbed phase in the recharge path (RSOLID) reduces this phase according to the FORTRAN statement

RSOLID = RSOLID*DEXP[–(HARATE/HALIFE)] ,

where HARATE is log 2.0 in double precision and HALIFE is the nuclide half-life in years. A similar statement is used for solution phase calculations.

D.3.4 Chemical Adsorption

The relationship between solution phase and solid phase partitioning of nuclide is calculated on two occasions in PADSIM. The first is for incorporation of the annual addition of nuclide from SOURCE1 into the soil column, and the second is the adjustment in nuclide partitioning after nuclide export from the soil column. Calculations of transport through the lateral flow path to surface water and through the recharge path to groundwater are conducted independently for independent soil volumes (Fig. 3.10 in text).

The key equations for adsorption calculations are shown using the recharge path (FORTRAN variables beginning with the letter R) as an example. The determination of the new solution

concentration (RSOLU) in the recharge path after the annual addition of nuclide and water from SOURCE1 calculations involves the following statements:

1. The sum of adsorbed chemical (RSOLID, μg) and chemical in solution (RLIQUD, μg) in the soil column from the previous time step plus the new nuclide addition [RLCH (I), μg] gives the total nuclide content of the soil column (RTCHEM, μg). New values for RSOLID and RLIQUD need to be determined for the revised total nuclide in the soil column.

$$\text{RSOLID} + \text{RLIQUD} = \text{RTCHEM} \ . \qquad \textbf{(D.2)}$$

2. The water content of the recharge path (RWATER, ml) is also adjusted from field capacity (RFDCAP, ml) by the addition of the vertical water flux (RFLOWV, ml) from SOURCE1 calculations. The current soil mass (RSMAS, g) in the flow path is given by the product of the current soil volume (RSVOL, ml) and the mean bulk density (BD, g/ml).

3. The K_d (CKD, ml/g) relationship has the form

$$\text{CKD} = \frac{\text{RSOLID/RSMAS}}{\text{RLIQUID/RWATER}} \ . \qquad \textbf{(D.3)}$$

4. The determination of solution concentration (RSOLU, μg/ml) at the new equilibrium is obtained in the following steps:

   a. The right-hand side of Eq. (D.3) is multiplied by RSVOL/RSVOL to give

$$\text{CKD} = \frac{\text{RSOLID/BD}}{\text{RLIQUD/RWPOR}} \ , \qquad \textbf{(D.4)}$$

where RWPOR is the water-filled matrix porosity given by RWATER/RSVOL in units of ml/ml.

   b. Substituting Eq. (D.2) in Eq. (D.4) to define RSOLID in terms of RLIQUD and rearranging to obtain an expression for RLIQUD:

$$(\text{RTCHEM} - \text{RLIQUD})/\text{BD} = \text{CKD}*\text{RLIQUD/RWPOR}$$

$$\text{RTCHEM} - \text{RLIQUD} = \text{CKD}*\text{BD}*\text{RLIQUD/RWPOR}$$

$$\text{RLIQUD}[1 + (\text{CKD}*\text{BD/RWPOR})] = \text{RTCHEM}$$

$$\text{RLIQUD} = \text{RTCHEM}/[1 + (\text{CKD}*\text{BD}*\text{RWPOR})] \ . \qquad \textbf{(D.5)}$$

c. Divide RLIQUD by RWATER to get RSOLU from Eq. (D.5):

RSOLU = RTCHEM/[RWATER + (CKD*BD*RSVOL)] .

5. The flux of nuclide to groundwater (RFLUX, μg) is given by the product of solution concentration (RSOLU, μg/ml) and the recharge volume (RFLOWV, ml).

The second adjustment of solid and liquid chemical partitioning is made after outflow of nuclide in recharge to groundwater. RTCHEM is reduced by the amount of chemical loss (RFLUX) in recharge, and RWPOR is reduced to RFDCAP/RSVOL. Thus, the total nuclide mass remaining in the soil path (RSOIL) is given by

RSOIL = RTCHEM – RFLUX .

The proportion of the total nuclide associated with the solution phase (RLIQUD) is given by

RLIQUD = RSOIL/[1 + (CKD*BD*RFDCAP/RSVOL)] .

and the adsorbed phase is given by

RSOLID = RSOIL – RLIQUD .

These revised values of RLIQUD and RSOLID are used in calculations at the next time step.

D.3.5 Mass Balance Test

PADSIM conducts a calculation to determine the difference between the sum of inflow and outflow of nuclide at a particular time step and the change in nuclide content within the soil column for the time step. An error message is printed if this difference exceeds machine round-off error.

D.4 REFERENCES

Beven, K. J., and M. J. Kirkby 1979. "A Physically-Based Variable Contributing Area Model of Basin Hydrology," *Hydrol. Sci. Bull.* **24**, 43–69.

Davis, E. C. et al. 1987. *Summary of Environmental Characterization Activities at the Oak Ridge National Laboratory Solid Waste Storage Area Six, FY 1986 though 1987,* ORNL/RAP/LTR-87/68, Martin Marietta Energy Systems, Inc., Oak Ridge Natl. Lab.

Huff, D. D. et al., 1977a. "The Application of Analytic and Mechanistic Hydrologic Models to the Study of Walker Branch Watershed," pp. 741–63 in *Watershed Research in Eastern North America*, ed. D. L. Correll, Chesapeake Bay Center for Environmental Studies, Smithsonian Institution, Edgewater, Md.

Huff, D. D. et al. 1977b. *TEHM: A Terrestrial Ecosystem Hydrology Model*, ORNL/NSF/EATC-27, Union Carbide Corp., Oak Ridge Natl. Lab.

Lietzke, D. A., S. Y. Lee, and R. E. Lambert 1988. *Soils, Surficial Geology, and Geomorphology of the Bear Creek Valley Low-Level Waste Disposal Development and Demonstration Program Site*, ORNL/TM-10573, Martin Marietta Energy Systems, Inc., Oak Ridge Natl. Lab.

Luxmoore, R. J. 1982. *Physical Characteristics of Soils of the Southern Region, Fullerton and Sequoia Series*, ORNL-5868. Union Carbide Corp., Oak Ridge Natl. Lab.

Luxmoore, R. J., and D. D. Huff 1989. "Water," pp. 164–96 in *Analysis of Biogeochemical Cycling Processes in Walker Branch Watershed*, ed. D. W. Johnson and R. I. Van Hook, Springer-Verlag, New York.

Luxmoore, R. J., B. P. Spalding, and I. M. Munro 1981. "Areal Variation and Chemical Modification of Weathered Shale Infiltration Characteristics," *Soil Sci. Soc. Am. J.* **45**, 687–91.

Moore, G. K. 1988. *Concepts of Groundwater Occurrence and Flow near Oak Ridge National Laboratory, Tennessee,* ORNL/TM-10969, Martin Marietta Energy Systems, Inc., Oak Ridge Natl. Lab.

Patterson, M. R. et al. 1974. *A User's Manual for the Fortran IV Version of the Wisconsin Hydrologic Transport Model*, ORNL/NSF/EATC-7, Union Carbide Corp., Oak Ridge Natl. Lab.

Quinn, P. et al. 1991. "The Prediction of Hillslope Flow Paths for Distributed Hydrological Modelling Using Digital Terrain Models," *Hydrol. Process.* **5**, 3–30.

Rothschild, E. R. et al. 1984. *Characterization of Soils at Proposed Solid Waste Storage Area (SWSA) 7*, ORNL/TM-9326, Martin Marietta Energy Systems, Inc., Oak Ridge Natl. Lab.

Schwartz, P. M. et al. 1995. *TERRAIN: A Computer Program to Process Digital Elevation Models for Modeling Surface Flow*, ORNL/TM-13071, Lockheed Martin Energy Systems, Inc., Oak Ridge Natl. Lab.

Timmins, S. P., M. A. Huston, and R. B. Clapp 1989. "Generation of Digital Elevation Models from Contours and Comparison of Topographic Indices," *Eos, Trans. Am. Geophys. Union* **70**, 1094.

Wilson, G. V., J. M. Alfonsi, and P. M. Jardine 1989. "Spatial Variability of Saturated Hydraulic Conductivity of the Subsoil of Two Forested Watersheds," *Soil Sci. Soc. Am. J.* **53**, 679–85.

Wilson, G. V., and R. J. Luxmoore 1988. "Infiltration, Macroporosity, and Mesoporosity Distributions on Two Forested Watersheds," *Soil Sci. Soc. Am. J.* **52**, 329–35.

Wilson, G. V. et al. 1993. "Field-Scale Transport from a Buried Line Source in Variably Saturated Soil," *J. Hydrol.* **145**, 83–109.

Appendix E

MODELING OF GROUNDWATER FLOW AND RADIONUCLIDE TRANSPORT AT THE CLASS L-II DISPOSAL FACILITY

J. D. Tauxe
M. W. Yambert

Appendix E

MODELING OF GROUNDWATER FLOW AND RADIONUCLIDE TRANSPORT AT THE CLASS L-II LLW DISPOSAL FACILITY

E.1 POROUS-MEDIUM CONTAMINANT TRANSPORT THEORY

Transport equations are founded on the principle of the conservation of mass: the net rate of increase of mass in a control volume is equal to net mass flux into the volume plus the increase of mass within the volume. This statement of continuity is expressed in the equation

$$\frac{\partial m}{\partial t} + \nabla \cdot \boldsymbol{J} = S^{+} \quad , \tag{E.1}$$

where

m ≡ bulk concentration (units of mass/length^3),

t ≡ time (units of time),

$\boldsymbol{J}$ ≡ the mass flux vector, representing the mass transport across a unit surface per unit time, normal to the surface (units of mass/length^2/time),

S^{+} ≡ strength of mass production within the control volume (units of mass/length^3/time),

and $\nabla \cdot \boldsymbol{J}$ is the divergence of the flux vector. The bulk concentration m of the constituent includes all of the mass in the volume, be it sorbed or in solution. Assuming local equilibrium and a linear sorption isotherm, the sorbed concentration C_s can be expressed as a function of the aqueous concentration C_{aq}:

$$C_s = K_d \, C_{aq} \quad , \tag{E.2}$$

where K_d is the distribution coefficient for the constituent. The bulk concentration is the sum of the aqueous and sorbed concentrations:

$$m = n \, C_{aq} + \rho_b \, C_s \quad , \tag{E.3}$$

or

$$m = (n + \rho_b K_d) C_{aq} \quad , \tag{E.4}$$

where

ρ_b ≡ soil density (units of mass/length³),
n ≡ total porosity (volume of voids/total volume).

The mass flux vector $\boldsymbol{J}$ includes both advective and dispersive components as described above:

$$\boldsymbol{J} = \boldsymbol{q} C - n \boldsymbol{D} \cdot \nabla C \quad , \tag{E.5}$$

where

$\boldsymbol{q}$ ≡ Darcy flux, or specific discharge vector (units of length³/time/length²),
$\boldsymbol{D}$ ≡ dispersion tensor (units of length²/time).

The right hand side of Eq. (A.1) contains the source term, S^+. The only process considered in the performance assessment (PA) which affects this value is decay as a first-order function of mass, so that

$$S^+ = -\lambda m \quad . \tag{E.6}$$

Substituting these expressions into Eq. (A.1) gives

$$\frac{\partial}{\partial t}\left[(n + \rho_b K_d) C\right] + \nabla \cdot \left[\boldsymbol{q} C - n \boldsymbol{D} \cdot \nabla C\right] = -\lambda \left[(n + \rho_b K_d) C\right] \quad . \tag{E.7}$$

To simplify, let us assume steady flow, with no volumetric sources or sinks. In this case,

$$\nabla \cdot \boldsymbol{q} = 0 \quad . \tag{E.8}$$

By the chain rule,

$$\nabla \cdot (\boldsymbol{q} C) = C \nabla \cdot \boldsymbol{q} + \boldsymbol{q} \cdot \nabla C \quad , \tag{E.9}$$

the second term of which disappears by Eq. (A.8). Assuming also a constant fluid density and porosity, Eq. (A.7) can be written

$$(n + \rho_b K_d) \frac{\partial C}{\partial t} + \boldsymbol{q} \cdot \nabla C - n \nabla \cdot (\boldsymbol{D} \cdot \nabla C) = -\lambda C (n + \rho_b K_d) \quad . \tag{E.10}$$

The definition of retardation $\left(R = \frac{m}{C \cdot n} = \frac{n + \rho_b K_d}{n} = 1 + \frac{\rho_b K_d}{n} \right)$ can simplify this equation further:

$$n R \frac{\partial C}{\partial t} + \boldsymbol{q} \cdot \nabla C - n \nabla \cdot (\boldsymbol{D} \cdot \nabla C) = -\lambda C n R \quad . \tag{E.11}$$

Dividing through by the porosity n gives the general form

$$R \frac{\partial C}{\partial t} - \nabla \cdot (\boldsymbol{D} \cdot \nabla C) + \boldsymbol{v} \cdot \nabla C + \lambda R C = 0 \quad . \tag{E.12}$$

This is the principal governing equation for the following exercise in modeling advection-dispersion.

One of the central issues in modeling contaminant transport is the derivation of the flow field. If the hydraulic conductivity tensor **K** is isotropic, groundwater flows in the direction of the largest gradient in the hydraulic head surface. While it is a common assumption that **K** is isotropic, in the vicinity of Oak Ridge it is strongly anisotropic, and groundwater flow does not simply follow the largest gradient, but rather follows the strike of the tilted geologic strata. This behavior still falls within the domain of classical porous medium physics and can be modeled by application of the head equation (Bear 1972),

$$\frac{\partial}{\partial x}\left(K_x \frac{\partial h}{\partial x} \right) + \frac{\partial}{\partial y}\left(K_y \frac{\partial h}{\partial y} \right) + \frac{\partial}{\partial z}\left(K_z \frac{\partial h}{\partial z} \right) = S_s \frac{\partial h}{\partial t} \quad , \tag{E.13}$$

together with appropriate initial and boundary conditions. Here K_x, K_y and K_z are x-, y- and z-components of the aquifer hydraulic conductivity tensor, h is the hydraulic head, and S_s is the specific storage. The solution of this equation may be constrained in several ways, principally by adjusting boundary conditions and flow in and out of the system. In the best case, the computed head replicates the measured head at measurement locations.

E.2 GROUNDWATER MODELING FOR THE CIIDF

E.2.1 Conceptual Model

CIIDF is situated on a knoll in Bear Creek Valley, straddling the contact between the Maryville and Nolichucky formations. Near the surface, the weathered regolith is fairly uniform in consistency, so the model does not distinguish between the two source lithologies. We assume that the regolith is of a uniform depth as well, following the natural topography. This upper layer of the subsurface is represented in the groundwater computer model by the upper two layers of cells. Below this lies more massive bedrock with a lower conductivity, which is represented as a third, tighter layer. The model

area is dissected by small intermittent streams between the knolls, which serve to drain the upper layers of meteoric recharge and may be outlets for deeper groundwater as well, so that no groundwater is expected to cross these tributary drainages. Bear Creek runs at the bottom of the valley and gains and loses water along its length to groundwater. It is the surface expression of the major drainage system for the valley, and all shallow groundwaters and surface waters are expected to eventually drain out via Bear Creek.

In order to assess the exposure to individuals from radionuclides in a waterborne environmental pathway, a model must be constructed. Given the site's hydrologic isolation, the only water input to the system would be from precipitation. That precipitation which does not run off to surface waters enters the subsurface by recharge, and that recharge which comes from water which has had contact with the waste will contain radionuclides and is modeled as a source of groundwater contamination. In the shallow subsurface, the recharge water is partitioned into that which discharges to the surface stream and that which enters groundwater, as described in the previous section. the groundwater flow model also discharges water to surface streams. The CIIDF groundwater model attempts to predict the fate of these contaminants with special attention paid to their concentration at the locus of compliance points over 100 m from the facility. For a given inventory, dose estimates are calculated through time for groundwater at the 100-m boundary and for surface waters at an integrating collection point in Bear Creek at the outlet of the modeling domain.

Major features of the groundwater conceptual model include a steady-state flow field, diffuse recharge (with that recharge through CIIDF being contaminated), chemical retardation, and discharge of groundwater to streams and surface water drains. Within an annual time step, all groundwater discharges to streams or drains is combined with the discharge from the subsurface transport model.

Since CIIDF has not yet been built or stocked with an inventory of radionuclides, there is an opportunity to use the PA process to define the limits of such an inventory. From the drinking water exposure pathway, the limit for a given radionuclide is defined as that inventory which corresponds to the upper limit of acceptable dose at any compliance point, whether from groundwater or surface waters. An inventory limit can thus be obtained for each radionuclide in question without considering contributing doses from other radionuclides in the inventory or from other sources.

For radionuclides whose expected aqueous concentrations are not limited by solubility, the modeling process used in the analysis (i.e, the combination of source, shallow subsurface, and groundwater models) is linear, and only two iterations of calculations were required to quantify maximum disposal limits. An initial estimate of a limiting inventory was made, and a corresponding dose was calculated. Taking advantage of the linearity of the system, a new limiting inventory was obtained, and the calculations rerun to confirm its acceptability.

For solubility-limited nuclides, the dose from consumption of drinking water may become nonlinear with regard to inventory. For these isotopes, several iterations were required to determine the inventory corresponding to the maximum allowable concentration in groundwater or surface water. The resulting graphs of dose as a function of inventory are displayed in Appendix F.

E.2.2 Computer Model

E.2.2.1 The FTWORK Computer Program

The computer model used to perform groundwater flow and transport analysis was built using FTWORK, a three-dimensional, block-centered finite-difference program developed by GeoTrans, Inc. (Faust et al. 1990). The program may be used to perform both steady-state and transient flow simulations, as well as contaminant transport calculations for multilayered, fully saturated, porous media. The "flow" portion of the program solves for hydraulic head (the state variable) and assumes an invariant water density. It can effectively model a wide range of processes and physical geometries which include the effects of source/sinks and layers with irregular thicknesses. The "transport" portion of the program incorporates the mechanisms of advection, dispersion, linear reversible adsorption, and radioactive decay. While there are numerous programs available for solving saturated flow and mass transport problems, FTWORK was chosen for the analysis for a number of reasons. Features which made it a desirable choice included the abilities to implement a "drain" boundary condition (making it possible to simulate the behavior of ephemeral streams without artificially constraining the head value at these locations), to handle multiple layers with varying thicknesses, and to specify both spatially and temporally dependent recharge and contaminant sources. FTWORK version 2.7, written in FORTRAN, has undergone significant verification and benchmarking exercises (Faust et al. 1990) and was used in the present analysis. All groundwater model runs were conducted on a Hewlett-Packard Model 9000 Series 730 UNIX workstation running HP-UX version 9.01.

E.2.2.2 Groundwater Flow Model

The ability to accurately assess the migration of contaminants in the groundwater requires the development of a calibrated groundwater flow model, consistent with the conceptual model for the site. Site characteristics are presented in Sect. 2.1, general assumptions about the site are discussed in Sect. 3.3, and the following sections discuss a variety of topics related to construction of this model. The linear dimensions of the model are measured in U.S. units (feet) rather than in the International System of Units (SI), since all current topographic data are recorded in these units. The Y-12 grid was used for layout of the site, and references to easting and northing are with respect to this grid.

E.2.2.2.1 Spatial Discretization

A region of Bear Creek Valley (BCV) about 2.1 km^2 (0.82 mi^2) in area surrounding the proposed CIIDF site was selected as the modeling domain based on the location a number of natural features which served as logical boundaries for a groundwater model. These include Bear Creek on south and west, Gum Branch (NT-14) to the east, and Pine Ridge to the north. This area was discretized into a variably spaced, finite-difference grid consisting of 160 cells in the X (easting, strike parallel) direction, 96 cells in the Y (northing, strike perpendicular) direction, and three layers in the Z (vertical)

direction for a total of 46,080 cells. A plan view of BCV showing the model grid in relation to selected features and the proposed CIIDF is shown in Fig. E.1. Cell dimensions in both the X and Y directions near the facility were uniformly set to 25 ft, whereas for areas located farther away from the site, X-Y cell dimensions ranged from 25 to 200 ft, as shown in the detailed grid cell plan presented in Fig. E.2.

As previously indicated, the model was discretized vertically into three layers. The extent of each of these layers was determined as follows: Surface elevations for Layer 1 (the uppermost layer) were first digitized from 10-ft contour maps of the BCV area (Y-12 1984). Fig. E.3 shows a contour plot of the resulting topographic surface. The EarthVision software package (Dynamic 1994) was used to interpolate elevations at the center of each model grid cell. Having established the elevation for the top of Layer 1, a series of iterative model flow calculations was performed in which model layer thicknesses were adjusted until the calculated water table was approximately 10 ft above the bottom of Layer 1. Thicknesses for Layer 1 were variable, ranging 150–180 ft underneath Pine Ridge near the northern boundary, to a prescribed minimum of 10 ft at locations near Bear Creek. The thickness of Layer 2 was set uniformly to 30 ft (roughly the distance from the water table to bedrock), and Layer 3 thicknesses were defined such that the bottom of Layer 3 corresponded to a constant elevation of 700 ft above mean sea level. Fig. E.4 depicts a cutaway view of the vertical discretization of the model before CIIDF construction modifications.

E.2.2.2.2 Hydrogeologic Properties

Hydrogeologic flow modeling requires a definition of material properties throughout the modeling domain, including thickness of the transmissive layer, porosity, and hydraulic conductivity. In the case of the CIIDF site, the porosity is assumed constant, the thickness is defined by the cell dimensions as defined by the modeling grid, and the hydraulic conductivity field is based on a geostatistical analysis of data obtained from well tests. A summary of hydrogeologic properties selected for the CIIDF model follows, with more detailed information on the development of the hydraulic conductivity field in the next section.

- Saturated thickness—The thickness of the saturated zone was variable, extending from the water table down to an elevation of 700 ft above mean sea level.
- Bulk density—The bulk density of all geologic materials was set at 1.35 g/mL, consistent with the shallow subsurface modeling.
- Porosity—A value of 0.05 (5%) effective porosity was used. This value is based on aquifer tests performed at the Engineering Test Facility, located in a similar geologic setting in Melton Valley.
- Dispersivity—The following constant values of dispersivity were used: $\alpha_L = 0.5$ ft, $\alpha_T = 0.25$ ft, and $\alpha_V = 0.25$ ft. These values are consistent with those reported by Lee et al. (1989).

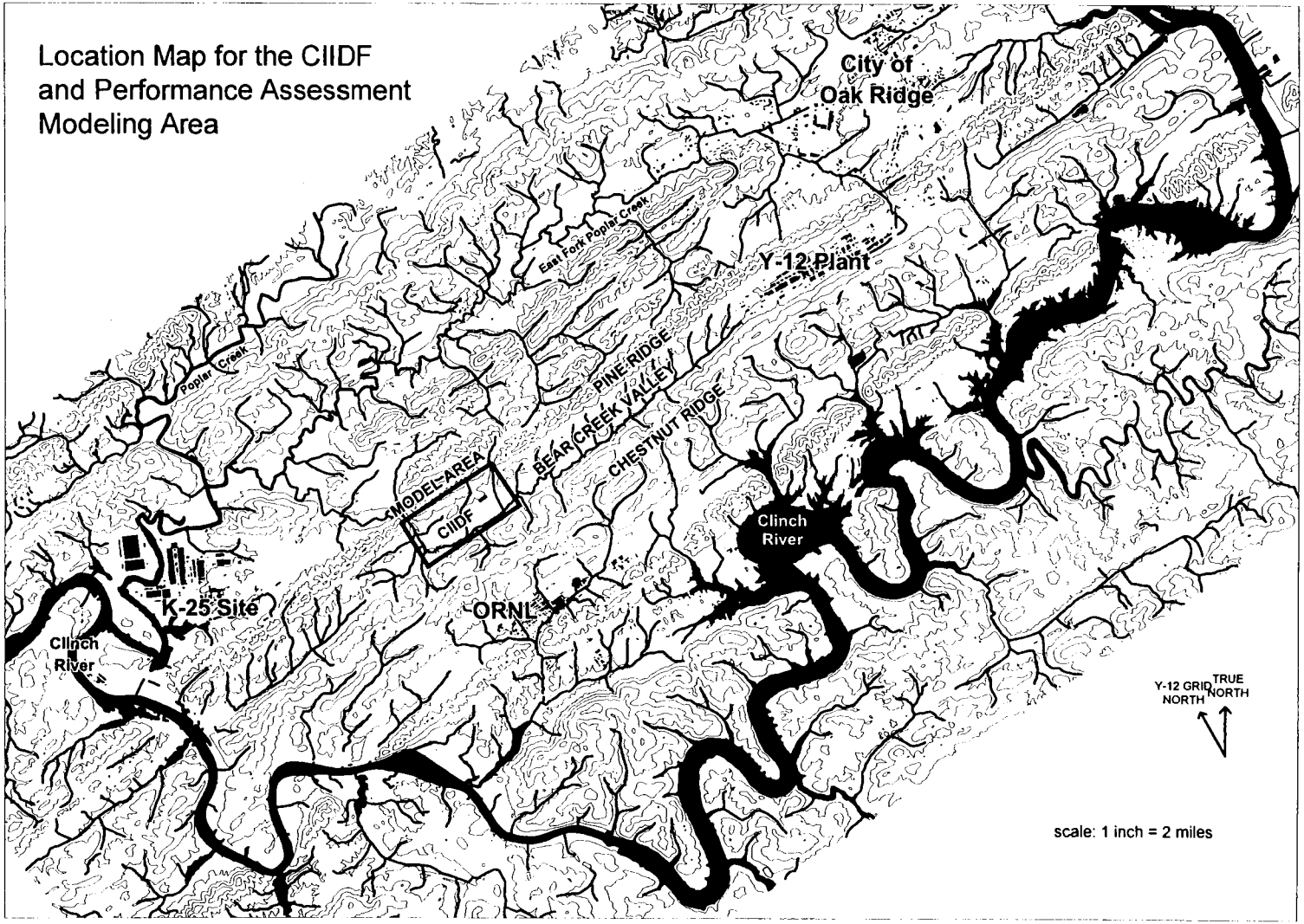

Fig. E.1. Location of CIIDF on the Oak Ridge Reservation.

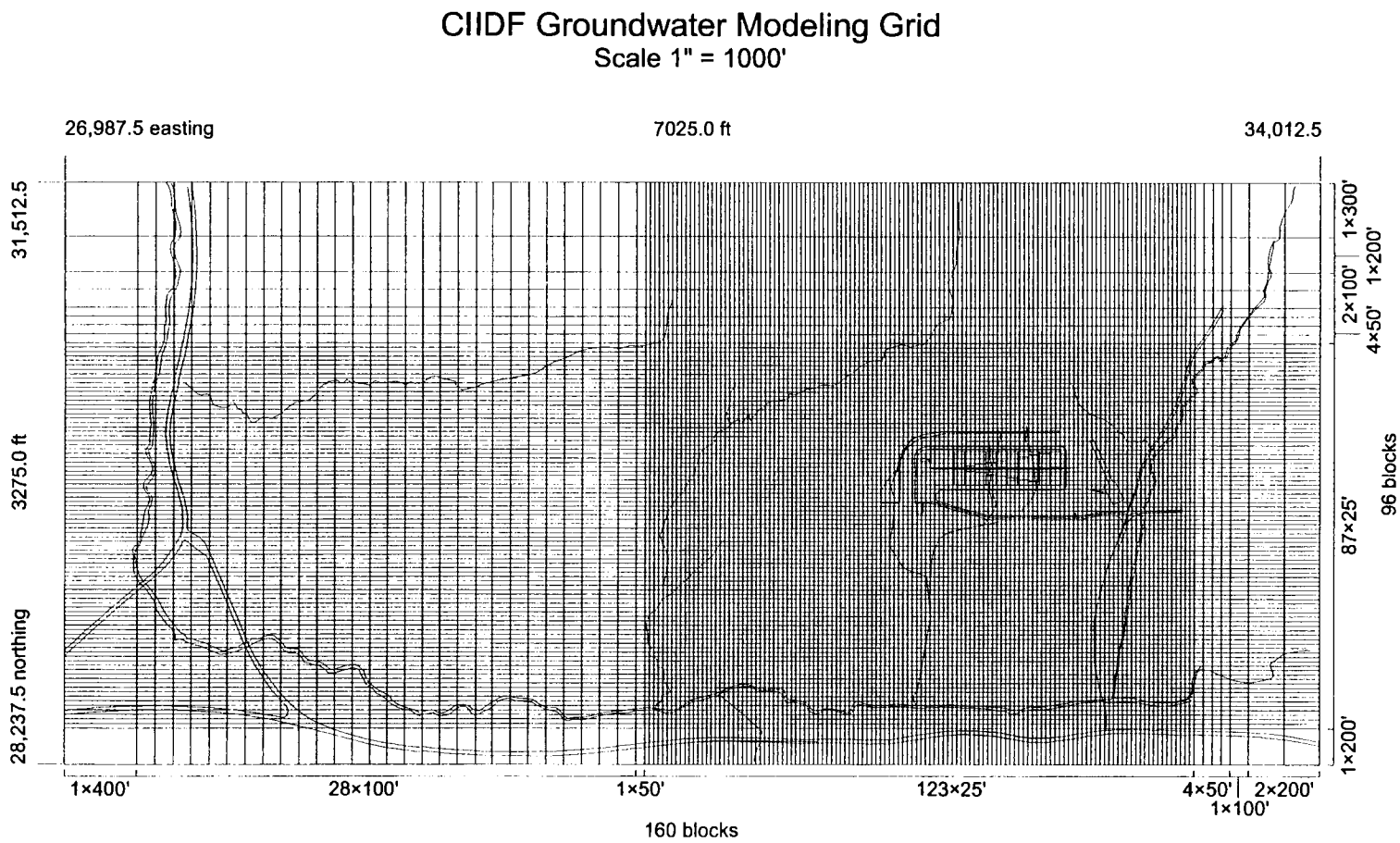

Fig. E.2. Finite difference horizontal discretization of the CIIDF groundwater model.

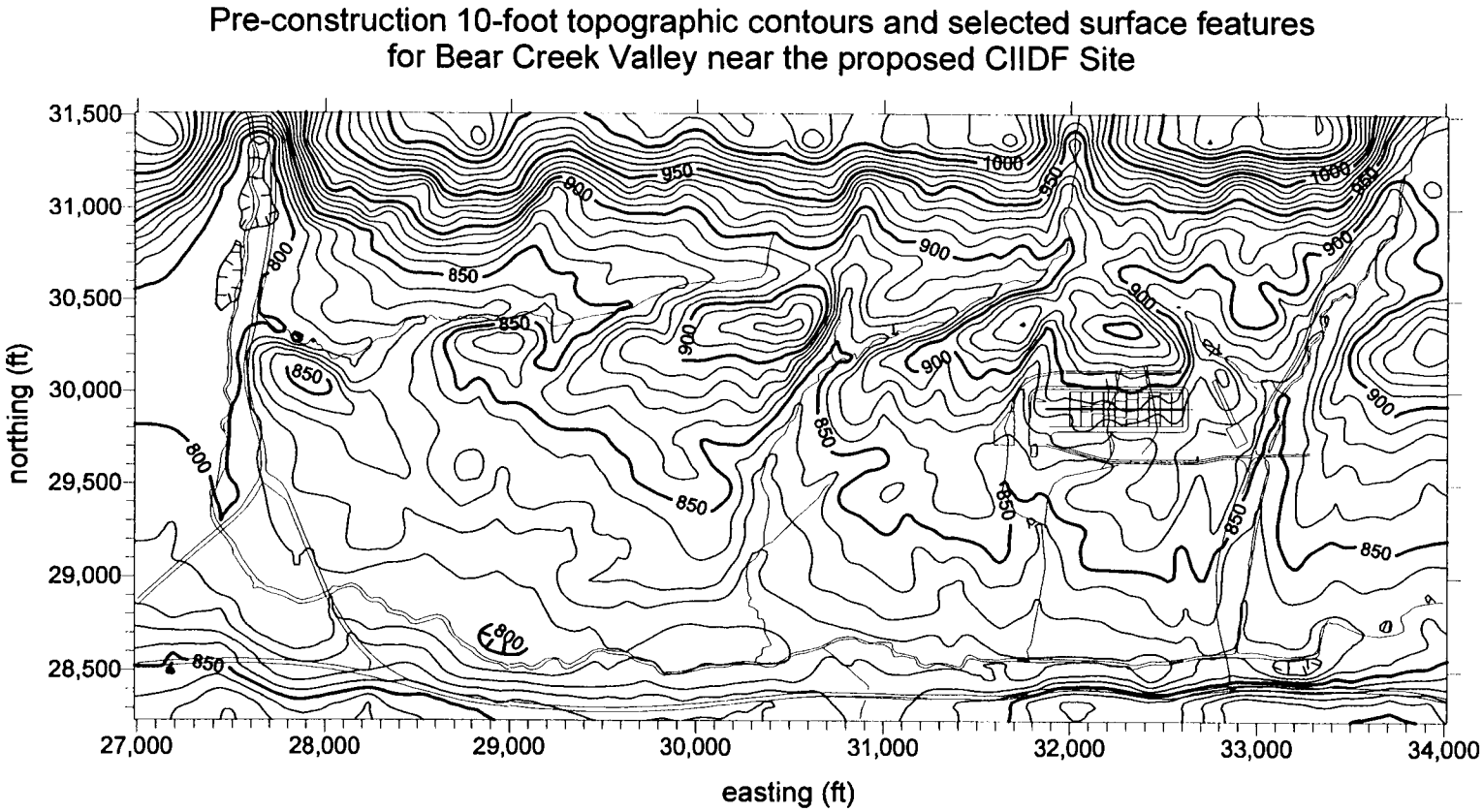

Fig. E.3. Preconstruction topography of the CIIDF model domain.

Cutaway through the CIIDF modeling domain in Bear Creek Valley
revealing layering used in the groundwater model
(pre-construction topography)

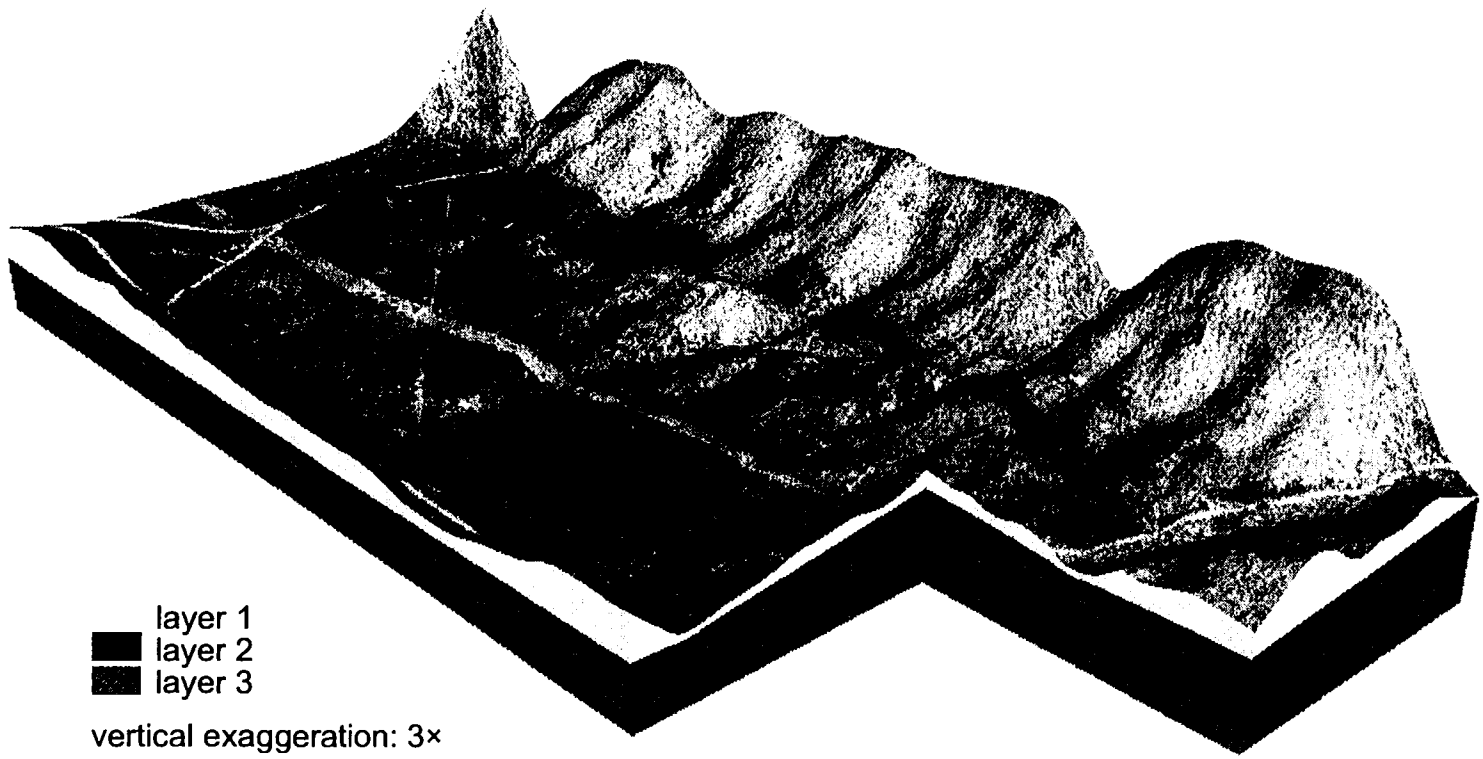

Fig. E.4. Vertical discretization of the preconstruction CIIDF groundwater model.

E.2.2.2.3 Hydrogeologic Conductivity

Hydraulic conductivity values for each model cell were assigned based on the following assumptions:

- The *X-Y* spatial variation is similar for all depths.
- The hydraulic conductivity field does not vary in time.
- Hydraulic conductivity decreases significantly below the bedrock surface (model Layer 3).
- Principal directions of the hydraulic conductivity tensor **K** are aligned with the strike parallel (*X*), strike perpendicular (*Y*), and vertical (*Z*) directions.
- The hydraulic conductivity tensor is anisotropic, with higher conductivity in the strike parallel direction than either the strike perpendicular or vertical directions.

Hydraulic conductivity data were obtained from a characterization study of the area by Golder Associates (1988). The values chosen as the basis for this PA, presented in Table E.1, are selected from rising head test data presented in Table 7.1 and well location data from Plate 1 of the Golder report. Since the PA modeling considers only the upper tens of meters of the subsurface, deeper wells (GW-136, -400, -403, -453, and -472) were excluded from the data set.

The log(*K*) values shown in Table E.1 were subjected to a geostatical analysis using the GeoEAS program (EPA 1988), in an effort to determine spatial characteristics for the field. A variogram is presented in Fig. E.5, with four curve fits overlain. These four curves were fitted by adjusting the nugget, sill, and range (where applicable) of the linear, exponential, spherical, and Gaussian variogram functions. The resulting best fits are presented in Table E.2.

Further analysis was performed with the GeoEAS program (EPA 1988) in order to determine if any anisotropy of the conductivity field was evident in the data set. Since variograms from data limited to an east-west window showed no better spatial correlation than those using a north-south window, no anisotropy in the value of hydraulic conductivity could be justified, although some might have been expected to follow the east-west trending geological structure. This result does not imply, however, that there is no anisotropy to the hydraulic conductivity tensor itself.

Once the best parameters for the four variograms ware determined, they were used to generate four continuous fields of log(*K*) conditioned (with allowance for the nugget) on the original data from Table E.1. These fields were generated by kriging using Surfer version 6.01 (Golden Software 1995), producing a regular grid of node-centered values covering the modeling domain, shown in Fig. E.6. Assuming a conductivity tensor anisotropy of K_x:K_y:K_z = 3:1:1 (Golder Associates 1988), the field based on a linear variogram produced the best fit of modeled heads to measured water table (as discussed in the model calibration section below) and was used for base case calculations, and the others were used in the sensitivity analysis. Based on the results of this analysis, several plausible fields were generated by kriging on a regular mesh covering the domain. The kriged fields were resampled onto the modeling grid, and the continuous values were discretized into sets, corresponding

Table E.1. Estimates of hydraulic conductivity used for the generation of synthetic hydraulic conductivity fields

Well ID	Well location		Open interval		Unit sampled[b]	Hydraulic conductivity		
	Northing (ft)	Easting (ft)	Top (TOC ft)[a]	Bottom (TOC ft)		*K* (cm/s)	*K* (ft/d)	log(*K*) (ft/d)
GW-405	30323.58	28253.06	25.5	36.7	MAR	1.77E-4	5.02E-1	-0.2995
GW-407	30434.65	28828.24	33.5	42.7	ROG	8.12E-6	2.30E-2	-1.6379
GW-409	30289.30	28916.54	48.3	60.5	MAR	4.24E-6	1.20E-2	-1.9201
GW-412	30629.78	29868.86	29.2	42.1	RUT/PV	2.47E-5	7.00E-2	-1.1548
GW-414	30199.96	29585.74	45.5	57.6	MAR	1.57E-5	4.45E-2	-1.3516
GW-415	30099.66	30018.45	26.6	30.0	MAR	3.35E-4	9.50E-1	-0.0225
GW-416	30096.84	30022.85	49.9	63.2	MAR	5.42E-5	1.54E-1	-0.8135
GW-417	29758.11	29655.75	36.5	50.9	NOL	1.16E-4	3.29E-1	-0.4830
GW-419	29473.36	29425.25	38.5	50.6	NOL	1.65E-5	4.68E-2	-1.3300
GW-421	28850.04	28843.60	28.9	40.4	MAY	4.33E-4	1.23E+0	0.0890
GW-422	28849.53	28855.92	4.1	9.4	MAY-SAP	1.25E-3	3.54E+0	0.5494
GW-423	28762.24	29314.19	29.1	41.1	MAY	2.81E-6	7.97E-3	-2.0988
GW-425	29037.15	29867.41	49.7	61.7	NOL	1.40E-4	3.97E-1	-0.4014
GW-427	28682.11	30210.83	38.8	49.8	MAY	1.16E-3	3.29E+0	0.5170
GW-428	28678.78	30217.99	11.3	15.9	MAY	3.05E-4	8.65E-1	-0.0632
GW-430	29522.24	30463.95	27.4	40.2	NOL	9.11E-6	2.58E-2	-1.5880
GW-432	30283.78	30821.16	34.3	46.1	MAR	5.94E-5	1.68E-1	-0.7737
GW-433	30390.62	31191.70	7.1	15.5	MAR/MAR-SAP	8.54E-5	2.42E-1	-0.6160
GW-434	30397.54	31195.83	30.2	42.2	ROG	2.70E-4	7.65E-1	-0.1161
GW-436	30250.71	31291.04	34.9	47.3	MAR	4.53E-6	1.28E-2	-1.8914
GW-437	29960.52	31457.62	53.3	65.1	MAR	1.52E-4	4.31E-1	-0.3657
GW-439	29582.44	31447.29	47.4	61.8	NOL	7.60E-5	2.15E-1	-0.6667
GW-440	29580.31	31453.12	23.1	28.7	NOL-SAP	7.08E-5	2.01E-1	-0.6975
GW-441	28967.71	31214.63	44.6	56.6	NOL	1.67E-5	4.73E-2	-1.3248
GW-448	29885.05	31738.31	32.6	46.1	MAR	6.49E-5	1.84E-1	-0.7353
GW-450	30430.33	31726.04	45.8	57.6	ROG	2.37E-5	6.72E-2	-1.1728
GW-452	29767.95	32590.72	10.6	21.1	NOL-SAP/NOL	2.08E-5	5.90E-2	-1.2294
GW-456	29621.30	29259.87	59.6	72.1	NOL	3.64E-5	1.03E-1	-0.9864
GW-457	29621.30	29259.87	18.3	28.1	NOL/NOL-SAP	1.92E-5	5.44E-2	-1.2642
GW-458	29581.22	29621.56	59.5	72.0	NOL	3.46E-5	9.81E-2	-1.0084
GW-459	29581.22	29621.56	19.5	29.0	NOL/NOL-SAP	1.41E-5	4.00E-2	-1.3983
GW-460	29601.91	29210.49	58.9	71.9	NOL	2.66E-5	7.54E-2	-1.1226
GW-461	29601.91	29210.49	16.9	27.8	NOL-SAP/NOL	1.85E-5	5.24E-2	-1.2803
GW-462	29601.15	29260.50	17.5	70.4	NOL/NOL-SAP	3.53E-6	1.00E-2	-1.9997
GW-463	28679.66	30111.11	45.4	58.2	MAY	2.21E-3	6.26E+0	0.7969
GW-464	28688.53	30111.26	11.8	24.0	MAY	5.17E-4	1.47E+0	0.1660
GW-465	28708.36	30154.55	29.5	42.3	MAY	1.17E-4	3.32E-1	-0.4793
GW-466	28650.90	30161.30	31.1	40.7	MAY	1.17E-3	3.32E+0	0.5207
GW-467	28678.88	30159.43	19.2	64.7	MAY/MAY-SAP	6.74E-3	1.91E+1	1.2812

[a]TOC = top of casing.

[b] Rock unit codes: MAY = Maynardville, MAR = Maryville, NOL = Nolichucky, PV = Pumpkin Valley, RUT = Rutledge, ROG = Rogersville, SAP = saprolite

Source: Data from Golder Associates (1988).

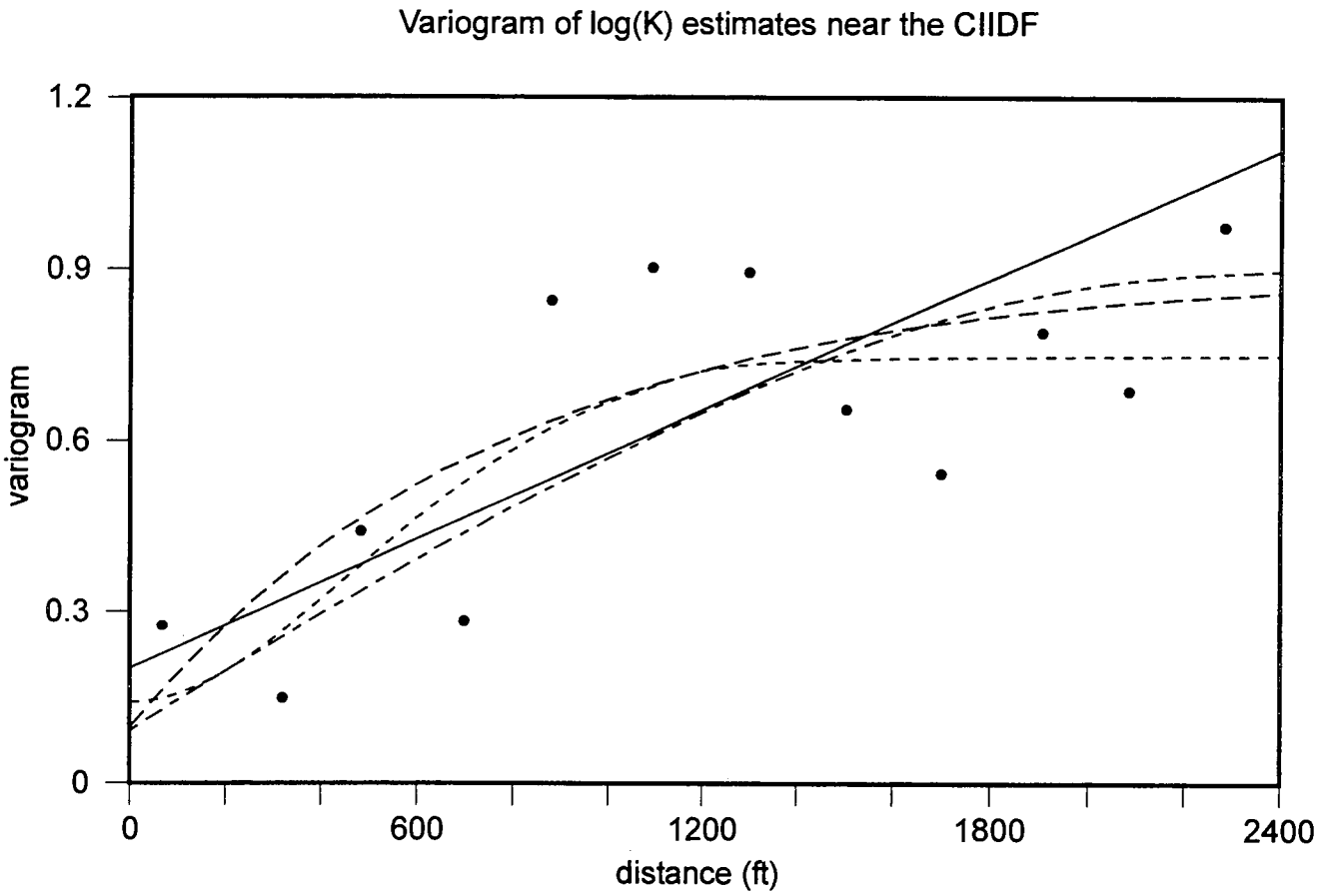

	model	nugget	sill	range
———	linear	0.2	N/A	N/A
- - - - -	gaussian	0.15	0.6	1200
— — — -	exponential	0.1	0.8	2400
- — - —	spherical	0.1	0.8	2400

Fig. E.5. Variograms of hydraulic conductivity field near the CIIDF site.

Table E.2. Variograms used to generate synthetic hydraulic conductivity fields at CIIDF

Variogram model	Mathematical formulation[a]	Fitted parameters		
		Nugget (ft/d)	Sill (ft/d)	Range (ft)
Exponential	$\gamma(h) = C\left[1 - e^{-h}\right]$	0.1	0.8	2400
Gaussian	$\gamma(h) = C\left[1 - e^{-h^2}\right]$	0.15	0.6	1200
Linear	$\gamma(h) = Ch$	0.2	0.9	None
Spherical	$\gamma(h) = \begin{cases} C\left[\frac{3}{2}h - \frac{1}{2}h^3\right] & 0 \le h \le 1 \\ C & h > 1 \end{cases}$	0.1	0.8	2400

[a] Mathematical symbols: γ = variogram function, h = relative separation distance between the measurement points, and C = scale for the structured component of the variogram (Journel and Huijbregts 1978).

to a series of material properties as required by FTWORK. Final hydraulic conductivity values were modified slightly to improve calibration of the calculated head field to measured values of the water table.

This analysis generated continuously distributed *X-Y* conductivity fields which were interpolated from sparse measured data. The FTWORK model, however, implements hydraulic conductivity as a material property, making the assignment of unique floating-point conductivity values for each model cell impractical. It was therefore necessary to convert these continuous distributions into a series of types, i.e., into a discrete zonal form. For each model layer, a set of seven zones, each representing a range of conductivities, was defined. A conductivity value associated with one of these seven zones (the median value of the zone's range) was then assigned to each model cell based on the interpolated, continuous conductivity value at the cell's center. Fig. E.7 shows the seven conductivity zones for a given layer.

K_x (conductivities in the strike parallel direction) values for each zone were assumed to be three times the K_y and K_z (conductivities in the strike perpendicular and vertical directions) values for each layer (K_x:K_y:K_z = 3:1:1). In addition, in order to reflect the decreased permeability which occurs at depth, the conductivities values for Layer 3 zones were assumed to be one order of magnitude less than the corresponding zones in Layers 1 and 2.

During calibration of the groundwater flow model, a number of proposed continuous conductivity fields were evaluated in order to ascertain which would produce the best model calibration. During this

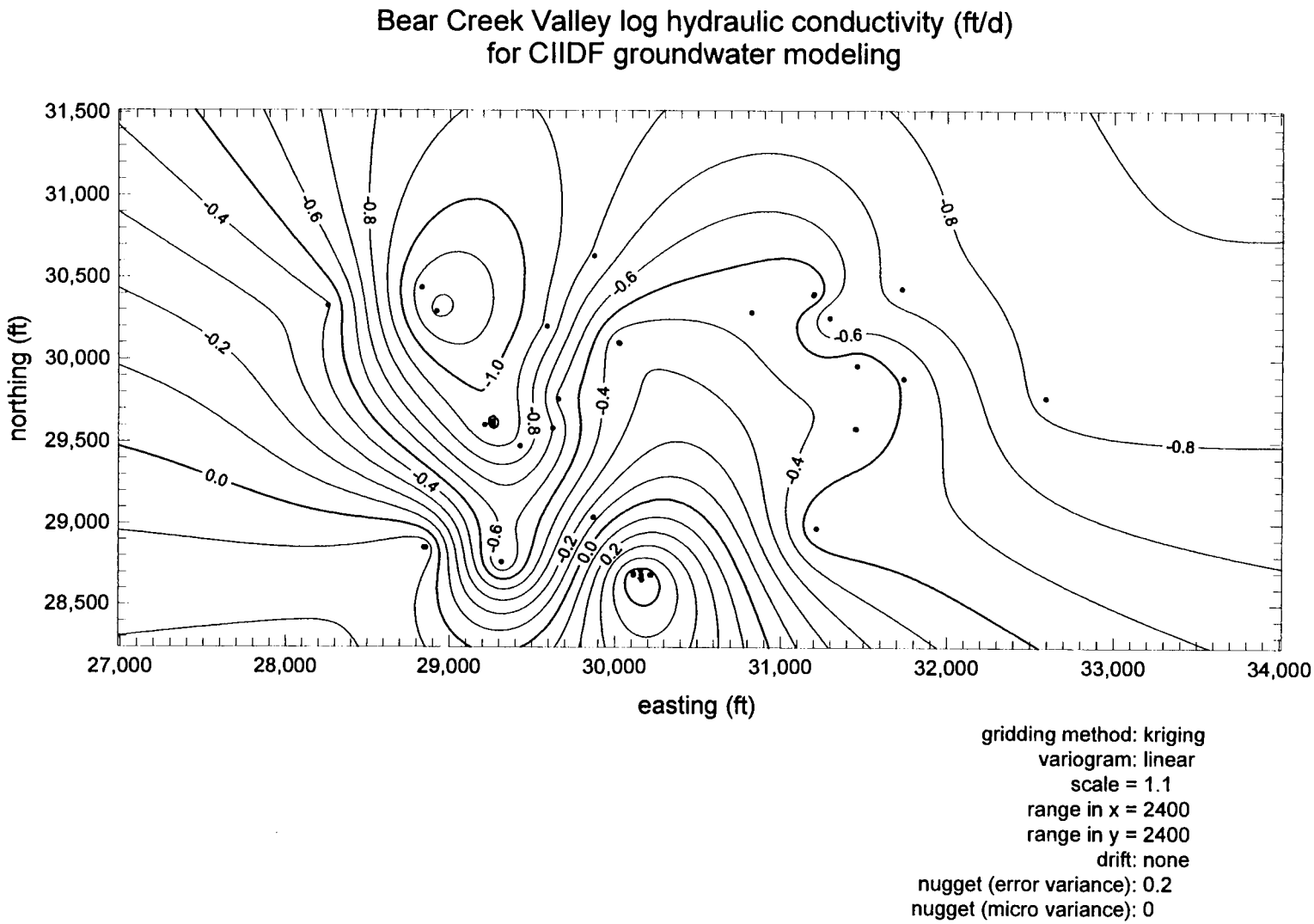

Fig. E.6. Continuous hydraulic conductivity field kriged from data.

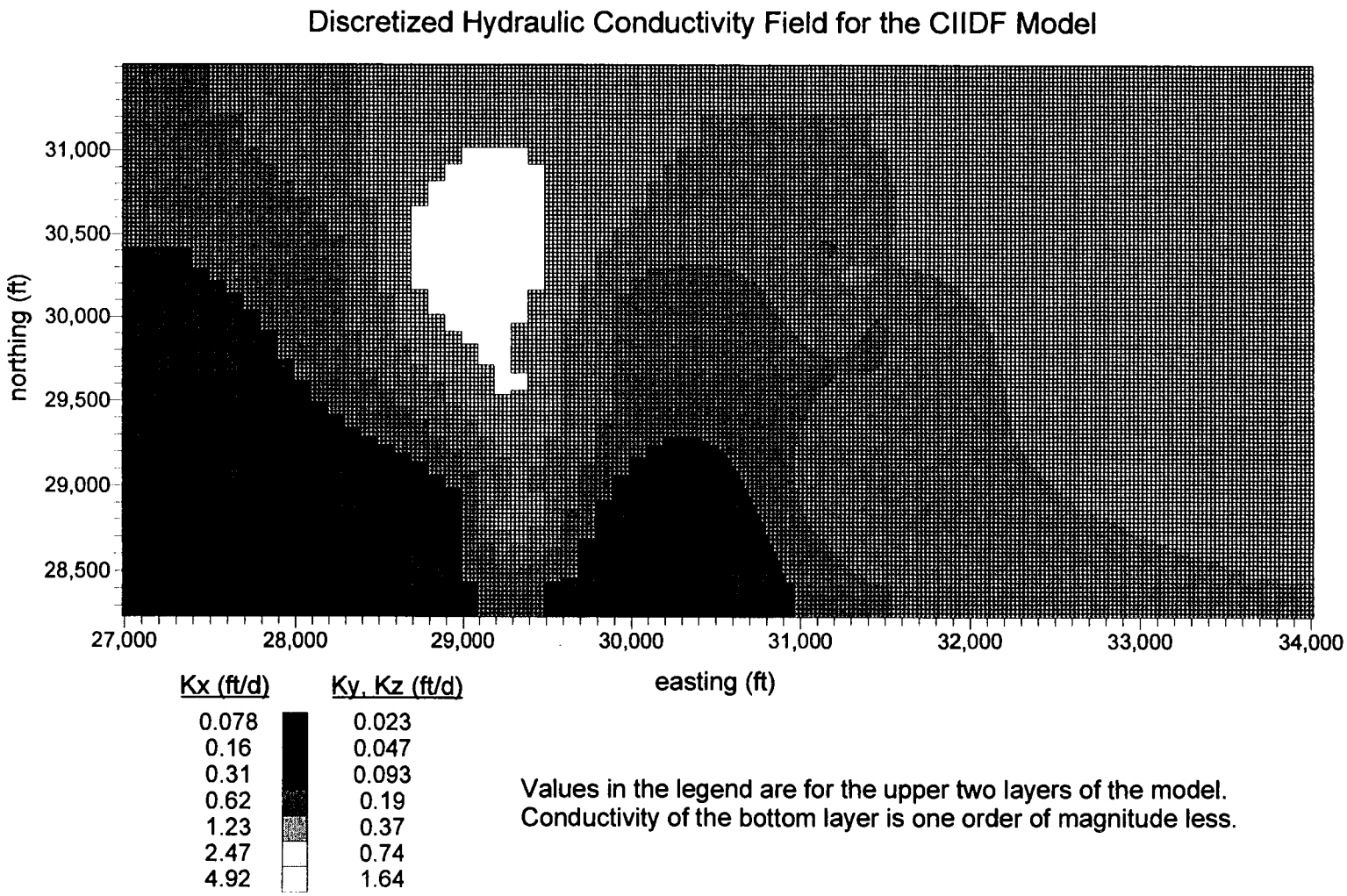

Fig. E.7. Zonal hydraulic conductivity field for the CIIDF model.

process, the corresponding zonal conductivity values were scaled by a single factor in order to improve the correlation between measured and calculated hydraulic head. Fig. E.7 shows the best fit K_x, K_y, and K_z values for each zone in Layer 1.

E.2.2.2.4 Surface Recharge

Diffuse recharge was applied to the Layer 1 of the model. Recharge rates were assumed to vary spatially over the domain and were based on results of the digital terrain analysis (see Sect. 3.4), which identified three separate recharge zones: preferential flow, stream channels, and remaining landscape. The recharge rates, used in the analysis for each of the three zones, are given in Table E.3. Fig. E.8 shows the recharge zone assigned to each model cell.

Table E.3. Model recharge rates

Model recharge zone	Recharge rate	
	(mm/year)	(in./year)
Preferential flow	140	5.25
Stream channels	180	7.0
Remaining landscape	90	3.5

E.2.2.2.5 Model Boundary Conditions

FTWORK automatically assigns no-flow boundary conditions to all outer edges of the modeled volume. In addition, for Layer 1, model cells coincident with Bear Creek on the southern and western edges of the model, as well as those coincident with Gum Branch near the eastern edge of the model, were treated as constant head locations, since these streams generally bear water year-round. The remaining, ephemeral streams were modeled as "drain" boundaries on Layer 1. The special "drain" boundary feature of FTWORK operates as follows: For conditions in which the head in a model cell is higher than the elevation of the drain, flow to the drain is treated as a head-dependent flux that is proportional to the area and conductance of the drain. Otherwise, for cases where the modeled head is lower than the drain elevation, no flow to the drain occurs.

For the purposes of calibration of the groundwater model, boundary conditions were assigned which corresponded to existing natural hydrologic features. Layer 1 model cells for which these boundary conditions were assigned are shown in Fig. E.9. To perform the contaminant transport simulations, however, boundary conditions were used which corresponded to postconstruction hydrology, as shown in Fig. E.16. A detailed discussion of both the model calibration and the construction modifications follows.

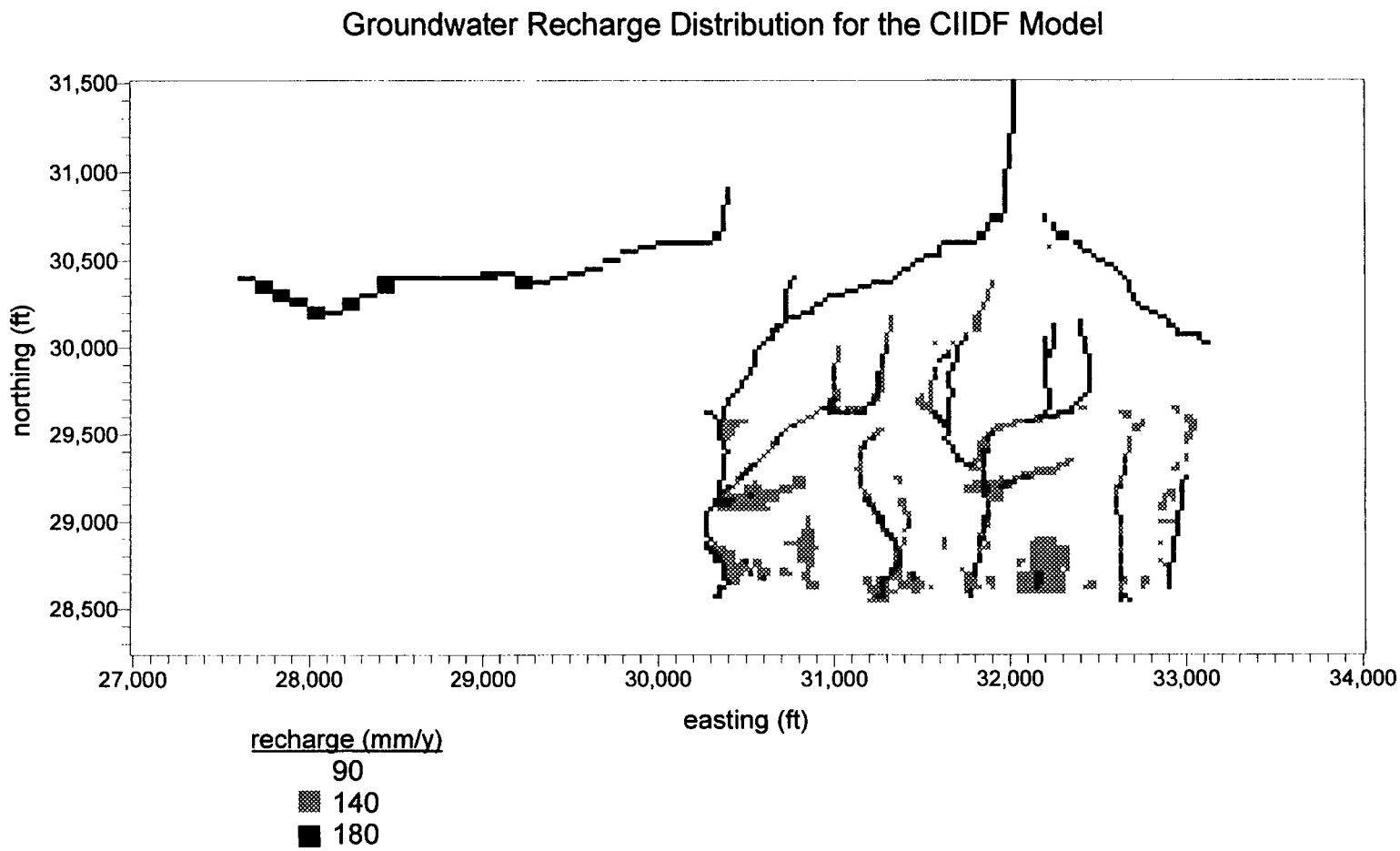

Fig. E.8. Diffuse recharge distribution for the CIIDF model.

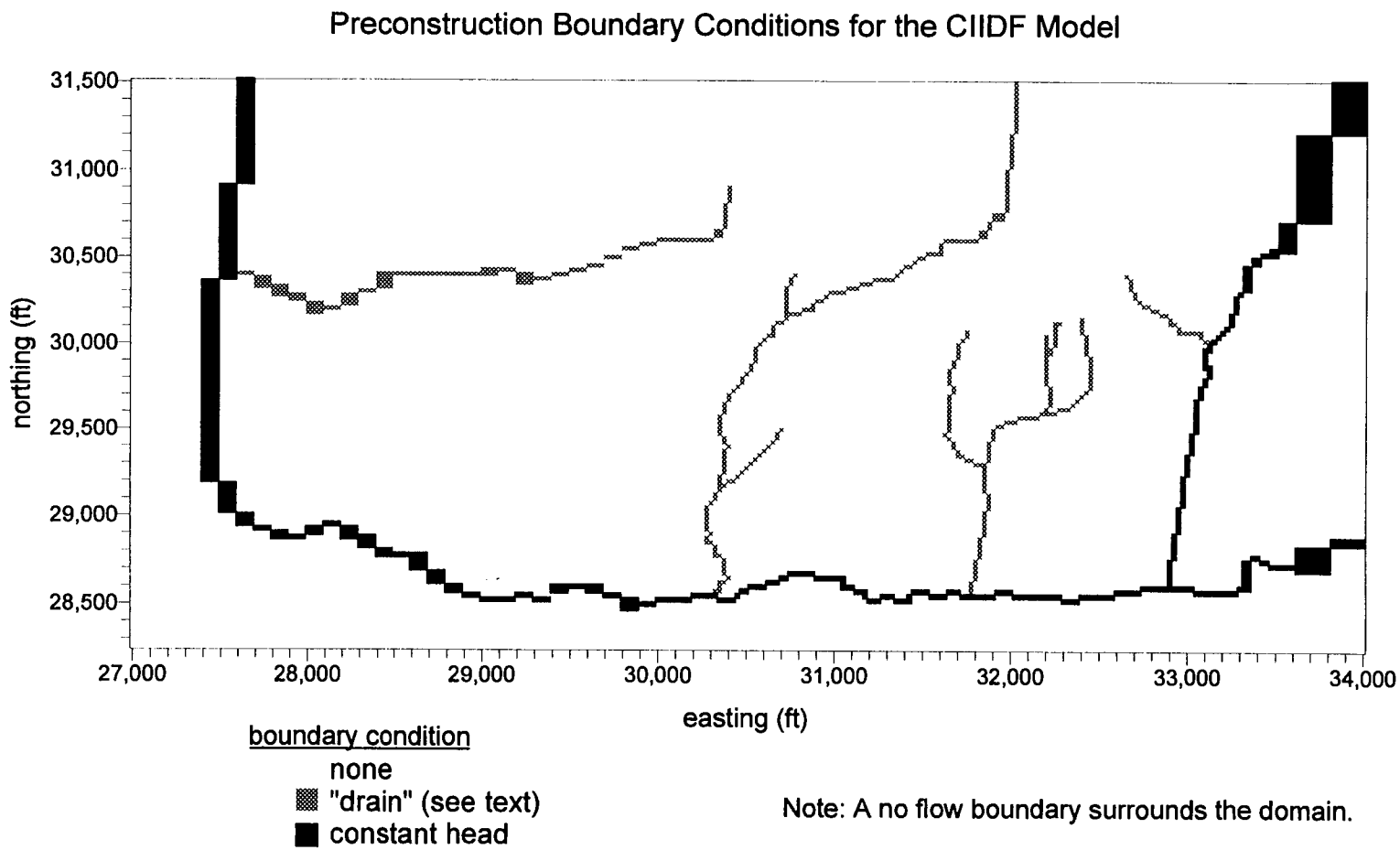

Fig. E.9. Preconstruction boundary conditions for the CIIDF model.

E.2.2.2.6 Groundwater Flow Model Calibration

Model calibration was accomplished by first generating steady-state solutions to the flow equation for a series of hydraulic conductivity distributions and the preconstruction boundary conditions. These solutions were then evaluated in order to determine which conductivity distribution produced the most accurate representation of the observed flow field, based on average residual error between calculated and actual measured head values at groundwater monitoring well locations. Although a large number of monitoring wells are located in Bear Creek Valley near the proposed disposal site, not all have a consistent, year-round distribution of recorded measurements. Furthermore, measured readings for other wells contain various obvious discrepancies. Thus, after careful screening of measured 1988–90 data for BCV monitoring wells, those with reliable, annual average water table measurements were selected for model calibration. The water table surface interpolated from these measurements is shown in Fig. E.10.

The calibrated head field compares well to the measured one, with differences of under a few feet in the vicinity of the CIIDF facility. A deviation of about 20 ft (6 m) exists in the western part of the modeling domain, beneath an anomalous local water table high. This mound is not accounted for in the recharge estimation, and so is not reflected in the flow model. At any rate, it is well outside the CIIDF region, and is not expected to have a significant effect on transport calculations.

Table E.4 lists the measured annual average water table values for these wells and the calculated head values for the flow solution which produced the least average residual error. Fig. E.11 shows the location of the wells used in the calibration process along with the corresponding error (i.e., measured minus calculated head value) for the best fit. The average difference between calculated and measured head for these wells was 6.4 ft. Finally, the calculated head surface for the entire model is depicted in Fig. E.12. A vector plot showing the corresponding Darcy velocity field for the area near the CIIDF for Layer 1 is given in Fig. E.13.

A secondary means of quantifying the model's ability to accurately represent actual flow conditions at the site was by comparison of measured discharges at surface water monitoring stations to the calculated discharge to drain cells which corresponded to stream locations upstream of a gauging station. Two U.S. Geological Survey (USGS) gauging stations are appropriately located so that their subwatersheds lie completely within the modeling domain (see Figure 3.10). USGS 03538272, located on a tributary to Bear Creek near at the western edge of the model boundary, had an annual mean discharge of 0.12 cfs (300 m^3/d) for its period of record, water years 1987–89 (USGS 1989). USGS 035382677, located on the tributary just west of the proposed disposal facility, recorded an average of 0.17 cfs (415 m^3/d) for its period of record, water years 1988–89 (USGS 1989). The water budget analysis in Sect. 3.3.2.2 indicates that only about 10% of surface water flow is directly attributed to discharge from groundwater, so the groundwater model should discharge about 10% of the gauge values, summing discharges to surface water from all nodes upstream of the gauge locations. These corresponding discharges from groundwater were calculated as 0.018 and 0.041 cfs, respectively, so

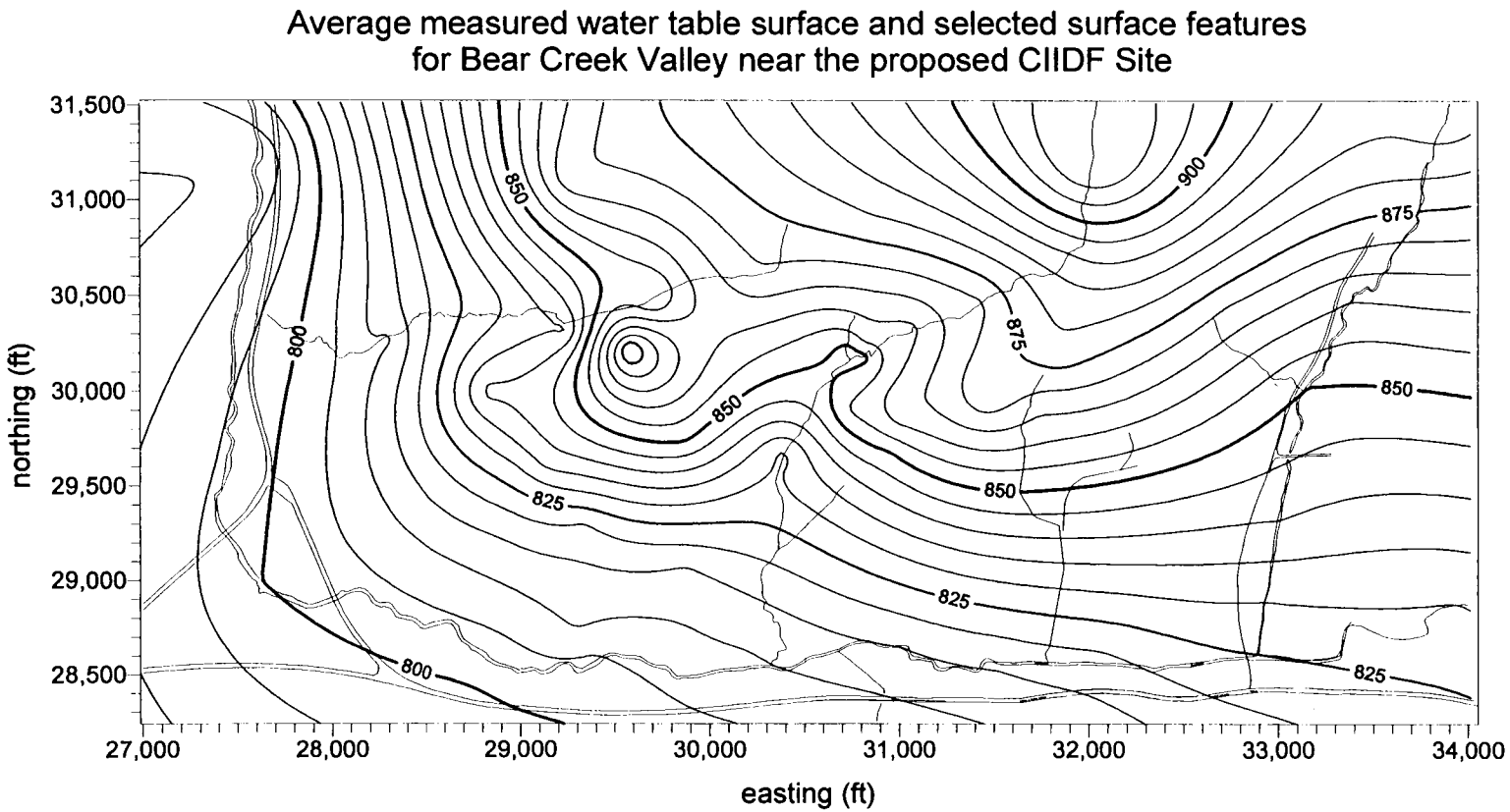

Fig. E.10. Water table interpolated from measured values near CIIDF.

Table E.4. Calculated vs measured head at target wells

Well ID	Easting (ft)	Northing (ft)	Measured head (ft)	Calculated head (ft)	Difference (ft)
gw406	28247.33	30330.43	812.19	812.08	0.11
gw408	28837.92	30442.79	827.83	838.23	–10.40
gw411	29868.24	30637.33	860.56	877.12	–16.56
gw413	29578.32	30211.02	880.39	862.31	18.08
gw418	29862.24	29752.14	851.24	848.10	3.14
gw420	29439.80	29473.57	831.38	841.39	–10.01
gw424	29299.44	28773.84	810.71	812.42	–1.71
gw426	29872.19	29042.83	814.02	821.46	–7.44
gw428	30217.99	28678.78	810.70	810.89	–0.19
gw429	30471.44	29521.94	832.23	833.92	–1.69
gw431	30828.81	30289.41	857.96	857.59	0.37
gw433	31191.70	30390.62	864.43	869.01	–4.58
gw438	31456.01	29967.91	873.90	866.35	7.55
gw440	31453.12	29580.31	853.66	854.40	–0.74
gw442	31206.30	28967.06	826.57	832.88	–6.31
gw447	31744.64	29893.72	865.56	868.07	–2.51
gw452	32590.72	29767.95	864.02	870.87	–6.85
gw475c	30737.01	29880.60	854.66	847.46	7.20
gw476c	30761.82	29899.50	855.54	848.35	7.19
gw477c	30738.54	29920.10	855.29	848.05	7.24
gw478c	30720.30	29900.61	853.89	847.31	6.58
gw480c	30737.11	29890.25	854.30	847.60	6.70
gw481c	30738.09	29910.66	855.05	847.91	7.14
gw482c	30747.28	29900.41	854.91	848.01	6.90
gw483	30773.45	29908.58	857.63	848.76	8.87
gw484	30751.92	29911.80	855.68	848.28	7.40
gw485	30718.88	29887.86	853.79	847.09	6.70
gw486	30713.65	29908.82	853.47	847.24	6.23
gw487	30708.68	29914.27	853.66	847.18	6.48
gw488	30711.37	29902.43	853.36	847.09	6.27
gw489	30706.85	29922.49	853.37	847.25	6.12
gw490	30692.75	29921.53	853.04	846.84	6.20
gw491	30693.65	29915.19	853.34	846.77	6.57
gw492	30694.68	29908.18	852.73	846.70	6.03
gw493	30694.15	29912.84	853.41	846.75	6.66
gw494	30693.18	29917.50	853.29	846.80	6.50

Table E.4 (continued)

Well ID	Easting (ft)	Northing (ft)	Measured head (ft)	Calculated head (ft)	Difference (ft)
gw495	30639.44	29920.31	849.32	845.21	4.11
gw492	30694.68	29908.18	852.73	846.70	6.03
gw495	30639.44	29920.31	849.32	845.21	4.11
gw496	30639.11	29917.51	849.12	845.15	3.97
gw497	30639.84	29914.47	850.02	845.14	4.88
gw498	30640.30	29911.65	850.41	845.11	5.30
gw499	30640.74	29908.62	849.61	845.09	4.52
gw499a	30638.43	29923.23	849.20	845.22	3.98
gw499b	30643.12	29898.85	850.33	845.05	5.28
gw499c	30642.22	29890.16	848.73	844.94	3.79
gw499d	30639.27	29882.73	847.20	844.78	2.42
gw499e	30636.15	29875.26	848.07	844.61	3.46
gw499f	30641.31	29903.81	851.51	845.05	6.46
gw499g	30667.88	29916.11	852.16	846.04	6.12
gw499h	30666.85	29913.72	852.28	845.97	6.31
gw499i	30665.71	29910.37	852.23	845.89	6.34
gw499j	30664.70	29907.68	852.21	845.82	6.39
gw499k	30680.58	29919.73	852.79	846.47	6.32
gw499l	30681.85	29922.96	852.59	846.55	6.04
gw499m	30679.86	29916.41	852.84	846.40	6.44
gw499n	30679.66	29913.23	852.67	846.34	6.33
gw499o	30681.70	29910.03	852.57	846.36	6.21
gw499p	30683.35	29907.35	852.45	846.37	6.08
gw499r	30668.56	29883.69	849.38	845.65	3.73
gw499s	30810.46	29825.00	857.62	848.46	9.16
gw499w	30633.18	29915.18	848.97	844.92	4.05
gw499aa	30947.52	29669.30	849.24	848.83	0.41
gw499ab	30637.55	29932.81	848.39	845.34	3.05
gw499ac	30583.29	29915.09	842.08	842.78	–0.70
gw499ad	30575.22	29911.03	841.65	842.25	–0.60
gw499ae	30581.64	29921.27	842.35	842.74	–0.39
gw499af	30583.48	29927.39	842.40	842.93	–0.53
gw499y	30980.25	29835.49	860.00	852.28	7.72
gw499z	31006.01	29937.06	863.84	855.43	8.41

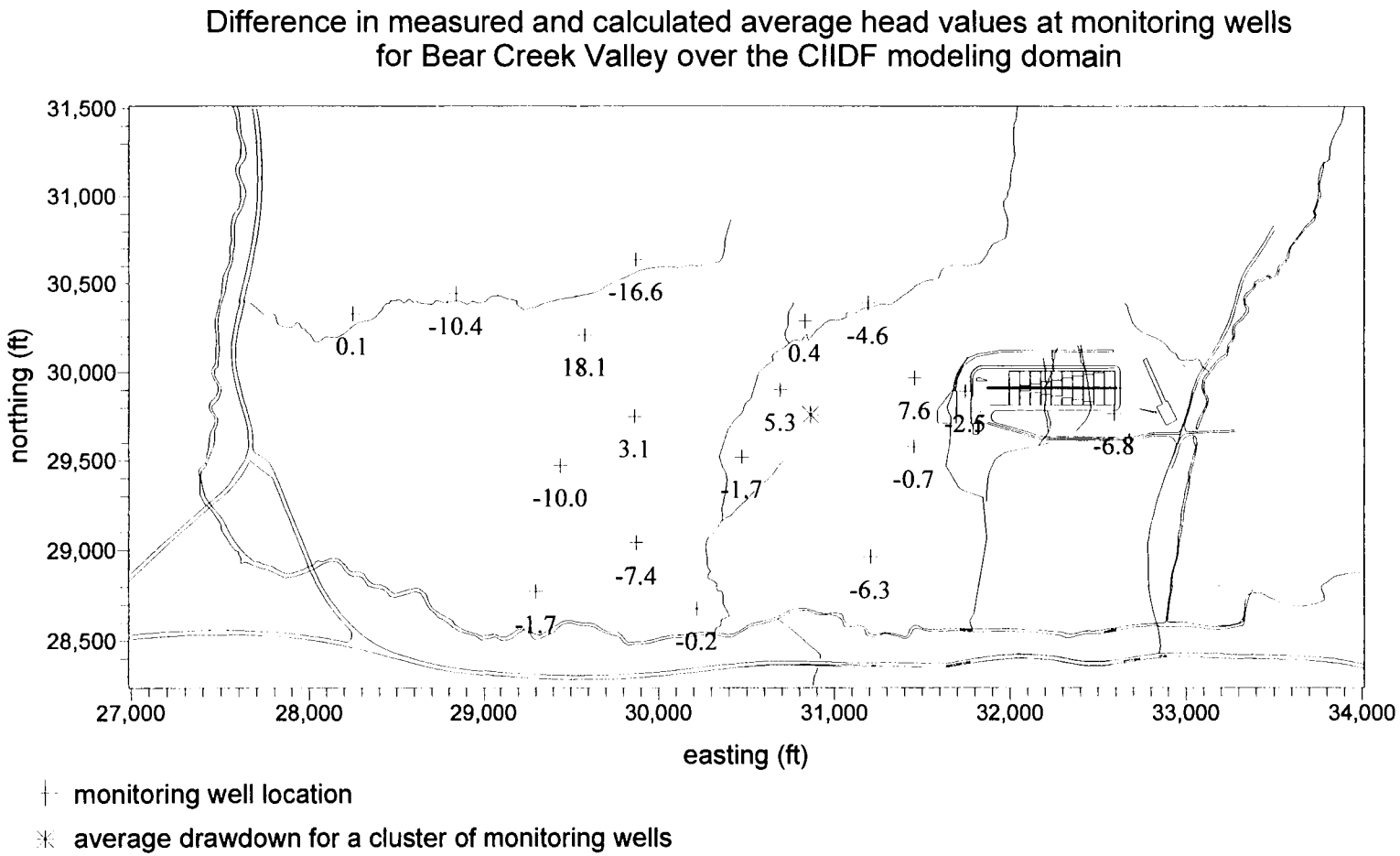

Fig. E.11. Water table residual error for flow model calibration.

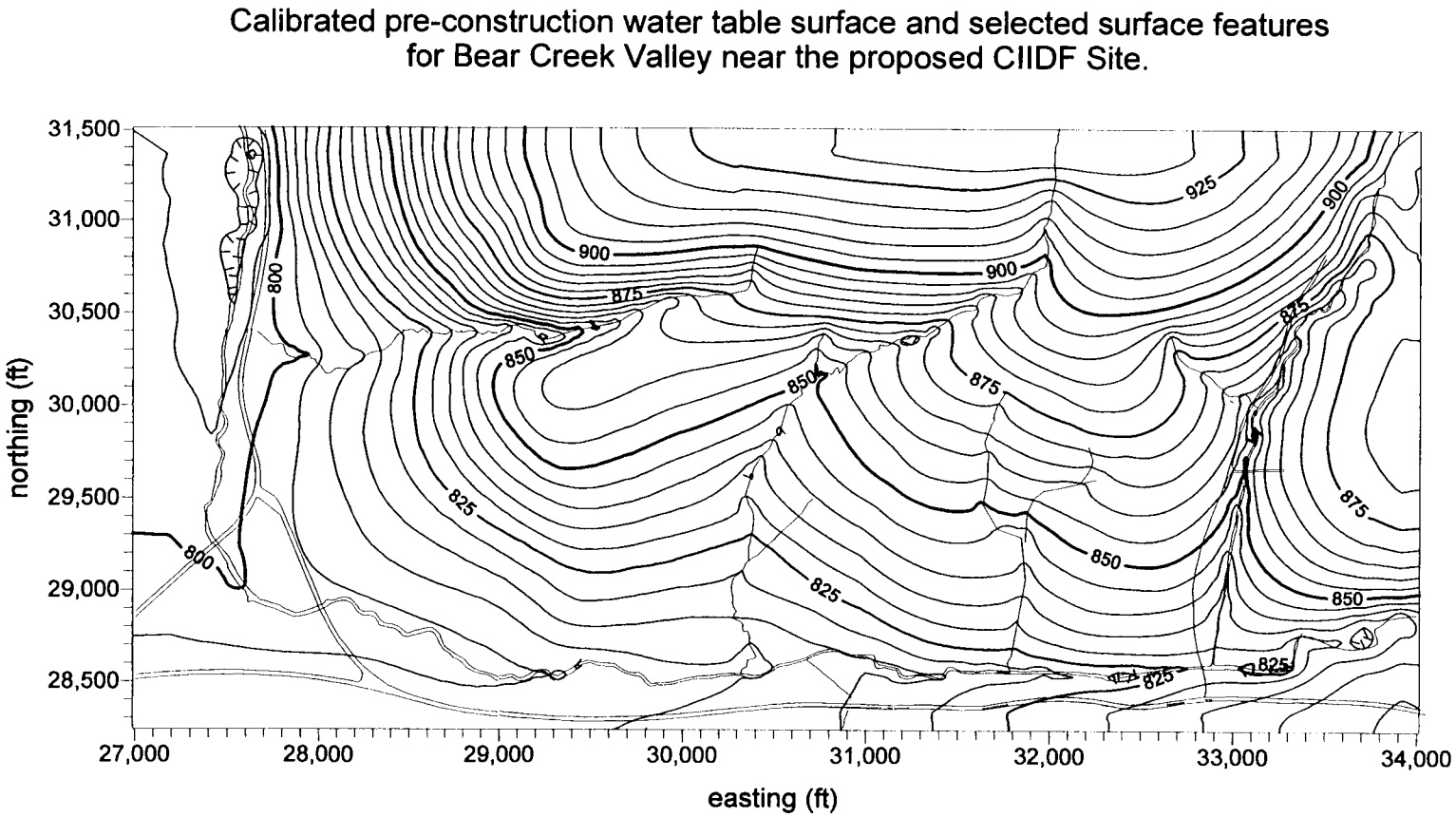

Fig. E.12. Calibrated preconstruction water table for the CIIDF region.

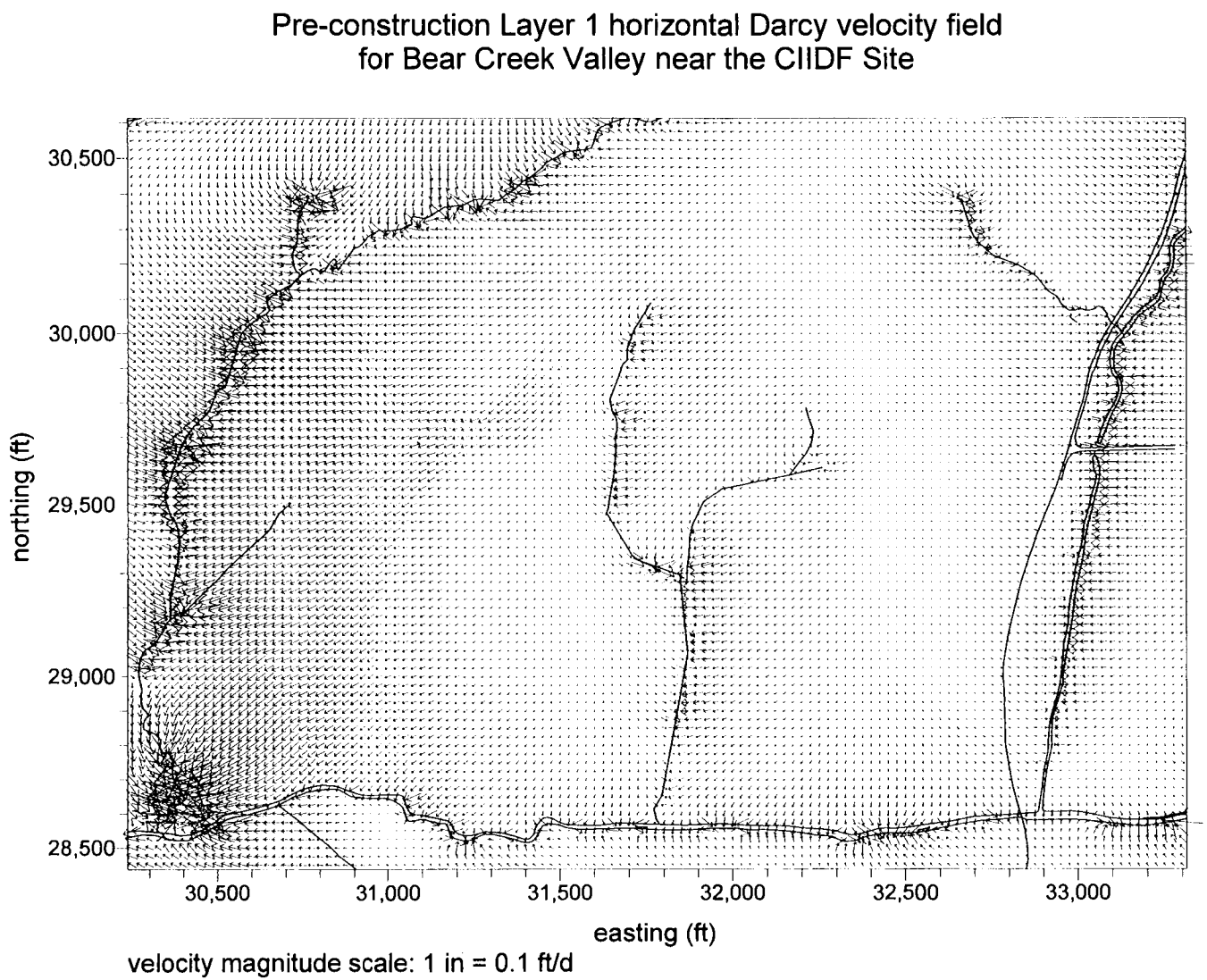

Fig. E.13. Calibrated preconstruction Darcy velocity near CIIDF.

estimates of total surface water flows would be 0.18 and 0.41 cfs. Although a 1.5 to 2.5 times higher than the measured values, the comparison is quite favorable given the uncertainty inherent in the modeling process.

E.2.2.2.7 Flow Model Modifications to Account for Site Modifications for Construction

Construction of CIIDF is expected to involve a number of significant engineering modifications to the site's terrain and drainage features, as discussed in Sect. 2.1.2. Such changes will have a significant influence on the near-surface groundwater flow field near the facility. To account for these local effects, it was necessary to perform a series of modifications to the calibrated flow model. The first of these was to alter Layer 1 surface elevations to match the revised site terrain based on preliminary engineering drawings from 16 August 1995 (Foster-Wheeler, 1995). Fig. E.14 shows the proposed topographical modifications near CIIDF based on these drawings. After incorporating the revised ground surface elevations, the thicknesses of Layer 1 cells were adjusted so that top elevation of Layer 2 remained unchanged, as shown in Fig. E.15. Next, the influence of additional, proposed drainage features was incorporated into the model by assigning additional drain boundaries to grid cells on Layer 1 of the model. Additional drainages features added during construction include french drains in those existing creekbeds which will be covered by the pads, a trench around the upslope and western sides of the facility, and another trench to the east. The intent of these drainages is both to maintain a depressed water table under CIIDF and to intercept contaminated surface and subsurface water emanating from the facility. The location special of boundary cells for the revised flow model are shown in Fig. E.16.

Once the proposed modifications were incorporated, the flow model was rerun in order to generate a steady-state flow field for use in all subsequent contaminant transport calculations. Fig. E.17 shows the calculated head surface obtained for the flow model based on the modified topography. The corresponding *X-Y* Darcy velocity field for Layer 1 near the proposed site location is presented in Fig. E.18.

E.2.2.3 Calculation of Contaminant Transport via Groundwater

Once the steady-state calibration of the flow model was completed and the proposed site modifications were incorporated into it, the next phase of the analysis was to use FTWORK to evaluate the groundwater transport of the 60 radionuclides from the site. For all transport calculations, the effects of radioactive decay and retardation of contaminant due to linear adsorption were considered. This step was done by (1) imposing the time-dependent release of contaminant from the disposal facility onto the calibrated, steady-state flow field and (2) performing a transient analysis for each nuclide to determine both (a) the concentration in groundwater at points 100 m from the facility and (b) the contaminant flux to surface water via discharge to ephemeral and perennial streams and constructed drains. This flux was then combined with contaminant fluxes from lateral runoff to

Existing topography at the CIIDF Site

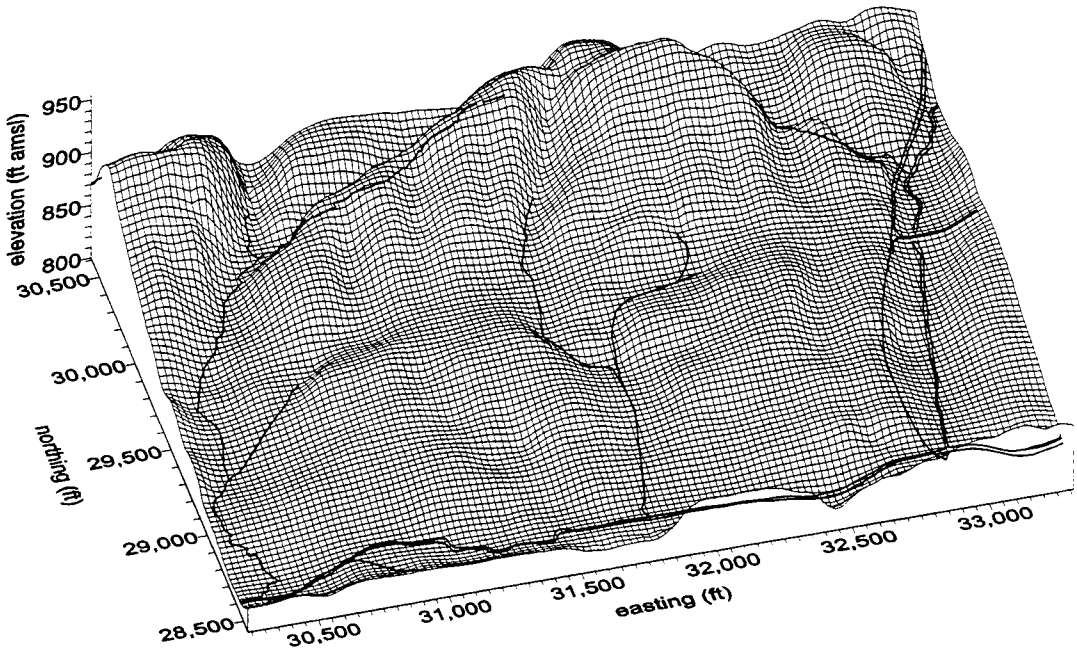

Modified topography proposed for the CIIDF Site

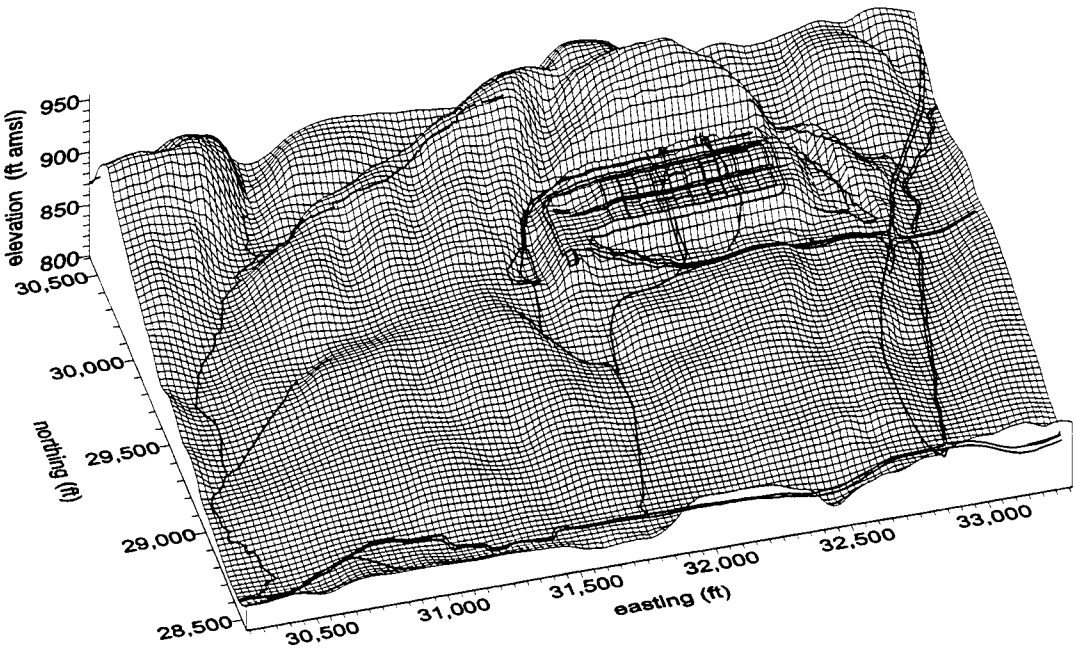

Fig. E.14. Proposed topographic modifications to the CIIDF site.

Cutaway through the CIIDF modeling domain in Bear Creek Valley
revealing layering used in the groundwater model
(post-construction topography)

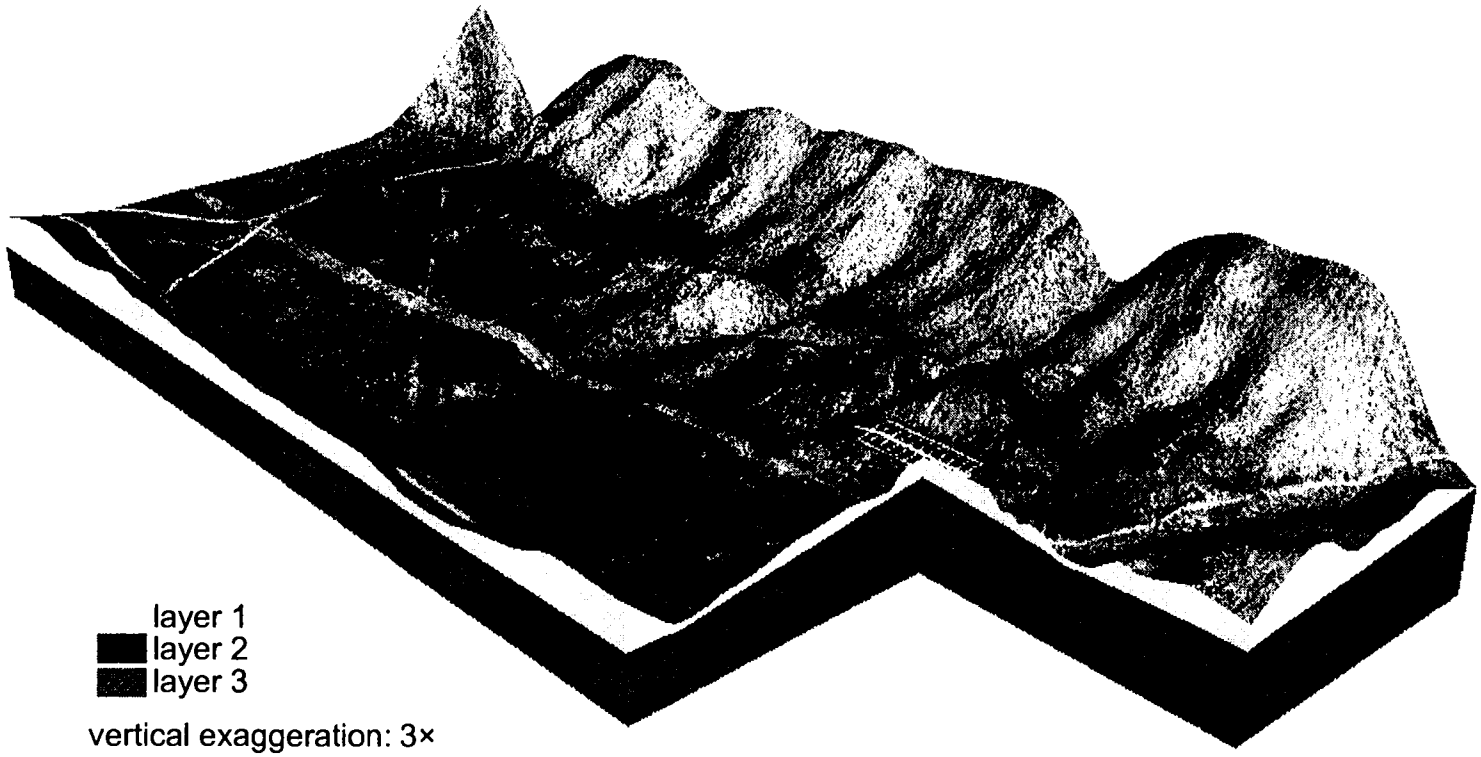

Fig. E.15. Vertical discretization of the postconstruction CIIDF groundwater model.

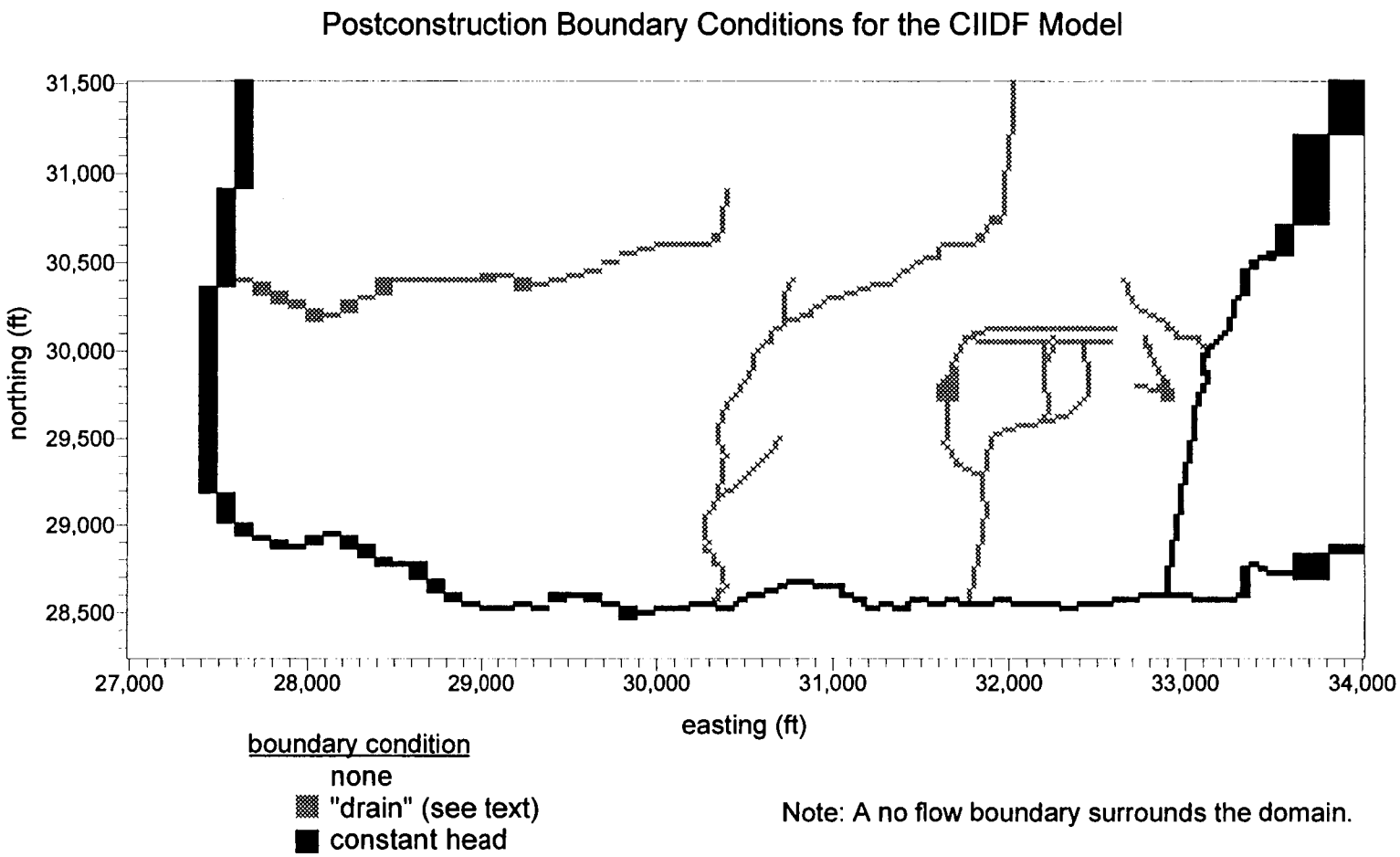

Fig. E.16. Postconstruction boundary conditions reflecting topographic modifications.

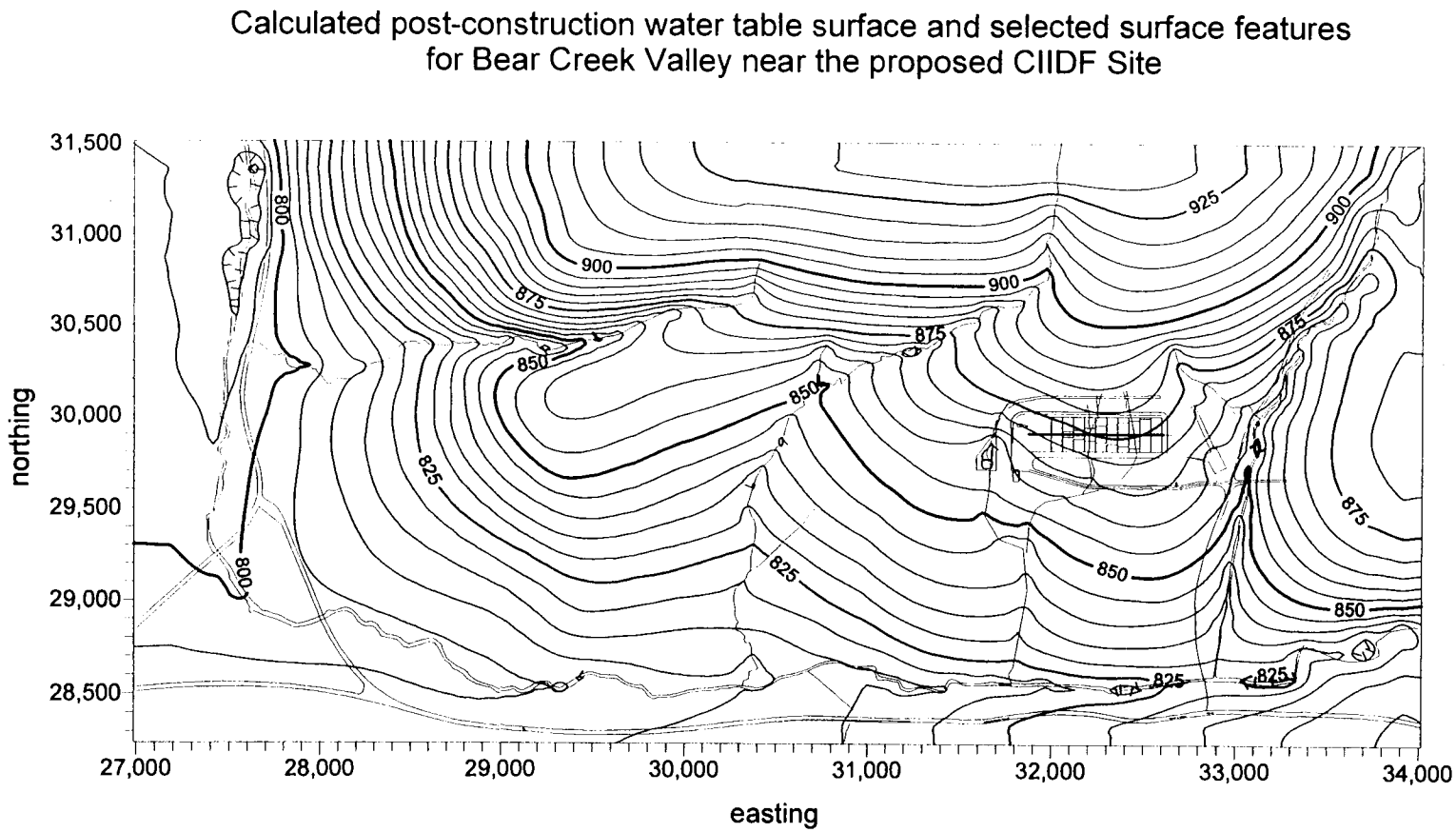

Fig. E.17. Calculated postconstruction water table for the CIIDF model.

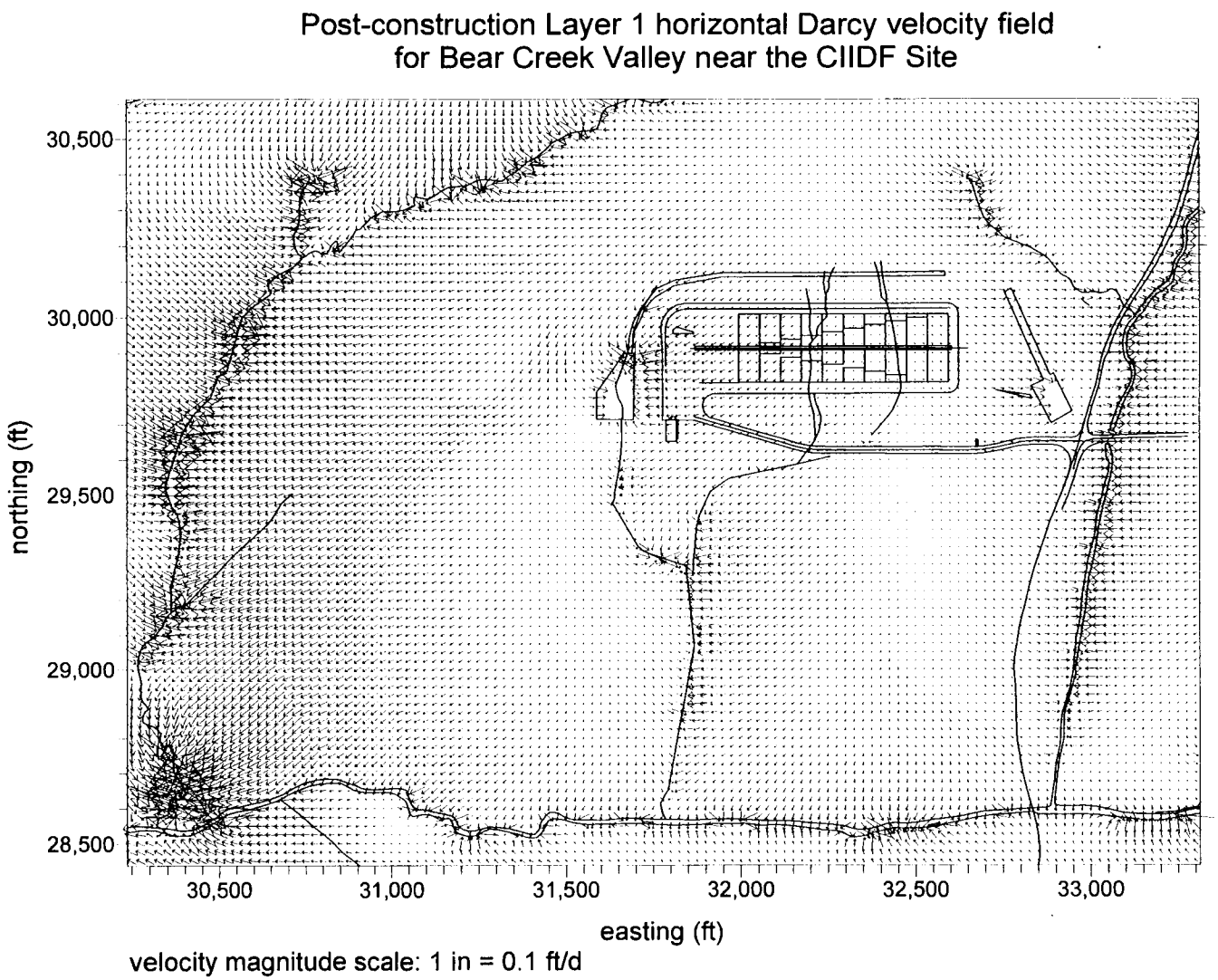

Fig. E.18. Calculated postconstruction Darcy velocity near the CIIDF site.

determine surface water contaminant concentrations in Bear Creek (see Sect. 3.3.4.3). For each radionuclide, the transient calculations were repeated for several hypothetical inventories in order to determine the disposal limit that corresponds to the maximum allowable drinking water concentrations (See Table 4.11).

E.2.2.3.1 Time-Dependent Contaminant Loading

As indicated previously, contaminant transport calculations were performed using the time-dependent mass fluxes calculated by the PADSIM program as input. Such time-dependent fluxes are approximated in FTWORK by assigning a contaminant concentration to the recharge associated with a model cell. It was therefore necessary to convert the mass fluxes calculated by PADSIM to a concentration based on the recharge rate associated with the six model grid cells which correspond to each of the CIIDF's physical pads.

The fluxes calculated by PADSIM represent the release of contaminant from any one of the facility's disposal pads. These 20 pads were assumed to be filled at the rate of one per year, and as a result, it would be possible for some pads to release contamination before others are loaded. For short-lived, highly mobile nuclides, it is conceivable that this irregular loading pattern could have considerable effect on the time, location, and magnitude of ground and surface water concentrations. Therefore, in order to reflect the one-pad-per-year loading rate, the fluxes calculated by PADSIM were applied at each pad location on a staggered basis. That is, contaminant fluxes were applied to Pad 1 beginning at year 1, to Pad 2 at year 2, etc. For nuclides that were long-lived or readily adsorbed onto the soil media, the effects of this variable loading pattern were assumed to be much less critical, and all 20 pads were assumed to be loaded in the first time step.

E.2.2.3.2 Location of 100-Meter Compliance Points

One of the primary goals of the contaminant transport analysis was to determine the maximum groundwater concentrations for each nuclide at any point greater than 100 m from the disposal facility, in accordance with the guidance presented in Sect. 1. For modeling purposes, this determination was made by recording concentrations at grid cells located approximately 100 m from the edge of the finished CIIDF closure cap (see Sect. 2.3) for all vertical layers of the model. This "ring" of monitoring points will capture the highest groundwater concentrations, under the assumption that concentrations will decrease with distance from the source. Figure E.19 shows the location of these model cells.

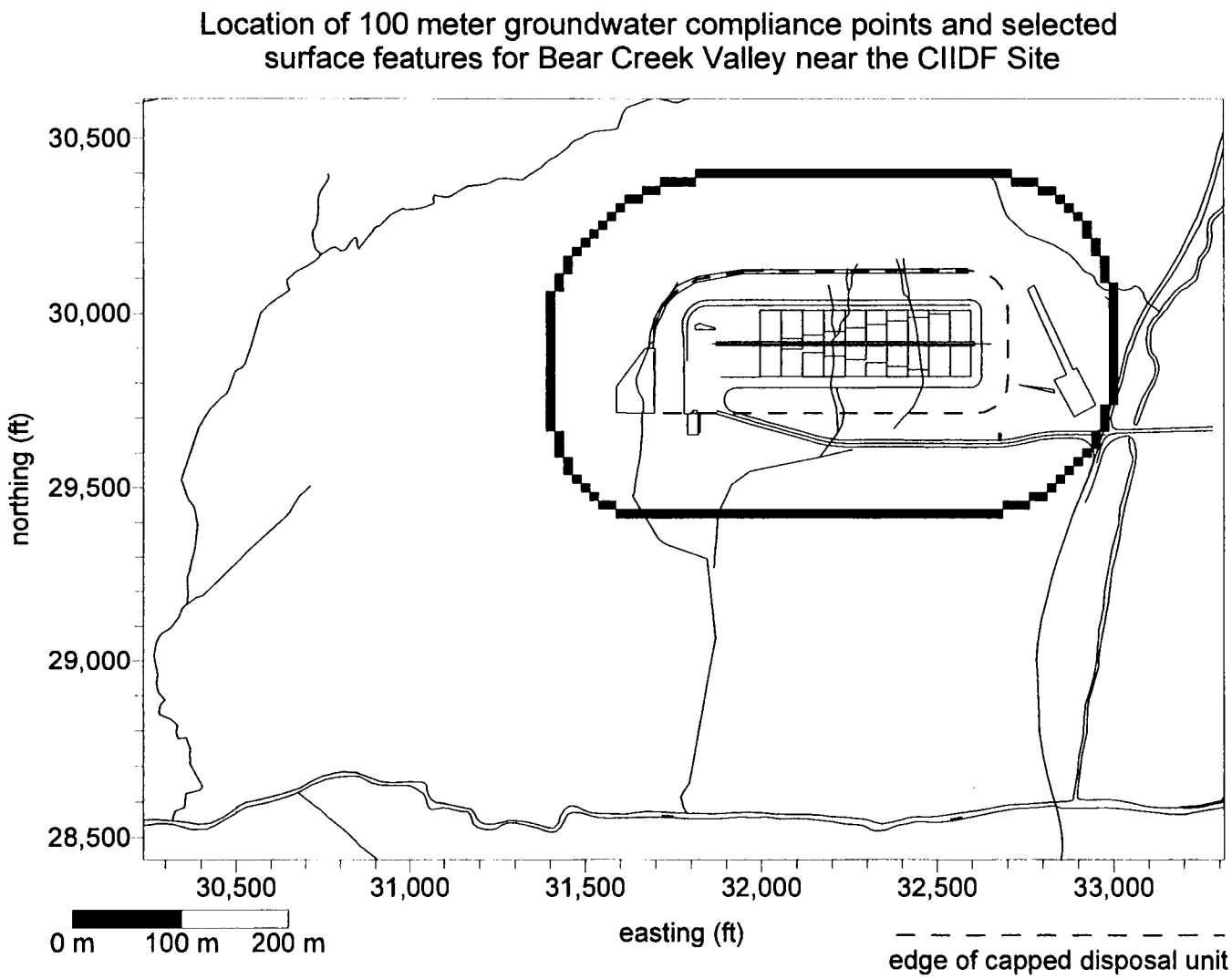

Fig. E.19. Grid cells representing the CIIDF 100-m compliance boundary.

E.3 REFERENCES

Bear, J. 1972. *Dynamics of Fluids in Porous Media*, Dover Publications, New York.

Dynamic Graphics, Inc. 1994, *EarthVision 2.0 Software*, Alameda, Calif.

EPA (U.S. Environmental Protection Agency) 1988. *Geo-EAS (Geostatistical Environmental Assessment Software)* [computer program by E. Englund and A. Sparks], EPA/600/4-88/033a, Washington, D.C.

Faust, C. R. et al. 1990. *FTWORK: Groundwater Flow and Solute Transport in Three Dimensions, Version 2.4* [computer code documentation], GeoTrans, Inc., Herndon, Va.

Foster-Wheeler Environmental Corporation / Parsons Engineering Science, Inc. 1995. *Class L-II LLW Disposal Facility*, engineering drawings C3E017096A004 and C3E017096A005.

Golden Software 1995. *Surfer*, Version 6.01 [computer program], Sept. 5, 1995, release, Golden, Colo.

Golder Associates 1988. *Task 2, Well Logging and Geohydrologic Testing, Site Characterization and Groundwater Flow Computer Model Application,* Vol. 1 of 6, ORNL/Sub/30X-SA706C, Martin Marietta Energy Systems, Inc., Oak Ridge Natl. Lab.

Journel, A. G., and Ch. J. Huijbregts 1978. *Mining Geostatistics*, Academic Press, New York.

Lee, R. R. 1989. *Calibration of a Groundwater Flow and Containment Transport Model: Progress Toward Model Validation,* ORNL/TM-11294, Martin Marietta Energy Systems, Inc., Oak Ridge Natl. Lab.

USGS (U.S. Geological Survey) 1989. *Water Resources Data, Tennessee, Water Year 1989,* Report TN-89-1, Reston, Va.

Y-12 (Oak Ridge Y-12 Plant) 1984. *Bear Creek Road Area,* engineering drawings based on aerial survey.

Appendix F

PLOTS OF MAXIMUM DRINKING WATER CONCENTRATION VS DISPOSAL INVENTORY

M. W. Yambert

Appendix F

PLOTS OF MAXIMUM DRINKING WATER CONCENTRATIONS VS DISPOSAL INVENTORY

This appendix contains plots of the predicted maximum groundwater and surface water concentrations vs per pad limiting inventory (assuming uniform loading of CIIDF's pads) for each of the 60 radionuclides considered in the analysis. Groundwater concentrations represent the maximum concentration for any of the 100-m compliance points (see Sect. 3.2.3.4) at any point in time. Surface water concentrations represent the maximum value at a hypothetical receptor located in Bear Creek (see Sect. 3.1.2.1) at any point in time due to the sum of all radionuclide discharges, via either shallow subsurface or groundwater transport, to surface water. In a few cases (^{3}H, ^{36}Cl, ^{79}Se, and ^{129}I), this peak concentration occurs before the 100-year period of institutional control.

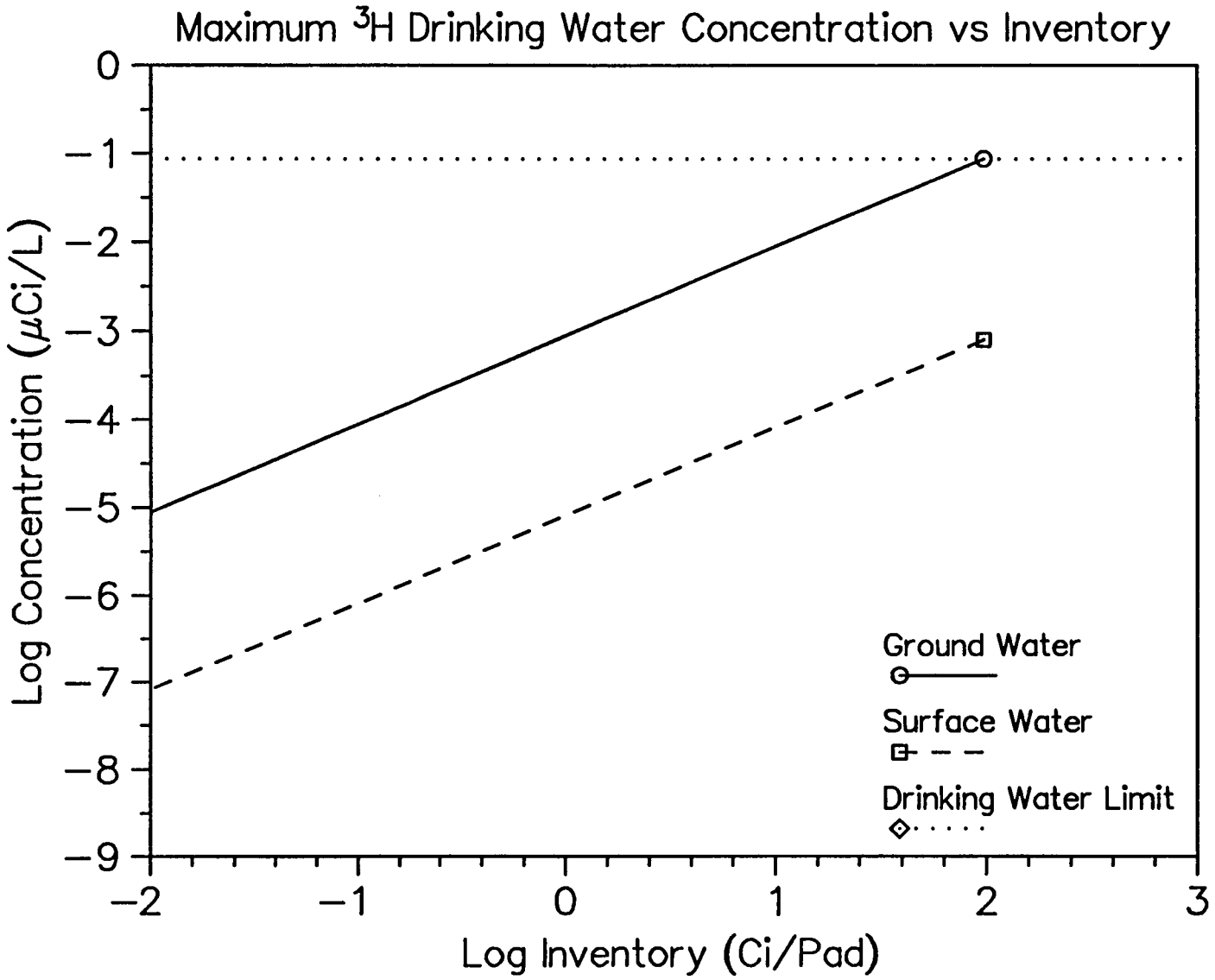

Fig. F.1. Maximum drinking water concentration as a function of CIIDF inventory for ^3H.

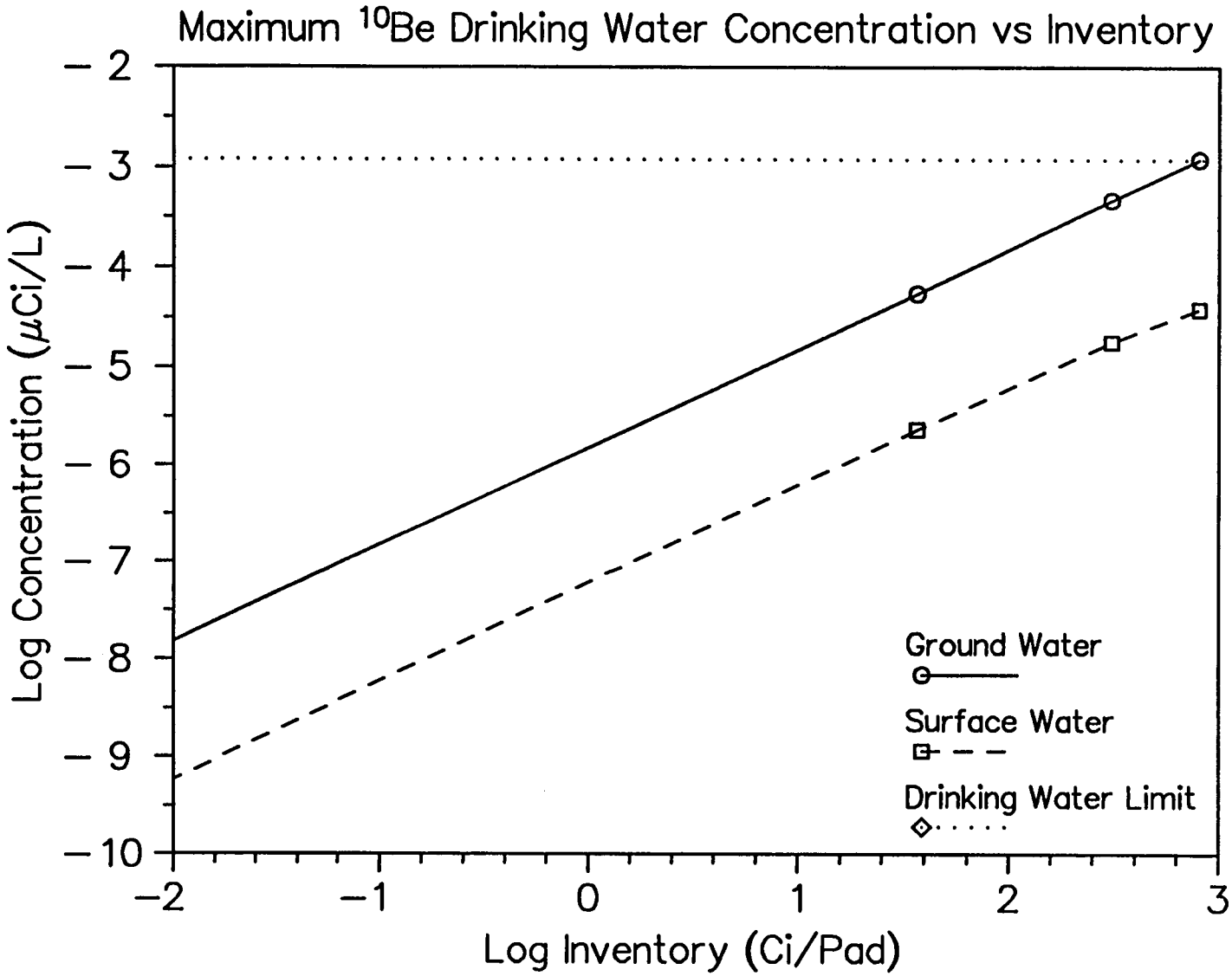

Fig. F.2. Maximum drinking water concentration as a function of CIIDF inventory for ^{10}Be.

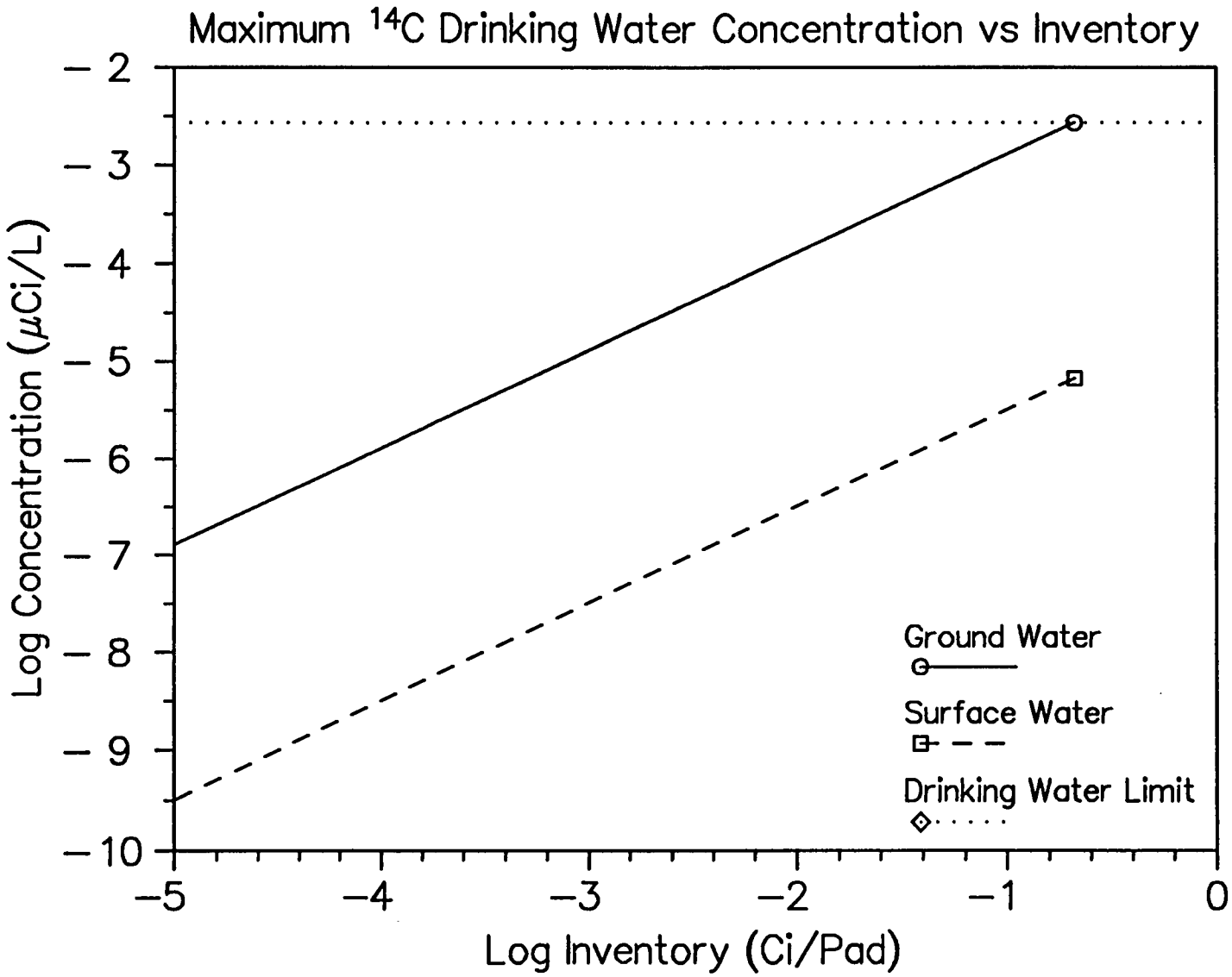

Fig. F.3. Maximum drinking water concentration as a function of CIIDF inventory for ^{14}C.

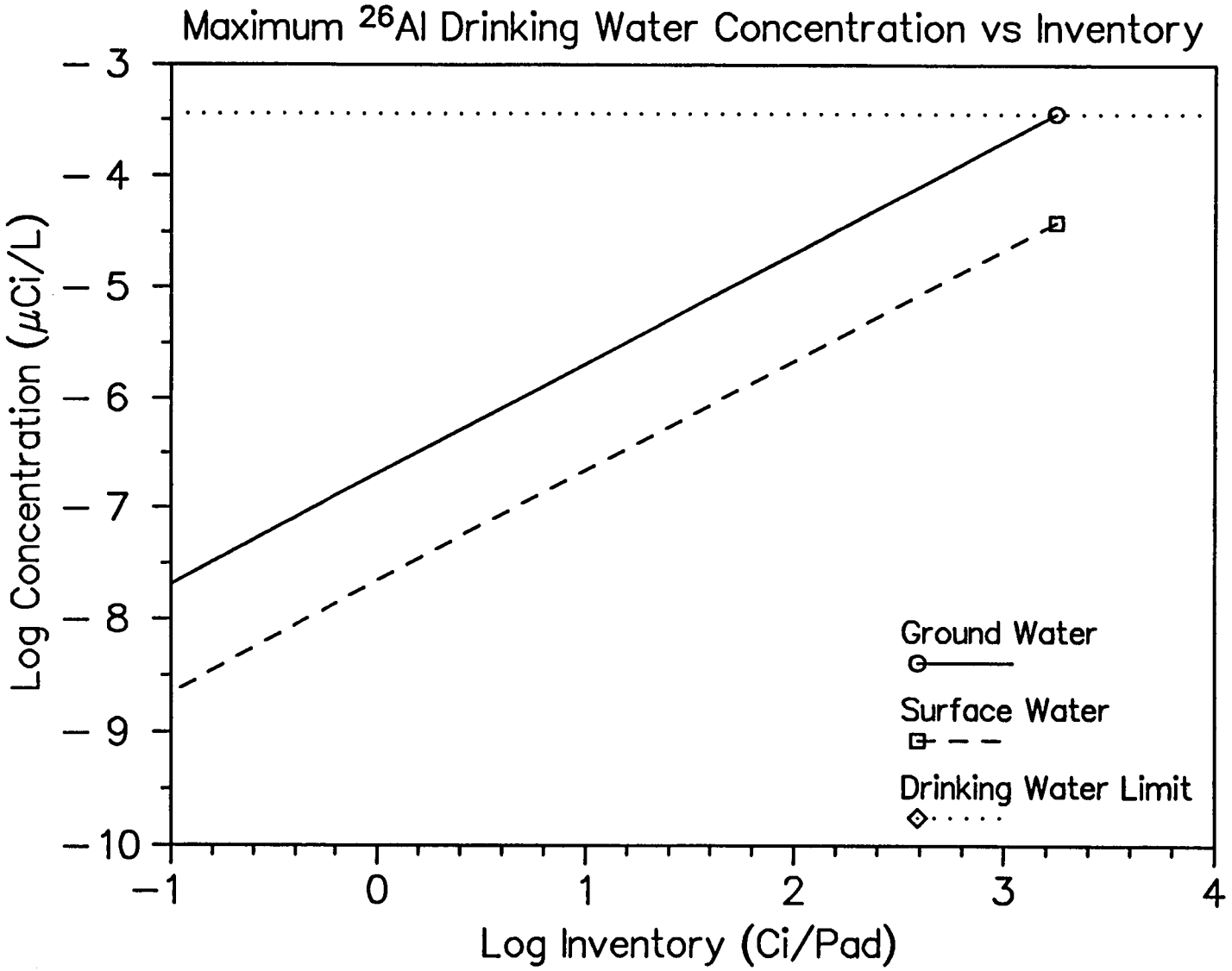

Fig. F.4. Maximum drinking water concentration as a function of CIIDF inventory for ^{26}Al.

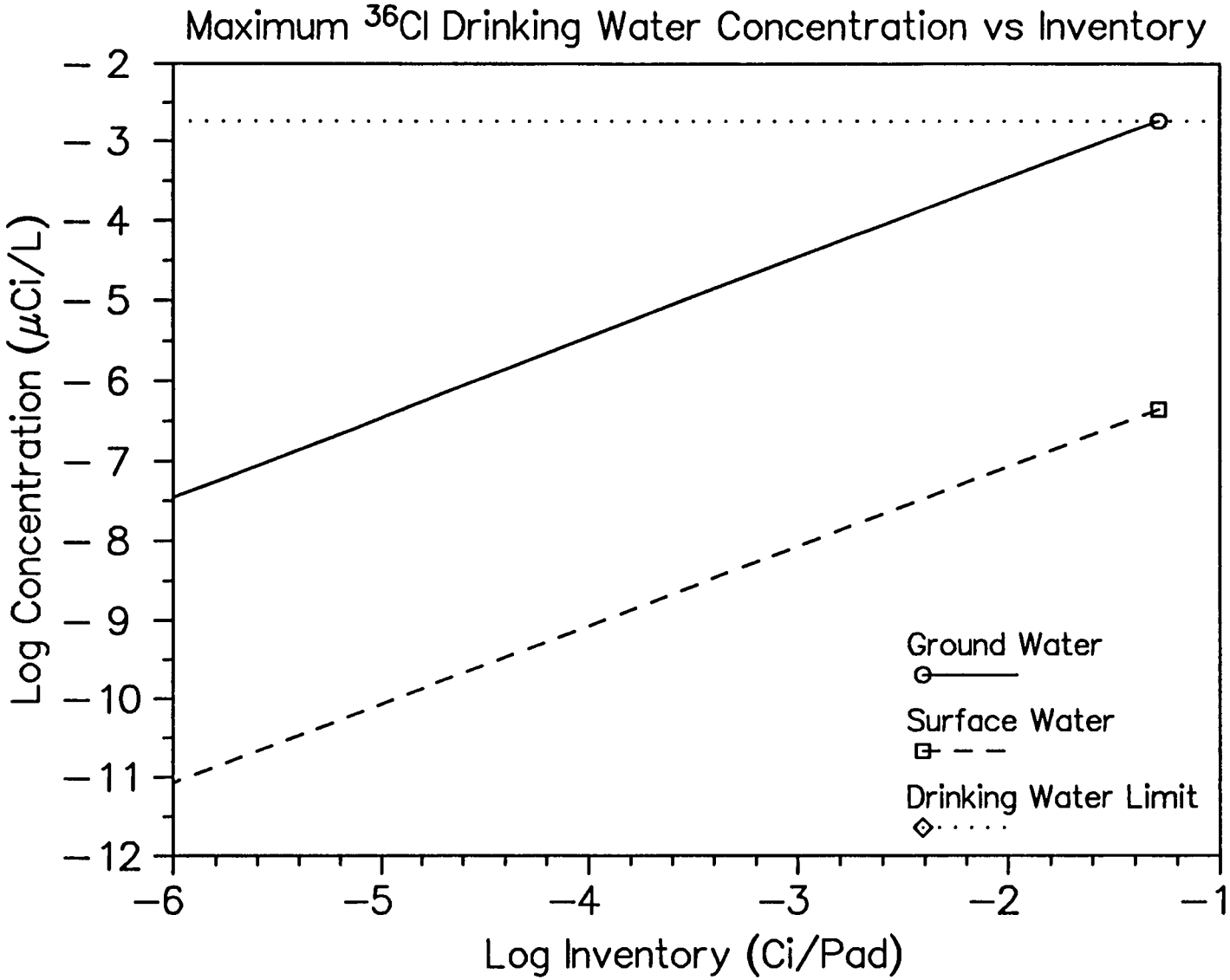

Fig. F.5. Maximum drinking water concentration as a function of CIIDF inventory for ^{36}Cl.

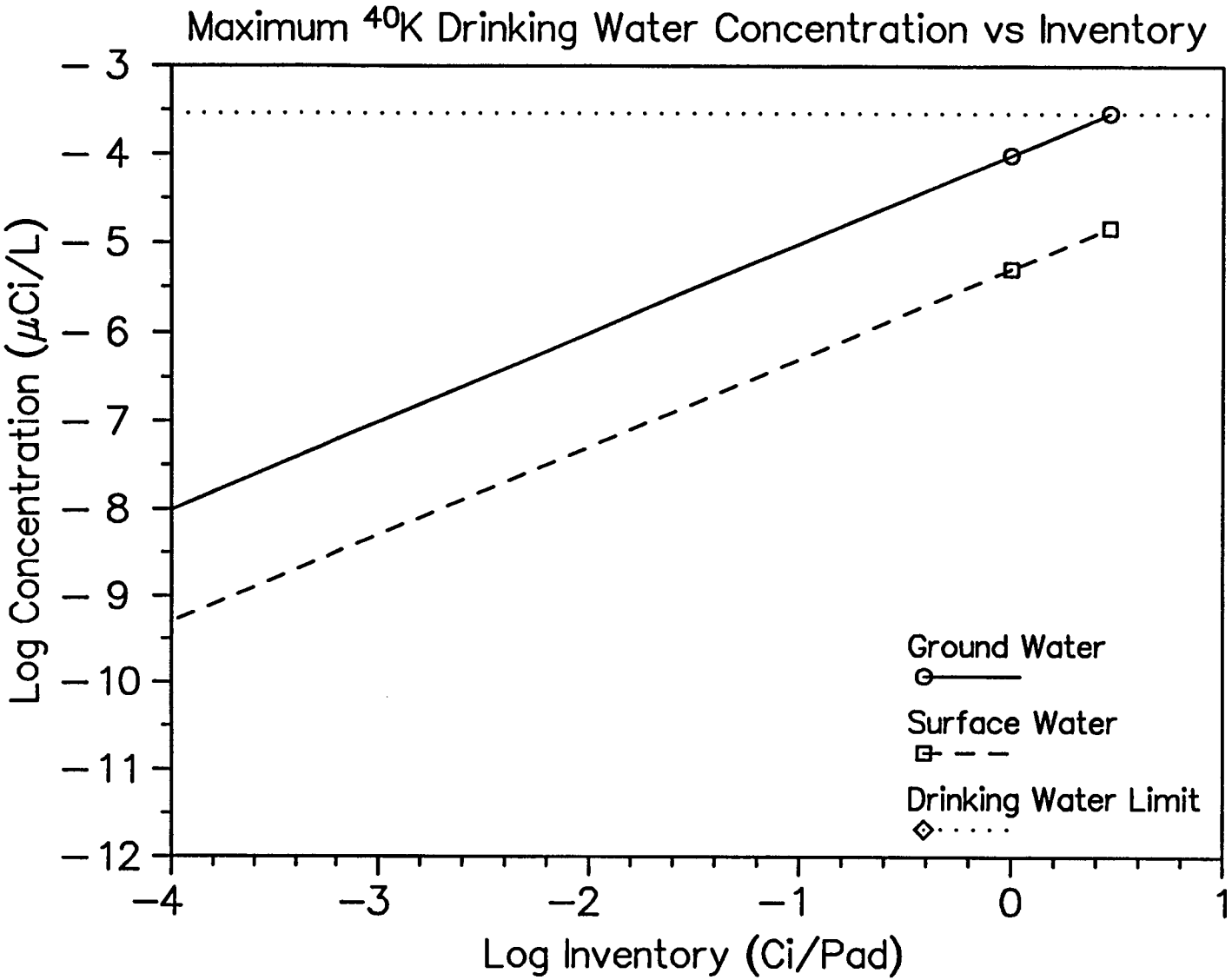

Fig. F.6. Maximum drinking water concentration as a function of CIIDF inventory for ^{40}K.

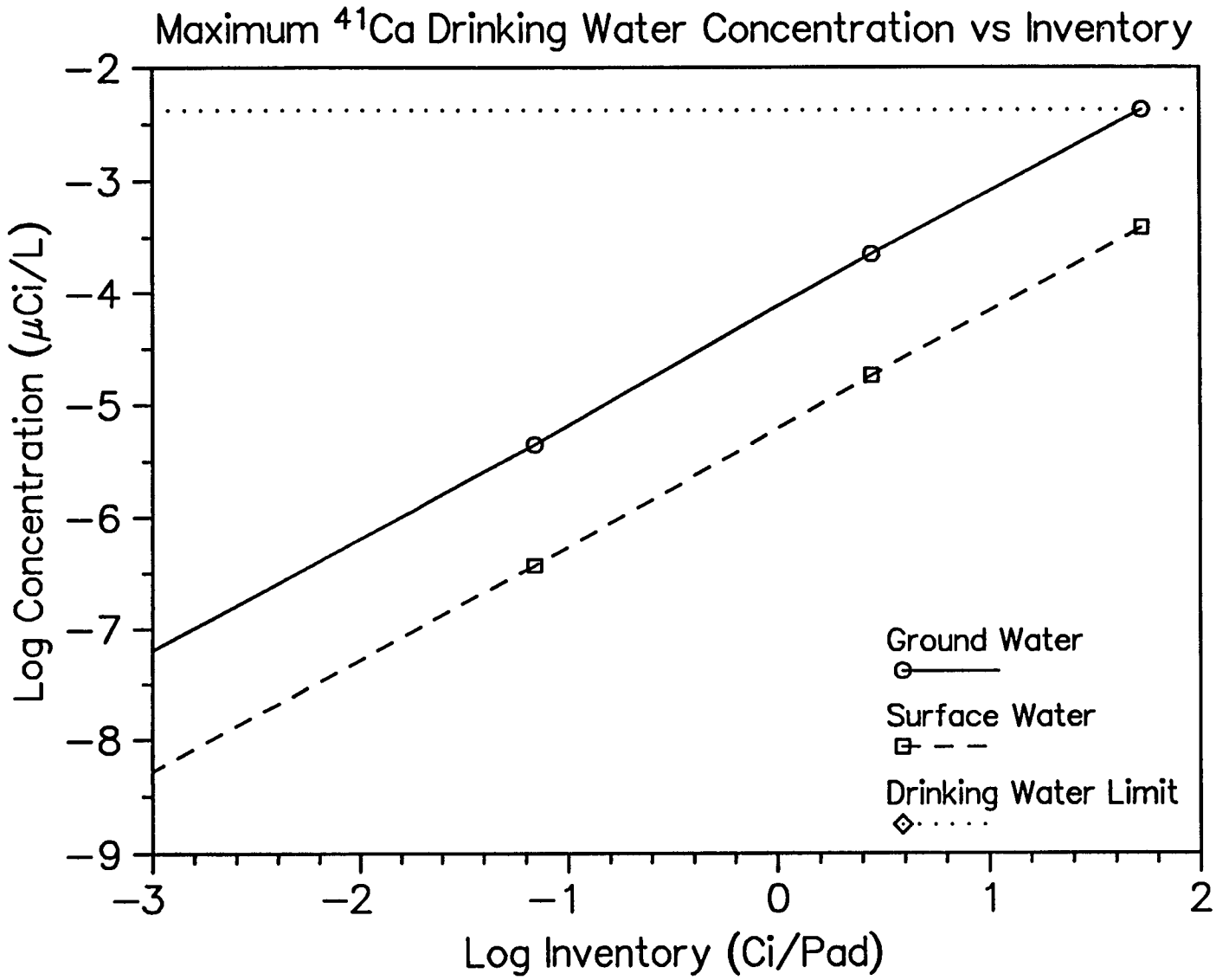

Fig. F.7. Maximum drinking water concentration as a function of CIIDF inventory for ^{41}Ca.

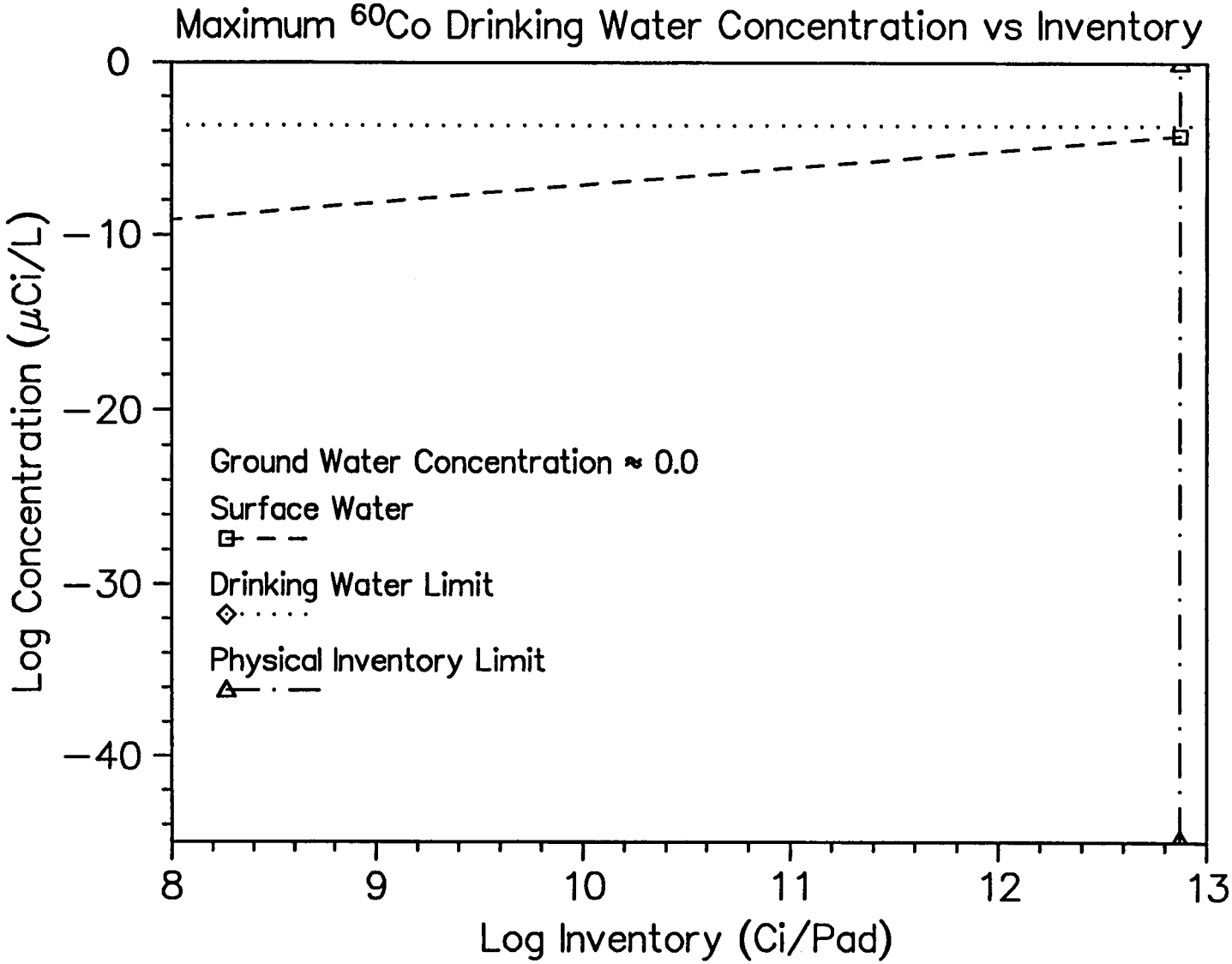

Fig. F.8. Maximum drinking water concentration as a function of CIIDF inventory for ^{60}Co.

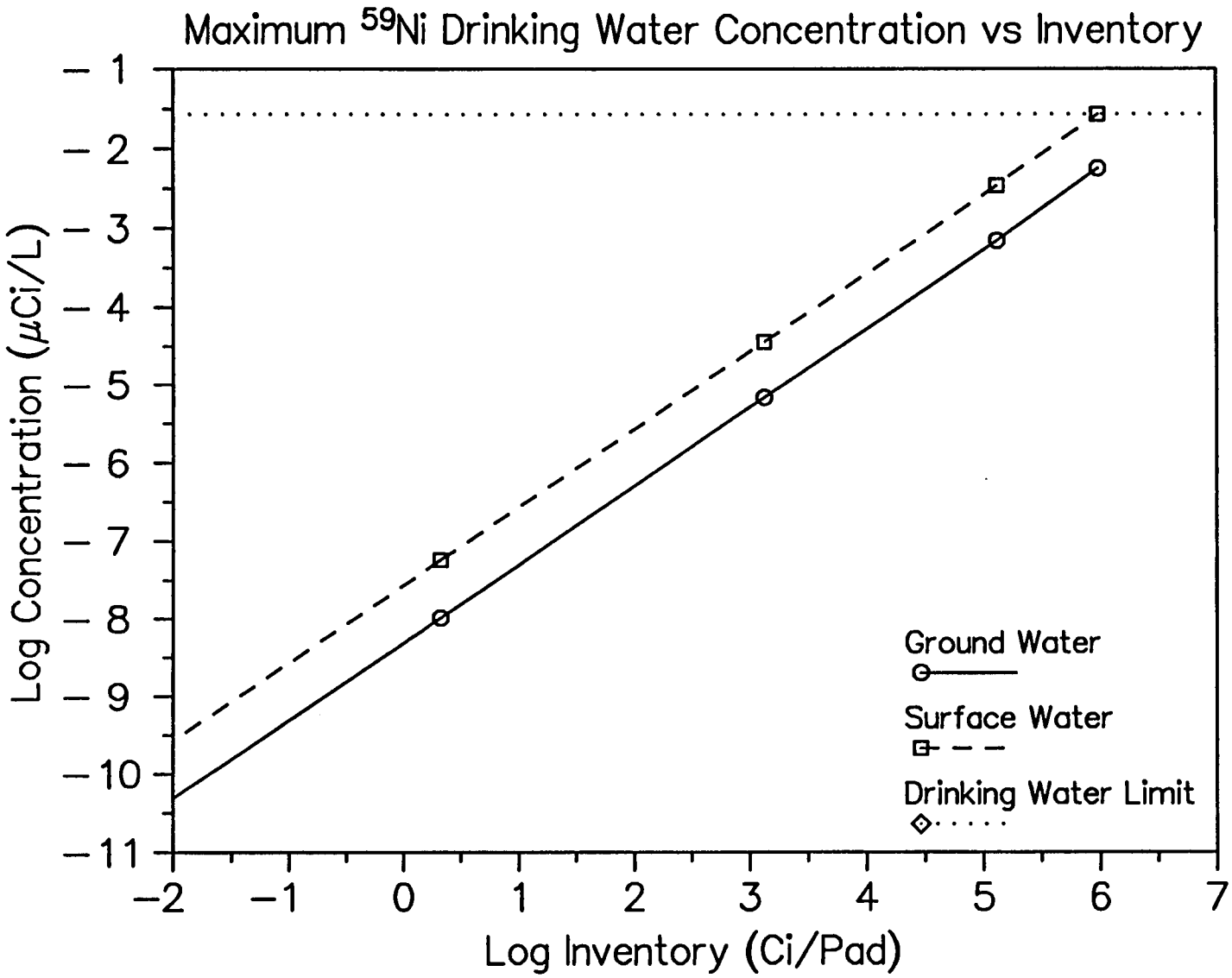

Fig. F.9. Maximum drinking water concentration as a function of CIIDF inventory for ^{59}Ni.

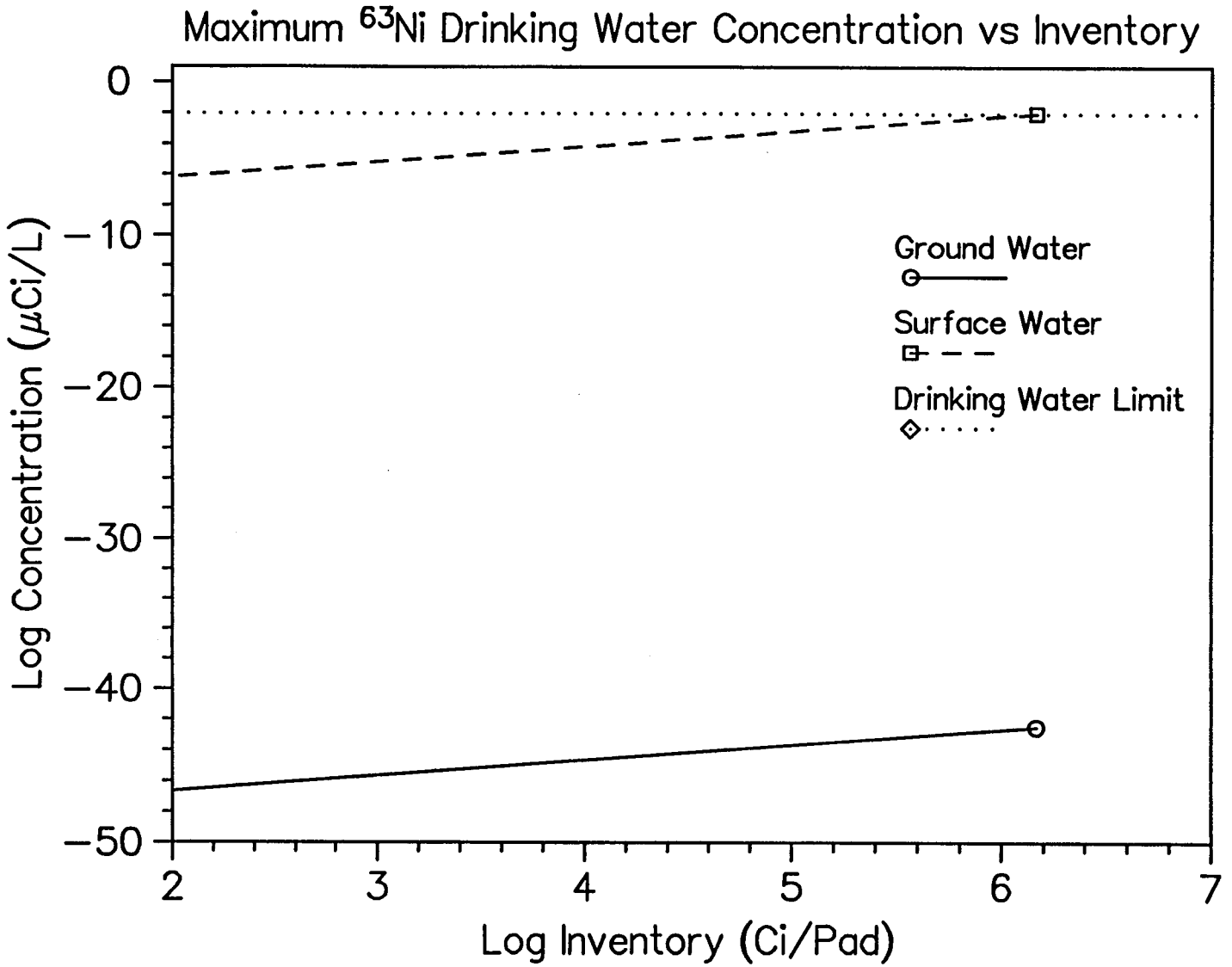

Fig. F.10. Maximum drinking water concentration as a function of CIIDF inventory for ^{63}Ni.

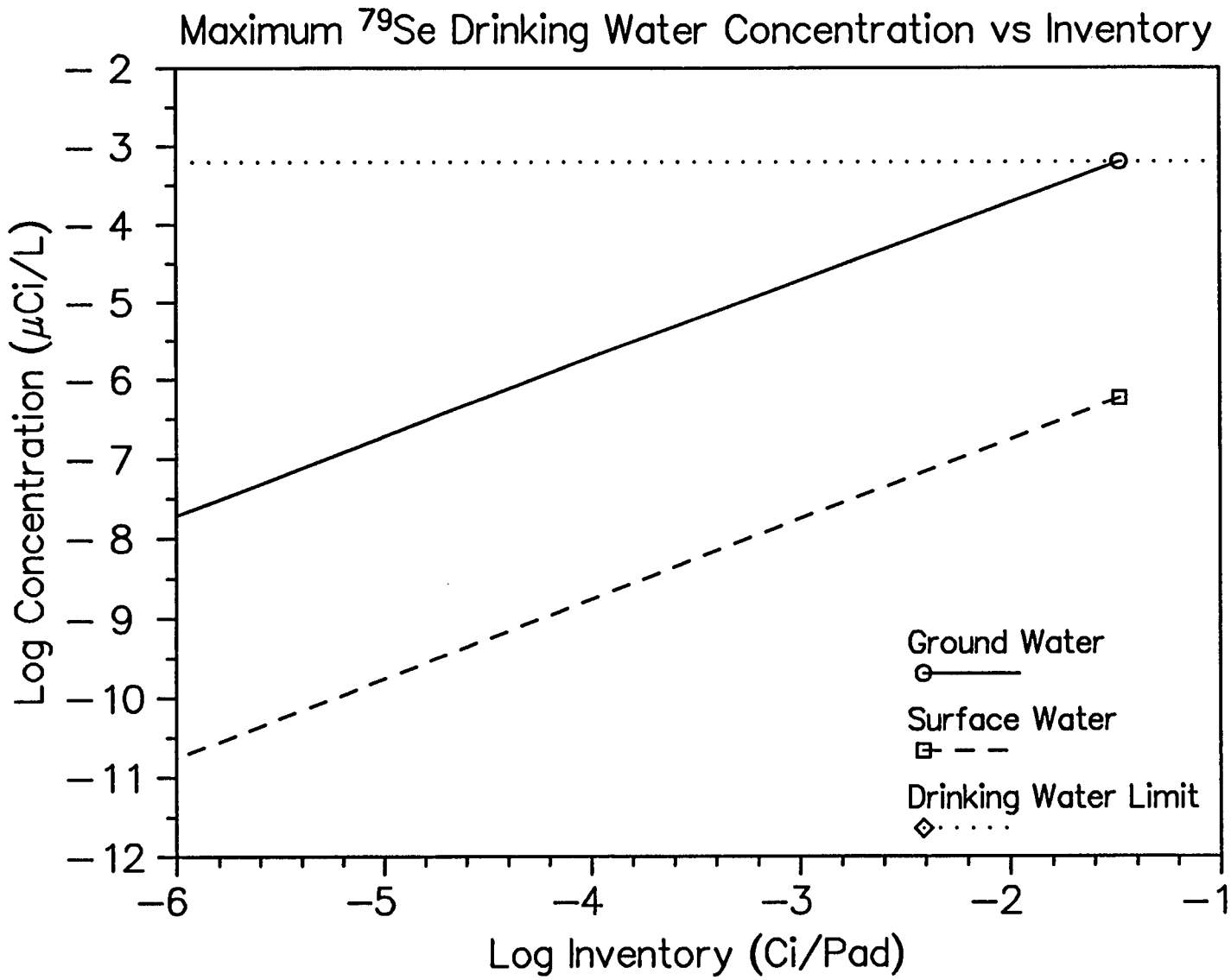

Fig. F.11. Maximum drinking water concentration as a function of CIIDF inventory for ^{79}Se.

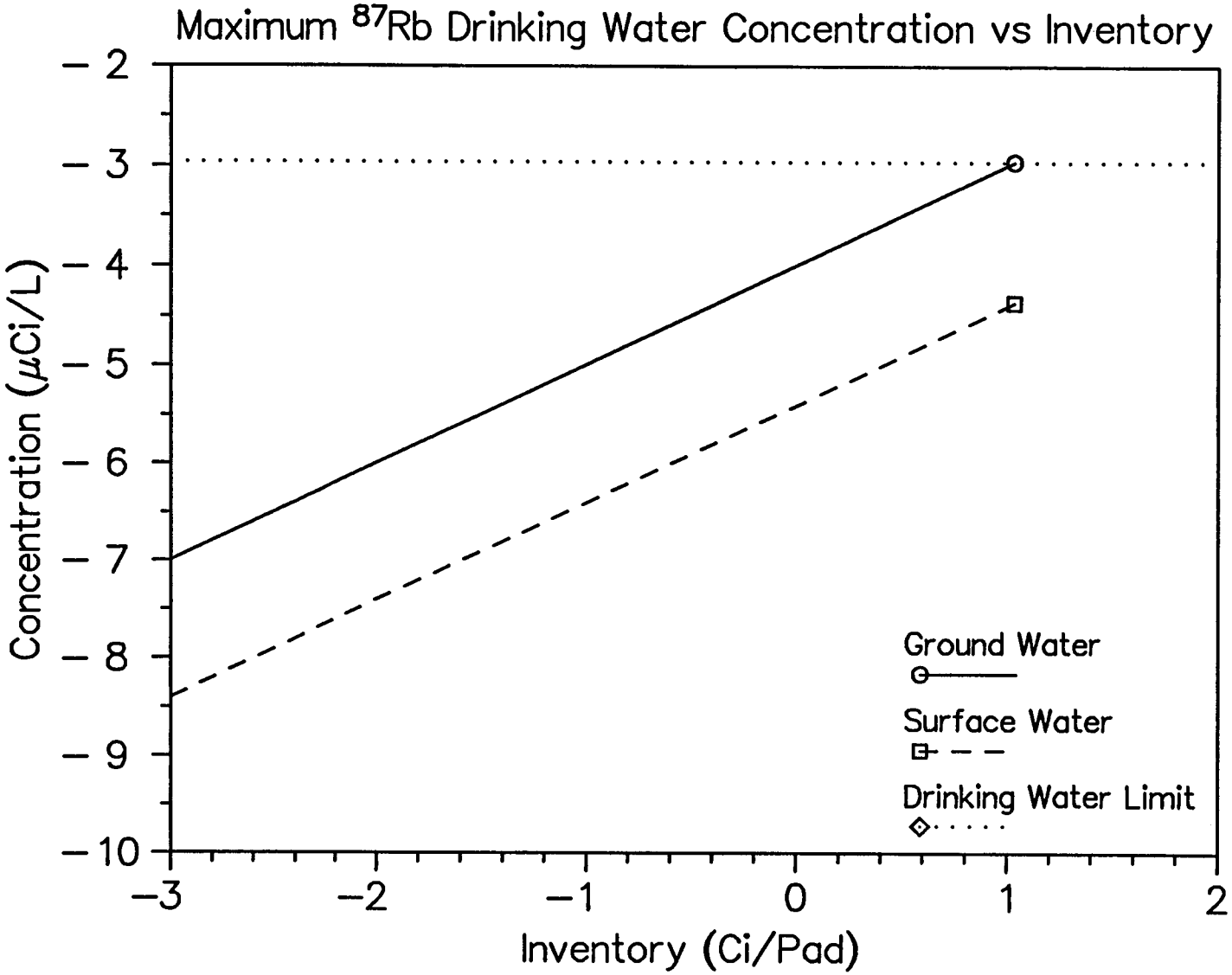

Fig. F.12. Maximum drinking water concentration as a function of CIIDF inventory for ^{87}Rb.

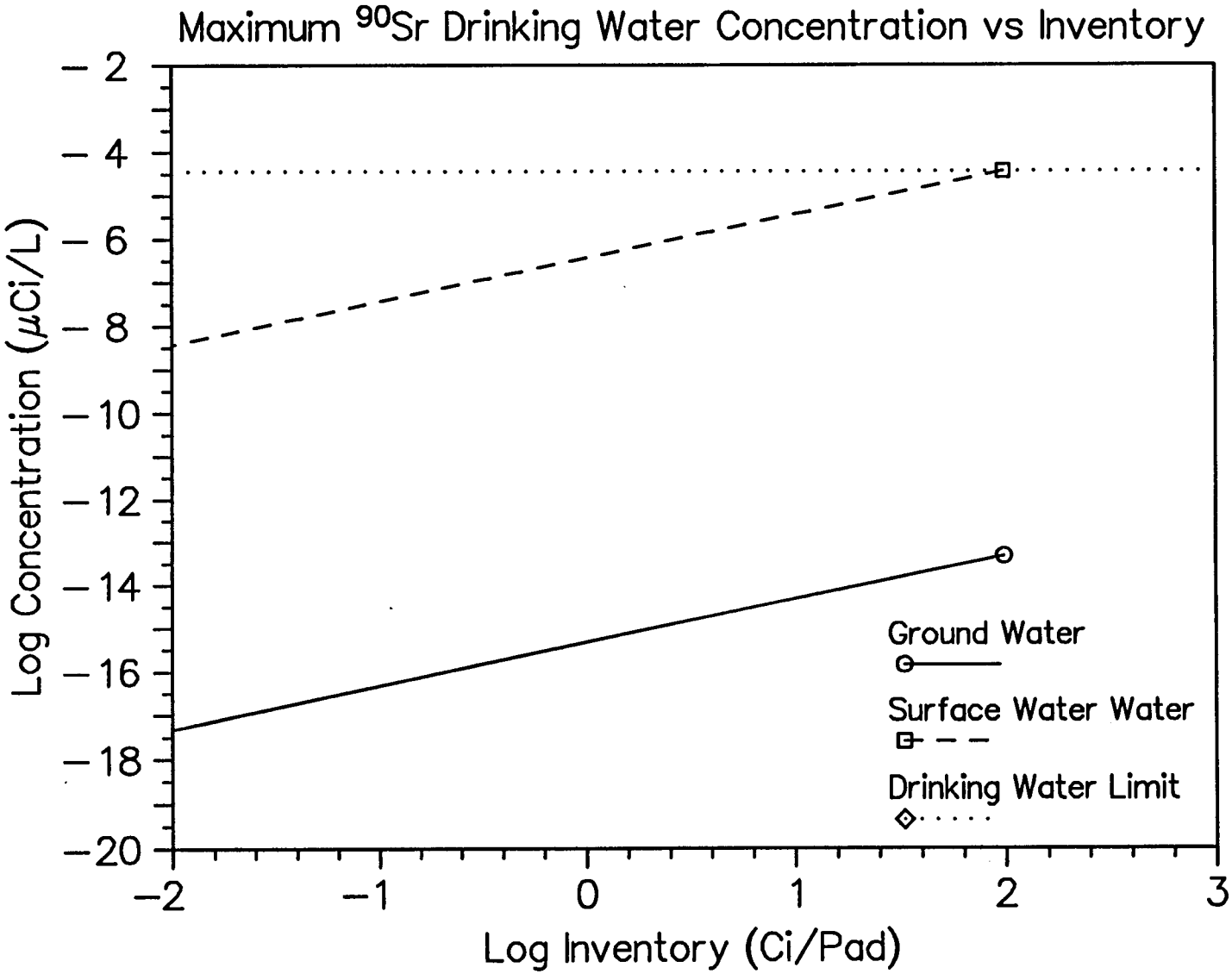

Fig. F.13. Maximum drinking water concentration as a function of CIIDF inventory for ^{90}Sr.

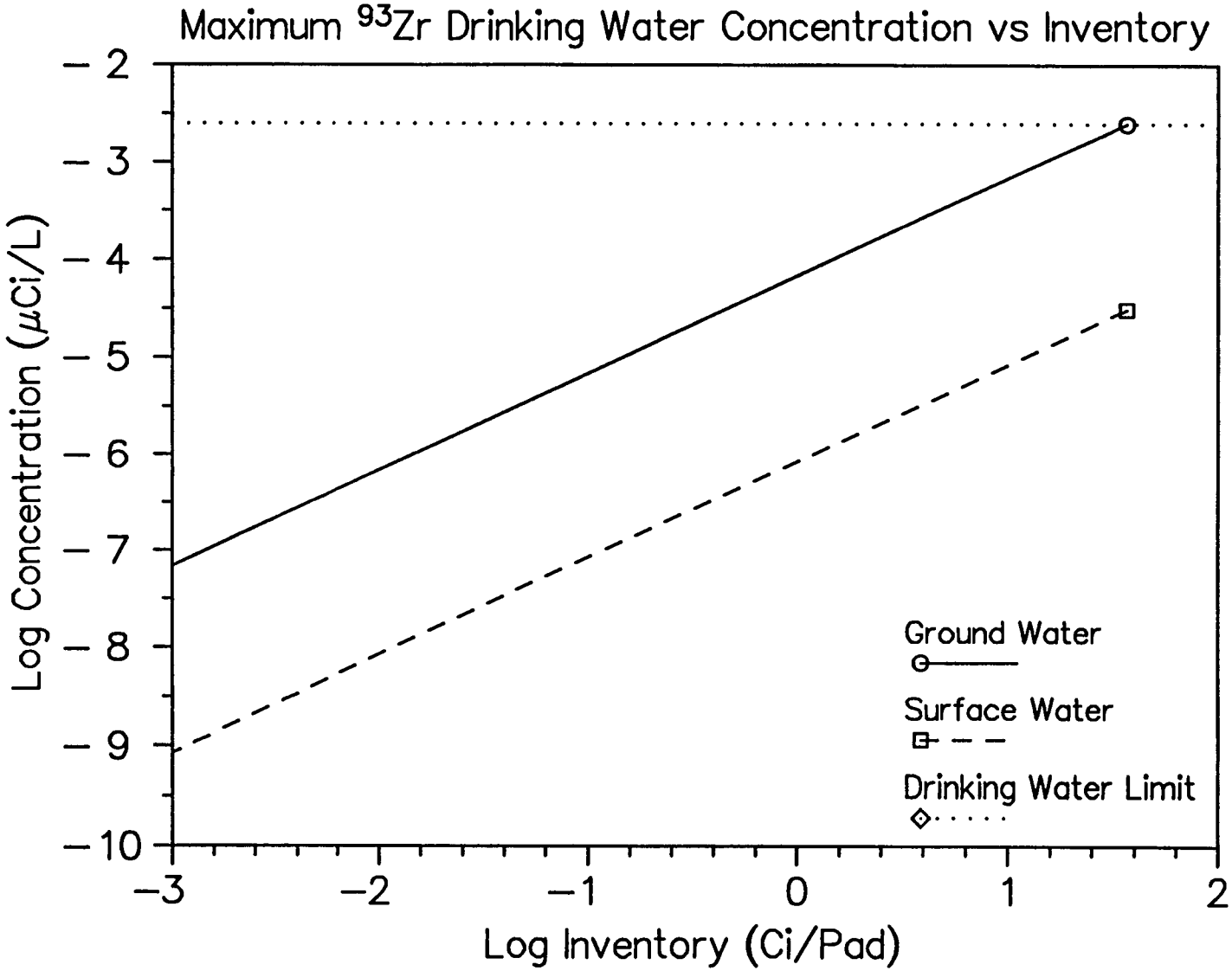

Fig. F.14. Maximum drinking water concentration as a function of CIIDF inventory for ^{93}Zr.

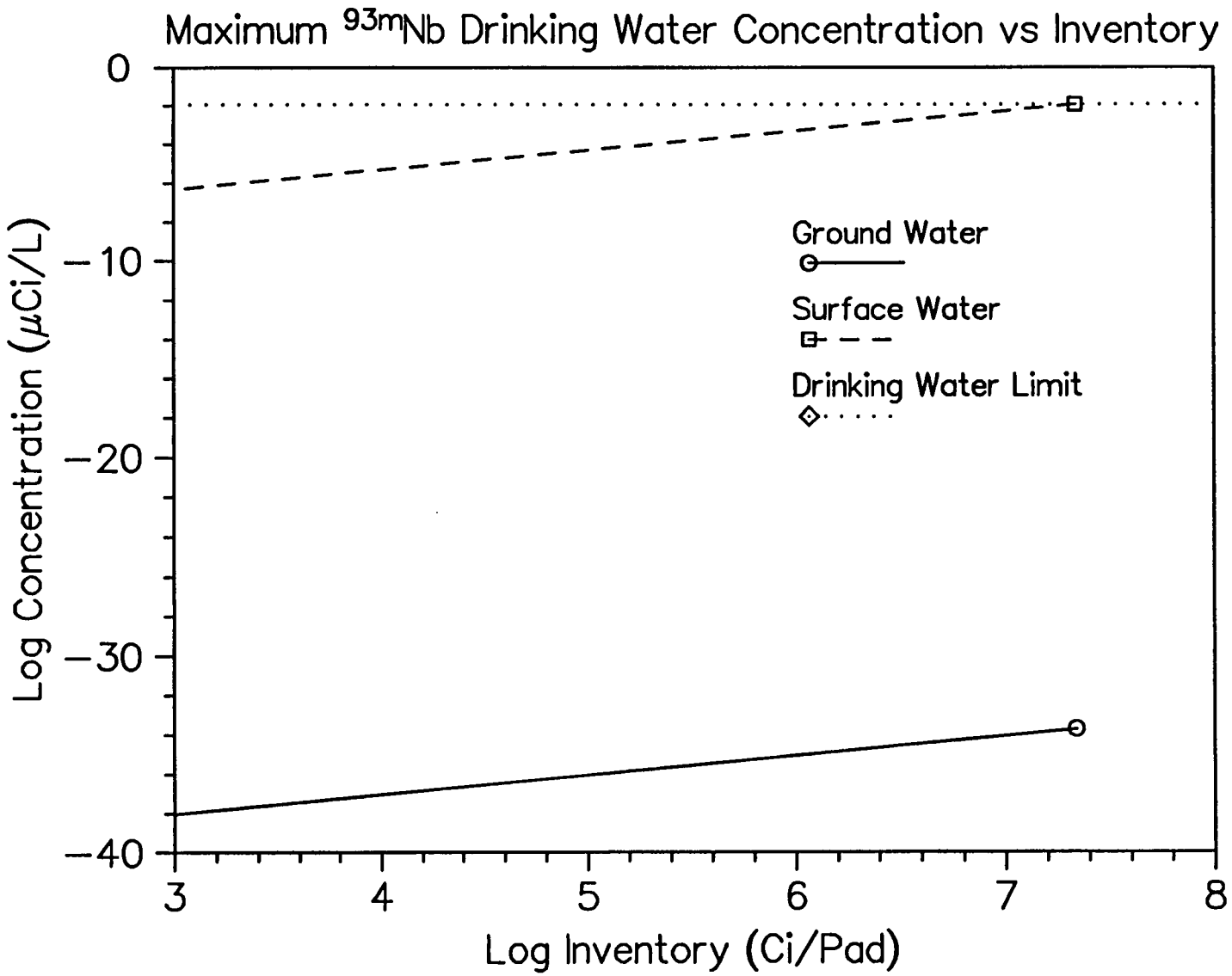

Fig. F.15. Maximum drinking water concentration as a function of CIIDF inventory for ^{93m}Nb.

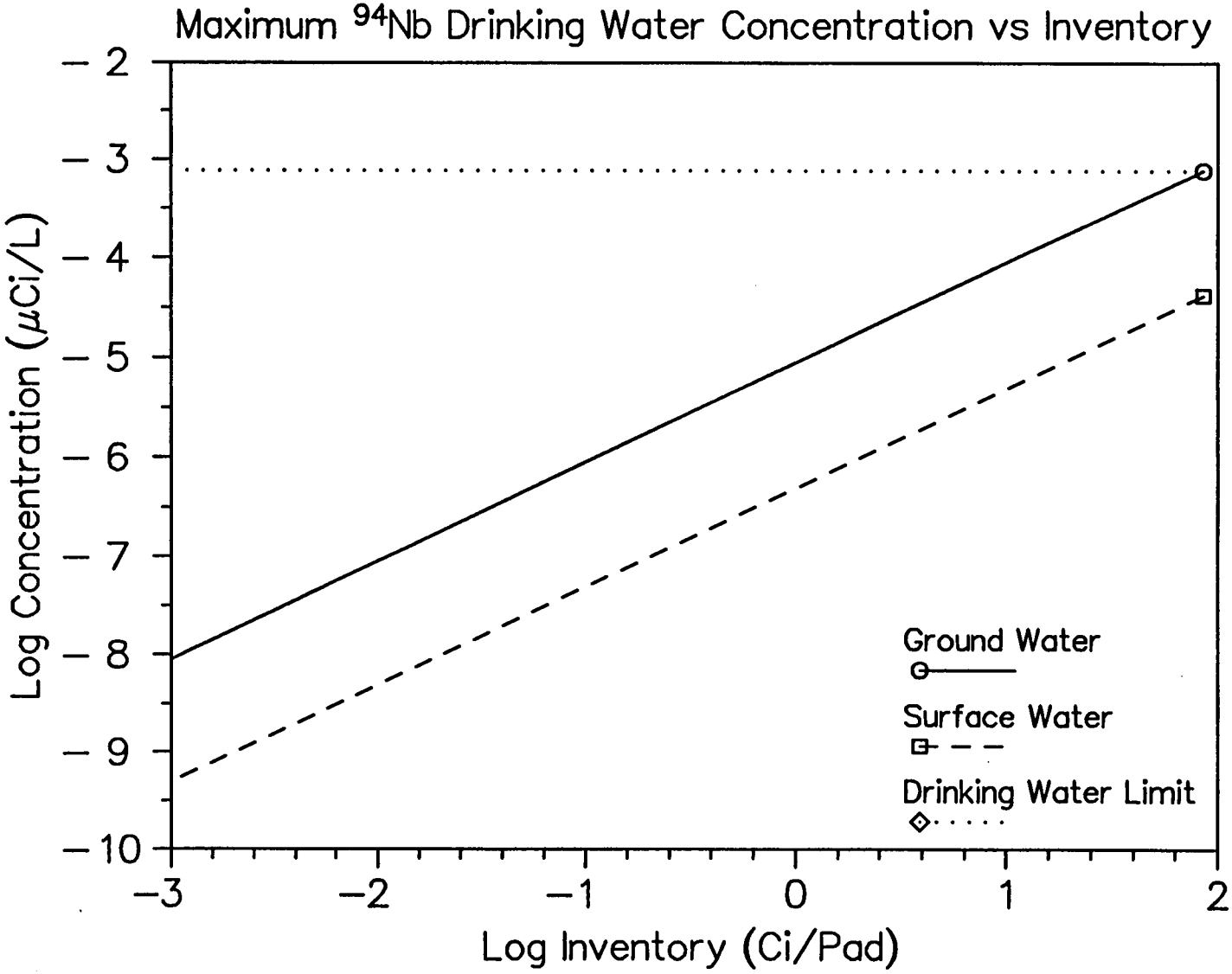

Fig. F.16. Maximum drinking water concentration as a function of CIIDF inventory for ^{94}Nb.

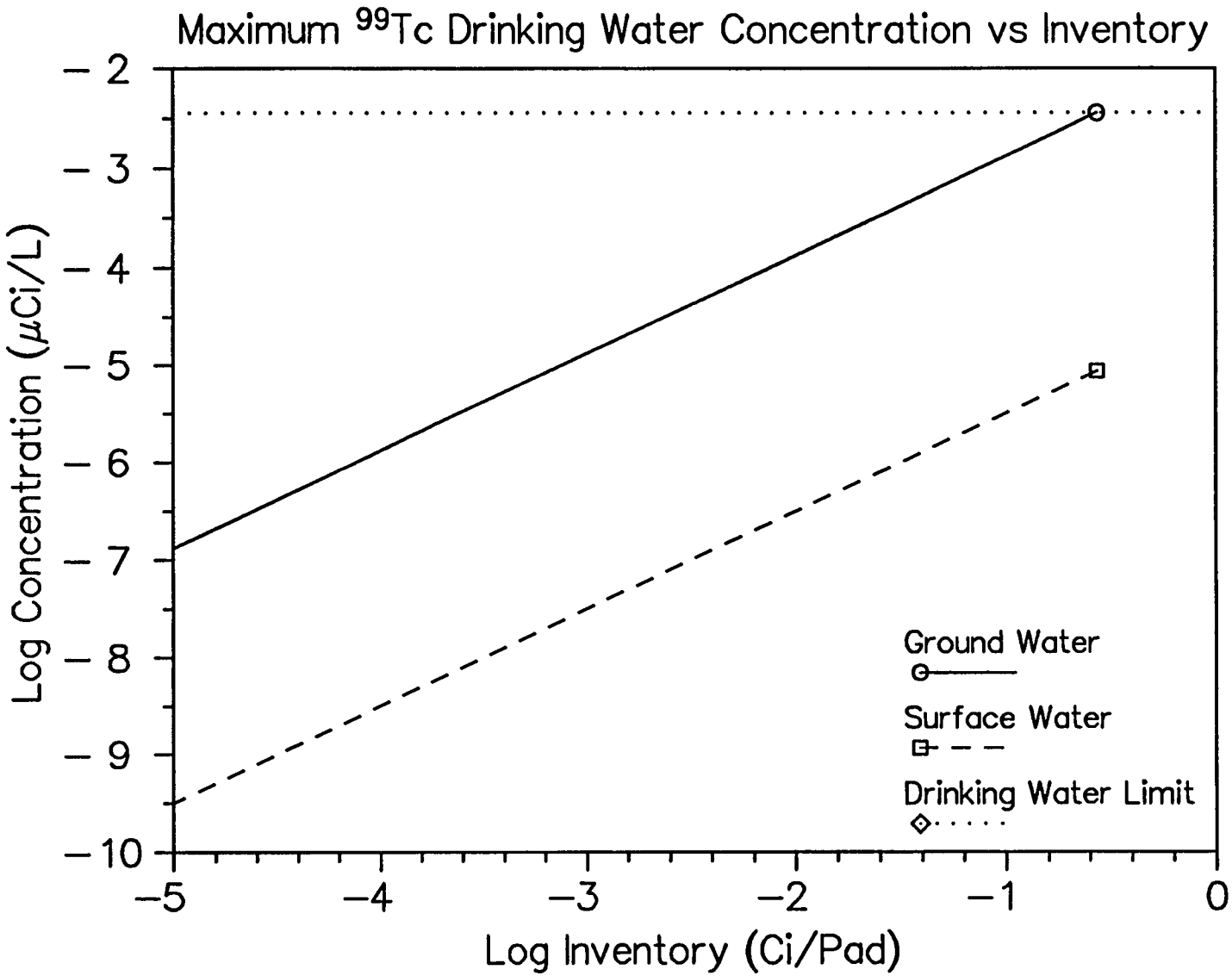

Fig. F.17. Maximum drinking water concentration as a function of CIIDF inventory for ^{99}Tc.

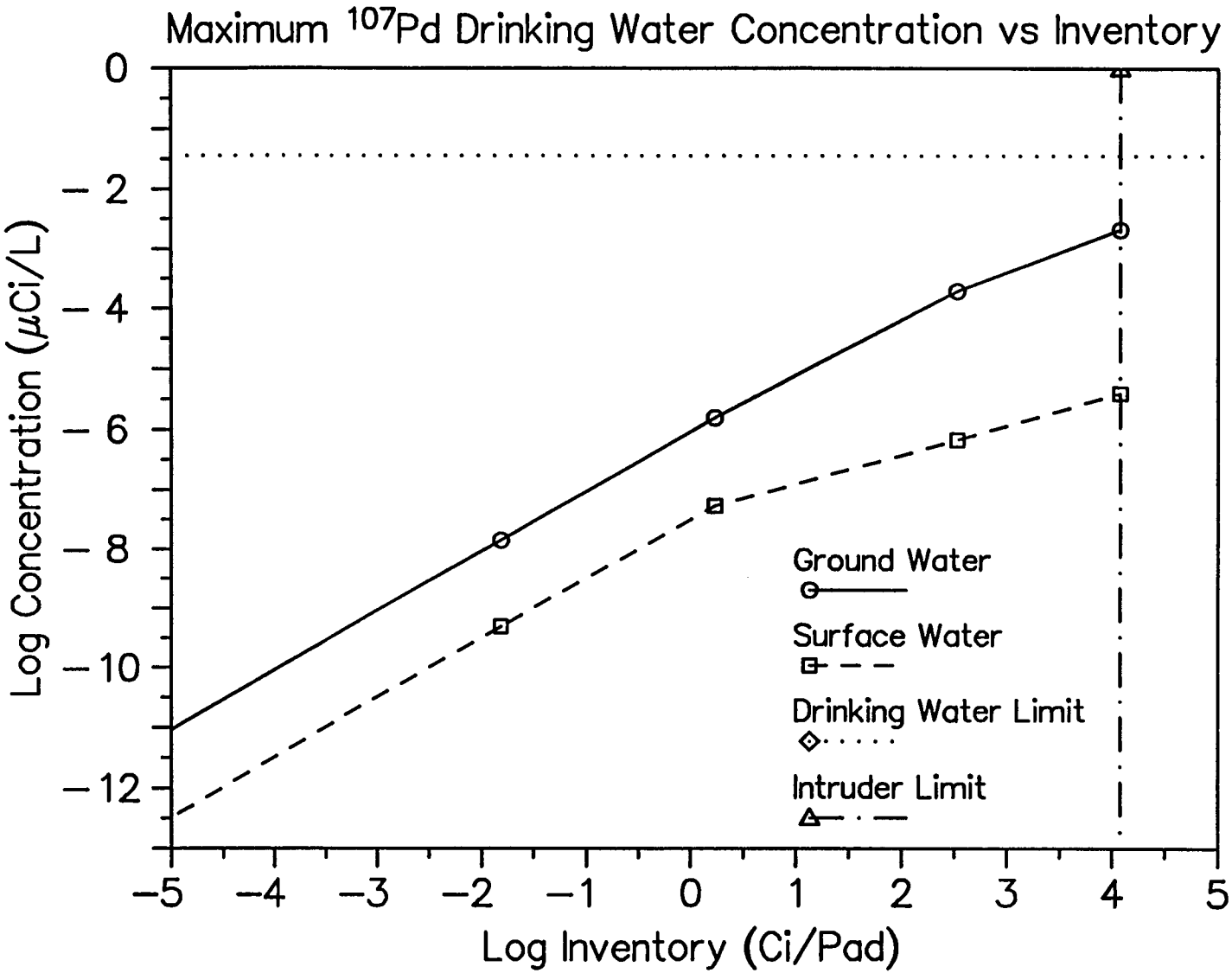

Fig. F.18. Maximum drinking water concentration as a function of CIIDF inventory for ^{107}Pd.

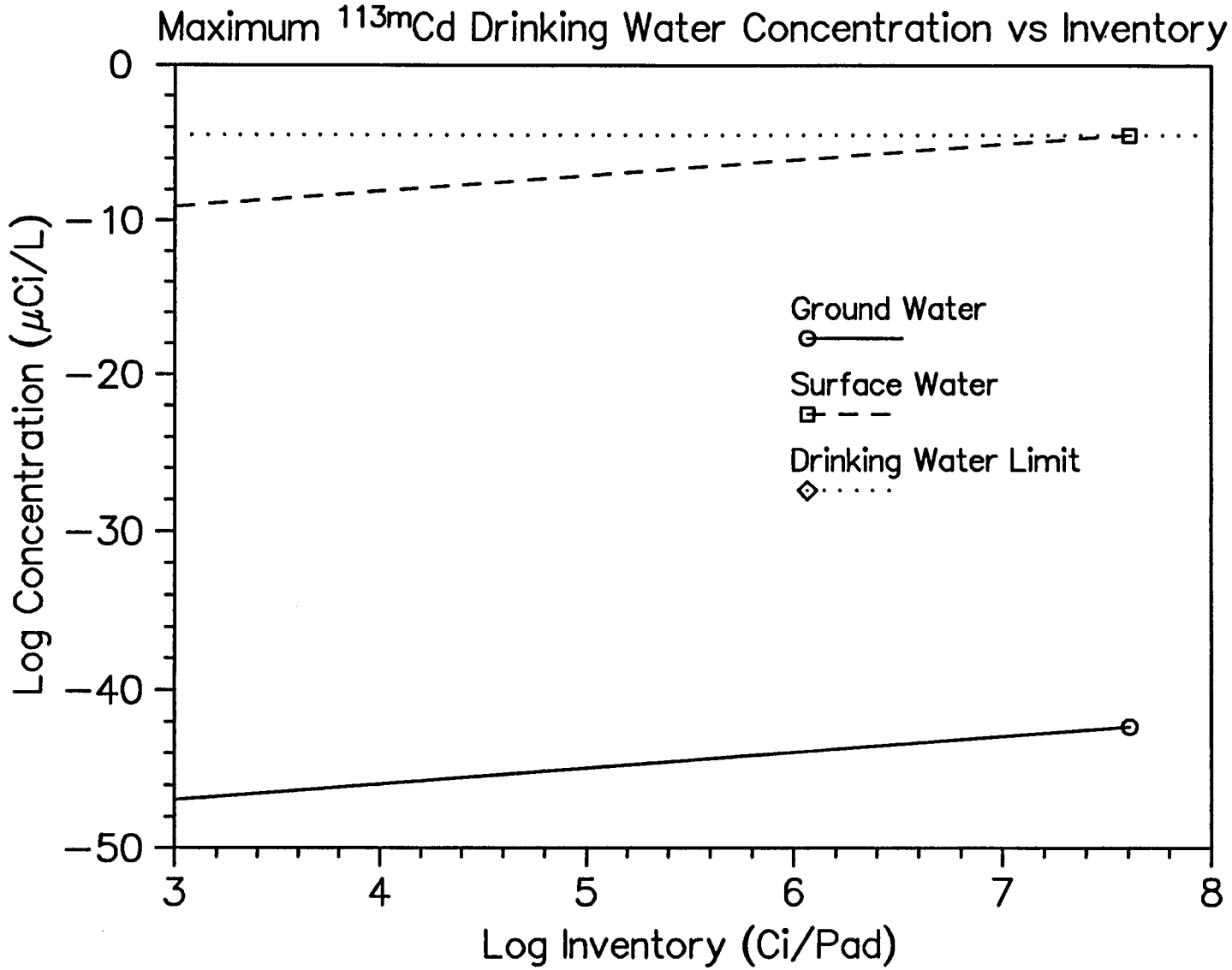

Fig. F.19. Maximum drinking water concentration as a function of CIIDF inventory for ^{113m}Cd.

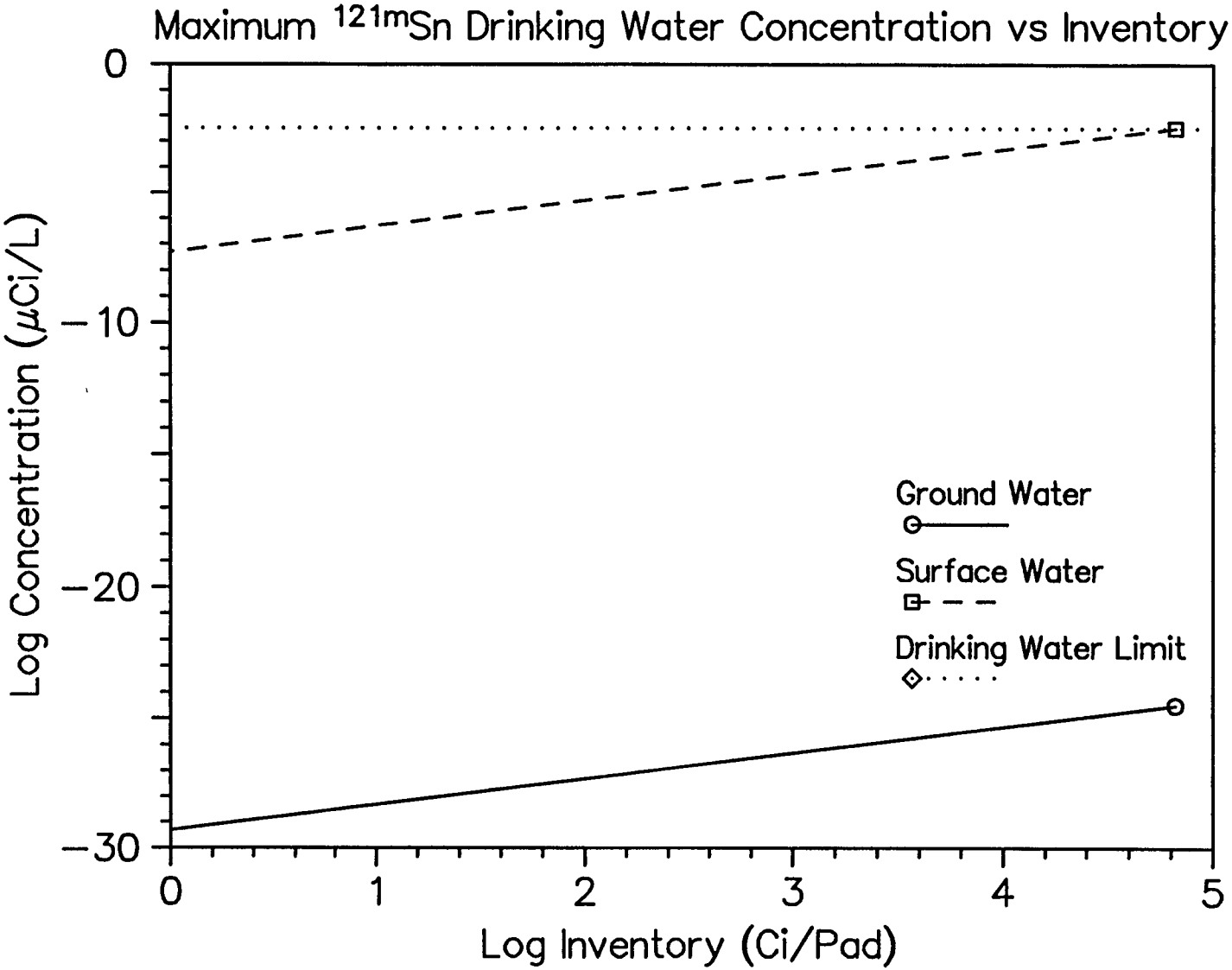

Fig. F.20. Maximum drinking water concentration as a function of CIIDF inventory for ^{121m}Sn.

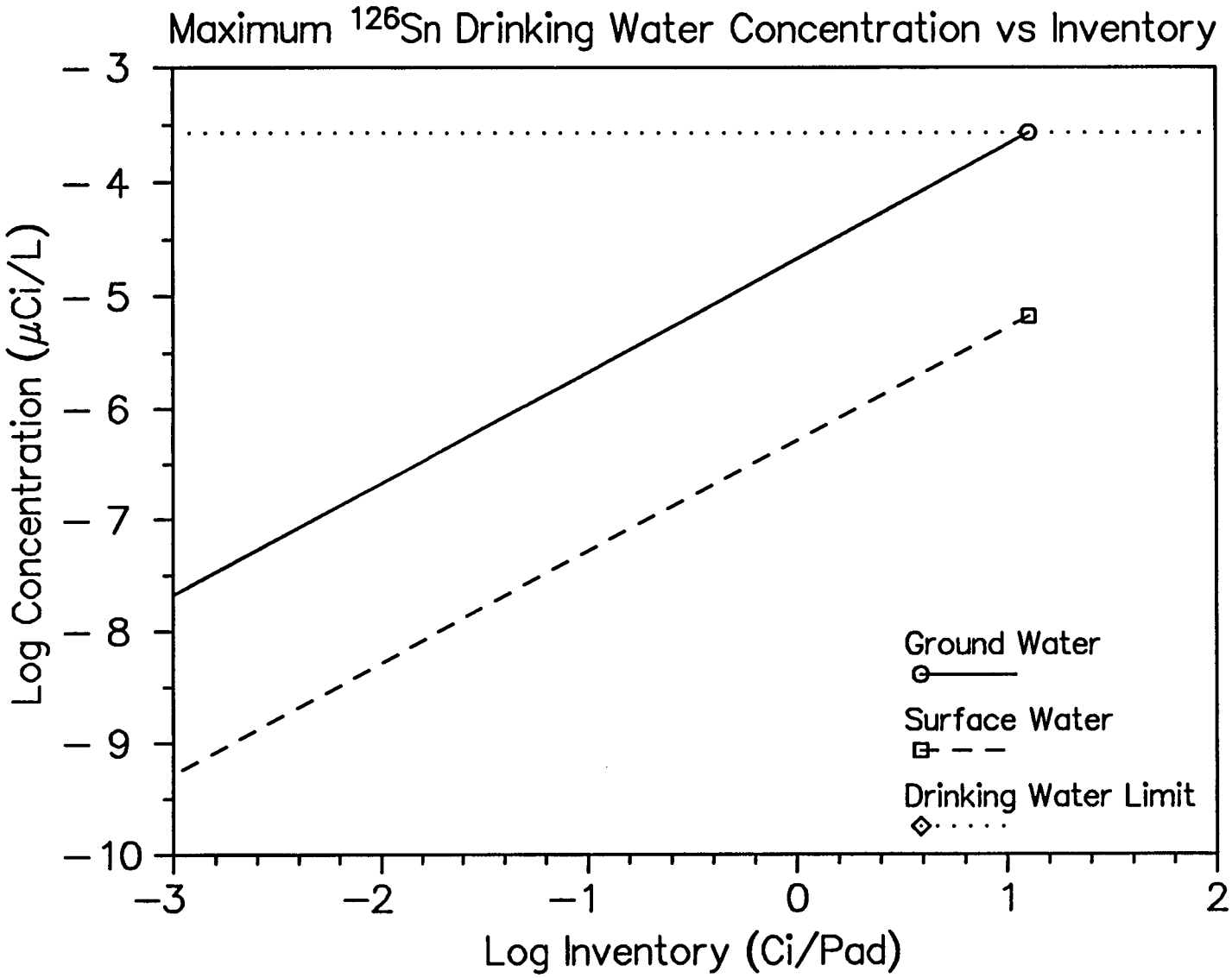

Fig. F.21. Maximum drinking water concentration as a function of CIIDF inventory for ^{126}Sn.

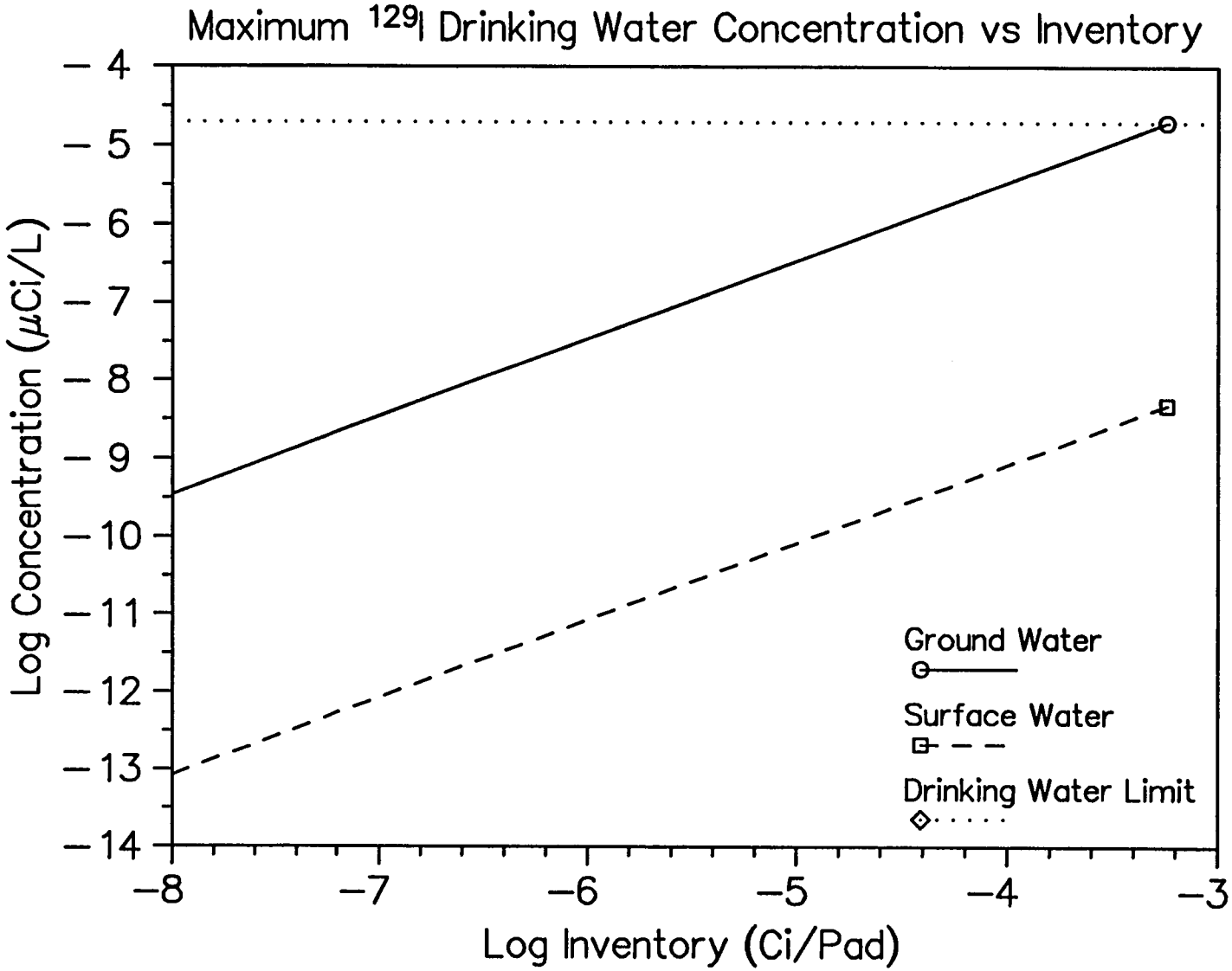

Fig. F.22. Maximum drinking water concentration as a function of CIIDF inventory for ^{129}I.

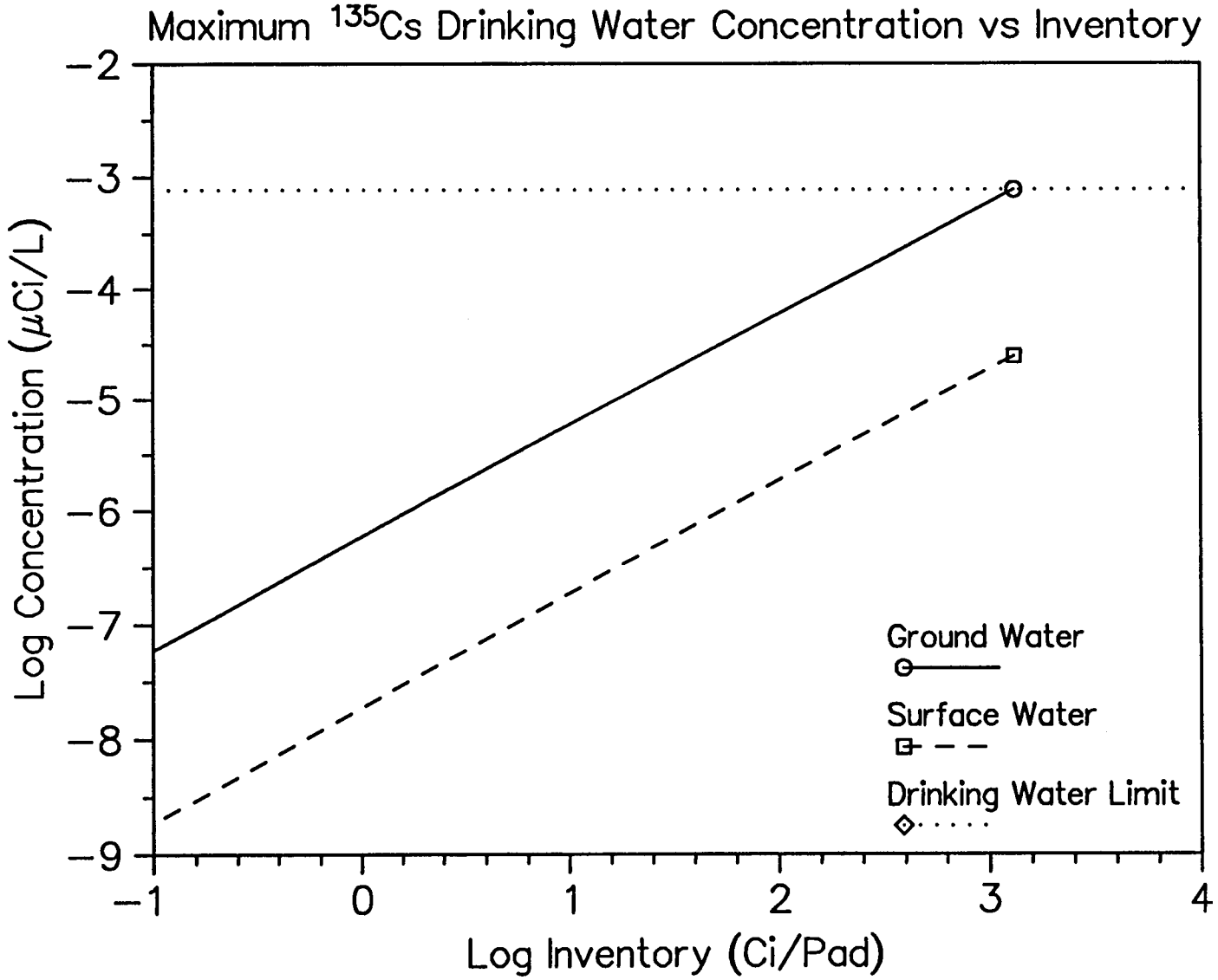

Fig. F.23. Maximum drinking water concentration as a function of CIIDF inventory for ^{135}Cs.

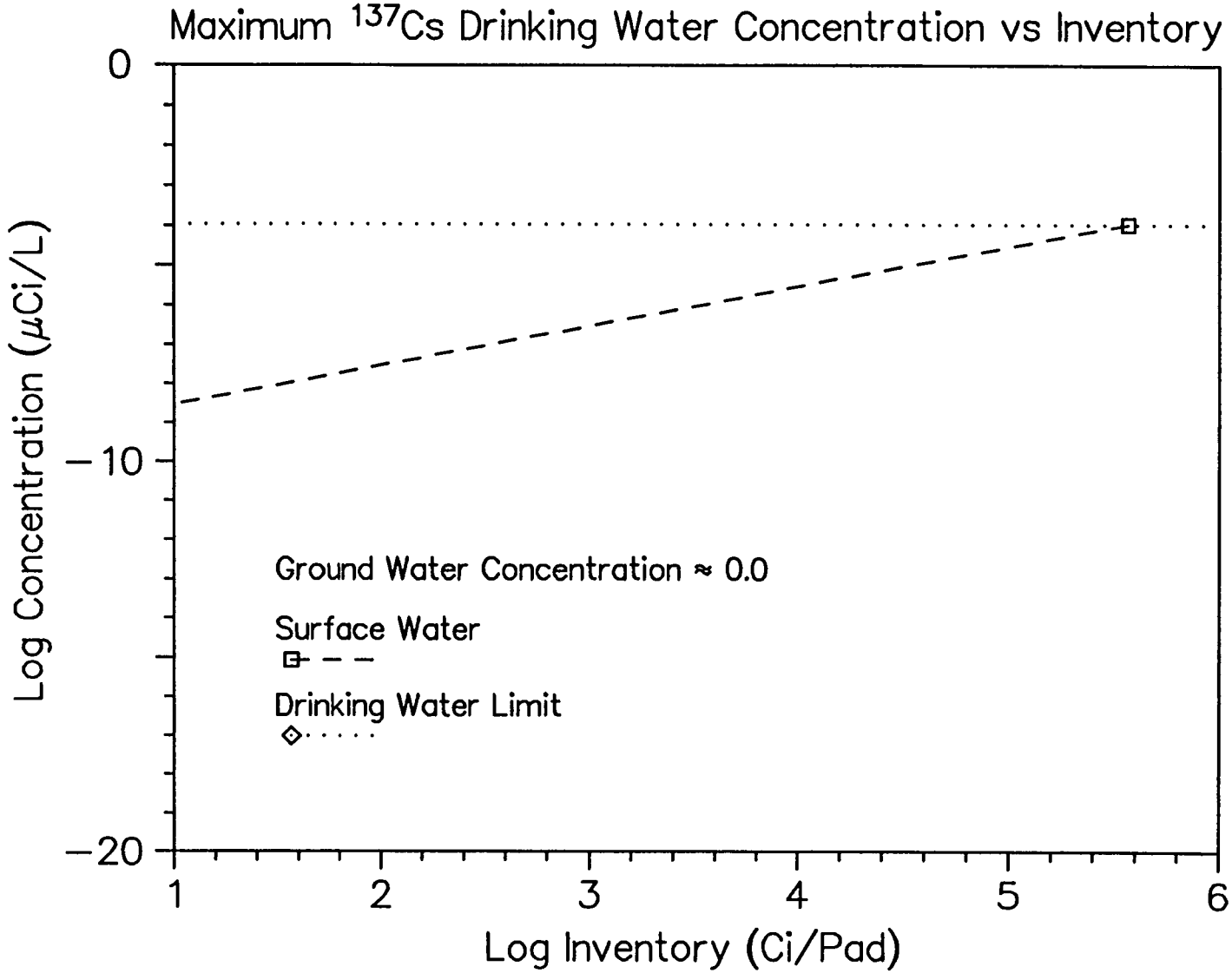

Fig. F.24. Maximum drinking water concentration as a function of CIIDF inventory for ^{137}Cs.

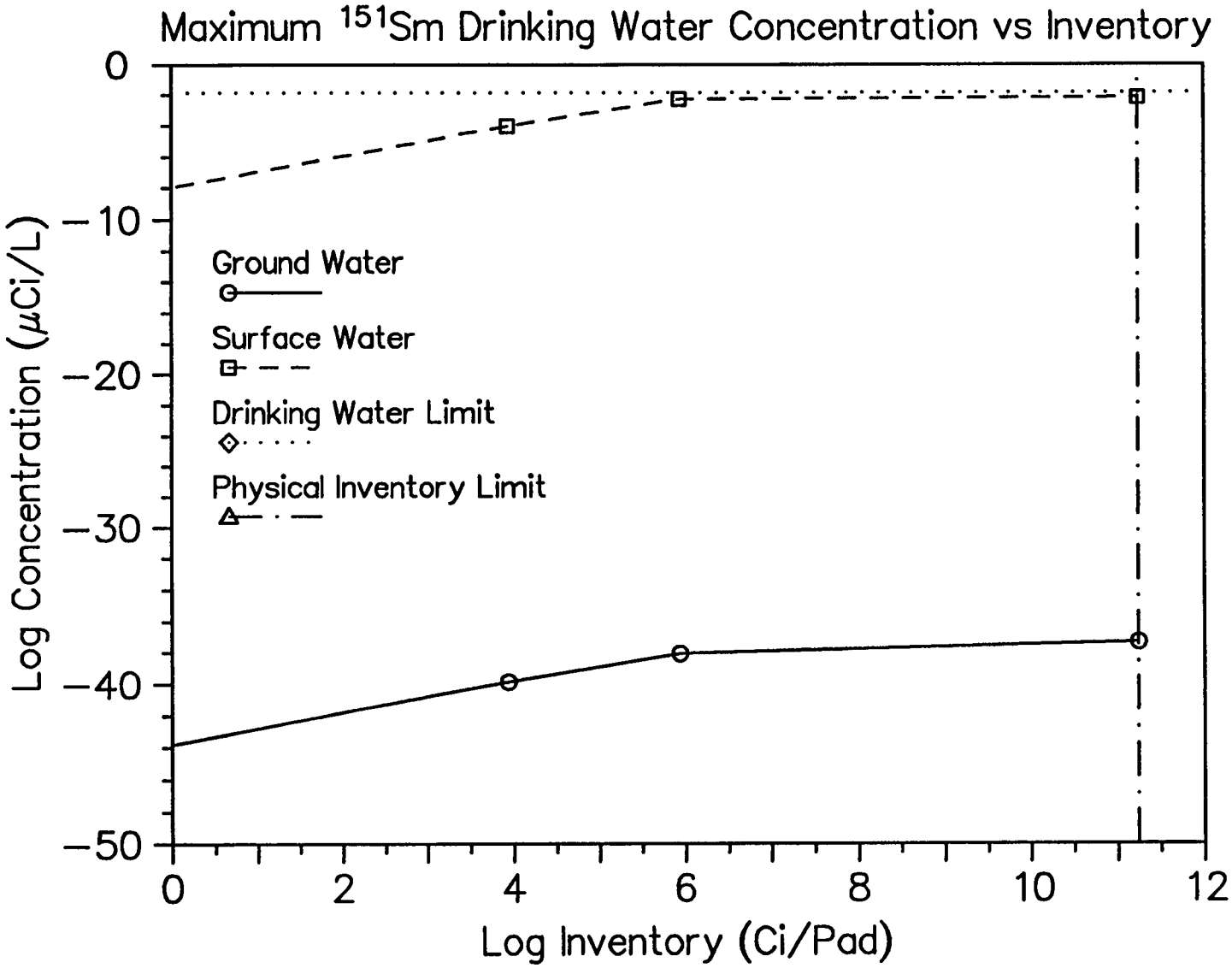

Fig. F.25. Maximum drinking water concentration as a function of CIIDF inventory for ^{151}Sm.

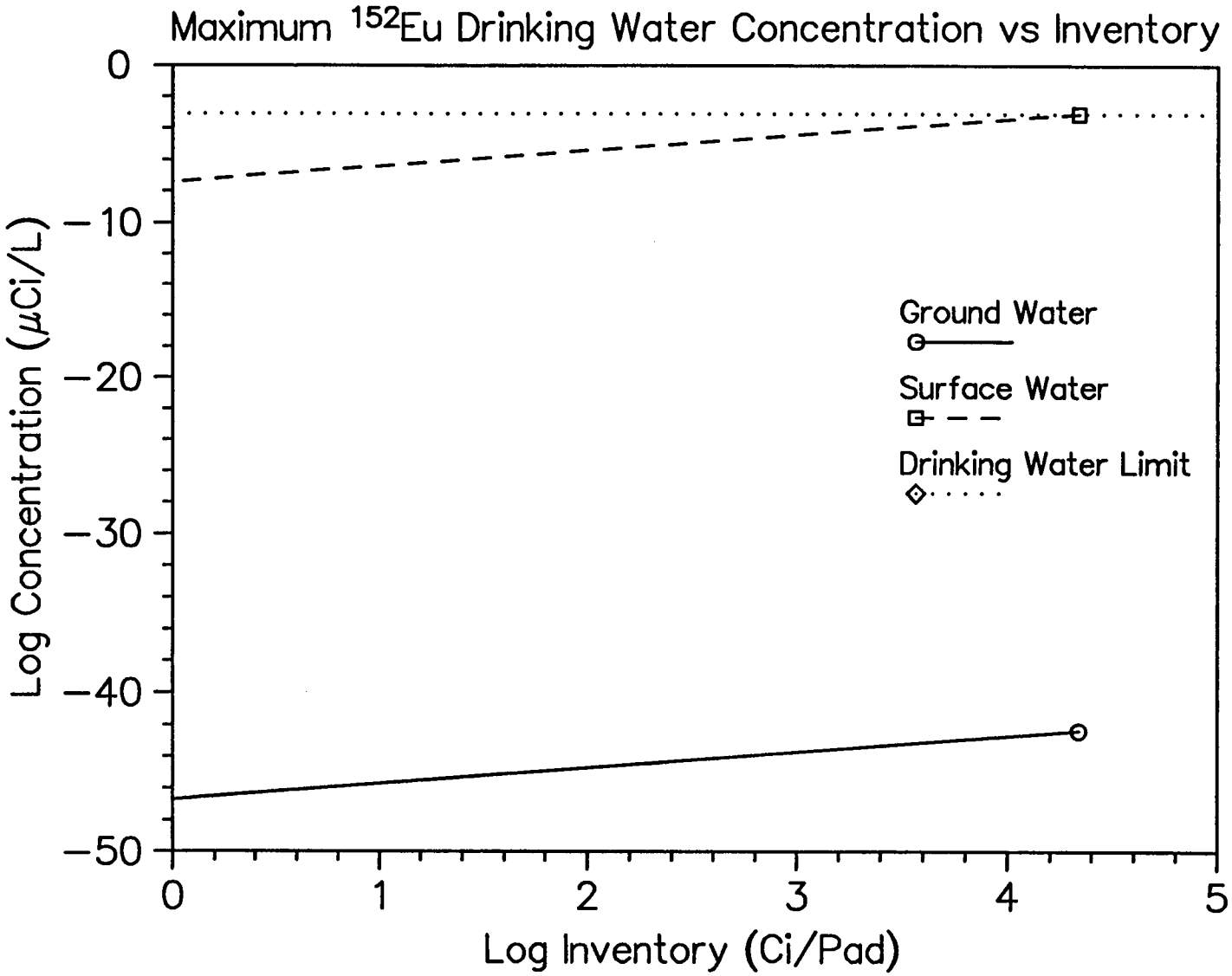

Fig. F.26. Maximum drinking water concentration as a function of CIIDF inventory for ^{152}Eu.

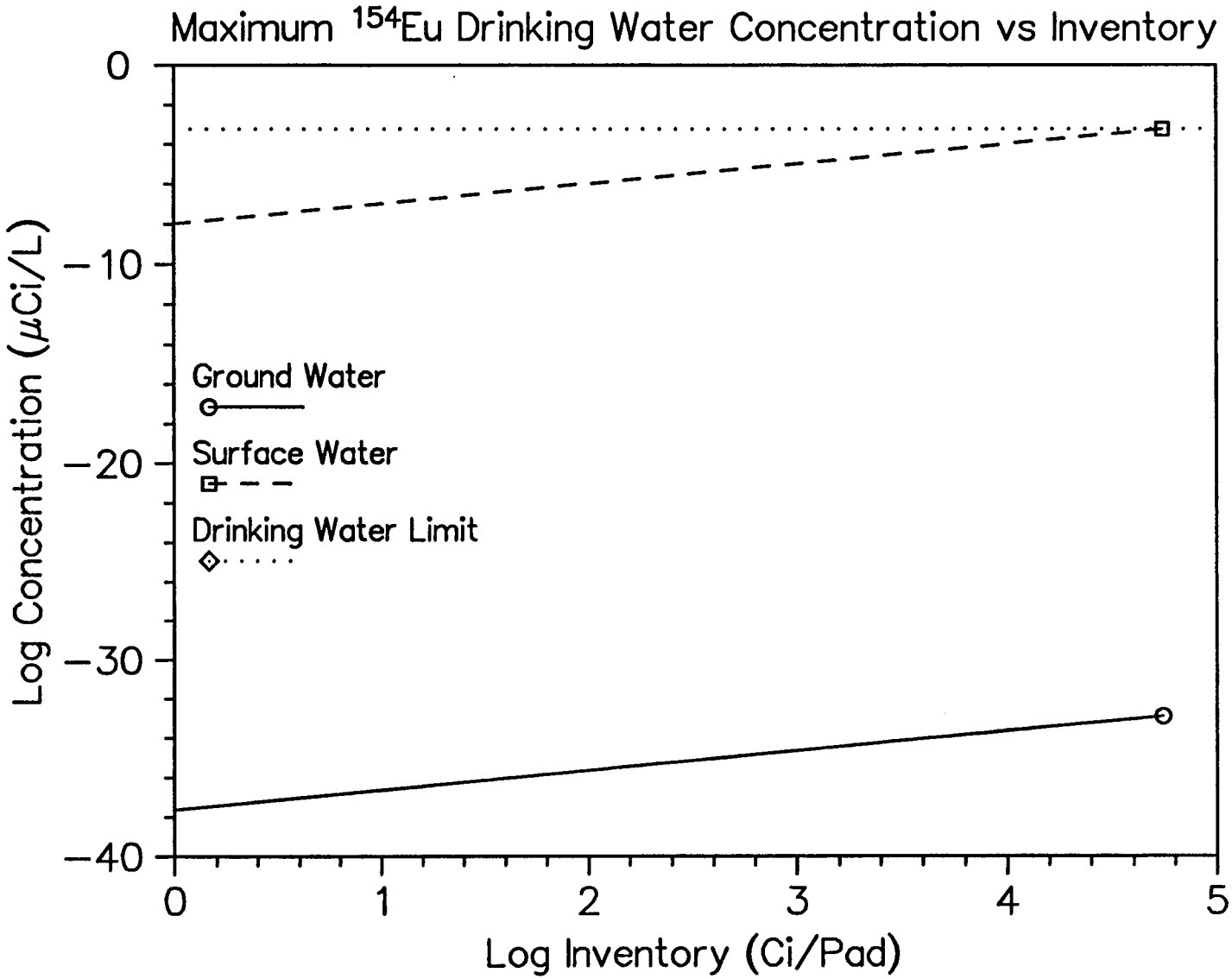

Fig. F.27. Maximum drinking water concentration as a function of CIIDF inventory for ^{154}Eu.

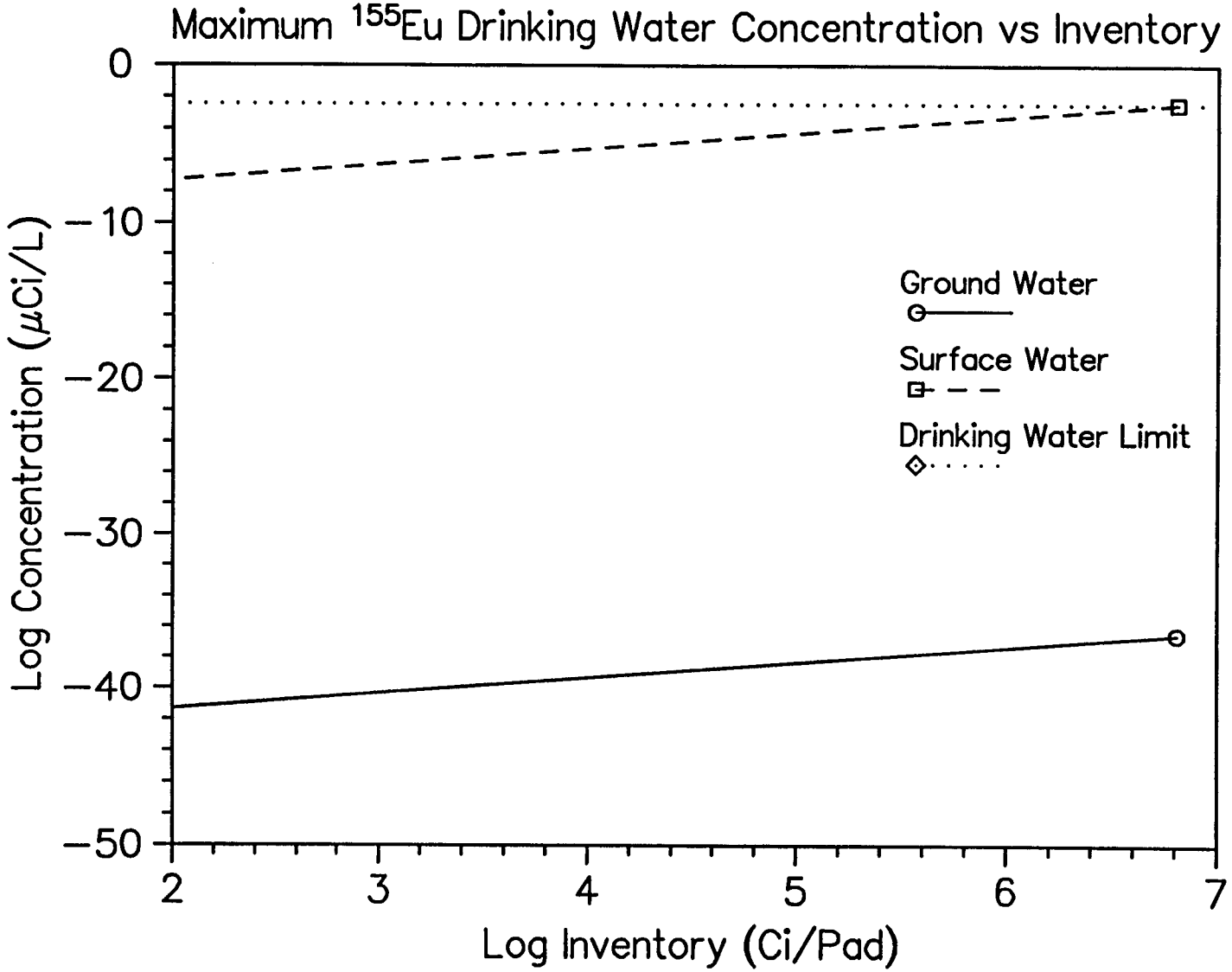

Fig. F.28. Maximum drinking water concentration as a function of CIIDF inventory for ^{155}Eu.

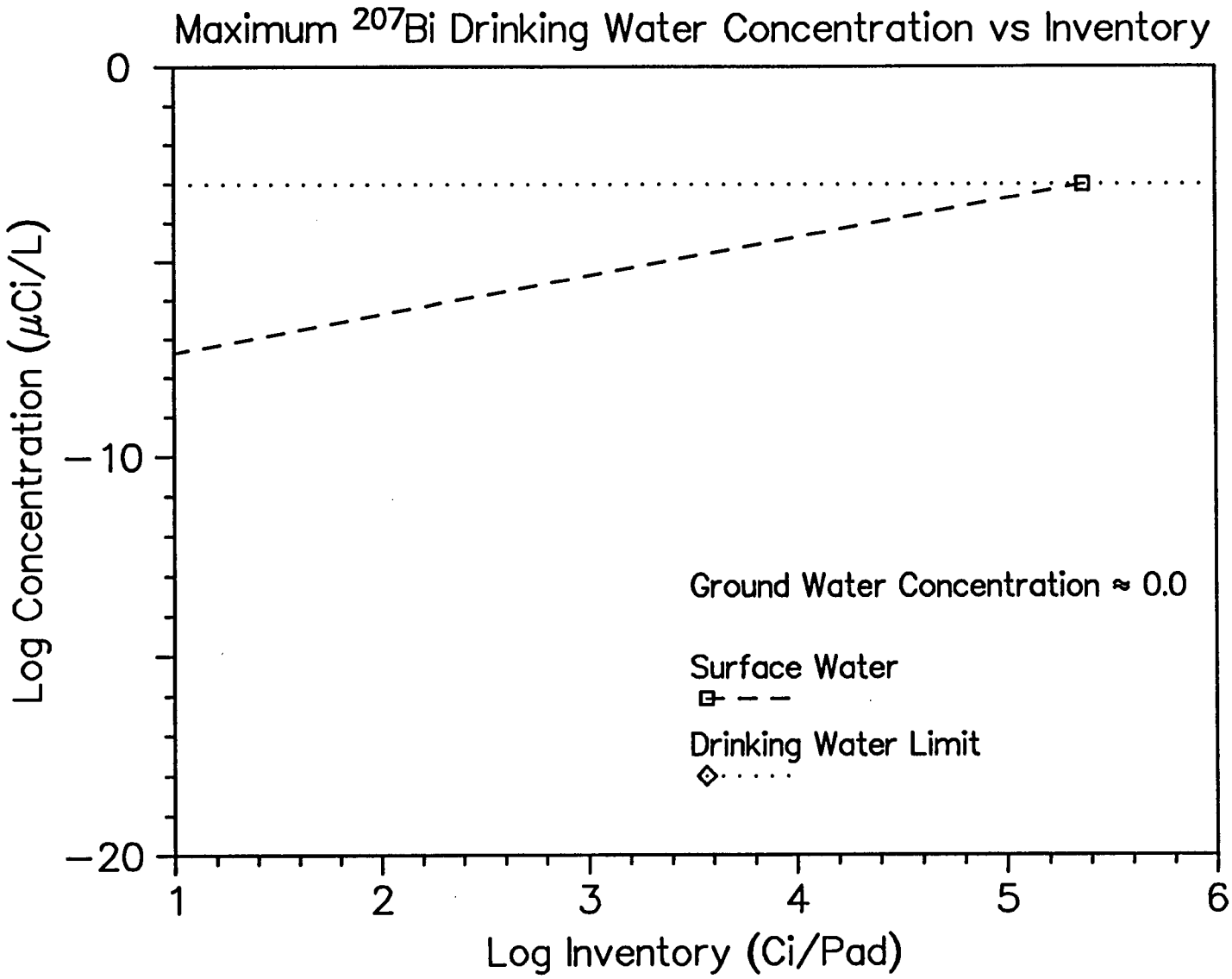

Fig. F.29. Maximum drinking water concentration as a function of CIIDF inventory for ^{207}Bi.

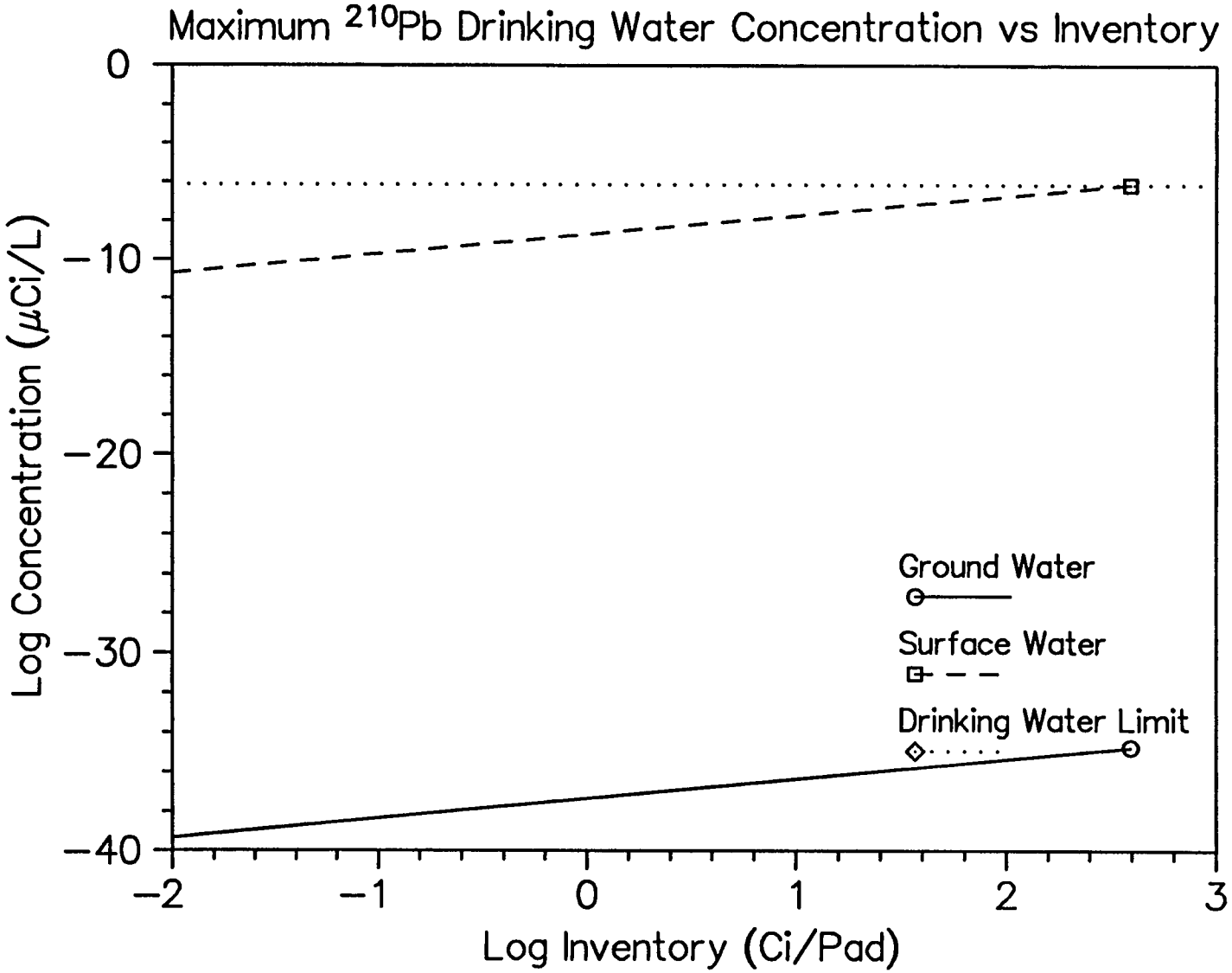

Fig. F.30. Maximum drinking water concentration as a function of CIIDF inventory for ^{210}Pb.

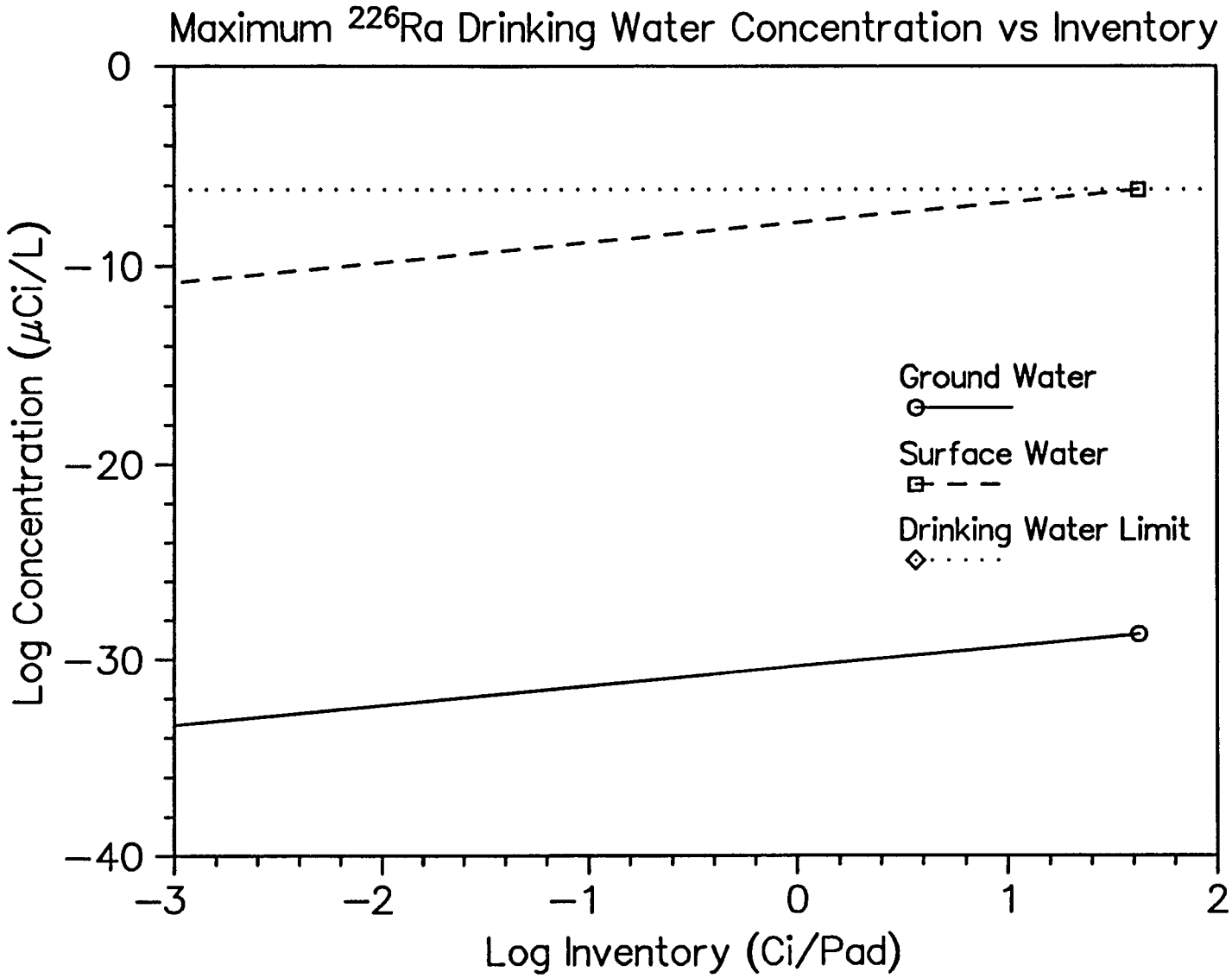

Fig. F.31. Maximum drinking water concentration as a function of CIIDF inventory for ^{226}Ra.

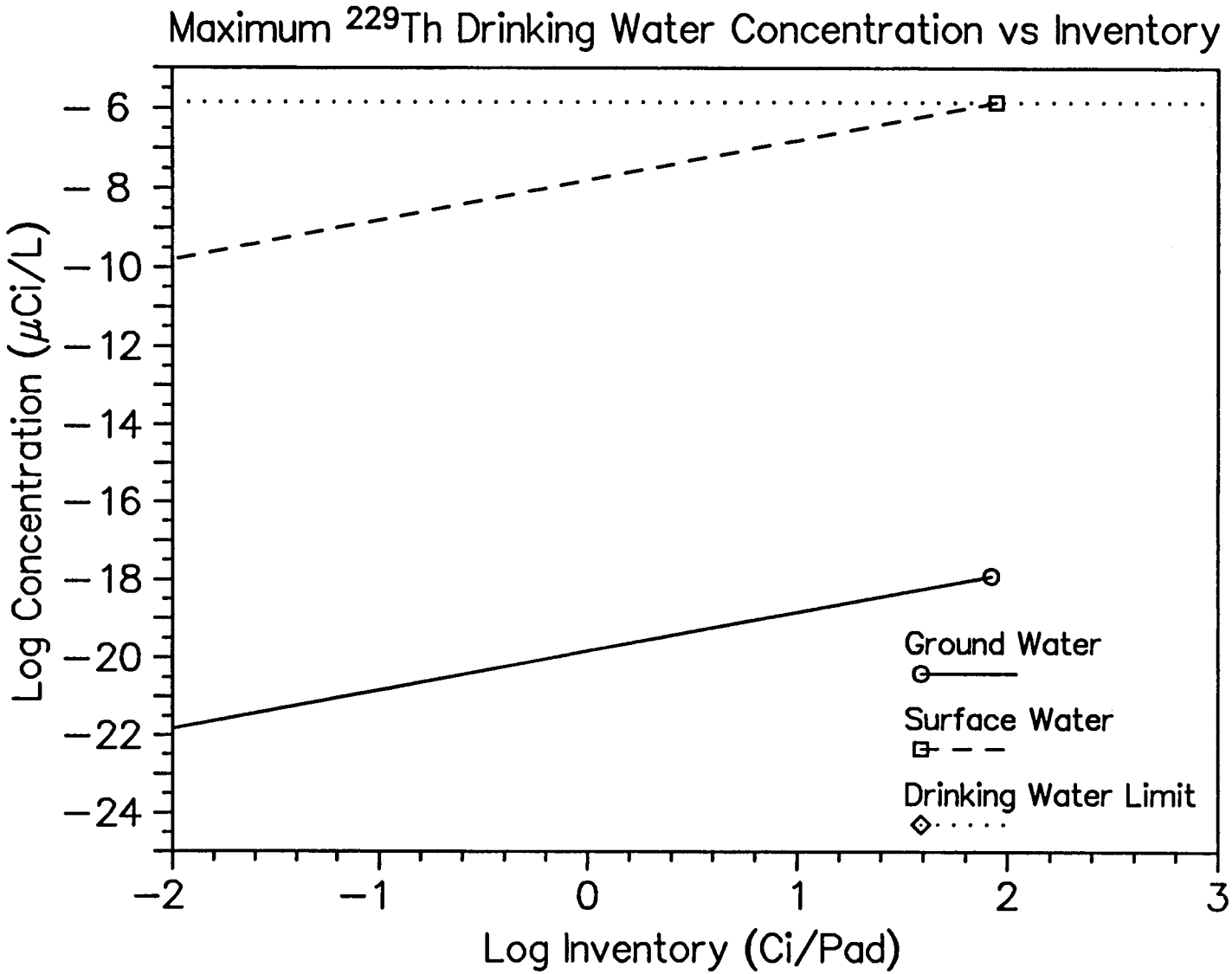

Fig. F.32. Maximum drinking water concentration as a function of CIIDF inventory for ^{229}Th.

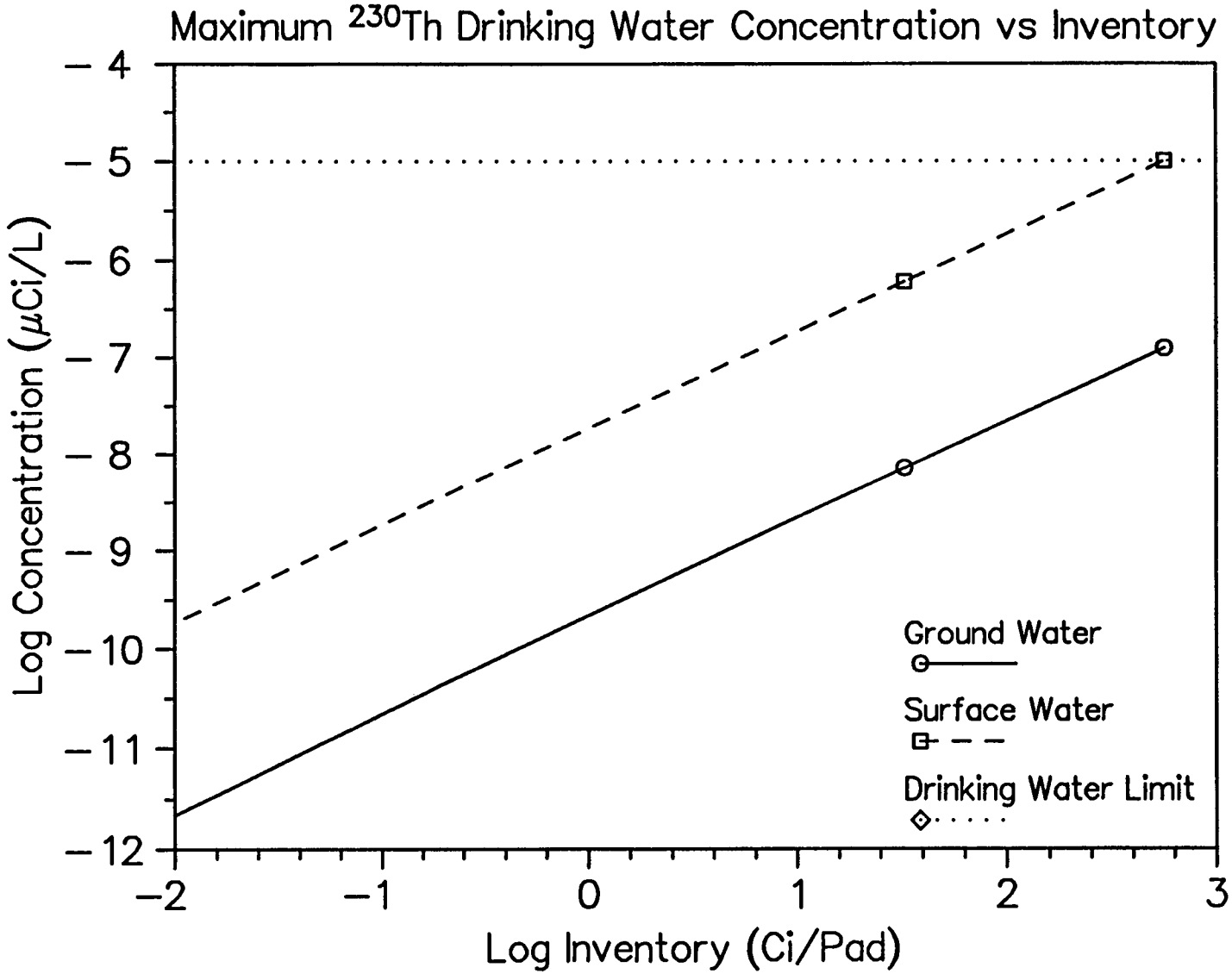

Fig. F.33. Maximum drinking water concentration as a function of CIIDF inventory for ^{230}Th.

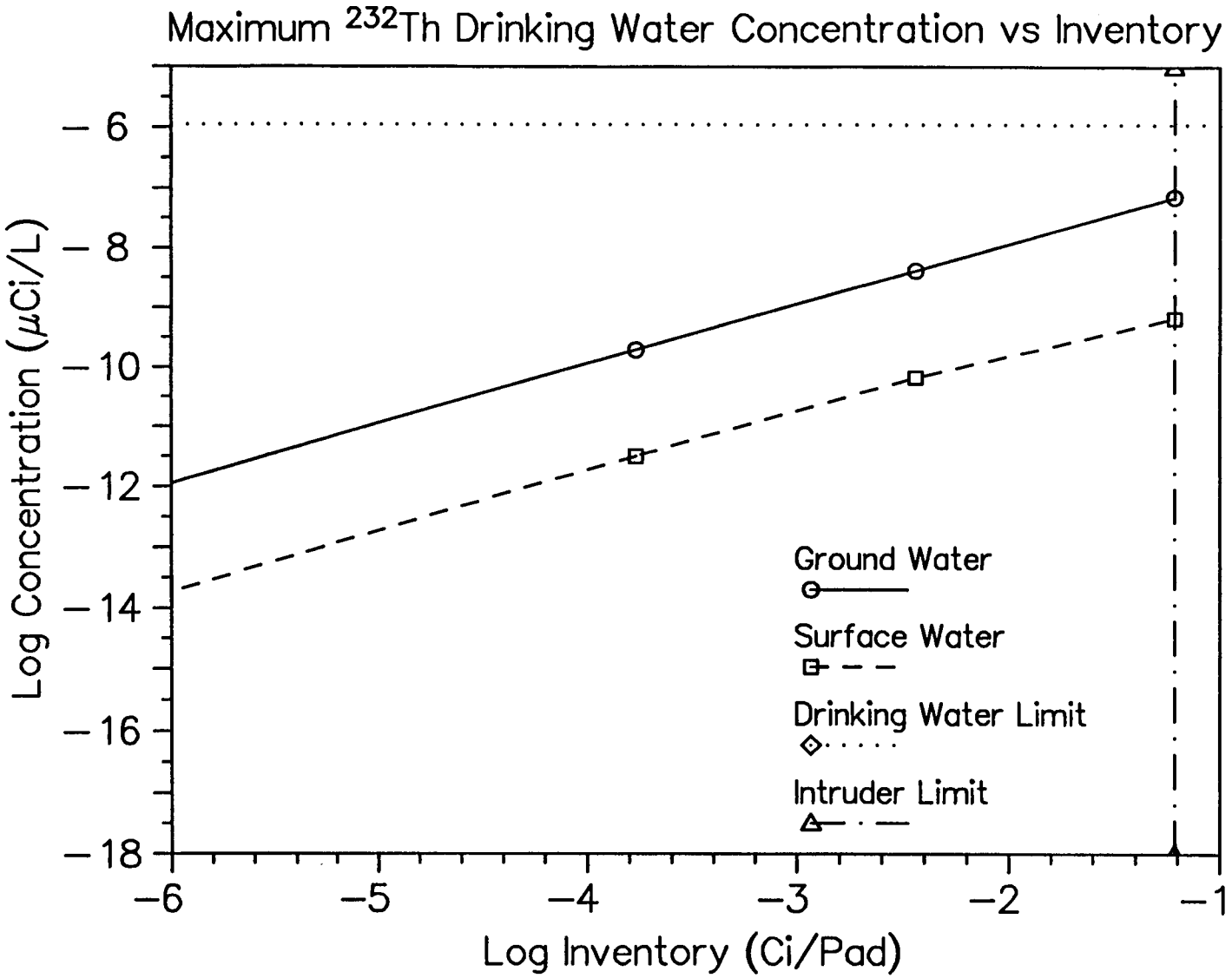

Fig. F.34. Maximum drinking water concentration as a function of CIIDF inventory for ^{232}Th.

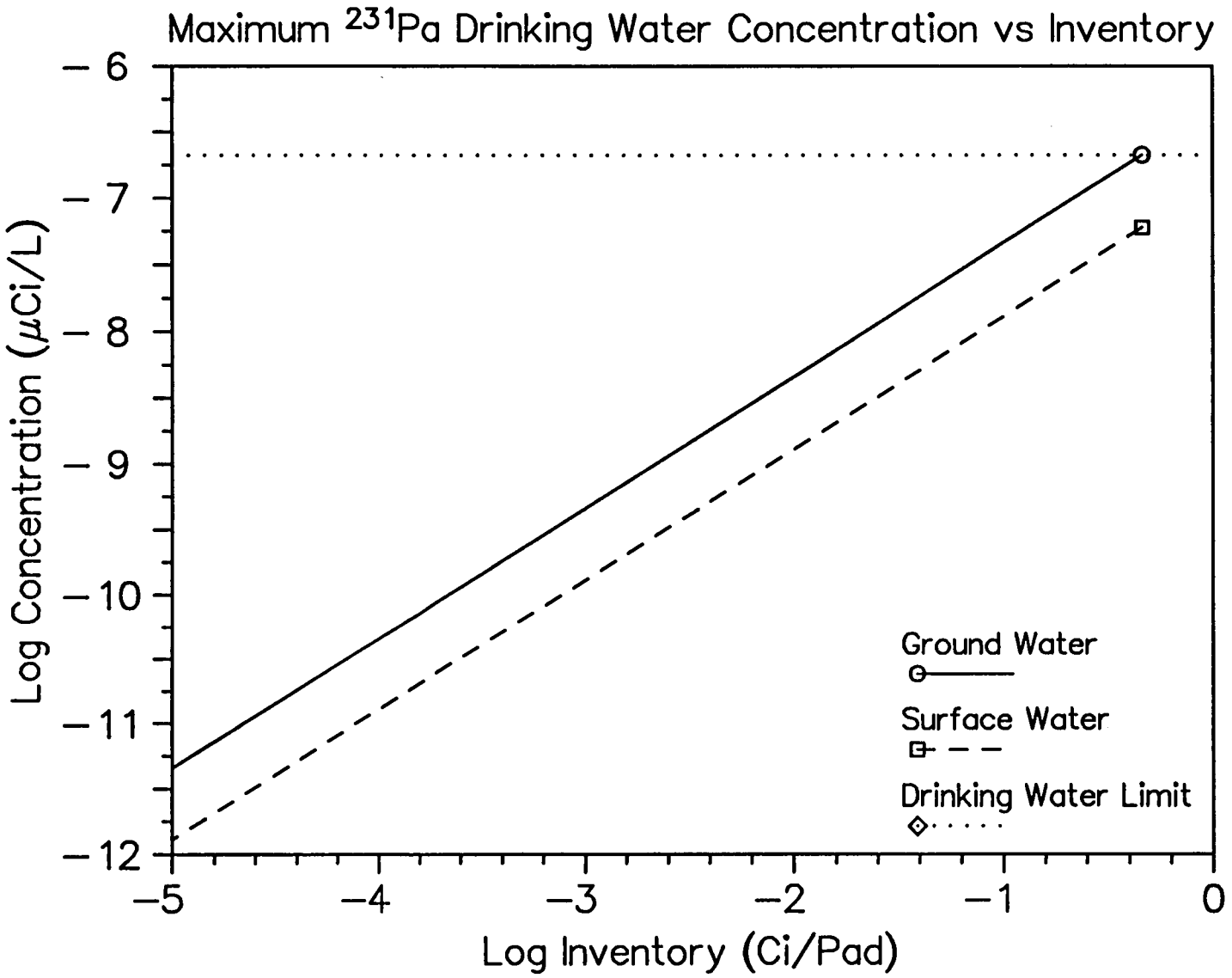

Fig. F.35. Maximum drinking water concentration as a function of CIIDF inventory for ^{231}Pa.

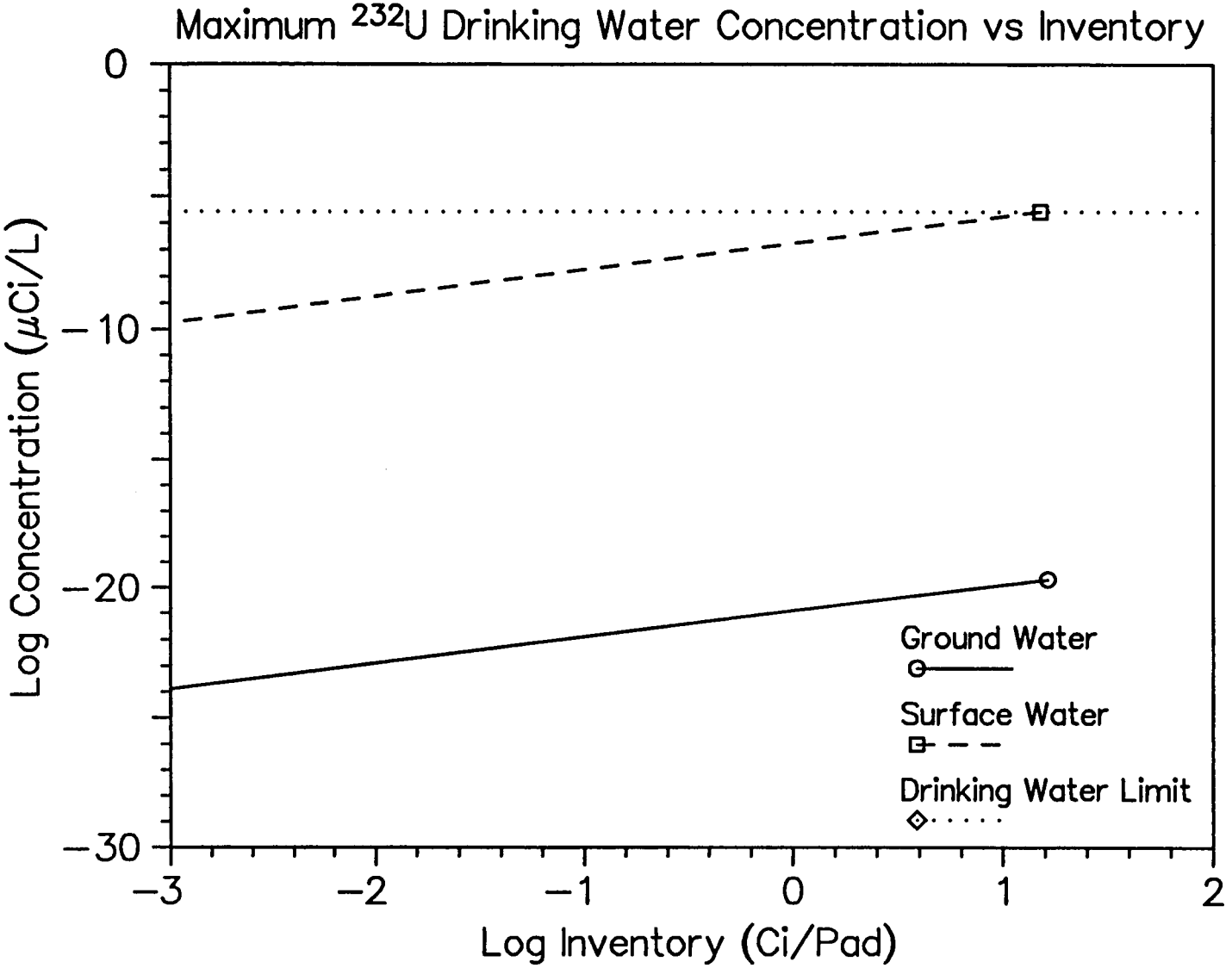

Fig. F.36. Maximum drinking water concentration as a function of CIIDF inventory for ^{232}U.

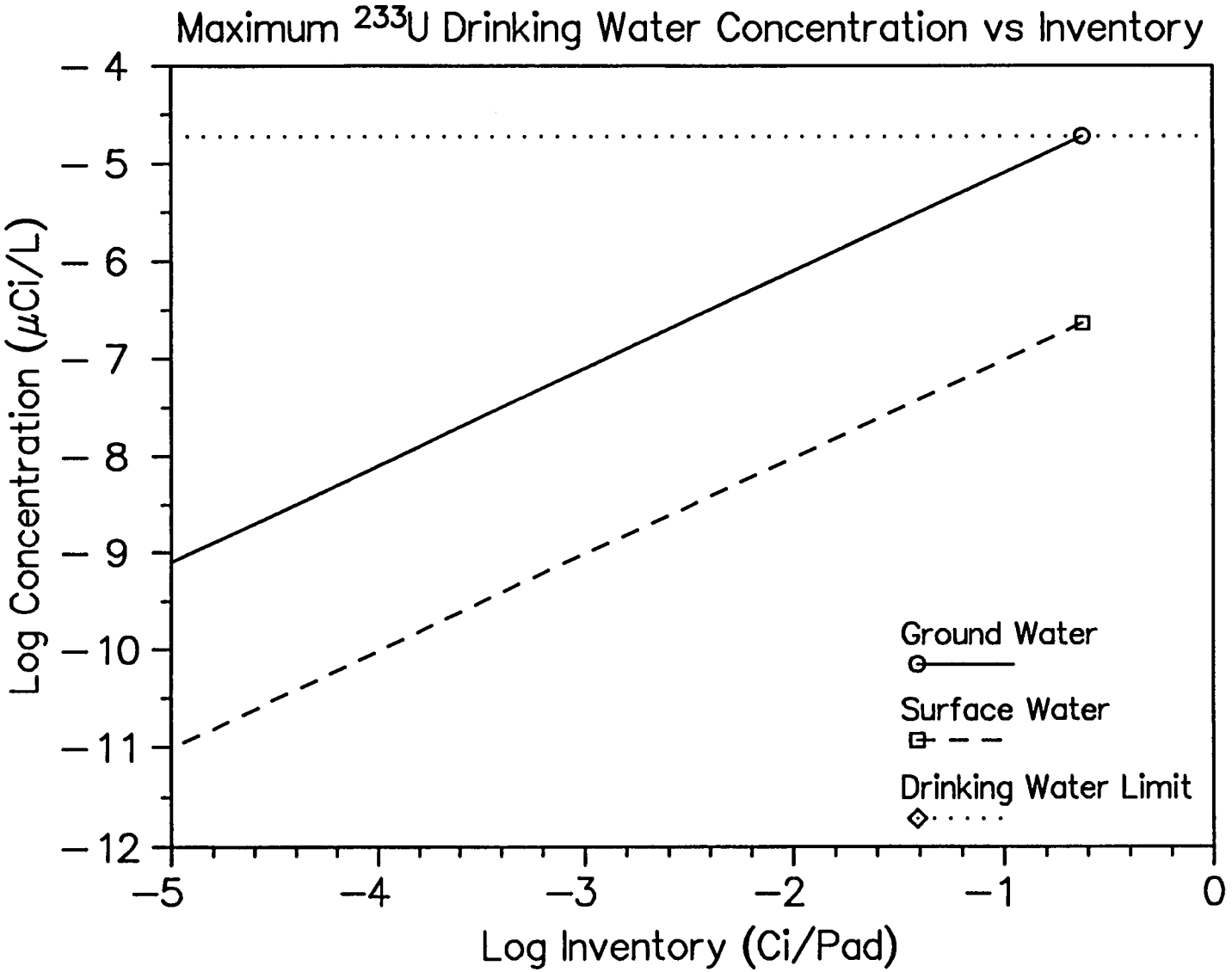

Fig. F.37. Maximum drinking water concentration as a function of CIIDF inventory for ^{233}U.

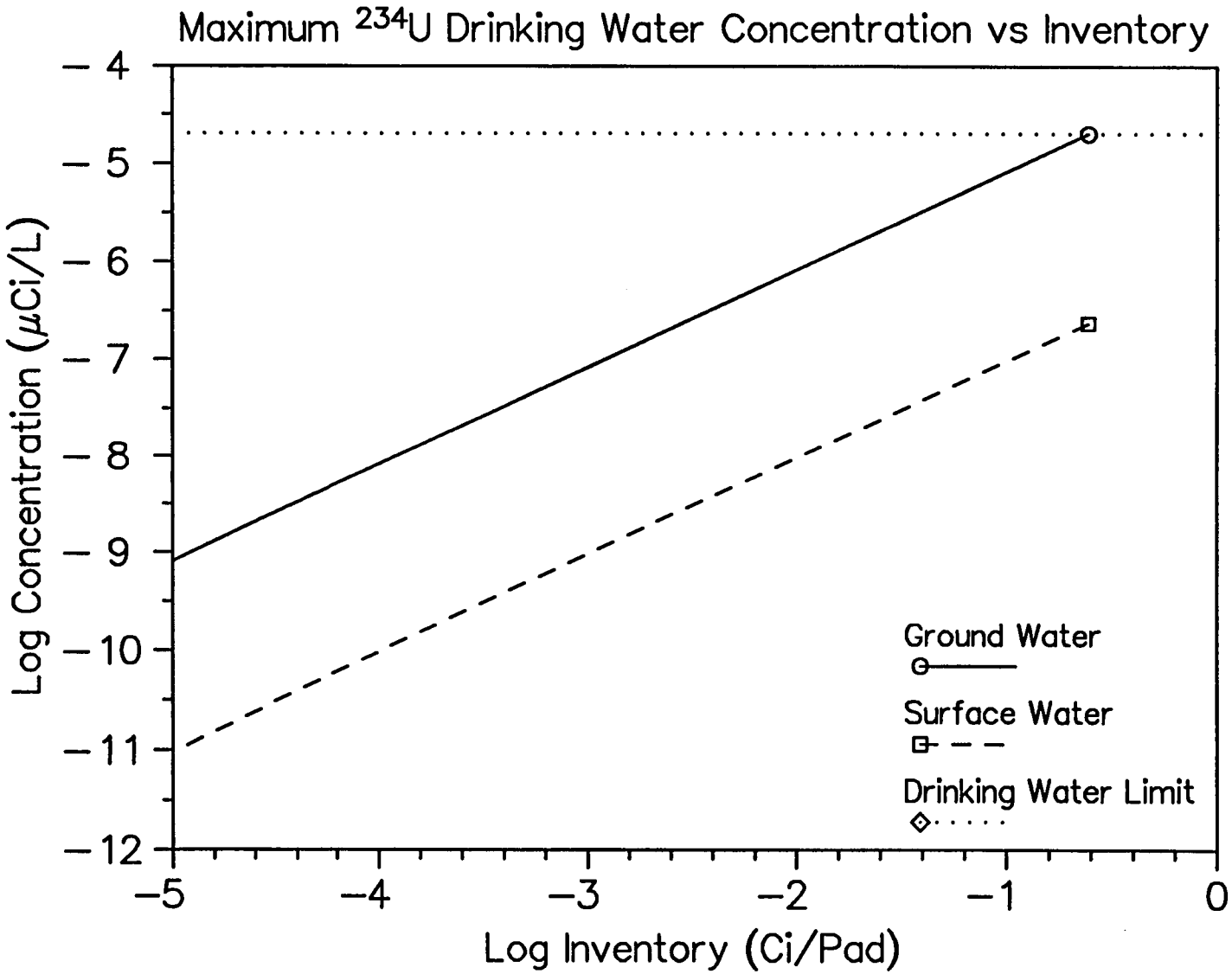

Fig. F.38. Maximum drinking water concentration as a function of CIIDF inventory for ^{234}U.

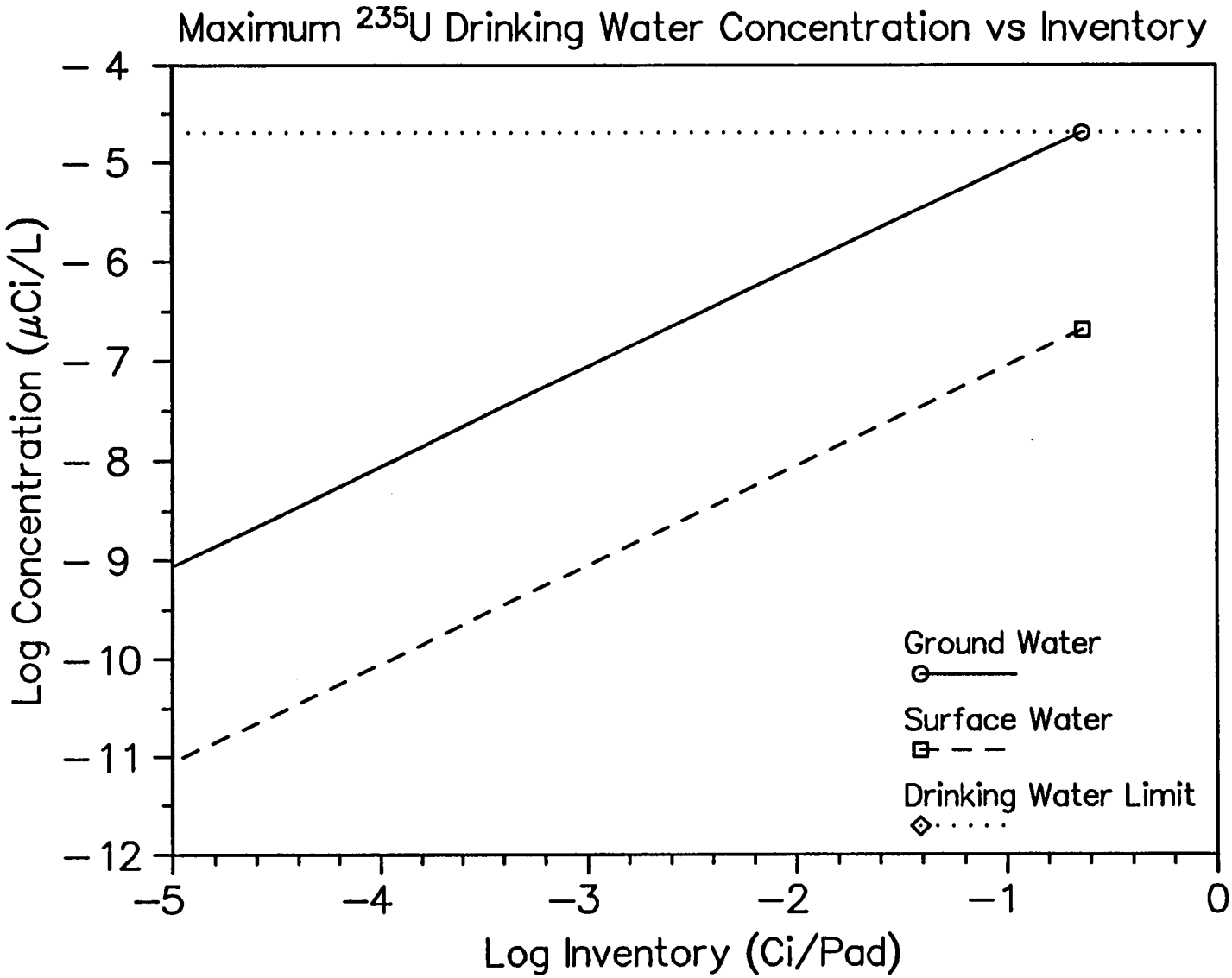

Fig. F.39. Maximum drinking water concentration as a function of CIIDF inventory for ^{235}U.

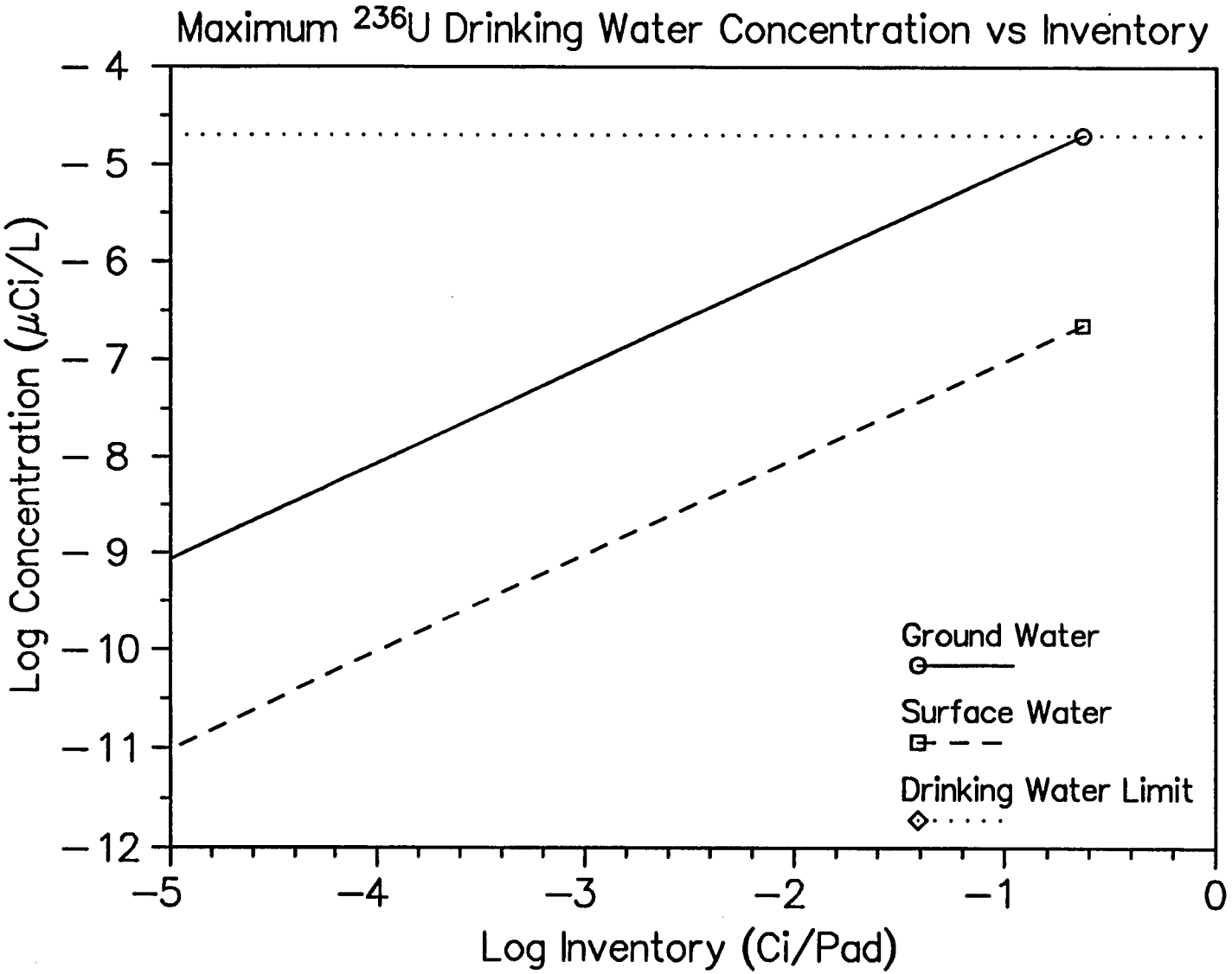

Fig. F.40. Maximum drinking water concentration as a function of CIIDF inventory for ^{236}U.

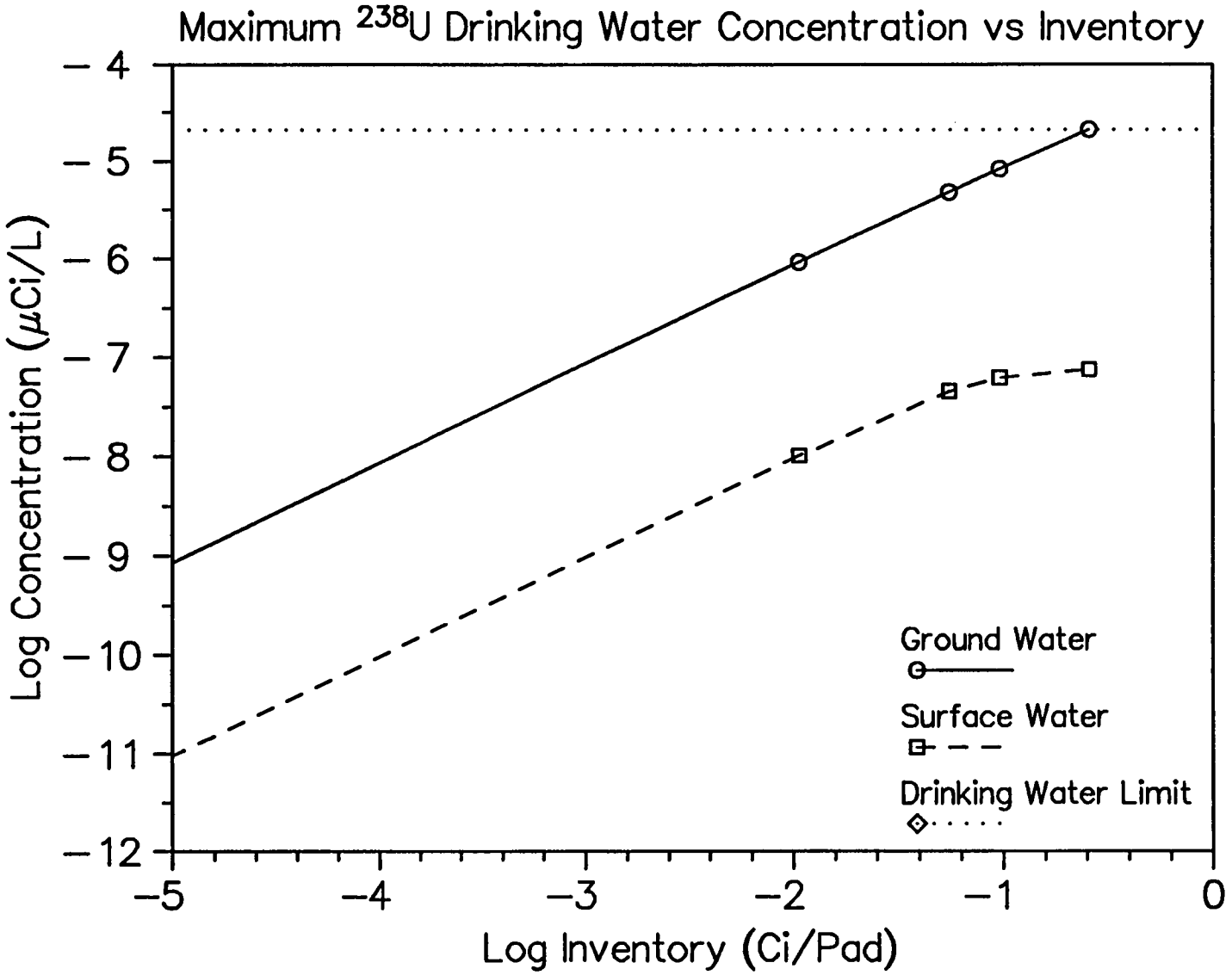

Fig. F.41. Maximum drinking water concentration as a function of CIIDF inventory for ^{238}U.

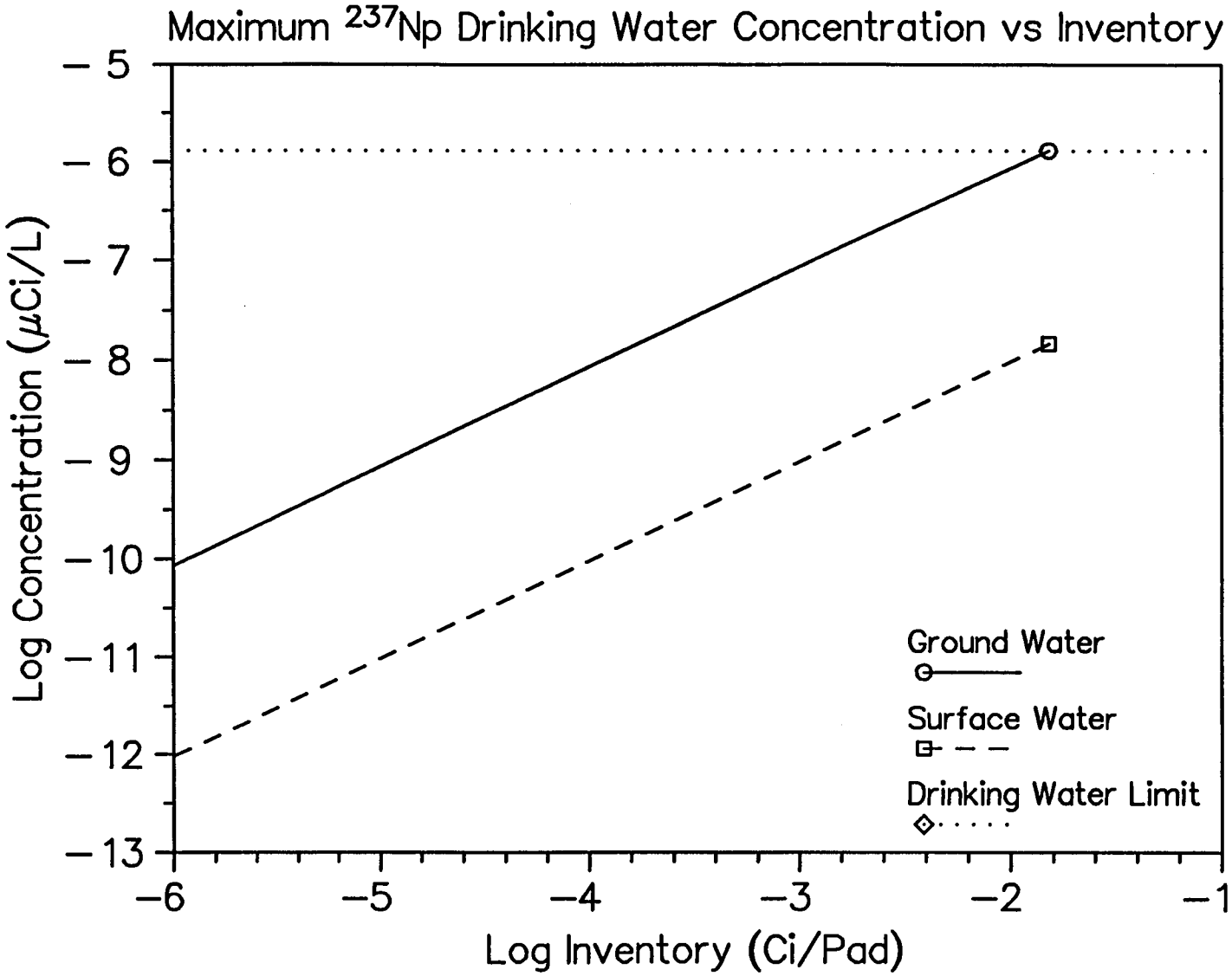

Fig. F.42. Maximum drinking water concentration as a function of CIIDF inventory for ^{237}Np.

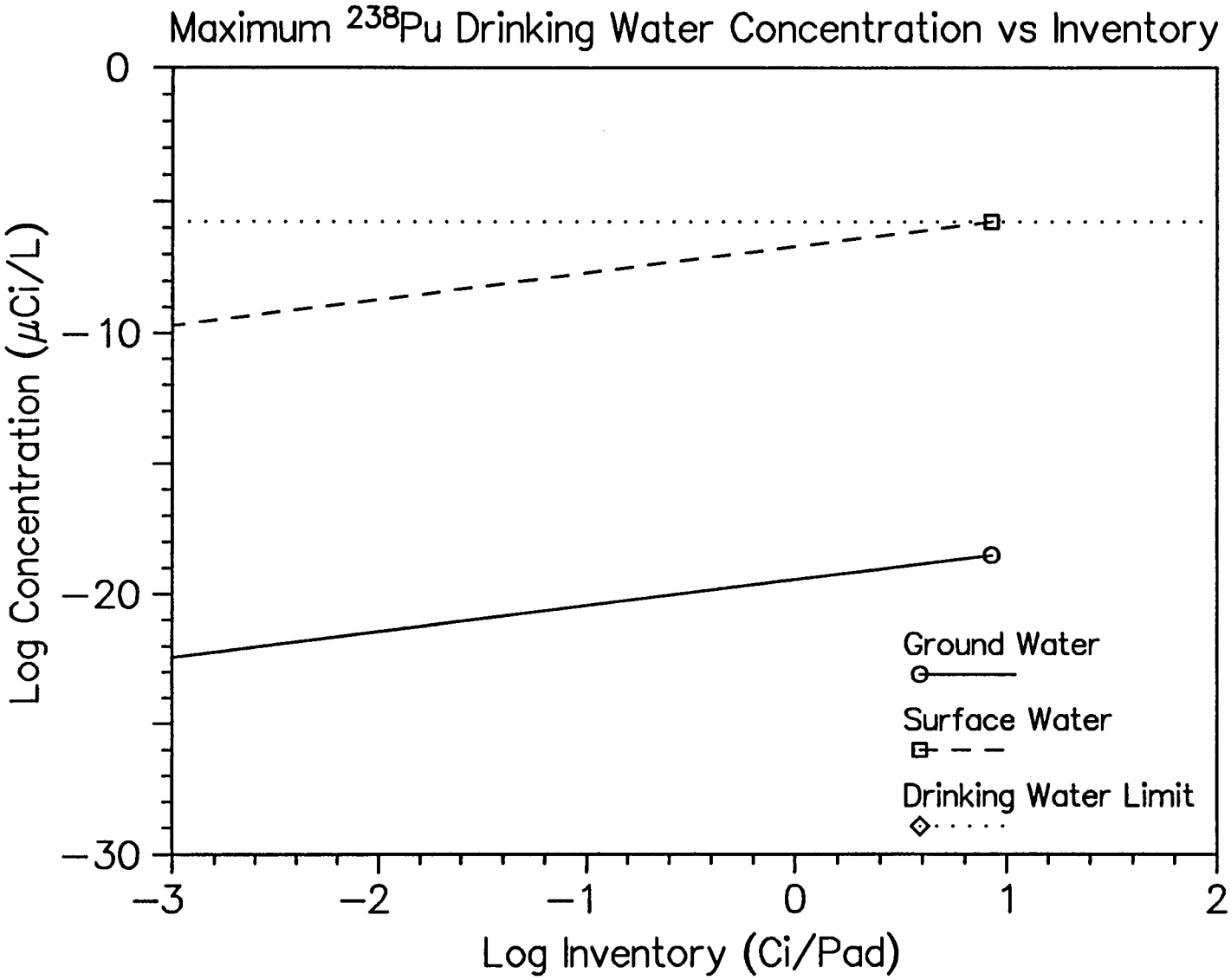

Fig. F.43. Maximum drinking water concentration as a function of CIIDF inventory for ^{238}Pu.

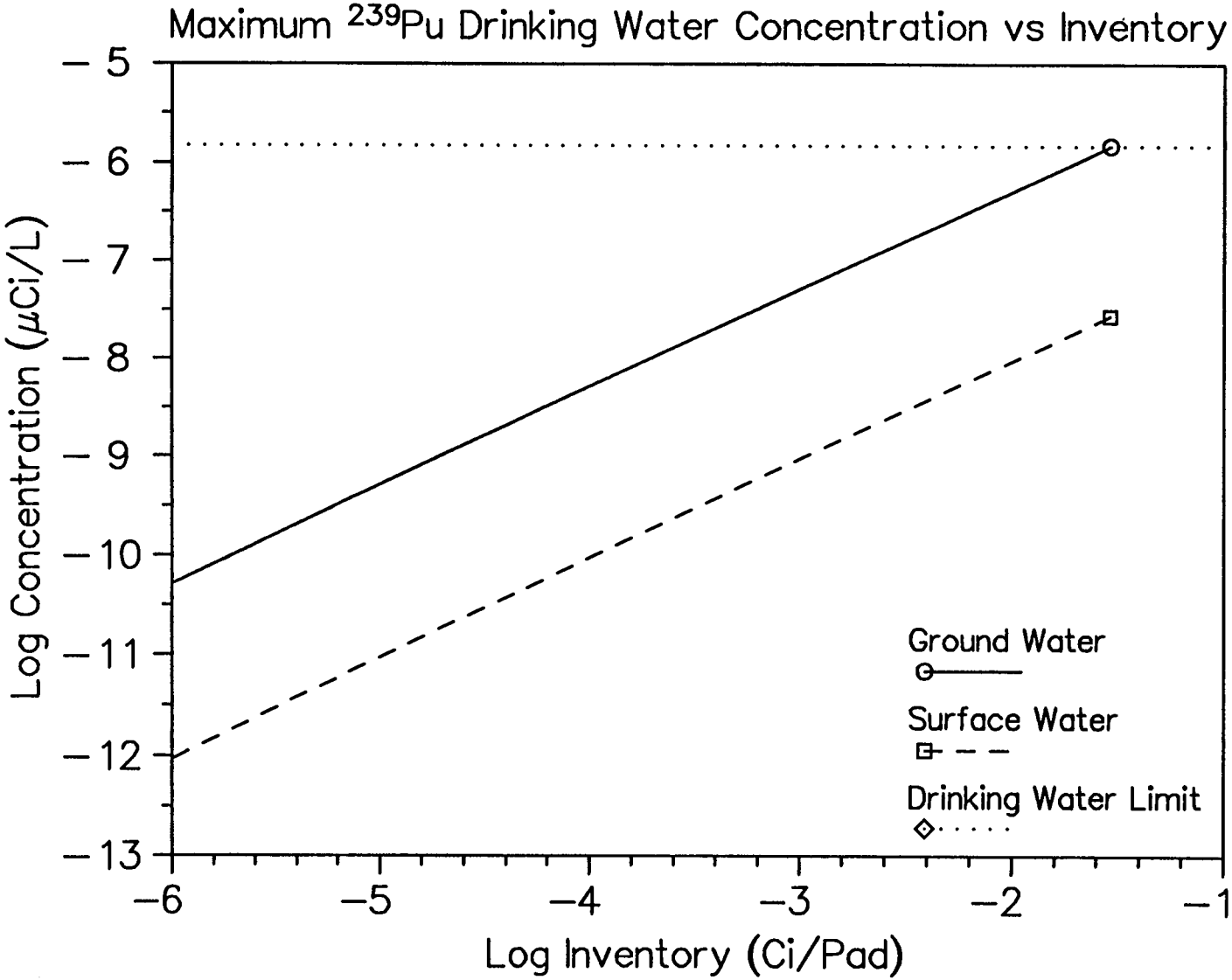

Fig. F.44. Maximum drinking water concentration as a function of CIIDF inventory for ^{239}Pu.

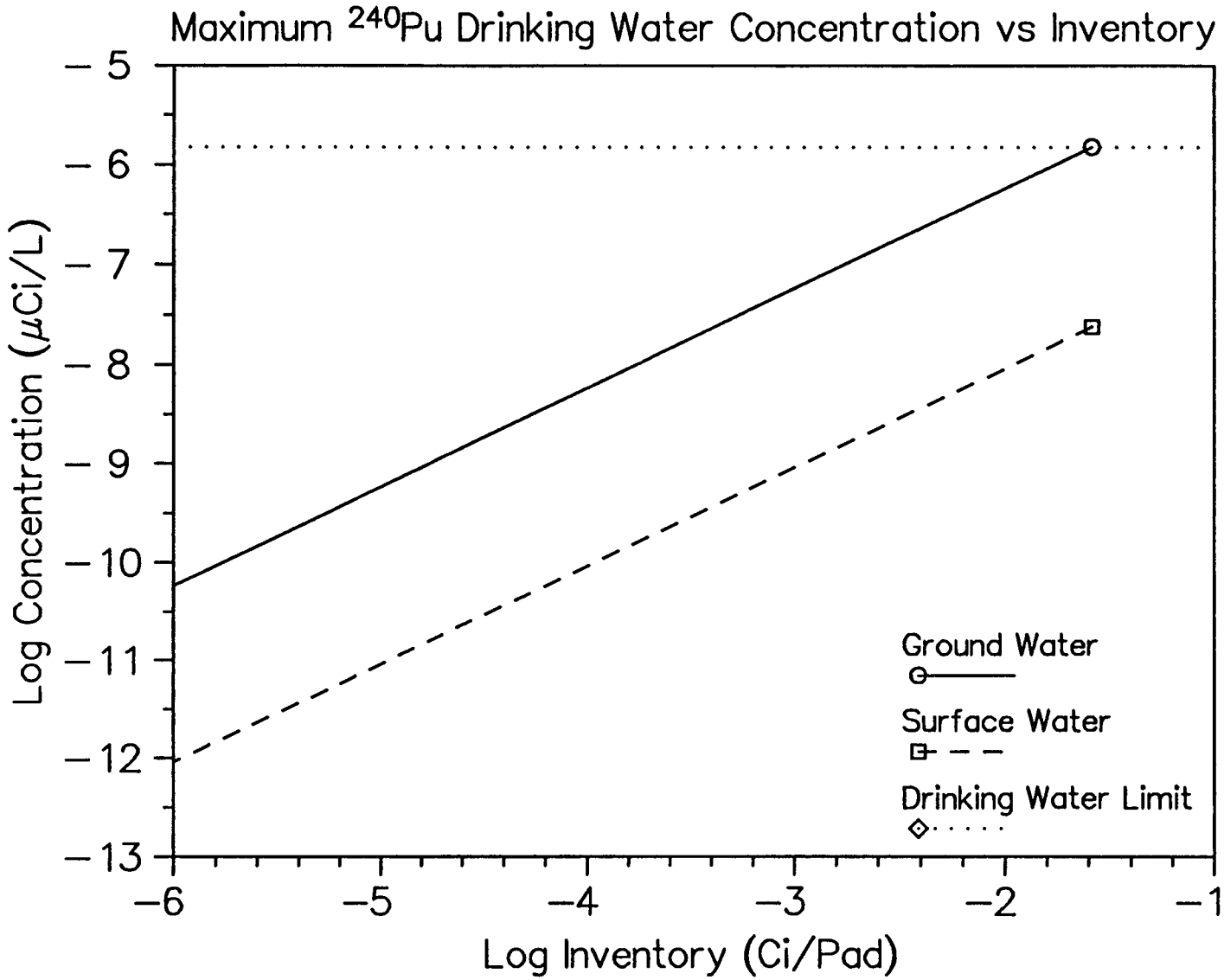

Fig. F.45. Maximum drinking water concentration as a function of CIIDF inventory for ^{240}Pu.

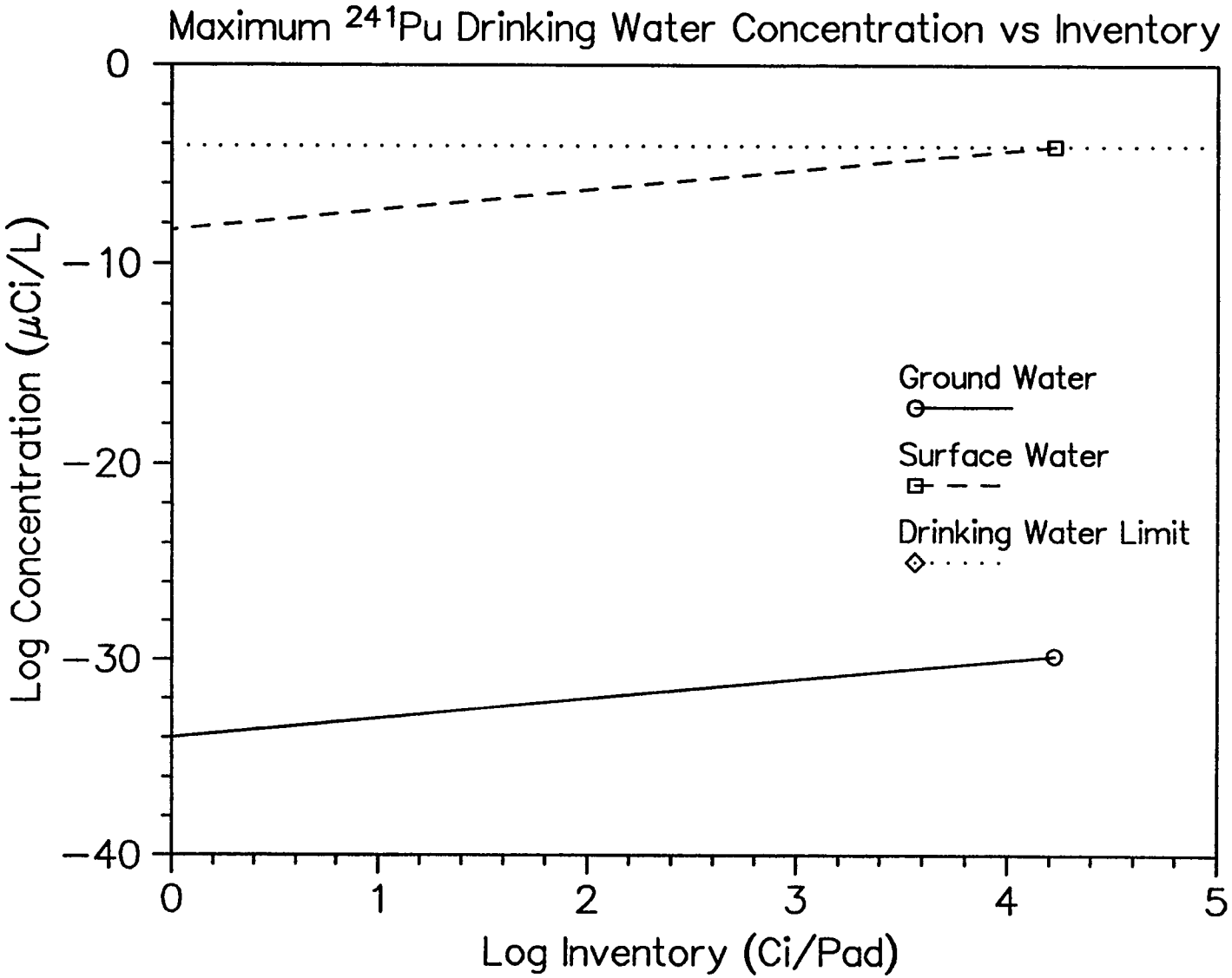

Fig. F.46. Maximum drinking water concentration as a function of CIIDF inventory for ^{241}Pu.

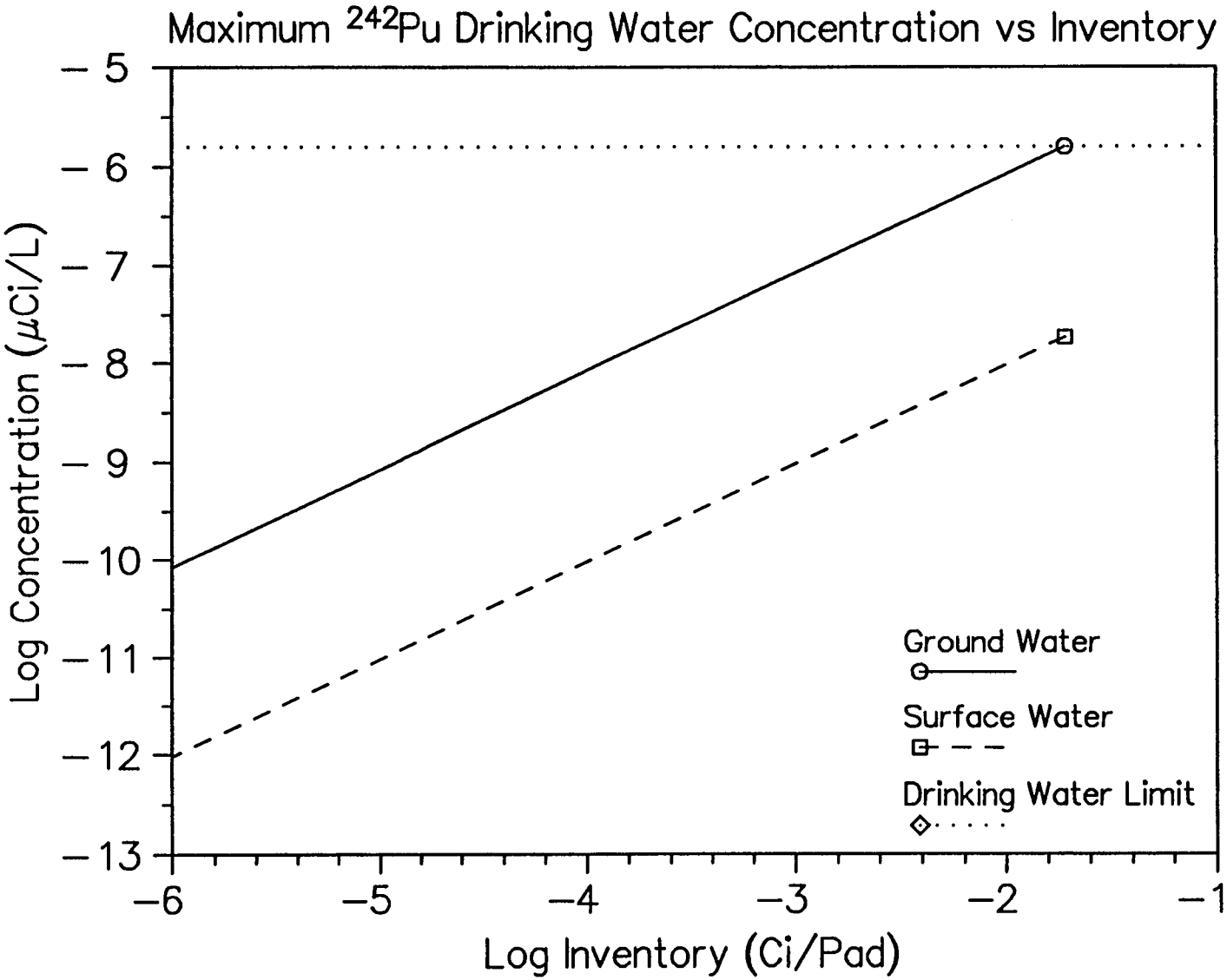

Fig. F.47. Maximum drinking water concentration as a function of CIIDF inventory for ^{242}Pu.

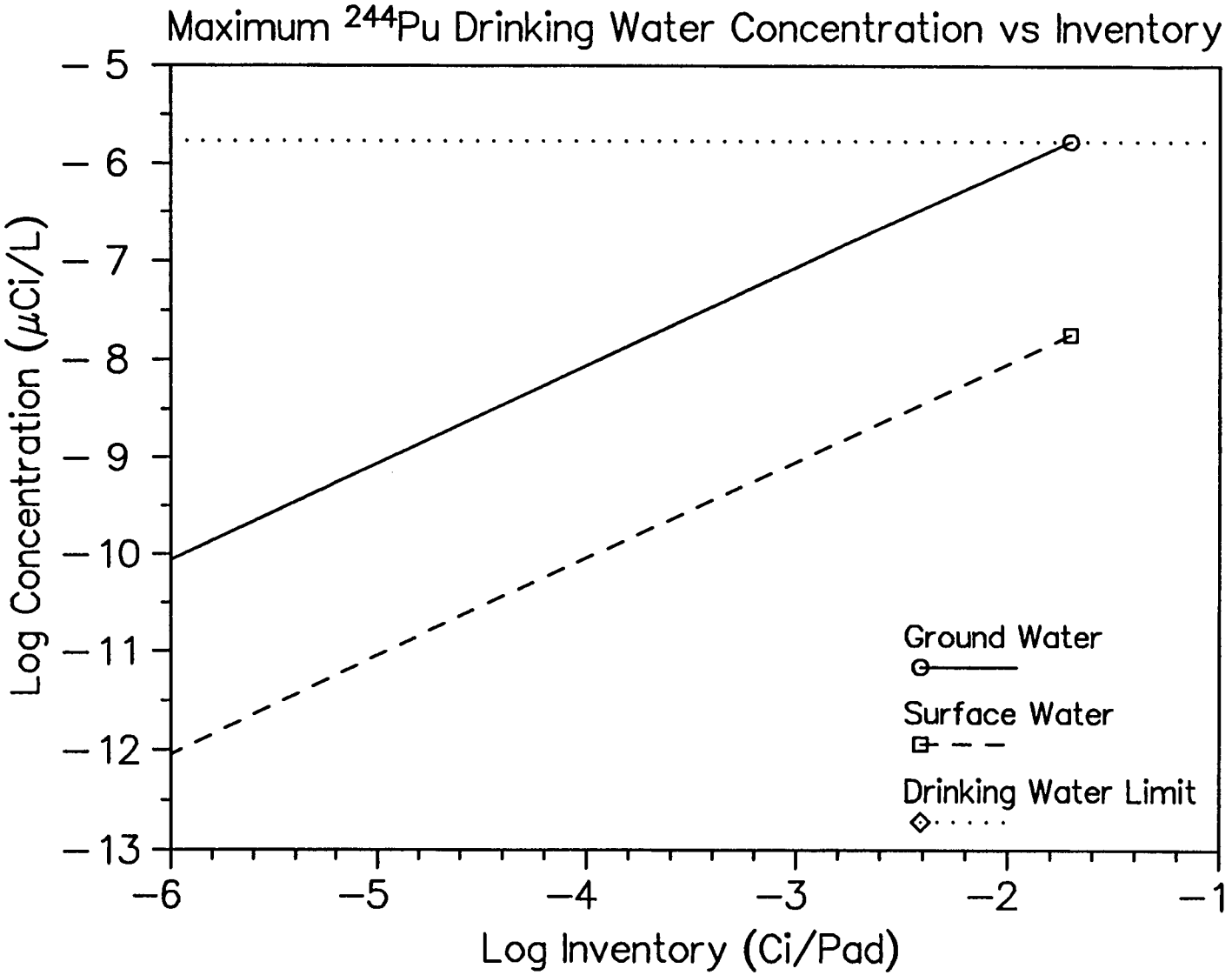

Fig. F.48. Maximum drinking water concentration as a function of CIIDF inventory for ^{244}Pu.

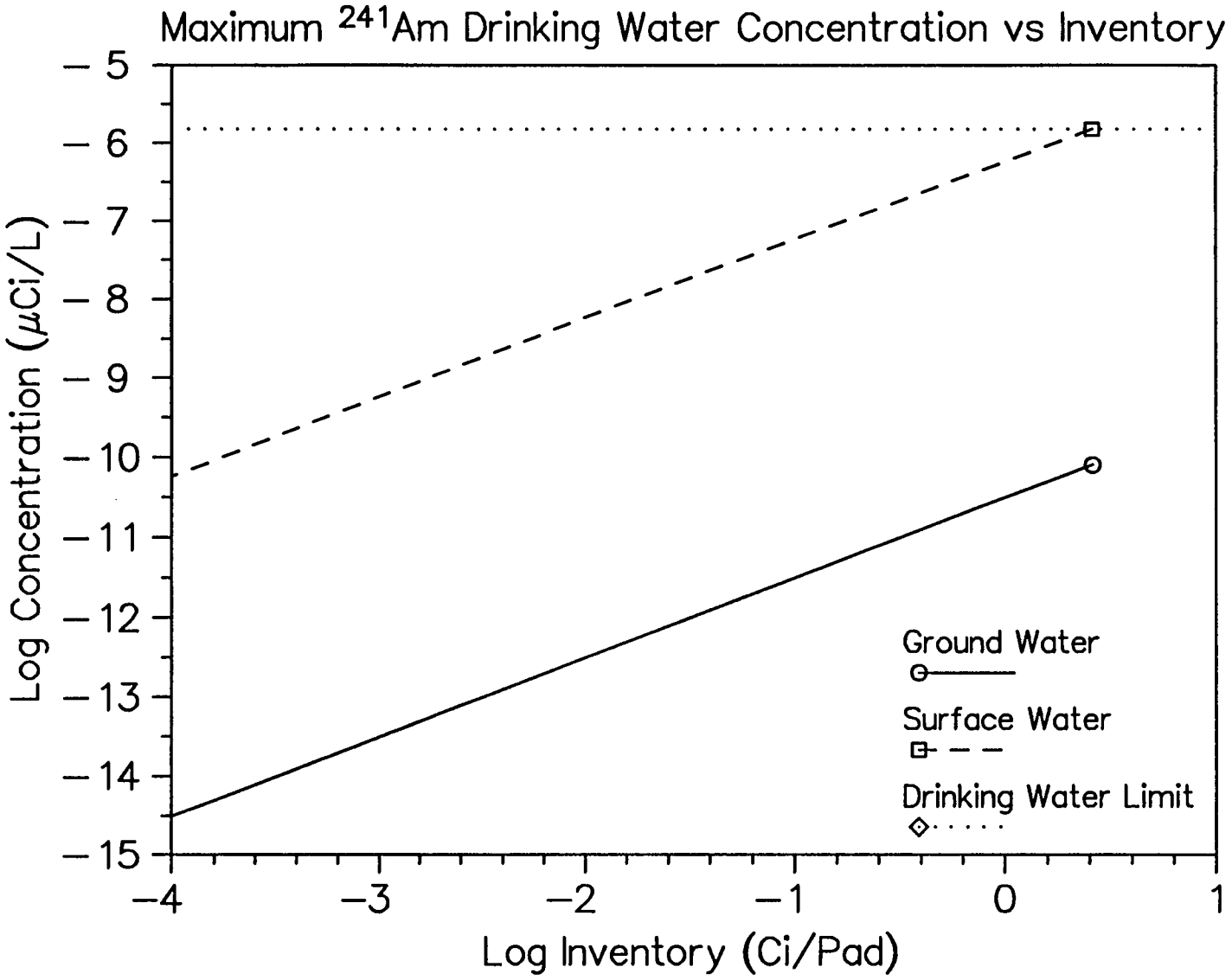

Fig. F.49. Maximum drinking water concentration as a function of CIIDF inventory for ^{241}Am.

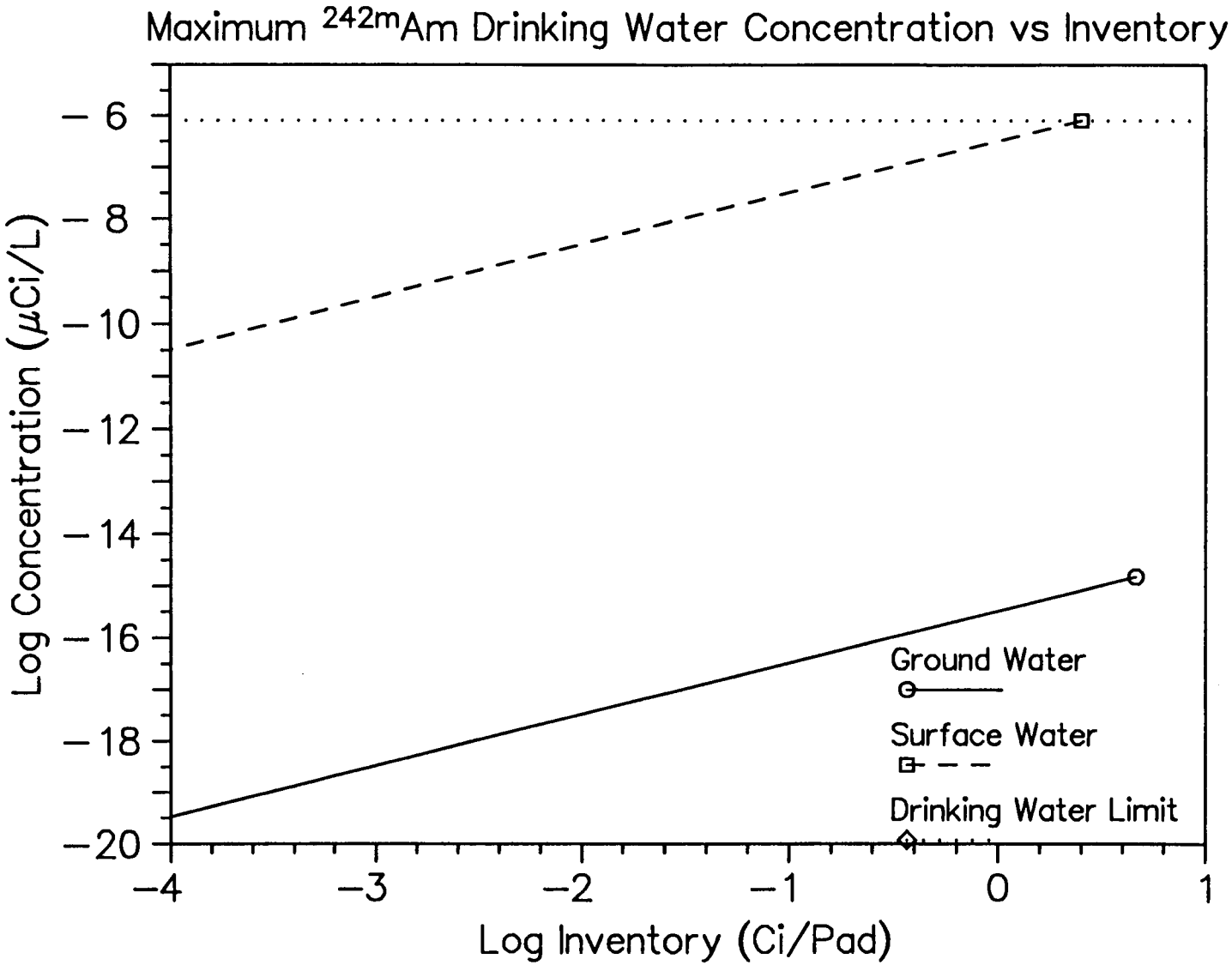

Fig. F.50. Maximum drinking water concentration as a function of CIIDF inventory for ^{242m}Am.

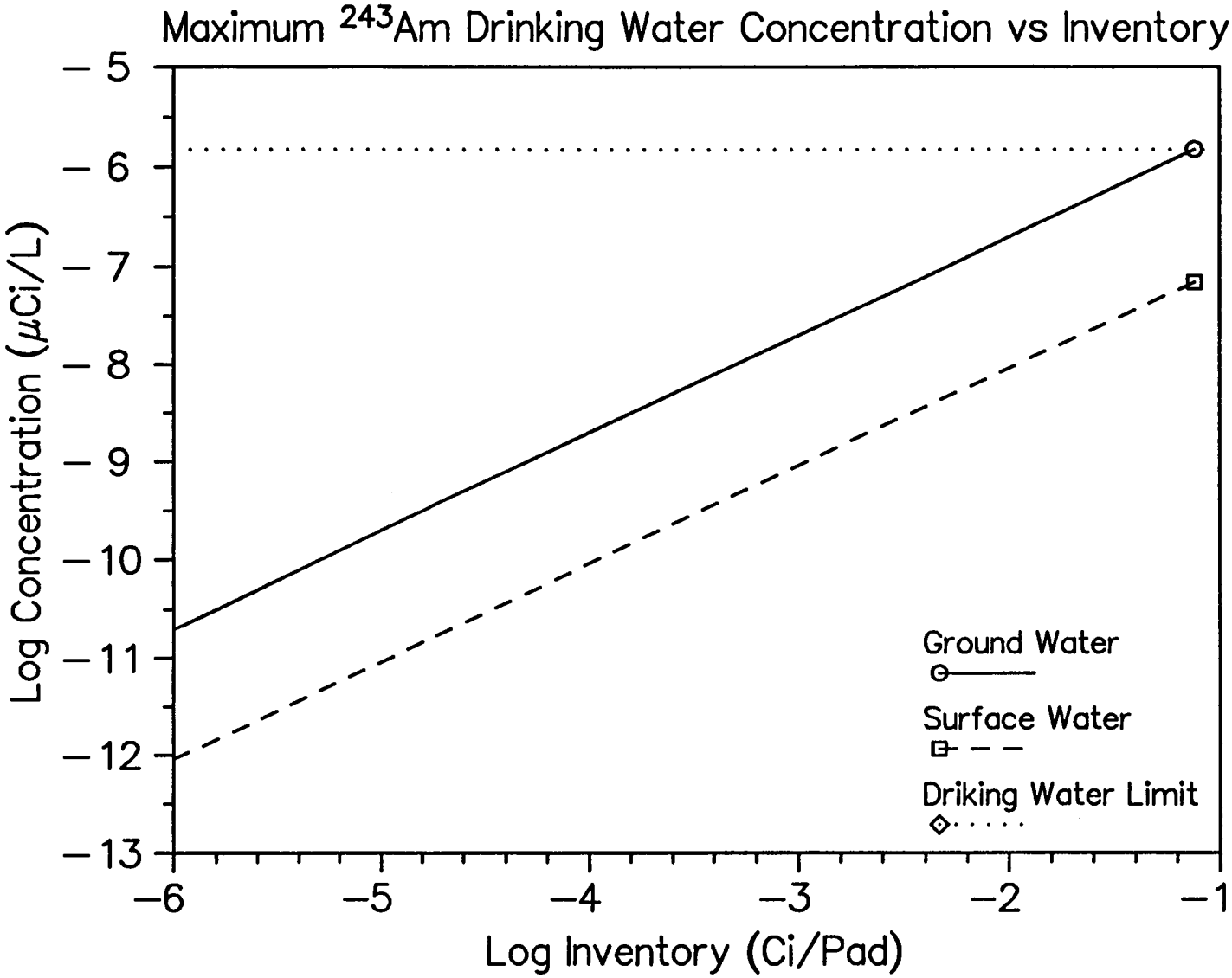

Fig. F.51. Maximum drinking water concentration as a function of CIIDF inventory for ^{243}Am.

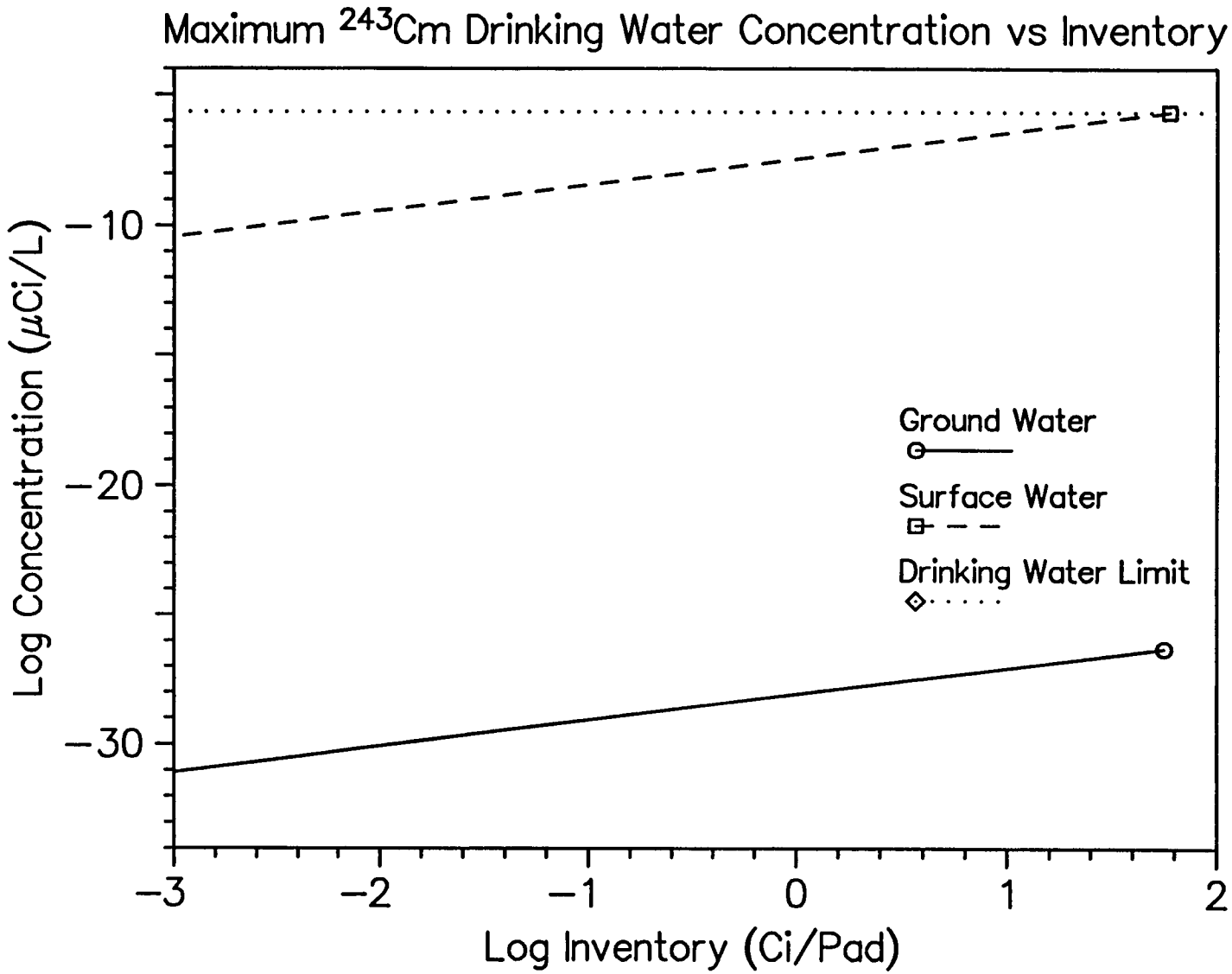

Fig. F.52. Maximum drinking water concentration as a function of CIIDF inventory for ^{243}Cm.

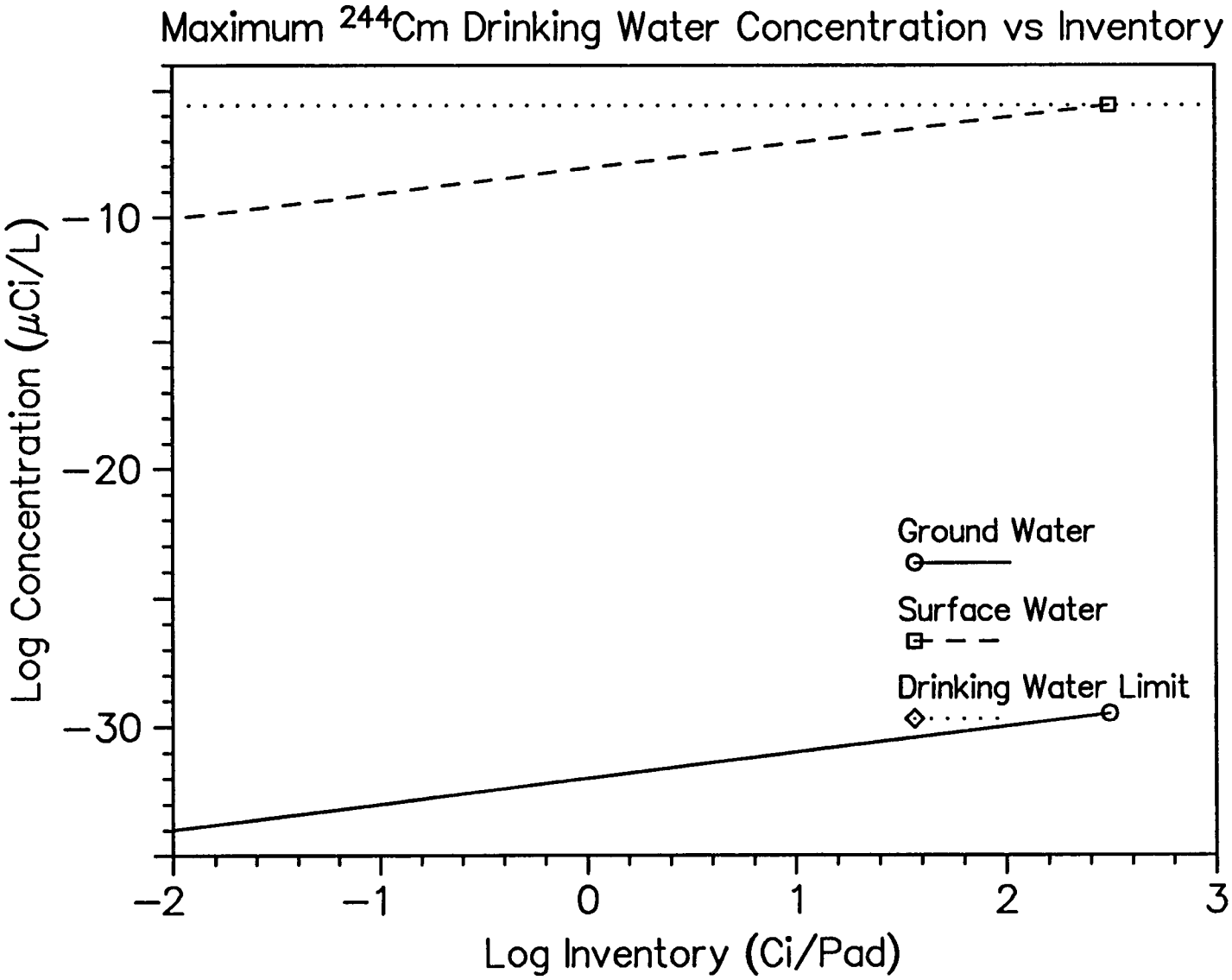

Fig. F.53. Maximum drinking water concentration as a function of CIIDF inventory for ^{244}Cm.

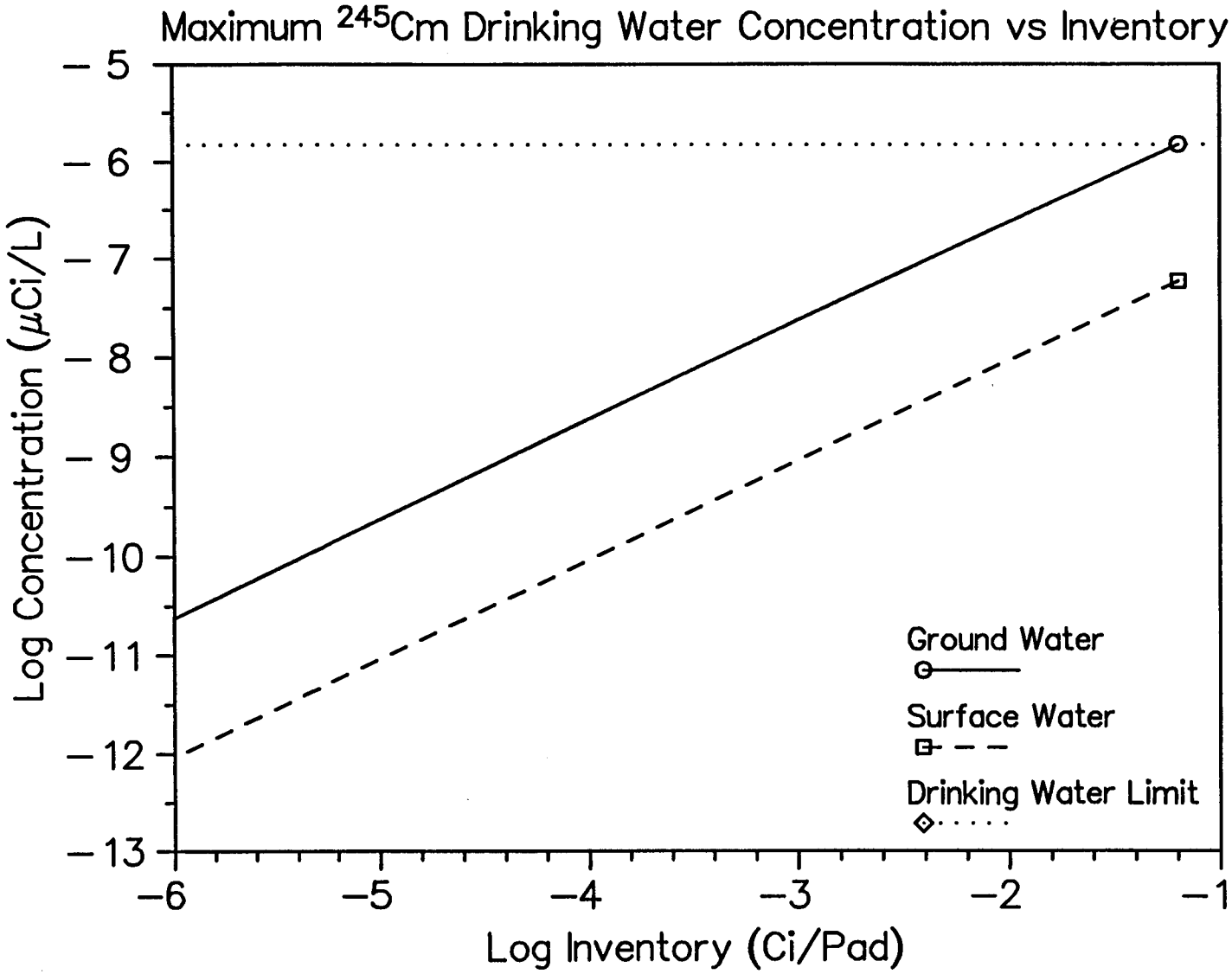

Fig. F.54. Maximum drinking water concentration as a function of CIIDF inventory for ^{245}Cm.

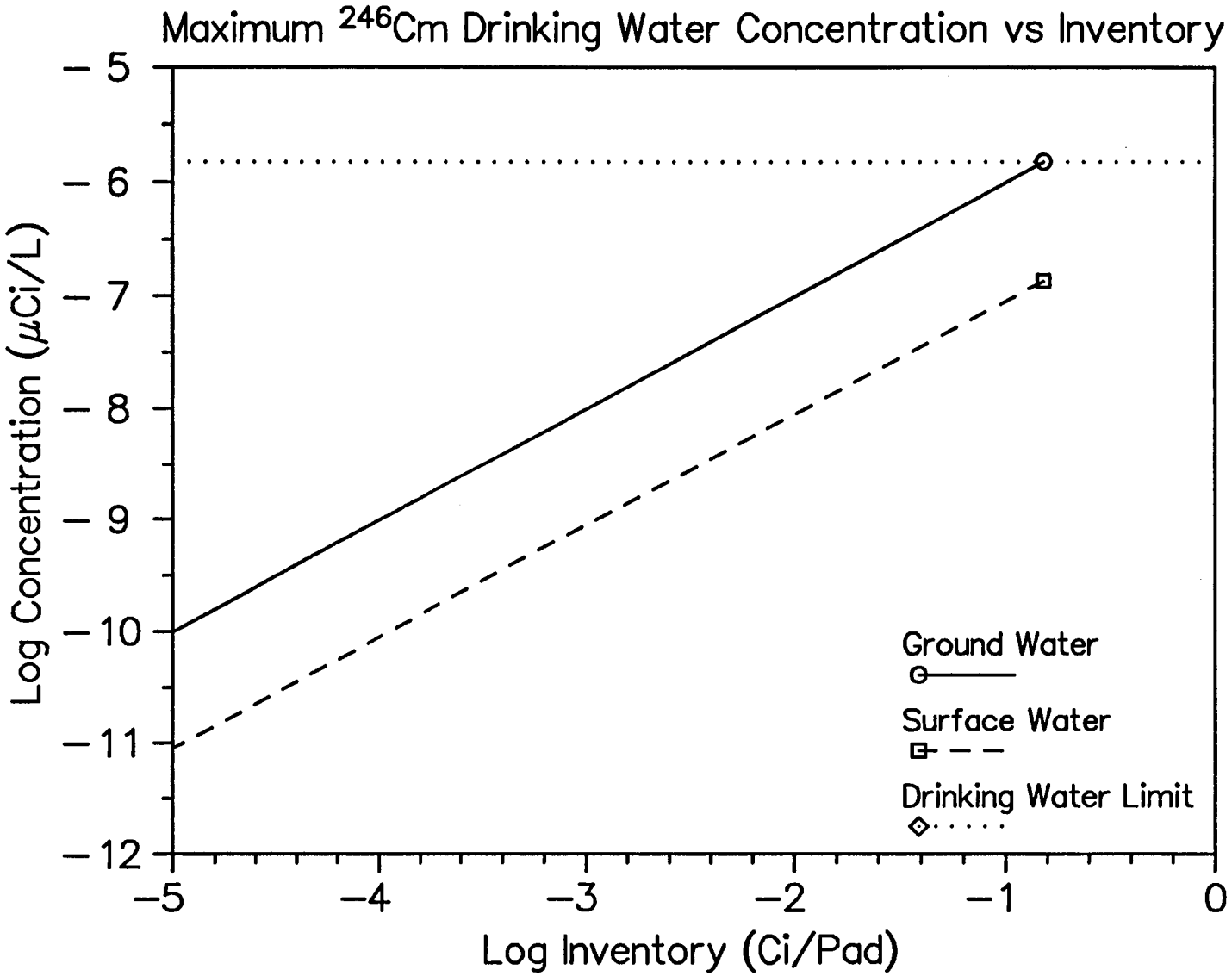

Fig. F.55. Maximum drinking water concentration as a function of CIIDF inventory for ^{246}Cm.

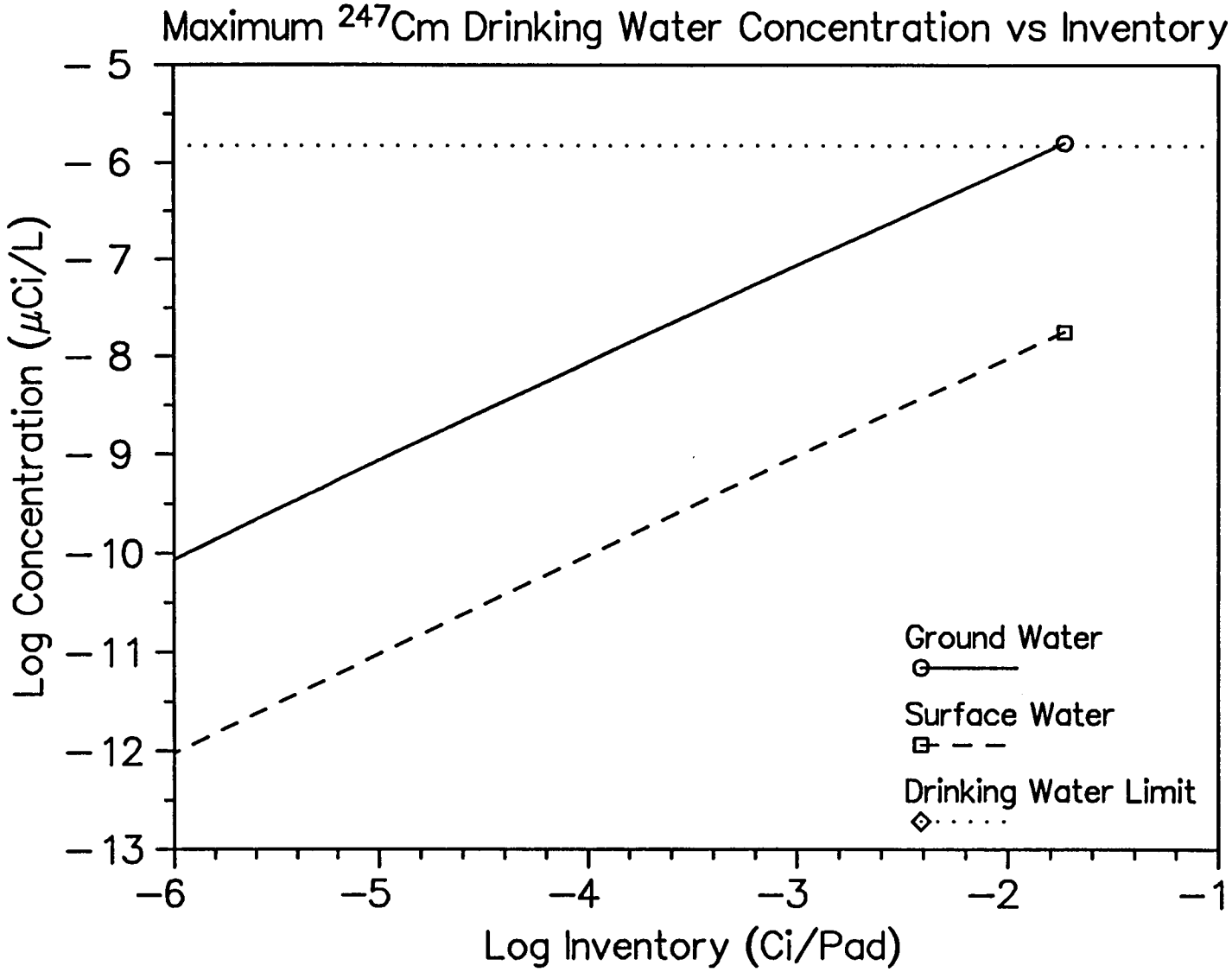

Fig. F.56. Maximum drinking water concentration as a function of CIIDF inventory for ^{247}Cm.

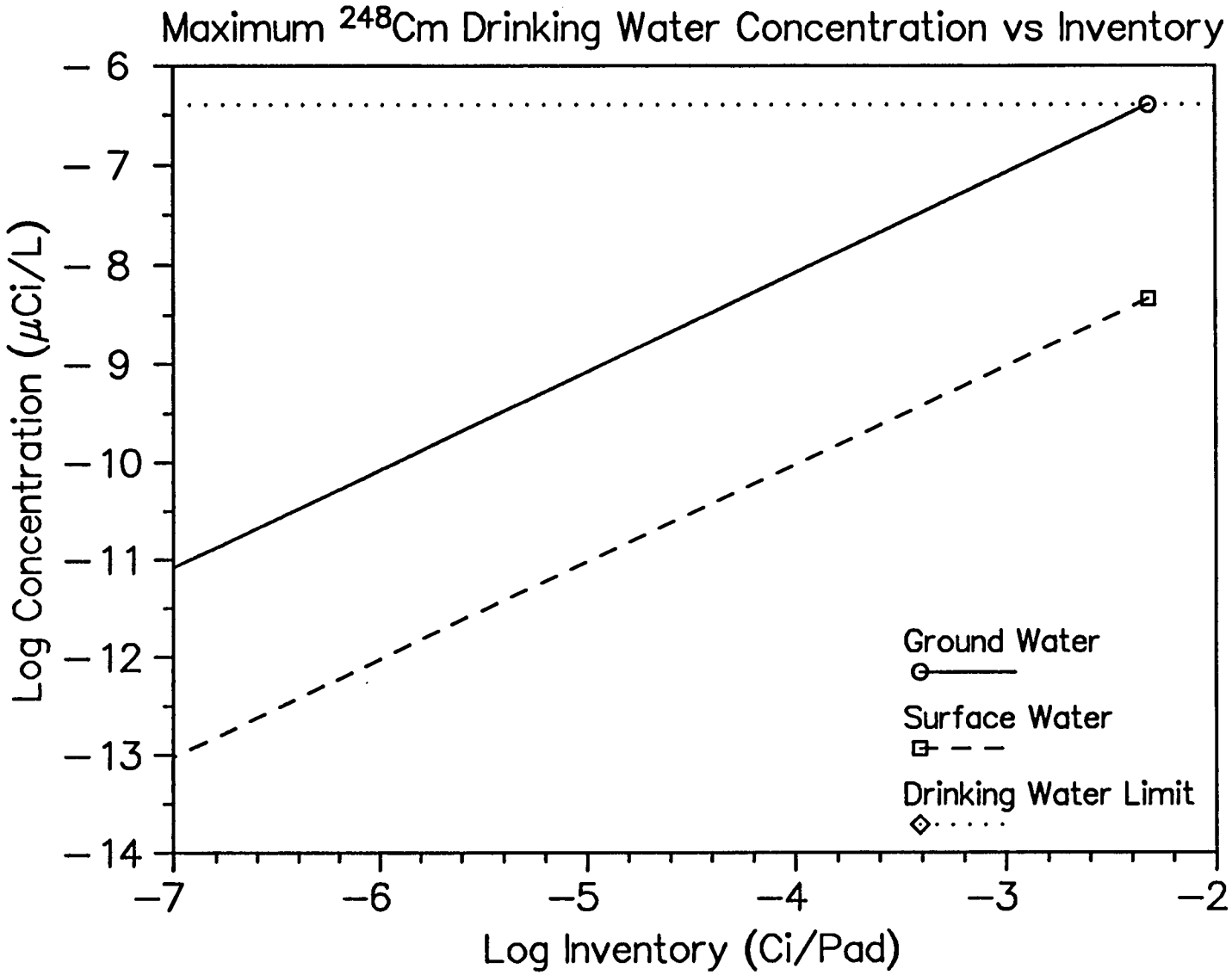

Fig. F.57. Maximum drinking water concentration as a function of CIIDF inventory for ^{248}Cm.

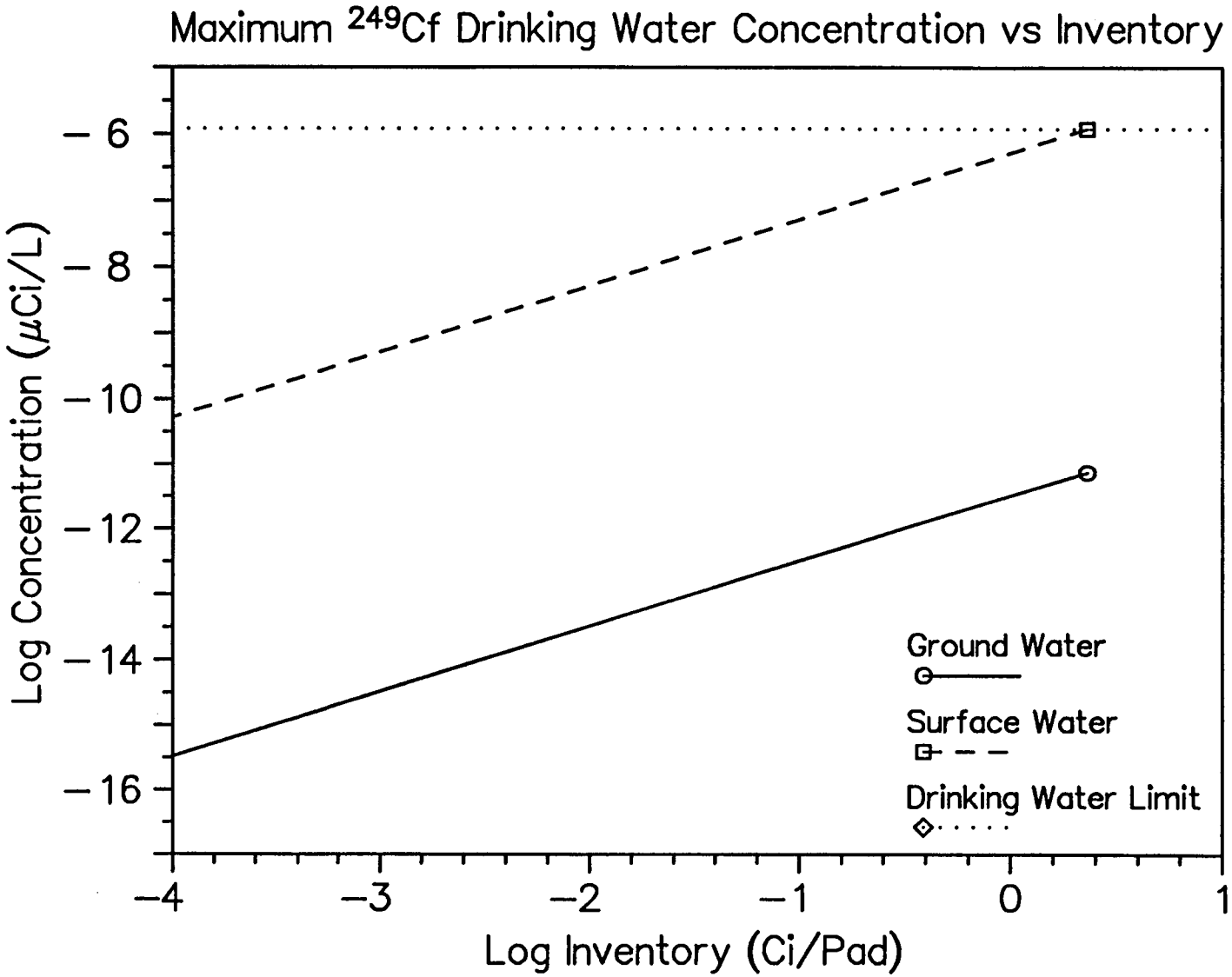

Fig. F.58. Maximum drinking water concentration as a function of CIIDF inventory for ^{249}Cf.

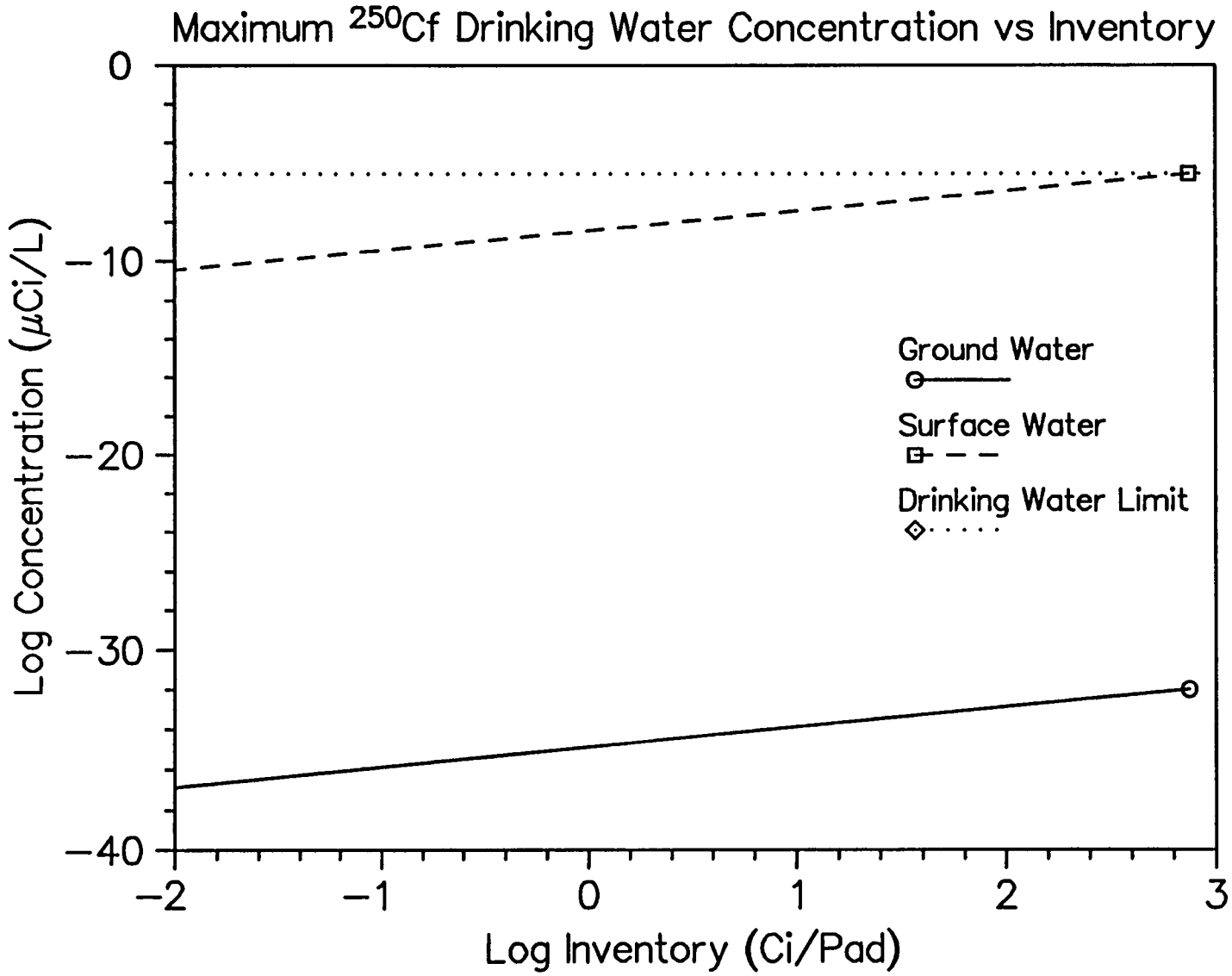

Fig. F.59. Maximum drinking water concentration as a function of CIIDF inventory for ^{250}Cf.

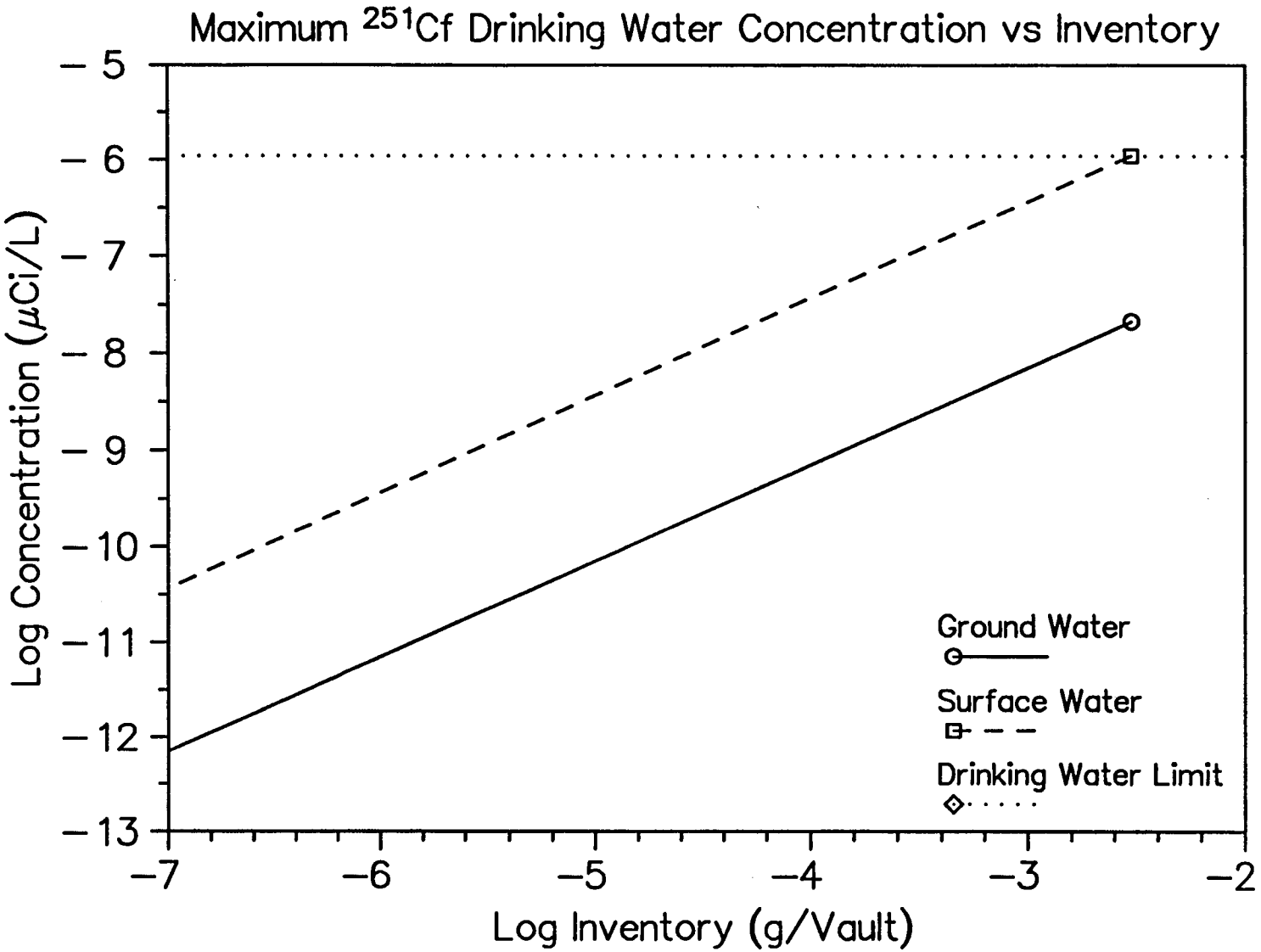

Fig. F.60. Maximum drinking water concentration as a function of CIIDF inventory for ^{251}Cf.

Appendix G

DOSE ANALYSIS FOR OFF-SITE INDIVIDUALS AND INADVERTENT INTRUDERS

D. C. Kocher

Appendix G

DOSE ANALYSIS FOR OFF-SITE INDIVIDUALS AND INADVERTENT INTRUDERS

G.1 INTRODUCTION

This appendix presents the models and data bases used in the performance assessment (PA) for the Class L-II Disposal Facility (CIIDF) to estimate radiation doses to individuals per unit concentration of radionuclides in the environment. Two groups of exposed individuals are considered:

- off-site individuals—members of the public who reside outside the boundary of the disposal facility, and
- inadvertent intruders—individuals who come onto the disposal site following loss of active institutional controls.

Off-site individuals may receive exposures from radionuclides that are transported beyond the facility boundary at any time after disposal. However, in accordance with current Department of Energy policy (DOE Order 5820.2A), inadvertent intrusion onto the disposal site is assumed to be precluded by active institutional controls for 100 years after disposal.

The PA for low-level waste (LLW) disposal in CIIDF assumes that transport in water is the principal pathway for removal of radionuclides from the disposal facility into the environment (see Sect. 3.2.1). Thus, for off-site individuals, only exposures to contaminated groundwater or surface water are evaluated.

The dose analysis for inadvertent intruders considers exposure scenarios involving direct intrusion into solid waste in the disposal facility, and three different scenarios involving direct intrusion are evaluated. Exposure of inadvertent intruders to contaminated groundwater obtained from a source within the facility boundary is not evaluated, because the performance objective limiting concentrations of radionuclides in groundwater beyond the facility boundary [i.e., a limit on effective dose equivalent (EDE) for the drinking water pathway of 4 mrem per year] is sufficiently restrictive that doses to inadvertent intruders from use of groundwater on the disposal site could be only a small fraction of the performance objective for protection of inadvertent intruders from all exposure pathways (i.e., a limit on effective dose equivalent of 100 mrem per year). Furthermore, the maximum predicted doses from use of contaminated groundwater on the disposal site would occur at different times than the maximum doses from direct intrusion into the disposal facility. There are no surface waters within the boundary of the disposal facility that could be used as a water supply by an inadvertent intruder.

The following sections discuss the assumed exposure scenarios and exposure pathways for off-site individuals or inadvertent intruders and the models and parameter values used in calculating doses for each exposure scenario and pathway. For exposures of off-site individuals to contaminated groundwater or surface water, the results of the dose analyses are presented in the form of annual EDEs per unit concentration of radionuclides in water. For exposures of inadvertent intruders resulting from direct intrusion into the disposal facility, the results are presented in the form of annual EDEs per unit concentration of radionuclides in the facility.

G.2 RADIONUCLIDES CONSIDERED IN DOSE ANALYSIS

The radionuclides considered in the dose analysis for off-site individuals or inadvertent intruders are listed in Table G.1. The choice of radionuclides to be analyzed was based on the following considerations.

First, the half-life of the radionuclide should be about 5 years or greater. Given the expected performance of the engineered barriers in the disposal facility and the assumption that active institutional controls will be maintained for 100 years after closure of the facility (DOE Order 5820.2A), radionuclides with half-lives less than about 5 years should decay to innocuous levels before significant transport into the environment beyond the 100-m buffer zone around the disposal facility or inadvertent intrusion into the facility could occur.

Second, the radionuclide should arise from operations of the nuclear fuel cycle or the production of nuclear weapons, including production in nuclear fission or by neutron activation of materials that would be present in reactors, because these are likely to be the most important sources of radionuclides in wastes on the Oak Ridge Reservation (ORR). However, if additional radionuclides from other sources or processes are found to be present in wastes intended for disposal, they can easily be included in the analysis.

Third, a few additional radionuclides have been included in the analysis based on records of past disposals on ORR; e.g., see Appendix A of the PA report for the Solid Waste Storage Area (SWSA) 6 disposal facility (ORNL 1994).

Table G.1. Radionuclides considered in dose analysis for off-site individuals and inadvertent intruders

Nuclide[a]	Half-life[b]	Nuclide	Half-life
^{3}H	12.28 y	^{137}Cs	30.17 y
^{10}Be	1.6×10^{6} y	^{137m}Ba (0.946)	2.552 m
^{14}C	5730 y	^{151}Sm	90 y
^{26}Al	7.2×10^{5} y	^{152}Eu	13.6 y
^{36}Cl	3.01×10^{5} y	^{154}Eu	8.8 y
^{40}K	1.277×10^{9} y	^{155}Eu	4.96 y
^{41}Ca	1.03×10^{5} y	^{207}Bi	33.4 y
^{60}Co	5.271 y	^{210}Pb	22.26 y
^{59}Ni	7.5×10^{4} y	^{210}Po (1.0)	138.378 d
^{63}Ni	100.1 y	^{226}Ra	1600 y
^{79}Se	6.5×10^{4} y	^{222}Rn (1.0)	3.8235 d
^{87}Rb	4.73×10^{10} y	^{214}Pb (1.0)	26.8 m
^{90}Sr	28.6 y	^{214}Bi (1.0)	19.9 m
^{90}Y (1.0)	64.1 h	^{229}Th	7.34×10^{3} y
^{93}Zr	1.53×10^{6} y	^{225}Ra (1.0)	14.8 d
^{93m}Nb	14.6 y	^{225}Ac (1.0)	10.0 d
^{94}Nb	2.03×10^{4} y	^{221}Fr (1.0)	4.8 m
^{99}Tc	2.13×10^{5} y	^{213}Bi	45.65 m
^{107}Pd	6.5×10^{6} y	^{209}Tl (0.0216)	2.20 m
^{113m}Cd	13.7 y	^{230}Th	7.7×10^{4} y
^{121m}Sn	55 y	^{232}Th	1.405×10^{10} y
^{126}Sn	1.0×10^{5} y	^{228}Ra (1.0)	5.75 y
^{126m}Sb (1.0)	19.0 m	^{228}Ac (1.0)	6.13 h
^{126}Sb (0.14)	12.4 d	^{228}Th (1.0)	1.9132 y
^{129}I	1.57×10^{7} y	^{224}Ra (1.0)	3.62 d
^{135}Cs	2.3×10^{6} y	^{220}Rn (1.0)	55.61 s

Table G.1 (continued)

Nuclide[a]	Half-life[b]	Nuclide	Half-life
^{232}Th (continued)		^{239}Pu	24131 y
^{212}Pb (1.0)	10.643 h	^{240}Pu	6569 y
^{212}Bi (1.0)	60.55 m	^{241}Pu	14.4 y
^{208}Tl (0.3593)	3.053 m	^{242}Pu	3.758×10^5 y
^{231}Pa	3.276×10^4 y	^{244}Pu	8.26×10^7 y
^{227}Ac (1.0)	21.773 y	^{240m}Np (1.0)	7.4 m
^{227}Th (0.9862)	18.718 d	^{241}Am	432.2 y
^{223}Ra (1.0)	11.434 d	^{242m}Am	152 y
^{211}Pb (1.0)	36.1 m	^{242}Am (0.99524)	16.02 h
^{211}Bi (1.0)	2.13 m	^{242}Cm (0.823)	163.2 d
^{207}Tl (0.99727)	4.77 m	^{238}Np (0.00476)	2.117 d
^{232}U[c]	72 y	^{243}Am	7380 y
^{233}U	1.5952×10^5 y	^{239}Np (1.0)	2.355 d
^{234}U	2.445×10^5 y	^{243}Cm	28.5 y
^{235}U	7.038×10^8 y	^{244}Cm	18.11 y
^{231}Th (1.0)	25.52 h	^{245}Cm	8.5×10^3 y
^{236}U	2.3415×10^7 y	^{246}Cm	4.75×10^3 y
^{238}U	4.468×10^9 y	^{247}Cm	1.56×10^7 y
^{234}Th (1.0)	24.10 d	^{243}Pu (1.0)	4.956 h
^{234m}Pa (1.0)	1.17 m	^{248}Cm	3.39×10^5 y
^{234}Pa (0.0016)	6.70 h	^{249}Cf	350.6 y
^{237}Np	2.14×10^6 y	^{250}Cf	13.08 y
^{233}Pa (1.0)	27.0 d	^{251}Cf	900 y
^{238}Pu	87.85 y		

[a]Indented entries are radiologically significant decay products of parent radionuclide listed. For each decay product, branching fraction in decay of parent radionuclide is given in parentheses.

[b]Values from Kocher (1981). Units are y = years, d = days, m = minutes, s = seconds.

[c]Entries for ^{228}Th, ^{224}Ra, ^{220}Rn, ^{212}Pb, ^{212}Bi, and ^{208}Tl decay products are listed following ^{232}Th.

G.3 ASSUMED EXPOSURE SCENARIOS AND EXPOSURE PATHWAYS

This section describes the exposure scenarios and exposure pathways assumed in the dose analyses for off-site individuals and inadvertent intruders. The model equations and parameter values for each exposure pathway are presented in Sects. G.4 and G.5.

G.3.1 Exposure Scenarios and Exposure Pathways for Off-Site Individuals

The CIIDF PA assumes that radionuclides are transported to locations beyond the facility boundary primarily via the groundwater pathway or by discharge to ephemeral surface streams within the facility boundary which flow into Bear Creek (see Sect. 3.2.1). Based on the design of the disposal facility and previous experience with waste disposals on ORR, off-site transport via the atmospheric pathway following suspension into the air of radionuclides in solid waste and transport by biotic pathways are believed to be relatively unimportant. An individual residing outside the boundary of the disposal facility is assumed to use contaminated surface water or groundwater for domestic purposes. The following pathways involving exposure to contaminated water are assumed to occur:

- direct ingestion of contaminated drinking water,
- ingestion of milk and meat from dairy and beef cattle that drink contaminated water,
- ingestion of vegetables grown in garden soil irrigated with contaminated water,
- direct ingestion of contaminated soil in conjunction with vegetable intakes from the garden,
- external exposure to contaminated soil while working in the garden, and
- inhalation of radionuclides suspended into air from contaminated soil while working in the garden.

However, as described below, most of these exposure pathways do not need to be evaluated in the dose analysis for off-site individuals.

In the CIIDF PA, off-site releases via water pathways are assumed to be subject to two performance objectives: an EDE of 25 mrem per year from all exposure pathways and an EDE of 4 mrem per year from consumption of 2 L per day of drinking water from a contaminated source. A previous analysis for a waste disposal facility at the Savannah River Site (MMES, EG&G, and WSRC 1994), supported by the previous analysis for SWSA 6 on ORR (ORNL 1994), showed that the performance objective for the drinking water pathway only should be considerably more restrictive for any radionuclide than the performance objective for all exposure pathways. That is, if the lower performance objective for the drinking water pathway is met, then the higher performance objective for all exposure pathways also should be met without the need for further analysis of the pathways involving use of contaminated water other than direct consumption of drinking water. This conclusion is even more appropriate for ORR than for the Savannah River Site because irrigation of food crops is not widely practiced at the present time due to the usually abundant rainfall.

An off-site individual might also receive exposures due to ingestion of fish obtained from contaminated surface waters and external exposure while swimming or boating in contaminated surface waters. However, these exposure pathways are not considered to be credible occurrences along Bear Creek near the boundary of the disposal site, where the concentrations of radionuclides in surface water would be the highest, but could occur only at locations near where the contaminated surface water enters the Clinch River. At these locations, the maximum concentrations in Bear Creek would be so diluted by the much greater flow of the Clinch River that the doses from these exposure pathways would be negligible compared with the dose from direct consumption of drinking water from Bear Creek near the disposal site.

Therefore, in the dose analysis for off-site individuals, only the following exposure pathway is evaluated: direct ingestion of contaminated drinking water from groundwater or surface water at the locations of maximum predicted concentrations of radionuclides beyond the 100-m buffer zone around the disposal facility.

G.3.2 Exposure Scenarios and Exposure Pathways for Inadvertent Intruders

Inadvertent intruders are assumed to establish a permanent homestead on the disposal site at any time after loss of active institutional controls over the site at 100 years after disposal. Furthermore, intruders are assumed to have no prior knowledge of waste disposal activities at the site. Inadvertent intruders then are assumed to receive radiation exposures from direct intrusion into solid waste in the disposal facility. As noted in Sect. G.1, potential exposures to inadvertent intruders from use of contaminated groundwater on the disposal site should be negligible compared to the maximum potential exposures from direct intrusion into solid waste in the disposal facility.

For direct intrusion into the disposal facility after loss of active institutional controls, exposures are assumed to occur according to one of three different scenarios, which are called the agriculture, resident, and post-drilling scenarios. Each of these scenarios involves chronic lifetime exposure. These scenarios are the same as those used in previous PAs for the SWSA 6 disposal facility on ORR (ORNL 1994) and a disposal facility at the Savannah River Site (MMES, EG&G, and WSRC 1994). The discovery scenario that also was included in the PA for the SWSA 6 disposal facility, which involves a single acute exposure, is not included in the assessment for CIIDF because this scenario is relevant only for disposal units constructed with engineered barriers that are thicker at the top than at the sides, a situation that does not occur at CIIDF. In all of the chronic exposure scenarios considered in this assessment, an inadvertent intruder is assumed to establish a permanent homestead on the disposal site. The three exposure scenarios and their associated exposure pathways are described as follows.

In the agriculture scenario, an inadvertent intruder is assumed to construct a home directly on top of the disposal facility, with the foundation extending into the disposal waste. Radioactive wastes and other waste materials in the facility, which are assumed to be indistinguishable from native soil,

are assumed to be exhumed during construction of the foundation. Some of the exhumed waste materials then are assumed to be mixed with native soil in the intruder's vegetable garden, and the following pathways involving exposure to radionuclides in solid waste are assumed to occur:

- ingestion of vegetables grown in the contaminated garden soil,
- direct ingestion of contaminated soil from the garden in conjunction with vegetable intakes,
- external exposure to contaminated soil while working in the garden or residing in the home on top of the disposal facility, and
- inhalation of radionuclides suspended into the air from contaminated soil while working in the garden or residing in the home.

In the resident scenario, an intruder also is assumed to dig a foundation for a home at the location of the disposal facility, as in the agriculture scenario described above, but is assumed to encounter an intact and impenetrable engineered barrier (e.g., reinforced concrete) on top of the facility. The intruder then is assumed to construct a home directly on top of the intact engineered barrier above the waste. Since the engineered barrier is assumed not to be breached during excavation, the only exposure pathway of concern for the resident scenario is external exposure to photon-emitting radionuclides in the waste during the time the intruder resides in the home on top of the facility. Because of the presence of an engineered barrier in the resident scenario, which provides considerable shielding, the external dose per unit concentration of radionuclides in disposed waste while residing in the home on top of facility will always be less in the resident scenario than in the agriculture scenario. Therefore, the resident scenario is intended to be applied only when inadvertent intrusion onto the disposal site first occurs at 100 years after disposal and the engineered barriers presumably are intact, at which time the external dose from shorter-lived radionuclides in the waste could be considerably higher than the dose at later times when the engineered barrier has degraded and residence on top of exposed waste could occur but the concentrations of the shorter-lived radionuclides would be reduced significantly by decay.

In the post-drilling scenario, direct intrusion into the disposal facility by excavation is assumed not to occur during construction of a home. Direct intrusion into disposal waste during construction could be precluded by the presence of impenetrable engineered barriers or by construction of a home at a location other than the location of the disposal facility. However, an intruder is assumed to access solid waste by drilling directly through the facility, e.g., while constructing a well for a domestic water supply. During drilling, a small volume of radioactive waste, which is assumed to be indistinguishable from native soil, is brought to the surface. All of the drilling waste then is assumed to be mixed with native soil in the intruder's vegetable garden, and the following pathways involving exposure to radionuclides in the solid waste are assumed to occur:

- ingestion of vegetables grown in the contaminated garden soil,
- direct ingestion of contaminated soil from the garden in conjunction with vegetable intakes,

- external exposure to contaminated soil while working in the garden, and
- inhalation of radionuclides suspended into air from contaminated soil while working in the garden.

These pathways correspond to some of the pathways assumed for the agriculture scenario. However, in the post-drilling scenario, external and inhalation exposures while residing in the home are not considered, because all of the drilling waste is assumed to be mixed with soil in the vegetable garden.

G.4 DOSE CONVERSION FACTORS FOR INTERNAL AND EXTERNAL EXPOSURE

From the descriptions of the assumed exposure scenarios given in Sect. G.3, doses to off-site individuals and inadvertent intruders are assumed to result from ingestion and inhalation of radionuclides and from external exposure to photons emitted by radionuclides in contaminated soil or in the disposal facility itself. This section presents the factors used in the dose analysis to convert intakes of radionuclides via ingestion and inhalation to internal doses and to convert concentrations of radionuclides in soil or the disposal facility to external dose rates.

The internal dose conversion factors for ingestion and inhalation of radionuclides used in this analysis are given in Tables G.2 and G.3, respectively. The dose conversion factors give 50-year committed EDEs per unit activity intake of each radionuclide. These values were developed by the International Commission on Radiological Protection and have been adopted by federal agencies for use in assessing radiation doses to the public (Eckerman, Wohlbarst, and Richardson 1988). Dose conversion factors for inhalation of isotopes of radon and their short-lived decay products are not listed in Table G.3 but are calculated using a natural analog model described in Sect. G.5.2.1.

For some radionuclides, more than one dose conversion factor for ingestion or inhalation is given by Eckerman, Wohlbarst, and Richardson (1988). If ingestion dose conversion factors are given for two values of the gastrointestinal-tract absorption fraction (f_1), the dose conversion factor corresponding to the higher absorption fraction is adopted in Table G.2, because radionuclides that are transported in water or through terrestrial food chains should be in relatively soluble form and more easily absorbed in the gastrointestinal tract. In all cases, this choice gives the higher dose conversion factor. If inhalation dose conversion factors are given for more than one lung clearance class (D, W, or Y), the clearance class giving the highest dose conversion factor is adopted in Table G.3 for most radionuclides. However, ^{90}Sr and ^{99}Tc are assumed to be Class D because their solubility in the environment is expected to be relatively high, and all isotopes of thorium are assumed to be Class Y because thorium in soil is expected to be highly insoluble (e.g., in oxide or hydroxide form). On the other hand, the particular choices of inhalation dose conversion factors for ^{90}Sr, ^{99}Tc, and isotopes of thorium do not have a significant impact on the results of a dose analysis, either because inhalation exposure pathways are relatively unimportant or because the dose conversion factors for other clearance classes are not significantly different.

Table G.2. Internal dose conversion factors for ingestion of radionuclides[a]

Nuclide[b]	f_1 [c]	Rem per μCi ingested	Nuclide	f_1	Rem per μCi ingested
^{3}H	1.0	6.4×10^{-5}	^{152}Eu	0.001	6.5×10^{-3}
^{10}Be	0.005	4.7×10^{-3}	^{154}Eu	0.001	9.5×10^{-3}
^{14}C	1.0	2.1×10^{-3}	^{155}Eu	0.001	1.5×10^{-3}
^{26}Al	0.01	1.5×10^{-2}	^{207}Bi	0.05	5.5×10^{-3}
^{36}Cl	1.0	3.0×10^{-3}	^{210}Pb	0.2	5.4
^{40}K	1.0	1.9×10^{-2}	^{210}Po	0.1	1.9
^{41}Ca	0.3	1.3×10^{-3}	^{226}Ra	0.2	1.3
^{60}Co	0.3	2.7×10^{-2}	^{229}Th	0.0002	3.5
^{59}Ni	0.05	2.1×10^{-4}	^{225}Ra	0.2	3.8×10^{-1}
^{63}Ni	0.05	5.8×10^{-4}	^{225}Ac	0.001	1.1×10^{-1}
^{79}Se	0.8	8.7×10^{-3}	^{230}Th	0.0002	5.5×10^{-1}
^{87}Rb	1.0	4.9×10^{-3}	^{232}Th	0.0002	2.7
^{90}Sr	0.3	1.4×10^{-1}	^{228}Ra	0.2	1.4
^{90}Y	0.0001	1.1×10^{-2}	^{228}Th	0.0002	4.0×10^{-1}
^{93}Zr	0.002	1.7×10^{-3}	^{224}Ra	0.2	3.7×10^{-1}
^{93m}Nb	0.01	5.2×10^{-4}	^{212}Pb	0.2	4.6×10^{-2}
^{94}Nb	0.01	7.1×10^{-3}	^{231}Pa	0.001	1.1×10^{1}
^{99}Tc	0.8	1.5×10^{-3}	^{227}Ac	0.001	1.4×10^{1}
^{107}Pd	0.005	1.5×10^{-4}	^{223}Ra	0.2	6.6×10^{-1}
^{113m}Cd	0.05	1.6×10^{-1}	^{232}U[d]	0.05	1.3
^{121m}Sn	0.02	1.6×10^{-3}	^{233}U	0.05	2.9×10^{-1}
^{126}Sn	0.02	1.9×10^{-2}	^{234}U	0.05	2.8×10^{-1}
^{126}Sb	0.1	1.0×10^{-2}	^{235}U	0.05	2.7×10^{-1}
^{129}I	1.0	2.8×10^{-1}	^{236}U	0.05	2.7×10^{-1}
^{135}Cs	1.0	7.1×10^{-3}	^{238}U	0.05	2.5×10^{-1}
^{137}Cs	1.0	5.0×10^{-2}	^{234}Th	0.0002	1.4×10^{-2}
^{151}Sm	0.0003	3.9×10^{-4}	^{237}Np	0.001	4.4

Table G.2 (continued)

Nuclide[b]	f_1[c]	Rem per μCi ingested	Nuclide	f_1	Rem per μCi ingested
^{238}Pu	0.001	3.2	^{243}Cm	0.001	2.5
^{239}Pu	0.001	3.5	^{244}Cm	0.001	2.0
^{240}Pu	0.001	3.5	^{245}Cm	0.001	3.7
^{241}Pu	0.001	6.8×10^{-2}	^{246}Cm	0.001	3.7
^{242}Pu	0.001	3.4	^{247}Cm	0.001	3.4
^{244}Pu	0.001	3.3	^{248}Cm	0.001	1.4×10^{1}
^{241}Am	0.001	3.6	^{249}Cf	0.001	4.7
^{242m}Am	0.001	3.5	^{250}Cf	0.001	2.1
^{242}Cm	0.001	1.1×10^{-1}	^{251}Cf	0.001	4.8
^{243}Am	0.001	3.6			

[a]Values from Eckerman, Wohlbarst, and Richardson (1988) give 50-year committed EDE per unit activity ingested.

[b]Indented entries are radiologically significant decay products of parent radionuclide listed.

[c]Fraction of ingested radionuclide absorbed into blood from gastrointestinal tract.

[d]Values for ^{228}Th, ^{224}Ra, and ^{212}Pb decay products are listed following ^{232}Th.

Table G.3. Internal dose conversion factors for inhalation of radionuclides[a]

Nuclide[b]	Clearance class[c]	Rem per μCi inhaled	Nuclide	Clearance class	Rem per μCi inhaled
^{3}H		6.4×10^{-5}	^{152}Eu	W	2.2×10^{-1}
^{10}Be	Y	3.5×10^{-1}	^{154}Eu	W	2.9×10^{-1}
^{14}C[d]		2.1×10^{-3}	^{155}Eu	W	4.1×10^{-2}
^{26}Al	D	8.0×10^{-2}	^{207}Bi	W	2.0×10^{-2}
^{36}Cl	W	2.2×10^{-2}	^{210}Pb	D	1.4×10^{1}
^{40}K	D	1.2×10^{-2}	^{210}Po	D	9.4
^{41}Ca	W	1.3×10^{-3}	^{226}Ra	W	8.6
^{60}Co	Y	2.2×10^{-1}	^{222}Rn[f]		
^{59}Ni[e]	D	1.3×10^{-3}	^{229}Th	Y	1.7×10^{3}
^{63}Ni[e]	D	3.1×10^{-3}	^{230}Th	Y	2.6×10^{2}
^{79}Se	W	6.5×10^{-3}	^{232}Th	Y	1.2×10^{3}
^{87}Rb	D	3.2×10^{-3}	^{228}Th	Y	3.4×10^{2}
^{90}Sr	D	2.4×10^{-1}	^{220}Rn[f]		
^{90}Y	Y	8.4×10^{-3}	^{231}Pa	W	1.3×10^{3}
^{93}Zr	D	3.2×10^{-1}	^{227}Ac	D	6.7×10^{3}
^{93m}Nb	Y	2.9×10^{-2}	^{232}U[g]	Y	6.6×10^{2}
^{94}Nb	Y	4.1×10^{-1}	^{233}U	Y	1.4×10^{2}
^{99}Tc	D	1.0×10^{-3}	^{234}U	Y	1.3×10^{2}
^{107}Pd	Y	1.2×10^{-2}	^{235}U	Y	1.2×10^{2}
^{113m}Cd	D	1.5	^{236}U	Y	1.3×10^{2}
^{121m}Sn	W	1.2×10^{-2}	^{238}U	Y	1.2×10^{2}
^{126}Sn	W	1.0×10^{-1}	^{237}Np	W	5.4×10^{2}
^{126}Sb	W	1.2×10^{-2}	^{238}Pu	W	3.9×10^{2}
^{129}I	D	1.7×10^{-1}	^{239}Pu	W	4.3×10^{2}
^{135}Cs	D	4.6×10^{-3}	^{240}Pu	W	4.3×10^{2}
^{137}Cs	D	3.2×10^{-2}	^{241}Pu	W	8.3
^{151}Sm	W	3.0×10^{-2}	^{242}Pu	W	4.1×10^{2}

Table G.3 (continued)

Nuclide[b]	Clearance class[c]	Rem per μCi inhaled	Nuclide	Clearance class	Rem per μCi inhaled
^{244}Pu	W	4.0×10^2	^{245}Cm	W	4.6×10^2
^{241}Am	W	4.4×10^2	^{246}Cm	W	4.5×10^2
^{242m}Am	W	4.3×10^2	^{247}Cm	W	4.1×10^2
^{242}Cm	W	1.7×10^1	^{248}Cm	W	1.7×10^3
^{243}Am	W	4.4×10^2	^{249}Cf	W	5.8×10^2
^{243}Cm	W	3.1×10^2	^{250}Cf	W	2.6×10^2
^{244}Cm	W	2.5×10^2	^{251}Cf	W	5.9×10^2

[a]Values from Eckerman, Wohlbarst, and Richardson (1988) give 50-year committed EDE per unit activity inhaled.

[b]Indented entries are radiologically significant decay products of parent radionuclide listed.

[c]Clearance from respiratory passages for radionuclides in particulate form in a matter of days (D), weeks (W), or years (Y).

[d]Radionuclide is assumed to be in organic form.

[e]Radionuclide is assumed to be in inorganic form.

[f]Inhalation doses from isotopes of radon and their short-lived decay products are estimated using model described in Sect. G.5.2.1.

[g]Values for ^{228}Th and ^{220}Rn decay products are listed following ^{232}Th.

The dose conversion factors for external exposure give EDE rates per unit concentration of radionuclides in the specified source regions. These factors depend on the distribution of radionuclides in the source region, the amount of self-shielding provided by the source region, and the amount of shielding between the source region and the location of the exposed individual. Therefore, separate sets of dose conversion factors are required for the assumed pathways involving exposure to contaminated soil while gardening and exposure to waste in the disposal facility during indoor residence on the site.

For external exposure to radionuclides in contaminated soil while gardening or to radionuclides in the disposal facility during indoor residence, the source region is assumed to be a uniformly contaminated slab of infinite lateral extent. Depending upon the exposure scenario, as described below, the slab source is assumed to have either finite or infinite thickness, and the shielding provided by any uncontaminated material between the source and receptor locations is taken into account. The idealized distributions of radionuclides in the source region assumed in the dose analysis probably are reasonable, because only about 1 m of soil-equivalent material between a slab source and a receptor location provides nearly complete shielding (Kocher and Sjoreen 1985). In all calculations of external dose from radionuclides in contaminated garden soil or the disposal facility, an exposed individual is assumed to be located at a distance of 1 m from the source region. The small amount of shielding provided by 1 m of air can be neglected in all cases compared with the much greater shielding provided by the soil in the source region itself or by an engineered barrier.

For external exposure while working in the vegetable garden, the source region is assumed to be a slab extending from the ground surface to a depth of 15 cm, which is a typical thickness of a plowed layer. The external dose-rate conversion factors for this case are given in Table G.4. For external exposure while residing in the home on top of exposed waste, the source region is assumed to be a slab of essentially infinite thickness, with no shielding assumed between the source region and the receptor location other than that provided by the soil in the source region (shielding provided by the walls of the home during indoor residence is taken into account in the exposure pathway analysis itself). The external dose-rate conversion factors for this case are given in the column in Table G.5 labeled "No shielding." In both of these cases, the external dose-rate conversion factors have been adopted by federal agencies in assessing radiation doses to the public (Eckerman and Ryman 1993). For all radioactive decay chains, the dose-rate factor for each short-lived decay product takes into account the branching fraction in the decay of its parent radionuclide (Kocher 1981).

For external exposure in the resident scenario, the source region also is assumed to be a slab of infinite thickness, but a thickness of uncontaminated shielding material between the source and receptor locations equivalent to 30 cm of soil is assumed to be provided by the engineered barrier used in constructing the disposal facility. The external dose-rate conversion factors for this thickness of shielding are given in the last column in Table G.5. Since values for this thickness of soil-equivalent material are not calculated by Eckerman and Ryman (1993), the dose-rate factors in Table G.5 for this case were obtained from calculations of absorbed dose rates in air for monoenergetic photon sources in soil (Kocher and Sjoreen 1985) and the spectrum of photons emitted by each radionuclide (Kocher 1981). For all radionuclides, absorbed dose in air was converted to EDE in an exposed individual by

multiplying by a factor of 0.8. This is an excellent approximation for all photon energies above about 0.1 MeV and provides a conservative overestimate of dose for lower photon energies. For the exposure pathways represented in Table G.4 and the second ("No shielding") column in Table G.5, the calculations from Kocher and Sjoreen (1985) agree with those from Eckerman and Ryman (1993) within a few tens of percent. The dose-rate factors for short-lived radionuclides in decay chains in Table G.5 take into account the branching fraction in the decay of the parent radionuclide (Kocher 1981).

G.5 MODELS AND PARAMETER VALUES FOR EXPOSURE PATHWAYS

This section presents the models used to calculate doses to off-site individuals and inadvertent intruders for the various exposure pathways involving use of contaminated water and direct intrusion into the disposal facility described in Sect. G.3. In each case, the parameter values assumed in implementing the models also are presented. For each exposure pathway, the results are presented in summary tables which give annual EDEs per unit concentration of radionuclides in water or in the disposal facility at the time exposures are assumed to occur.

The parameter values selected for use in the models usually are intended to represent reasonable best estimates or prudently conservative values, rather than worst-case assumptions. This approach is regarded as appropriate when one considers the hypothetical and conservative nature of the assumed exposure scenarios, particularly the assumptions that exposures occur only at the locations of greatest estimated radionuclide concentrations.

G.5.1 Exposure of Off-Site Individuals to Radionuclides in Contaminated Water

As described in Sect. G.3.1, exposures of off-site individuals to contaminated groundwater or surface water are assumed to result from use of the contaminated source as a drinking water supply, but other exposure pathways involving use of contaminated water from the same source do not need to be considered for the purpose of demonstrating compliance with the applicable performance objectives for limiting off-site releases by water pathways.

Table G.4. External dose-rate conversion factors for radionuclides uniformly distributed in 15 cm of surface soil[a]

Nuclide[b]	Dose-rate factor (rem/year per μCi/m³)	Nuclide	Dose-rate factor (rem/year per μCi/m³)
^{26}Al	9.0×10^{-3}	^{232}Th	—
^{40}K	5.3×10^{-4}	^{228}Ac	3.2×10^{-3}
^{60}Co	8.5×10^{-3}	^{212}Pb	4.2×10^{-4}
^{94}Nb	5.3×10^{-3}	^{212}Bi	6.3×10^{-4}
^{121m}Sn	1.2×10^{-6}	^{208}Tl	4.1×10^{-3}
^{126}Sn	9.2×10^{-5}	^{231}Pa	1.1×10^{-4}
^{126m}Sb	5.2×10^{-3}	^{227}Th	3.1×10^{-4}
^{126}Sb	1.3×10^{-3}	^{223}Ra	3.6×10^{-4}
^{129}I	8.1×10^{-6}	^{211}Pb	1.7×10^{-4}
^{137}Cs	—	^{211}Bi	1.5×10^{-4}
^{137m}Ba	1.9×10^{-3}	^{207}Tl	1.1×10^{-5}
^{152}Eu	3.8×10^{-3}	^{232}U[c]	—
^{154}Eu	4.1×10^{-3}	^{235}U	4.6×10^{-4}
^{155}Eu	1.1×10^{-4}	^{231}Th	2.3×10^{-5}
^{207}Bi	5.1×10^{-3}	^{238}U	—
^{226}Ra	—	^{234}Th	1.5×10^{-5}
^{214}Pb	7.8×10^{-4}	^{234m}Pa	4.9×10^{-5}
^{214}Bi	5.1×10^{-3}	^{234}Pa	1.0×10^{-5}
^{229}Th	2.0×10^{-4}	^{237}Np	4.9×10^{-5}
^{225}Ra	6.9×10^{-6}	^{233}Pa	6.0×10^{-4}
^{225}Ac	3.9×10^{-5}	^{244}Pu	—
^{221}Fr	9.2×10^{-5}	^{240m}Np	1.1×10^{-3}
^{213}Bi	4.4×10^{-4}	^{241}Am	2.7×10^{-5}
^{209}Tl	1.5×10^{-4}		

Table G.4 (continued)

Nuclide[b]	Dose-rate factor (rem/year per μCi/m^3)	Nuclide	Dose-rate factor (rem/year per μCi/m^3)
^{242m}Am	1.1×10^{-6}	^{245}Cm	2.1×10^{-4}
^{242}Am	3.1×10^{-5}	^{247}Cm	1.0×10^{-3}
^{238}Np	8.8×10^{-6}	^{243}Pu	4.9×10^{-5}
^{243}Am	8.9×10^{-5}	^{249}Cf	1.1×10^{-3}
^{239}Np	4.6×10^{-4}	^{251}Cf	3.2×10^{-4}
^{243}Cm	3.5×10^{-4}		

[a]Values from Eckerman and Ryman (1993), and assuming branching fractions for radioactive decay chains from Kocher (1981), give external EDE rate per unit activity concentration in soil at distance of 1 m from source region.

[b]Indented entries are radiologically significant decay products of parent radionuclide listed.

[c]Values for ^{212}Pb, ^{212}Bi, and ^{208}Tl decay products are listed following ^{232}Th.

Table G.5. External dose-rate conversion factors for radionuclides uniformly distributed in infinite thickness of soil[a]

	Dose-rate factor (rem/year per μCi/m³)			Dose-rate factor (rem/year per μCi/m³)	
Nuclide[b]	No shielding[c]	30-cm shielding[d]	Nuclide	No shielding	30-cm shielding
^{26}Al	1.1×10^{-2}	9.4×10^{-4}	^{232}Th	—	—
^{40}K	6.5×10^{-4}	5.9×10^{-5}	^{228}Ac	3.7×10^{-3}	2.2×10^{-4}
^{60}Co	1.0×10^{-2}	8.2×10^{-4}	^{212}Pb	4.4×10^{-4}	—
^{94}Nb	6.1×10^{-3}	3.1×10^{-4}	^{212}Bi	7.3×10^{-4}	4.8×10^{-5}
^{121m}Sn	1.2×10^{-6}	—	^{208}Tl	5.2×10^{-3}	6.0×10^{-4}
^{126}Sn	9.2×10^{-5}	—	^{231}Pa	1.2×10^{-4}	1.3×10^{-6}
^{126m}Sb	5.8×10^{-3}	2.4×10^{-4}	^{227}Th	3.2×10^{-4}	3.2×10^{-6}
^{126}Sb	1.5×10^{-3}	6.3×10^{-5}	^{223}Ra	3.8×10^{-4}	3.8×10^{-6}
^{129}I	8.1×10^{-6}	—	^{211}Pb	1.9×10^{-4}	8.0×10^{-6}
^{137}Cs	—	—	^{211}Bi	1.6×10^{-4}	3.2×10^{-6}
^{137m}Ba	2.1×10^{-3}	9.0×10^{-5}	^{207}Tl	1.2×10^{-5}	5.0×10^{-7}
^{152}Eu	4.4×10^{-3}	2.8×10^{-4}	^{232}U[e]	—	—
^{154}Eu	4.8×10^{-3}	3.2×10^{-4}	^{235}U	4.5×10^{-4}	1.6×10^{-6}
^{155}Eu	1.1×10^{-4}	5.7×10^{-8}	^{231}Th	2.3×10^{-5}	—
^{207}Bi	5.9×10^{-3}	3.5×10^{-4}	^{238}U	—	—
^{226}Ra	—	—	^{234}Th	1.5×10^{-5}	—
^{214}Pb	8.4×10^{-4}	1.6×10^{-5}	^{234m}Pa	5.6×10^{-5}	2.7×10^{-6}
^{214}Bi	6.1×10^{-3}	5.2×10^{-4}	^{234}Pa	1.2×10^{-5}	6.8×10^{-7}
^{229}Th	2.0×10^{-4}	3.7×10^{-7}	^{237}Np	4.9×10^{-5}	5.1×10^{-8}
^{225}Ra	6.9×10^{-6}	—	^{233}Pa	6.4×10^{-4}	9.9×10^{-6}
^{225}Ac	4.0×10^{-5}	1.1×10^{-7}	^{244}Pu	—	—
^{221}Fr	9.6×10^{-5}	4.9×10^{-7}	^{240m}Np	1.3×10^{-3}	6.0×10^{-5}
^{213}Bi	4.8×10^{-4}	1.4×10^{-5}	^{241}Am	2.7×10^{-5}	—
^{209}Tl	1.7×10^{-4}	1.5×10^{-5}			

Table G.5 (continued)

Nuclide[b]	Dose-rate factor (rem/year per μCi/m³) No shielding[c]	Dose-rate factor (rem/year per μCi/m³) 30-cm shielding[d]	Nuclide	Dose-rate factor (rem/year per μCi/m³) No shielding	Dose-rate factor (rem/year per μCi/m³) 30-cm shielding
^{242m}Am	1.1×10^{-6}	4.2×10^{-10}	^{245}Cm	3.6×10^{-4}	2.8×10^{-7}
^{242}Am	3.1×10^{-5}	2.8×10^{-8}	^{247}Cm	1.1×10^{-3}	2.4×10^{-5}
^{238}Np	1.0×10^{-5}	6.7×10^{-7}	^{243}Pu	5.0×10^{-5}	2.0×10^{-7}
^{243}Am	8.9×10^{-5}	—	^{249}Cf	1.2×10^{-3}	2.3×10^{-5}
^{239}Np	4.7×10^{-4}	3.0×10^{-6}	^{251}Cf	3.3×10^{-4}	1.1×10^{-6}
^{243}Cm	3.6×10^{-4}	2.2×10^{-6}			

[a]Values from indicated sources, and assuming branching fractions for radioactive decay chains from Kocher (1981), give external EDE rate per unit activity concentration in soil at distance of 1 m from source region and assumed thicknesses of shielding by soil-equivalent material between source and receptor locations.

[b]Indented entries are radiologically significant decay products of parent radionuclide listed.

[c]Values from Eckerman and Ryman (1993).

[d]Values based on calculations for monoenergetic sources by Kocher and Sjoreen (1985) and radioactive decay data from Kocher (1981).

[e]Values for ^{212}Pb, ^{212}Bi, and ^{208}Tl decay products are listed following ^{232}Th.

The annual committed EDE (rem/year) from direct ingestion of radionuclide i in drinking water (w) is given by

$$H_{iw} = C_{iw} U_w D_i \ , \qquad \textbf{(G.1)}$$

where

C_{iw} = concentration of radionuclide i in drinking water (μCi/L),
U_w = annual consumption of drinking water (L/year),
D_i = dose conversion factor for ingestion of radionuclide i (rem/μCi ingested).

In implementing the model, a daily consumption of contaminated drinking water of 2 L (i.e., an annual consumption of 730 L) is assumed.

The model for estimating the dose from the drinking water pathway is summarized in Table G.6. The annual dose per unit concentration of a radionuclide in water is obtained by multiplying the assumed annual consumption of drinking water by the ingestion dose conversion factor given in Table G.2.

G.5.2 Exposure Pathways for Inadvertent Intruders into Disposal Facility

Exposures of inadvertent intruders resulting from direct intrusion into the disposal facility after loss of active institutional control over the disposal site are assumed to occur according to the agriculture, resident, or post-drilling scenarios. This section presents the models and parameter values used to estimate annual EDEs per unit concentration of radionuclides in the disposal facility for the different exposure pathways assumed for each of these exposure scenarios.

G.5.2.1 Agriculture Scenario

In the agriculture scenario, an inadvertent intruder is assumed to exhume waste materials from the disposal facility in digging a foundation for a home on top of the facility, and some of the exhumed material is assumed to be mixed with native soil in the intruder's vegetable garden. The pathways for chronic exposure assumed for this scenario then include (1) ingestion of vegetables grown in contaminated soil, (2) direct ingestion of contaminated soil from the garden in conjunction with vegetable intakes, (3) external exposure to contaminated soil while working in the garden and during indoor residence on top of the disposal facility, and (4) inhalation of activity suspended in air while working in the garden and during indoor residence.

Table G.6. Annual effective dose equivalents from drinking water pathway per unit concentration of radionuclides in water[a]

Nuclide[b]	Annual dose (rem/year per μCi/L)	Nuclide	Annual dose (rem/year per μCi/L)
^{3}H	4.7×10^{-2}	^{151}Sm	2.8×10^{-1}
^{10}Be	3.4	^{152}Eu	4.7
^{14}C	1.5	^{154}Eu	6.9
^{26}Al	1.1×10^{1}	^{155}Eu	1.1
^{36}Cl	2.2	^{207}Bi	4.0
^{40}K	1.4×10^{1}	^{210}Pb + d	5.3×10^{3}
^{41}Ca	9.5×10^{-1}	^{226}Ra[d]	9.5×10^{2}
^{60}Co	2.0×10^{1}	^{229}Th + d	2.9×10^{3}
^{59}Ni	1.5×10^{-1}	^{230}Th	4.0×10^{2}
^{63}Ni	4.2×10^{-1}	^{232}Th + d	3.6×10^{3}
^{79}Se	6.4	^{231}Pa + d	1.9×10^{4}
^{87}Rb	3.6	^{232}U + d	1.5×10^{3}
^{90}Sr + d	1.1×10^{2}	^{233}U	2.1×10^{2}
^{93}Zr[c]	1.2	^{234}U	2.0×10^{2}
^{93m}Nb	3.8×10^{-1}	^{235}U	2.0×10^{2}
^{94}Nb	5.2	^{236}U	2.0×10^{2}
^{99}Tc	1.1	^{238}U + d	1.9×10^{2}
^{107}Pd	1.1×10^{-1}	^{237}Np	3.2×10^{3}
^{113m}Cd	1.2×10^{2}	^{238}Pu	2.3×10^{3}
^{121m}Sn	1.2	^{239}Pu	2.6×10^{3}
^{126}Sn + d	1.5×10^{1}	^{240}Pu	2.6×10^{3}
^{129}I	2.0×10^{2}	^{241}Pu	5.0×10^{1}
^{135}Cs	5.2	^{242}Pu	2.5×10^{3}
^{137}Cs	3.7×10^{1}	^{244}Pu	2.4×10^{3}

Table G.6 (continued)

Nuclide[b]	Annual dose (rem/year per μCi/L)	Nuclide	Annual dose (rem/year per μCi/L)
^{241}Am	2.6×10^3	^{246}Cm	2.7×10^3
^{242m}Am + d[e]	2.6×10^3	^{247}Cm	2.5×10^3
^{243}Am	2.6×10^3	^{248}Cm	1.0×10^4
^{243}Cm	1.8×10^3	^{249}Cf	3.4×10^3
^{244}Cm	1.5×10^3	^{250}Cf	1.5×10^3
^{245}Cm	2.7×10^3	^{251}Cf	3.5×10^3

[a]Values give 50-year committed EDE from one year's intakes of drinking water.

[b]The notation "+ d" with some entries denotes short-lived decay products that are assumed to be in secular equilibrium with parent radionuclide; see Table G.1 for decay products and branching fractions.

[c]Possible contributions to dose from ^{93m}Nb decay product are not included.

[d]Possible contributions to dose from ^{210}Pb decay product are not included.

[e]Possible contributions to dose from ^{238}Pu decay product are not included.

Vegetable pathway

The annual committed effective dose equivalent (rem/year) from ingestion of radionuclide i in vegetables (v) is given by

$$H_{iv} = C_{iv} U_v D_i \ , \tag{G.2}$$

where

C_{iv} = concentration of radionuclide i in vegetables (μCi/kg),
U_v = annual consumption of vegetables (kg/year),
D_i = dose conversion factor for ingestion of radionuclide i (rem/μCi ingested).

Radionuclides are assumed to be transferred to vegetables via root uptake from the contaminated soil. Radionuclide concentrations in vegetables then are given by

$$\begin{aligned} C_{iv} &= B_{iv} C_{is} / \rho_s \ , \\ &= B_{iv} f_s C_{it} / \rho_s \ , \end{aligned} \tag{G.3}$$

where

B_{iv} = plant-to-soil concentration ratio for radionuclide i (μCi/kg wet weight in vegetation per μCi/kg dry weight in soil),
C_{is} = concentration of radionuclide i in soil in vegetable garden (μCi/m^3),
ρ_s = density of soil (kg/m^3),
C_{it} = concentration of radionuclide i in disposal facility (μCi/m^3),
f_s = dilution factor for mixing of exhumed waste materials from disposal facility into soil in vegetable garden.

In implementing the model, the assumed plant-to-soil concentration ratios in vegetables are given in Table G.7. Although some data from ORR are available [e.g., see Garten et al. (1987)], site-specific data for most of the radionuclides of concern to this assessment and for a variety of food crops are lacking. Therefore, most of the values adopted in this analysis are generic and were obtained from an evaluation of published data by Baes et al. (1984). This approach clearly is judgmental for application to ORR, but selection of the concentration ratios primarily from a single source at least ensures some degree of consistency among the values for the different elements, because similar biases presumably were applied in developing the adopted concentration ratios from the published data.

Table G.7. Elemental plant-to-soil concentration ratios in vegetables

Element	B_v [a]	Element	B_v
H	4.8[b]	Sb	1.3×10^{-2}
Be	6.5×10^{-4}	I	2.2×10^{-2}
C	5.6×10^{-1}[c]	Cs	1.3×10^{-2}
Al	2.8×10^{-4}	Sm	1.7×10^{-3}
Cl	3.0×10^{1}	Eu	1.7×10^{-3}
K	2.4×10^{-1}	Pb	3.9×10^{-3}
Ca	1.5×10^{-1}	Bi	2.2×10^{-3}
Co	3.0×10^{-3}	Po	1.7×10^{-4}
Ni	2.6×10^{-2}	Ra	6.5×10^{-4}
Se	1.1×10^{-2}	Ac	1.5×10^{-4}
Rb	3.0×10^{-2}	Th	3.7×10^{-5}
Sr	1.1×10^{-1}	Pa	1.1×10^{-4}
Y	2.6×10^{-3}	U	1.7×10^{-3}
Zr	2.2×10^{-4}	Np	4.3×10^{-3}
Nb	2.2×10^{-3}	Pu	1.9×10^{-5}
Tc	6.5×10^{-1}	Am	1.1×10^{-4}
Pd	1.7×10^{-2}	Cm	6.5×10^{-6}
Cd	6.5×10^{-2}	Cf	6.5×10^{-6}[d]
Sn	2.6×10^{-3}		

[a]μCi/kg wet weight of vegetation per μCi/kg dry weight of soil; unless otherwise noted, values are obtained from concentration ratios on dry-weight basis of vegetation given in Fig. 2.2 of Baes et al. (1984) multiplied by factor of 0.43 to convert to fresh-weight basis of vegetation (Baes et al. 1984).

[b]Value from Table E-1 of NRC (1977).

[c]Value from Sheppard, Sheppard, and Amiro (1991) for carbonate form in acidic soil with low organic matter content; concentration ratio on dry-weight basis of vegetation is multiplied by factor of 0.43 to convert to fresh-weight basis of vegetation (Baes et al. 1984).

[d]Value is assumed to be the same as that for Cm.

Baes et al. (1984) give two sets of plant-to-soil concentration ratios—one for vegetative portions of food crops, which generally apply to leafy vegetables, and the other for nonvegetative (reproductive) portions, which generally apply to nonleafy vegetables. The values for nonvegetative portions of food crops were adopted for use in this analysis, becauseconsumption of nonleafy vegetables is about an order of magnitude greater than consumption of leafy vegetables (Baes et al. 1984; Hamby 1992). In addition, the adopted concentration ratios on a dry-weight basis of nonleafy vegetation were converted to fresh weight by multiplying by a factor of 0.43, which represents the average dry-weight to fresh-weight conversion factor for all types of nonleafy vegetables (Baes et al. 1984). Taking into account the concentration ratios for leafy vegetables would not significantly change the adopted values in Table G.7, due to the relatively low consumption of leafy vegetables and the much higher fresh-weight-to-dry-weight ratio for leafy vegetables than for nonleafy vegetables (Peterson 1983).

The other parameter values assumed in the model for the vegetable pathway are as follows: a dilution factor for mixing of exhumed waste materials, including both contaminated and uncontaminated materials, from the disposal facility into native soil in the vegetable garden of 0.2 (Oztunali et al. 1981; NRC 1982; Napier et al. 1984), a density of soil of 1,400 kg/m^3 (Baes and Sharp 1983), and an annual consumption of contaminated vegetables, including both leafy and nonleafy vegetables, of 90 kg. The dilution factor for mixing of exhumed waste materials with native soil in a vegetable garden is based on the reasonable assumption that no more than a relatively small fraction of the soil in the garden could consist of such materials if the garden were to be fertile, since essentially all of the exhumed waste would be nonfertile materials from below ground. The assumed annual consumption of leafy and nonleafy vegetables from the garden is consistent with data obtained near the Savannah River Site (Hamby 1992), which should be reasonably representative of data near ORR, and the assumption that half of an intruder's entire intakes of vegetables would be obtained from the home garden. An assumption that an intruder's entire intakes of vegetables would be obtained from the home garden is unreasonably conservative.

The model for estimating dose from the vegetable pathway is summarized in Table G.8. The annual dose per unit concentration of a radionuclide in exhumed waste from the disposal facility at the time intrusion occurs is based on the model and parameter values described above and the ingestion dose conversion factors given in Table G.2.

Soil ingestion pathway

The annual committed effective dose equivalent (rem per year) from direct ingestion of radionuclide i in contaminated soil (s) is given by

$$H_{is} = C_{is} U_s D_i \ , \qquad \textbf{(G.4)}$$

Table G.8. Annual effective dose equivalents to inadvertent intruders from vegetable pathway per unit concentration of radionuclides in disposal facility for agriculture scenario[a]

Nuclide[b]	Annual dose (rem/year per μCi/m^3)	Nuclide	Annual dose (rem/year per μCi/m^3)
^{3}H	4.0×10^{-6}	^{137}Cs	8.5×10^{-6}
^{10}Be	4.0×10^{-8}	^{151}Sm	8.6×10^{-9}
^{14}C	1.5×10^{-5}	^{152}Eu	1.4×10^{-7}
^{26}Al	5.5×10^{-8}	^{154}Eu	2.1×10^{-7}
^{36}Cl	1.2×10^{-3}	^{155}Eu	3.3×10^{-8}
^{40}K	5.9×10^{-5}	^{207}Bi	1.6×10^{-7}
^{41}Ca	2.5×10^{-6}	^{210}Pb	2.7×10^{-4}
^{60}Co	1.1×10^{-6}	^{226}Ra[d]	1.1×10^{-5}
^{59}Ni	7.1×10^{-8}	^{229}Th + d	5.1×10^{-6}
^{63}Ni	2.0×10^{-7}	^{230}Th	2.6×10^{-7}
^{79}Se	1.2×10^{-6}	^{232}Th + d	1.9×10^{-5}
^{87}Rb	1.9×10^{-6}	^{231}Pa + d	4.9×10^{-5}
^{90}Sr	2.0×10^{-4}	^{232}U + d	3.5×10^{-5}
^{93}Zr[c]	4.9×10^{-9}	^{233}U	6.4×10^{-6}
^{93m}Nb	1.5×10^{-8}	^{234}U	6.2×10^{-6}
^{94}Nb	2.0×10^{-7}	^{235}U	6.0×10^{-6}
^{99}Tc	1.3×10^{-5}	^{236}U	6.0×10^{-6}
^{107}Pd	3.3×10^{-8}	^{238}U	5.5×10^{-6}
^{113m}Cd	1.4×10^{-4}	^{237}Np	2.5×10^{-4}
^{121m}Sn	5.4×10^{-8}	^{238}Pu	7.9×10^{-7}
^{126}Sn + d	8.8×10^{-7}	^{239}Pu	8.6×10^{-7}
^{129}I	8.0×10^{-5}	^{240}Pu	8.6×10^{-7}
^{135}Cs	1.2×10^{-6}	^{241}Pu	1.7×10^{-8}

Table G.8 (continued)

Nuclide[b]	Annual dose (rem/year per μCi/m^3)	Nuclide	Annual dose (rem/year per μCi/m^3)
^{242}Pu	8.4×10^{-7}	^{245}Cm	3.1×10^{-7}
^{244}Pu	8.2×10^{-7}	^{246}Cm	3.1×10^{-7}
^{241}Am	5.1×10^{-6}	^{247}Cm	2.9×10^{-7}
^{242m}Am[e]	5.0×10^{-6}	^{248}Cm	1.2×10^{-6}
^{243}Am	5.1×10^{-6}	^{249}Cf	4.0×10^{-7}
^{243}Cm	2.1×10^{-7}	^{250}Cf	1.8×10^{-7}
^{244}Cm	1.7×10^{-7}	^{251}Cf	4.1×10^{-7}

[a]Values give 50-year committed EDEs from one year's intakes of vegetables.

[b]The notation "+ d" with some entries denotes short-lived decay products that are assumed to be in secular equilibrium with parent radionuclide; see Table G.1 for decay products and branching fractions.

[c]Possible contributions to dose from ^{93m}Nb decay product are not included.

[d]Possible contributions to dose from ^{210}Pb decay product are not included.

[e]Possible contributions to dose from ^{238}Pu decay product are not included.

where

C_{is}	=	concentration of radionuclide i in soil in vegetable garden (μCi/kg),
U_s	=	annual consumption of contaminated soil (kg/year),
D_i	=	dose conversion factor for ingestion of radionuclide i (rem/μCi ingested).

In this analysis, ingestion of contaminated soil is assumed to occur as a result of incomplete washing of vegetables from the garden before consumption. At humid sites with extensive vegetation, such as ORR, direct ingestion of contaminated soil from sources other than the garden should be relatively unimportant for an average adult. Radionuclide concentrations in soil in the vegetable garden are given by

$$C_{is} = f_s C_{it} / \rho_s \ , \qquad \textbf{(G.5)}$$

where

C_{it}	=	concentration of radionuclide i in disposal facility (μCi/m^3),
f_s	=	dilution factor for mixing of exhumed waste materials from disposal facility into soil in vegetable garden,
ρ_s	=	density of soil (kg/m^3).

In implementing the model, a dilution factor for mixing of exhumed waste materials from the disposal facility into native soil in the vegetable garden of 0.2 and a density of soil of 1,400 kg/m^3 are assumed, as in the model for the vegetable pathway described above. The consumption of contaminated soil from the vegetable garden is assumed to be 0.1 g per day (i.e., 0.037 kg per year), a value which is appropriate for average adults (EPA 1989).

The model for estimating dose from the soil ingestion pathway is summarized in Table G.9. The annual dose per unit concentration of a radionuclide in exhumed waste from the disposal facility at the time intrusion occurs is based on the model and parameter values described above and the ingestion dose conversion factors given in Table G.2.

External exposure pathways

External exposure of inadvertent intruders in the agriculture scenario is assumed to occur while working in the vegetable garden containing contaminated soil and while residing in the home on top of disposed waste. For external exposure (e) to contaminated soil while working in the vegetable garden, the annual EDE (rem per year) from radionuclide i is given by

$$H_{ie} = C_{is} U_s D_{is} \ , \qquad \textbf{(G.6)}$$

Table G.9. Annual effective dose equivalents to inadvertent intruders from soil ingestion pathway per unit concentration of radionuclides in disposal facility for agriculture scenario[a]

Nuclide[b]	Annual dose (rem/year per μCi/m³)	Nuclide	Annual dose (rem/year per μCi/m³)
^{3}H	3.4×10^{-10}	^{137}Cs	2.7×10^{-7}
^{10}Be	2.5×10^{-8}	^{151}Sm	2.1×10^{-9}
^{14}C	1.1×10^{-8}	^{152}Eu	3.4×10^{-8}
^{26}Al	8.0×10^{-8}	^{154}Eu	5.0×10^{-8}
^{36}Cl	1.6×10^{-8}	^{155}Eu	8.0×10^{-9}
^{40}K	1.0×10^{-7}	^{207}Bi	2.9×10^{-8}
^{41}Ca	4.9×10^{-9}	$^{210}Pb + d$	3.9×10^{-5}
^{60}Co	1.4×10^{-7}	^{226}Ra[d]	6.9×10^{-6}
^{59}Ni	1.1×10^{-9}	$^{229}Th + d$	2.1×10^{-5}
^{63}Ni	3.1×10^{-9}	^{230}Th	2.9×10^{-6}
^{79}Se	4.6×10^{-8}	$^{232}Th + d$	2.6×10^{-5}
^{87}Rb	2.6×10^{-8}	$^{231}Pa + d$	1.4×10^{-4}
$^{90}Sr + d$	8.0×10^{-7}	$^{232}U + d$	1.1×10^{-5}
^{93}Zr[c]	9.0×10^{-9}	^{233}U	1.5×10^{-6}
^{93m}Nb	2.8×10^{-9}	^{234}U	1.5×10^{-6}
^{94}Nb	3.8×10^{-8}	^{235}U	1.4×10^{-6}
^{99}Tc	8.0×10^{-9}	^{236}U	1.4×10^{-6}
^{107}Pd	8.0×10^{-10}	$^{238}U + d$	1.4×10^{-6}
^{113m}Cd	8.5×10^{-7}	^{237}Np	2.3×10^{-5}
^{121m}Sn	8.5×10^{-9}	^{238}Pu	1.7×10^{-5}
$^{126}Sn + d$	1.1×10^{-7}	^{239}Pu	1.9×10^{-5}
^{129}I	1.5×10^{-6}	^{240}Pu	1.9×10^{-5}
^{135}Cs	3.7×10^{-8}	^{241}Pu	3.6×10^{-7}

Table G.9 (continued)

Nuclide[b]	Annual dose (rem/year per μCi/m^3)	Nuclide	Annual dose (rem/year per μCi/m^3)
^{242}Pu	1.8×10^{-5}	^{245}Cm	2.0×10^{-5}
^{244}Pu	1.7×10^{-5}	^{246}Cm	2.0×10^{-5}
^{241}Am	1.9×10^{-5}	^{247}Cm	1.8×10^{-5}
^{242m}Am + d[e]	1.9×10^{-5}	^{248}Cm	7.4×10^{-5}
^{243}Am	1.9×10^{-5}	^{249}Cf	2.5×10^{-5}
^{243}Cm	1.3×10^{-5}	^{250}Cf	1.1×10^{-5}
^{244}Cm	1.1×10^{-5}	^{251}Cf	2.5×10^{-5}

[a]Values give 50-year committed EDEs from one year's intakes of soil.

[b]The notation "+ d" with some entries denotes short-lived decay products that are assumed to be in secular equilibrium with parent radionuclide; see Table G.1 for decay products and branching fractions.

[c]Possible contributions to dose from ^{93m}Nb decay product are not included.

[d]Possible contributions to dose from ^{210}Pb decay product are not included.

[e]Possible contributions to dose from ^{238}Pu decay product are not included.

where

C_{is} = concentration of radionuclide i in soil in vegetable garden (μCi/m^3),

U_s = fraction of the year during which external exposure to contaminated soil in vegetable garden occurs,

D_{is} = dose conversion factor for external exposure to radionuclide i in garden soil (rem/year per μCi/m^3).

As in the models for the vegetable and soil ingestion pathways described previously, the radionuclide concentrations in soil in the vegetable garden are given by

$$C_{is} = f_s C_{it} \ , \qquad \textbf{(G.7)}$$

where

C_{it} = concentration of radionuclide i in disposal facility (μCi/m^3),

f_s = dilution factor for mixing of exhumed waste materials from disposal facility into soil in vegetable garden.

In implementing the model, a dilution factor for mixing of exhumed waste materials from the disposal facility into native soil in the vegetable garden of 0.2 is assumed, as in the models for the vegetable and soil ingestion pathways described above. The fraction of the year during which external exposure while working in the garden occurs is assumed to be 0.01 (Oztunali et al. 1981); i.e., the assumed exposure time is about 100 hours per year.

The model for estimating external dose while working in the garden is summarized in Table G.10. The annual dose per unit concentration of a radionuclide in exhumed waste in the disposal facility at the time intrusion occurs is based on the model and parameter values described above and the external dose-rate conversion factors given in Table G.4.

For external exposure to exposed waste during indoor residence on top of the disposal facility, the annual EDE (rem per year) from radionuclide i is given by

$$H_{ie} = C_{it} U_t D_{it} S \ , \qquad \textbf{(G.8)}$$

where

C_{it} = concentration of radionuclide i in disposal facility (μCi/m^3),

U_t = fraction of the year during which external exposure to waste in disposal facility during indoor residence occurs,

D_{it} = dose conversion factor for external exposure to radionuclide i in disposal facility (rem/year per μCi/m^3),

S = shielding factor for radionuclides during indoor residence.

The shielding factor takes into account the reduction in external dose provided by the walls and floor of the home.

Table G.10. Annual effective dose equivalents to inadvertent intruders from external exposure while working in vegetable garden per unit concentration of radionuclides in disposal facility for agriculture scenario

Nuclide[a]	Annual dose (rem/year per μCi/m^3)	Nuclide	Annual dose (rem/year per μCi/m^3)
^{26}Al	1.8×10^{-5}	^{231}Pa + d	2.2×10^{-6}
^{40}K	1.1×10^{-6}	^{232}U + d	1.0×10^{-5}
^{60}Co	1.7×10^{-5}	^{235}U + d	9.6×10^{-7}
^{94}Nb	1.1×10^{-5}	^{238}U + d	1.5×10^{-7}
^{121m}Sn	2.4×10^{-9}	^{237}Np + d	1.3×10^{-6}
^{126}Sn + d	1.3×10^{-5}	^{244}Pu + d	2.2×10^{-6}
^{129}I	1.6×10^{-8}	^{241}Am	5.4×10^{-8}
^{137}Cs + d	3.8×10^{-6}	^{242m}Am + d	8.2×10^{-8}
^{152}Eu	7.6×10^{-6}	^{243}Am + d	1.1×10^{-6}
^{154}Eu	8.2×10^{-6}	^{243}Cm	7.0×10^{-7}
^{155}Eu	2.2×10^{-7}	^{245}Cm	4.2×10^{-7}
^{207}Bi	1.0×10^{-5}	^{247}Cm + d	2.1×10^{-6}
^{226}Ra + d	1.2×10^{-5}	^{249}Cf	2.2×10^{-6}
^{229}Th + d	1.9×10^{-6}	^{251}Cf	6.4×10^{-7}
^{232}Th + d	1.7×10^{-5}		

[a]The notation "+ d" with some entries denotes short-lived decay products that are assumed to be in secular equilibrium with parent radionuclide; see Table G.1 for decay products and branching fractions.

In implementing the model, the fraction of the year during which exposure in the home is assumed to occur is 0.5 (Oztunali et al. 1981); i.e., the assumed exposure time is about 4000 hours per year. The exposure time could be as much as a factor of two higher, but the assumed value is intended to be representative of an average individual residing on the disposal site. A shielding factor during indoor residence of 0.7 is assumed for all photon-emitting radionuclides (NRC 1977). This is a good approximation for all photon energies of concern.

The model for estimating external dose during indoor residence is summarized in Table G.11. The annual dose per unit concentration of a radionuclide in the disposal facility at the time intrusion occurs is based on the model and parameter values described above and the external dose-rate conversion factors for "No shielding" given in Table G.5.

Inhalation pathways

Inhalation exposure of inadvertent intruders in the agriculture scenario is assumed to occur while working in the vegetable garden containing contaminated soil and while residing in the home on top of disposed waste. For either exposure pathway, the annual committed EDE (rem per year) from inhalation of radionuclide i suspended into air (a) in particulate form is given by

$$H_{ia} = C_{ia} f_a U_a D_i \ , \qquad \textbf{(G.9)}$$

where

C_{ia} = concentration of radionuclide i in air (μCi/m^3),
f_a = fraction of the year during which inhalation exposure occurs,
U_a = annual air intake (m^3/year),
D_i = dose conversion factor for inhalation of radionuclide i (rem/μCi inhaled).

Concentrations of suspended radionuclides in air are estimated using a mass-loading model (Anspaugh et al. 1975), which is based on observations of airborne concentrations of naturally occurring materials, such as uranium and thorium, relative to their concentrations in surface soil. In a mass-loading model, airborne concentrations of radionuclides are given by

$$C_{ia} = C_{is} L_a / \rho_s \ , \qquad \textbf{(G.10)}$$

where

C_{is} = concentration of radionuclide i in surface soil (μCi/m^3),
L_a = atmospheric mass loading of surface soil (kg/m^3),
ρ_s = density of soil (kg/m^3).

This model is applied to all radionuclides except isotopes of radon and their short-lived decay products. The model for estimating inhalation dose due to radon released from contaminated soil or the disposal facility is described later in this section.

Table G.11. Annual effective dose equivalents to inadvertent intruders from external exposure during indoor residence per unit concentration of radionuclides in disposal facility for agriculture scenario

Nuclide[a]	Annual dose (rem/year per μCi/m³)	Nuclide	Annual dose (rem/year per μCi/m³)
^{26}Al	3.9×10^{-3}	$^{231}Pa + d$	4.2×10^{-4}
^{40}K	2.3×10^{-4}	$^{232}U + d$	2.2×10^{-3}
^{60}Co	3.5×10^{-3}	$^{235}U + d$	1.6×10^{-4}
^{94}Nb	2.1×10^{-3}	$^{238}U + d$	2.9×10^{-5}
^{121m}Sn	4.2×10^{-7}	$^{237}Np + d$	2.4×10^{-4}
$^{126}Sn + d$	2.6×10^{-3}	$^{244}Pu + d$	4.6×10^{-4}
^{129}I	2.8×10^{-6}	^{241}Am	9.5×10^{-6}
$^{137}Cs + d$	7.4×10^{-4}	$^{242m}Am + d$	1.5×10^{-5}
^{152}Eu	1.5×10^{-3}	$^{243}Am + d$	2.0×10^{-4}
^{154}Eu	1.7×10^{-3}	^{243}Cm	1.3×10^{-4}
^{155}Eu	3.9×10^{-5}	^{245}Cm	7.4×10^{-5}
^{207}Bi	2.1×10^{-3}	$^{247}Cm + d$	4.0×10^{-4}
$^{226}Ra + d$	2.4×10^{-3}	^{249}Cf	4.2×10^{-4}
$^{229}Th + d$	3.5×10^{-4}	^{251}Cf	1.2×10^{-4}
$^{232}Th + d$	3.5×10^{-3}		

[a]The notation "+ d" with some entries denotes short-lived decay products that are assumed to be in secular equilibrium with parent radionuclide; see Table G.1 for decay products and branching fractions.

For inhalation exposure while working in the vegetable garden, the concentration of radionuclide i in soil again is given by

$$C_{is} = f_s C_{it} \ , \qquad \textbf{(G.11)}$$

where

C_{it} = concentration of radionuclide i in disposal facility (μCi/m³),

f_s = dilution factor for mixing of exhumed waste materials from disposal facility into soil in vegetable garden.

In implementing the model, a dilution factor for mixing of exhumed waste materials from the disposal facility into native soil in the garden of 0.2, a density of soil of 1400 kg/m^3, and a fraction of the year during which exposure while working in the garden occurs of 0.01 (i.e., about 100 hours per year) again are assumed, as in the model for external exposure while working in the garden described above. The annual air intake (i.e., breathing rate) is assumed to be 8000 m^3 (NRC 1977). Finally, the atmospheric mass loading of contaminated soil while working in the garden is assumed to be 10^{-7} kg/m^3.

The assumed atmospheric mass loading of contaminated soil while working in the vegetable garden of 10^{-7} kg/m^3 is somewhat greater than the average background dust loading for nonurban areas in the United States of about 4×10^{-8} kg/m^3 (Anspaugh et al. 1975). Furthermore, the assumed value is in good agreement with an average dust loading of 6×10^{-8} kg/m^3 measured above two agricultural fields at the Savannah River Site (Shinn, Norman, and Gay 1982), where meteorological conditions and soil moisture levels should be similar to those on ORR. The choice of an atmospheric mass loading for this exposure pathway is based primarily on these data, but it also takes into account the following considerations.

Some gardening activities should increase atmospheric concentrations of suspended soil well above average background levels. However, for the following reasons, the average concentration during all gardening activities on ORR probably would not be much greater than the average background level in the United States. First, the average background level of suspended soil originating from ORR should be substantially lower than the average level in the United States due to the high annual precipitation, extensive vegetation, and low average wind speed at the site. Second, at any location, airborne concentrations of suspended soil consist of material originating from a wide area, not just from the particular location where inhalation exposures occur. Finally, the model assumes that all suspended soil particles are respirable. However, particularly during more vigorous gardening activities, such as hoeing and tilling, which could result in unusually high atmospheric mass loadings, some particles are likely to be too large to be respirable.

Taking the available data and the other factors described above into account, the choice of 10^{-7} kg/m^3 to represent the average atmospheric mass loading during gardening activities on ORR appears to be a reasonable assumption for this parameter.

The model for estimating inhalation dose while working in the garden is summarized in Table G.12. The annual dose per unit concentration of a radionuclide in exhumed waste in the disposal facility at the time intrusion occurs is based on the model and parameter values described above and the inhalation dose conversion factors given in Table G.3. Again, the results for isotopes of radon are estimated using a model described later in this section.

Table G.12. Annual effective dose equivalents to inadvertent intruders from inhalation exposure while working in vegetable garden per unit concentration of radionuclides in disposal facility for agriculture scenario[a]

Nuclide[b]	Annual dose (rem/year per μCi/m^3)	Nuclide	Annual dose (rem/year per μCi/m^3)
^{3}H	7.0×10^{-14}	^{137}Cs	3.5×10^{-11}
^{10}Be	3.9×10^{-10}	^{151}Sm	3.3×10^{-11}
^{14}C	2.5×10^{-12}	^{152}Eu	2.4×10^{-10}
^{26}Al	8.8×10^{-11}	^{154}Eu	3.2×10^{-10}
^{36}Cl	2.4×10^{-11}	^{155}Eu	4.5×10^{-11}
^{40}K	1.3×10^{-11}	^{207}Bi	2.2×10^{-11}
^{41}Ca	1.4×10^{-12}	^{210}Pb + d	2.5×10^{-8}
^{60}Co	2.4×10^{-10}	^{226}Ra[d,e]	9.5×10^{-9}
^{59}Ni	1.4×10^{-12}	^{222}Rn	1.3×10^{-4}
^{63}Ni	3.4×10^{-12}	^{229}Th	1.9×10^{-6}
^{79}Se	7.2×10^{-12}	^{230}Th	2.9×10^{-7}
^{87}Rb	3.5×10^{-12}	^{232}Th + d[e]	1.7×10^{-6}
^{90}Sr + d	2.8×10^{-10}	^{220}Rn	2.1×10^{-5}
^{93}Zr[c]	3.5×10^{-10}	^{231}Pa + d	8.8×10^{-6}
^{93m}Nb	3.2×10^{-11}	^{232}U + d[e]	1.1×10^{-6}
^{94}Nb	4.5×10^{-10}	^{220}Rn	2.1×10^{-5}
^{99}Tc	1.1×10^{-12}	^{233}U	1.5×10^{-7}
^{107}Pd	1.3×10^{-11}	^{234}U	1.4×10^{-7}
^{113m}Cd	1.7×10^{-9}	^{235}U	1.3×10^{-7}
^{121m}Sn	1.3×10^{-11}	^{236}U	1.4×10^{-7}
^{126}Sn + d	1.1×10^{-10}	^{238}U	1.3×10^{-7}
^{129}I	1.9×10^{-10}	^{237}Np	5.9×10^{-7}
^{135}Cs	5.1×10^{-12}	^{238}Pu	4.3×10^{-7}

Table G.12 (continued)

Nuclide[b]	Annual dose (rem/year per μCi/m^3)	Nuclide	Annual dose (rem/year per μCi/m^3)
^{239}Pu	4.7×10^{-7}	^{244}Cm	2.8×10^{-7}
^{240}Pu	4.7×10^{-7}	^{245}Cm	5.1×10^{-7}
^{241}Pu	9.1×10^{-9}	^{246}Cm	5.0×10^{-7}
^{242}Pu	4.5×10^{-7}	^{247}Cm	4.5×10^{-7}
^{244}Pu	4.4×10^{-7}	^{248}Cm	1.9×10^{-6}
^{241}Am	4.8×10^{-7}	^{249}Cf	6.4×10^{-7}
^{242m}Am + d[f]	4.9×10^{-7}	^{250}Cf	2.9×10^{-7}
^{243}Am	4.8×10^{-7}	^{251}Cf	6.5×10^{-7}
^{243}Cm	3.4×10^{-7}		

[a]Values give 50-year committed effective dose equivalents from one year's intakes of air.

[b]The notation "+ d" with some entries denotes short-lived decay products that are assumed to be in secular equilibrium with parent radionuclide; see Table G.1 for decay products and branching fractions.

[c]Possible contributions to dose from ^{93m}Nb decay product are not included.

[d]Possible contributions to dose from ^{210}Pb decay product are not included.

[e]Contribution to dose from radon decay product is listed separately.

[f]Possible contributions to dose from ^{238}Pu decay product are not included.

For inhalation exposures while residing in the home, the airborne concentration of radionuclide i is given by

$$C_{ia} = C_{it} L_a / \rho_s \ , \qquad \textbf{(G.12)}$$

where

C_{it} = concentration of radionuclide i in disposal facility (μCi/m^3),
L_a = mass loading of soil in the atmosphere (kg/m^3),
ρ_s = density of soil (kg/m^3).

In implementing the model, a density of soil of 1400 kg/m^3, a fraction of the year during which exposure in the home occurs of 0.5 (i.e., about 4000 hours per year), and an annual air intake of 8000 m^3 again are assumed, as in the models for other exposure pathways. The atmospheric mass loading of contaminated soil at the location of the home on top of the disposal facility is assumed to be 10^{-8} kg/m^3, which is approximately one-fourth of the average dust loading in the United States (Anspaugh et al. 1975). The assumed atmospheric mass loading is based on the following considerations.

From the previous discussion of the atmospheric mass loading of contaminated soil while working in the vegetable garden, it seems unreasonable to assume that the mass loading of largely undisturbed surface soil on ORR during indoor residence would be as high as the average dust loading in the United States. The assumption that the average mass loading at the disposal site is one-fourth of the average background level in the United States is intended to take into account the abundant precipitation, extensive vegetation, and low average wind speed at the disposal site, as well as the presence of uncontaminated soil suspended from other locations. In addition, the model for inhalation exposure indoors does not take into account that indoor concentrations of suspended soil particles may be somewhat less than the concentrations outdoors, e.g., due to filtering of air by doors and windows.

The model for estimating inhalation dose during indoor residence is summarized in Table G.13. The annual dose per unit concentration of a radionuclide in the disposal facility at the time intrusion occurs is based on the model and parameter values described above and the inhalation dose conversion factors given in Table G.3. The results for isotopes of radon are estimated using the model described below.

In this analysis, doses from inhalation of radon and its short-lived decay products while working in the vegetable garden containing contaminated soil or while residing in a home of top of exposed waste in the disposal facility are estimated using a natural analog model. Specifically, estimated average doses from indoor and outdoor exposure to ^{222}Rn and ^{220}Rn, which result from known average concentrations of their respective parent radionuclides ^{226}Ra and ^{232}Th in surface soil, are used to estimate doses from the radon isotopes per unit concentration of the parent radionuclides in disposed waste for the inhalation pathways considered in the agriculture scenario. The analysis based on the natural analog model proceeds as follows.

Table G.13. Annual effective dose equivalents to inadvertent intruders from inhalation exposure during indoor residence per unit concentration of radionuclides in disposal facility for agriculture scenario[a]

Nuclide[b]	Annual dose (rem/year per μCi/m³)	Nuclide	Annual dose (rem/year per μCi/m³)
^{3}H	1.9×10^{-12}	^{137}Cs	9.3×10^{-10}
^{10}Be	1.0×10^{-8}	^{151}Sm	8.7×10^{-10}
^{14}C	6.1×10^{-11}	^{152}Eu	6.4×10^{-9}
^{26}Al	2.3×10^{-9}	^{154}Eu	8.4×10^{-9}
^{36}Cl	6.4×10^{-10}	^{155}Eu	1.2×10^{-9}
^{40}K	3.5×10^{-10}	^{207}Bi	5.8×10^{-10}
^{41}Ca	3.8×10^{-11}	$^{210}Pb + d$	6.7×10^{-7}
^{60}Co	6.4×10^{-9}	^{226}Ra[d,e]	2.5×10^{-7}
^{59}Ni	3.8×10^{-11}	^{222}Rn	1.2×10^{-1}
^{63}Ni	9.0×10^{-11}	^{229}Th	4.9×10^{-5}
^{79}Se	1.9×10^{-10}	^{230}Th	7.5×10^{-6}
^{87}Rb	9.3×10^{-11}	$^{232}Th + d$[e]	4.4×10^{-5}
$^{90}Sr + d$	7.3×10^{-9}	^{220}Rn	1.0×10^{-2}
^{93}Zr[c]	9.3×10^{-9}	$^{231}Pa + d$	2.3×10^{-4}
^{93m}Nb	8.4×10^{-10}	$^{232}U + d$[e]	2.9×10^{-5}
^{94}Nb	1.2×10^{-8}	^{220}Rn	1.0×10^{-2}
^{99}Tc	2.9×10^{-11}	^{233}U	4.1×10^{-6}
^{107}Pd	3.5×10^{-10}	^{234}U	3.8×10^{-6}
^{113m}Cd	4.4×10^{-8}	^{235}U	3.5×10^{-6}
^{121m}Sn	3.5×10^{-10}	^{236}U	3.8×10^{-6}
$^{126}Sn + d$	2.9×10^{-9}	^{238}U	3.5×10^{-6}
^{129}I	4.9×10^{-9}	^{237}Np	1.6×10^{-5}
^{135}Cs	1.3×10^{-10}	^{238}Pu	1.1×10^{-5}

Table G.13 (continued)

Nuclide[b]	Annual dose (rem/year per μCi/m³)	Nuclide	Annual dose (rem/year per μCi/m³)
^{239}Pu	1.2×10^{-5}	^{244}Cm	7.3×10^{-6}
^{240}Pu	1.2×10^{-5}	^{245}Cm	1.3×10^{-5}
^{241}Pu	2.4×10^{-7}	^{246}Cm	1.3×10^{-5}
^{242}Pu	1.2×10^{-5}	^{247}Cm	1.2×10^{-5}
^{244}Pu	1.2×10^{-5}	^{248}Cm	4.9×10^{-5}
^{241}Am	1.3×10^{-5}	^{249}Cf	1.7×10^{-5}
^{242m}Am + d[f]	1.3×10^{-5}	^{250}Cf	7.5×10^{-6}
^{243}Am	1.3×10^{-5}	^{251}Cf	1.7×10^{-5}
^{243}Cm	9.0×10^{-6}		

[a]Values give 50-year committed EDEs from one year's intakes of air.

[b]The notation "+ d" with some entries denotes short-lived decay products that are assumed to be in secular equilibrium with parent radionuclide; see Table G.1 for decay products and branching fractions.

[c]Possible contributions to dose from ^{93m}Nb decay product are not included.

[d]Possible contributions to dose from ^{210}Pb decay product are not included.

[e]Contribution to dose from radon decay product is listed separately.

[f]Possible contributions to dose from ^{238}Pu decay product are not included.

The National Council on Radiation Protection and Measurements (NCRP 1987) has estimated that the average EDE from exposure to radon in the United States is about 0.2 rem per year. This estimate applies only to exposure to ^{222}Rn and its short-lived decay products in homes and, furthermore, assumes continuous residence indoors (NCRP 1987). The estimated dose from ^{222}Rn indoors results from an average concentration of the parent radionuclide ^{226}Ra in surface soil of about 0.6 pCi/g (NCRP 1984), which, for an average bulk density of soil of 1.4 g/cm^3 (Baes and Sharp 1983), corresponds to 0.84 μCi/m^3. Therefore, for continuous residence indoors, the annual EDE from exposure to ^{222}Rn and its short-lived decay products per unit concentration of ^{226}Ra in surface soil is estimated as follows:

^{222}Rn, continuous residence indoors

(0.2 rem/year)/(0.84 μCi/m^3) = 0.24 rem/year per μCi/m^3 .

For application to the agriculture scenario, the average dose from ^{222}Rn during continuous residence indoors can be used to estimate the dose from inhalation during indoor residence in a home on top of exposed waste in the disposal facility containing ^{226}Ra by taking into account the fraction of the year during which residence in the home at the disposal site occurs. As described previously, this factor is assumed to be 0.5. Therefore, for inhalation exposure while residing in a home on top of exposed waste in the disposal facility, the annual EDE from ^{222}Rn and its short-lived decay products per unit concentration of ^{226}Ra in the disposal facility is estimated as follows:

^{222}Rn, indoor residence in agriculture scenario

(0.24 rem/year per μCi/m^3)(0.5) = 0.12 rem/year per μCi/m^3 .

This dose estimate is given in Table G.13.

The agriculture scenario also considers inhalation doses while working in a vegetable garden containing contaminated soil. The inhalation dose from ^{222}Rn while working in the vegetable garden contaminated with ^{226}Ra is estimated as follows. The United Nations Scientific Committee on the Effects of Atomic Radiation (UNSCEAR 1988) has estimated that, for continuous exposure, the average EDE from outdoor ^{222}Rn would be about 28% of the average dose from indoor ^{222}Rn. Therefore, for continuous exposure outdoors, the annual EDE from ^{222}Rn and its short-lived decay products per unit concentration of ^{226}Ra in surface soil is estimated from the previous result for continuous indoor residence as follows:

^{222}Rn, continuous exposure outdoors

(0.24 rem/year per μCi/m^3)(0.28) = 0.067 rem/year per μCi/m^3 .

The dose from ^{222}Rn during continuous exposure outdoors can be used to estimate the dose from inhalation while working in the vegetable garden containing ^{226}Ra by applying two corrections. The first is the fraction of the year that an intruder spends working in the garden, which is assumed to be 0.01. The second is the dilution factor for mixing of radionuclides in exhumed waste materials from the disposal facility into soil in the garden, which is assumed to be 0.2. Therefore, for inhalation exposure while working in the vegetable garden, the annual EDE from ^{222}Rn and its short-lived decay products per unit concentration of ^{226}Ra in exhumed waste is estimated as follows:

^{222}Rn, exposure in vegetable garden in agriculture scenario

$(0.067 \text{ rem/year per } \mu\text{Ci/m}^3)(0.01)(0.2) = 1.3 \times 10^{-4} \text{ rem/year per } \mu\text{Ci/m}^3$.

This dose estimate is given in Table G.12.

The dose estimates for inhalation exposure to ^{220}Rn and its short-lived decay products during indoor residence and while working in the vegetable garden are obtained from the data on average doses from indoor and outdoor exposure to ^{222}Rn presented above and the following information. First, for continuous residence, the average dose from indoor ^{220}Rn is estimated to be about 14% of the average dose from indoor ^{222}Rn, and the average dose from outdoor ^{220}Rn is estimated to be about 26% of the average dose from outdoor ^{222}Rn (UNSCEAR 1988). Second, the estimated doses from ^{220}Rn result from an average concentration of the parent radionuclide ^{232}Th in surface soil of about 1 pCi/g (NCRP 1984), which, for an average bulk density of soil of 1.4 g/cm^3 (Baes and Sharp 1983), corresponds to 1.4 μCi/m^3.

Using the data on doses from ^{222}Rn for continuous residence indoors and outdoors presented previously, the data on doses from ^{220}Rn relative to the doses from ^{222}Rn and the average concentration of ^{232}Th in surface soil given above, and the assumptions in the agriculture scenario for the indoor residence time, the residence time while working in the vegetable garden, and the dilution factor for mixing of exhumed waste materials in garden soil, the following dose estimates for ^{220}Rn are obtained. For inhalation exposure while residing in a home on top of exposed waste in the disposal facility, the annual effective dose equivalent from ^{220}Rn and its short-lived decay products per unit concentration of ^{232}Th in the disposal facility is estimated as follows:

^{220}Rn, indoor residence in agriculture scenario

$(0.2 \text{ rem/year})(0.14)(0.5)/(1.4\ \mu\text{Ci/m}^3) = 0.010 \text{ rem/year per } \mu\text{Ci/m}^3$.

This dose estimate is given in Table G.13.

For inhalation exposure while working in the vegetable garden, the annual EDE from ^{220}Rn and its short-lived decay products per unit concentration of ^{232}Th in exhumed waste is estimated as follows:

^{220}Rn, exposure in vegetable garden in agriculture scenario

$$(0.2 \text{ rem/year})(0.28)(0.26)(0.01)(0.2)/(1.4\ \mu\text{Ci/m}^3) = 2.1 \times 10^{-5} \text{ rem/year per } \mu\text{Ci/m}^3 \ .$$

This dose estimate is given in Table G.12. The annual doses per unit concentration for ^{220}Rn during indoor residence and while working in the vegetable garden given above also apply to ^{220}Rn produced in the decay of ^{232}U.

All pathways

For the agriculture scenario, the annual doses to an inadvertent intruder from all exposure pathways per unit concentration of radionuclides in the disposal facility at the time intrusion is assumed to occur are summarized in Table G.14. The total dose for each radionuclide is the sum of the doses from the vegetable, soil ingestion, external exposure, and inhalation pathways summarized in Tables G.8–G.13.

On the basis of the models and parameter values assumed in the dose analysis for the agriculture scenario, the most important exposure pathways depend on the particular radionuclide. For the fission and activation products and ^{210}Pb, the vegetable pathway is the most important unless the radionuclide is a photon emitter, in which case external exposure while residing in the home is the most important pathway. For ^{226}Ra, ^{232}Th, and ^{232}U, inhalation of radon and its short-lived decay products while residing in the home is the most important pathway. However, if the dose from radon is excluded, external exposure while residing in the home is the most important pathway for ^{226}Ra and the actinide radioelements when the isotope emits significant intensities of high-energy photons, but the vegetable and soil ingestion pathways and inhalation exposure while residing in the home usually are significant contributors to the total dose when the isotope is not a high-energy photon emitter. For many of the actinide radioelements, the soil ingestion pathway is more important than the vegetable pathway, due to the low plant-to-soil concentration ratios in vegetables assumed for most of these elements.

The different pathways assumed in the agriculture scenario can be divided into those involving exposure to contaminated soil in the intruder's vegetable garden (i.e., vegetable, soil ingestion, external exposure, and inhalation pathways) and exposure to waste during indoor residence on top of the disposal facility (i.e., external exposure and inhalation pathways). For some radionuclides (e.g., ^{90}Sr), the total dose from all exposure pathways is dominated by the exposures to contaminated soil in the vegetable garden, whereas for other radionuclides (e.g., ^{137}Cs), the total dose is dominated by the exposures to waste in the disposal facility.

Table G.14. Annual effective dose equivalents to inadvertent intruders from all exposure pathways per unit concentration of radionuclides in disposal facility for agriculture scenario[a]

Nuclide[b]	Annual dose (rem/year per μCi/m^3)	Nuclide	Annual dose (rem/year per μCi/m^3)
^{3}H	4.0×10^{-6}	^{137}Cs + d	7.5×10^{-4}
^{10}Be	7.5×10^{-8}	^{151}Sm	1.2×10^{-8}
^{14}C	1.5×10^{-5}	^{152}Eu	1.5×10^{-3}
^{26}Al	3.9×10^{-3}	^{154}Eu	1.7×10^{-3}
^{36}Cl	1.2×10^{-3}	^{155}Eu	3.9×10^{-5}
^{40}K	2.9×10^{-4}	^{207}Bi	2.1×10^{-3}
^{41}Ca	2.5×10^{-6}	^{210}Pb + d	3.1×10^{-4}
^{60}Co	3.5×10^{-3}	^{226}Ra + d[d,e]	2.4×10^{-3}
^{59}Ni	7.2×10^{-8}	^{222}Rn	1.2×10^{-1}
^{63}Ni	2.0×10^{-7}	^{229}Th + d	4.3×10^{-4}
^{79}Se	1.2×10^{-6}	^{230}Th	1.1×10^{-5}
^{87}Rb	1.9×10^{-6}	^{232}Th + d[e]	3.6×10^{-3}
^{90}Sr + d	2.0×10^{-4}	^{220}Rn	1.0×10^{-2}
^{93}Zr[c]	2.4×10^{-8}	^{231}Pa + d	8.5×10^{-4}
^{93m}Nb	1.9×10^{-8}	^{232}U + d[e]	2.3×10^{-3}
^{94}Nb	2.1×10^{-3}	^{220}Rn	1.0×10^{-2}
^{99}Tc	1.3×10^{-5}	^{233}U	1.2×10^{-5}
^{107}Pd	3.4×10^{-8}	^{234}U	1.2×10^{-5}
^{113m}Cd	1.4×10^{-4}	^{235}U + d	1.7×10^{-4}
^{121m}Sn	4.8×10^{-7}	^{236}U	1.1×10^{-5}
^{126}Sn + d	2.6×10^{-3}	^{238}U + d	4.0×10^{-5}
^{129}I	8.4×10^{-5}	^{237}Np + d	5.3×10^{-4}
^{135}Cs	1.2×10^{-6}	^{238}Pu	2.9×10^{-5}

Table G.14 (continued)

Nuclide[b]	Annual dose (rem/year per μCi/m³)	Nuclide	Annual dose (rem/year per μCi/m³)
^{239}Pu	3.2×10^{-5}	^{244}Cm	1.9×10^{-5}
^{240}Pu	3.2×10^{-5}	^{245}Cm	1.1×10^{-4}
^{241}Pu	6.3×10^{-7}	^{246}Cm	3.4×10^{-5}
^{242}Pu	3.1×10^{-5}	$^{247}Cm + d$	4.3×10^{-4}
$^{244}Pu + d$	4.9×10^{-4}	^{248}Cm	1.3×10^{-4}
^{241}Am	4.7×10^{-5}	^{249}Cf	4.7×10^{-4}
$^{242m}Am + d$[f]	5.3×10^{-5}	^{250}Cf	1.9×10^{-5}
$^{243}Am + d$	2.4×10^{-4}	^{251}Cf	1.6×10^{-4}
^{243}Cm	1.5×10^{-4}		

[a]Values give sum of EDEs per unit concentration in disposal facility for vegetable, soil ingestion, external exposure, and inhalation pathways given in Tables G.8, G.9, G.10 and G.11, and G.12 and G.13, respectively.

[b]The notation "+ d" with some entries denotes short-lived decay products that are assumed to be in secular equilibrium with parent radionuclide; see Table G.1 for decay products and branching fractions.

[c]Possible contributions to dose from ^{93m}Nb decay product are not included.

[d]Possible contributions to dose from ^{210}Pb decay product are not included.

[e]Contribution to dose from radon decay product is listed separately.

[f]Possible contributions to dose from ^{238}Pu decay product are not included.

Summing the doses from all exposure pathways to obtain the results in Table G.14 assumes implicitly that the ratio of the volume of radioactive waste to the volume of uncontaminated waste materials which is excavated from the disposal facility and mixed with native soil in the vegetable garden is the same as the ratio of the volume of radioactive waste to the volume of uncontaminated waste materials in the disposal facility itself. However, the disposal facility is expected to be constructed with a cover of uncontaminated material, and the fraction of the volume of excavated material that contains radioactive waste thus would be substantially less than the corresponding fraction of the volume of exposed materials remaining in the disposal facility after excavation. Therefore, for the agriculture scenario, it is useful to separate the dose per unit concentration for the vegetable, soil ingestion, external exposure, and inhalation pathways due to exposure to contaminated soil in the vegetable garden given in Tables G.8, G.9, G.10, and G.12, respectively, from the dose for the external exposure and inhalation pathways due to exposure during indoor residence on top of the disposal facility given in Tables G.11 and G.13, respectively. A summary of the results of the dose analysis for the agriculture scenario in this form is given in Table G.15.

G.5.2.2 Resident Scenario

In the resident scenario, an inadvertent intruder is assumed to construct a home on top of the disposal facility, as in the agriculture scenario described in Sect. G.5.2.1. However, in digging a foundation for a home, an intruder is assumed to encounter an intact engineered barrier above the waste that cannot be penetrated by normal excavation procedures, and the home is assumed to be located on top of the intact barrier, rather than on top of exposed waste as in the agriculture scenario. An intruder then is assumed to receive external exposure while residing in the home on top of the disposal facility, but ingestion exposure and inhalation exposure to radionuclides in particulate form are precluded by the presence of an intact engineered barrier. Inhalation of radon and its short-lived decay products during indoor residence also is assumed to be mitigated by the presence of an intact barrier above the waste.

External exposure while residing in the home in the resident scenario is estimated using the model given in Eq. (G.8). As in the agriculture scenario described in Sect. G.5.2.1, the fraction of the year during which external exposure in the home occurs is assumed to be 0.5, and the shielding factor for all photon-emitting radionuclides during indoor residence is assumed to be 0.7. For each photon-emitting radionuclide, the dose conversion factor for external exposure is the dose-equivalent rate per unit concentration in the disposal facility taking into account the shielding provided by the source region and by the engineered barrier on top of the disposal facility. The intact engineered barrier consists essentially of the reinforced concrete top of each waste vault plus the layer of grout between the top of the waste box and the top of the vault, and these layers are assumed to provide shielding equivalent to a layer of soil 30 cm thick.

The model for estimating external dose in the resident scenario is summarized in Table G.16. The annual dose per unit concentration of a radionuclide in the disposal facility at the time intrusion

Table G.15. Annual effective dose equivalents (rem/year per μCi/m³) for agriculture scenario for inadvertent intruders per unit concentration of radionuclides in disposal facility from exposure to contaminated soil in vegetable garden and exposure during residence on disposal site[a]

Nuclide[b]	Garden pathways	Residence pathways	Nuclide	Garden pathways	Residence pathways
^{3}H	4.0×10^{-6}	1.9×10^{-12}	$^{126}Sn + d$	1.4×10^{-5}	2.6×10^{-3}
^{10}Be	6.5×10^{-8}	1.0×10^{-8}	^{129}I	8.2×10^{-5}	2.8×10^{-6}
^{14}C	1.5×10^{-5}	6.1×10^{-11}	^{135}Cs	1.2×10^{-6}	1.3×10^{-10}
^{26}Al	1.8×10^{-5}	3.9×10^{-3}	$^{137}Cs + d$	1.3×10^{-5}	7.4×10^{-4}
^{36}Cl	1.2×10^{-3}	6.4×10^{-10}	^{151}Sm	1.1×10^{-8}	8.7×10^{-10}
^{40}K	6.0×10^{-5}	2.3×10^{-4}	^{152}Eu	7.8×10^{-6}	1.5×10^{-3}
^{41}Ca	2.5×10^{-6}	3.8×10^{-11}	^{154}Eu	8.5×10^{-6}	1.7×10^{-3}
^{60}Co	1.8×10^{-5}	3.5×10^{-3}	^{155}Eu	2.6×10^{-7}	3.9×10^{-5}
^{59}Ni	7.2×10^{-8}	3.8×10^{-11}	^{207}Bi	1.0×10^{-5}	2.1×10^{-3}
^{63}Ni	2.0×10^{-7}	9.0×10^{-11}	$^{210}Pb + d$	3.1×10^{-4}	6.7×10^{-7}
^{79}Se	1.2×10^{-6}	1.9×10^{-10}	$^{226}Ra + d$[d,e]	3.0×10^{-5}	2.4×10^{-3}
^{87}Rb	1.9×10^{-6}	9.3×10^{-11}	^{222}Rn	1.3×10^{-4}	1.2×10^{-1}
$^{90}Sr + d$	2.0×10^{-4}	7.3×10^{-9}	$^{229}Th + d$	3.0×10^{-5}	4.0×10^{-4}
^{93}Zr[c]	1.4×10^{-8}	9.3×10^{-9}	^{230}Th	3.5×10^{-6}	7.5×10^{-6}
^{93m}Nb	1.8×10^{-8}	8.4×10^{-10}	$^{232}Th + d$[e]	6.4×10^{-5}	3.5×10^{-3}
^{94}Nb	1.1×10^{-5}	2.1×10^{-3}	^{220}Rn	2.1×10^{-5}	1.0×10^{-2}
^{99}Tc	1.3×10^{-5}	2.9×10^{-11}	$^{231}Pa + d$	2.0×10^{-4}	6.5×10^{-4}
^{107}Pd	3.4×10^{-8}	3.5×10^{-10}	$^{232}U + d$[e]	5.7×10^{-5}	2.2×10^{-3}
^{113m}Cd	1.4×10^{-4}	4.4×10^{-8}	^{220}Rn	2.1×10^{-5}	1.0×10^{-2}
^{121m}Sn	6.5×10^{-8}	4.2×10^{-7}	^{233}U	8.1×10^{-6}	4.1×10^{-6}

Table G.15 (continued)

Nuclide[b]	Garden pathways	Residence pathways	Nuclide	Garden pathways	Residence pathways
^{234}U	7.8×10^{-6}	3.8×10^{-6}	$^{242m}Am + d$[f]	2.5×10^{-5}	2.8×10^{-5}
$^{235}U + d$	8.5×10^{-6}	1.6×10^{-4}	$^{243}Am + d$	2.6×10^{-5}	2.1×10^{-4}
^{236}U	7.5×10^{-6}	3.8×10^{-6}	^{243}Cm	1.4×10^{-5}	1.4×10^{-4}
$^{238}U + d$	7.2×10^{-6}	3.3×10^{-5}	^{244}Cm	1.1×10^{-5}	7.3×10^{-6}
$^{237}Np + d$	2.7×10^{-4}	2.6×10^{-4}	^{245}Cm	2.1×10^{-5}	8.7×10^{-5}
^{238}Pu	1.8×10^{-5}	1.1×10^{-5}	^{246}Cm	2.1×10^{-5}	1.3×10^{-5}
^{239}Pu	2.0×10^{-5}	1.2×10^{-5}	$^{247}Cm + d$	2.1×10^{-5}	4.1×10^{-4}
^{240}Pu	2.0×10^{-5}	1.2×10^{-5}	^{248}Cm	7.7×10^{-5}	4.9×10^{-5}
^{241}Pu	3.9×10^{-7}	2.4×10^{-7}	^{249}Cf	2.8×10^{-5}	4.4×10^{-4}
^{242}Pu	1.9×10^{-5}	1.2×10^{-5}	^{250}Cf	1.1×10^{-5}	7.5×10^{-6}
$^{244}Pu + d$	2.0×10^{-5}	4.7×10^{-4}	^{251}Cf	2.7×10^{-5}	1.4×10^{-4}
^{241}Am	2.5×10^{-5}	2.3×10^{-5}			

[a]Values for pathways involving exposure to contaminated soil in vegetable garden are sum of values given in Tables G.8, G.9, G.10, and G.12, and values for pathways involving exposure during indoor residence on top of disposal facility are sum of values given in Tables G.11 and G.13.

[b]The notation "+ d" with some entries denotes short-lived decay products that are assumed to be in secular equilibrium with parent radionuclide; see Table G.1 for decay products and branching fractions.

[c]Possible contributions to dose from ^{93m}Nb decay product are not included.

[d]Possible contributions to dose from ^{210}Pb decay product are not included.

[e]Contribution to dose from radon decay product is listed separately.

[f]Possible contributions to dose from ^{238}Pu decay product are not included.

Table G.16. Annual effective dose equivalents to inadvertent intruders per unit concentration of radionuclides in disposal facility for resident scenario[a]

Nuclide[b]	Annual dose (rem/year per μCi/m³)	Nuclide	Annual dose (rem/year per μCi/m³)
^{26}Al	3.3×10^{-4}	$^{231}Pa + d$	7.0×10^{-6}
^{40}K	2.1×10^{-5}	$^{232}U + d$	2.3×10^{-4}
^{60}Co	2.9×10^{-4}	$^{235}U + d$	5.6×10^{-7}
^{94}Nb	1.1×10^{-4}	$^{238}U + d$	1.2×10^{-6}
$^{126}Sn + d$	1.1×10^{-4}	$^{237}Np + d$	3.5×10^{-6}
$^{137}Cs + d$	3.2×10^{-5}	$^{244}Pu + d$	2.1×10^{-5}
^{152}Eu	9.8×10^{-5}	$^{242m}Am + d$	2.5×10^{-7}
^{154}Eu	1.1×10^{-4}	$^{243}Am + d$	1.1×10^{-6}
^{155}Eu	2.0×10^{-8}	^{243}Cm	1.1×10^{-7}
^{207}Bi	1.2×10^{-4}	^{245}Cm	9.8×10^{-8}
$^{226}Ra + d$	1.9×10^{-4}	$^{247}Cm + d$	8.4×10^{-6}
$^{229}Th + d$	1.1×10^{-5}	^{249}Cf	8.1×10^{-6}
$^{232}Th + d$	3.0×10^{-4}	^{251}Cf	3.9×10^{-7}

[a]Values give EDEs per unit concentration of radionuclides in disposal facility from one year's external exposure during indoor residence on top of waste covered with intact engineered barriers of thickness 30 cm.

[b]The notation "+ d" with some entries denotes short-lived decay products that are assumed to be in secular equilibrium with parent radionuclide; see Table G.1 for decay products and branching fractions.

occurs is obtained from the assumed exposure time and shielding factor during indoor residence given above and the external dose-rate conversion factors for "30-cm shielding" given in Table G.5.

G.5.2.3 Post-Drilling Scenario

In the post-drilling scenario, an inadvertent intruder is assumed to drill through a disposal unit (e.g., for the purpose of constructing a well for a domestic water supply), and the entire amount of drilling waste is assumed to be mixed with native soil in the intruder's vegetable garden. The intruder then receives a chronic exposure to the contaminated garden soil, and the exposure pathways assumed for this scenario include (1) ingestion of vegetables grown in the contaminated garden soil, (2) direct ingestion of contaminated soil in conjunction with vegetable intakes, (3) external exposure to contaminated soil while working in the garden, and (4) inhalation of suspended activity while working in the garden.

The exposure pathways for the post-drilling scenario are conceptually the same as the corresponding four garden pathways for the agriculture scenario described in Sect. G.5.2.1. External and inhalation exposures during indoor residence do not occur in the post-drilling scenario, because all of the exhumed waste is assumed to be mixed with native soil in the vegetable garden and the intruder's home is assumed not to be located on top of the disposal facility. Therefore, the models given by Eqs. (G.2) and (G.3) for the vegetable pathway, Eqs. (G.4) and (G.5) for the soil ingestion pathway, Eqs. (G.6) and (G.7) for external exposure while working in the garden, and Eqs. (G.9), (G.10), and (G.11) for inhalation exposure while working in the garden, as well as the natural analog model for estimating inhalation dose from exposure to radon and its short-lived decay products while working in the garden, also apply to the post-drilling scenario.

In implementing the exposure pathway models for the post-drilling scenario, most of the parameter values are the same as the values assumed for the agriculture scenario. The one exception is the dilution factor for mixing of exhumed waste materials from the disposal facility with native soil in the vegetable garden, which is denoted by f_s. For all exposure pathways in the post-drilling scenario, the dose per unit concentration of a radionuclide in the disposal facility is directly proportional to this dilution factor.

With the assumption in the post-drilling scenario that all drilling waste is mixed with native soil in the vegetable garden, the dilution factor for mixing of waste in garden soil is given by the ratio of the volume of waste exhumed by drilling to the volume of garden soil into which the exhumed waste is mixed. These two volumes are estimated as follows.

The volume of radioactive waste that would be exhumed by drilling can be estimated from the thickness of buried waste in the disposal facility and the diameter of a well. For the current design of CIIDF, each disposal pad will consist of three layers of waste vaults, with each vault containing a waste box 1.2 m high. Therefore, the total thickness of buried waste is expected to be about 3.6 m. The diameter of a well drilled through the waste then is assumed to be 0.15 m. This value should not

underestimate the diameter of a well that would be established for domestic use on the disposal site. From the assumed thickness of buried waste and diameter of a well, the assumed volume of waste exhumed by drilling then is about 0.06 m^3.

The intruder's vegetable garden into which all of the exhumed drilling waste is mixed is assumed to be about 200 m^2 in area. A garden of this size should be sufficient to provide half of the entire yearly intake of vegetables by an intruder, as assumed in this analysis. The waste is assumed to be mixed to a depth of 0.15 m, which is a typical depth of a plowed layer in garden soil. Therefore, the volume of soil into which the waste exhumed from the disposal facility is mixed is assumed to be about 30 m^3.

From the estimated volume of contaminated drilling waste of 0.06 m^3 and the assumed volume into which this waste is mixed of 30 m^3, the dilution factor (f_s) assumed in the analysis for the post-drilling scenario then is 0.002. This value is 1% of the corresponding dilution factor assumed in the agriculture scenario. This difference reflects the much smaller volume of waste that would be exhumed by drilling compared to the volume of waste that would be exhumed while digging a foundation for a home.

In a previous analysis of the post-drilling scenario for the SWSA 6 disposal facility (ORNL 1994), the dilution factor for mixing of exhumed drilling waste with native soil in the intruder's vegetable garden was assumed to be 0.02, which is a factor of ten greater than the value assumed in this analysis. In the previous analysis, the volume of contaminated material exhumed by drilling was assumed to be 0.5 m^3, based on an estimate for a disposal site on the Hanford Reservation (Kennedy, Napier, and Soldat 1983). However, this value clearly is much too large for CIIDF, based on the current design of the facility.

For the post-drilling scenario, the annual doses to an inadvertent intruder from all exposure pathways per unit concentration of radionuclides in the disposal facility at the time intrusion is assumed to occur, as obtained from the models and parameter values described above, are summarized in Table G.17. Based on the comparison of the waste dilution factors (f_s) for the post-drilling and agriculture scenarios described above, the total dose for each radionuclide is 1% of the sum of the doses from the garden pathways given in Table G.15.

G.6 SUMMARY

This appendix has presented the models and data bases used in estimating EDEs to (1) off-site individuals resulting from exposure to radionuclides in contaminated groundwater or surface water and (2) inadvertent intruders resulting from direct intrusion into the waste disposal facility. In each case, particular exposure scenarios and associated exposure pathways have been evaluated. For each exposure pathway, simple models for estimating dose have been developed, and annual doses per unit concentration of radionuclides in water or in the disposal facility have been estimated on the basis of assumed parameter values for the particular pathway models. In the absence of site-specific data for most parameters in the models, the assumed parameter values were based on generic data available in the literature.

Table G.17. Annual effective dose equivalents to inadvertent intruders per unit concentration of radionuclides in exhumed waste from all exposure pathways for post-drilling scenario[a]

Nuclide[b]	Annual dose (rem/year per μCi/m^3)	Nuclide	Annual dose (rem/year per μCi/m^3)
^{3}H	4.0×10^{-8}	^{137}Cs + d	1.3×10^{-7}
^{10}Be	6.5×10^{-10}	^{151}Sm	1.1×10^{-10}
^{14}C	1.5×10^{-7}	^{152}Eu	7.8×10^{-8}
^{26}Al	1.8×10^{-7}	^{154}Eu	8.5×10^{-8}
^{36}Cl	1.2×10^{-5}	^{155}Eu	2.6×10^{-9}
^{40}K	6.0×10^{-7}	^{207}Bi	1.0×10^{-7}
^{41}Ca	2.5×10^{-8}	^{210}Pb + d	3.1×10^{-6}
^{60}Co	1.8×10^{-7}	^{226}Ra[d,e]	3.0×10^{-7}
^{59}Ni	7.2×10^{-10}	^{222}Rn	1.3×10^{-6}
^{63}Ni	2.0×10^{-9}	^{229}Th + d	3.0×10^{-7}
^{79}Se	1.2×10^{-8}	^{230}Th	3.5×10^{-8}
^{87}Rb	1.9×10^{-8}	^{232}Th + d[e]	6.4×10^{-7}
^{90}Sr + d	2.0×10^{-6}	^{220}Rn	2.1×10^{-7}
^{93}Zr[c]	1.4×10^{-10}	^{231}Pa + d	2.0×10^{-6}
^{93m}Nb	1.8×10^{-10}	^{232}U + d[e]	5.7×10^{-7}
^{94}Nb	1.1×10^{-7}	^{220}Rn	2.1×10^{-7}
^{99}Tc	1.3×10^{-7}	^{233}U	8.1×10^{-8}
^{107}Pd	3.4×10^{-10}	^{234}U	7.8×10^{-8}
^{113m}Cd	1.4×10^{-6}	^{235}U + d	8.5×10^{-8}
^{121m}Sn	6.5×10^{-10}	^{236}U	7.5×10^{-8}
^{126}Sn + d	1.4×10^{-7}	^{238}U + d	7.2×10^{-8}
^{129}I	8.2×10^{-7}	^{237}Np + d	2.7×10^{-6}
^{135}Cs	1.2×10^{-8}	^{238}Pu	1.8×10^{-7}

Table G.17 (continued)

Nuclide[b]	Annual dose (rem/year per μCi/m³)	Nuclide	Annual dose (rem/year per μCi/m³)
^{239}Pu	2.0×10^{-7}	^{244}Cm	1.1×10^{-7}
^{240}Pu	2.0×10^{-7}	^{245}Cm	2.1×10^{-7}
^{241}Pu	3.9×10^{-9}	^{246}Cm	2.1×10^{-7}
^{242}Pu	1.9×10^{-7}	$^{247}Cm + d$	2.1×10^{-7}
$^{244}Pu + d$	2.0×10^{-7}	^{248}Cm	7.7×10^{-7}
^{241}Am	2.5×10^{-7}	^{249}Cf	2.8×10^{-7}
$^{242m}Am + d$[f]	2.5×10^{-7}	^{250}Cf	1.1×10^{-7}
$^{243}Am + d$	2.6×10^{-7}	^{251}Cf	2.7×10^{-7}
^{243}Cm	1.4×10^{-7}		

[a]Values are 1% of annual EDEs per unit concentration in disposal facility for garden pathways given in Table G.15.

[b]The notation "+ d" with some entries denotes short-lived decay products that are assumed to be in secular equilibrium with parent radionuclide; see Table G.1 for decay products and branching fractions.

[c]Possible contributions to dose from ^{93m}Nb decay product are not included.

[d]Possible contributions to dose from ^{210}Pb decay product are not included.

[e]Contribution to dose from radon decay product is listed separately.

[f]Possible contributions to dose from ^{238}Pu decay product are not included.

For each exposure scenario, the annual doses per unit concentration of a radionuclide for each exposure pathway have been added to obtain the total annual dose per unit concentration from all pathways. However, the exposure scenario for off-site individuals considered only a single exposure pathway (the drinking water pathway), and only a single exposure pathway (external exposure during indoor residence) was relevant for the resident scenario for inadvertent intruders. In addition, for the agriculture scenario for inadvertent intruders, the total dose from all pathways involving exposure to contaminated garden soil was listed separately from the total dose from all exposure pathways during indoor residence, because the concentration of radionuclides per unit volume of material exhumed from the disposal facility during excavation generally would be different from the concentration per unit volume of waste in the disposal facility, due to the presence of a cap above the facility. The following summary tables give the total annual dose per unit concentration of radionuclides in water or the disposal facility for the different exposure scenarios:

- Table G.6, exposure of off-site individuals to contaminated groundwater or surface water;
- Table G.15, agriculture scenario for exposure of inadvertent intruders;
- Table G.16, resident scenario for exposure of inadvertent intruders; and
- Table G.17, post-drilling scenario for exposure of inadvertent intruders.

In the dose analysis for each exposure scenario and exposure pathway, some of the model parameters depend on the particular radionuclide or chemical element, whereas other parameters are the same for all radionuclides. The radionuclide- or element-specific parameter values are given in Tables G.2–G.5, and G.7. The parameter values that are independent of radionuclide are summarized in Table G.18.

For the three scenarios involving direct intrusion into solid waste in the disposal facility, the radionuclide concentrations to which the doses are normalized are the concentrations in the facility at the time intrusion is assumed to occur, rather than the concentrations at the time of disposal. The dose analyses for these scenarios presented in this appendix do not include any assumptions about the time after disposal at which intrusion occurs. Such assumptions are applied when the results of the intruder dose analyses are combined with the results of the PA for the disposal facility, which yield predictions of the concentrations of radionuclides remaining in the disposal facility as a function of time after disposal.

Table G.18. Summary of radionuclide-independent parameter values used in dose analyses for off-site individuals and inadvertent intruders

Parameter description	Symbol	Parameter value
Consumption of contaminated drinking water[a]	U_w	730 L/year
Consumption of contaminated vegetables[b]	U_v	90 kg/year (fresh weight)
Density of soil[b]	ρ_s	1400 kg/m^3
Dilution factor for mixing of exhumed waste with native soil in vegetable garden	f_s	0.2[c] 0.002[d]
Consumption of contaminated soil[b]	U_s	0.037 kg/year
Exposure times		
Working in garden[b]	U_s, f_a	1% per year
Residing in home[e]	U_r, f_a	50% per year
Shielding factor for external exposure during indoor residence[e]	S	0.7
Air intake (breathing rate)[b]	U_a	8,000 m^3/year
Atmospheric mass loading of contaminated surface soil	L_a	
Working in garden[b]		10^{-7} kg/m^3
Residing in home[c]		10^{-8} kg/m^3

[a]Parameter applies to exposure of off-site individuals from use of contaminated groundwater or surface water.

[b]Parameter applies to agriculture and post-drilling scenarios for inadvertent intruders.

[c]Parameter applies to agriculture scenario for inadvertent intruders.

[d]Parameter applies to post-drilling scenario for inadvertent intruders.

[e]Parameter applies to agriculture and resident scenarios for inadvertent intruders.

G.7 REFERENCES

Anspaugh, L. R. et al. 1975. "Resuspension and Redistribution of Plutonium in Soils," *Health Phys.* **29**, 571.

Baes, C. F. III, and R. D. Sharp 1983. "A Proposal for Estimation of Soil Leaching Constants for Use in Assessment Models," *J. Environ. Qual.* **12**(1), 17–28.

Baes, C. F. et al. 1984. *A Review and Analysis of Parameters for Assessing Transport of Environmentally Released Radionuclides Through Agriculture,* ORNL-5786, Martin Marietta Energy Systems, Inc., Oak Ridge Natl. Lab.

Eckerman, K. F., A. B. Wohlbarst, and A. C. B. Richardson 1988. *Limiting Values of Radionuclide Intake and Air Concentration and Dose Conversion Factors for Inhalation, Submersion, and Ingestion*, Federal Guidance Report No. 11, EPA-520/1-88-020, Oak Ridge Natl. Lab. and U.S. Environmental Protection Agency, Washington, D.C.

Eckerman, K. F., and J. C. Ryman 1993. *External Exposure to Radionuclides in Air, Water, and Soil,* Federal Guidance Report No. 12, EPA 402-R-93-081, Oak Ridge Natl. Lab. and U.S. Environmental Protection Agency, Washington, D.C.

EPA (U.S. Environmental Protection Agency) 1989. *Risk Assessment Guidance for Superfund, Vol. I. Human Health Evaluation Manual (Part A)*, EPA/540/1-89/002, Washington, D.C.

Garten, C. T., Jr., et al. 1987. "Field Studies on the Terrestrial Behavior of Actinide Elements in East Tennessee," p. 109 in *Environmental Research on Actinide Elements*, ed. J. E. Pinder III et al. CONF-841142, U.S. Department of Energy, Washington, D.C.

Hamby, D. M. 1992. "Site-Specific Parameter Values for the Nuclear Regulatory Commission's Food Pathway Dose Model," *Health Phys.* **62**, 136.

Kennedy, W. E., Jr., B. A. Napier, and J. K. Soldat 1983. "Advanced Disposal Systems for Transuranic Waste: Preliminary Disposal Criteria for Plutonium-239 at Hanford," *Nucl. Chem. Waste Manage.* **4**, 103.

Kocher, D. C. 1981. *Radioactive Decay Data Tables*, DOE/TIC-11026, U.S. Department of Energy, Washington, D.C.

Kocher, D. C., and A. L. Sjoreen 1985. "Dose-Rate Conversion Factors for Photon Emitters in Soil," *Health Phys.* **48**, 193.

MMES, EG&G, and WSCR (Martin Marietta Energy Systems, Inc.; EG&G Idaho, Inc.; and Westinghouse Savannah River Company) 1994. *Radiological Performance Assessment for the E-Area Vaults Disposal Facility*, WSRC-RP-94-218, Westinghouse Savannah River Company, Aiken, S.C.

Napier, B. A. et al. 1984. *Intruder Dose Pathway Analysis for the Onsite Disposal of Radioactive Waste: The ONSITE/MAXI1 Computer Program*, NUREG/CR-3620, PNL-4054, Pacific Northwest Laboratory, Richland, Wash.

NCRP (National Council on Radiation Protection and Measurements) 1984. *Exposures from the Uranium Series with Emphasis on Radon and Its Daughters*, NCRP Report No. 77, Bethesda, Md.

NCRP (National Council on Radiation Protection and Measurements) 1987. *Exposure of the Population in the United States and Canada from Natural Background Radiation*, NCRP Report No. 94, Bethesda, Md.

NRC (U.S. Nuclear Regulatory Commission) 1977. "Calculation of Annual Doses to Man from Routine Releases of Reactor Effluents for the Purpose of Evaluating Compliance with 10 CFR Part 50, Appendix I," Regulatory Guide 1.109, Washington, D.C.

NRC (U.S. Nuclear Regulatory Commission) 1982. *Final Environmental Impact Statement on 10 CFR Part 61 "Licensing Requirements for Land Disposal of Radioactive Waste,"* NUREG-0945, Vol. 1, Washington, D.C.

ORNL (Oak Ridge National Laboratory) 1994. *Performance Assessment for Continuing and Future Operations at Solid Waste Storage Area 6*, ORNL-6783, Martin Marietta Energy Systems, Inc., Oak Ridge, Tenn.

Oztunali, O. I. et al. 1981. *Data Base for Radioactive Waste Management*, NUREG/CR-1759, Vol. 3, Dames and Moore, Inc., and U.S. Nuclear Regulatory Commission, Washington, D.C.

Peterson, H. T., Jr. 1983. "Terrestrial and Aquatic Food Chain Pathways," Chap. 5 in *Radiological Assessment*, ed. J. E. Till and H. R. Meyer, NUREG/CR-3332, ORNL-5968, U.S. Nuclear Regulatory Commission and Oak Ridge Natl. Lab., Washington, D.C.

Sheppard, M. I., S. C. Sheppard, and B. D. Amiro 1991. "Mobility and Plant Uptake of Inorganic ^{14}C and ^{14}C-Labelled PCB in Soils of High and Low Retention," *Health Phys.* **61**, 481.

Shinn, J. H., D. N. Norman, and D. D. Gay 1982. "Plutonium Aerosol Fluxes and Pulmonary Exposure Rates During Resuspension from Bare Soils Near a Chemical Separation Facility," p. 1131 in *Precipitation Scavenging, Dry Deposition, and Resuspension*, Vol. 2, ed. H. R. Pruppacher, R. G. Semonin, and W. G. N. Slinn, Elsevier Science Publishing Co., New York.

UNSCEAR (United Nations Scientific Committee on the Effects of Atomic Radiation) 1988. *Sources, Effects and Risks of Ionizing Radiation*, United Nations, New York.

INTERNAL DISTRIBUTION

1. J. K. Bailey
2 K.A. Balo
3. G. E. Courville
4. G. R. Cunningham
5. J. R. Forgy, Jr.
6. W. C. Gilbert
7. S. C. Howard
8. A. S. Icenhour
9. L. S. Jones
10. D. C. Kocher
11. D. W. Lee
12. S. L. Loghry
13. D. A. Lombardi
14. R. J. Luxmoore
15. C. I. Moser
16. R. M. Reed
17. R. B. Shelton
18. M. L. Socolof
19. J. D. Tauxe
20. M. L. Tharp
21. S. M. Trotter
22. M. W. Tull
23. M. W. Yambert
24. ORNL Patent Office
25. Central Research Library
26. Document Reference Section
27-28. Laboratory Records
29. Laboratory Records - RC

EXTERNAL DISTRIBUTION

30. Dr. Lilia A. Abron, President, PEER Consultants, P.C., 1000 N. Ashley Drive, Suite 312, Tampa, FL 33602
31. Dr. Thomas E. Drabek, Professor, Department of Sociology, University of Denver, Denver, CO 80208-0209
32. Dr. Stephen G. Hildebrand, Director, Environmental Sciences Division, Oak Ridge National Laboratory, P.O. Box 2008, Oak Ridge, TN 37831-6037
33. Dr. Susan F. Tierney, The Economic Resource Group, Inc., One Mifflin Place, Cambridge, MA 02138
34. Dr. C. Michael Walton, Ernest H. Cockrell Centennial Chair in Engineering and Chairman, Department of Civil Engineering, University of Texas at Austin, Austin, TX 78712-1076
35. Herschel W. Godbee, 104 Tidewater Lane, Oak Ridge, TN 37830
36. ORNL Site Manager, U.S. Department of Energy, Oak Ridge National Laboratory, P.O. Box 2008, Oak Ridge, TN 37831-6269

37-38. OSTI, U.S. Department of Energy, P.O. Box 62, Oak Ridge, TN 37831